이학박사 학위논문

Development of Catalytic Transformations of Isocyanides and Allylic Compounds

아이소사이아나이드와 알릴 화합물의 촉매적 변환 개발

2020 년 8 월

서울대학교 대학원

화학부 유기화학 전공

김 정 원

아이소사이아나이드와
알릴 화합물의 촉매적 변환 개발

지도교수 이 홍 근

이 논문을 이학박사 학위논문으로 제출함
2020 년 7 월

서울대학교 대학원
화학부 유기화학전공
김 정 원

김정원의 이학박사 학위논문을 인준함
2020 년 7 월

위 원 장 최태림 (인)

부위원장 이홍근 (인)

위 원 David Chem (인)

위 원 정 영 근 (인)

위 원 홍 순 혁 (인)

Abstract

Development of Catalytic Transformations of Isocyanides and Allylic Compounds

Jungwon Kim

Department of Chemistry

The Graduate School

Seoul National University

Catalytic transformations of the organic compounds provide useful strategies to produce valuable structures efficiently. The control of catalytic conditions, based on the chemical property of the substrate and the previously established strategies, is the key to achieving the unprecedented and novel organic transformations. This thesis covers the discovery of an array of catalytic transformations of isocyanides and allylic compounds toward the synthetically meaningful chemical structures.

In Part 1, the chemistry and the catalytic utilization of isocyanides will be discussed. The ability of the terminal carbon of the isocyanide as both a nucleophile and an electrophile has enabled the various types of activation modes in the catalysis. Chapter 1 describes the detailed mechanistic strategies for the activation of the terminal carbon of isocyanides, together with the representative

examples reported so far. Chapters 2 and 3 introduce a new approach for the catalytic nucleophilic activation of the isocyanides. Especially, the utilization of N-heterocyclic carbene (NHC) as an organocatalyst for the transformations of isocyanides will be demonstrated. The reactions with ketones provide several types of enaminones in high efficiency (Chapter 2), and the novel formamidine structure is accessible through the reaction between indoles and isocyanides using the developed activation strategy (Chapter 3).

Part 2 discusses the achievement of the catalytic C(sp^3)–H bond functionalizations via visible light photoredox catalysis. The use of visible light as an energy source to conduct a challenging C(sp^3)–H bond activation reaction has been widely investigated in the organic synthesis. Chapter 4 reviews the currently established approaches for the C(sp^3)–H bond functionalizations with visible light photoredox catalysis, based on the categorized strategies and the representative transformations. Chapter 5 discloses a new method to synthesize allyl thioethers from simple allylic compounds and disulfides via visible light photoredox catalysis. The design of the target catalytic cycle for the prevention of the side reaction (hydrothiolation) enabled the selective allylic C(sp^3)–H bond thiolation, and the in-depth mechanistic studies expanded the substrate scope through the introduction of tailored unsymmetrical disulfides.

Keywords : Isocyanide, nucleophilic activation, organocatalysis, N-heterocyclic carbene, allylic compound, visible light, photoredox catalysis, allyl thioether

Student Number : 2014-21250

Table of Contents

Chapter 3. Dual Activation of Nucleophiles and Electrophiles by N-Heterocyclic Carbene Organocatalysis: Chemoselective N-Imination of Indoles with Isocyanides

Chapter 5. Direct Allylic C(sp^3)–H Thiolation with Disulfides via Visible Light Photoredox Catalysis

Appendix

NMR Spectra

Cartesian Coordinates for DFT Calculation

List of Tables

Chapter 2

Chapter 3

Chapter 5

List of Schemes

Chapter 1

Chapter 2

Chapter 3

Chapter 4

Chapter 5

List of Figures

Chapter 2

Chapter 3

Chapter 5

List of Abbreviations

%	Percent
[PC]	Photocatalyst
°C	Degree Celsius
1°	Primary
^{13}C NMR	Carbon thirteen nuclear magnetic resonance
^{19}F NMR	Fluorine nineteen nuclear magnetic resonance
^{1}H NMR	Proton nuclear magnetic resonance
2°	Secondary
3°	Tertiary
9-BBN	9-Borabicyclo[3.3.1]nonane
A	Absorbance
Å	Angstrom
acac	Acetylacetone
Ad	Adamantyl
AIBN	2,2′-Azobis(2-methylpropionitrile)
Alk	Alkyl
aq.	Aqueous
AQN	Anthraquinone
Ar	Aryl
BAr_F	Tetrakis[3,5-bis(trifluoromethyl)phenyl]borate
BDE	Bond dissociation energy
BiOx or BOX	Bis(oxazoline)
Bn	Benzyl
Boc	*tert*-Butyloxycarbonyl
bpy	2,2-Bipyridine
cat.	Catalytic
C–C	Carbon-carbon single bond
C–C	Carbon-carbon single bond
CCDC	The Cambridge Crystallographic Data Centre
CF_3ppy	2-(4-(Trifluoromethyl)phenyl)pyridine
CFL	Compact fluorescent lamp
C–H	Carbon-hydrogen single bond
cm	Centimeter(s)
COD	1,5-Cyclooctadiene
Cp*	1,2,3,4,5-Pentamethylcyclopentadienyl anion

C–S	Carbon-sulfur single bond
C–Te	Carbon-tellurium single bond
CV	Cyclic voltammetry
Cy	Cyclohexyl
Cz	Carbazole
$_D$	*Dexter*
d	Distance
DABCO	1,4-Diazabicyclooctane
dba	Dibenzylideneacetone
DBU	1,8-Diazabicyclo(5.4.0)undec-7-ene
DCE	Dichloroethane
$dFCF_3ppy$	2-(2,4-Difluorophenyl)-5-(trifluoromethyl)pyridine
DFT	Density-functional theory
DIPEA	*N*,*N*-Diisopropylethylamine
DMA	*N*,*N*-Dimethylacetamide
DMBP	Bis(4-methoxyphenyl)methanone
DME	1,2-Dimethoxyethane
DMF	Dimethylformamide
dmg	Dimethylglyoxime dianion
DMPU	1,3-Dimethyl-3,4,5,6-tetrahydro-2-pyrimidinone
DMSO	Dimethylsulfoxide
DNB	Dinitrobenzene
DPA	Diphenylamine
dppe	1,2-Bis(diphenylphosphino)ethane
dppf	1,1'-Bis(diphenylphosphino)ferrocene
dppp	1,3-Bis(diphenylphosphino)propane
dr	Diastereomeric ratio
dtbbpy	4,4′-Di-*tert*-butyl-2,2′-dipyridyl
DTBP	Di-*tert*-butyl peroxide
E	*Entgegen*
e.g.	For example (exempli gratia)
E^+	Electrophile
EI	Electron ionization
EnT	Energy transfer
$E°$	Standard reduction potential
E^{ox}	Electrochemical oxidation potential
E_p	Peak potential

equiv	Equivalents
E^{red}	Electrochemical reduction potential
ESI	Electrospray ionization
Et	Ethyl
E_T	Triplet-state energy
EWG	Electron-withdrawing group
EY	Eosin Y
FAB	Fast atom bombardment
fac	Facial
Fc	Ferrocene
FG	Functional group
g	Gram(s)
GC	Gas chromatography
glyme	1,2-Dimethoxyethane
h	Hour(s)
HAT	Hydrogen atom transfer
HFIP	Hexafluoroisopropanol
HOMO	Highest occupied molecular orbital
HRMS	High resolution mass spectrometer
hν	Photon of light
Hz	Hertz
I	Intensity
i. e.	That is (id est)
IPN	Isophthalonitrile
iPr	Isopropyl
IPrHCl	1,3-Bis-(2,6-diisopropylphenyl)imidazolinium chloride
ISC	Intersystem crossing
kcal	Kilocalories
KHMDS	Potassium bis(trimethylsilyl)amide
KIE	Kinetic isotope effect
L	Liter(s)
LDA	Lithium diisopropylamide
LED	Light emitting diode
LiHMDS	Lithium bis(trimethylsilyl)amide
LMCT	Ligand-to-metal charge transfer
LTMP	Lithium 2,2,6,6-tetramethylpiperidide
LUMO	Lowest occupied molecular orbital

m	*meta*
M	Molar concentration
m/z	Mass to charge ratio
MCR	Multicomponent reactions
Me	Methyl
MeCN	Acetonitrile
Mes	Mesityl
mg	Milligram(s)
MHz	Megahertz
min	Minute(s)
mL	Milliliter(s)
mM	Millimolar concentration
mmol	Millimolar
mol%	Molar percentage
MS	Molecular sieve
N	Equivalent concentration (normality)
*n*Bu	Normal butyl
NFSI	*N*-fluorobenzenesulfonimide
N–H	Nitrogen-hydrogen single bond
NHC	N-heterocyclic carbene
NHK	Nozaki–Hiyama–Kishi
NHPI	*N*-Hydroxyphthalimide
nm	Nanometer(s)
NMR	Nuclear magnetic resonance
Nu or Nu^-	Nucleophile
o	*ortho*
OAc	Acetate
O–H	Oxygen-hydrogen single bond
O–O	Oxygen-oxygen single bond
O–Si	Oxygen-silicon single bond
p	*para*
PCET	Proton-coupled electron transfer
Ph	Phenyl
P–H	Phosphorous-hydrogen single bond
Phen	1,10-Phenanthroline
Phth	Phthalimidyl
PIDA	(Diacetoxyiodo)benzene

Piv	Trimethylacetyl
pK_a	Logarithm of acidity equilibrium constant
PMP	*para*-Methoxyphenyl
PPh_3	Triphenylphosphine
ppm	Parts per million
ppy	2-Phenylpyridine
PTFE	Poly(tetrafluoroethylene)
p-tol	*para*-Tolyl
RBF	Round-bottom flask
R_f	Fluorinated alkyl
rr	Regioisomeric ratio
rt	Room temperature
s	Second(s)
salen	*N*,*N*′-ethylenebis(salicylimine)
SCE	Saturated calomel electrode
SET	Single electron transfer
S–H	Sulfur-hydrogen single bond
Si–H	Silicon-hydrogen single bond
SIPrHCl	1,3-Bis-(2,6-diisopropylphenyl)imidazolinium chloride
S–S	Sulfur-sulfur single bond
TBHP	*tert*-Butyl hydroperoxide
*t*Bu	*tert*-Butyl
*t*BuOH	*tert*-Butanol
TEMPO	(2,2,6,6-Tetramethylpiperidin-1-yl)oxyl
Tf	Trifluoromethylsulfonyl
TFA	Trifluoroacetic acid
THF	Tetrahydrofuran
THIQ	Tetrahydroisoquinoline
TLC	Thin layer chromatography
TMS	Trimethylsilyl
*t*Pent	*tert*-Pentyl
tpy	2, 2′:6′, 2″-Terpyridine
Ts	*para*-Toluenesulfonyl
UV	Ultraviolet
V	Volt(s)
vis	Visible
W	Watt(s)

wt%	weight percent
Z	*Zusammen*
ΔG	Free energy change
$\Delta G^{\ddagger}$	Transition state free energy
ε	Extinction coefficient
λ	Wavelength
μA	Microampere(s)
μL	Microliter(s)
μM	Micromolar

Chapter 1. Utilization of Isocyanides in Organic Transformations

1.1 Introduction

Isocyanides, first obtained in 1867 by Gautier[1] and Hofmann[2], are an important class of molecules in organic synthesis.[3] Although a characteristic odor from isocyanides make chemists unpleasant to work with in the laboratory, a unique reactivity derived from the isomeric structure of cyanides has stimulated the usage in inorganic chemistry as a ligand and organic synthesis as a reactive functional group.[4] Because the electronic structure of an isocyanide can be described by either a carbenic form or a zwitterionic form (Scheme 1.1), the terminal carbon acts as both a nucleophile and an electrophile, depending on the reaction conditions or the coupling partners. This unique property enabled characteristic reactivities of isocyanides with wide ranges of nucleophiles, electrophiles, and catalysts.

In this Chapter, an array of organic transformations involving isocyanide will be discussed, classified by the activation strategy, together with the representative examples reported so far.

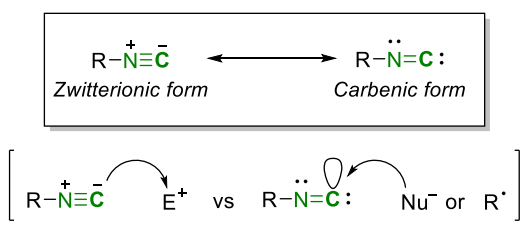

Scheme 1.1 Description of the electronic structure of isocyanide

1.2 Activation of the isocyanides with electrophilic component

1.2.1 Passerini and Ugi multicomponent reaction (MCR)

Multicomponent reactions (MCRs) are described as the convergent reactions involving more than two starting reaction components. Pioneered by the Strecker reaction discovered in 1850,[5] Hantzch MCR,[6] Biginelli MCR,[7] and Mannich MCR[8] have been developed as versatile methodologies for the construction of molecular complexity from readily available starting materials. Passerini MCR, reported firstly in 1921, produces α-acyloxyamides from isocyanide, ketone, and carboxylic acid (Scheme 1.2A).[9] In 1959, Ugi reported an extended version of Passerini MCR by the addition of amine as a fourth component, enabling four-multicomponent reaction (4-MCR) to produce peptoid structures in high efficiency (Scheme 1.2B).[10]

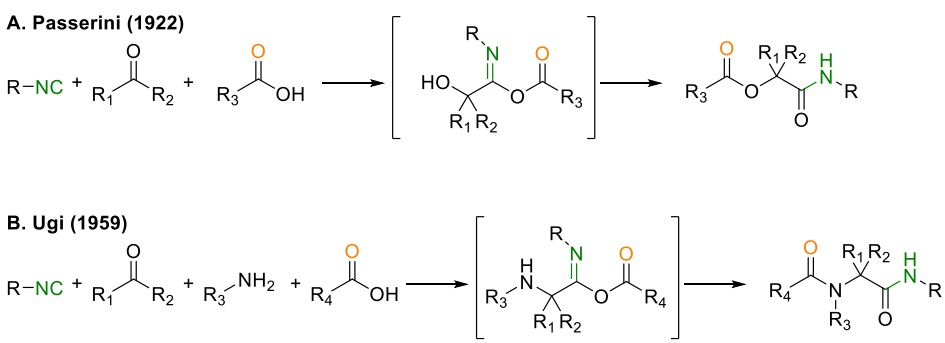

Scheme 1.2 Passerini and Ugi multicomponent reactions

After the initial observation of such reactivity, numerous applications have been reported in several transformations. For example, intramolecular Ugi 4-MCR enabled the synthesis of multicyclic structures from readily available precursors (Scheme 1.3A).[11] Also, the generated product after Ugi 4-MCR (peptoid) can be further transformed into other structures (post Ugi 4-MCR). Recently, Domling demonstrated a synthesis of highly functionalized imidazoles containing Uracil motif using sequential Ugi 4-MCR and condensation with ammonia, taking advantage of high functional group tolerance (Scheme 1.3B).[12] Another direction in the development of isocyanide-based MCR is the synthesis of enantio-enriched products via a catalytic asymmetric induction. A recent work by Houk and Tan elegantly demonstrated that such transformation could be realized by the incorporation of chiral phosphoric acid, which can deliver chiral information during the addition steps (Scheme 1.3C).[13]

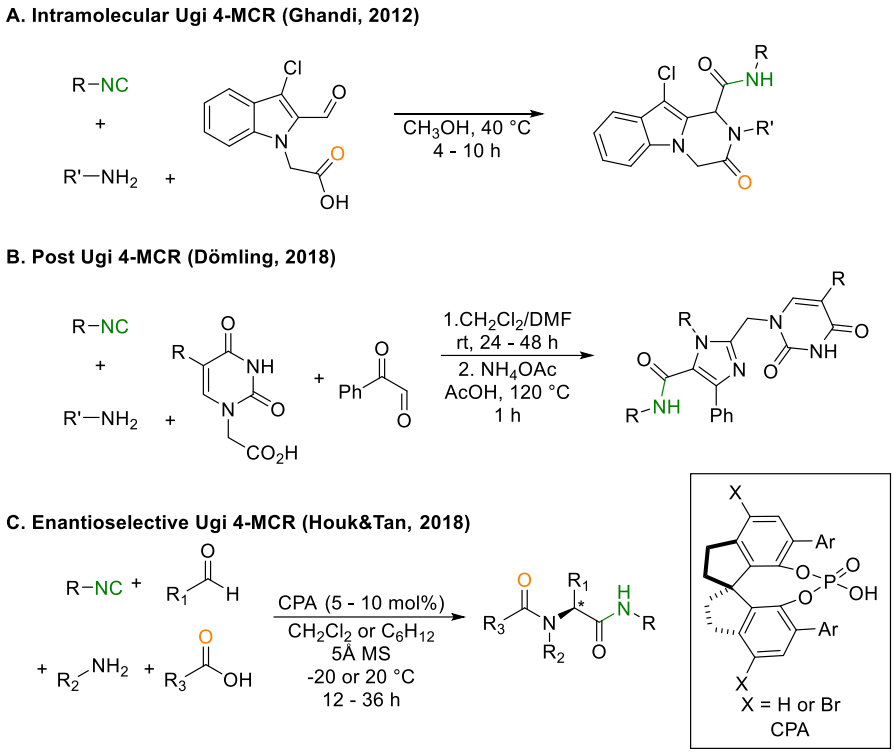

Scheme 1.3 Variations of Ugi 4-multicomponent reaction

1.2.2 Activation of isocyanides by other electrophilic partners

A major mechanistic feature of the isocyanide-based multicomponent reactions is an initial activation of the terminal carbon of isocyanide by electrophilic species, such as a protonated carbonyl or an iminium compound, further enhancing the electrophilicity of the isocyanide. This activation strategy can also be applied in the reactions with other electrophilic moieties, providing a generalized electrophilic activation protocol (Scheme 1.4).[14]

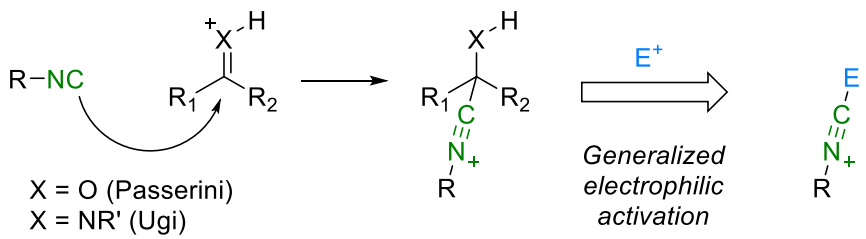

Scheme 1.4 Electrophilic activation strategy

In 1892, Nef utilized an acyl chloride as an electrophilic partner, instead of conventional carbonyl species, to generate an imidoyl chloride as a reactive intermediate. Further incorporation of an external nucleophile provides an α-iminocarbnyl compound (Scheme 1.5A).[15] For example, the use of H_2O or H_2S as a nucleophile produces corresponding amide or thioamide via the subsequent isomerization of the generated imine intermediate.[16] Further utilization of the produced imine product was also possible, as El Kaim and Grimaud demonstrated a further Huisgen rearrangement to form 1,2,4-triazole.[17]

The proposed strategy was extensively applied in the synthesis of cyclic structures, which was mainly developed by Livinghouse (Scheme 1.5B).[18] Because of the proximity effect, facile trapping of activated isocyanide species with the nucleophilic part in the molecule was possible, enabling the construction of diverse

cyclic structures. With the developed strategy, the synthesis of Dendrobine was achieved through the formation of key ring skeletons from the corresponding isocyanide precursors.[18d]

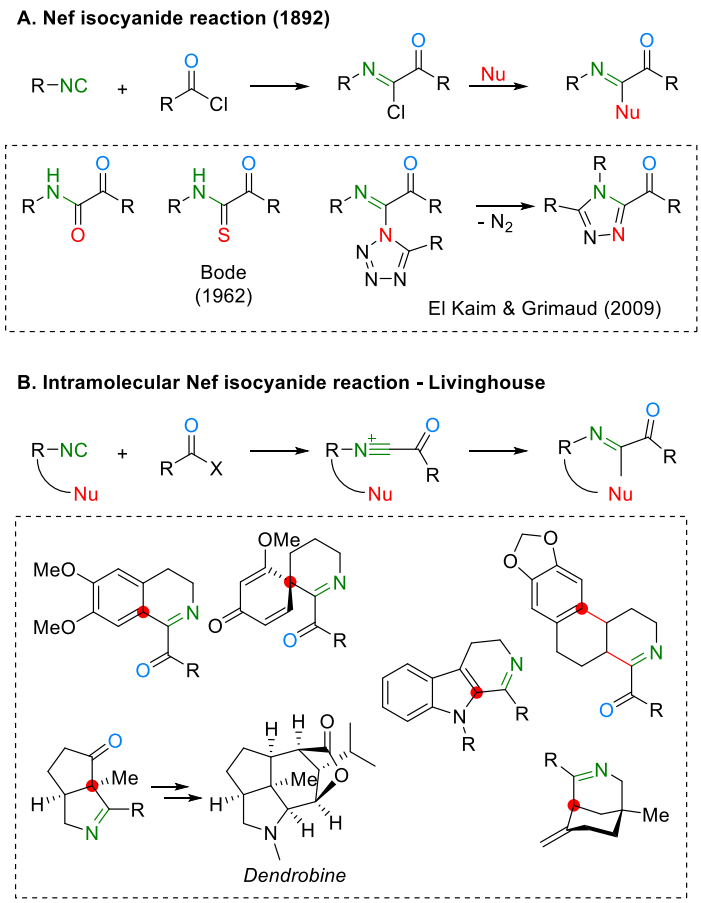

Scheme 1.5 Inter- and intra-molecular Nef isocyanide reaction

Electrophilic activation of isocyanide with other electrophilic coupling partners was also developed. In 1997, Shaabini reported the introduction of 1,1-dicarbonyl olefin which led the facile Michael addition of isocyanide toward the double bond. Further intramolecular trapping of the nitrilium intermediate with oxygen nucleophile generated 5-membered oxygen heterocyclic compounds.[19] Inspired by the initial observation, variation of the enone structure was performed, providing the novel route toward the 2-aminofuran skeleton (Scheme 1.6A).[20]

Highly electron-deficient alkynes, such as 1,2-dicarbonyl alkynes, can initiate a similar mechanistic scenario (Scheme 1.6B). After the addition of isocyanide, zwitterionic nitrilium-carbanion intermediate would be produced, which can act as a base for the activation of pronucleophilic species (NuH). In 2004, Yavari reported that the use of pronucleophilic N-heterocycles, such as pyrrole, indole, and carbazole, generates conjugated iminoamides as final products.[21] Interestingly, when isatoic anhydride was used as a pronucleophile, a 1,2-addition pattern was observed, producing ketenimine as the final product.[22] Similar reactivity was also found in the case of 4-hydroxycoumarine, and further annulation enabled the construction of pyrano[3,2-*c*]coumarins.[23]

1,1-dicyano alkene, similar to electron-deficient alkyne, is another category that can activate the terminal carbon of isocyanide (Scheme 1.6C). In this case, phenol and thiophenol are generally used for the trapping nucleophiles, and further cyclization produces the heteroatom-enriched nitrogen heterocycles in excellent efficiency.[24]

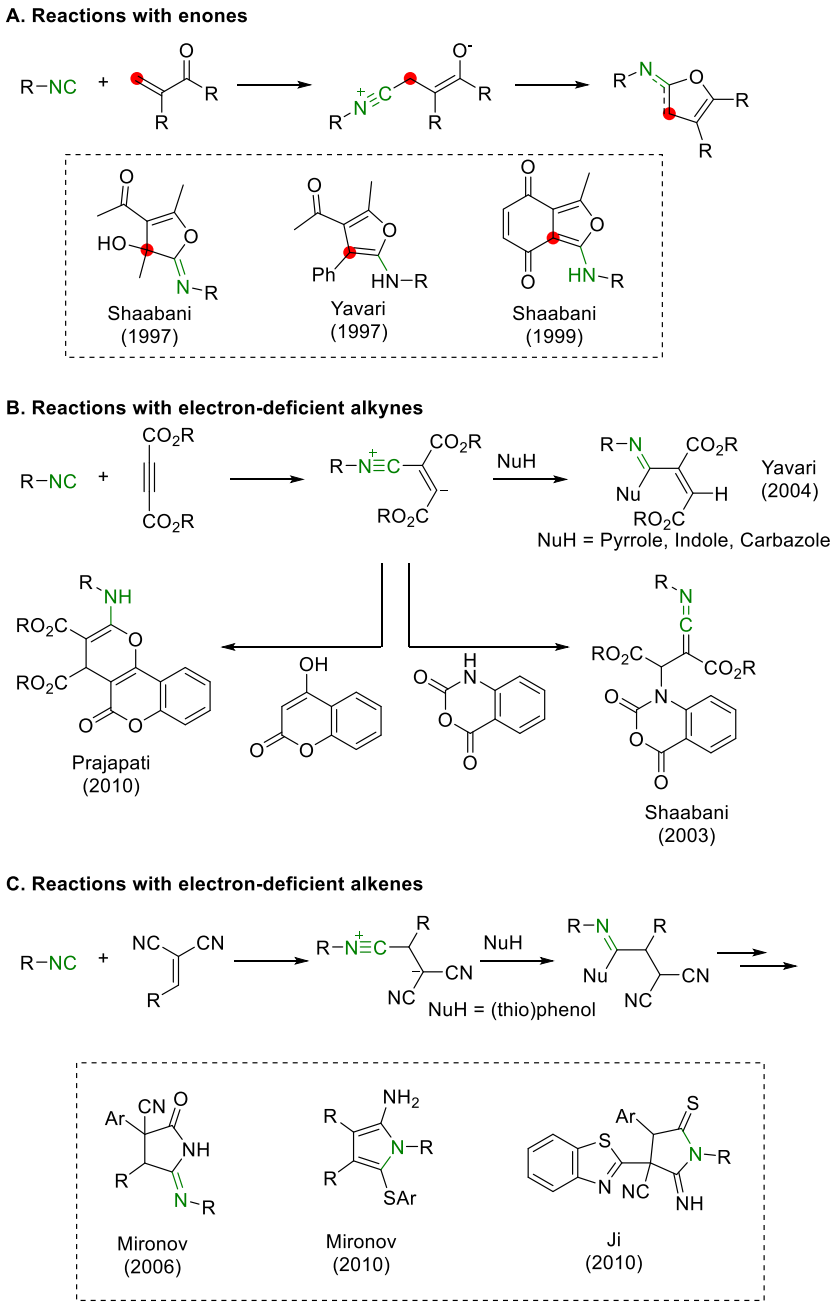

Scheme 1.6 Activation of isocyanides with electron-deficient π-systems

The combination of electrophile and Lewis acid is another method to activate the terminal carbon of isocyanide (Scheme 1.7). However, the choice of a Lewis acid is highly important, due to the competing polymerization and uncontrolled insertion of isocyanide toward the electrophile. Chatani observed that gallium (III) chloride ($GaCl_3$) has a moderate Lewis acidity, which is enough to activate the heteroatoms of the electrophiles but prevents the over-insertion process, for the reaction with isocyanide species.[25] The $GaCl_3$-catalyzed reaction between unactivated enone systems and aryl isocyanides produced γ-lactone derivatives.[26] Not only enones, but also other coupling partners, such as epoxide,[27] acetal,[28] and thioacetal,[29] can be applied with the developed strategy, forming isocyanide-inserted products.

In some cases, stronger Lewis acids, such as Et_2AlCl or $AlCl_3$, were used, together with the subsequent cyclization process, to prevent over-insertion. In 2006, Winkler provided the method to utilize α-furanoenone as a coupling partner, performing double-insertion and aromatization to produce a benzo-fused ring product.[30] Masson and Zhu applied in situ formed α,β-unsaturated imidoyl cyanide, performing isocyanide insertion, and cyclization to form substituted pyrroles under strong Lewis acidic conditions.[31] Recently, Shi demonstrated a silver-catalyzed synthesis of dihydrocyclobuta[*b*]quinoline from methylenecyclopropane, which is initiated by the activation of olefin by a silver catalyst, followed by nucleophilic attack of isocyanide and ring expansion process.[32]

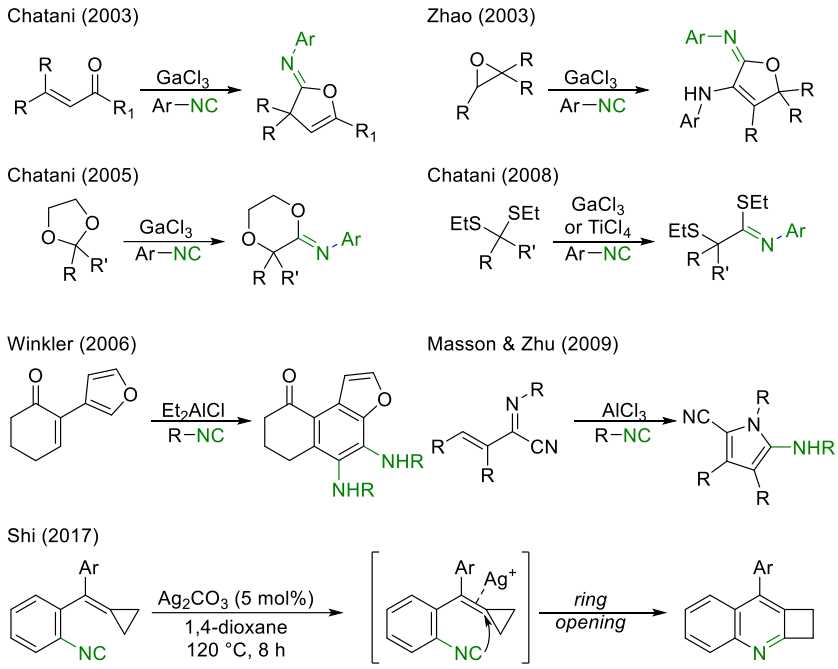

Scheme 1.7 Activation of isocyanides with electrophile-Lewis acid combination

The use of a stoichiometric amount of Lewis acid solely to increase the electrophilicity of the terminal carbon of isocyanide could be applied in the reactions with other nucleophiles (Scheme 1.8). Based on the previous reports about the formation of α-adduct between isocyanides and Lewis acids, a few examples adopted such a mechanistic strategy. For instance, Chatani reported a C3-imination of indole with isocyanide using aluminum (III) chloride as a Lewis acid.[33] Wang and Zhu applied zinc(II) bromide to activate isocyanide, producing functionalized oxazoles from carboxylic acid.[34] In both cases, the formation of α-adduct between Lewis acid and isocyanide facilitates the nucleophilic attack.

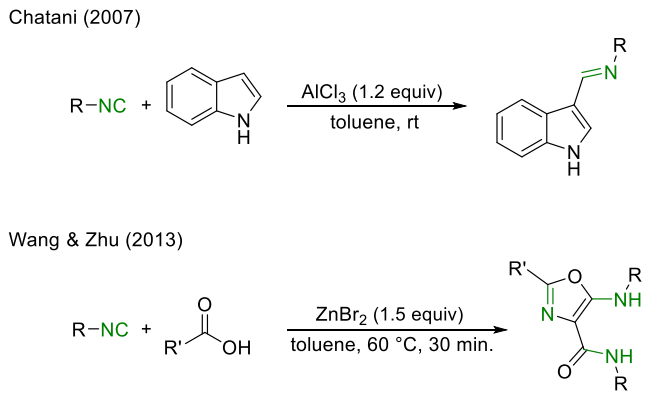

Scheme 1.8 Activation of isocyanides with Lewis acid

1.2.3 Activation of isocyanides by transition-metal catalysts

The introduction of transition-metal catalysis expanded the scope of the reactivity of isocyanide for various functionalizations. Taking advantage of the well-established elementary transformations of transition-metal complexes, a wide variety of coupling reactions onto the terminal carbon of isocyanide have been developed.

The seminal work of transition-metal catalyzed transformation of isocyanide was studied by Saegusa and Ito, utilizing a simple copper salt as a catalyst for the activation of terminal carbon of isocyanide (Scheme 1.9). With this highly electrophilic nitrilinium species, various heteroatom-based nucleophiles, including N–H,[35] O–H,[36] S–H,[37] Si–H,[38] and P–H nucleophiles,[39] can be cooupled, forming corresponding imino esters. Also, an activated methylene position, which can be easily deprotonated, participate in the reaction as a nucleophile, achieving C–C bond formation reactions.[40]

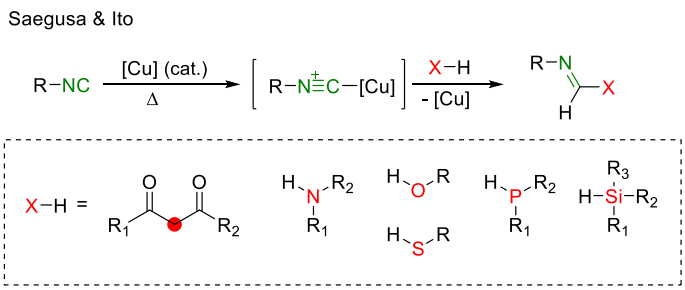

Scheme 1.9 Copper-catalyzed isocyanide insertion – early examples

The concept of electrophilic activation of the terminal carbon of isocyanide via the coordination of a copper catalyst provided numerous applications in various catalytic transformations (Scheme 1.10). In 2009, de Meijere reported an intramolecular version of copper-catalyzed isocyanide insertion into the O–H bond, generating imine-containing 6-membered ring structures.[41] Depending on the substituent on the benzyl position, rearrangement can occur to form 5-membered iminolactones. Hong reported the reactions of isocyanides with carbon-pronucleophiles, especially benzyl isocyanides and benzyl cyanides. The former case performs cyclization, producing 1,4-diaryl imidazole.[42] In contrast, the latter case provides β-enaminonitrile as the final product.[43] Mechanistic studies revealed that the use of *tert*-butoxide is crucial, which acts as a base and a mediator to form the key formimidate intermediate from isocyanide. Very recently, Wang and Ji developed an intramolecular cyclization process between carbonyl compounds and isocyanides, producing substituted quinolines.[44]

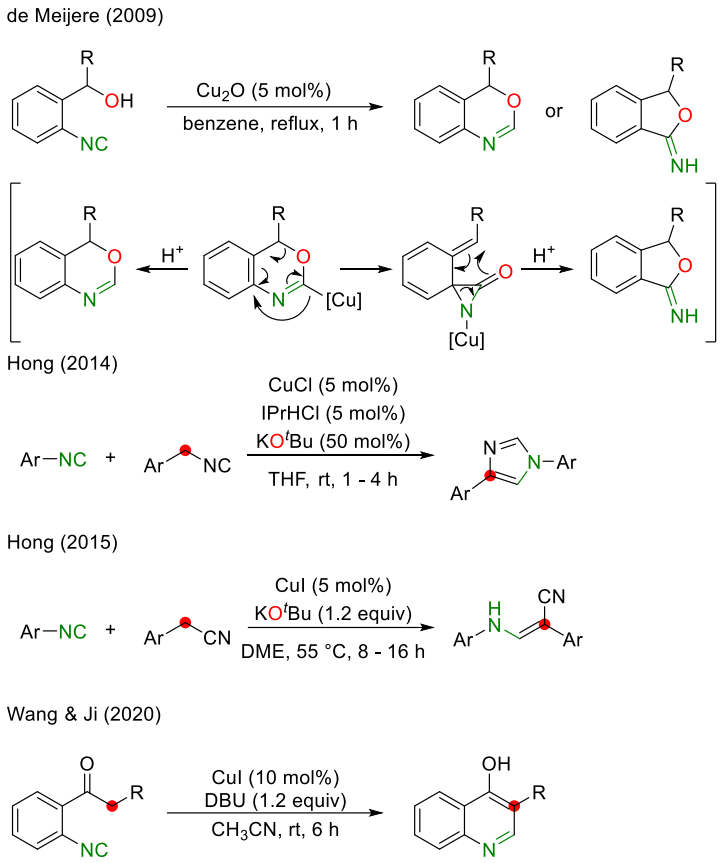

Scheme 1.10 Copper-catalyzed isocyanide insertion – recent applications

The use of a palladium catalyst achieved a breakthrough in the utilization of transition metal catalysts for the transformation of isocyanide.[45] The application of elementary reactions mediated by the palladium catalyst can be combined with the isocyanide insertion step, enabling the synthesis of an imino-substituted scaffold in a one-pot process (Scheme 1.11). Specifically, the oxidative addition of the palladium catalyst into aryl (pseudo)halides generates reactive Pd(II) species, which can undergo isocyanide coordination and insertion. Because of the similarity in the electronic structure between isocyanide and carbon monoxide, such an insertion step is highly facile and well-established. Further elaboration of the metal center via various elementary steps and reductive elimination produces an imine species from multiple starting molecules.

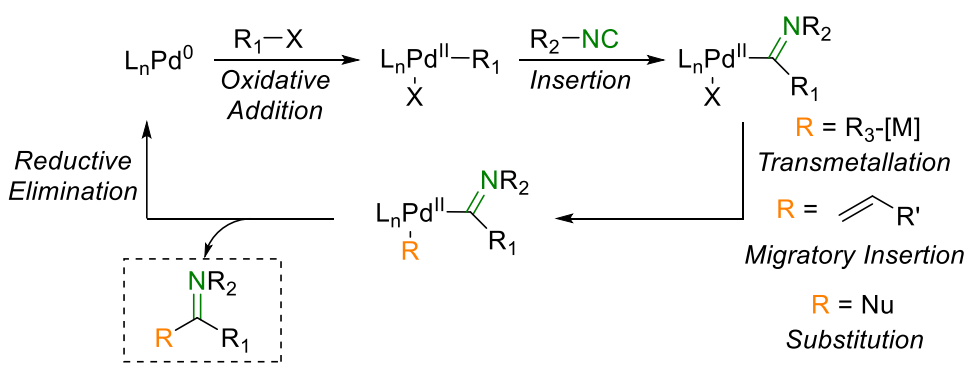

Scheme 1.11 Palladium-catalyzed isocyanide insertion – general mechanisms

An early example of the palladium-catalyzed isocyanide transformation was reported in 1986 by Kosugi and Migita (Scheme 1.12A).[46] The combination of the Stille coupling protocol with the isocyanide insertion process enabled the one-pot synthesis of functionalized imines under the aid of simple $Pd(PPh_3)_4$ precatalyst. This was also the case when the Suzuki coupling reaction was applied by replacing the organotin compound into an organoboron reagent.[47] Recently, a more practical protocol using Negishi coupling with organozinc reagent was developed by Dechert-Schmitt and Blackmond.[48] In this case, double insertion of *tert*-butyl isocyanide was performed, producing a 1,2-dicarbonyl compound after the hydrolysis. Migratory insertion steps can also be applied in the catalytic cycle via the introduction of an olefinic coupling partner (Scheme 1.12B). In 2002, Takahashi demonstrated the formation of indole via isocyanide insertion of arylpalladium(II) intermediate, followed by migratory insertion and nucleophilic substitution reaction.[49]

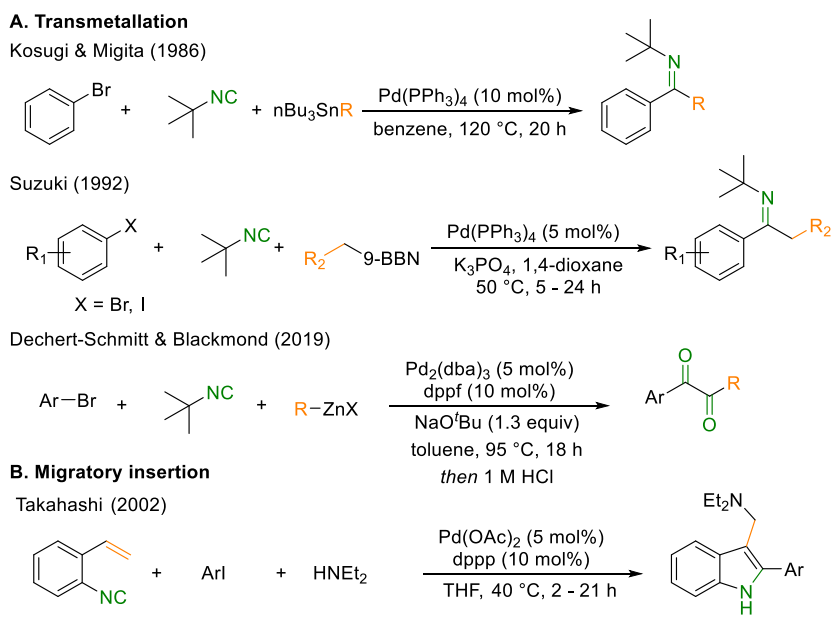

Scheme 1.12 Palladium-catalyzed transformation of isocyanides through transmetallation and migratory insertion

Palladium catalysis has been generally utilized in nucleophilic substitution of isocyanides, enabling the formation of numerous substituted imidate compounds (Scheme 1.13). Taking advantage of ready availability of aryl halides and nucleophilic sources, many transformations were developed using the proposed strategy (Scheme 1.13A). Amines,[50] alkoxides,[51] thiolates,[51] and even water[52] can be incorporated into the imidate structure. Terminal alkynes also serve as a reactive nucleophile after deprotonation, producing alkyne imines.[53]

Incorporation of two components in a single molecule can easily lead the intramolecular transformation, providing a powerful tool for the synthesis of heterocycles (Scheme 1.13B). For example, aryl halides bearing nucleophilic tether engage in the formation of an imine-containing cyclic motif.[54] Depending on the trapping nucleophiles and reaction conditions, the formed imine can be further isomerized to an amine or hydrolyzed into the carbonyl moiety. In 2017, Wang and Ji reported a trapping of carbon dioxide with 2-iodoaniline and further utilization of the generated carbamate for the synthesis of heteroatom-rich cyclic compounds.[55] Pu and Wu installed a carbodiimide electrophile to lead the nucleophilic attack, thereby the created nitrogen nucleophile further reacts with the *tert*-butyl isocyanide under palladium catalysis.[56] Takemoto provided an elegant procedure to utilize the oxypalladation process in the isocyanide insertion chemistry, so as to produce functionalized indoles.[57]

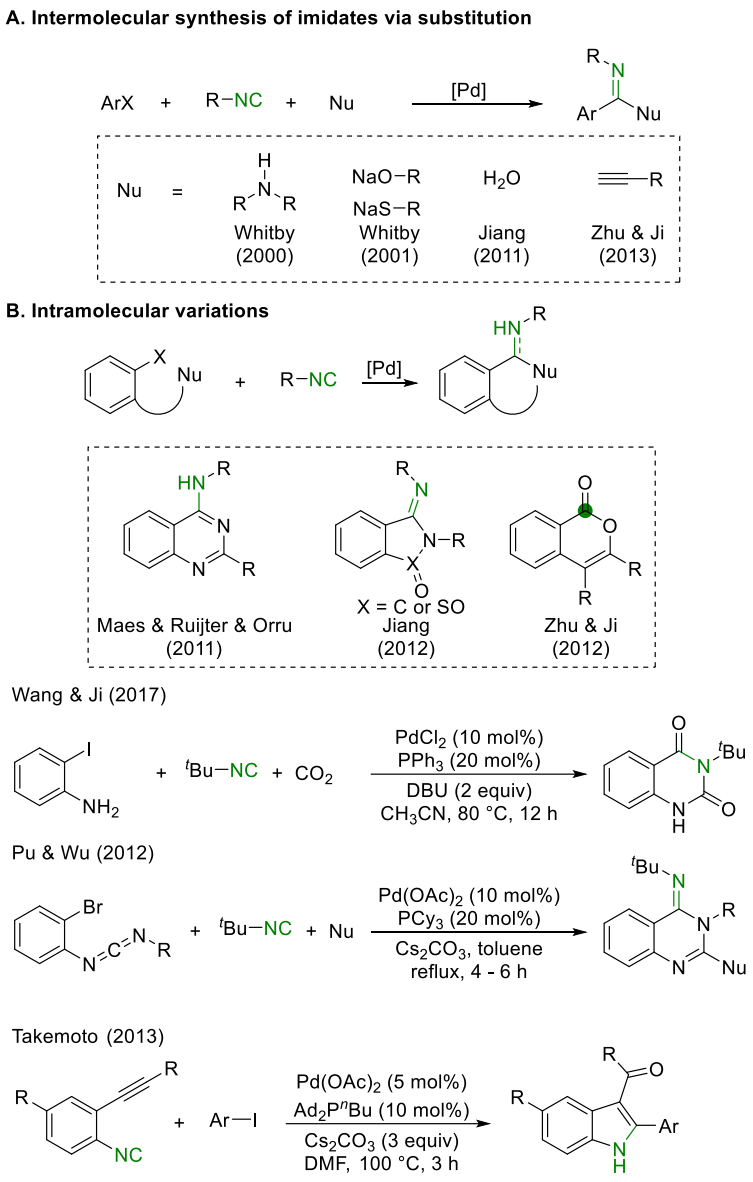

Scheme 1.13 Palladium-catalyzed transformation of isocyanides through nucleophilic substitution

In recent decades, the thriving chemistry of palladium-catalyzed C–H bond activation enabled the use of more readily available simple aromatic systems (Scheme 1.14).[58] Initially performed by Curran in 2002 during the synthesis of ring-fused quinoline systems,[59] diverse methods applied the C–H bond activation process to achieve a straightforward synthesis of target ring structures. In 2010, Chatani reported a reaction between aryl isocyanide and 2-halobiphenyl, which efficiently produced 9-fluorenone imines.[60] After oxidative addition and isocyanide insertion, C–H bond cleavage can be facilitated via proximity effect. Zhu achieved the synthesis of amino-substituted quinazoline via *ortho*-C–H bond activation of *N*-phenylamidine.[61] Synthesis and functionalization of the indole system using isocyanides were also performed via corresponding palladium-catalyzed benzylic C–H bond activation[62] and C3–H bond activation of indole.[63]

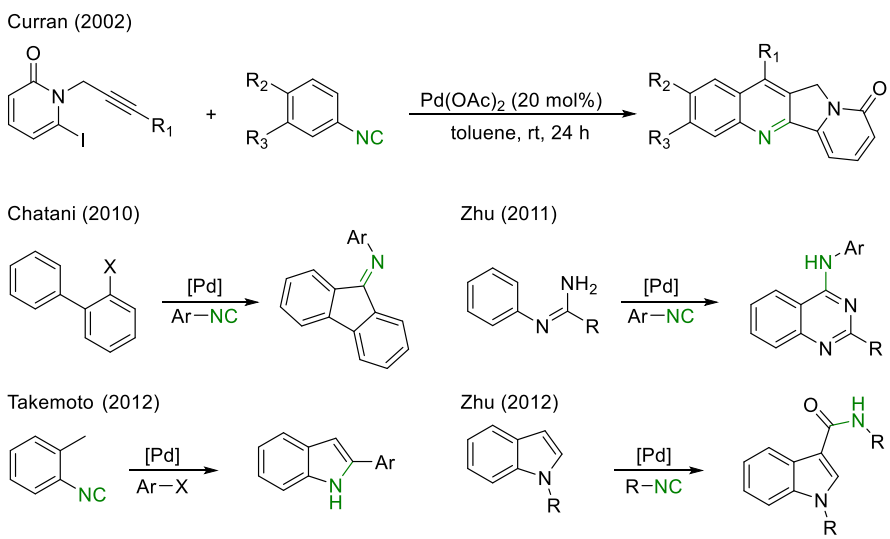

Scheme 1.14 Palladium-catalyzed transformation of isocyanides through C–H bond activation

Not only copper and palladium catalysts, which have extensively utilized in the transformations of isocyanides, but also other transition-metal-based catalysts have been employed in the reactions (Scheme 1.15). For example, rhodium-catalyzed C–H bond activation is one of the well-established strategies, which could be combined with isocyanide insertion chemistry.[64] Additionally, replacing rare-transition-metal into base-metal catalysts, such as nickel[65] and silver catalysts,[66] has been also reported.[67] Those approaches enabled the previously reported transformations, including oxidative addition of aryl bromides and the activation of terminal carbon of isocyanide, with readily available earth-abundant metal catalysts.

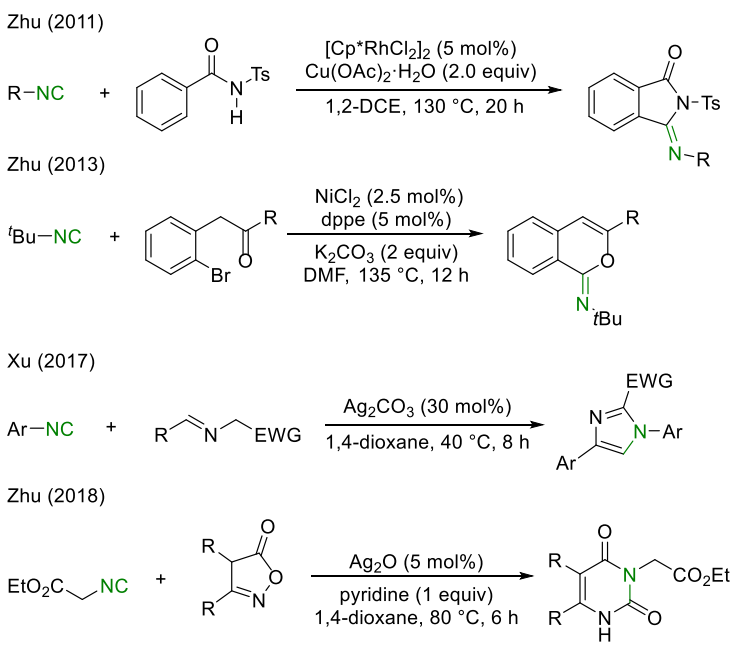

Scheme 1.15 Utilization of other transition-metal catalysis for the transformation of isocyanides

1.3 Activation of the isocyanides with nucleophilic component

1.3.1 Intermolecular reactions

The terminal carbon of isocyanide can react directly with a nucleophile without the aid of an electrophilic activator, but the process is not as efficient as that of electrophilic activation. Therefore, most of the reported examples are usually limited to the coupling reactions with highly reactive nucleophiles, mainly organometallic reagents. The direct addition of nucleophile into the terminal carbon of isocyanide produced an imidoyl anion intermediate, which can be further quenched by external electrophiles (Scheme 1.16).

Early example demonstrating such mechanism was reported by Walborsky in 1969, which utilized organolithium to generate imidoyl anion.[68] Quenching of the lithium aldimine with various types of electrophiles, such as alkyl halide, epoxide, carbonyl compounds, and carbon dioxide, produced a variety of functionalized carbonyl compounds in a divergent manner. In 1989, Ito discovered the generation of zinc aldimine and further utilization of it in the cross-coupling reactions with aryl iodides under palladium or nickel-catalyzed conditions.[69]

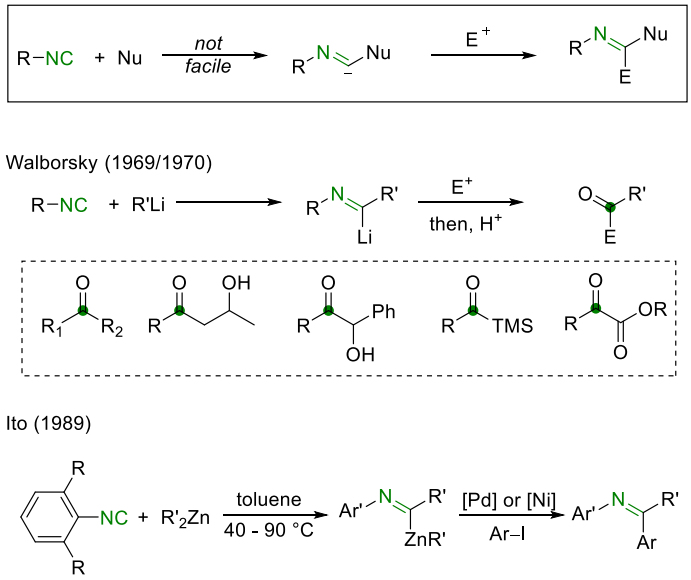

Scheme 1.16 Nucleophilic activation of isocyanide via external nucleophiles

1.3.2 Intramolecular reactions

The more general usage of the nucleophilic activation of isocyanide has been studied in the intramolecular system to form a nitrogen-containing cyclic compound. Isocyanides containing an internal pronucleophilic motif can smoothly perform cyclization under certain activation conditions, and the generated cyclic imidoyl anion reacts readily with various electrophiles to produce cyclic compounds (Scheme 1.17). Because of the proximity effect, equilibrium can be shifted more toward the imidoyl anion. Saegusa demonstrated that a lithiation of the benzylic position initiates the cyclization with isocyanide group and sequential protonation by water generated indole as a product.[70] Later on, lithiation-free protocol was developed applying a copper catalyst to generate adjacent carbon nucleophile.[71]

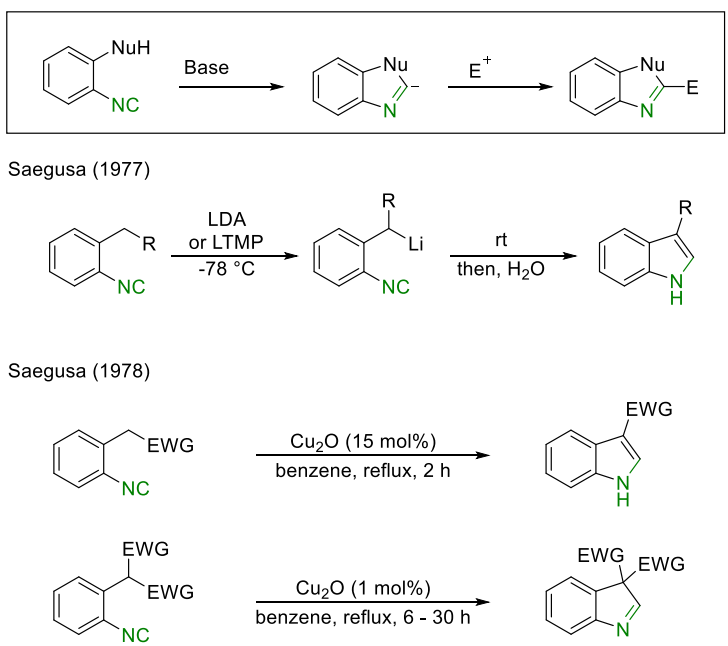

Scheme 1.17 Nucleophilic activation of isocyanide via an adjacent nucleophilic motif

If the isocyanide contains an adjacent electrophile, the addition of nucleophile toward the terminal carbon of isocyanide becomes much more facile, due to the immediate stabilization of imidoyl anion via the reaction with the electrophilic part (Scheme 1.18). For example, Kobayashi demonstrated the reaction of *ortho*-isocyano-β-methoxystyrene with organolithium for the synthesis of substituted quinolines.[72] Sequential addition of organolithium to isocyanide, imidoyl anion to olefin, and the elimination of methoxy group provides the aromatized product. The adjacent electrophile can be replaced to another electron-deficient olefin,[73] benzyl chloride,[74] and ketone.[75] One advantage of this protocol is that the use of Grignard reagent, which showed the low reactivity or gave a sluggish reaction mixture in the intermolecular reaction with isocyanide,[68] smoothly performed the desired cyclization, enhancing the scope of the protocol. Ito discovered that triple-bond electrophile could initiate the cyclization even when much milder nucleophiles, such as alcohol, amine, and 1,3-dicarbonyl compound, were employed.[76] Because the direct intermolecular introduction of the weak nucleophile into the terminal position of isocyanide via the nucleophilic activation is not available, those observations imply the importance of the coupling system to achieve a rather challenging activation process. Later, the scope of nucleophile was further extended to a simple chloride anion, which enabled the direct access toward the chlorinated heterocycles for further syntheses.[77]

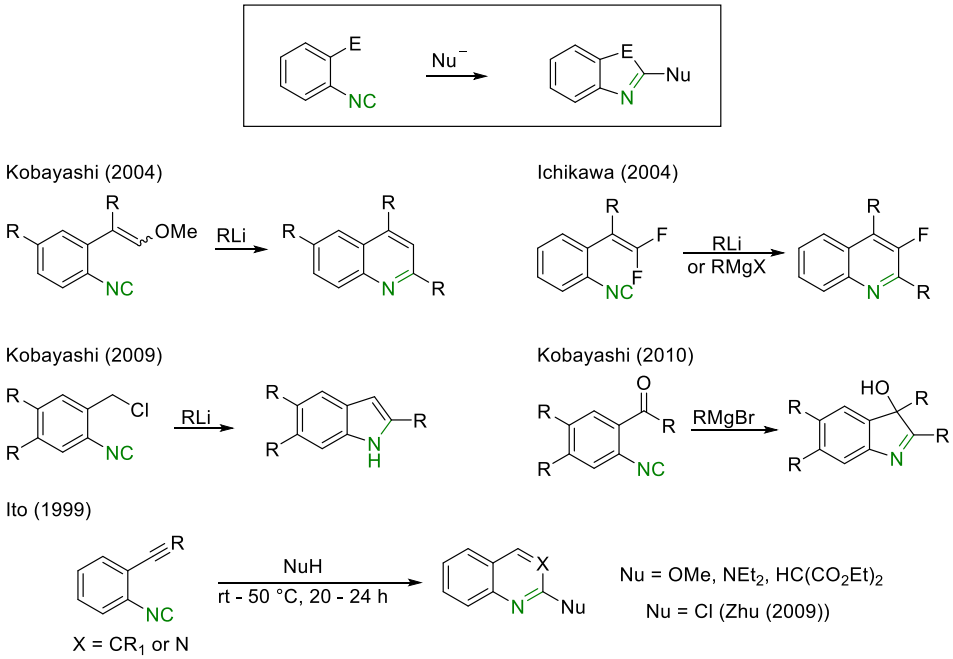

Scheme 1.18 Nucleophilic activation of isocyanide in the aid of adjacent electrophilic groups

1.4 Activation of the isocyanides with radical components

1.4.1 Radical cyclization

Addition of radical species into the isocyanide is another approach to convert the terminal carbon into different types of reactive intermediates, so-called imidoyl radicals. Because of the higher stability of imidoyl radicals than that of imidoyl anions, this radical activation strategy has been extended toward a variety of organic transformations.[78] Fukuyama reported one of the early examples in 1994, which performed radical cyclization with a stilbene bearing an isocyano group (Scheme 1.19).[79] In this case, tetra-n-butyltin hydride was used as a radical source, and further protonation can provide indole as the product. In the case of the reaction with an alkyne, both 5-exo-dig and 6-endo-dig cyclization can happen, depending on the substituent on the alkyne group.[80] Studer recently reported the utilization of Togni's reagent, which provides trifluoromethyl radical in the reaction mixture, to synthesize CF_3-containing indoles.[81]

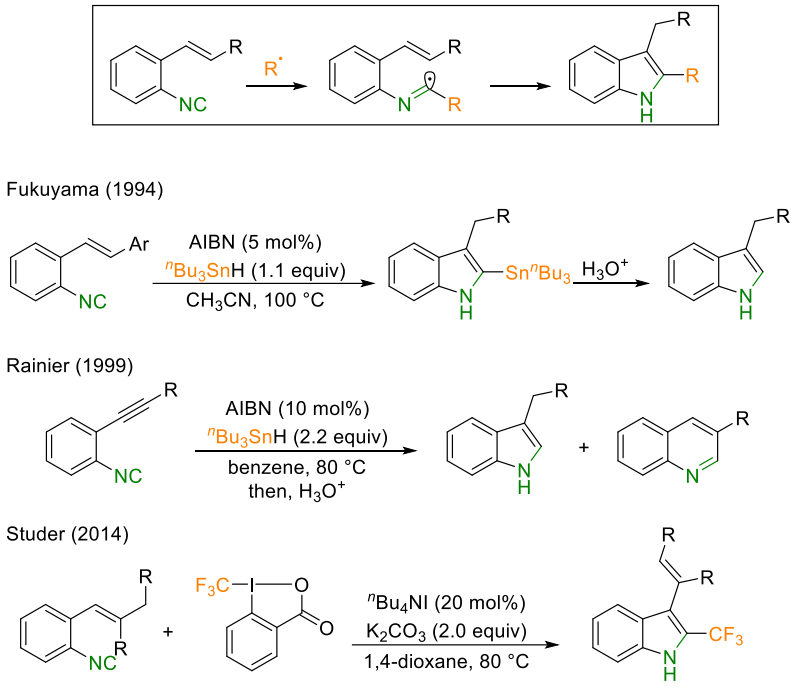

Scheme 1.19 Radical activation of isocyanide and cyclization with olefins and alkynes

An aromatic ring system can also act as a coupling partner in the radical cyclization of biphenyl compounds bearing an *ortho*-isocyano group (Scheme 1.20). Because the reaction between aromatic compounds and radical species is well-established (homolytic aromatic substitution),[82] the generated imidoyl radical readily attacks to the adjacent phenyl ring, and further aromatization provides phenanthridine as the product. Numerous examples for the use of proposed strategy have been reported by varying the radical precursors, which enable the facile synthesis of substituted phenanthridine derivatives in an efficient manner.[83]

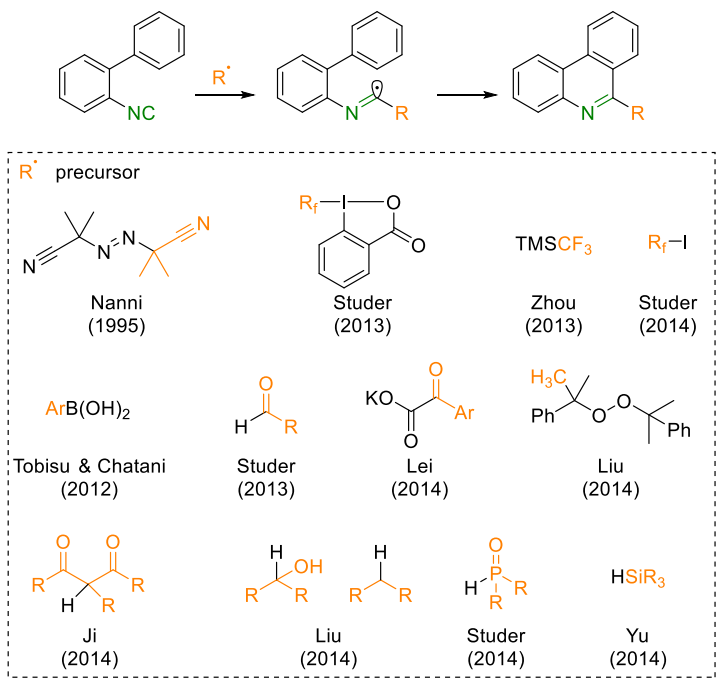

Scheme 1.20 Radical activation of isocyanide and cyclization with aromatic system

Sulfur-based radical precursors were reported to be highly competent with isocyanide cyclization reactions (Scheme 1.21). Ogawa demonstrated the incorporation of thiyl radicals generated from homolytic cleavage under UV irradiation.[84] Very recently, Wu devised the in situ formation of thiyl radical bearing isocyano group via C–S bond cleavage, producing benzothiazole as a cyclized product.[85]

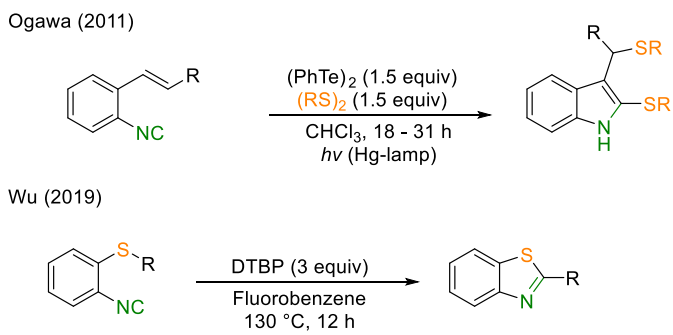

Scheme 1.21 Radical activation of isocyanide and cyclization via thiyl radical

1.4.2 Intermolecular radical coupling

Unlike the intramolecular radical transformations, which follow general cyclization protocols, intermolecular reactions between isocyanide and radical species provide much diverse imine-insertion products (Scheme 1.22). Yamago and Yoshida discovered that a new C–Te bond formation reaction could be realized, together with the C–C bond and O–Si bond formation process, under thermal Si–Te bond cleavage conditions.[86] Bi reported a C–C bond formation reaction under silver-catalysis, which is governed by the carbon-centered radical from 1,3-dicarbonyl species.[87] Ruijiter and Maes suggested an unusual coupling between isocyanide and sulfonethioate, producing carbamothioate as a major product.[88] Similar transformation was realized by Lei, using acyl peroxides to produce amides.[89] Li and Liu developed a double incorporation of CF_3 radical and cyanide into the isocyanide to provide CF_3-containing imidoyl cyanides.[90] This reaction is proceeded through a radical insertion into the terminal carbon of isocyanide, trapping of imidoyl radical by copper catalyst, and reductive elimination with cyanide moiety.

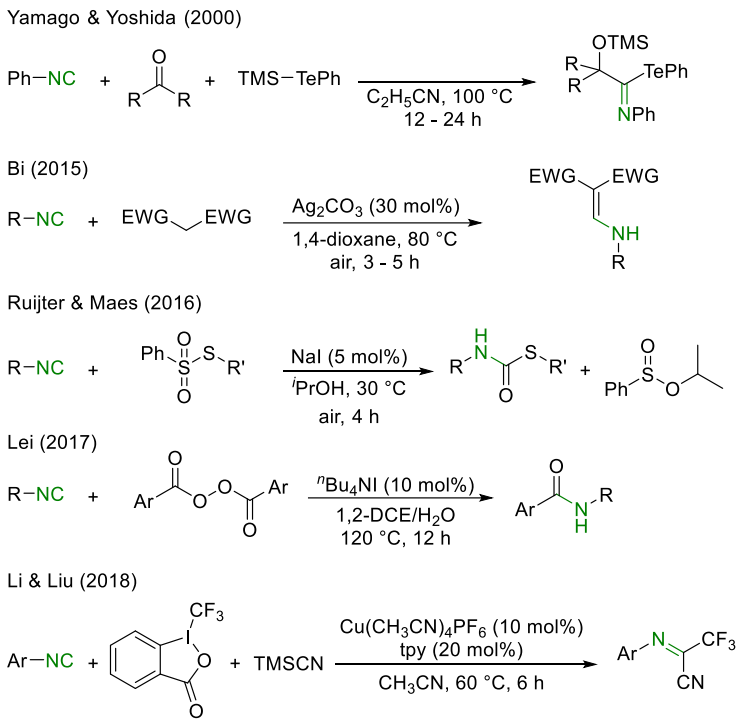

Scheme 1.22 Radical activation of isocyanide: intermolecular transformations

1.4.3 Reactions initiated by visible light photoredox catalysis

A recent development of visible light photoredox catalysis in organic chemistry enabled the generation of target radical species from readily accessible source under mild reaction conditions.[91] This approach is easily implemented into the isocyanide chemistry, providing the expanded scope of substrates, higher availability of the reaction, and the use of previously unreactive coupling partners (Scheme 1.23). For example, Zhang and Yu demonstrated the replacement of conventional radical source in the cyclization of *ortho*-isocyanobiphenyl into the alkyl bromide, expanding the scope of the substituent in the synthesized phenanthridine.[92] Yang also demonstrated the advantage of visible light photoredox catalysis in the synthesis of phosphine-containing indoles, which do not require strong radical initiators to activate the P–H bond.[93] Yadav and Liu utilized the alkylamine[94] and Katritzky salt[95] for alkyl radical sources, respectively, and the target cyclizations proceeded smoothly under mild reaction conditions. This was also the case when simple thiol was applied as a source of thiyl radical, achieving C–S bond formation to generate carbamothioate.[96] Very recently, a multicomponent cyclization of isocyanide, alkyne, and 1,3-dicarbonyl bromide was performed to produce furan-2(5*H*)-imines.[97]

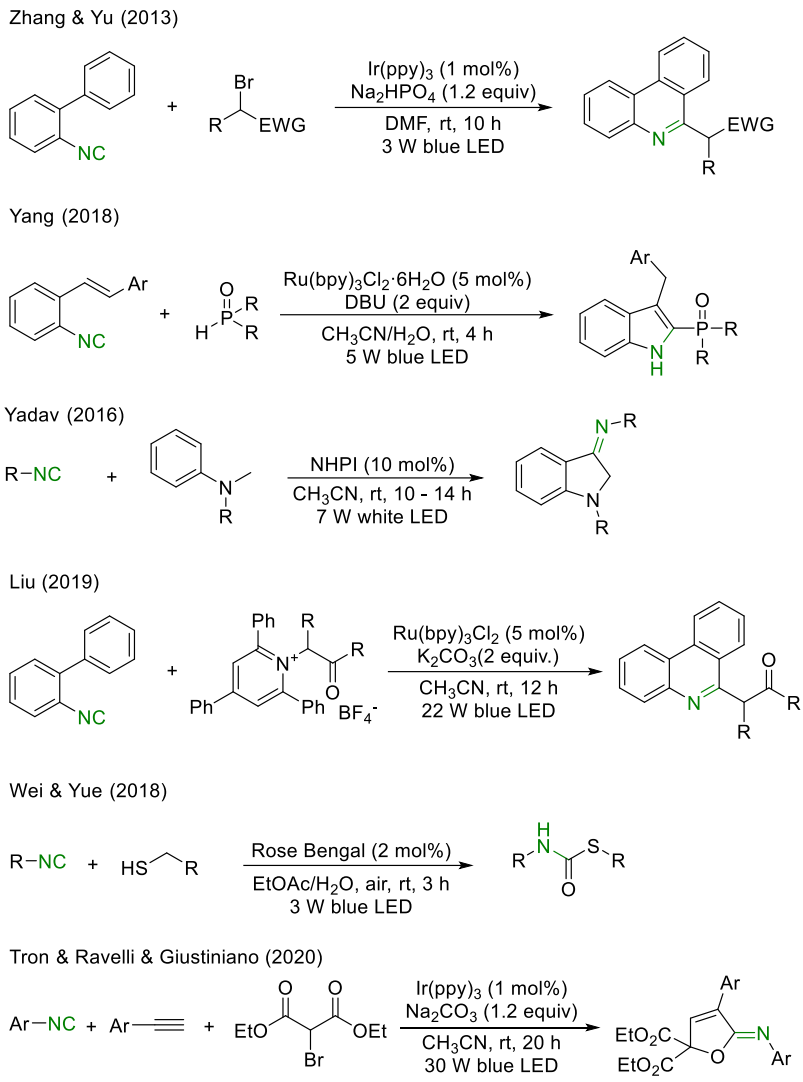

Scheme 1.23 Radical activation of isocyanide under visible-light photoredox catalysis conditions

1.5 Other utilization strategies

1.5.1 Activation of α-proton of isocyanides

Aliphatic isocyanide bearing electron-withdrawing group readily undergoes deprotonation at the α-position, providing the stabilized carbon nucleophiles (Scheme 1.24).[98] This process could be further accelerated by the electrophilic activation of isocyanide, which enhances the electron-withdrawing property. The generated intermediate can act as a formal 1,3-dipole, conducting dipolar cycloaddition reactions. One of the well-established categories of the isocyanides for this purpose is *p*-toluenesulfonylmethyl isocyanide (TosMIC), which performs a facile deprotonation, 1,3-cycloaddition, and desulfonylation.[99] Other electron-withdrawing groups, such as ester, benzotriazole, and aryl groups, can participate in a similar process, providing several 5-/6-membered nitrogen-containing heterocycles.[100]

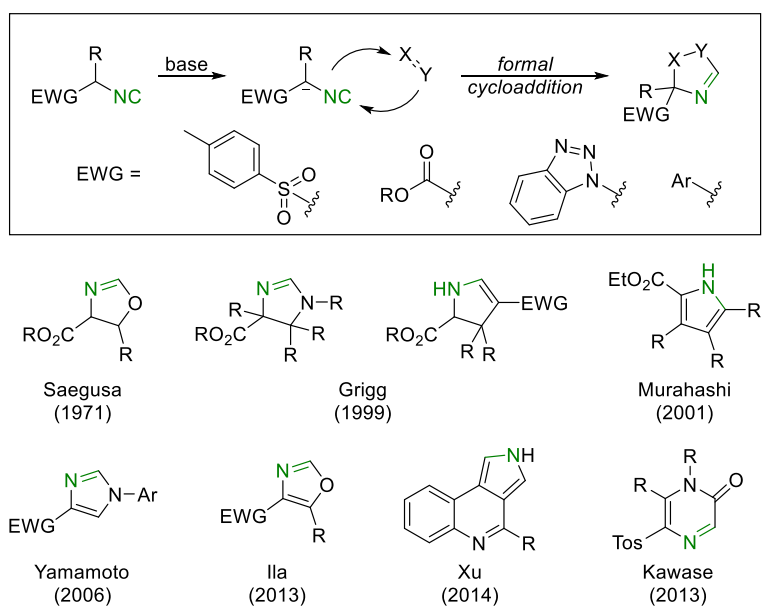

Scheme 1.24 Activation of α-proton of alkyl isocyanides and the applications

1.5.2 Reactions with carbenoid species

Due to the carbonic character of the terminal carbon of isocyanide, reaction with other carbenoid species generates two new bonds via carbene transfer process, producing ketene or ketenimine as the product (Scheme 1.25). In 2006, Barluenga demonstrated the reaction between *tert*-butyl isocyanide and in situ generated Cr-carbene complex, forming an aromatized ring-fused skeleton in one-pot.[101] Catalytic use of metal species with a combination of carbene precursor was achieved by Zhao utilizing trifluoromethyl diazomethane to synthesize functionalized imines.[102]

When an azide is used as a nitrene precursor, corresponding ketenimine can be produced. Holland demonstrated the catalytic use of iron β-diiminate complex to realize the proposed mechanism.[103] The identical reaction was performed under milder reaction conditions with a palladium catalyst replacing the iron catalyst.[104] The synthesized ketenimine could be further used for the synthesis of cyclic structure, as demonstrated by Zhang in 2016.[105]

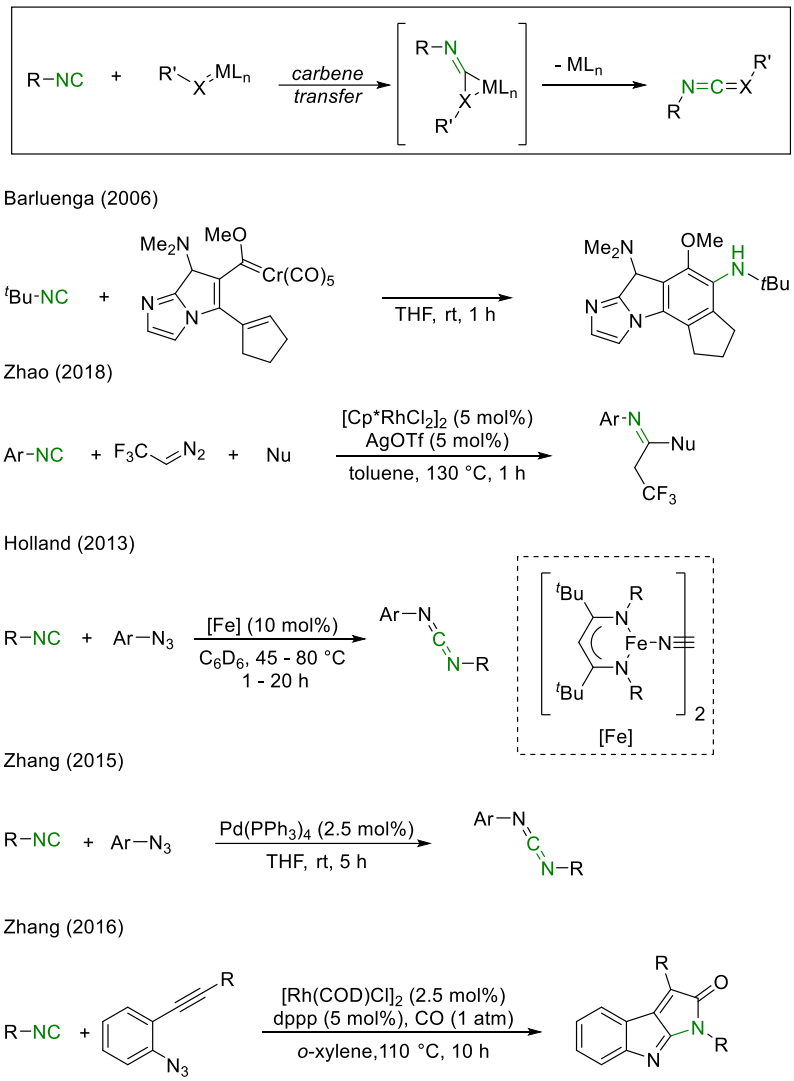

Scheme 1.25 Reactions of isocyanides with carbenoid species

1.6 Summary and outlook

Over past decades, the transformations of various isocyanide-containing molecules have been developed via a diverse array of activations strategies. Based on the characteristic property of the terminal carbon of isocyanide, almost all kinds of reactive species, including electrophiles, nucleophiles, and radicals, can be coupled to produce different types of imine-related structures. A relay of electrophilic activation of isocyanide and nucleophilic attack enabled the novel multicomponent reactions, providing a useful tool for the synthesis of peptoid structures. In addition, a number of electrophilic-/nucleophilic-/radical-cyclization processes have been extensively developed for the production of various nitrogen-containing cyclic molecules. Recent studies about the introduction of transition-metal catalysis, especially palladium catalysis, facilitated the insertion of isocyanide species toward the diverse bonds, including relatively inactive C–H bonds.

Despite the continuous developments of the isocyanide utilization, the remaining problems observed from the previous reports should be resolved. The most problematic issue is the requirement of an excess amount of isocyanide in most cases, due to the facile oligomerization[106]/polymerization[107] of isocyanide under various reaction conditions. Also, a limitation of the scope of isocyanide, mainly to the *tert*-butyl isocyanide, control of the reactivity to prevent over-insertion process, and accessibility of the isocyanide itself are remaining hurdles to be overcome. Finally, the introduction of different mechanistic aspects in the activation of isocyanide has to be pursued to widen the scope of reactivity, accessible functional groups, and understanding of the property of isocyanide groups in the organic transformations.

1.7 References

(1) Gautier, A. *Liebigs Ann.* **1867**, *142*, 289.

(2) Hofmann, A. W. *Liebigs Ann.* **1867**, *144*, 114.

(3) Nenajdenko, V. G. *Isocyanide Chemistry: Applications in Synthesis and Material Science*; Wiley-VCH Verlag GmbH & Co. KGaA: Weinheim, 2012.

(4) (a) Lygin, A. V.; de Meijere, A. *Angew. Chem., Int. Ed.* **2010**, *49*, 9094. (b) Ivachtchenko, A. V.; Ivanenkov, Y. A.; Kysil, V. M.; Krasavin, M. Y.; Ilyin, A. P. *Russ. Chem. Rev.* **2010**, *79*, 787. (c) Kaïm, L.; Grimaud, L. *Tetrahedron* **2009**, *65*, 2153. (d) van Berkel, S. S.; Bögels, B. G. M.; Wijdeven, M. A.; Westermann, B.; Rutjes, F. P. J. T. *Eur. J. Org. Chem.* **2012**, 3543. (e) Boyarskiy, V. P.; Bokach, N. A.; Luzyanin, K. V.; Kukushkin, V. Y. *Chem. Rev.* **2015**, *115*, 2698. (f) Heravi, M. M.; Moghimi, S. *J. Iran. Chem. Soc.* **2011**, *8*, 306. (g) Domling, A. *Chem. Rev.* **2006**, *106*, 17. (h) Zhu, J. *Eur. J. Org. Chem.* **2003**, 1133. (i) Giustiniano, M.; Basso, A.; Mercalli, V.; Massarotti, A.; Novellino, E.; Tron, G. C.; Zhu, J. *Chem. Soc. Rev.* **2017**, *46*, 1295. (j) Sadjadi, S.; Heravi, M. M. *Tetrahedron* **2011**, *67*, 2707. (k) Qiu, G.; Ding, Q.; Wu, J. *Chem. Soc. Rev.* **2013**, *42*, 5257.

(5) Strecker, A. *Liebigs Ann.* **1850**, *75*, 27.

(6) Hantzsch, A. *Liebigs Ann.* **1882**, *215*, 1.

(7) Biginelli, P. *Ber. Dtsch. Chem. Ges.* **1891**, *24*, 1317.

(8) Mannich, C.; Krösche, W. *Arch. Pharm.* **1912**, *250*, 647.

(9) Passerini, M.; Simone, L. *Gazz. Chim. Ital.* **1921**, *51*, 126

(10) Ugi, I.; Meyr, R.; Fetzer, U.; Steinbrückner, C. *Angew. Chem.* **1959**, *71*, 386.

(11) Ghandi, M.; Zarezadeh, N.; Taheri, A. *Tetrahedron Lett.* **2012**, *53*, 3353.

(12) Madhavachary, R.; Zarganes-Tzitzikas, T.; Patil, P.; Kurpiewska, K.;

Kalinowska-Tluscik, J.; Dömling, A. *ACS. Comb. Sci.* **2018**, *20*, 192.

(13) Zhang, J.; Yu, P.; Li, S. Y.; Sun, H.; Xiang, S. H.; Wang, J. J.; Houk, K. N.; Tan, B. *Science* **2018**, *361*, eaas8707.

(14) Chakrabarty, S.; Choudhary, S.; Doshi, A.; Liu, F.-Q.; Mohan, R.; Ravindra, M. P.; Shah, D.; Yang, X.; Fleming, F. F. *Adv. Synth. Catal.* **2014**, *356*, 2135.

(15) Nef, J. U. *Liebigs Ann.* **1892**, *270*, 267.

(16) Walter, W.; Bode, K. D. *Angew. Chem., Int. Ed. Engl.* **1962**, *1*, 510.

(17) Grimaud, L.; El Kaim, L.; Wagschal, S. *Synlett* **2009**, 1315.

(18) (a) Westling, M.; Livinghouse, T. *Tetrahedron Lett.* **1985**, *26*, 5389. (b) Westling, M.; Smith, R.; Livinghouse, T. *J. Org. Chem.* **1986**, *51*, 1159. (c) Westling, M.; Livinghouse, T. *J. Am. Chem. Soc.* **1987**, *109*, 590. (d) Lee, C. H.; Westling, M.; Livinghouse, T.; Williams, A. C. *J. Am. Chem. Soc.* **1992**, *114*, 4089. (e) Luedtke, G.; Westling, M.; Livinghouse, T. *Tetrahedron* **1992**, *48*, 2209. (f) Hughes, D. J.; Livinghouse, T. *J. Chem. Soc., Perkin Trans. 1* **1995**, 2373. (g) Luedtke, G.; Livinghouse, T. *J. Chem. Soc., Perkin Trans. 1* **1995**, 2369. (h) Kercher, T.; Livinghouse, T. *J. Org. Chem.* **1997**, *62*, 805. (i) Livinghouse, T. *Tetrahedron* **1999**, *55*, 9947.

(19) Shaabani, A.; Farrokhzad, F. *J. Chem. Res.* **1997**, 344.

(20) (a) Yavari, I.; Shaabani, A.; Maghsoodlou, M. T. *Monatsh. Chem.* **1997**, *128*, 697. (b) Shaabani, A.; Ajabi, S.; Farrokhzad, F.; Bijanzadeh, H. R. *J. Chem. Res.* **1999**, 582.

(21) Yavari, I.; Djahaniani, H.; Nasiri, F. *Monatsh. Chem.* **2004**, *135*, 543.

(22) Shaabani, A.; Teimouri, M. B.; Mirzaei, P.; Bijanzadeh, H. R. *J. Chem. Res.* **2003**, *2003*, 82.

(23) Prajapati, D.; Sarma, R.; Sarmah, M.; Lekhok, K. *Synlett* **2010**, 2847.

(24) (a) Mironov, M. A.; Ivantsova, M. N.; Mokrushin, V. S. *Synlett* **2006**, 615. (b) Kolontsova, A. N.; Ivantsova, M. N.; Tokareva, M. I.; Mironov, M. A. *Mol. Divers.* **2010**, *14*, 543. (c) Zhu, X.; Xu, X. P.; Sun, C.; Wang, H. Y.; Zhao, K.; Ji, S. J. *J. Comb. Chem.* **2010**, *12*, 822.

(25) Tobisu, M.; Chatani, N. *Chem. Lett.* **2011**, *40*, 330.

(26) (a) Chatani, N.; Oshita, M.; Tobisu, M.; Ishii, Y.; Murai, S. *J. Am. Chem. Soc.* **2003**, *125*, 7812. (b) Oshita, M.; Yamashita, K.; Tobisu, M.; Chatani, N. *J. Am. Chem. Soc.* **2005**, *127*, 761.

(27) Bez, G.; Zhao, C. G. *Org. Lett.* **2003**, *5*, 4991.

(28) Yoshioka, S.; Oshita, M.; Tobisu, M.; Chatani, N. *Org. Lett.* **2005**, *7*, 3697.

(29) Tobisu, M.; Ito, S.; Kitajima, A.; Chatani, N. *Org. Lett.* **2008**, *10*, 5223.

(30) Winkler, J. D.; Asselin, S. M. *Org. Lett.* **2006**, *8*, 3975.

(31) Fontaine, P.; Masson, G.; Zhu, J. *Org. Lett.* **2009**, *11*, 1555.

(32) Liu, H.-L.; Yuan, Y.-C.; Wei, Y.; Shi, M. *Adv. Synth. Catal.* **2017**, *359*, 3437.

(33) Tobisu, M.; Yamaguchi, S.; Chatani, N. *Org. Lett.* **2007**, *9*, 3351.

(34) Odabachian, Y.; Tong, S.; Wang, Q.; Wang, M. X.; Zhu, J. *Angew. Chem., Int. Ed.* **2013**, *52*, 10878.

(35) Saegusa, T.; Ito, Y.; Kobayashi, S.; Hirota, K.; Yoshioka, H. *Tetrahedron Lett.* **1966**, *7*, 6121.

(36) Saegusa, T.; Ito, Y.; Kobayashi, S.; Hirota, K. *Tetrahedron Lett.* **1967**, *8*, 521.

(37) Saegusa, T.; Kobayashi, S.; Hirota, K.; Okumura, Y.; Ito, Y. *Bull. Chem. Soc. Jpn.* **1968**, *41*, 1638.

(38) Saegusa, T.; Ito, Y.; Kobayashi, S.; Hirota, K. *J. Am. Chem. Soc.* **1967**, *89*, 2240.

(39) Saegusa, T.; Ito, Y.; Kobayashi, S. *Tetrahedron Lett.* **1968**, *9*, 935.

(40) Saegusa, T.; Murase, I.; Ito, Y. *Synth. Commun.* **2007**, *1*, 145.

(41) Lygin, A. V.; de Meijere, A. *J. Org. Chem.* **2009**, *74*, 4554.

(42) Pooi, B.; Lee, J.; Choi, K.; Hirao, H.; Hong, S. H. *J. Org. Chem.* **2014**, *79*, 9231.

(43) Kim, S.; Hong, S. H. *Adv. Synth. Catal.* **2015**, *357*, 1004.

(44) Yuan, Q.; Rao, W.; Wang, S. Y.; Ji, S. J. *J. Org. Chem.* **2020**, *85*, 1279.

(45) (a) Lang, S. *Chem. Soc. Rev.* **2013**, *42*, 4867. (b) Vlaar, T.; Ruijter, E.; Maes, B. U. W.; Orru, R. V. A. *Angew. Chem., Int. Ed.* **2013**, *52*, 7084.

(46) Kosugi, M.; Ogata, T.; Tamura, H.; Sano, H.; Migita, T. *Chem. Lett.* **1986**, *15*, 1197.

(47) Ishiyama, T.; Oh-e, T.; Miyaura, N.; Suzuki, A. *Tetrahedron Lett.* **1992**, *33*, 4465.

(48) Dechert-Schmitt, A.-M.; Garnsey, M. R.; Wisniewska, H. M.; Murray, J. I.; Lee, T.; Kung, D. W.; Sach, N.; Blackmond, D. G. *ACS Catal.* **2019**, *9*, 4508.

(49) Onitsuka, K.; Suzuki, S.; Takahashi, S. *Tetrahedron Lett.* **2002**, *43*, 6197.

(50) Saluste, C. G.; Whitby, R. J.; Furber, M. *Angew. Chem.* **2000**, *39*, 4156.

(51) Saluste, C. G.; Whitby, R. J.; Furber, M. *Tetrahedron Lett.* **2001**, *42*, 6191.

(52) Jiang, H.; Liu, B.; Li, Y.; Wang, A.; Huang, H. *Org. Lett.* **2011**, *13*, 1028.

(53) Tang, T.; Fei, X. D.; Ge, Z. Y.; Chen, Z.; Zhu, Y. M.; Ji, S. J. *J. Org. Chem.* **2013**, *78*, 3170.

(54) (a) Van Baelen, G.; Kuijer, S.; Rycek, L.; Sergeyev, S.; Janssen, E.; de Kanter, F. J.; Maes, B. U.; Ruijter, E.; Orru, R. V. *Chem.–Eur. J.* **2011**, *17*, 15039. (b) Liu, B.; Li, Y.; Jiang, H.; Yin, M.; Huang, H. *Adv. Synth. Catal.* **2012**, *354*, 2288. (c) Fei, X. D.; Ge, Z. Y.; Tang, T.; Zhu, Y. M.; Ji, S. J. *J. Org. Chem.* **2012**, *77*, 10321.

(55) Xu, P.; Wang, F.; Wei, T. Q.; Yin, L.; Wang, S. Y.; Ji, S. J. *Org. Lett.* **2017**, *19*,

4484.

(56) Qiu, G.; Liu, G.; Pu, S.; Wu, J. *Chem. Commun*. **2012**, *48*, 2903.

(57) Nanjo, T.; Yamamoto, S.; Tsukano, C.; Takemoto, Y. *Org. Lett.* **2013**, *15*, 3754.

(58) (a) Rouquet, G.; Chatani, N. *Angew. Chem., Int. Ed.* **2013**, *52*, 11726. (b) Neufeldt, S. R.; Sanford, M. S. *Acc. Chem. Res.* **2012**, *45*, 936. (c) He, J.; Wasa, M.; Chan, K. S. L.; Shao, Q.; Yu, J.-Q. *Chem. Rev.* **2017**, *117*, 8754.

(59) Curran, D. P.; Du, W. *Org. Lett.* **2002**, *4*, 3215.

(60) Tobisu, M.; Imoto, S.; Ito, S.; Chatani, N. *J. Org. Chem.* **2010**, *75*, 4835.

(61) Wang, Y.; Wang, H.; Peng, J.; Zhu, Q. *Org. Lett.* **2011**, *13*, 4604.

(62) Nanjo, T.; Tsukano, C.; Takemoto, Y. *Org. Lett.* **2012**, *14*, 4270.

(63) Peng, J.; Liu, L.; Hu, Z.; Huang, J.; Zhu, Q. *Chem. Commun.* **2012**, *48*, 3772.

(64) Zhu, C.; Xie, W.; Falck, J. R. *Chem.–Eur. J.* **2011**, *17*, 12591.

(65) Fei, X.-D.; Tang, T.; Ge, Z.-Y.; Zhu, Y.-M. *Synth. Commun.* **2013**, *43*, 3262.

(66) (a) Hu, Z.; Dong, J.; Xu, X. *Adv. Synth. Catal.* **2017**, *359*, 3585. (b) Liang, H. W.; Yang, Z.; Jiang, K.; Ye, Y.; Wei, Y. *Angew. Chem., Int. Ed.* **2018**, *57*, 5720.

(67) Collet, J. W.; Roose, T. R.; Ruijter, E.; Maes, B. U. W.; Orru, R. V. A. *Angew. Chem., Int. Ed.* **2020**, *59*, 540.

(68) (a) Walborsky, H. M.; Niznik, G. E. *J. Am. Chem. Soc.* **1969**, *91*, 7778.

(69) Murakami, M.; Ito, H.; Bakar, W. A. b. W. A.; Baba, A. B. b.; Ito, Y. *Chem. Lett.* **1989**, *18*, 1603.

(70) Ito, Y.; Kobayashi, K.; Saegusa, T. *J. Am. Chem. Soc.* **1977**, *99*, 3532.

(71) Ito, Y.; Inubushi, Y.; Sugaya, T.; Kobayashi, K.; Saegusa, T. *Bull. Chem. Soc. Jpn.* **1978**, *51*, 1186.

(72) Kobayashi, K.; Yoneda, K.; Miyamoto, K.; Morikawa, O.; Konishi, H. *Tetrahedron* **2004**, *60*, 11639.

(73) Ichikawa, J.; Mori, T.; Miyazaki, H.; Wada, Y. *Synlett* **2004**, 1219.

(74) Kobayashi, K.; Iitsuka, D.; Fukamachi, S.; Konishi, H. *Tetrahedron* **2009**, *65*, 7523.

(75) Kobayashi, K.; Okamura, Y.; Fukamachi, S.; Konishi, H. *Tetrahedron* **2010**, *66*, 7961.

(76) Suginome, M.; Fukuda, T.; Ito, Y. *Org. Lett.* **1999**, *1*, 1977.

(77) Liu, L.; Wang, Y.; Wang, H.; Peng, C.; Zhao, J.; Zhu, Q. *Tetrahedron Lett.* **2009**, *50*, 6715.

(78) Zhang, B.; Studer, A. *Chem. Soc. Rev.* **2015**, *44*, 3505.

(79) Fukuyama, T.; Chen, X.; Peng, G. *J. Am. Chem. Soc.* **1994**, *116*, 3127.

(80) Rainier, J. D.; Kennedy, A. R.; Chase, E. *Tetrahedron Lett.* **1999**, *40*, 6325.

(81) Zhang, B.; Studer, A. *Org. Lett.* **2014**, *16*, 1216.

(82) Bowman, W. R.; Storey, J. M. D. *Chem. Soc. Rev.* **2007**, *36*, 1803.

(83) (a) Nanni, D.; Pareschi, P.; Rizzoli, C.; Sgarabotto, P.; Tundo, A. *Tetrahedron* **1995**, *51*, 9045. (b) Zhang, B.; Muck-Lichtenfeld, C.; Daniliuc, C. G.; Studer, A. *Angew. Chem., Int. Ed.* **2013**, *52*, 10792. (c) Wang, Q.; Dong, X.; Xiao, T.; Zhou, L. *Org. Lett.* **2013**, *15*, 4846. (d) Zhang, B.; Studer, A. *Org. Lett.* **2014**, *16*, 3990. (e) Tobisu, M.; Koh, K.; Furukawa, T.; Chatani, N. *Angew. Chem., Int. Ed.* **2012**, *51*, 11363. (f) Leifert, D.; Daniliuc, C. G.; Studer, A. *Org. Lett.* **2013**, *15*, 6286. (g) Liu, J.; Fan, C.; Yin, H.; Qin, C.; Zhang, G.; Zhang, X.; Yi, H.; Lei, A. *Chem. Commun.* **2014**, *50*, 2145. (h) Xu, Z.; Yan, C.; Liu, Z. Q. *Org. Lett.* **2014**, *16*, 5670. (i) Cao, J. J.; Wang, X.; Wang, S. Y.; Ji, S. J. *Chem. Commun.* **2014**, *50*, 12892. (j) Li, Z.; Fan, F.; Yang, J.; Liu, Z. Q. *Org. Lett.* **2014**, *16*, 3396. (k) Zhang, B.; Daniliuc, C. G.; Studer, A. *Org. Lett.* **2014**, *16*, 250. (l) Wang, L.; Zhu, H.; Guo, S.; Cheng, J.; Yu, J. T. *Chem. Commun.* **2014**, *50*, 10864.

(84) Mitamura, T.; Iwata, K.; Ogawa, A. *J. Org. Chem.* **2011**, *76*, 3880.

(85) Luo, K.; Yang, W. C.; Wei, K.; Liu, Y.; Wang, J. K.; Wu, L. *Org. Lett.* **2019**, *21*, 7851.

(86) Miyazoe, H.; Yamago, S.; Yoshida, J.-i. *Angew. Chem.* **2000**, *39*, 3669.

(87) Liu, J.; Liu, Z.; Liao, P.; Zhang, L.; Tu, T.; Bi, X. *Angew. Chem., Int. Ed.* **2015**, *54*, 10618.

(88) Mampuys, P.; Zhu, Y.; Sergeyev, S.; Ruijter, E.; Orru, R. V.; Van Doorslaer, S.; Maes, B. U. *Org. Lett.* **2016**, *18*, 2808.

(89) Chen, M.; Li, Y.; Tang, H.; Ding, H.; Wang, K.; Yang, L.; Li, C.; Gao, M.; Lei, A. *Org. Lett.* **2017**, *19*, 3147.

(90) Chen, S.; Feng, D. F.; Li, D. Y.; Liu, P. N. *Org. Lett.* **2018**, *20*, 5418.

(91) (a) Tucker, J. W.; Stephenson, C. R. J. *J. Org. Chem.* **2012**, *77*, 1617. (b) Prier, C. K.; Rankic, D. A.; MacMillan, D. W. C. *Chem. Rev.* **2013**, *113*, 5322. (c) Romero, N. A.; Nicewicz, D. A. *Chem. Rev.* **2016**, *116*, 10075.

(92) Jiang, H.; Cheng, Y.; Wang, R.; Zheng, M.; Zhang, Y.; Yu, S. *Angew. Chem., Int. Ed.* **2013**, *52*, 13289.

(93) Wang, C. H.; Li, Y. H.; Yang, S. D. *Org. Lett.* **2018**, *20*, 2382.

(94) Yadav, A. K.; Yadav, L. D. *Chem. Commun.* **2016**, *52*, 10621.

(95) Zhu, Z. F.; Zhang, M. M.; Liu, F. *Org. Biomol. Chem.* **2019**, *17*, 1531.

(96) Wei, W.; Bao, P.; Yue, H.; Liu, S.; Wang, L.; Li, Y.; Yang, D. *Org. Lett.* **2018**, *20*, 5291.

(97) Pelliccia, S.; Alfano, A. I.; Luciano, P.; Novellino, E.; Massarotti, A.; Tron, G. C.; Ravelli, D.; Giustiniano, M. *J. Org. Chem.* **2020**, *85*, 1981.

(98) Elders, N.; Ruijter, E.; Nenajdenko, V. G.; Orru, R. V. A. In *Synthesis of Heterocycles via Multicomponent Reactions I*; Orru, R. V. A., Ruijter, E., Eds.;

Springer Berlin Heidelberg: Berlin, Heidelberg, 2010, pp 129–159.

(99) (a) Mathiyazhagan, A. D.; Anilkumar, G. *Org. Biomol. Chem.* **2019**, *17*, 6735. (b) Kaur, T.; Wadhwa, P.; Sharma, A. *RSC Adv.* **2015**, *5*, 52769.

(100) (a) Saegusa, T.; Ito, Y.; Kinoshita, H.; Tomita, S. *J. Org. Chem.* **1971**, *36*, 3316. (b) Grigg, R.; Lansdell, M. I.; Thornton-Pett, M. *Tetrahedron* **1999**, *55*, 2025. (c) Takaya, H.; Kojima, S.; Murahashi, S. *Org. Lett.* **2001**, *3*, 421. (d) Kanazawa, C.; Kamijo, S.; Yamamoto, Y. *J. Am. Chem. Soc.* **2006**, *128*, 10662. (e) Yugandar, S.; Acharya, A.; Ila, H. *J. Org. Chem.* **2013**, *78*, 3948. (f) Hu, Z.; Li, Y.; Pan, L.; Xu, X. *Adv. Synth. Catal.* **2014**, *356*, 2974. (g) Saijo, R.; Kurihara, K.-i.; Akira, K.; Uno, H.; Kawase, M. *Tetrahedron Lett.* **2013**, *54*, 4418.

(101) Barluenga, J.; Garcia-Rodriguez, J.; Martinez, S.; Suarez-Sobrino, A. L.; Tomas, M. *Chem.–Eur. J.* **2006**, *12*, 3201.

(102) Bu, X.-B.; Wang, Z.; Wang, X.-D.; Meng, X.-H.; Zhao, Y.-L. *Adv. Synth. Catal.* **2018**, *360*, 2945.

(103) Cowley, R. E.; Golder, M. R.; Eckert, N. A.; Al-Afyouni, M. H.; Holland, P. L. *Organometallics* **2013**, *32*, 5289.

(104) Zhang, Z.; Li, Z.; Fu, B.; Zhang, Z. *Chem. Commun.* **2015**, *51*, 16312.

(105) Zhang, Z.; Xiao, F.; Huang, B.; Hu, J.; Fu, B.; Zhang, Z. *Org. Lett.* **2016**, *18*, 908.

(106) (a) Saegusa, T.; Takaishi, N.; Ito, Y. *J. Org. Chem.* **1969**, *34*, 4040. (b) Boeyens, J. C.; Cook, L. M.; Ding, Y.; Fernandes, M. A.; Reid, D. H. *Org. Biomol. Chem.* **2003**, *1*, 2168.

(107) Suginome, M.; Ito, Y. Transition Metal-Mediated Polymerization of Isocyanides. In *Polymer Synthesis. Advances in Polymer Science*; Vol.171; Springler: Berlin, Heidelberg, 2004; pp 77−136.

Chapter 2. Organocatalytic Activation of Isocyanides: N-Heterocyclic Carbene-Catalyzed Enaminone Synthesis from Ketones*

2.1 Introduction

Isocyanides are useful building blocks for the synthesis of various acyclic and cyclic compounds.[1] Because the terminal carbon of isocyanide can act as both a nucleophile and the carbene center, control of its reactivity is key to developing novel transformations. In many cases, the isocyanide group can act as a mild nucleophile, meaning that it undergoes electrophilic activation in the presence of an electrophilic compound. In addition, various metal-based catalysts allow further transformations after the incorporation of the isocyanide motif into the starting substrate. Pd-catalyzed insertion reactions,[2] Cu(Ag)-mediated electrophilic activation,[3] and Cu-alkoxide systems[4] for the generation of formimidate intermediates are well developed isocyanide activation strategies (Scheme 2.1A). Because of the mild nucleophilicity of the carbon atom of the isocyanide group, its utilization as a nucleophile has been limited to the use of highly electrophilic reaction partners, such as carbonyl compounds and metal catalysts. This has been a critical hurdle for achieving metal-free, non-Ugi-type transformations. In order to overcome this shortcoming, we envisioned a new approach where the isocyanide

∗ The majority of this work has been published: Jungwon Kim and Soon Hyeok Hong*, *Chem. Sci.* **2017**, *8*, 2401.

group is activated by a 'nucleophilic moiety' to transform the isocyanide into a highly basic intermediate. The reactions of isocyanides with external nucleophiles are relatively rare and most of them require highly reactive organometallic nucleophiles (Scheme 2.1B).[5] The incorporation of milder nucleophiles into the isocyanide is possible only in the presence of an electrophilic group near the reactive center to trigger intramolecular cyclization reactions (Scheme 2.1B).[6] To the best of our knowledge, the catalytic nucleophilic activation of isocyanides has not yet been reported.

We chose N-heterocyclic carbenes (NHCs) as potential nucleophilic activators.[7] There have been several reports on the formation of ketenimines from the reaction between carbenes and isocyanides,[8] such as diamidocarbene (DAC),[8c,8d] cyclic (alkyl)(amino)carbene (CAAC),[8e] and acyclic di(amino)carbene (ADAC) (Scheme 2.1C).[8e] Among them, a computational study on the formation of an imidoyl intermediate from the reaction between an imidazole-based NHC and an isocyanide, which proposed a zwitterionic imidoyl adduct as a favorable structure, attracted our attention (Scheme 2.1C).[8c,8e] Although this intermediate was not stable enough to be isolated, the transient zwitterionic imidoyl intermediate containing a localized anion charge on the terminal carbon of the isocyanide structure could be highly reactive.[7a] On the basis of this report, we envisioned the possibility to enhance the nucleophilicity (basicity) of the terminal carbon atom of the isocyanide group by conversion into an imidoyl intermediate (Scheme 2.1D). This intermediate would abstract a proton from an unactivated substrate, generating activated nucleophilic and electrophilic species. Thus, formal X–H insertion without the aid of a metal catalyst could be achieved. To realize this strategy, we

first attempted the reaction between isocyanide and ketone derivatives, which can form an enaminone as the final product (Scheme 2.1E). The proposed methodology provides an unprecedented synthetic route to enaminones via C–C bond formation. Although various synthetic strategies have been developed for the preparation of enaminones, the limited scope and relatively low availability of reagents are significant drawbacks to these procedures.[9] Herein, we report a novel organocatalytic enaminone synthesis from isocyanides and ketones with excellent functional group tolerance. This methodology is applicable to the preparation of a wide range of enaminones via the first catalytic activation of isocyanides by an NHC.

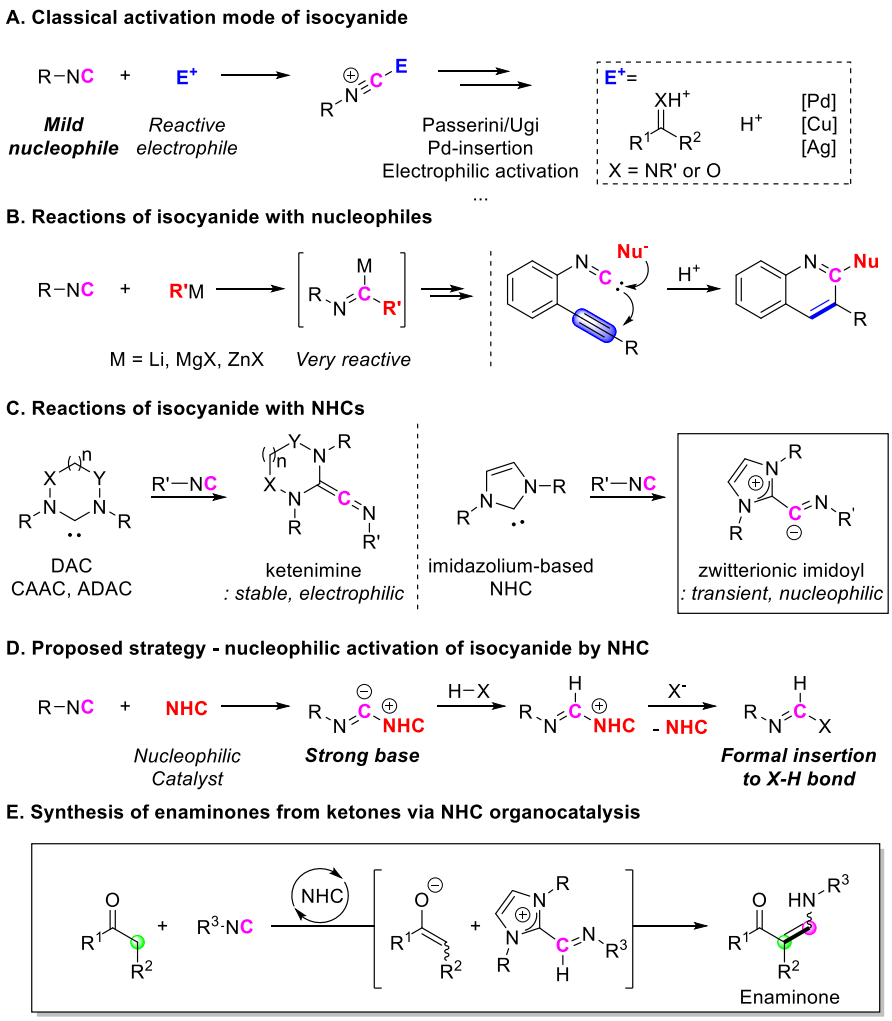

Scheme 2.1 Strategies for isocyanide activation

2.2 Result and discussion

2.2.1 Optimization

At the outset, the reaction between acetophenone (**1a**) and 4-methylphenyl isocyanide (**2a**) was conducted, and in our first attempt the desired (*Z*)-enaminone (**3a**) was isolated in 19% yield. The exclusive (*Z*)-selectivity of **3a** can be explained by intramolecular hydrogen bonding, which was confirmed by ^{1}H NMR spectroscopy.[10] To further increase the reactivity, several reaction parameters were varied (Table 2.1). Among the several solvents examined, DMA afforded the highest yields of **3aa** (entries 1–4). Next, various bases were evaluated, showing that replacing a strong base (NaO*t*Bu) with a relatively weak one (K_2CO_3) did not significantly affect the reactivity (entry 5). Interestingly, the use of IMes as an organocatalyst was critical to obtain the desired product, and the reaction did not proceed at all in the presence of other related imidazolium salts (entries 6 and 7). Screening of the amount of NHC salt, base, and solvent and increasing the reaction temperature resulted in further enhancement of the reaction efficiency (entries 8–10). The reaction time could be reduced to 6 h without significant decrease in reactivity (entry 11). The reaction without NHC salt did not generate the desired product (entry 12) or showed lower reactivity (entry 13), proving that this transformation cannot be catalyzed only by a base.

Table 2.1 Optimization of reaction conditions[a]

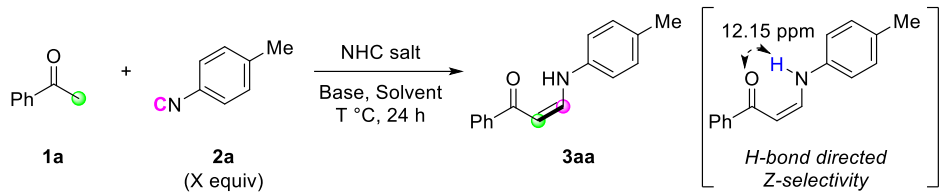

entry	NHC salt (mol%)	Base (mol%)	Solvent (M)	T	X	Yield 3aa (%)
1	IMesHCl (20)	NaO*t*Bu (30)	1,4-Dioxane (0.25)	50	1.0	30
2	IMesHCl (20)	NaO*t*Bu (30)	CH_3CN (0.25)	50	1.0	19
3	IMesHCl (20)	NaO*t*Bu (30)	Toluene (0.25)	50	1.0	36
4	IMesHCl (20)	NaO*t*Bu (30)	DMA (0.25)	50	1.0	43
5	IMesHCl (20)	K_2CO_3 (30)	DMA (0.25)	50	1.0	45
6	IPrHCl (20)	K_2CO_3 (30)	DMA (0.25)	50	1.0	N. R.
7	IAdHBF$_4$ (20)	K_2CO_3 (30)	DMA (0.25)	50	1.0	N. R.
8	IMesHCl (15)	K_2CO_3 (20)	DMA (0.25)	50	1.0	50
9	IMesHCl (15)	K_2CO_3 (20)	DMA (0.125)	80	1.0	73
10	IMesHCl (15)	K_2CO_3 (20)	DMA (0.125)	80	1.5	92
11[b]	IMesHCl (15)	K_2CO_3 (20)	DMA (0.083)	80	1.5	93 (86)[c]
12	None	K_2CO_3 (20)	DMA (0.125)	80	1.0	N. R.
13[b]	None	NaO*t*Bu (20)	DMA (0.083)	80	1.5	13[c]

[a]Reaction conditions: **1a** (0.2 mmol), **2a**, NHC salt, base, and solvent for 24 h, including the 5 min. induction period. Yields determined by GC using mesitylene as an internal standard. [b]6 h, without induction time. [c]Isolated yields. IMesHCl = 1,3-bis(2,4,6-trimethylphenyl)imidazolium chloride. IPrHCl = 1,3-bis(2,6-diisopropylphenyl)imidazolium chloride. IAdHBF$_4$ = 1,3-bis(1-adamantyl)imidazolium tetrafluoroborate. DMA = *N*,*N*-dimethylacetamide. N. R. = no reaction.

2.2.2 Substrate scope evaluation

With the optimized conditions in hand, the scope of the reaction was investigated. First, the reactions of various methyl ketones were performed (Table 2.2). *para*-Substituted acetophenones produced the corresponding enaminones in good to excellent yields (**3aa**–**3ea**). In particular, halide-containing substrates were tolerated under the reaction conditions demonstrating the advantage of this organocatalytic approach (**3ca** and **3da**). *ortho*-Substituted acetophenones also gave excellent yields within 6 h (**3fa** and **3ga**), and bis-substituted acetophenone **1h** produced the corresponding (*Z*)-enaminone **3ha** in 75% yield. In addition, heteroaromatic methyl ketones exhibited excellent reactivity (**3ia**–**3ma**). Non-aromatic methyl ketones could also be used in the reaction, albeit lower yields were obtained (**3na** and **3oa**).

Table 2.2 Substrate scope of methyl ketones[a]

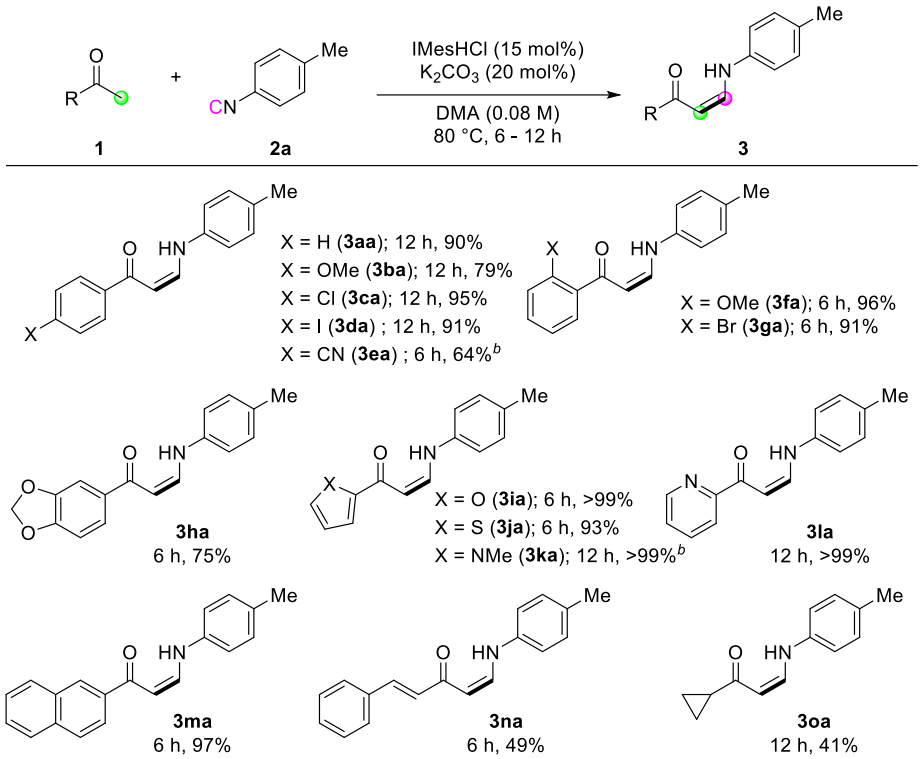

[a]Reaction conditions: **1** (0.2 mmol), **2a** (0.3 mmol), IMesHCl (0.03 mmol), K_2CO_3 (0.04 mmol), and DMA (2.4 mL) at 80 °C. Isolated yields. [b]0.4 mmol of **2a** was used.

Next, we turned our attention toward the synthesis of trisubstituted enaminones. The synthesis of α-alkyl enaminones has been sparsely reported using specifically prepared starting materials,[11] such as triazolyl alkanols,[11a,11b] β-dicarbonyl compounds,[11c,11d] and α,β-unsaturated carbonyl compounds.[11e] To our delight, our strategy could provide an alternative approach starting from readily available ketones (Table 2.3). Ring-fused acetophenone derivatives efficiently produced the corresponding trisubstituted (*Z*)-enaminones under the optimized conditions (**3pa**–**3ra**). In the case of propiophenone and other α-alkyl-substituted acetophenones, stoichiometric amounts of NaO*t*Bu were used to facilitate enolate formation and protonation of the imidoyl intermediate by in situ generated *t*BuOH. Under these modified reaction conditions, *α*-substituted ketones with a linear alkyl chain or a branched alkyl group were all reactive, affording α-alkyl (*E*)-enaminones in good to excellent yields (**3sa**–**3xa**). The exclusive (*E*)-selectivity can be rationalized by the steric repulsion between the phenyl group and the α-alkyl substituent, as previously reported,[12] and the (*E*)-configuration of **3sa** was further determined by X-ray crystallography.

Table 2.3 Synthesis of trisubstituted enaminones[a]

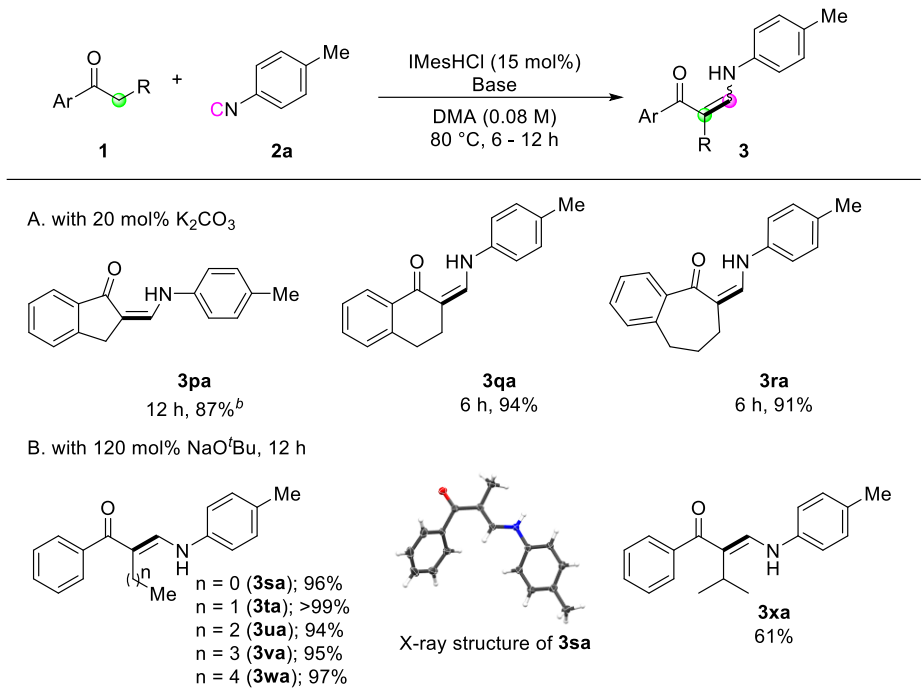

[a]Reaction conditions: **1** (0.2 mmol), **2a** (0.3 mmol), IMesHCl (0.03 mmol), base, and DMA (2.4 mL) at 80 °C for the indicated time. Isolated yields. [b]0.4 mmol of **2a** was used.

The reaction of various isocyanides was evaluated (Table 2.4). Phenyl isocyanide (**2b**) and *p*-methoxyphenyl isocyanide (**2c**) exhibited good to excellent reactivity. However, halogen-substituted isocyanides gave only moderate yields under several reaction conditions (**3ad** and **3ae**). *ortho*-Substituted isocyanides (**3af** and **3ai**), 4-styryl isocyanide (**3ag**), and disubstituted isocyanide (**3ah**) were all tolerated under the reaction conditions, with moderate to good reactivity. Biphenyl isocyanide (**2i**) and naphthyl isocyanide (**2j**) afforded the corresponding (*Z*)-enaminones in good yields (**3ai** and **3aj**). Unfortunately, alkyl isocyanides were not reactive, presumably because the relatively low electrophilicity of the terminal carbon atom of the alkyl isocyanides prevents the nucleophilic attack of the NHC catalyst.

Table 2.4 Substrate scope of isocyanides[a]

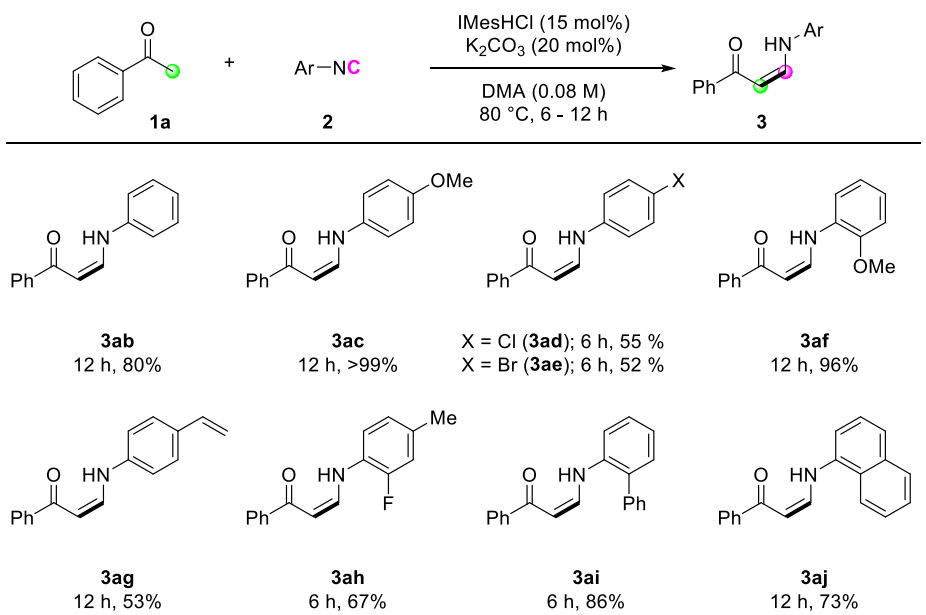

[a]Reaction conditions: **1a** (0.2 mmol), **2** (0.3 mmol), IMesHCl (0.03 mmol), K_2CO_3 (0.04 mmol), and DMA (2.4 mL) at 80 °C for the indicated time. Isolated yields.

Encouraged by the high efficiency of the developed reaction, we further evaluated the scope of the carbon nucleophiles (Scheme 2.2). When bis-acetyl compounds (**1y** and **1z**) were treated with excess amounts of **2a**, formation of bis-(*Z*)-enaminones was observed (**3ya** and **3za**). It is noteworthy that such bis-enaminones have been synthesized using highly activated formamide acetal under harsh conditions, limiting the applicability.[13] These examples clearly demonstrate the utility of our methodology for the synthesis of various complex enaminones. In addition, diethyl malonate (**1A**) and benzyl cyanide (**1B**) efficiently participated in the reaction (**3Aa** and **3Ba**). To check the utility of the reaction further, a gram-scale synthesis was conducted with ketone **1f**, and enaminone **3fa** was produced in 75% yield (Scheme 2.2).

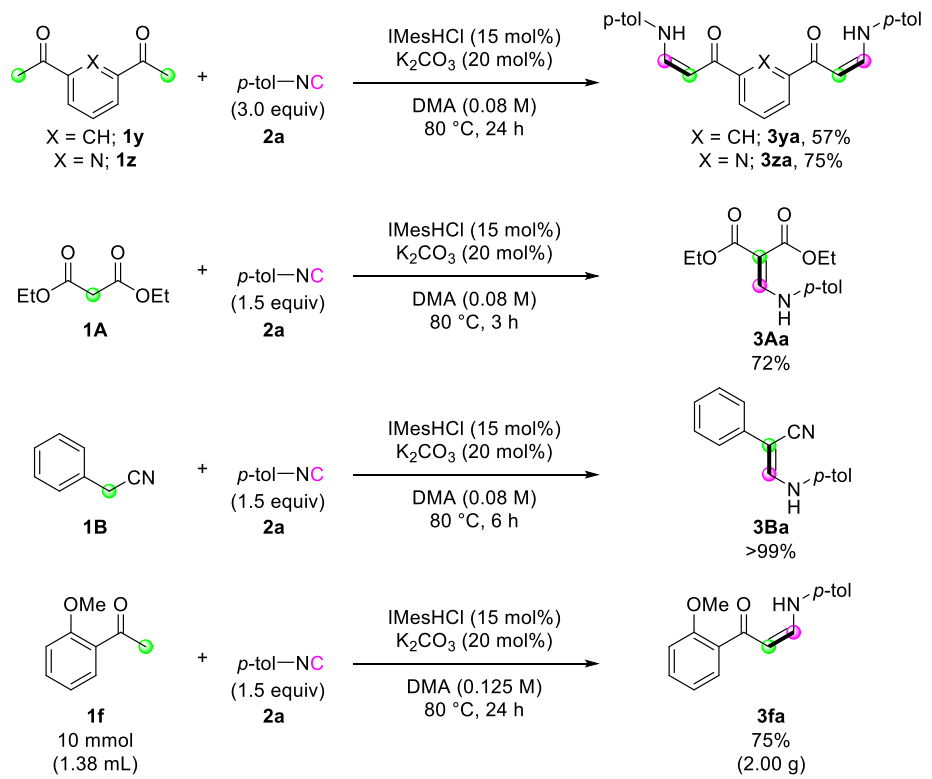

Scheme 2.2 Expansion of the scope of carbon nucleophiles and gram scale synthesis

2.2.3 Mechanistic investigation

In order to gain mechanistic insight into this transformation, control experiments were conducted (Scheme 2.3). When the standard reaction was performed with free carbene (IMes), a comparable yield of the desired product was obtained, suggesting that free carbene is involved in the catalytic cycle (Scheme 2.3A). To further reveal the role of the NHC catalyst, ethyl *N*-phenylformimidate (**2b′**), which can be considered as an analogue of the imine–azolium intermediate, was treated with **1a** (Scheme 2.3B). Even in the presence of stoichiometric amounts of IMes, the reaction yield of **3ab** was not improved, suggesting that the major role of NHC is not ketone deprotonation. In contrast, the use of stoichiometric amounts of a strong base led to full conversion of the ketone **1a** to enaminone **3ab**. This was further supported by the direct alkylation reaction via a stepwise approach with **1a** and benzyl bromide (Scheme 2.3C). When a stoichiometric amount of KO*t*Bu was used in the deprotonation step, enolate **1a′** was observed and α-benzylated product **4** was produced, whereas the use of IMes as a base was not effective for the same transformation. Even at an elevated temperature of 60 °C in THF, we could not observe **1a′** with IMes. From these observations,[14] together with the literature data for the pK_a values of **1a** and related NHC salt,[15] we concluded that the major role of the NHC catalyst is to activate the terminal carbon atom of the isocyanide, generating a more basic imidoyl intermediate, which deprotonates the ketone. Besides, we performed a stoichiometric reaction between an independently generated enolate **1a′** and isocyanide **2a** to check the possibility of the direct addition of **1a′** to isocyanide. **3aa** was obtained in a decreased isolated yield than that of the original catalytic conditions (55% vs. 86%), suggesting that a minor

pathway of direct addition of enolate to isocyanide could exist (Scheme 2.3D). Considering the use of a stoichiometric amount of enolate anions for the reaction under an excess amount of isocyanide as the sole coupling partner, such direct addition process between isocyanide and enolate would not be the major pathway in our reaction.

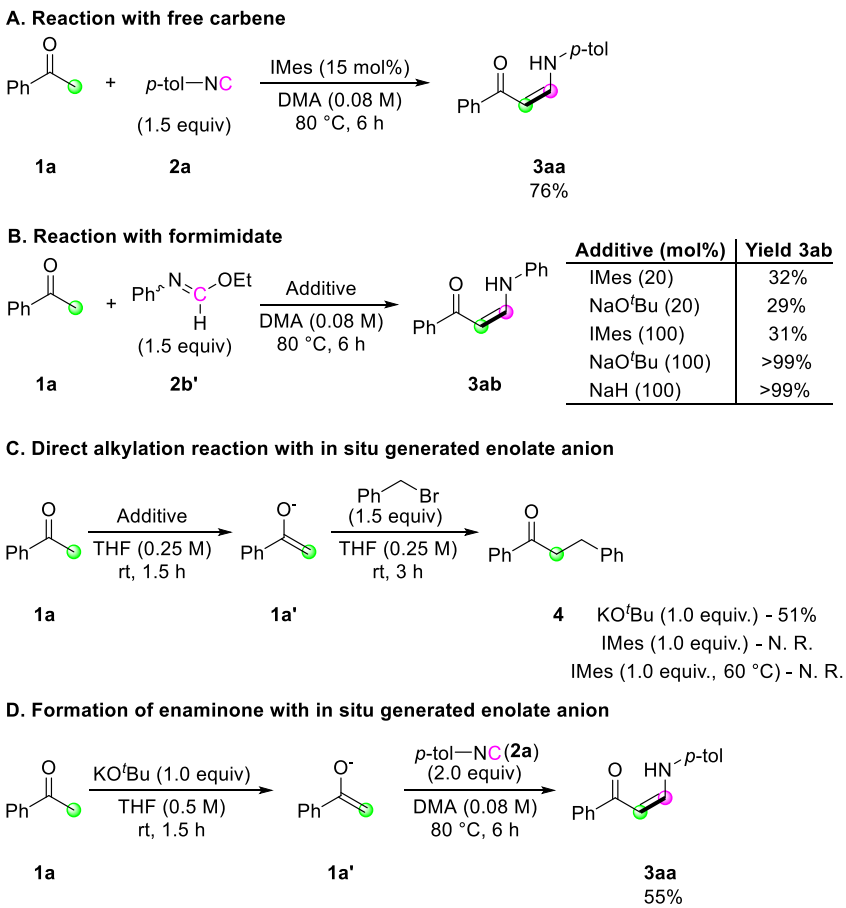

Scheme 2.3 Control experiments

Based on the control experiments and earlier literatures, a catalytic cycle is proposed in Scheme 2.4. The reaction of IMes with isocyanide generates an imidoyl intermediate (**Int A**), which can perform deprotonation to afford an imine–azolium intermediate (**Int B**). During this step, the proton source can be either the ketone, which directly produces the corresponding enolate (Path A), or unreacted imidazolium salt/protonated base (Path B). Trials for the observation of **Int A** or **Int B** through stepwise nucleophilic attack and protonation via ^{1}H NMR spectroscopy were conducted, but promising species were not detectable.[16] We reasoned that those intermediates derived from IMes are transient species in catalytic conditions, which structures are relatively different from that of the stable ketenimine adduct. However, the instability of the intermediates would be a driving force to achieve overall turnover of the catalytic cycle in the reaction mixture. Deprotonation of the ketone by the regenerated base, i.e., Path B, is dominant when Path A is disfavored by steric repulsion interactions such as in the case of bulky ketones. These steps lead to the formation of activated nucleophiles (enolate) and electrophiles (**Int B**). Subsequent coupling and isomerization reactions produce the desired enaminone, together with the regeneration of IMes. Direct coupling between the generated enolate and isocyanide could be also possible, although it would be a minor pathway in the catalytic cycle.

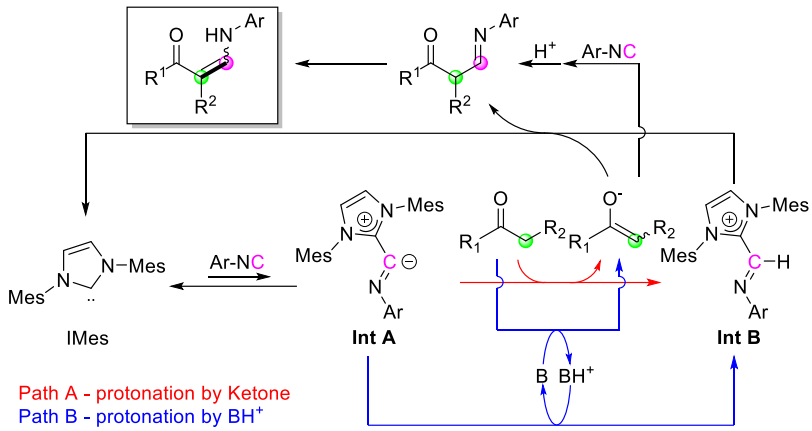

Scheme 2.4 Proposed catalytic cycle.

2.3 Conclusion

We demonstrated the first NHC-catalyzed C–C bond formation reaction between ketones and isocyanides. Using an imidazolium-based NHC catalyst, diverse enaminones were synthesized in excellent yields. We believe that the major role of the NHC in the catalytic cycle is to transform the isocyanide moiety into an imidoyl intermediate, followed by the formation of a highly electrophilic imine–azolium intermediate via a proton transfer process with concomitant nucleophile (enolate) generation. The in situ generated enolate attacks the terminal carbon atom of the isocyanide to complete the catalytic cycle. In this strategy, isocyanides are used as new substrates for NHC organocatalysis.

2.4 Experimental section

2.4.1 General information

Unless otherwise noted, all reactions were performed in a 4mL screw-capped reaction vial. All anhydrous solvents were purchased from commercial suppliers and degassed with dry argon before use. NMR spectra were recorded in $CDCl_3$ or DMSO-d_6, and the residue solvent signals were used as reference. Chemical shifts were reported in ppm, and coupling constants in Hz. Multiplicity is indicated by one or more of the following: s (singlet), d (doublet), t (triplet), q (quartet), quint (quintet), m (multiplet). Unless otherwise note, all reagents and solvents as well as all starting ketones, benzyl bromide, **2b'**, and **2c** were purchased from commercial suppliers and used as received without further purification. Previously reported isocyanides (**2a**, **2b**, **2d**, **2e**, **2f**, **2g**, **2i**, and **2j**) were prepared from their corresponding amines by methods described in the literature,[4a] and their identity was confirmed by comparison with reported data. New isocyanide **2h** was synthesized by a previously reported method, and its structure was confirmed by spectroscopic analysis.[4a] The free carbene (IMes) was synthesized from the corresponding salt (IMesHCl), according to a previous method.[17] All enaminone products were purified by silica gel column chromatography (hexane/ethyl acetate with 3% triethylamine). We are grateful to the Organic Chemistry Research Center of Sogang University for HRMS-ESI analysis, the Korea Basic Science Institute (KBSI) for HRMS-EI analysis, and the Research Institute of Pharmaceutical Science (SNU) for single-crystal X-ray diffraction analysis.

2.4.2 Initial experiment of (*Z*)-enaminone synthesis

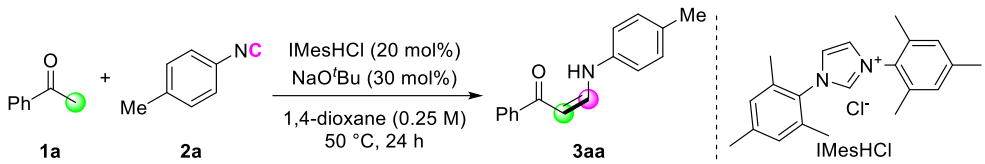

Scheme 2.5 Reaction between **1a** and **2a**

IMesHCl (54.5 mg, 0.16 mmol) and NaO*t*Bu (23.1 mg, 0.24 mmol) were charged in a 25mL Schlenk tube under argon atmosphere. The tube was then sealed with a rubber septum, and 1,4-dioxane (1.6 mL) was added. The mixture was stirred for 5 min. at room temperature, and a solution of **1a** (93.5 μL, 0.8 mmol) and **2a** (95.6 μl, 0.8 mmol) in 1,4-dioxane (1.6 mL) was added via syringe. The mixture was stirred for 24 h at 50 °C. After cooling to room temperature, the volatiles were removed in vacuo and the remaining residue was purified by flash column chromatography (silica gel, hexane/ethyl acetate) to afford **3aa** as a yellow solid (36.1 mg, 19 % yields).

2.4.3 General procedure for the synthesis of enaminone (3)

IMesHCl (10.2mg, 0.03 mmol) and the base were charged in a 4 mL vial under argon atmosphere. The vial was then sealed with a Teflon-lined septum, and the ketone (0.2 mmol), aryl isocyanide (0.3 mmol), and DMA (2.4 mL) were added via syringe. The solution was stirred for the indicated time at 80 °C. After cooling to room temperature, the volatiles were removed in vacuo and the remaining residue was purified by flash column chromatography (silica gel, hexane/ethyl acetate with 3% triethylamine) to afford the corresponding enaminone.

2.4.4 Optimization tables

Table 2.5 Variation of solvent

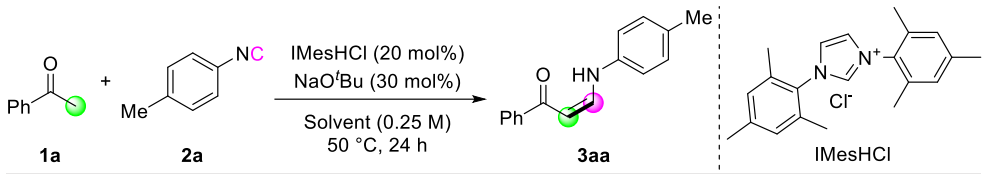

1a **2a** **3aa** IMesHCl

entry	Solvent	Yield 3aa (%)
1	1,4-Dioxane	30
2	CH_3CN	19
3	THF	35
4	Isopropyl acetate	25
5	DCM	13
6	1,2-DCE	Trace
7	Benzene	33
8	Toluene	36
9	*o*-Xylene	38
10	*p*-Xylene	32
11	Cyclohexane	32
12	Hexane	38
13	DMF	42
14	**DMA**	**43**
15	DMSO	40

Table 2.6 Variation of base

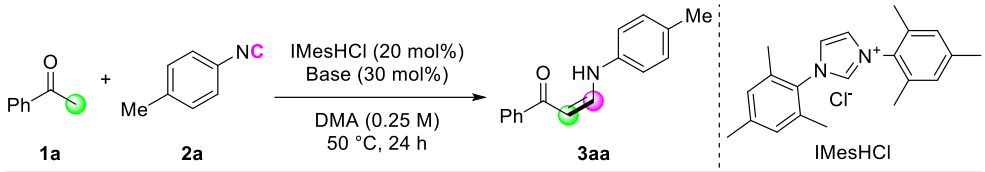

entry	Base	Yield 3aa (%)
1	NaO*t*Bu	39
2	LiO*t*Bu	27
3	KO*t*Bu	37
4	NaOMe	45
5	LiHMDS	38
6	KHMDS	32
7	NaH	45
8	Li_2CO_3	N. R.
9	Na_2CO_3	7
10	K_2CO_3	45
11	Cs_2CO_3	45
12	K_3PO_4	48
13	K_2HPO_4	N. R.
14	KH_2PO_4	N. R.
15	NaOAc	N. R.
16	CsOAc	30
17	Et_3N	N. R.
18	DIPEA	N. R.
19	Pyridine	N. R.

Table 2.7 Variation of NHC salt

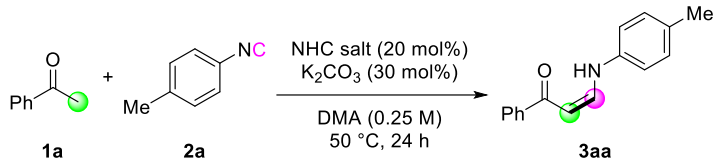

1a **2a** **3aa**

entry	NHC Salt	X	Yield 3aa (%)
1	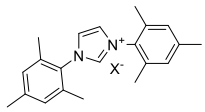	**Cl**	**45**
2		BF_4	42
3		PF_6	32
4	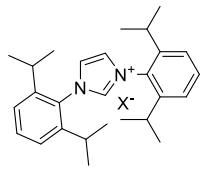	Cl	N. R.
5		BF_4	N. R.
6		PF_6	N. R.
7	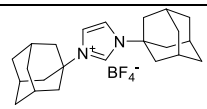	BF_4	N. R.
8	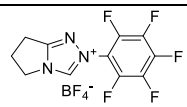	BF_4	N. R.
9		I	N. R.

Table 2.8 Variation of equivalence, time, and temperature

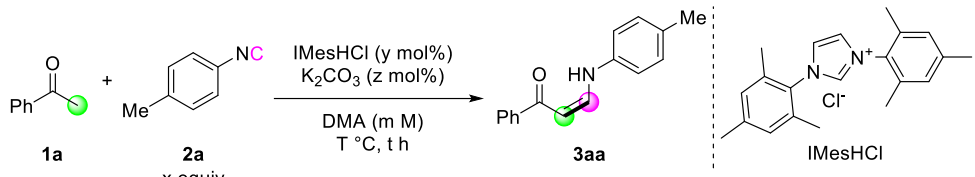

1a 2a x equiv 3aa IMesHCl

entry	x	y	z	m	T	t	Yield 3aa (%)
1	1.0	20	30	0.25	50	24	46
2	1.5	20	30	0.25	50	24	58
3	2.0	20	30	0.25	50	24	54
4	1.0	20	25	0.25	50	24	47
5	1.0	20	20	0.25	50	24	48
6	1.0	15	20	0.25	50	24	50
7	1.0	10	20	0.25	50	24	42
8	1.5	15	20	0.25	50	48	64
9	1.5	15	20	0.25	80	48	81
10	1.5	15	20	0.125	80	48	87
11	1.5	15	20	0.125	80	24	92
12	1.5	15	20	0.125	80	12	94
13	1.5	15	20	0.125	80	6	91
14	1.5	15	20	0.125	80	3	74
15	**1.5**	**15**	**20**	**0.083**	**80**	**6**	**93**

2.4.5 Experimental procedures for the control experiments

IMes (9.1mg, 0.03 mmol) was charged in a 4 mL vial under argon atmosphere. The vial was then sealed with a Teflon-lined septum, and **1a** (23.4 μl, 0.2 mmol), **2a** (48 μL, 0.3 mmol), and DMA (2.4 mL) were added via syringe. The solution was stirred for 6 h at 80 °C. After cooling to room temperature, the volatiles were removed in vacuo and the remaining residue was purified by flash column chromatography (silica gel, hexane/ethyl acetate with 3% triethylamine) to afford the corresponding enaminone **3aa** in 76% yields.

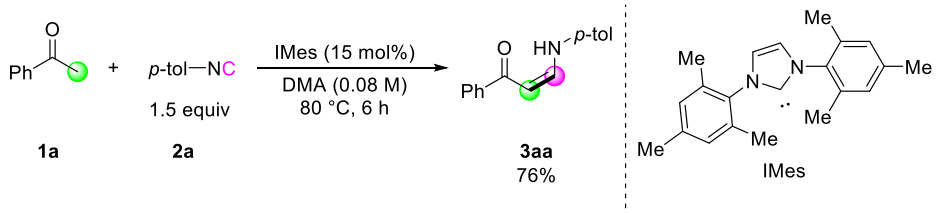

1a 2a 3aa 76%

Scheme 2.6 Reaction between **1a** and **2a** with IMes

Additive (0.04 or 0.2 mmol) was charged in a 4 mL vial under argon atmosphere. The vial was then sealed with a Teflon-lined septum, and **1a** (23.4 μL, 0.2 mmol), **2b'** (44.5 μl, 0.3 mmol), and DMA (2.4 mL) were added via syringe. The solution was stirred for 6 h at 80 °C. After cooling to room temperature, the volatiles were removed in vacuo and the remaining residue was purified by flash column chromatography (silica gel, hexane/ethyl acetate with 3% triethylamine) to afford the corresponding enaminone **3ab**.

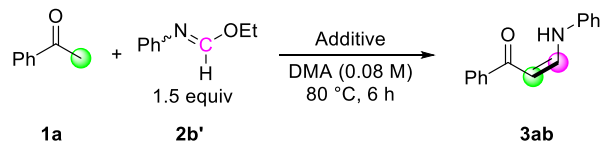

1a 2b' 3ab

Scheme 2.7 Reaction between **1a** and **2b'**

Additive (0.5 mmol) and THF (2 mL) were charged in a 10 mL Schlenk tube under argon atmosphere, and the tube was then sealed with rubber septum. **1a** (58.3 μL, 0.5 mmol) was slowly added to the solution under argon flow at room temperature, and the solution was further stirred for 1.5 h at room temperature. Benzyl bromide (71.4 μL, 0.6 mmol) was added in the reaction mixture under argon flow, and the solution was further stirred for 3 h at room temperature. After the reaction was finished, the reaction mixture was diluted with ethyl acetate (10 mL), washed with aqueous sat. $NaHCO_3$ solution (10 mL) and brine (10 mL), dried with $MgSO_4$, and concentrated in vacuo. The crude mixture was analysed by ^1H NMR using nitromethane as an internal standard.

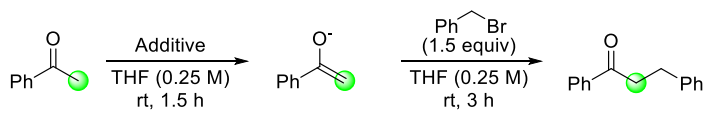

Scheme 2.8 Direct alkylation reaction with in situ generated enolate anion

KO*t*Bu (56 mg, 0.5 mmol) and THF (1 mL) were charged in a 25 mL Schlenk tube under argon atmosphere, and the tube was then sealed with rubber septum. **1a** (58.3 μL, 0.5 mmol) was slowly added to the solution under argon flow at room temperature, and the solution was further stirred for 1.5 h at room temperature. After removing all volatiles via manifold vacuum (white solid **1a'** was observed), **2b** (120 μL, 1.0 mmol), and DMA (6 mL) were added in the tube under argon flow. The solution was stirred for 6 h at 80 °C. After cooling to room temperature, the reaction mixture was diluted with ethyl acetate (20 ml), washed with aqueous sat. $NaHCO_3$ solution (20 mL × 2) and brine (20 mL), dried with $MgSO_4$, and concentrated in vacuo. The crude mixture was purified by flash column chromatography (silica gel, hexane/ethyl acetate with 3% triethylamine) to afford the corresponding enaminone **3aa** in 55% yields.

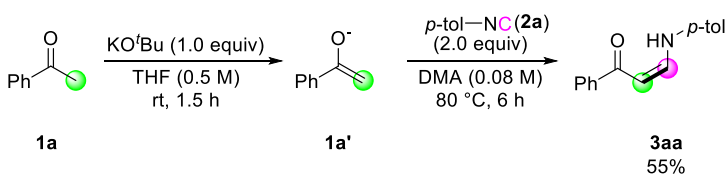

Scheme 2.9 Reaction of **2a** with in-situ generated enolate anion

2.4.6 Experimental procedures for the gram-scale reaction

IMesHCl (511 mg, 1.5 mmol), K_2CO_3 (276 mg, 2.0 mmol), and DMA (80 mL) were charged in a 250 mL oven-dried round-bottom flask (RBF) under argon atmosphere, and the flask was then sealed with rubber septum. **1f** (1.38 mL, 10 mmol) and **2a** (1.8 mL, 15 mmol) were added to the solution under argon flow, and the solution was further stirred for 24 h at 80 °C. After reaction was finished, the reaction mixture was cooled to room temperature and diluted with ethyl acetate (170 mL). The organic solution was washed with aqueous 5% LiCl solution (250 mL × 4) and brine (250 mL), dried with $MgSO_4$ and concentrated in vacuo. The residual mixture was further purified by flash column chromatography (silica gel, hexane/ethyl acetate with 3% triethylamine) to afford the corresponding enaminone **3fa** in 75% yield.

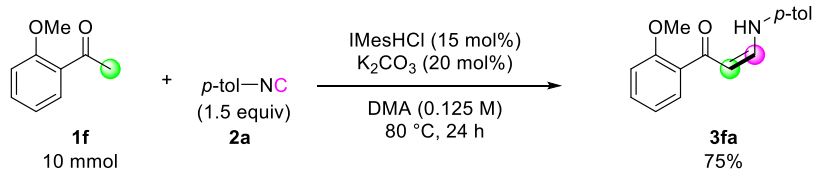

Scheme 2.10 Gram-scale reaction of **1f** with **2a**

2.4.7 Crystallographic data of 3sa

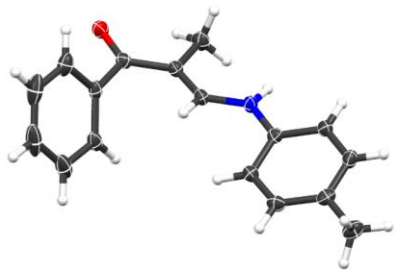

Figure 2.1 Solid-state structure of **3sa** at 50 % probability ellipsoids

Single crystals of **3sa** were obtained by slow evaporation of saturated DMA solution of **3sa**, and one of them was chosen for the analysis by X-ray diffractometer.

Table 2.9 Crystal data and structure refinement for **3sa**

CCDC number	1503347
Empirical formula	$C_{17}H_{17}ON$
Formula weight	251.31
Temperature/K	101(2)
Crystal system	monoclinic
Space group	$P2_1/n$
a/Å	6.39890(8)
b/Å	11.27072(15)
c/Å	19.0731(3)
α/°	90
β/°	92.0107(13)
γ/°	90

Volume/$Å^3$	1374.71(3)
Z	4
$\rho_{calc}g/cm^3$	1.214
μ/mm^{-1}	0.587
F(000)	536.0
Crystal size/mm^3	0.289 × 0.148 × 0.031
Radiation	CuKα (λ = 1.54184)
2Theta range for data collection/°	9.116 to 152.968
Index ranges	$-7 \leq h \leq 5$, $-14 \leq k \leq 14$, $-23 \leq l \leq 23$
Reflections collected	16312
Independent reflections	2863 [R_{int} = 0.0287, R_{sigma} = 0.0191]
Data/restraints/parameters	2863/0/174
Goodness-of-fit on F^2	1.048
Final R indexes [I>=2σ (I)]	R_1 = 0.0411, wR_2 = 0.1095
Final R indexes [all data]	R_1 = 0.0441, wR_2 = 0.1128
Largest diff. peak/hole / $e.Å^{-3}$	0.26/-0.27

2.4.8 Spectroscopic data

2-Fluoro-1-isocyano-4-methylbenzene (**2h**)

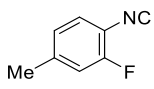

^{1}H NMR (499 MHz, $CDCl_3$) δ 7.27 (t, *J* = 7.7 Hz, 1H), 7.00 (d, *J* = 10.2 Hz, 1H), 6.97 – 6.94 (m, 1H), 2.38 (s, 3H); ^{13}C NMR (75 MHz, $CDCl_3$) δ 169.4, 157.1 (d, *J* = 255.9 Hz), 142.3 (d, *J* = 7.3 Hz), 127.4, 125.3 (d, J = 3.5 Hz), 117.0 (d, *J* = 18.1 Hz), 112.6 (d, *J* = 14.8 Hz), 21.4 (d, *J* = 1.3 Hz); ^{19}F NMR (376 MHz, $CDCl_3$) δ -119.3; HRMS-EI (m/z) $[M]^+$ calculated for C_8H_6FN, 135.0484; found: 135.0483.

(*Z*)-1-phenyl-3-(*p*-tolylamino)prop-2-en-1-one (**3aa**)

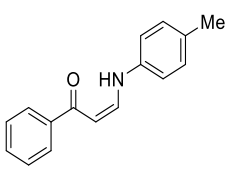

^{1}H NMR (499MHz, $CDCl_3$) δ 12.15 (d, *J* = 11.7 Hz, 1 H), 7.94 (d, *J* = 7.8 Hz, 2 H), 7.44 – 7.52 (m, 4 H), 7.15 (d, *J* = 8.3 Hz, 2 H), 7.02 (d, *J* = 8.3 Hz, 2 H), 6.00 (d, *J* = 7.8 Hz, 1 H), 2.33 (s, 3 H). Identity confirmed by comparing with reported literature.[18]

(*Z*)-1-(4-methoxyphenyl)-3-(*p*-tolylamino)prop-2-en-1-one (**3ba**)

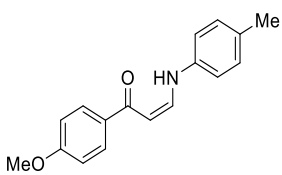

^{1}H NMR (400 MHz, $CDCl_3$) δ 12.08 (d, *J* = 11.8 Hz, 1H), 7.92 (d, *J* = 8.8 Hz, 2H), 7.45 (dd, *J* = 11.8 Hz, 7.9 Hz, 1H), 7.14 (d, *J* = 8.2 Hz, 2H), 6.99 (d, *J* = 8.2 Hz, 2H), 6.94 (d, *J* = 8.8 Hz, 2H), 5.95 (d, *J* = 7.9 Hz, 1H), 3.86 (s, 3H), 2.32 (s, 3H); ^{13}C NMR (101 MHz, $CDCl_3$) δ 189.9, 162.5, 144.8, 138.1, 133.2, 132.2, 130.3, 129.4, 116.3, 113.7, 93.1, 55.5, 20.9; HRMS-ESI (m/z) $[M+Na]^+$ calculated for $C_{17}H_{17}NNaO_2$, 290.1151; found: 290.1150.

(*Z*)-1-(4-chlorophenyl)-3-(*p*-tolylamino)prop-2-en-1-one (**3ca**)

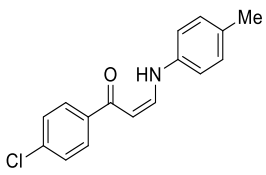

^{1}H NMR (400 MHz, $CDCl_3$) δ 12.14 (d, *J* = 12.3 Hz 1H), 7.87 (d, *J* = 6.7 Hz, 2H), 7.51 (dd, *J* = 11.4 Hz, 7.5 Hz, 1H), 7.42 (d, *J* = 6.7 Hz, 1H), 7.16 (d, *J* = 7.2 Hz, 2H), 7.02 (d, *J* = 7.2 Hz, 2H), 5.95 (d, *J* = 7.5 Hz, 1H), 2.33 (s, 3H); ^{13}C NMR (101 MHz, $CDCl_3$) δ 189.4, 145.8, 145.8, 137.8, 137.8, 133.9, 130.4, 128.8, 116.6, 93.00, 20.9; HRMS-ESI (m/z) $[M+Na]^+$ calculated for $C_{16}H_{14}ClNNaO$, 294.0656; found: 294.0658.

(*Z*)-1-(4-iodophenyl)-3-(*p*-tolylamino)prop-2-en-1-one (**3da**)

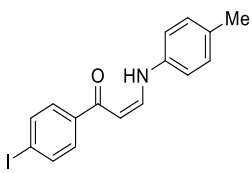

^{1}H NMR (400 MHz, $CDCl_3$) δ 12.15 (d, *J* = 12.0 Hz, 1H), 7.80 (d, *J* = 8.3 Hz, 2H), 7.64 (d, *J* = 8.4 Hz, 2H), 7.50 (dd, *J* = 12.5 Hz, 7.7 Hz, 1H), 7.15 (d, *J* = 8.2 Hz, 2H), 7.01 (d, *J* = 8.3 Hz, 2H), 5.93 (d, *J* = 7.7 Hz, 1H), 2.33 (s, 3H); ^{13}C NMR (75 MHz, $CDCl_3$) δ 189.7, 145.9, 138.8, 137.8, 133.9, 130.4, 129.0, 116.6, 98.8, 92.9, 20.9.; HRMS-ESI (m/z) $[M+H]^+$ calculated for $C_{16}H_{15}INO$, 364.0913; found: 364.0913.

(*Z*)-4-(3-(*p*-tolylamino)acryloyl)benzonitrile (**3ea**)

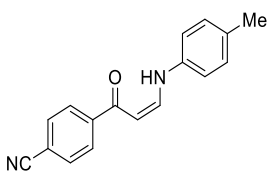

^{1}H NMR (400 MHz, $CDCl_3$) δ 12.24 (d, *J* = 12.2 Hz, 1H), 7.99 (d, *J* = 8.2 Hz, 2H), 7.73 (d, *J* = 8.4 Hz, 2H), 7.56 (dd, *J* = 12.6 Hz, 7.7 Hz, 1H), 7.17 (d, *J* = 8.2 Hz, 2H), 7.03 (d, *J* = 8.3 Hz, 2H), 5.95 (d, *J* = 7.6 Hz, 1H), 2.33 (s, 3H); ^{13}C NMR (101 MHz, $CDCl_3$) δ 188.4, 146.8, 143.0, 137.4, 134.4, 132.4, 130.5, 127.8, 118.6, 116.9, 114.6, 93.1, 21.0; HRMS-ESI (m/z) $[M+Na]^+$ calculated for $C_{17}H_{14}N_2NaO$, 285.0998; found: 285.0997.

(*Z*)-1-(2-methoxyphenyl)-3-(*p*-tolylamino)prop-2-en-1-one (**3fa**)

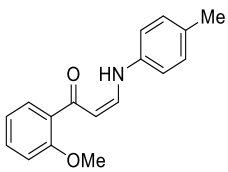

^{1}H NMR (499 MHz, $CDCl_3$) δ 12.05 (d, *J* = 12.6 Hz, 1H), 7.71 (dd, *J* = 7.6 Hz, 1.8 Hz, 1H), 7.44 – 7.39 (m, 2H), 7.15 (d, *J* = 8.2 Hz, 2H), 7.05 – 6.96 (m, 4H), 6.01 (d, *J* = 7.8 Hz, 1H), 3.92 (s, 3H), 2.33 (s, 3H); ^{13}C NMR (101 MHz, $CDCl_3$) δ 191.7, 157.7, 144.4, 138.2, 133.3, 132.0, 130.3, 130.2, 120.7, 116.5, 111.7, 98.5, 55.8, 20.9; HRMS-ESI (m/z) $[M+Na]^+$ calculated for $C_{17}H_{17}NNaO_2$, 290.1151; found: 290.1152.

(*Z*)-1-(2-bromophenyl)-3-(*p*-tolylamino)prop-2-en-1-one (**3ga**)

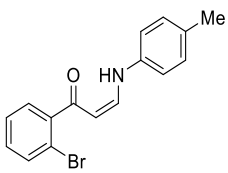

^{1}H NMR (400 MHz, $CDCl_3$) δ 11.92 (d, *J* = 11.6 Hz, 1H), 7.60 (d, *J* = 8.0 Hz, 1H), 7.46 (dd, *J* = 12.5 Hz, 7.7 Hz, 2H), 7.35 (t, *J* = 7.5 Hz, 1H), 7.23 (t, *J* = 8.2 Hz, 2H), 7.02 (d, *J* = 8.3 Hz, 2H), 5.63 (d, *J* = 7.6 Hz, 1H), 2.33 (s, 3H); ^{13}C NMR (101 MHz, $CDCl_3$) δ 193.0, 145.5, 142.6, 137.7, 134.0, 133.6, 130.7, 130.4, 129.3, 127.4, 119.5, 116.8, 97.2, 20.9.; HRMS-ESI (m/z) $[M+Na]^+$ calculated for $C_{16}H_{14}BrNNaO$, 338.0151; found: 338.0152.

(*Z*)-1-(benzo[*d*][1,3]dioxol-5-yl)-3-(*p*-tolylamino)prop-2-en-1-one (**3ha**)

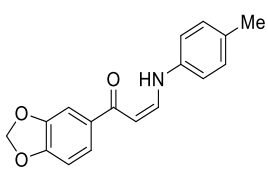

^{1}H NMR (400 MHz, $CDCl_3$) δ 12.04 (d, *J* = 11.7Hz, 1H), 7.52 (d, *J* = 8.2Hz, 1H), 7.49 – 7.41 (m, 2H), 7.14 (d, *J* = 8.2 Hz, 2H), 6.99 (d, *J* = 8.3 Hz, 2H), 6.85 (d, *J* = 8.1 Hz, 1H), 6.03 (s, 2H), 5.90 (d, *J* = 7.8 Hz, 1H), 2.32 (s, 3H); ^{13}C NMR (101 MHz, $CDCl_3$) δ 189.4, 150.6, 148.1, 145.0, 138.0, 134.1, 133.4, 130.4, 122.8, 116.4, 108.0, 107.6, 101.7, 93.0, 20.9; HRMS-ESI (m/z) $[M+Na]^+$ calculated for $C_{17}H_{15}NNaO_3$, 304.0944; found: 304.0943.

(*Z*)-1-(furan-2-yl)-3-(*p*-tolylamino)prop-2-en-1-one (**3ia**)

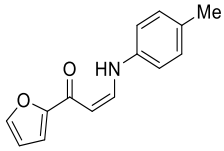

^{1}H NMR (400 MHz, $CDCl_3$) δ 11.91 (d, *J* = 11.6 Hz, 1H), 7.53 (s, 1H), 7.45 (dd, *J* = 12.5, 7.8 Hz, 1H), 7.14 (d, *J* = 8.1 Hz, 2H), 7.09 (d, *J* = 3.4 Hz, 1H), 6.98 (d, *J* = 8.3 Hz, 2H), 6.51 (dd, *J* = 3.3, 1.5 Hz, 1H), 5.90 (d, *J* = 7.8 Hz , 1H), 2.31 (s, 3H); ^{13}C NMR (101 MHz, $CDCl_3$) δ 180.0, 154.0, 145.3, 145.0, 137.8, 133.6, 130.4, 116.4, 114.0, 112.2, 112.2, 93.1, 20.9; HRMS-ESI (m/z) $[M+Na]^+$ calculated for $C_{14}H_{13}NNaO_2$, 250.0838; found: 250.0836.

(*Z*)-1-(thiophen-2-yl)-3-(*p*-tolylamino)prop-2-en-1-one (**3ja**)

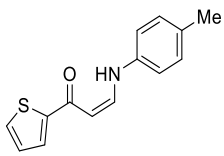

^{1}H NMR (400 MHz, $CDCl_3$) δ 11.87 (d, *J* = 11.6 Hz, 1H), 7.63 (d, *J* = 3.7 Hz, 1H), 7.54 (d, *J* = 4.9 Hz, 1H), 7.44 (dd, *J* = 12.5, 7.7 Hz, 1H), 7.14 (d, *J* = 8.3 Hz, 2H), 7.11 (t, *J* = 3.9 Hz, 1H), 6.98 (d, *J* = 8.3 Hz, 2H), 5.86 (d, *J* = 7.7 Hz, 1H), 2.32 (s, 3H); ^{13}C NMR (101 MHz, $CDCl_3$) δ 183.7, 146.4, 145.0, 137.9, 133.6, 131.5, 130.4, 128.9, 128.12, 116.4, 93.4, 20.9; HRMS-ESI (m/z) $[M+Na]^+$ calculated for $C_{14}H_{13}NNaOS$, 266.0610; found: 266.0610.

(*Z*)-1-(1-methyl-1*H*-pyrrol-2-yl)-3-(*p*-tolylamino)prop-2-en-1-one (**3ka**)

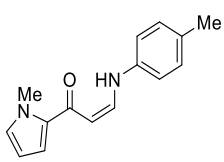

^{1}H NMR (400 MHz, $CDCl_3$) δ 11.53 (d, *J* = 11.9Hz, 1H), 7.29 (dd, *J* = 12.3, 8.1 Hz, 1H), 7.12 (d, *J* = 8.2 Hz, 2H), 6.96 (d, *J* = 8.3 Hz, 2H), 6.86 - 6.82 (m, 1H), 6.76 (s, 1H), 6.14 - 6.10 (m, 1H), 5.79 (d, *J* = 8.1 Hz, 1H), 4.02 (s, 3H), 2.31 (s, 3H); ^{13}C NMR (101 MHz, $CDCl_3$) δ 183.6, 142.9, 138.5, 132.5, 132.1, 130.3, 129.8, 116.0, 116.0, 107.8, 95.1, 37.7, 20.8.; HRMS-ESI (m/z) $[M+Na]^+$ calculated for $C_{15}H_{16}N_2NaO$,

263.1155; found: 263.1156.

(*Z*)-1-(pyridin-2-yl)-3-(*p*-tolylamino)prop-2-en-1-one (**3la**)

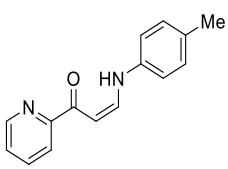

^{1}H NMR (400 MHz, $CDCl_3$) δ 12.16 (d, *J* = 12.0 Hz, 1H), 8.66 (d, *J* = 4.1 Hz, 1H), 8.13 (d, *J* = 7.8 Hz, 1H), 7.83 (t, *J* = 7.7 Hz, 1H), 7.60 (dd, *J* = 12.3, 7.7 Hz, 1H), 7.39 (dd, *J* = 7.7, 4.8 Hz, 1H), 7.15 (d, *J* = 7.9 Hz, 2H), 7.03 (d, *J* = 7.7 Hz, 2H), 6.71 (d, *J* = 7.7 Hz, 1H), 2.32 (s, 3H); ^{13}C NMR (101 MHz, $CDCl_3$) δ 189.4, 155.4, 148.8, 146.4, 137.8, 137.0, 133.8, 130.4, 125.8, 121.8, 116.7, 92.9, 20.9.; HRMS-ESI (m/z) $[M+Na]^+$ calculated for $C_{15}H_{14}N_2NaO$, 261.0998; found: 261.0998.

(*Z*)-1-(naphthalen-2-yl)-3-(*p*-tolylamino)prop-2-en-1-one (**3ma**)

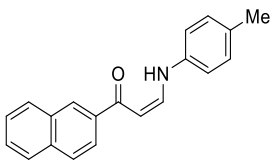

^{1}H NMR (400 MHz, $CDCl_3$) δ 12.23 (d, *J* = 11.9 Hz, 1H), 8.45 (s, 1H), 8.04 (d, *J* = 8.6 Hz, 1H), 7.96 (d, *J* = 8.1 Hz, 1H), 7.90 (d, *J* = 8.7 Hz, 1H), 7.87 (d, *J* = 7.7 Hz, 1H), 7.59 – 7.49 (m, 3H), 7.16 (d, *J* = 8.1 Hz, 2H), 7.04 (d, *J* = 8.3 Hz, 2H), 6.16 (d, *J* = 7.8 Hz, 1H), 2.33 (s, 3H); ^{13}C NMR (101 MHz, $CDCl_3$) δ 190.7, 145.4, 138.0, 136.8, 135.1, 133.6, 133.0, 130.4, 129.5, 128.3, 128.1, 127.8, 127.7, 126.6, 124.1, 116.6, 93.6, 20.9; HRMS-ESI (m/z) $[M+Na]^+$ calculated for $C_{20}H_{17}NNaO$, 310.1202; found: 310.1204.

(1*E*,4*Z*)-1-phenyl-5-(*p*-tolylamino)penta-1,4-dien-3-one (**3na**)

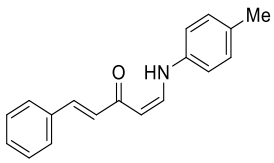

^{1}H NMR (499 MHz, $CDCl_3$) δ 12.18 (d, *J* = 12.3 Hz, 1H), 7.60 – 7.54 (m, 3H), 7.44 – 7.33 (m, 4H), 7.14 (d, *J* = 8.0 Hz, 2H), 6.99 (d, *J* = 8.4 Hz, 2H), 6.78 (d, *J* = 15.9 Hz, 2H), 5.50 (d, *J* = 7.5 Hz, 1H), 2.32 (s, 3H); ^{13}C NMR (75 MHz, $CDCl_3$) δ 189.1, 145.1, 139.5, 137.9, 135.6, 133.6, 130.4, 129.7, 128.9, 128.2, 127.9, 116.5, 97.8, 20.9; HRMS-ESI (m/z) $[M+Na]^+$ calculated for $C_{18}H_{17}NNaO$, 286.1202; found: 286.1200.

(*Z*)-1-cyclopropyl-3-(*p*-tolylamino)prop-2-en-1-one (**3oa**)

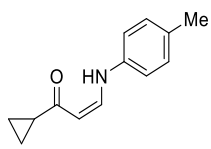

^{1}H NMR (499 MHz, $CDCl_3$) δ 11.56 (d, *J* = 10.9 Hz, 1H), 7.18 (dd, *J* = 12.4, 7.7 Hz, 1H), 7.10 (d, *J* = 8.3 Hz, 2H), 6.90 (d, *J* = 8.4 Hz, 2H), 5.41 (d, *J* = 7.7 Hz, 1H), 2.29 (s, 3H), 1.83 – 1.78 (m, 1H), 1.05 – 1.02 (m, 2H), 0.85 – 0.81 (m, 2H); ^{13}C NMR (75 MHz, $CDCl_3$) δ 200.5, 142.6, 138.1, 132.9, 130.2, 115.9, 96.7, 20.7, 20.5, 9.9; HRMS-ESI (m/z) $[M+Na]^+$ calculated for $C_{13}H_{15}NNaO$, 224.1046; found: 224.1043.

(*Z*)-2-((*p*-tolylamino)methylene)-2,3-dihydro-1*H*-inden-1-one (**3pa**)

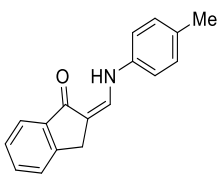

^{1}H NMR (499 MHz, $CDCl_3$) δ 11.35 (d, *J* = 11.3 Hz, 1H), 7.84 (d, *J* = 7.6 Hz, 1H), 7.55 – 7.46 (m, 3H), 7.14 (d, *J* = 8.0 Hz, 2H), 7.00 (d, *J* = 8.5 Hz, 2H), 3.66 (s, 2H), 2.32 (s, 3H); ^{13}C NMR (75 MHz, $CDCl_3$) δ 193.3, 148.8, 141.0, 139.3, 138.2, 132.9, 132.2, 130.4, 127.2, 125.8, 122.9, 115.8, 107.8, 30.9, 20.9; HRMS-ESI (m/z) $[M+Na]^+$ calculated for $C_{17}H_{15}NNaO$, 272.1046; found: 272.1048.

(*Z*)-2-((*p*-tolylamino)methylene)-3,4-dihydronaphthalen-1(2*H*)-one (**3qa**)

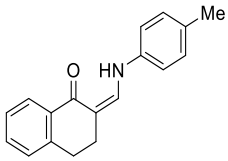

^{1}H NMR (400 MHz, $CDCl_3$) δ 11.97 (d, *J* = 11.4 Hz, 1H), 8.03 (d, *J* = 7.6 Hz, 1H), 7.44 – 7.31 (m, 3H), 7.22 (d, *J* = 7.4 Hz, 1H), 7.13 (d, *J* = 8.1 Hz, 2H), 6.99 (d, *J* = 8.3 Hz, 2H), 2.92 (t, *J* = 6.5 Hz, 2H), 2.68 (t, *J* = 6.5 Hz, 2H), 2.31 (s, 3H); ^{13}C NMR (101 MHz, $CDCl_3$) δ 187.6, 142.4, 142.1, 138.3, 135.3, 132.8, 131.9, 130.4, 128.0, 126.9, 126.7, 116.1, 104.8, 30.0, 27.9, 20.9.; HRMS-ESI (m/z) $[M+Na]^+$ calculated for $C_{18}H_{17}NNaO$, 286.1202; found: 286.1201.

(*Z*)-6-((*p*-tolylamino)methylene)-6,7,8,9-tetrahydro-5*H*-benzo[7]annulen-5-one (**3ra**)

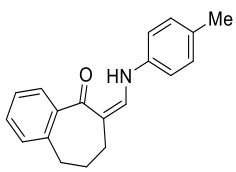

^{1}H NMR (499 MHz, $CDCl_3$) δ 12.01 (d, *J* = 11.6 Hz, 1H), 7.61 (dd, *J* = 7.3, 1.7 Hz, 1H), 7.39 – 7.31 (m, 2H), 7.28 (d, *J* = 12.2 Hz, 1H), 7.16 (d, *J* = 8.2 Hz, 1H), 7.14 (d, *J* = 8.3 Hz, 2H), 7.00 (d, J = 8.4 Hz, 2H), 2.74 (t, *J* = 7.0 Hz, 2H), 2.32 (s, 3H), 2.18 (t, *J* = 6.8 Hz, 2H), 1.95 (quint, *J* = 6.9 Hz, 2H); ^{13}C NMR (75 MHz, $CDCl_3$) δ 197.1, 143.0, 141.7, 138.9, 138.3, 132.8, 130.7, 130.3, 128.6, 127.5, 126.8, 116.2, 107.6, 31.0, 30.6, 28.1, 20.8; HRMS-ESI (m/z) $[M+Na]^+$ calculated for $C_{19}H_{19}NNaO$, 300.1359; found: 300.1360.

(*E*)-2-methyl-1-phenyl-3-(*p*-tolylamino)prop-2-en-1-one (**3sa**)

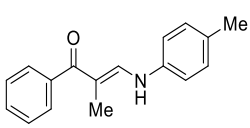

^{1}H NMR (499 MHz, DMSO-d_6) δ 8.96 (d, *J* = 13.1 Hz, 1H), 7.52 – 7.42 (m, 5H), 7.40 (d, *J* = 13.1 Hz, 1H), 7.06 (d, *J* = 8.3, 2H), 6.85 (d, *J* = 8.4 Hz, 2H), 2.20 (s, 3H), 1.93 (s, 3H); ^{13}C NMR (75 MHz, DMSO-d_6) δ 194.8, 145.6, 141.4, 139.7, 131.6, 130.4, 130.1, 128.5, 116.3, 110.0,

20.7, 10.3; HRMS-ESI (m/z) $[M+Na]^+$ calculated for $C_{17}H_{17}NNaO$, 274.1202; found: 274.1200.

(*E*)-1-phenyl-2-((*p*-tolylamino)methylene)butan-1-one (**3ta**)

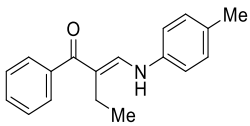

^{1}H NMR (499 MHz, DMSO-d_6) δ 9.01 (d, *J* = 13.2 Hz, 1H), 7.50 – 7.40 (m, 5H), 7.32 (d, *J* = 13.2 Hz, 1H), 7.05 (d, *J* = 8.3 Hz, 2H), 6.84 (d, *J* = 8.5 Hz, 2H), 2.48 (t, *J* = 7.3 Hz, 2H), 2.19 (s, 3H), 1.03 (t, *J* = 7.4 Hz, 3H); ^{13}C NMR (101 MHz, DMSO-d_6) δ 194.2, 144.4, 141.0, 139.3, 131.0, 129.9, 129.6, 128.0, 116.1, 115.8, 20.2, 16.8, 13.1; HRMS-ESI (m/z) $[M+Na]^+$ calculated for $C_{18}H_{19}NNaO$, 288.1359; found: 288.1358.

(*E*)-1-phenyl-2-((*p*-tolylamino)methylene)pentan-1-one (**3ua**)

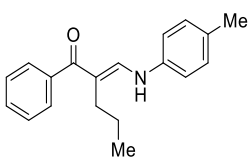

^{1}H NMR (499 MHz, DMSO-d_6) δ 8.96 (d, *J* = 13.3 Hz, 1H), 7.50 – 7.42 (m, 5H), 7.05 (d, *J* = 8.4 Hz, 2H), 6.83 (d, *J* = 8.5 Hz, 2H), 2.46 (t, *J* = 7.3 Hz, 2H), 2.19 (s, 3H), 1.49 – 1.41 (m, 2H), 0.95 (t, *J* = 7.3 Hz, 3H); ^{13}C NMR (75 MHz, DMSO-d_6) δ 194.5, 145.0, 141.1, 139.3, 131.1, 129.9, 129.6, 128.0, 115.9, 114.5, 25.2, 21.2, 20.2, 13.9.; HRMS-ESI (m/z) $[M+Na]^+$ calculated for $C_{19}H_{21}NNaO$, 302.1515; found: 302.1517.

(*E*)-1-phenyl-2-((*p*-tolylamino)methylene)hexan-1-one (**3va**)

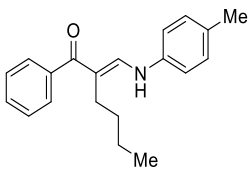

^{1}H NMR (499 MHz, DMSO-d_6) δ 8.94 (d, *J* = 13.2 Hz, 1H), 7.51 – 7.40 (m, 5H), 7.33 (d, *J* = 13.2 Hz, 1H), 7.04 (d, *J* = 8.2 Hz, 2H), 6.83 (d, *J* = 8.4 Hz, 2H), 2.49 (t, *J* = 7.3 Hz, 2H), 2.19 (s, 3H), 1.47 – 1.31 (m, 4H), 0.91 (t, *J* = 6.9 Hz, 3H); ^{13}C NMR (75 MHz, DMSO-d_6) δ 194.5, 144.8, 141.1, 139.3, 131.0, 129.9, 129.6, 128.0, 128.0, 115.9, 114.8, 30.4, 23.1, 22.2, 20.2, 14.1; HRMS-ESI (m/z) $[M+Na]^+$ calculated for $C_{20}H_{23}NNaO$, 316.1672; found: 316.1670.

(*E*)-1-phenyl-2-((*p*-tolylamino)methylene)heptan-1-one (**3wa**)

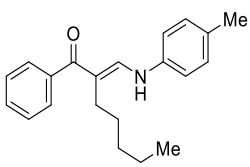

^{1}H NMR (499 MHz, DMSO-d_6) δ 8.94 (d, *J* = 13.2 Hz, 1H), 7.50 – 7.39 (m, 5H), 7.32 (d, *J* = 13.2 Hz, 1H), 7.05 (d, *J* = 8.3 Hz, 2H), 6.83 (d, *J* = 8.4 Hz, 2H), 2.47 (t, *J* = 7.6 Hz, 2H), 2.19 (s, 3H), 1.46 – 1.38 (m, 2H), 1.38 – 1.28 (m, 4H), 0.88 (t, *J* = 7.0 Hz, 3H); ^{13}C NMR (101 MHz, DMSO-d_6) δ 194.5, 144.8, 141.1, 139.3, 131.0, 129.9, 129.6, 128.0, 115.8, 114.8, 31.3, 27.8, 23.3, 22.3, 20.2, 14.1; HRMS-ESI (m/z) $[M+Na]^+$ calculated for $C_{21}H_{25}NNaO$, 330.1828; found: 330.1827.

3-Methyl-1-phenyl-2-((*p*-tolylamino)methylene)butan-1-one (**3xa**)

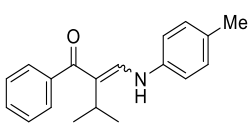

^{1}H NMR (499 MHz, DMSO-d_6) (*E*)-form (major): δ 8.91 (d, *J* = 13.2 Hz, 1H), 7.51 – 7.41 (m, 5H), 7.16 (d, *J* = 13.2 Hz, 1H), 7.03 (d, J = 8.2 Hz, 2H), 6.79 (d, *J* = 8.4 Hz, 2H), 3.19 – 3.05 (m, 1H), 2.18 (s, 3H), 1.28 (d, *J* = 6.9 Hz, 6H), (*Z*)-form (minor): δ 12.14 (d, *J* = 12.1 Hz, 1H), 7.68 (d, *J* = 12.1 Hz, 1H), 7.51 – 7.41 (m, 5H), 7.22 (d, *J* = 8.5 Hz, 2H), 7.15 (d, *J* = 8.3 Hz, 2H), 2.71 – 2.64 (m, 1H), 2.27 (s, 3H), 1.08 (d, *J* = 6.9 Hz, 6H); ^{13}C NMR (101

MHz, DMSO-d_6) δ 195.1, 144.0, 141.7, 139.4, 130.8, 129.9, 129.8, 128.2, 128.0, 118.8, 115.7, 25.1, 20.3, 20.2; HRMS-ESI (m/z) $[M+Na]^+$ calculated for $C_{19}H_{21}NNaO$, 302.1515; found: 302.1515.

(2*Z*,2'*Z*)-1,1'-(1,3-phenylene)bis(3-(*p*-tolylamino)prop-2-en-1-one) (**3ya**)

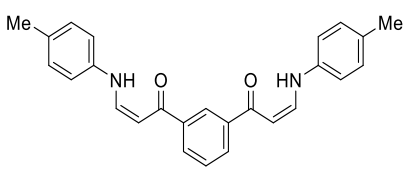

^{1}H NMR (499 MHz, $CDCl_3$) δ 12.18 (d, *J* = 12.4 Hz, 2H), 8.48 (t, *J* = 1.6 Hz, 1H), 8.07 (dd, *J* = 7.7, 1.8 Hz, 2H), 7.54 (t, *J* = 7.6 Hz, 1H), 7.53 (dd, *J* = 12.4, 7.7 Hz, 2H), 7.16 (d, *J* = 8.1 Hz, 4H), 7.03 (d, *J* = 8.4 Hz, 4H), 6.07 (d, *J* = 7.8 Hz, 2H), 2.33 (s, 6H); ^{13}C NMR (75 MHz, $CDCl_3$) δ 190.2, 145.8, 139.6, 137.9, 133.8, 130.4, 130.3, 128.8, 126.3, 116.6, 93.4, 20.9.; HRMS-ESI (m/z) $[M+Na]^+$ calculated for $C_{26}H_{24}N_2NaO_2$, 419.1730; found: 419.1732.

(2*Z*,2'*Z*)-1,1'-(pyridine-2,6-diyl)bis(3-(*p*-tolylamino)prop-2-en-1-one) (**3za**)

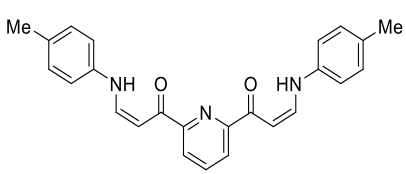

^{1}H NMR (499 MHz, $CDCl_3$) δ 12.18 (d, *J* = 12.4 Hz, 2H), 8.24 (d, *J* = 7.7 Hz, 2H), 7.98 (t, *J* = 7.7 Hz, 1H), 7.63 (dd, *J* = 12.4, 7.7 Hz, 2H), 7.17 (d, *J* = 7.9 Hz, 4H), 7.05 (d, *J* = 8.0 Hz, 4H), 6.87 (d, *J* = 7.7 Hz, 2H), 2.34 (s, 6H); ^{13}C NMR (75 MHz, CDCl3) δ 189.0, 154.3, 146.4, 138.0, 137.9, 133.9, 130.5, 123.6, 116.7, 93.0, 20.9; HRMS-ESI (m/z) $[M+Na]^+$ calculated for $C_{25}H_{23}N_3NaO_2$, 420.1682; found: 420.1684.

Diethyl 2-((*p*-tolylamino)methylene)malonate (**3Aa**)

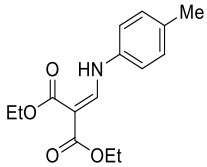

^{1}H NMR (499 MHz, $CDCl_3$) δ 10.97 (d, *J* = 13.7 Hz, 1H), 8.50 (d, *J* = 13.8 Hz, 1H), 7.17 (d, *J* = 8.1 Hz, 2H), 7.03 (d, *J* = 8.4 Hz, 2H), 4.30 (q, *J* = 7.1 Hz, 2H), 4.24 (q, *J* = 7.1 Hz, 2H), 2.33 (s, 3H), 1.38 (t, *J* = 7.1 Hz, 3H), 1.32 (t, *J* = 7.1 Hz, 3H). Identity confirmed by comparing with reported literature.[19]

(*Z*)-2-phenyl-3-(*p*-tolylamino)acrylonitrile (**3Ba**)

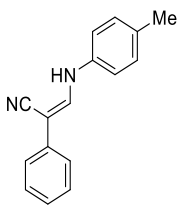

^{1}H NMR (499 MHz, DMSO-d_6) δ 9.61 (d, *J* = 12.9 Hz, 1H), 8.05 (d, J = 12.9 Hz, 1H), 7.50 (dd, *J* = 8.4, 1.1 Hz, 2H), 7.34 (t, *J* = 7.9 Hz, 2H), 7.28 (d, *J* = 8.5 Hz, 2H), 7.16 (t, *J* = 7.3 Hz, 1H), 7.11 (d, *J* = 8.2 Hz, 2H), 2.25 (s, 3H). Identity confirmed by comparing with reported literature.[4b]

(*Z*)-1-phenyl-3-(phenylamino)prop-2-en-1-one (**3ab**)

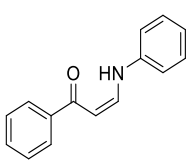

^{1}H NMR (400 MHz, $CDCl_3$) δ 12.15 (d, *J* = 10.8 Hz, 1H), 7.95 (d, *J* = 7.0 Hz, 2H), 7.56 – 7.44 (m, 4H), 7.35 (t, *J* = 7.8 Hz, 2H), 7.11 (d, *J* = 7.9 Hz, 2H), 7.08 (t, *J* = 7.4 Hz, 1H), 6.04 (d, *J* = 7.8 Hz, 1H). Identity confirmed by comparing with reported literature.[20]

(*Z*)-3-((4-methoxyphenyl)amino)-1-phenylprop-2-en-1-one (**3ac**)

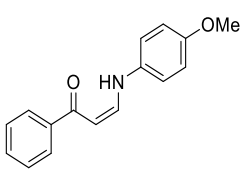

^{1}H NMR (499 MHz, $CDCl_3$) δ 12.20 (d, *J* = 11.9 Hz, 1H), 7.95 - 7.91 (m, 2H), 7.52 – 7.39 (m, 4H), 7.05 (d, *J* = 8.9 Hz, 2H), 6.89 (d, *J* = 8.9 Hz, 2H), 5.97 (d, *J* = 7.7 Hz, 1H), 3.79 (s, 3H). Identity confirmed by comparing with reported literature.[21]

(*Z*)-3-((4-chlorophenyl)amino)-1-phenylprop-2-en-1-one (**3ad**)

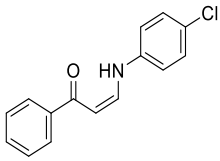

^{1}H NMR (499 MHz, $CDCl_3$) δ 12.14 (d, *J* = 11.6 Hz, 1H), 7.93 (d, *J* = 7.0 Hz, 2H), 7.54 – 7.42 (m, 4H), 7.31 (d, *J* = 8.9 Hz, 2H), 7.03 (d, *J* = 8.9 Hz, 2H), 6.05 (d, *J* = 7.9 Hz, 1H). Identity confirmed by comparing with reported literature.[21]

(*Z*)-3-((4-bromophenyl)amino)-1-phenylprop-2-en-1-one (**3ae**)

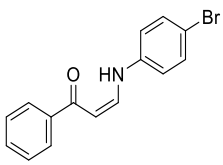

^{1}H NMR (400 MHz, $CDCl_3$) δ 12.13 (d, *J* = 11.5 Hz, 1H), 7.93 (d, *J* = 7.2 Hz, 2H), 7.55 – 7.40 (m, 6H), 6.98 (d, *J* = 8.7 Hz, 2H), 6.06 (d, *J* = 7.9 Hz, 1H); ^{13}C NMR (101 MHz, $CDCl_3$) δ 191.4, 144.5, 139.5, 139.1, 132.8, 131.9, 128.6, 127.5, 117.9, 116.3, 94.5; HRMS-ESI (m/z) $[M+Na]^+$ calculated for $C_{15}H_{12}BrNNaO$, 323.9994; found: 323.9991.

(*Z*)-3-((2-methoxyphenyl)amino)-1-phenylprop-2-en-1-one (**3af**)

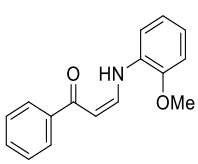

^{1}H NMR (400 MHz, $CDCl_3$) δ 12.22 (d, *J* = 11.4 Hz, 1H), 7.97 (d, *J* = 7.1 Hz, 2H), 7.54 (dd, *J* = 12.7, 7.9 Hz, 1H), 7.51 – 7.41 (m, 3H), 7.17 (d, *J* = 7.7 Hz, 1H), 7.03 (t, *J* = 7.7 Hz, 1H), 6.94 (dd, *J* = 12.9, 7.8 Hz, 2H), 6.06 (d, *J* = 7.8 Hz, 1H), 3.97 (s, 3H); ^{13}C NMR (101 MHz, CDCl3) δ 190.8, 148.6, 143.7 (d, *J* = 3.8 Hz), 139.5, 131.5, 129.9, 128.4, 127.5, 123.6, 121.1, 113.3, 111.2, 94.2 (d, *J* = 3.8 Hz), 56.0 (d, *J* = 4.9 Hz); HRMS-ESI (m/z) $[M+Na]^+$ calculated for $C_{16}H_{15}NNaO_2$, 276.0995; found: 276.0996.

(*Z*)-3-([1,1'-biphenyl]-2-ylamino)-1-phenylprop-2-en-1-one (**3ag**)

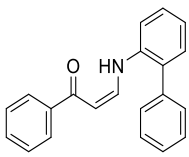

^{1}H NMR (400 MHz, $CDCl_3$) δ 12.03 (d, *J* = 10.9 Hz, 1H), 7.86 (d, *J* = 6.9 Hz, 2H), 7.61 – 7.31 (m, 11H), 7.28 (d, *J* = 8.1 Hz, 1H), 7.17 (t, *J* = 7.4 Hz, 1H), 5.97 (d, *J* = 7.9 Hz, 1H); ^{13}C NMR (101 MHz, CDCl3) δ 190.6, 144.9, 144.9, 139.4, 138.0, 137.9, 132.2, 131.4, 129.4, 129.2, 128.8, 128.3, 128.1, 127.4, 123.7, 115.3, 94.5; HRMS-ESI (m/z) $[M+Na]^+$ calculated for $C_{21}H_{17}NNaO$, 322.1202; found: 322.1203.

(*Z*)-1-phenyl-3-((4-vinylphenyl)amino)prop-2-en-1-one (**3ah**)

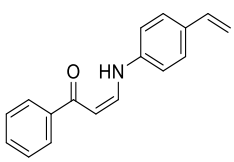

^{1}H NMR (499 MHz, $CDCl_3$) δ 12.19 (d, *J* = 11.9 Hz, 1H), 7.94 (d, *J* = 7.1 Hz, 2H), 7.55 – 7.43 (m, 4H), 7.39 (d, *J* = 8.5 Hz, 2H), 7.06 (d, *J* = 8.5 Hz, 2H), 6.67 (dd, *J* = 17.6, 10.9 Hz, 1H), 6.04 (d, *J* = 7.8 Hz, 1H), 5.68 (d, *J* = 17.6 Hz, 1H), 5.20 (d, *J* = 10.9 Hz, 1H); ^{13}C NMR (101 MHz, $CDCl_3$) δ 191.1, 144.6 (d, *J* = 3.7 Hz), 139.8, 139.3, 136.0, 133.4, 131.7, 128.6, 127.7, 127.4, 116.4, 113.0, 94.1 (d, *J* = 3.7 Hz); HRMS-ESI (m/z) $[M+Na]^+$ calculated for $C_{17}H_{15}NNaO$, 272.1046; found: 272.1048.

(*Z*)-3-((2-fluoro-4-methylphenyl)amino)-1-phenylprop-2-en-1-one (**3ai**)

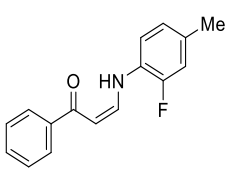

^{1}H NMR (400 MHz, CDCl3) δ 12.17 (d, *J* = 11.5 Hz, 1H), 7.95 (d, *J* = 7.1 Hz, 2H), 7.52 – 7.43 (m, 4H), 7.09 (t, *J* = 8.2 Hz, 1H), 6.94 (t, *J* = 11.0 Hz, 1H), 6.93 (s, 1H), 6.07 (d, *J* = 7.8 Hz, 1H), 2.31 (s, 3H); 13C NMR (101 MHz, CDCl3) δ 191.2, 152.4 (d, *J* = 245.7 Hz), 144.6, 139.2, 134.3 (d, *J* = 6.9 Hz), 131.7, 128.5, 127.5, 126.4 (d, *J* = 11.0 Hz), 125.4 (d, *J* = 3.3 Hz), 116.9 (d, *J* = 18.6 Hz), 115.6 (d, *J* = 1.4 Hz), 94.5, 20.9; ^{19}F NMR (376 MHz, $CDCl_3$) δ -130.9; HRMS-ESI (m/z) $[M+Na]^+$ calculated

for $C_{16}H_{14}FNNa$, 278.0952; found: 278.0951.

(*Z*)-3-(naphthalen-1-ylamino)-1-phenylprop-2-en-1-one (**3aj**)

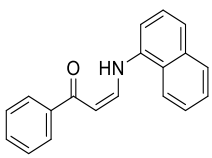

^{1}H NMR (499 MHz, $CDCl_3$) δ 13.08 (d, *J* = 11.0 Hz, 1H), 8.26 (d, *J* = 8.5 Hz, 1H), 8.01 (d, *J* = 6.8 Hz, 2H), 7.88 (d, *J* = 8.1 Hz, 1H), 7.74 (dd, *J* = 11.8, 7.7 Hz, 1H), 7.62 (t, *J* = 8.1 Hz, 2H), 7.56 (t, *J* = 7.5 Hz, 1H), 7.54 – 7.45 (m, 4H), 7.31 (d, *J* = 7.6 Hz, 1H), 6.18 (d, *J* = 7.7 Hz, 1H); ^{13}C NMR (101 MHz, $CDCl_3$) δ 191.5, 146.3, 146.3, 139.4, 136.6, 134.5, 131.8, 128.6, 127.5, 126.8, 126.8, 125.9, 125.0, 124.3, 121.2, 111.2, 94.8; HRMS-ESI (m/z) $[M+Na]^+$ calculated for $C_{19}H_{15}NNaO$, 296.1046; found: 296.1047.

2.5 References

(1) (a) Lygin, A. V.; de Meijere, A. *Angew. Chem., Int. Ed.* **2010**, *49*, 9094. (b) Sadjadi, S.; Heravi, M. M. *Tetrahedron* **2011**, *67*, 2707. (c) Tobisu, M.; Chatani, N. *Chem. Lett.* **2011**, *40*, 330. (d) Boyarskiy, V. P.; Bokach, N. A.; Luzyanin, K. V.; Kukushkin, V. Y. *Chem. Rev.* **2015**, *115*, 2698. (e) Nenajdenko, V. G. *Isocyanide Chemistry: Applications in Synthesis and Materials Science*; Wiley-VCH Verlag GmbH & Co. KGaA: Weinheim, 2012.

(2) (a) Vlaar, T.; Ruijter, E.; Maes, B. U.; Orru, R. V. *Angew. Chem., Int. Ed.* **2013**, *52*, 7084. (b) Qiu, G.; Ding, Q.; Wu, J. *Chem. Soc. Rev.* **2013**, *42*, 5257.

(3) (a) Ito, Y.; Inubushi, Y.; Saegusa, T. *Tetrahedron Lett.* **1974**, *15*, 1283. (b) Saegusa, T.; Ito, Y.; Kobayashi, S.; Hirota, K.; Yoshioka, H. *Tetrahedron Lett.* **1966**, *7*, 6121. (c) Saegusa, T.; Ito, Y.; Kobayashi, S.; Takeda, N.; Hirota, K. *Tetrahedron Lett.* **1967**, *8*, 1273. (d) Saegusa, T.; Murase, I.; Ito, Y. *Synth. Commun.* **1971**, *1*, 145. (e) Saegusa, T.; Ito, Y.; Kobayashi, S.; Hirota, K. *Tetrahedron Lett.* **1967**, *8*, 521.

(4) (a) Pooi, B.; Lee, J.; Choi, K.; Hirao, H.; Hong, S. H. *J. Org. Chem.* **2014**, *79*, 9231. (b) Kim, S.; Hong, S. H. *Adv. Synth. Catal.* **2015**, *357*, 1004.

(5) (a) Walborsky, H. M.; Niznik, G. E. *J. Am. Chem. Soc.* **1969**, *91*, 7778. (b) Niznik, G. E.; Morrison, W. H.; Walborsky, H. M. *J. Org. Chem.* **1974**, *39*, 600. (c) Murakami, M.; Ito, H.; Ito, Y. *J. Org. Chem.* **1988**, *53*, 4158.

(6) (a) Kobayashi, K.; Yoneda, K.; Mano, M.; Morikawa, O.; Konishi, H. *Chem. Lett.* **2003**, *32*, 76. (b) Kobayashi, K.; Iitsuka, D.; Fukamachi, S.; Konishi, H. *Tetrahedron* **2009**, *65*, 7523. (c) Zhao, J.; Peng, C.; Liu, L.; Wang, Y.; Zhu, Q. *J. Org. Chem.* **2010**, *75*, 7502. (d) Suginome, M.; Fukuda, T.; Ito, Y. *Org. Lett.* **1999**,

1, 1977. (e) Mitamura, T.; Nomoto, A.; Sonoda, M.; Ogawa, A. *Bull. Chem. Soc. Jpn.* **2010**, *83*, 822.

(7) (a) Hopkinson, M. N.; Richter, C.; Schedler, M.; Glorius, F. *Nature* **2014**, *510*, 485. (b) Bugaut, X.; Glorius, F. *Chem. Soc. Rev.* **2012**, *41*, 3511. (c) Enders, D.; Niemeier, O.; Henseler, A. *Chem. Rev.* **2007**, *107*, 5606. (d) Hirano, K.; Piel, I.; Glorius, F. *Chem. Lett.* **2011**, *40*, 786. (e) Flanigan, D. M.; Romanov-Michailidis, F.; White, N. A.; Rovis, T. *Chem. Rev.* **2015**, *115*, 9307.

(8) (a) Halleux, A. *Angew. Chem., Int. Ed.* **1964**, *3*, 752. (b) Ciganek, E. *J. Org. Chem.* **1970**, *35*, 862. (c) Hudnall, T. W.; Moorhead, E. J.; Gusev, D. G.; Bielawski, C. W. *J. Org. Chem.* **2010**, *75*, 2763. (d) Hudnall, T. W.; Tennyson, A. G.; Bielawski, C. W. *Organometallics* **2010**, *29*, 4569. (e) Martin, D.; Canac, Y.; Lavallo, V.; Bertrand, G. *J. Am. Chem. Soc.* **2014**, *136*, 5023.

(9) (a) Elassar, A.-Z. A.; El-Khair, A. A. *Tetrahedron* **2003**, *59*, 8463. (b) Negri, G.; Kascheres, C.; Kascheres, A. J. *J. Heterocycl. Chem.* **2004**, *41*, 461. (c) Greenhill, J. V. *Chem. Soc. Rev.* **1977**, *6*, 277. (d) Lue, P.; Greenhill, J. V. In *Adv. Heterocycl. Chem.*; Alan, R. K., Ed.; Academic Press: Cambridge, Massachusetts, 1996; Vol. 67, pp 207–343. (e) Seki, H.; Georg, G. I. *J. Am. Chem. Soc.* **2010**, *132*, 15512. (f) Koduri, N. D.; Scott, H.; Hileman, B.; Cox, J. D.; Coffin, M.; Glicksberg, L.; Hussaini, S. R. *Org. Lett.* **2012**, *14*, 440. (g) Xu, X.; Du, P.; Cheng, D.; Wang, H.; Li, X. *Chem. Commun.* **2012**, *48*, 1811. (h) Yu, D.; Sum, Y. N.; Ean, A. C. C.; Chin, M. P.; Zhang, Y. *Angew. Chem., Int. Ed.* **2013**, *52*, 5125. (i) Kang, Y.-W.; Cho, Y. J.; Han, S. J.; Jang, H.-Y. *Org. Lett.* **2016**, *18*, 272.

(10) Gilli, P.; Bertolasi, V.; Ferretti, V.; Gilli, G. *J. Am. Chem. Soc.* **2000**, *122*, 10405.

(11) (a) Miura, T.; Funakoshi, Y.; Morimoto, M.; Biyajima, T.; Murakami, M. *J. Am.*

Chem. Soc. **2012**, *134*, 17440. (b) Selander, N.; Worrell, B. T.; Fokin, V. V. *Angew. Chem., Int. Ed.* **2012**, *51*, 13054. (c) Sridharan, V.; Avendaño, C.; Menéndez, J. C. *Synlett* **2007**, 0881. (d) Khodaei, M. M.; Khosropour, A. R.; Kookhazadeh, M. *Synlett* **2004**, 1980. (e) Reddy, D. S.; Judd, W. R.; Aubé, J. *Org. Lett.* **2003**, *5*, 3899.

(12) (a) Zhuo, J.-C.; Schenk, K. *Helv. Chim. Acta* **1997**, *80*, 2137. (b) Zhuo, J.-C. *Magn. Reson. Chem.* **1998**, *36*, 565.

(13) (a) Abdulla, R. F.; Brinkmeyer, R. S. *Tetrahedron* **1979**, *35*, 1675. (b) Pleier, A.-K.; Glas, H.; Grosche, M.; Sirsch, P.; Thiel, W. R. *Synthesis* **2001**, 55.

(14) We tried to observe any interaction or reaction between IMes and **1a** in C_6D_6 via ^1H NMR at various temperatures, but no change was observed. Although deuterium incorporation on the α-position of 3-pentanone by IMes was reported in the previous GC-MS analysis, it was hard to observe the generation of significant amount of enolate anion directly from IMes and acetophenone in our experiments. See: E. M. Phillips, M. Riedrich, K. A. Scheidt, *J. Am. Chem. Soc.* **2010**, *132*, 13179.

(15) The pK_a value of acetophenone in DMSO is 24.7, whereas the calculated pK_a value of 1,3-bis(2,6-dimethylphenyl)imidazolium cation is ~17. See: (a) W. S. Matthews, J. E. Bares, J. E. Bartmess, F. G. Bordwell, F. J. Conforth, G. E. Drucker, Z. Margolin, R. J. McCallum, G. J. McCollum, N. R. Vanier, *J. Am. Chem. Soc.* **1975**, *97*, 7006; (b) A. M. Magill, K. J. Cavell, B. F. Yates, *J. Am. Chem. Soc.* **2004**, *126*, 8717.

(16) Reactions between stoichiometric amount of IMes and **2a** were monitored by ^1H NMR in benzene-d_6 and THF-d_8 respectively, but unidentificable broadened peaks were observed in both cases. We think that generated imidoyl intermediate could initiate oligomerization process, because fast conversion of **2a** was observed.

In the developed reaction, an appropriate pronucleophile, ketone in our reaction, could intercept reactive imidoyl intermediate and prevent the unwanted side reactions. For anion mediated oligomerization of isocyanide, see: (a) C. Grundmann, *Chem. Ber.* **1958**, *91*, 1380; (b) I. Ugi, U. Fetzer, *Chem. Ber.* **1961**, *94*, 2239; (c) M. A. Mironov, V. S. Mokrushin, *Mendeleev Commun.* **1998**, *8*, 242; (d) E. Iravani, B. Neumuller, *Organometallics* **2005**, *24*, 842.

(17) Arduengo, A. J.; Dias, H. V. R.; Harlow, R. L.; Kline, M. *J. Am. Chem. Soc.* **1992**, *114*, 5530.

(18) Katritzky, A. R.; Barcock, R. A.; Long, Q.-H.; Balsubramanian, M.; Malhotra, N.; Greenhill, J. V. *Synthesis* **1993**, 233.

(19) Heikkilä, T.; Ramsey, C.; Davies, M.; Galtier, C.; Stead, A. M. W.; Johnson, A. P.; Fishwick, C. W. G.; Boa, A. N.; McConkey, G. A. *J. Med. Chem.* **2007**, *50*, 186.

(20) Haak, E. *Eur. J. Org. Chem.* **2007**, 2815.

(21) Yang, J.; Wang, C.; Xie, X.; Li, H.; Li, Y. *Eur. J. Org. Chem.* **2010**, 4189.

Chapter 3. Dual Activation of Nucleophiles and Electrophiles by N-Heterocyclic Carbene Organocatalysis: Chemoselective N-Imination of Indoles with Isocyanides*

3.1 Introduction

Selective functionalization of indoles is one of the most actively pursued research areas in organic synthesis, due to its privileged structure in natural products, drugs, agrochemicals, and materials.[1] Especially, chemoselectivity control between C3- and N-positions of indole is a very important issue in the synthesis of functionalized indoles. Generally, either the starting indole or its coupling partner requires an activation step, which determines the chemoselectivity of the overall transformation. For example, direct alkylation of indole at C3-position can be achieved by using alkyl halides or alcohols activated by Lewis acids (Friedel-Crafts alkylation),[2] whereas direct N-alkylation can be performed with the deprotonated indole anion, such as indole sodium salt, which has an enhanced nucleophilicity at the nitrogen position (Scheme 3.1A).[3] Apart from alkylation, several other types of reactions such as vinylation,[3c,4] allylation,[5] acylation,[6] and carboxylation,[7] have also been developed to achieve selective introduction of functionality at the indole moiety, enhancing the diversity of synthetic pathways.

* The majority of this work has been published: Jungwon Kim and Soon Hyeok Hong*, *Org. Lett.* **2017**, 19, 3259.

The isocyanide functional group is versatile and has been utilized for the synthesis of many useful molecules.[8] Generally, isocyanides have been employed in metal-based activation strategies as an iminating reagent for coupling reactions with different types of nucleophiles.[9,10] Chatani et al. have demonstrated the first C3-imination of indoles by using a stoichiometric amount of $AlCl_3$ for activation of the isocyanide (Scheme 3.1B).[11] To the best of our knowledge, no practical approach towards the direct N-imination of indoles for the synthesis of indole-formamidines has been reported to date.[12] Initial trial reactions for N-imination of indole using indole anion species gave very low yields, which may be due to the low electrophilicity of isocyanide itself (Scheme 3.1B). Therefore, a new strategy for concurrent activation of the indole and the isocyanide is required. We envisioned that the use of N-heterocyclic carbene (NHC) as an organocatalyst would have a chance to induce a new reaction pathway for the selective N-imination reaction of indole. NHC has been widely applied in several types of organocatalysis, including nucleophilic catalysis for the activation of carbonyl compounds and base catalysis for the activation of nucleophiles.[13] Recently, an activation strategy to enhance the basicity of the terminal carbon of isocyanides was developed by introducing NHC organocatalysis.[14] On the basis of the result, it was envisioned that the NHC organocatalyst can generate the basic imidoyl intermediate, which can further activate the indole substrate via deprotonation. Thus, an activated nucleophile (indole anion) and an activated electrophile (imine-azolium) can be produced together, which can be coupled to produce indole-based formamidines (Scheme 3.1C).[15]

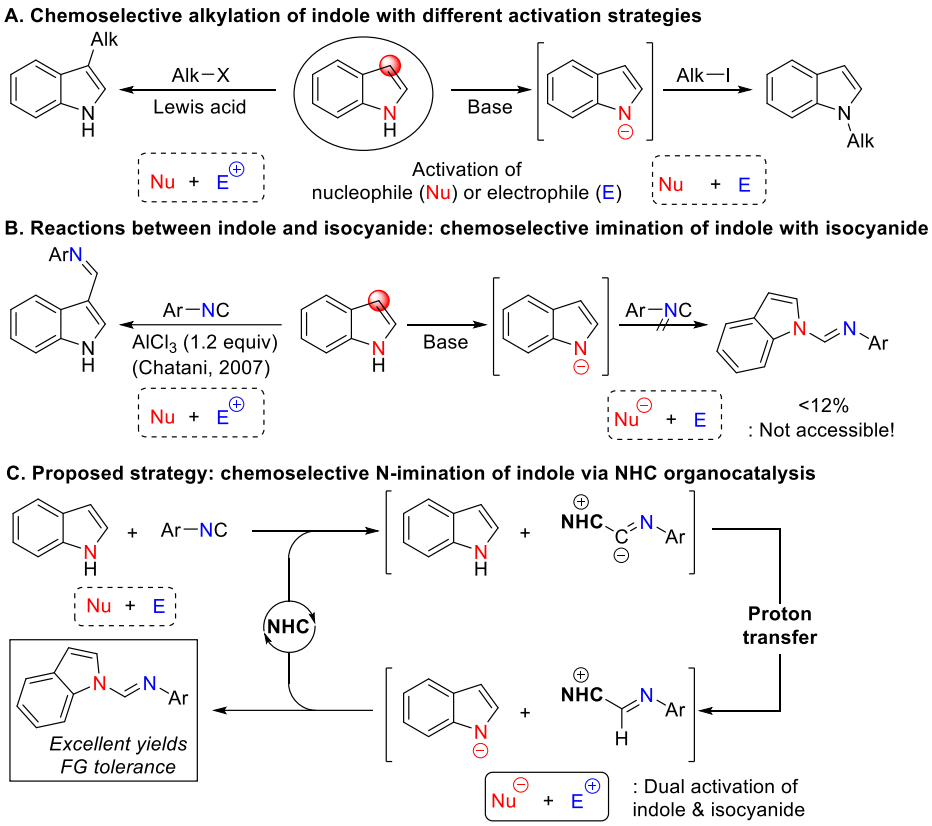

Scheme 3.1 Chemoselective functionalization of indole

3.2 Result and discussion

3.2.1 Optimization

To check the viability of our proposed approach for N-imination of indoles, the reaction of indole (**1a**) with 4-methylphenyl isocyanide (**2a**) was investigated. After an extensive screening process with the model substrates, we found the reaction conditions which gave desired product in 85% yields. With this result, further variations of reaction conditions from the standard conditions were evaluated to check effect of each component of the reaction (Table 3.1). Among several NHC precursors tested, a triazolium salt **3a** containing electron-deficient aryl group gave the highest yield (entries 1-4). Choice of a base and a solvent was also crucial to get high yields of the desired product (entries 5-10). Omission of an NHC salt from reaction conditions showed dramatic decrease of yield (20%), suggesting the role of **3a** as an organocatalyst (entry 11). The use of catalytic amount of a base for the generation of free NHC did not significantly drop the reactivity (entry 12). This clearly supports that deprotonation of indole could be performed by in situ generated imidoyl anion via proton abstraction process in a catalytic manner. Notably, no C3-iminated product was observed for all entries. Thus, NHC-based organocatalytic dual activation of neutral indole (**1a**) and isocyanide (**2a**) enabled the coupling process under mild reaction conditions (at 28 °C) without the use of a stoichiometric amount of an activator.

Table 3.1 Variations of reaction conditions[a]

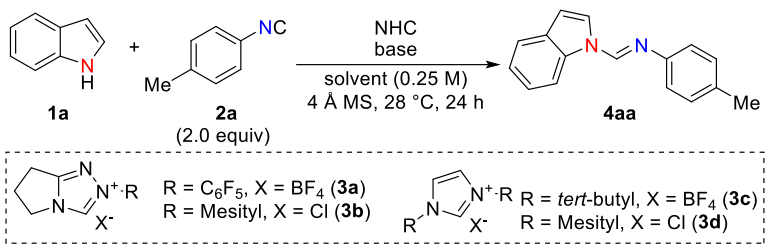

entry	NHC (mol%)	Base (mol%)	Solvent	Yield (%)[b]
1	**3a** (20)	NaO*t*Bu (130)	1,4-Dioxane	85
2	**3b** (20)	NaO*t*Bu (130)	1,4-Dioxane	48
3	**3c** (20)	NaO*t*Bu (130)	1,4-Dioxane	43
4	**3d** (20)	NaO*t*Bu (130)	1,4-Dioxane	31
5	**3a** (20)	KO*t*Bu (130)	1,4-Dioxane	45
6	**3a** (20)	NaH (130)	1,4-Dioxane	43
7	**3a** (20)	DIPEA (130)	1,4-Dioxane	trace
8	**3a** (20)	NaO*t*Bu (130)	THF	61
9	**3a** (20)	NaO*t*Bu (130)	Toluene	10
10	**3a** (20)	NaO*t*Bu (130)	CH_3CN	26
11	None	NaO*t*Bu (130)	1,4-Dioxane	20
12[c]	**3a** (20)	NaO*t*Bu (30)	1,4-Dioxane	83

[a]Reaction conditions: **1a** (0.2 mmol), **2a** (0.4 mmol), NHC salt, 4 Å MS, base and solvent (0.8 mL) for 24 h at 28 °C, including 5 min. induction period. [b]Yields were determined by GC using mesitylene as an internal standard. [c]Without 4 Å MS. THF = tetrahydrofuran.

3.2.2 Substrate scope evaluation

Under the optimized conditions, the substrate scope for the reaction was evaluated (Table 3.2). Phenyl isocyanide (**2b**) gave an excellent yield of the corresponding formamidine (**4ab**). Gratifyingly, the halide-containing isocyanides (**2c**–**2f**, **2l**) were all tolerated and produced halogenated formamidines in excellent yields (**4ac**–**4af**, **4al**). Other electron-withdrawing groups such as—cyanide (**4ag**), ester (**4ah**), and sulfone (**4ai**)—present in isocyanides also tolerable and showed excellent yields of the formamidines, illustrating the advantages of the mild reaction conditions. Furthermore, scale-up of the reaction with isocyanide **2i** proceeded smoothly, showing the practicality of the developed reaction conditions. In contrast, an introduction of electron-donating group on the isocyanide resulted in a decreased yield of the formamidine even when excess amount of a base was used (**4ak**). *ortho*-Substituted isocyanides also showed good to excellent reactivity, despite their increased steric hindrance (**4al** and **4am**). 4-Styryl isocyanide (**2j**) and 3-pyridyl isocyanide (**2n**) gave corresponding formamidines (**4aj** and **4an**) in high yields. However, several reaction attempts with alkyl isocyanides were not successful for the synthesis of corresponding formamidines, presumably due to the low electrophilicity of alkyl isocyanides.[14] Reactions with substituted indoles proceeded smoothly under the mild reaction conditions, regardless of the position of substituents. Indoles containing electron-donating groups, such as methyl (**1b**) and alkoxy (**1d**–**1f**), gave excellent yields of corresponding formamidines, whereas relatively electron-deficient indoles (**1c** and **1g**) required an excess amount of the base to afford moderate yields of formamidines (**4ca** and **4ga**). The use of more electron-deficient indole, such as 5-nitroindole, was not successful, showing no

reactivity under the optimized conditions. Substitution on the C2-/C3-positions of indole, which can affect the steric environment of the reactive center, was also tolerated and corresponding products (**4ha** and **4ia**) were obtained. Other nitrogen-heterocycles, such as carbazole (**1j**) and pyrrole (**1k**), gave the desired products in good to excellent yields (**4ja** and **4ka**). The scalability of the reaction was further confirmed with a gram-scale reaction with isocyanide **2f**, and formamidine **4af** was obtained in 98% yield.

Table 3.2 Substrate scope[a]

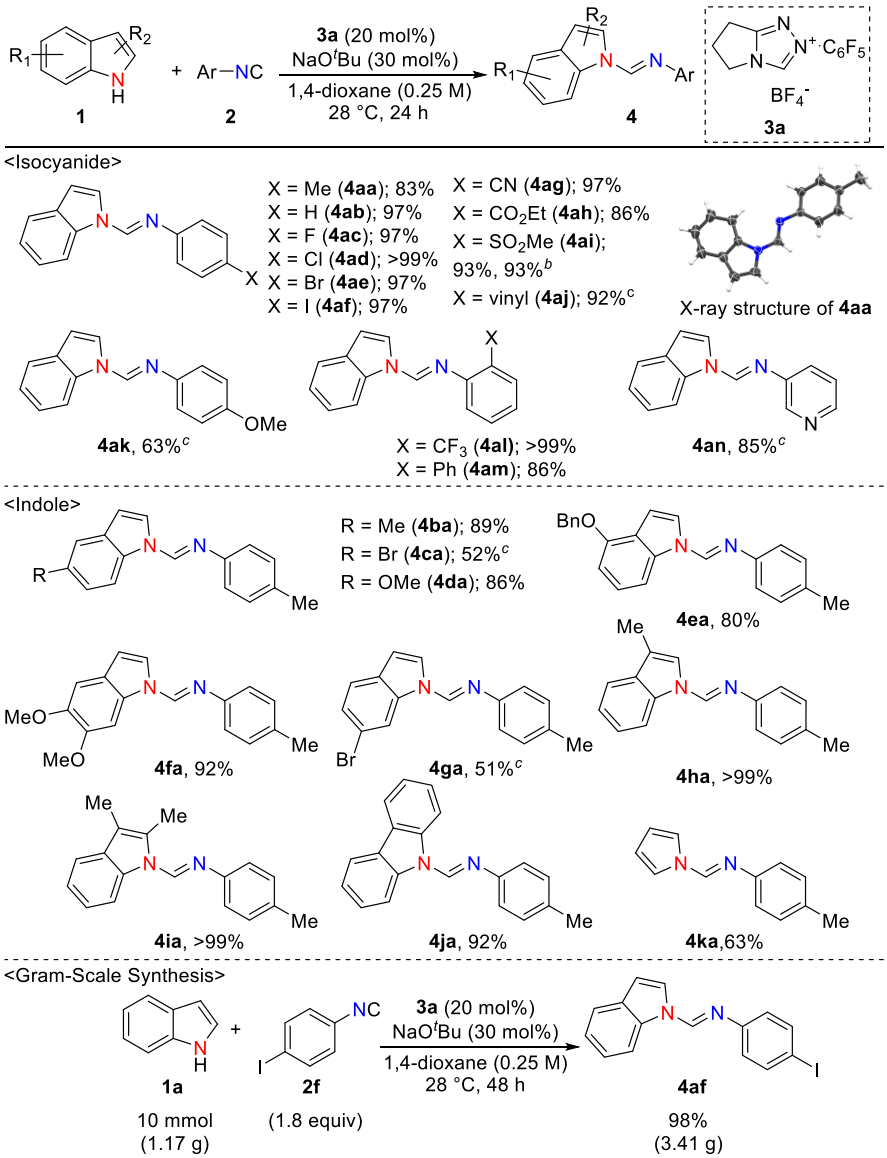

[a]Reaction conditions: **1** (0.2 mmol), **2** (0.4 mmol), **3a** (0.04 mmol), NaO*t*Bu (0.06 mmol) and 1,4-dioxane (0.8 mL) for 24 h at 28 °C, including 5 min. induction period. All yields are isolated yields. [b]**1a** (0.6 mmol), **2i** (1.2 mmol), **3a** (0.12 mmol), NaO*t*Bu (0.18 mmol) and 1,4-dioxane (2.4 mL) for 24 h at 28 °C. [c]1.3 equivalence of NaO*t*Bu & 4 Å MS.

3.2.3 Mechanistic investigation

To get detailed insight on the reaction, comparisons with previously reported strategies were conducted (Scheme 3.2). First, reactions of isocyanide with deprotonated indole species using a strong base were tested (Scheme 3.2A). Among several attempts, a stepwise reaction with sodium hydride (NaH) afforded formamidine **4aa** in less than 12% yield, which proves that the use of unactivated isocyanide as an electrophile is not effective for the imination of indole. Next, several reported strategies for the activation of isocyanides into electrophilic intermediates were investigated (Scheme 3.2B). Cu-based catalytic systems which can generate an electrophilic isocyanide analogue such as Cu-bound isocyanide (intermediate A)[10a] or formimidate (intermediate B)[16] have been previously developed. However, the reported reaction conditions for the synthesis of formamidine from indole were not as efficient as those discussed in this work. Based on the knowledge that a non-activated isocyanide cannot react with the indole anion efficiently (Scheme 3.2A), these observations clearly suggest that the dual activation of indole and isocyanide substrates via NHC organocatalysis is essential for the coupling reaction.

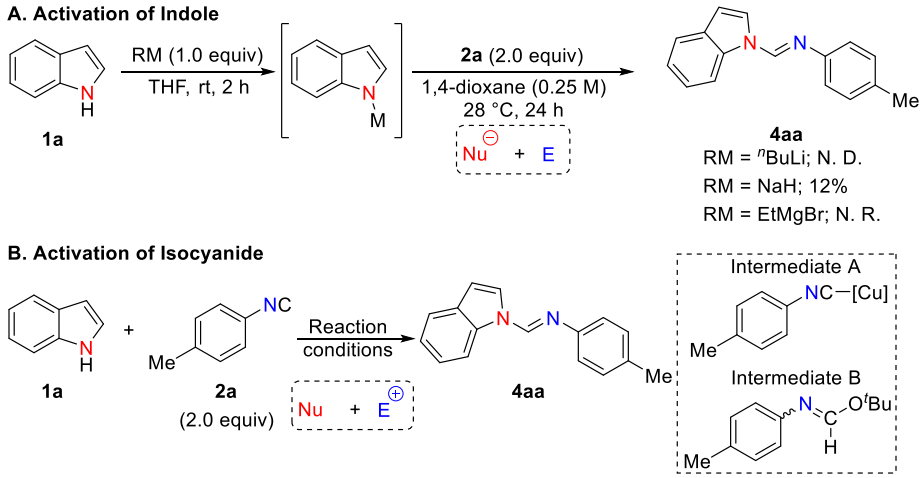

entry	Reaction conditions	Intermediate	Yield
1	CuCl (10 mol%), THF (0.5 M), reflux, 24 h	A	Trace
2	CuCl (20 mol%), NaH (1.0 equiv) 1,4-dioxane (0.25 M), 28 °C, 24 h	A	42%
3	CuI (5 mol%), KO^{t}Bu (1.2 equiv), DME (0.5M), 55 °C, 24 h	B	10%
4	CuI (20 mol%), KO^{t}Bu (1.2 equiv), DME (0.5 M), 28 °C, 24 h	B	44%

Scheme 3.2 Previous activation strategies

The involvement of indole anion is further supported by the correlation between reaction parameters and the yield of formamidines (Scheme 3.3). First, it was observed that the yields of the formamidines obtained from indole (**1a**), carbazole (**1j**) and pyrrole (**1k**) are found to increase as the acidity of NH-proton increases, and benzylamine did not show any reactivity at all (Scheme 3.3A). Those observations indicate that the proton transfer process from the nucleophile to the isocyanide is necessary to generate the deprotonated nucleophilic species and the electrophilic imine-azolium intermediate.[17] Moreover, a higher yield was observed when oxygen-containing solvents were used during the optimization of the reaction conditions (Scheme 3.3B). This could be related to dissociation of indole anion with solvation of counter cation (Na^+). The generation of the naked anionic species might be necessary to perform the desired transformation of indoles under our reaction conditions.[3a,3b,18] To further test this hypothesis, several indole anion salts were prepared and used for the synthesis of formamidine **4ab**. It was previously known that the use of indole anion salts (potassium or sodium salts of indole) that dissociate easily result in N-selectivity, whereas the use of magnesium[19] or zinc[20] salts exhibits C3-selectivity, due to the high degree of covalent character in the N–M bond.[18a,21] In the reaction of the indole anion salt with readily available ethyl *N*-phenylformimidate (**5**), an activated analogue of isocyanide, different reaction yields were obtained depending on the counter cations of the indole salts (Scheme 3.3C). In the case of reactions with a more ionic salt (**1a'-Na** or **1a'-Li**), a higher degree of reactivity was observed. In contrast, the reaction with a more covalent salt (**1a'-MgBr**) exhibited significantly decreased yield. These results strongly indicate the involvement of naked indole anion in the reaction system.

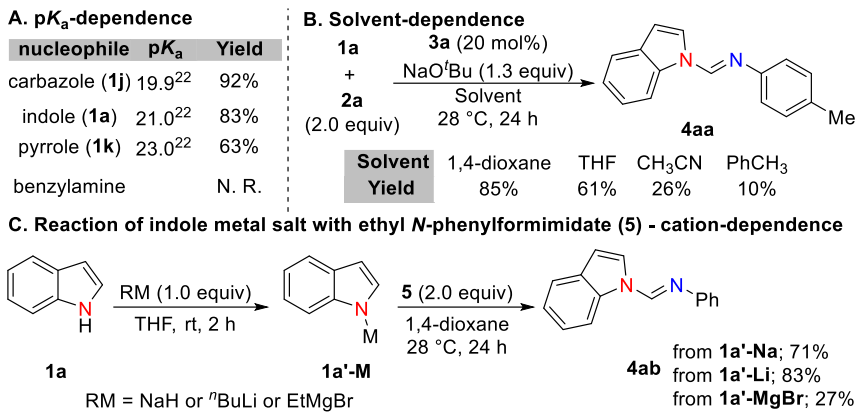

Scheme 3.3 Evidence of the involvement of indole anion[22]

Based on the aforementioned experimental results, a plausible mechanism was proposed (Scheme 3.4). After the imidoyl intermediate (**Int B**) is produced from NHC catalyst and isocyanide, deprotonation of acidic proton of indole, the activated nucleophile (indole-N^-) and electrophile (**Int C**) can be generated simultaneously, and the subsequent coupling reaction produces the desired formamidine.[14,17] Besides the stepwise process (red arrow), a concerted mechanism (blue arrow), based on the reported interaction between acidic proton and NHC, is also possible (**Int A**).[23] However, the direct insertion of isocyanide into N–H bond would not be favorable due to the innate low electrophilicity of isocyanide (Scheme 3.2A). Therefore, a concerted addition/deprotonation for the generation of **Int C** is proposed to be more plausible under our reaction conditions. The involvement of in situ generated *t*BuOH as a proton source[23c] is also less likely, due to relatively big difference in pK_a values between *t*BuOH (32.2 in DMSO)[24] and indole (21.0 in DMSO).[22] Additionally, reactions with *t*BuOD as an additive showed rather low yield and limited deuterium incorporation ratio, even in the existence of excess *t*BuOD, supporting the exclusion of *t*BuOH as the proton source. Participation of formimidate as an alternative electrophile is also not plausible, based on the trials for the detection of formimidate intermediates. As previously reported,[14] attempts to observe **Int B** or **Int C** with various experimental approaches were unsuccessful, presumably due to transient nature of the proposed intermediates.[17,25] Although those results provided the challenges for the detailed elucidation of the catalytic cycle, the involvement of imidoyl intermediate (**Int B**)[25] and imine-azolium intermediate (**Int C**)[17] would be the most plausible scenario in our catalytic cycle, based on the previous literature studies[10,14,17,23,25] and discussed mechanistic aspects of the reaction.

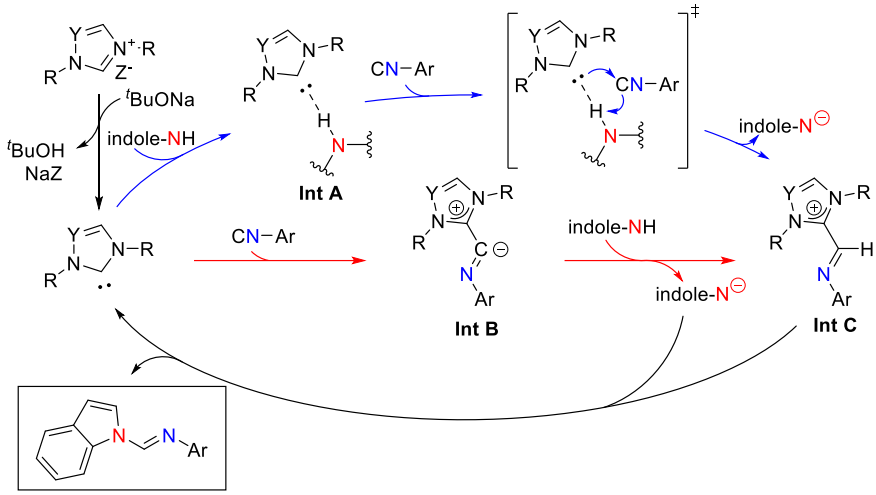

Scheme 3.4 Proposed mechanism

3.3 Conclusion

To conclude, the first chemoselective N-imination of indoles with aryl isocyanides for the synthesis of formamidines was successfully achieved via NHC-catalyzed concurrent activation of both nucleophile and electrophile substrates. Several new indole-based formamidines were obtained in high degree of reactivity and wide substrate scope under mild reaction conditions.

3.4 Experimental section

3.4.1 General information

Unless otherwise stated, all reactions were performed in an argon filled glove box. All anhydrous solvents were purchased from commercial suppliers and degassed with dry argon before use. NMR spectra were recorded in $CDCl_3$ or THF-d_8, and its residual solvent signal was used as a reference. Chemical shifts are reported in ppm and coupling constants in Hz. Multiplicity is indicated by one or more of the following: s (singlet), d (doublet), t (triplet), q (quartet), m (multiplet). All reagents, unless otherwise noted, were purchased from commercial suppliers and used as received without further purification. All of the starting indoles, isocyanide **2k**, and formimidate **5** were purchased from commercial sources and used without further purification. Previously reported isocyanides (**2a**, **2b**, **2c**, **2d**, **2e**, **2g**, **2h**, **2j**, **2l**, **2m**, **2n**, and **2o**) were prepared from their corresponding amines according to literature,[16a] and the identify was confirmed by comparing with reported data. New isocyanides (**2f** and **2i**) were synthesized by a previously reported method, and their structures were confirmed by spectroscopic analysis.[16a] All formamidine products were purified by silica gel flash column chromatography (1% triethylamine in diethyl ether/hexane or ethyl acetate/hexane).

3.4.2 Initial experiment of formamidine 4aa synthesis

1a (23.4 mg, 0.2 mmol), iPrHBF$_4$ (9.6 mg, 0.04 mmol), potassium *tert*-butoxide (29.2 mg, 0.26 mmol), 4 Å molecular sieves (10 mg), and THF (0.4 mL) were charged in a 4 mL reaction vial under argon atmosphere. The vial was then sealed with a Teflon lined septum and the solution was allowed to stir for 5 min. at 28 °C. **2a** (26.7 µL, 0.22 mmol) and THF (0.4 mL) were added quickly via a gas-tight syringe, and the solution was allowed to stir for 24 h at 28 °C. After the reaction was complete, all volatiles were removed in vacuo and the remaining residue was purified by silica gel flash column chromatography (diethyl ether/hexane, 1:9) to afford formamidine **4aa** as a light brown solid (8.0 mg, 17%).

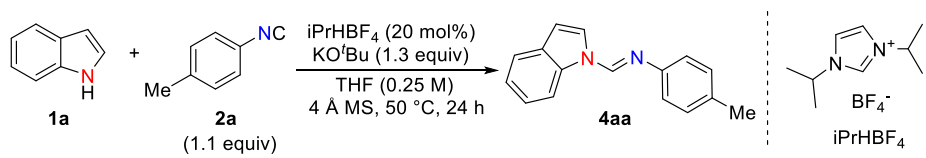

1a 2a (1.1 equiv) 4aa iPrHBF$_4$

Scheme 3.5 Synthesis of formamidine **4aa** with **1a** and **2a** using NHC organocatalyst

3.4.3 Characterization of formamidine 4aa

3.4.3.1 Crystallographic data

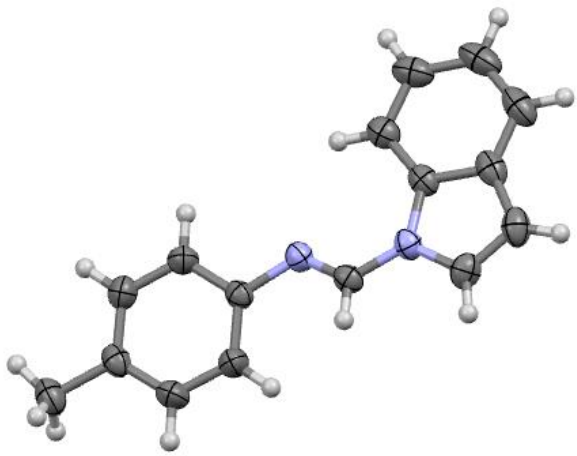

Figure 3.1 Solid state structure of **4aa** at 50 % probability ellipsoids

Single crystals of **4aa** were obtained by vapor diffusion of cyclooctane into the saturated THF solution of **4aa**, and one of them was chosen for X-ray diffraction analysis.

Table 3.3 Crystal data and structure refinement for **4aa**

CCDC number	1527016
Empirical formula	$C_{16}H_{14}N_2$
Formula weight	234.29
Temperature/K	223.15
Crystal system	monoclinic
Space group	$P2_1/c$

a/Å	11.3407(15)
b/Å	9.2307(14)
c/Å	12.6634(17)
α/°	90
β/°	109.296(6)
γ/°	90
Volume/Å^3	1251.2(3)
Z	4
ρ_{calc}g/cm^3	1.244
μ/mm^{-1}	0.074
F(000)	496.0
Crystal size/mm^3	0.16 × 0.11 × 0.05
Radiation	MoKα (λ = 0.71073)
2Θ range for data collection/°	5.576 to 56.984
Index ranges	-15 ≤ h ≤ 15, -12 ≤ k ≤ 12, -16 ≤ l ≤ 16
Reflections collected	34491
Independent reflections	3136 [R_{int} = 0.0778, R_{sigma} = 0.0349]
Data/restraints/parameters	3136/0/164
Goodness-of-fit on F^2	1.038
Final R indexes [I>=2σ (I)]	R_1 = 0.0502, wR_2 = 0.1103
Final R indexes [all data]	R_1 = 0.0978, wR_2 = 0.1309
Largest diff. peak/hole / e Å^{-3}	0.20/-0.19

3.4.3.2 2D-ROESY spectra

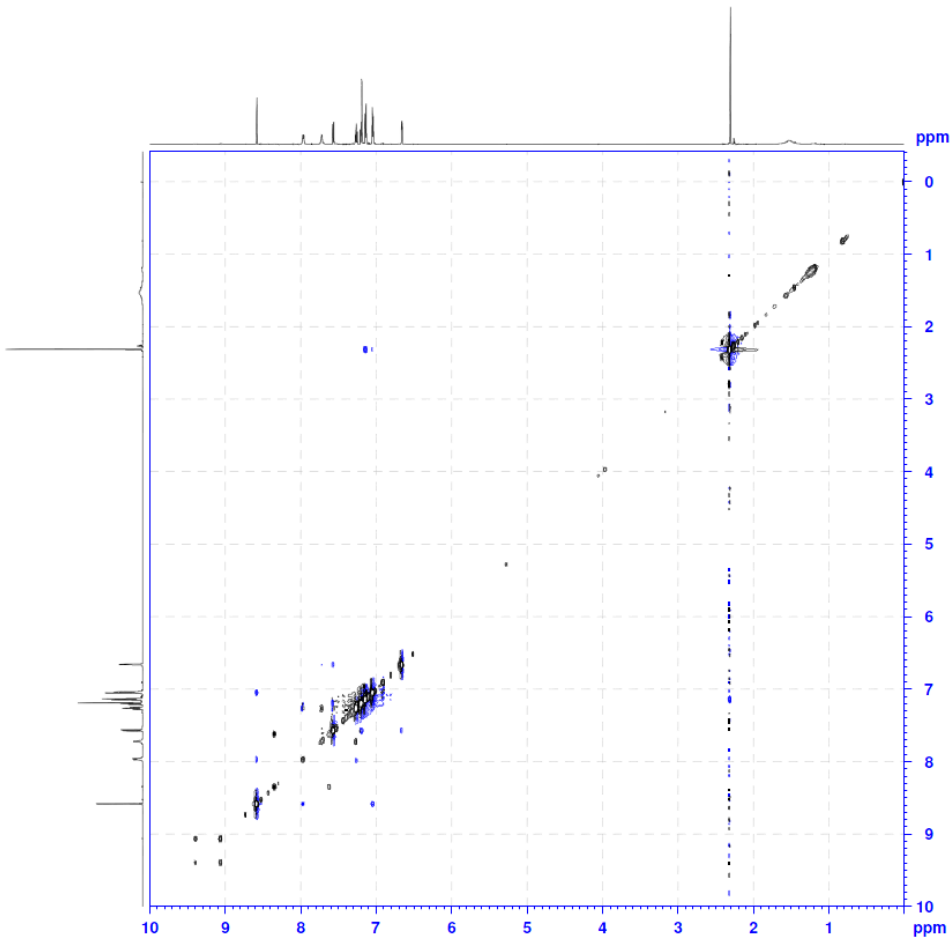

Figure 3.2 2D-ROESY spectrum for **4aa** ($CDCl_3$, 600 MHz)

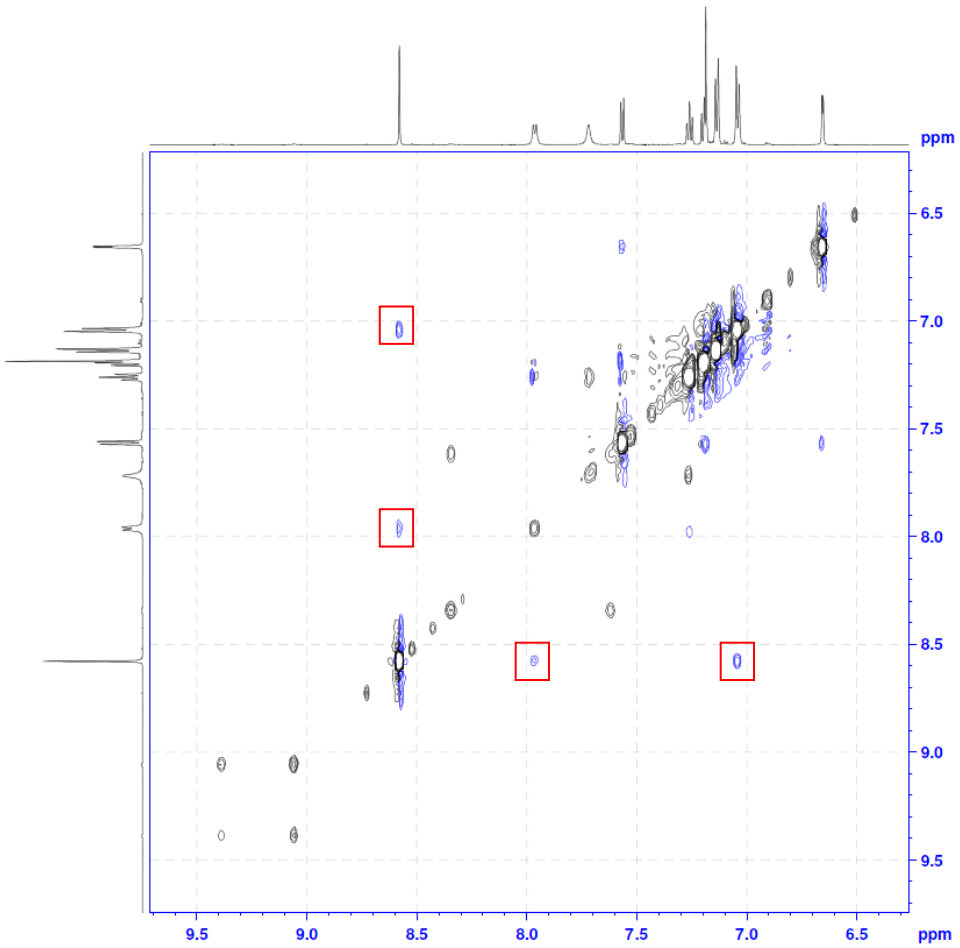

Figure 3.3 2D-ROESY spectrum for **4aa** ($CDCl_3$, 600 MHz, 6.0 - 10.0 ppm)

2D-ROESY correlation of **4aa** in $CDCl_3$ indicated that a different rotamer is favored in the solution, when compared to that of solid-state structure of **4aa**.

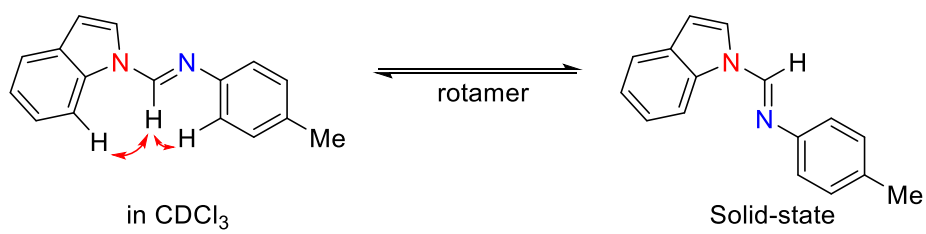

Scheme 3.6 Different conformation of **4aa** in solution and solid state

3.4.4 Optimization Tables

Table 3.4 Effect of different solvents on the yield of **4aa**

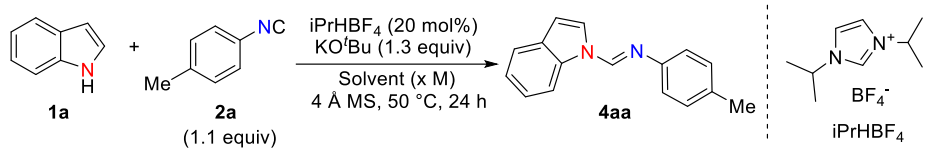

entry	Solvent	x	Yield 4aa (%)
1	THF	0.25	8
2	Toluene	0.25	10
3	*p*-xylene	0.25	11
4	*o*-xylene	0.25	15
5	CH_3CN	0.25	Trace
6	**1,4-Dioxane**	**0.25**	**17**
7	1,4-Dioxane	0.125	14
8	1,4-Dioxane	0.4	11

Table 3.5 Effect of different bases on the yield of **4aa**

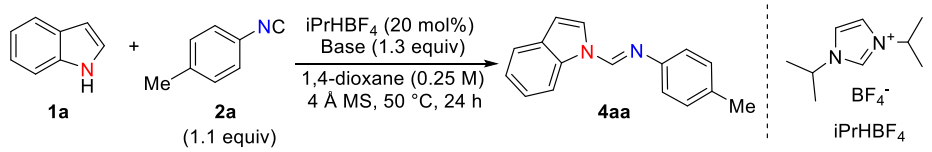

entry	Base	Yield 4aa (%)
1	KO*t*Bu	17
2	**NaO*t*Bu**	**41**
3	NaOMe	27
4	KO*t*Pent	5
5	NaO*t*Pent	31
6	NaH	15

Table 3.6 Effect of different NHC organocatalysts on the yield of **4aa**

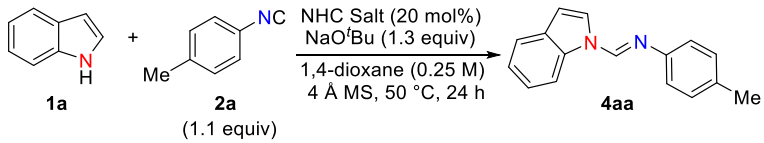

1a + **2a** (1.1 equiv) → **4aa**

entry	NHC Salt	R, X	Yield 4aa (%)
1	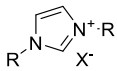	R = isopropyl, X = BF_4	41
2		R = isopropyl, X = Br	36
3		R = cyclohexyl, X = BF_4	27
4		R = cyclohexyl, X = Cl	31
5		R = methyl, X = I	38
6		R = *tert*-butyl, X = BF_4 (**3c**)	55
7		R = 1-adamantyl, X = BF_4	53
8	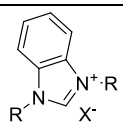	R = methyl, X = I	54
9		R = 1-adamantyl, X = Cl	46
10		R = cyclohexyl, X = Cl	48
11	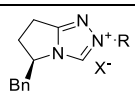	R = (4-trifluoromethyl)phenyl, X = BF_4	55
12	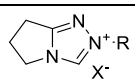	**R = pentafluorophenyl, X = BF_4 (3a)**	**66**
13		R = 1,3,5-trimethylphenyl, X = Cl (**3b**)	47
14	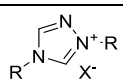	R = methyl, X = I	35

Table 3.7 Effect of varying amounts of isocyanide **2a** and NHC organocatalyst **3a** under different temperature

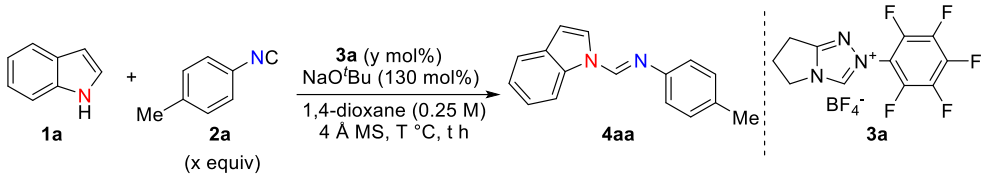

entry	x	y	T	t	Yield 4aa (%)
1	1.1	20	50	24	66
2	1.5	20	50	24	73
3	2.0	20	50	24	83
4	2.0	20	50	12	65
5	2.0	20	23	24	81
6	2.0	20	23	36	77
7	**2.0**	**20**	**28**	**24**	**85**
8	2.0	15	28	24	65

3.4.5 Experimental procedure for the synthesis of 4aa via indole anion

1a (0.5 mmol, 58.6 mg) and NaH (0.5 mmol, 12 mg) were charged in a 10 mL Schlenk tube under argon atmosphere, which was then sealed with a rubber septum. After an argon filled balloon was attached to the Schlenk tube, THF (2 mL) was slowly added to the mixture, and the solution was stirred for 2 h at room temperature.[26] After removing all volatiles via manifold vacuum line, **2a** (120 µL, 1.0 mmol) and 1,4-dioxane (2 mL) were added in the tube under a flow of argon. The solution was stirred for 24 h at 28 °C. After cooling to room temperature, the reaction mixture was diluted with ethyl acetate (20 mL), washed with brine (2 x 20 mL), dried with $MgSO_4$, filtered and concentrated in vacuo. The crude mixture was analyzed by ^1H NMR spectroscopy using mesitylene as an internal standard. Although the reaction with NaH gives 12% NMR yield of **4aa**, reactions using *n*BuLi (1.6 M in hexane, 313 µL, 0.5 mmol) or EtMgBr (1.0 M in THF, 500 µL, 0.5 mmol) either did not proceed or gave unidentifiable oligomers of **2a**.

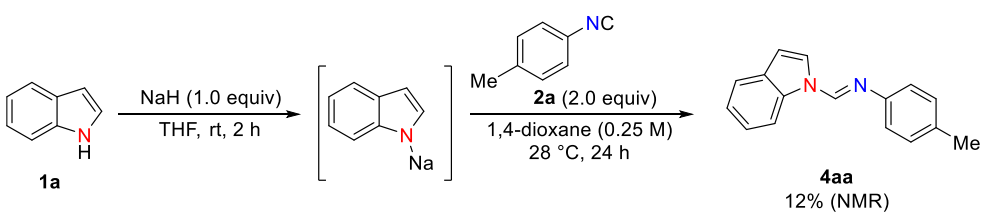

Scheme 3.7 Synthesis of formamidine **4aa** from in situ generated indole anion and **2a**

3.4.6 Experimental procedures for the control experiments

In a 4 mL reaction vial, **1a** (23.4 mg, 0.2 mmol) and indicated amounts of the catalysts, base, and solvent were charged under argon atmosphere. The vial was then sealed with a Teflon lined septum, and **2a** (49 µL) was added quickly via a gas-tight syringe. The reaction mixture was allowed to stir at indicated temperature for 24 h. After the reaction was complete, all volatiles were removed in vacuo, and the residue was further analyzed by GC using mesitylene as an internal standard.

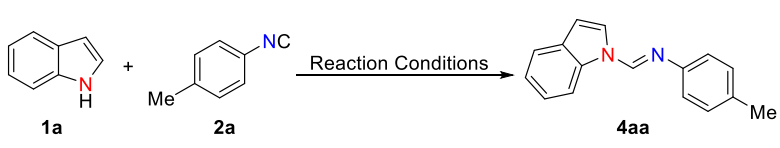

Scheme 3.8 Synthesis of formamidine **4aa** using previously reported strategies for isocyanide activation

1a (0.5 mmol, 58.6mg) and NaH (0.5 mmol, 12 mg) were charged in a 10 mL Schlenk tube under argon atmosphere, and the tube was then sealed with rubber septum. After an argon balloon was attached to the Schlenk tube, THF (2 mL) was slowly added to the mixture, and the solution was stirred for 2 h at room temperature.[26] After removing all volatiles via manifold vacuum line, ethyl *N*-phenylformimidate (**5**) (74.2 µL, 1.0 mmol) and 1,4-dioxane (2 mL) were added in the tube under argon flow, and the solution was stirred for 24 h at 28 °C. After cooling to room temperature, the reaction mixture was diluted with ethyl acetate (20 mL), washed with brine (2 × 20 mL), dried with $MgSO_4$, filtered and concentrated in vacuo. The crude mixture was analyzed by ^1H NMR spectroscopy using mesitylene as an internal standard. The reaction using NaH gave 71% NMR yield of **4ab**, and the reaction using with *n*BuLi (1.6 M in hexane, 313 µL, 0.5 mmol) or EtMgBr (1.0 M in THF, 500 µL, 0.5 mmol) gave 83% and 27% NMR yield of **4ab**, respectively.

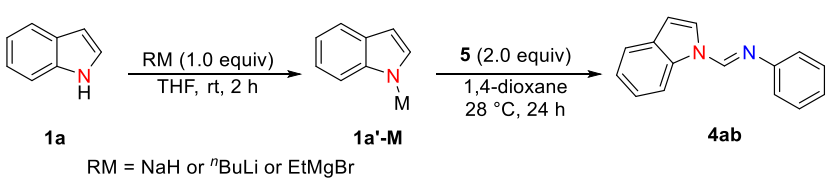

Scheme 3.9 Synthesis of formamidine 4ab from in situ generated indole anion and formimidate (**5**)

3.4.7 Experimental procedures for deuterium incorporation experiments

Indole (**1a**, 23.4 mg, 0.2 mmol), **3a** (14.5 mg, 0.04 mmol), sodium *tert*-butoxide (5.8 mg, 0.06 mmol), and 1,4-dioxane (0.4 mL) were charged in a 4 mL reaction vial under argon atmosphere. The vial was then sealed with a Teflon-lined septum and the solution was allowed to stir for 5 min at 28 °C. 4-Methylphenyl isocyanide (**2a**, 48.3 μL, 0.4 mmol), *t*BuOD (19.4 μL, 0.2 mmol), and 1,4-dioxane (0.4 mL) were added quickly via a gas tight syringe, and the solution was allowed to stir for 24 h at 28 °C. After the reaction was complete, the reaction mixture was diluted with ethyl acetate (1.2 mL) and directly injected into the silica gel flash column chromatography (1% triethylamine in diethyl ether/hexane, 1:9) to afford the formamidine **4aa** in 73% yield. 29% deuteration on the C8-position of **4aa** was observed via ^{1}H NMR spectroscopy. When 1.0 mmol of *t*BuOD (97 μL) was used in the reaction, 46% of **4aa** was isolated, and 69% deuteration on the C8-position of **4aa** was observed.

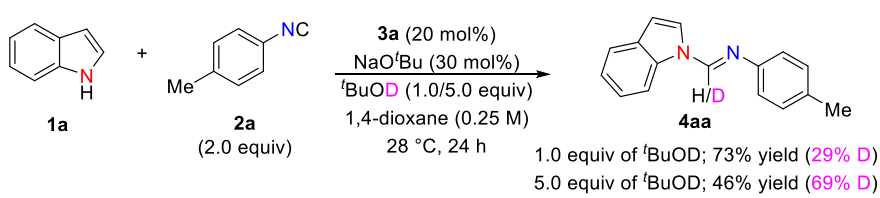

Scheme 3.10 Deuterium incorporation experiment with *t*BuOD

Formamidine (**4aa**, 46.9 mg, 0.2 mmol), **3a** (14.5 mg, 0.04 mmol), sodium *tert*-butoxide (5.8 mg, 0.06 mmol), and 1,4-dioxane (0.8 mL) were charged in a 4 mL reaction vial under argon atmosphere. The vial was then sealed with a Teflon-lined septum and the solution was allowed to stir for 24 h at 28 °C. After the reaction was complete, the reaction mixture was diluted with ethyl acetate (1.2 mL) and directly injected into the silica gel flash column chromatography (1% triethylamine in diethyl ether/hexane). The formamidine **4aa** was recovered in 91% yield, and no deuteration on the C8-position of **4aa** was observed via ^{1}H NMR spectroscopy. From this result, post-incorporation of deuterium by *t*BuOD can be excluded in the reaction.

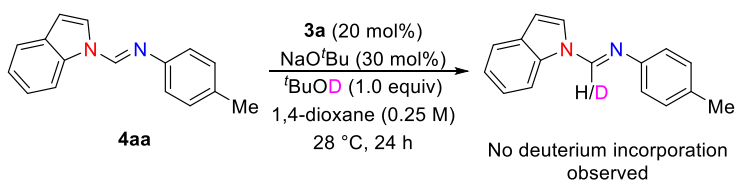

Scheme 3.11 H/D exchange experiment with *t*BuOD and **4aa**

Indole (**1a**, 23.4 mg, 0.2 mmol), sodium *tert*-butoxide (5.8 mg, 0.06 mmol), *t*BuOD (19.4 μL, 0.2 mmol), and 1,4-dioxane (0.8 mL) were charged in a 4 mL reaction vial under argon atmosphere. The vial was then sealed with a Teflon-lined septum and the solution was allowed to stir for 24 h at 28 °C. After the reaction was complete, the reaction mixture was concentrated in vacuo, and deuterium incorporation ratio was determined by ^{1}H NMR spectroscopy using $CDCl_3$ as a solvent. 31% deuteration on the N-position of indole **1a** was observed, and when 1.0 mmol of *t*BuOD (97 μL) was used in the reaction, 67% deuteration on the N-position of indole **1a** was observed.

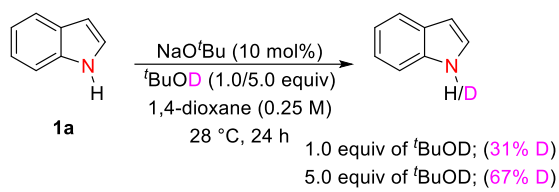

Scheme 3.12 H/D exchange experiment with *t*BuOD and **1a**

When comparing with the results of Scheme 3.10, similar deuterium incorporation ratio in **4aa** to that of simple deuterium exchange equilibrium process with indole and *t*BuOD was observed. In addition, only partial deuteration was observed even under large excess amount (5 equiv) of *t*BuOD. These results imply that the observed deuterium incorporation could be from the initial deuteration of indole. Although the role of HFIP as a proton source in enantioselective Michael addition catalyzed by NHC was reported,[23c,27] the role of *t*BuOH as an independent proton donor in our reaction would be negligible, considering low amount of existing *t*BuOH (~20 mol%) under the reaction conditions.

3.4.8 Experimental procedures for trials for the detection of formimidate intermediate

Stoichiometric reaction: **3a** (14.5 mg, 0.04 mmol), sodium *tert*-butoxide (5.8 mg, 0.06 mmol), and THF-d_8 (0.4 mL) were charged in a 4 mL reaction vial under argon atmosphere. The vial was then sealed with a Teflon-lined septum and the solution was allowed to stir for 5 min. at 28 °C. A solution of 4-bromophenyl isocyanide (**2e**, 36.4 mg, 0.2 mmol) and *tert*-butyl alcohol (19.1 μL, 0.2 mmol) in THF-d_8 (0.4 mL) was added quickly via syringe, and the solution was allowed to stir for 6 h at 28 °C. 0.4 mL of the solution was then transferred to the NMR tube and analyzed by ^{1}H NMR spectroscopy. No corresponding formimidate species was observed.

Reaction with in situ generated substoichiometric amount of *tert*-butanol: **3a** (36.3 mg, 0.1 mmol), sodium *tert*-butoxide (11.5 mg, 0.12 mmol), and THF-d_8 (0.4 mL) were charged in a 4 mL reaction vial under argon atmosphere. The vial was then sealed with a Teflon-lined septum and the solution was allowed to stir for 5 min. at 28 °C. A solution of 4-bromophenyl isocyanide (**2e**, 36.4 mg, 0.2 mmol) in THF-d_8 (0.4 mL) was added quickly via syringe, and the solution was allowed to stir for 6 h at 28 °C. 0.4 mL of the solution was then transferred to the NMR tube and analyzed by ^{1}H NMR spectroscopy. No corresponding formimidate species was observed.

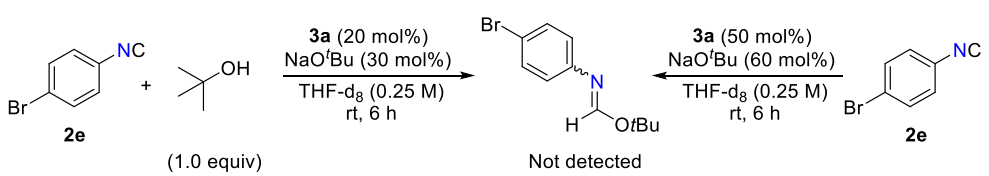

Scheme 3.13 Trials for the observation of formimidate via ^{1}H NMR spectroscopy

α-Methylbenzyl isocyanide (**2o**, 27.0 μL, 0.2 mmol), **3a** (14.5 mg, 0.04 mmol), sodium *tert*-butoxide (25 mg, 0.26 mmol), and 1,4-dioxane (0.4 mL) were charged in a 4 mL reaction vial under argon atmosphere. The vial was then sealed with a Teflon-lined septum and the solution was allowed to stir for 5 min. at room temperature. A solution of 4-methylphenyl isocyanide (**2a**, 48.3 μL, 0.4 mmol) in 1,4-dioxane (0.4 mL) was added quickly via syringe, and the solution was allowed to stir for 24 h at room temperature. Reaction was analyzed by TLC, but no promising species was observed at all.

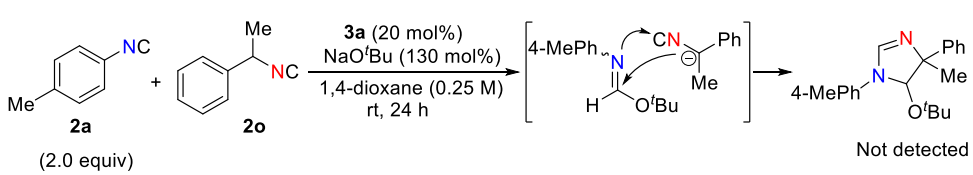

Scheme 3.14 Trial for the trapping of formimidate with *α*-methylbenzyl isocyanide

3.4.9 General procedures for the synthesis of new compounds and characterization data

3.4.9.1 Synthetic procedures and characterization of new isocyanides

1-Iodo-4-isocyanobenzene (**2f**)

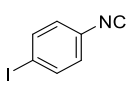

In a 25 mL RBF, 4-iodoaniline (4.38 g, 20 mmol), thiamine hydrochloride (134.8 mg, 0.4 mmol), and formic acid (4 mL) were added, and the reaction mixture was stirred under 80 °C for 2 h. After reaction was complete, the reaction mixture was diluted with ethyl acetate (20 mL), washed with 1 N aqueous HCl solution (25 mL × 2), saturated aqueous $NaHCO_3$ solution (25 mL × 2), and brine (25 mL). The organic layer was dried ($MgSO_4$), filtered, and concentrated in vacuo, which was directly used in next step. In a 500 mL RBF, previous reaction mixture was dissolved in dichloromethane/triethylamine solution (40 mL, 1:1 volumetric ratio) and stirred at room temperature vigorously. Phenyl dichlorophosphate (2.8 mL, 30 mmol) was added via syringe, and the reaction mixture was further stirred at room temperature for 3 h (vigorous reaction was observed right after the addition of reagent). After the reaction was complete, the reaction mixture was diluted with diethyl ether (100 mL) and cooled to 0 °C. Brine (20 mL) was carefully added to the reaction mixture, and the organic layer was further washed with saturated aq. $NaHCO_3$ solution (100 mL × 2). After drying with $MgSO_4$, the organic layer was filtered and concentrated in vacuo, which was further purified by silica gel flash column chromatography (ether) to afford desired isocyanide **2f** as a beige solid (3.50 g, 76%). ^{1}H NMR (400 MHz, $CDCl_3$) δ 7.73 (d, *J* = 8.7 Hz, 2H), 7.11 (d, *J* = 8.7 Hz, 2H); ^{13}C NMR (100 MHz, $CDCl_3$) δ 166.1, 138.8, 128.0, 95.1; HRMS-EI (m/z) $[M]^+$ calculated for C_7H_4NI, 228.9389; found:

228.9390.

1-Isocyano-4-(methylsulfonyl)benzene (**2i**)

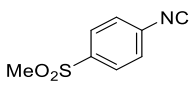

In a 25 mL RBF, 4-(methylsulfonyl)aniline (3.53 g, 20 mmol), thiamine hydrochloride (270 mg, 0.8 mmol), and formic acid (4 mL) were added, and the reaction mixture was stirred under 80 °C for 3 h. After reaction was complete, the reaction mixture was diluted with ethyl acetate (20 mL), washed with 1 N aqueous HCl solution (25 mL × 2), saturated aqueous $NaHCO_3$ solution (25 mL × 2), and brine (25 mL). The organic layer was dried ($MgSO_4$), filtered, and concentrated in vacuo, which was directly used in next step. To a 500 mL RBF charged with stirring bar, dropping funnel was connected and back-filled with argon (× 3). A solution of previous reaction mixture dissolved in dichloromethane/triethylamine solution (40 mL, 1:1 volumetric ratio) was added to the RBF through dropping funnel and cooled to -78 °C. Phosphoryl chloride (2.8 mL, 30 mmol) was added via dropping funnel in a dropwise manner, and the reaction mixture was further stirred for 2 h at room temperature (vigorous reaction was observed during warming up of the reaction mixture). After the reaction was complete, the reaction mixture was diluted with ethyl acetate (100 mL) and cooled to 0 °C. Brine (20 mL) was carefully added to the reaction mixture, and the organic layer was further washed with saturated aq. $NaHCO_3$ solution (100 mL × 2). After drying with $MgSO_4$, the organic layer was filtered and concentrated in vacuo, which was further purified by silica gel flash column chromatography (ether) to afford desired isocyanide **2i** as an off-white solid (663 mg, 18%). ^{1}H NMR (400 MHz, $CDCl_3$) δ 8.02 (d, J = 8.7 Hz, 2H), 7.59 (d, J = 8.6 Hz, 2H), 3.08 (s, 3H); ^{13}C NMR (75MHz, $CDCl_3$) δ 168.5, 141.3, 130.5, 129.0, 127.5, 44.3; HRMS-EI (m/z) $[M]^+$ calculated for $C_8H_7NO_2S$, 181.0198; found: 181.0199.

3.4.9.2 Synthetic procedures and characterization of formamidines (4)

General procedure: indole (0.2 mmol), **3a** (14.5 mg, 0.04 mmol), sodium *tert*-butoxide (5.8 mg, 0.06 mmol or 25 mg, 0.26 mmol), and 1,4-dioxane (0.4 mL) were charged in a 4 mL reaction vial under argon atmosphere. The vial was then sealed with a Teflon-lined septum and the solution was allowed to stir for 5 min. at 28 °C. Isocyanide (0.4 mmol) and 1,4-dioxane (0.4 mL) were added quickly via a gas-tight syringe, and the solution was allowed to stir for 24 h at 28 °C. After the reaction was complete, all volatiles were removed in vacuo and the remaining residue was purified by silica gel flash column chromatography to afford the corresponding formamidine.

(*E*)-1-(1*H*-indol-1-yl)-*N*-(*p*-tolyl)methanimine (**4aa**)

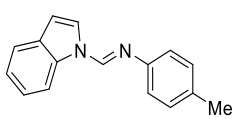

Following the general procedure, indole (**1a**, 23.4 mg, 0.2 mmol), 4-methylphenyl isocyanide (**2a**, 48.3 μL, 0.4 mmol), **3a** (14.5 mg, 0.04 mmol), sodium *tert*-butoxide (5.8 mg, 0.06 mmol), and 1,4-dioxane (0.8 mL) were used. After the reaction was complete, all volatiles were removed, and the remaining residue was purified by silica gel flash column chromatography (1% triethylamine in diethyl ether/hexane, 1:9) to afford formamidine **4aa** as a light brown solid (83%, 38.9 mg). ^{1}H NMR (300MHz, $CDCl_3$) δ 8.65 (s, 1 H), 8.06 (d, *J* = 8.0 Hz, 2 H), 7.75 (d, *J* = 3.5 Hz, 1 H), 7.64 (d, *J* = 7.5 Hz, 1 H), 7.23 – 7.36 (m, 2 H), 7.21 (d, *J* = 8.2 Hz, 2 H), 7.10 (d, *J* = 8.2 Hz, 2 H), 6.72 (d, *J* = 3.4 Hz, 1H), 2.38 ppm (s, 3 H); ^{13}C NMR ($CDCl_3$,100MHz): δ 147.1, 143.1, 135.5, 135.0, 130.7, 130.1, 124.9, 123.9, 122.9, 121.4, 121.1, 112.1, 108.0, 21.1; HRMS-ESI (m/z) $[M+H]^+$ calculated for $C_{16}H_{15}N_2$, 235.1230; found: 235.1230.

(*E*)-1-(1*H*-indol-1-yl)-*N*-phenylmethanimine (**4ab**)

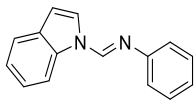

Following the general procedure, indole (**1a**, 23.4 mg, 0.2 mmol), phenyl isocyanide (**2b**, 38 μL, 0.4 mmol), 3a (14.5 mg, 0.04 mmol), sodium *tert*-butoxide (5.8 mg, 0.06 mmol), and 1,4-dioxane (0.8 mL) were used. After the reaction was complete, all volatiles were removed, and the remaining residue was purified by silica gel flash column chromatography (1% triethylamine in diethyl ether/hexane, 1:9) to afford formamidine **4ab** as a beige solid (44.1 mg, 99%). ^{1}H NMR (300 MHz, $CDCl_3$) δ 8.67 (s, 1H), 8.10 (d, *J* = 8.0 Hz, 1H), 7.77 (d, *J* = 3.5 Hz, 1H), 7.68 (d, *J* = 7.6 Hz, 1H), 7.44 (t, *J* = 7.7 Hz, 2H), 7.37 (t, *J* = 7.4 Hz, 1H), 7.29 (m, 2H), 7.22 (d, *J* = 7.4 Hz, 2H), 6.76 (d, *J* = 3.5 Hz, 1H); ^{13}C NMR (75 MHz, $CDCl_3$) δ 149. 7, 143.5, 135.5, 130.7, 129.5, 125.3, 124.9, 124.0, 123.0, 121. 5, 121.3, 112.2, 108.1; HRMS-ESI (m/z) $[M+H]^+$ calculated for $C_{15}H_{13}N_2$, 221.1073; found: 221.1071.

(*E*)-N-(4-fluorophenyl)-1-(1*H*-indol-1-yl)methanimine (**4ac**)

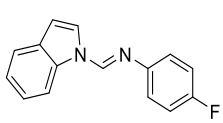

Following the general procedure, indole (**1a**, 23.4 mg, 0.2 mmol), 4-fluorophenyl isocyanide (**2c**, 37.3 μL, 0.4 mmol), **3a** (14.5 mg, 0.04 mmol), sodium *tert*-butoxide (5.8 mg, 0.06 mmol), and 1,4-dioxane (0.8 mL) were used. After the reaction was complete, all volatiles were removed, and the remaining residue was purified by silica gel flash column chromatography (1% triethylamine in diethyl ether/hexane, 1:9) to afford formamidine **4ac** as a beige solid (46.1 mg, 97%). ^{1}H NMR (300 MHz, $CDCl_3$) δ 8.52 (s, 1H), 7.98 (d, *J* = 8.0 Hz, 1H), 7.63 (d, *J* = 3.5 Hz, 1H), 7.56 (d, *J* = 7.4 Hz, 1H), 7.26 (t, *J* = 7.7 Hz, 1H), 7.22 – 7.15 (m, 1H), 7.12 – 6.91 (m, 4H), 6.64 (d, *J* = 3.5 Hz, 1H); ^{13}C NMR (75 MHz, $CDCl_3$) δ 160.8 (d, *J* = 243.5 Hz), 145.7, 143.5, 135.4, 130.7, 124.9,

124.0, 123.0, 122.5 (d, J = 8.2 Hz), 121.5, 116.1 (d, J = 22.5 Hz), 112.24, 108.25; ^{19}F NMR (376 MHz, $CDCl_3$) δ -118.5 (m); HRMS-ESI (m/z) $[M+H]^+$ calculated for $C_{15}H_{12}FN_2$, 239.0979; found: 239.0981.

(*E*)-*N*-(4-chlorophenyl)-1-(1*H*-indol-1-yl)methanimine (**4ad**)

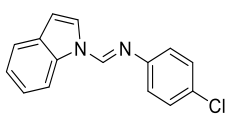

Following the general procedure, indole (**1a**, 23.4 mg, 0.2 mmol), 4-chlorophenyl isocyanide (**2d**, 55 mg, 0.4 mmol), **3a** (14.5 mg, 0.04 mmol), sodium *tert*-butoxide (5.8 mg, 0.06 mmol), and 1,4-dioxane (0.8 mL) were used. After the reaction was complete, all volatiles were removed, and the remaining residue was purified by silica gel flash column chromatography (1% triethylamine in diethyl ether/hexane, 1:9) to afford formamidine **4ad** as a beige solid (50.9 mg, >99%). ^{1}H NMR (499 MHz, $CDCl_3$) δ 8.61 (s, 1H), 8.06 (d, J = 7.8 Hz, 1H), 7.71 (d, J = 2.9 Hz, 1H), 7.64 (d, J = 7.8 Hz, 1H), 7.36, (d, J = 8.2 Hz, 2H), 7.34 (d, J = 8.2 Hz, 1H), 7.28 (t, J = 7.5 Hz, 1H), 7.12 (d, J = 8.1 Hz, 2H), 6.74 (d, J = 3.4 Hz, 1H); ^{13}C NMR (126 MHz, $CDCl_3$) δ 148.2, 143.7, 135.4, 130.8, 130.7, 129.5, 129.3, 124.9, 124.1, 123.2, 122.6, 121.5, 112.3, 108.5; HRMS-ESI (m/z) $[M+H]^+$ calculated for $C_{15}H_{12}ClN_2$, 255.0684; found: 255.0685.

(*E*)-*N*-(4-bromophenyl)-1-(1*H*-indol-1-yl)methanimine (**4ae**)

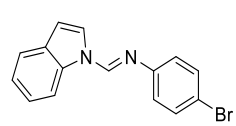

Following the general procedure, indole (**1a**, 23.4 mg, 0.2 mmol), 4-bromophenyl isocyanide (**2e**, 73 mg, 0.4 mmol), **3a** (14.5 mg, 0.04 mmol), sodium *tert*-butoxide (5.8 mg, 0.06 mmol), and 1,4-dioxane (0.8 mL) were used. After the reaction was complete, all volatiles were removed, and the remaining residue was purified by silica gel flash column chromatography (1% triethylamine in diethyl ether/hexane, 1:9) to afford formamidine **4ae** as a

white solid (58.2 mg, 97%). ^{1}H NMR (499 MHz, $CDCl_3$) δ 8.58 (s, 1H), 8.08 (d, *J* = 7.7 Hz, 1H), 7.70 (d, *J* = 3.2 Hz, 1H), 7.66 (d, *J* = 7.8 Hz, 1H), 7.52 (d, *J* = 8.6 Hz, 2H), 7.36 (t, *J* = 7.4 Hz, 1H), 7.30 (t, *J* = 7.4 Hz, 1H), 7.07 (d, *J* = 8.6 Hz, 2H), 6.75 (d, *J* = 3.6 Hz, 1H); ^{13}C NMR (126 MHz, $CDCl_3$) δ 148.5, 143.6, 135.3, 132.3, 130.7, 124.9, 124.0, 123.1, 123.0, 121.4, 118.4, 112.3, 108.4; HRMS-ESI (m/z) $[M+H]^+$ calculated for $C_{15}H_{12}BrN_2$, 299.0178; found: 299.0179.

(*E*)-1-(1*H*-indol-1-yl)-*N*-(4-iodophenyl)methanimine (**4af**)

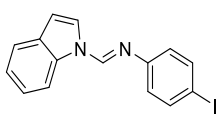

Following the general procedure, indole (**1a**, 23.4 mg, 0.2 mmol), 4-iodophenyl isocyanide (**2f**, 91.6 mg, 0.4 mmol), **3a** (14.5 mg, 0.04 mmol), sodium *tert*-butoxide (5.8 mg, 0.06 mmol), and 1,4-dioxane (0.8 mL) were used. After the reaction was complete, all volatiles were removed, and the remaining residue was purified by silica gel flash column chromatography (1% triethylamine in diethyl ether/hexane, 1:9) to afford formamidine **4af** as a light yellow solid (67.2 mg, 97%). ^{1}H NMR (499 MHz, $CDCl_3$) δ 8.59 (s, 1H), 8.06 (d, *J* = 7.7 Hz, 1H), 7.70 (m, 3H), 7.64 (d, *J* = 7.8 Hz, 1H), 7.34 (t, *J* = 7.7 Hz, 1H), 7.28 (t, *J* = 7.5 Hz, 1H), 6.95 (d, *J* = 8.6 Hz, 2H), 6.74 (d, *J* = 3.5 Hz, 1H); ^{13}C NMR (75 MHz, $CDCl_3$) δ 148.9, 143.3, 138.1, 135.0, 130.4, 124.8, 123.8, 123.3, 122.9, 121.2, 112.3, 108.2, 89.2; HRMS-ESI (m/z) $[M+H]^+$ calculated for $C_{15}H_{12}IN_2$, 347.0040; found: 347.0042.

Multigram-scale (10 mmol) synthesis: In a 100 mL RBF charged with stirring bar, indole (**1a**, 1.17 g, 10 mmol), **3a** (726 mg, 2 mmol), and sodium *tert*-butoxide (288 mg, 3 mmol) were added under argon atmosphere, and the RBF was sealed with rubber septum. After an argon filled balloon was attached to the RBF, 1,4-dioxane (20 mL) was added, and the reaction mixture was stirred for 10 min. at

room temperature. A solution of 4-iodophenyl isocyanide (**2f**, 4.12 g, 18 mmol) in 1,4-dioxane (20 mL) was added, and the reaction mixture was further stirred at 28 °C for 48 h. After the reaction was complete, the reaction mixture was diluted with ethyl acetate (80 mL), and the organic layer was washed with saturated aqueous NH_4Cl solution (80 mL × 3). The resulting aqueous solution was further extracted with dichloromethane (80 mL × 3). The combined organic layer was dried ($MgSO_4$) and concentrated in vacuo, which was further purified by silica gel flash column chromatography (1% triethylamine in diethyl ether/hexane, 1:9) to afford formamidine **4af** in 98% yield (3.41 g).

(*E*)-4-(((1*H*-indol-1-yl)methylene)amino)benzonitrile (**4ag**)

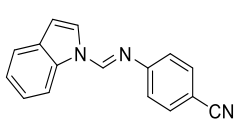

Following the general procedure, indole (**1a**, 23.4 mg, 0.2 mmol), 4-isocyanobenzonitrile (**2g**, 51.3 mg, 0.4 mmol), **3a** (14.5 mg, 0.04 mmol), sodium *tert*-butoxide (5.8 mg, 0.06 mmol), and 1,4-dioxane (0.8 mL) were used. After the reaction was complete, all volatiles were removed, and the remaining residue was purified by silica gel flash column chromatography (1% triethylamine in diethyl ether/hexane, 1:3) to afford formamidine **4ag** as a white solid (47.8 mg, 97%). ^{1}H NMR (499 MHz, $CDCl_3$) δ 8.58 (s, 1H), 8.09 (s, 1H), 7.65 (m, 4H), 7.36 (t, *J* = 7.6 Hz, 1H), 7.30 (t, *J* = 7.4 Hz, 1H), 7.22 (d, *J* = 8.3 Hz, 2H), 6.76 (d, *J* = 3.4 Hz, 1H); ^{13}C NMR (75 MHz, $CDCl_3$) δ 153.6, 144.6, 135.3, 133.6, 130.9, 125.0, 124.4, 123.6, 122.2, 121.6, 119.2, 112.6, 109.2, 108.4; HRMS-ESI (m/z) $[M+Na]^+$ calculated for $C_{16}H_{11}N_3Na$, 268.0845; found: 268.0843.

Ethyl (*E*)-4-(((1*H*-indol-1-yl)methylene)amino)benzoate (**4ah**)

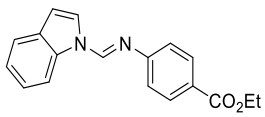

Following the general procedure, indole (**1a**, 23.4 mg, 0.2 mmol), ethyl 4-isocyanobenzoate (**2h**, 70.1 mg, 0.4 mmol), **3a** (14.5 mg, 0.04 mmol), sodium *tert*-butoxide (5.8 mg, 0.06 mmol), and 1,4-dioxane (0.8 mL) were used. After the reaction was complete, all volatiles were removed, and the remaining residue was purified by silica gel flash column chromatography (1% triethylamine in diethyl ether/hexane, 1:3) to afford formamidine **4ah** as a white solid (50.2 mg, 86%). ^{1}H NMR (499 MHz, $CDCl_3$) δ 8.59 (s, 1H), 8.10 (d, *J* = 8.5 Hz, 3H), 7.69 (s, 1H), 7.64 (d, *J* = 7.7 Hz, 1H), 7.35 (t, *J* = 7.6 Hz, 1H), 7.29 (t, *J* = 7.3 Hz, 1H), 7.20 (d, *J* = 8.5 Hz, 2H), 6.74 (d, *J* = 3.4 Hz, 1H), 4.40 (q, *J* = 7.1 Hz, 2H), 1.43 (t, *J* = 7.1 Hz, 3H); ^{13}C NMR (126 MHz, $CDCl_3$) δ 166.3, 153.5, 144.0, 135.2, 130.9, 130.7, 127.0, 124.9, 124.0, 123.1, 121.3, 121.1, 112.5, 108.5, 60.9, 14.4; HRMS-ESI (m/z) $[M+Na]^+$ calculated for $C_{18}H_{16}N_2NaO_2$, 315.1104; found: 315.1102.

(*E*)-1-(1*H*-indol-1-yl)-*N*-(4-(methylsulfonyl)phenyl)methanimine (**4ai**)

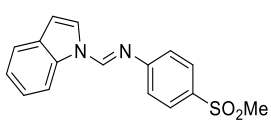

Following the general procedure, indole (**1a**, 23.4 mg, 0.2 mmol), 4-(methylsulfonyl)phenyl isocyanide (**2i**, 72.5 mg, 0.4 mmol), **3a** (14.5 mg, 0.04 mmol), sodium *tert*-butoxide (5.8 mg, 0.06 mmol), and 1,4-dioxane (0.8 mL) were used. After the reaction was complete, all volatiles were removed, and the remaining residue was purified by silica gel flash column chromatography (1% triethylamine in ethyl acetate/hexane, 1:1) to afford formamidine **4ai** as a white solid (58.2 mg, 93%). For the scaled-up reaction, indole (**1a**, 70.3 mg, 0.6 mmol), 4-(methylsulfonyl)phenyl isocyanide (**2i**, 217.5 mg, 1.2 mmol), **3a** (43.6 mg, 0.12 mmol), sodium *tert*-butoxide (17.3 mg, 0.18 mmol),

and 1,4-dioxane (2.4 mL) were used, and formamidine **4ai** was isolated in 93% yield (166.2 mg). ^{1}H NMR (499 MHz, $CDCl_3$) δ 8.61 (s, 1H), 8.10 (brs, 1H), 7.95 (d, *J* = 7.9 Hz, 2H), 7.68 (brs, 1H), 7.64 (d, *J* = 7.7 Hz, 1H), 7.36 (t, *J* = 7.7 Hz, 1H), 7.30 (m, 3H), 6.76 (d, *J* = 3.4 Hz, 1H), 3.08 (s, 3H); ^{13}C NMR (126 MHz, $CDCl_3$) δ 154.6, 144.8, 136.6, 135.3, 130.9, 129.0, 125.1, 124.4, 123.6, 122.2, 121.6, 112.6, 109.2, 44.9; HRMS-ESI (m/z) $[M+Na]^+$ calculated for $C_{16}H_{14}N_2NaO_2S$, 321.0668; found: 321.0667.

(*E*)-1-(1*H*-indol-1-yl)-*N*-(4-vinylphenyl)methanimine (**4aj**)

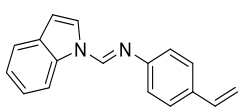

Following the general procedure, indole (**1a**, 23.4 mg, 0.2 mmol), 4-styryl isocyanide (**2j**, 47 μL, 0.4 mmol), **3a** (14.5 mg, 0.04 mmol), sodium *tert*-butoxide (25 mg, 0.26 mmol), 1,4-dioxane (0.8 mL), and 4Å molecular sieve (~12 mg) were used. After the reaction was complete, all volatiles were removed, and the remaining residue was purified by silica gel flash column chromatography (1% triethylamine in hexane) to afford formamidine **4aj** as a light-yellow solid (45.3 mg, 92%). ^{1}H NMR (499 MHz, $CDCl_3$) δ 8.65 (s, 1H), 8.07 (d, *J* = 8.2 Hz, 1H), 7.74 (d, *J* = 3.3 Hz, 1H), 7.64 (d, *J* = 7.8 Hz, 1H), 7.45 (d, *J* = 8.3 Hz, 2H), 7.34 (t, *J* = 7.6 Hz, 1H), 7.27 (d, *J* = 7.3 Hz, 1H), 7.16 (d, *J* = 8.2 Hz, 2H), 6.79 – 6.70 (m, 2H), 5.74 (dd, *J* = 17.6, 1.2 Hz, 1H), 5.24 (dd, *J* = 10.9, 1.3 Hz, 1H); ^{13}C NMR (75 MHz, $CDCl_3$) δ 149.2, 143.3, 136.4, 135.5, 134.9, 130.8, 127.4, 124.9, 124.0, 123.0, 121.5, 121.5, 113.2, 112.2, 108.3; HRMS-ESI (m/z) $[M+H]^+$ calculated for $C_{17}H_{15}N_2$, 247.1230; found: 247.1230.

(*E*)-1-(1*H*-indol-1-yl)-*N*-(4-methoxyphenyl)methanimine (**4ak**)

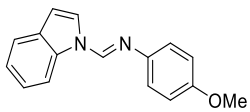

Following the general procedure, indole (**1a**, 23.4 mg, 0.2 mmol), 4-methoxyphenyl isocyanide (**2k**, 53.3 mg, 0.4 mmol), **3a** (14.5 mg, 0.04 mmol), sodium *tert*-butoxide (25 mg, 0.26 mmol), 1,4-dioxane (0.8 mL), and 4 Å molecular sieve (~12 mg) were used. After the reaction was complete, all volatiles were removed, and the remaining residue was purified by silica gel flash column chromatography (1% triethylamine in diethyl ether/hexane, 1:9) to afford formamidine **4ak** as a brown solid (31.5 mg, 63%). ^{1}H NMR (499 MHz, $CDCl_3$) δ 8.66 (s, 1H), 8.06 (d, *J* = 8.2 Hz, 1H), 7.75 (d, *J* = 3.5 Hz, 1H), 7.64 (d, *J* = 8.4 Hz, 1H), 7.33 (t, *J* = 7.7 Hz, 1H), 7.26 (t, *J* = 7.5 Hz, 1H), 7.16 (d, *J* = 8.9 Hz, 2H), 6.95 (d, *J* = 8.3 Hz, 2H), 6.72 (d, *J* = 3.5 Hz, 1H), 3.84 (s, 3H); ^{13}C NMR (75 MHz, $CDCl_3$) δ 157.7, 142.7, 142.6, 135.4, 130.7, 124.9, 123.9, 122.8, 122.2, 121.4, 114.7, 112.1, 107.8, 55.7; HRMS-ESI (m/z) $[M+H]^+$ calculated for $C_{16}H_{15}N_2O$, 251.1179; found: 251.1179.

(*E*)-1-(1*H*-indol-1-yl)-*N*-(2-(trifluoromethyl)phenyl)methanimine (**4al**)

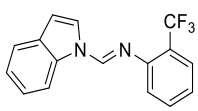

Following the general procedure, indole (**1a**, 23.4 mg, 0.2 mmol), 2-(trifluoromethyl)phenyl isocyanide (**2l**, 63.6 μL, 0.4 mmol), **3a** (14.5 mg, 0.04 mmol), sodium *tert*-butoxide (5.8 mg, 0.06 mmol), and 1,4-dioxane (0.8 mL) were used. After the reaction was complete, all volatiles were removed, and the remaining residue was purified by silica gel flash column chromatography (1% triethylamine in diethyl ether/hexane, 1:3) to afford formamidine **4al** as a dark green solid (57.6 mg, >99%). ^{1}H NMR (300 MHz, $CDCl_3$) δ 8.56 (s, 1H), 8.22 (d, *J* = 7.8 Hz, 1H), 7.71 (d, *J* = 7.8 Hz, 1H), 7.68 – 7.61 (m, 2H), 7.56 (t, *J* = 7.6 Hz, 1H), 7.37 (t, *J* = 7.5 Hz, 1H), 7.33 – 7.24 (m, 2H),

7.11 (d, J = 7.9 Hz, 1H), 6.75 (d, J = 3.5 Hz, 1H); ^{13}C NMR (75 MHz, $CDCl_3$) δ 148.1, 144.0, 135.3, 133.1, 130.9, 126.8 (d, J = 5.2 Hz), 125.5, 124.5 (d, J = 20.5 Hz), 124.2 (q, J = 271.5 Hz), 123.9 (d, J = 29.9 Hz), 123.4, 121.4, 120.3, 118.7, 113.2, 108.8; ^{19}F NMR (376 MHz, $CDCl_3$) δ -60.5; HRMS-ESI (m/z) $[M+Na]^+$ calculated for $C_{16}H_{11}F_3N_2Na$, 311.0767; found: 311.0768.

(*E*)-*N*-([1,1'-biphenyl]-2-yl)-1-(1*H*-indol-1-yl)methanimine (**4am**)

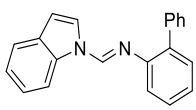

Following the general procedure, indole (**1a**, 23.4 mg, 0.2 mmol), 2-isocyano-1,1'-biphenyl (**2m**, 85.3 μL, 0.4 mmol), **3a** (14.5 mg, 0.04 mmol), sodium *tert*-butoxide (5.8 mg, 0.06 mmol), and 1,4-dioxane (0.8 mL) were used. After the reaction was complete, all volatiles were removed, and the remaining residue was purified by silica gel flash column chromatography (1% triethylamine in diethyl ether/hexane, 1:9) to afford formamidine **4am** as a colorless liquid (51.0 mg, 86%). ^{1}H NMR (300 MHz, $CDCl_3$) δ 8.61 (s, 1H), 7.98 (d, J = 8.1 Hz, 1H), 7.63 (m, 4H), 7.53 (d, J = 7.5 Hz, 1H), 7.43 (m, 3H), 7.39 – 7.32 (m, 2H), 7.30 (m, 2H), 7.17 (d, J = 7.7 Hz, 1H), 6.70 (d, J = 3.4 Hz, 1H); ^{13}C NMR (75 MHz, $CDCl_3$) δ 147.0, 143.4, 139.8, 135.8, 135.3, 130.8, 130.6, 130.2, 128.6, 127.9, 126.9, 125.5, 125.1, 123.9, 122.9, 121.2, 119.8, 112.6, 107.9; HRMS-ESI (m/z) $[M+H]^+$ calculated for $C_{21}H_{17}N_2$, 297.1386; found: 297.1384.

(*E*)-1-(1H-indol-1-yl)-*N*-(pyridin-3-yl)methanimine (**4an**)

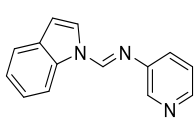

Following the general procedure, indole (**1a**, 23.4 mg, 0.2 mmol), 3-pyridyl isocyanide (**2n**, 30.2 μL, 0.4 mmol), **3a** (14.5 mg, 0.04 mmol), sodium *tert*-butoxide (25 mg, 0.26 mmol), 1,4-dioxane (0.8 mL), and 4 Å molecular sieve (~12 mg) were used. After the reaction was complete, all

volatiles were removed, and the remaining residue was purified by silica gel flash column chromatography (1% triethylamine in ethyl acetate) to afford formamidine **4an** as a brown solid (37.8 mg, 85%).^{1}H NMR (499 MHz, $CDCl_3$) δ 8.57 (s, 1H), 8.48 (s, 1H), 8.46 (d, *J* = 4.1 Hz, 1H), 8.07 (d, *J* = 5.1 Hz, 1H), 7.66 (s, 1H), 7.62 (d, *J* = 7.7 Hz, 1H), 7.47 (d, *J* = 6.3 Hz, 1H), 7.35 – 7.26 (m, 3H), 6.72 (d, *J* = 3.3 Hz, 1H); ^{13}C NMR (126 MHz, $CDCl_3$) δ 146.3, 145.5, 144.4, 142.8, 135.2, 130.7, 128.4, 124.9, 124.1, 123.8, 123.2, 121.4, 112.4, 108.7; HRMS-ESI (m/z) $[M+H]^+$ calculated for $C_{14}H_{12}N_3$, 222.1026; found: 222.1027.

(*E*)-1-(5-methyl-1*H*-indol-1-yl)-*N*-(*p*-tolyl)methanimine (**4ba**)

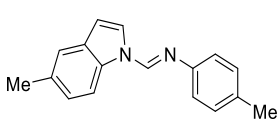

Following the general procedure, 5-methylindole (**1b**, 26.2 mg, 0.2 mmol), 4-methylphenyl isocyanide (**2a**, 48.3 μL, 0.4 mmol), **3a** (14.5 mg, 0.04 mmol), sodium *tert*-butoxide (5.8 mg, 0.06 mmol), and 1,4-dioxane (0.8 mL) were used. After the reaction was complete, all volatiles were removed, and the remaining residue was purified by silica gel flash column chromatography (1% triethylamine in diethyl ether/hexane, 1:9) to afford formamidine **4ba** as a light green solid (44.3 mg, 89%). ^{1}H NMR (300 MHz, $CDCl_3$) δ 8.61 (s, 1H), 7.97 (d, *J* = 8.3 Hz, 1H), 7.70 (d, *J* = 3.4 Hz, 1H), 7.45 (s, 1H), 7.23 (d, *J* = 8.1 Hz, 2H), 7.18 (d, *J* = 8.5 Hz, 1H), 7.12 (d, *J* = 8.2 Hz, 2H), 6.66 (d, *J* = 3.4 Hz, 1H), 2.50 (s, 3H), 2.41 (s, 3H); ^{13}C NMR (75 MHz, $CDCl_3$) δ 147.2, 143.2, 134.9, 133.7, 132.3, 130.9, 130.0, 125.3, 125.0, 121.2, 121.1, 111.9, 107.6, 21.6, 21.1; HRMS-ESI (m/z) $[M+H]^+$ calculated for $C_{17}H_{17}N_2$, 249.1386; found: 249.1387.

(*E*)-1-(5-bromo-1*H*-indol-1-yl)-*N*-(*p*-tolyl)methanimine (**4ca**)

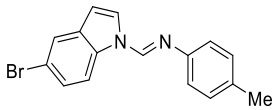

Following the general procedure, 5-bromoindole (**1c**, 39.2 mg, 0.2 mmol), 4-methylphenyl isocyanide (**2a**, 48.3 μL, 0.4 mmol), **3a** (14.5 mg, 0.04 mmol), sodium *tert*-butoxide (25 mg, 0.26 mmol), 1,4-dioxane (0.8 mL), and 4 Å molecular sieve (~12 mg) were used. After the reaction was complete, all volatiles were removed, and the remaining residue was purified by silica gel flash column chromatography (1% triethylamine in diethyl ether/hexane, 1:9) to afford formamidine **4ca** as a light yellow solid (32.3 mg, 52%). ^{1}H NMR (499 MHz, $CDCl_3$) δ 8.57 (s, 1H), 8.05 (d, *J* = 8.7 Hz, 1H), 7.76 (d, *J* = 1.4 Hz, 1H), 7.67 (d, *J* = 3.4 Hz, 1H), 7.42 (dd, *J* = 8.7, 1.4 Hz, 1H), 7.21 (d, *J* = 8.0 Hz, 2H), 7.10 (d, *J* = 8.1 Hz, 2H), 6.65 (d, *J* = 3.5 Hz, 1H), 2.39 (s, 3H); ^{13}C NMR (126 MHz, $CDCl_3$) δ 146.7, 143.0, 135.3, 134.0, 132.4, 130.1, 126.8, 126.4, 124.0, 121.1, 116.0, 114.2, 107.1, 21.1; HRMS-ESI (m/z) $[M+H]^+$ calculated for $C_{16}H_{14}BrN_2$, 313.0335; found: 313.0334.

(*E*)-1-(5-methoxy-1*H*-indol-1-yl)-*N*-(*p*-tolyl)methanimine (**4da**)

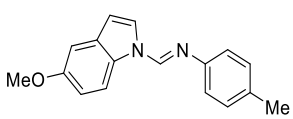

Following the general procedure, 5-methoxylindole (**1d**, 29.4 mg, 0.2 mmol), 4-methylphenyl isocyanide (**2a**, 48.3 μL, 0.4 mmol), **3a** (14.5 mg, 0.04 mmol), sodium *tert*-butoxide (5.8 mg, 0.06 mmol), and 1,4-dioxane (0.8 mL) were used. After the reaction was complete, all volatiles were removed, and the remaining residue was purified by silica gel flash column chromatography (1% triethylamine in diethyl ether/hexane, 1:3) to afford formamidine **4da** as a yellow liquid (45.3 mg, 86%). ^{1}H NMR (499 MHz, $CDCl_3$) δ 8.55 (s, 1H), 8.07 (d, *J* = 8.8 Hz, 1H), 7.62 (d, *J* = 3.1 Hz, 1H), 7.20 (d, *J* = 8.0 Hz, 2H), 7.09 (m, 3H), 6.96 (dd, *J* = 8.9, 2.3 Hz, 1H), 6.64 (d, *J* = 3.3 Hz, 1H), 3.88 (s,

3H), 2.38 (s, 3H); ^{13}C NMR (75 MHz, $CDCl_3$) δ 156.2, 147.2, 143.4, 134.9, 131.5, 130.2, 130.0, 125.9, 121.1, 113.6, 113.1, 107.7, 103.7, 55.9, 21.1; HRMS-ESI (m/z) $[M+H]^+$ calculated for $C_{17}H_{17}N_2O$, 265.1335; found: 265.1333.

(*E*)-1-(4-(benzyloxy)-1*H*-indol-1-yl)-*N*-(*p*-tolyl)methanimine (**4ea**)

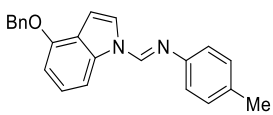

Following the general procedure, 4-(benzyloxy)indole (**1e**, 44.7 mg, 0.2 mmol), 4-methylphenyl isocyanide (**2a**, 48.3 μL, 0.4 mmol), **3a** (14.5 mg, 0.04 mmol), sodium *tert*-butoxide (5.8 mg, 0.06 mmol), and 1,4-dioxane (0.8 mL) were used. After the reaction was complete, all volatiles were removed, and the remaining residue was purified by silica gel flash column chromatography (1% triethylamine in diethyl ether/hexane, 1:3) to afford formamidine **4ea** as a light green solid (54.2 mg, 80%). ^{1}H NMR (499 MHz, $CDCl_3$) δ 8.63 (s, 1H), 7.68 (d, *J* = 3.6 Hz, 1H), 7.61 (d, *J* = 8.3 Hz, 1H), 7.51 (dd, *J* = 7.9, 0.8 Hz, 2H), 7.41 (dd, *J* = 8.1, 6.7 Hz, 2H), 7.34 (t, *J* = 7.3 Hz, 1H), 7.23 (d, *J* = 8.1 Hz, 1H), 7.20 (d, *J* = 8.4 Hz, 2H), 7.11 – 7.08 (m, 2H), 6.89 (d, *J* = 3.6 Hz, 1H), 6.75 (d, *J* = 7.9 Hz, 1H), 5.24 (s, 2H), 2.38 (s, 3H); ^{13}C NMR (101 MHz, $CDCl_3$) δ 152.6, 147.0, 143.1, 137.3, 137.0, 135.0, 130.0, 128.7, 128.0, 127.5, 124.8, 123.2, 121.2, 121.1, 105.3, 105.3, 104.6, 70.2, 21.1; HRMS-ESI (m/z) $[M+H]^+$ calculated for $C_{23}H_{21}N_2O$, 341.1648; found: 341.1648.

(*E*)-1-(5,6-dimethoxy-1*H*-indol-1-yl)-*N*-(*p*-tolyl)methanimine (**4fa**)

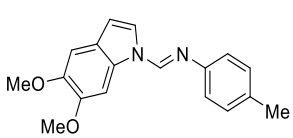

Following the general procedure, 5,6-dimethoxyindole (**1f**, 35.4 mg, 0.2 mmol), 4-methylphenyl isocyanide (**2a**, 48.3 μL, 0.4 mmol), **3a** (14.5 mg, 0.04 mmol), sodium *tert*-butoxide (5.8 mg, 0.06 mmol), and 1,4-dioxane (0.8 mL) were used. After the reaction was complete, all

volatiles were removed, and the remaining residue was purified by silica gel flash column chromatography (1% triethylamine in ethyl acetate/hexane, 1:3) to afford formamidine **4fa** as a yellow solid (54.1 mg, 92%). ^{1}H NMR (300 MHz, $CDCl_3$) δ 8.53 (s, 1H), 7.89 (s, 2H), 7.47 (d, *J* = 3.0 Hz, 2H), 7.21 (d, *J* = 8.1 Hz, 4H), 7.11 (d, *J* = 8.3 Hz, 6H), 7.08 (s, 1H), 6.61 (d, *J* = 3.4 Hz, 2H), 3.97 (s, 7H), 3.95 (s, 6H), 2.38 (s, 6H); ^{13}C NMR (75 MHz, $CDCl_3$) δ 147.8, 147.2, 146.8, 144.1, 134.8, 130.0, 129.5, 124.3, 123.4, 121.1, 107.6, 102.7, 97.5, 56.4, 56.3, 21.0; HRMS-ESI (m/z) $[M+Na]^+$ calculated for $C_{18}H_{18}N_2NaO_2$, 317.1260; found: 317.1261.

(*E*)-1-(6-bromo-1*H*-indol-1-yl)-*N*-(*p*-tolyl)methanimine (**4ga**)

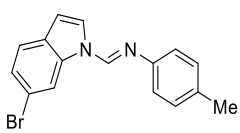

Following the general procedure, 6-bromoindole (**1g**, 39.2 mg, 0.2 mmol), 4-methylphenyl isocyanide (**2a**, 48.3 μL, 0.4 mmol), **3a** (14.5 mg, 0.04 mmol), sodium *tert*-butoxide (25 mg, 0.26 mmol), 1,4-dioxane (0.8 mL), and 4 Å molecular sieve (~12 mg) were used. After the reaction was complete, all volatiles were removed, and the remaining residue was purified by silica gel flash column chromatography (1% triethylamine in diethyl ether/hexane, 1:9) to afford formamidine **4ga** as a white solid (31.8 mg, 51%). ^{1}H NMR (499 MHz, $CDCl_3$) δ 8.55 (s, 1H), 8.37 (s, 1H), 7.64 (d, *J* = 3.0 Hz, 1H), 7.48 (d, *J* = 8.3 Hz, 1H), 7.37 (d, *J* = 8.3 Hz, 1H), 7.21 (d, *J* = 7.8 Hz, 2H), 7.10 (d, *J* = 7.9 Hz, 2H), 6.67 (d, *J* = 3.2 Hz, 1H), 2.39 (s, 3H); ^{13}C NMR (126 MHz, $CDCl_3$) δ 146.6, 143.0, 136.0, 135.3, 130.1, 129.5, 126.1, 125.9, 122.4, 121.1, 117.6, 116.1, 107.6, 21.1; HRMS-ESI (m/z) $[M+H]^+$ calculated for $C_{16}H_{14}BrN_2$, 313.0335; found: 313.0337.

(*E*)-1-(3-methyl-1*H*-indol-1-yl)-*N*-(*p*-tolyl)methanimine (**4ha**)

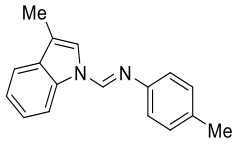

Following the general procedure, 3-methylindole (**1h**, 26.2 mg, 0.2 mmol), 4-methylphenyl isocyanide (**2a**, 48.3 μL, 0.4 mmol), **3a** (14.5 mg, 0.04 mmol), sodium *tert*-butoxide (5.8 mg, 0.06 mmol), and 1,4-dioxane (0.8 mL) were used. After the reaction was complete, all volatiles were removed, and the remaining residue was purified by silica gel flash column chromatography (1% triethylamine in diethyl ether/hexane, 1:9) to afford formamidine **4ha** as a yellow solid (49.6 mg, >99%). ^{1}H NMR (499 MHz, $CDCl_3$) δ 8.60 (s, 1H), 7.96 (d, *J* = 7.6 Hz, 1H), 7.59 (d, *J* = 7.8 Hz, 1H), 7.58 (s, 1H), 7.35 (t, *J* = 7.6 Hz, 1H), 7.30 (t, *J* = 7.4 Hz, 1H), 7.22 (d, *J* = 7.9 Hz, 2H), 7.11 (d, *J* = 8.0 Hz, 2H), 2.40 (s, 3H), 2.37 (s, 3H); ^{13}C NMR (126 MHz, $CDCl_3$) δ 147.3, 142.6, 135.8, 134.7, 131.5, 130.0, 123.9, 122.4, 121.8, 121.1, 119.5, 117.5, 111.6, 21.1, 9.9; HRMS-ESI (m/z) $[M+H]^+$ calculated for $C_{17}H_{17}N_2$, 249.1386; found: 249.1386.

(*E*)-1-(2,3-dimethyl-1*H*-indol-1-yl)-*N*-(*p*-tolyl)methanimine (**4ia**)

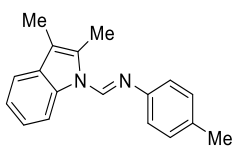

Following the general procedure, 2,3-dimethylindole (**1i**, 29.0 mg, 0.2 mmol), 4-methylphenyl isocyanide (**2a**, 48.3 μL, 0.4 mmol), **3a** (14.5 mg, 0.04 mmol), sodium *tert*-butoxide (5.8 mg, 0.06 mmol), and 1,4-dioxane (0.8 mL) were used. After the reaction was complete, all volatiles were removed, and the remaining residue was purified by silica gel flash column chromatography (1% triethylamine in diethyl ether/hexane, 1:9) to afford formamidine **4ia** as a yellow solid (52.4 mg, >99%). ^{1}H NMR (499 MHz, $CDCl_3$) δ 8.62 (d, *J* = 8.1 Hz, 1H), 8.58 (s, 1H), 7.46 (d, *J* = 7.2 Hz, 1H), 7.32 – 7.22 (m, 3H), 7.20 (d, *J* = 8.3 Hz, 2H), 7.08 (d, *J* = 8.2 Hz, 2H), 2.50 (s, 3H),

2.38 (s, 3H), 2.24 (s, 3H); ^{13}C NMR (75 MHz, $CDCl_3$) δ 148.2, 144.2, 135.2, 134.4, 131.2, 129.9, 126.3, 123.6, 122.6, 121.1, 118.0, 115.4, 113.1, 21.0, 11.0, 8.8; HRMS-ESI (m/z) $[M+H]^+$ calculated for $C_{18}H_{19}N_2$, 263.1543; found: 263.1543.

(*E*)-1-(9*H*-carbazol-9-yl)-*N*-(*p*-tolyl)methanimine (**4ja**)

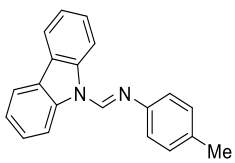

Following the general procedure, carbazole (**1j**, 33.4 mg, 0.2 mmol), 4-methylphenyl isocyanide (**2a**, 48.3 μL, 0.4 mmol), **3a** (14.5 mg, 0.04 mmol), sodium *tert*-butoxide (5.8 mg, 0.06 mmol), and 1,4-dioxane (0.8 mL) were used. After the reaction was complete, all volatiles were removed, and the remaining residue was purified by silica gel flash column chromatography (1% triethylamine in diethyl ether/hexane, 1:9) to afford formamidine **4ja** as an off-yellow solid (52.3 mg, 92%). ^{1}H NMR (499 MHz, $CDCl_3$) δ 9.01 (s, 1H), 8.31 (d, *J* = 8.2 Hz, 2H), 8.06 (d, *J* = 7.7 Hz, 2H), 7.51 (t, *J* = 7.8 Hz, 2H), 7.39 (t, *J* = 7.9 Hz, 2H), 7.24 (d, *J* = 8.4 Hz, 2H), 7.16 (d, *J* = 8.2 Hz, 2H), 2.40 (s, 3H); ^{13}C NMR (75 MHz, $CDCl_3$) δ 147.9, 143.1, 138.8, 134.7, 130.1, 127.1, 125.6, 123.0, 121.2, 120.3, 113.3, 21.1; HRMS-ESI (m/z) $[M+H]^+$ calculated for $C_{20}H_{17}N_2$, 285.1386; found: 285.1387.

(*E*)-1-(1*H*-pyrrol-1-yl)-*N*-(*p*-tolyl)methanimine (**4ka**)

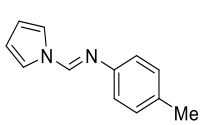

Following the general procedure, pyrrole (**1k**, 13.9 μL, 0.2 mmol), 4-methylphenyl isocyanide (**2a**, 48.3 μL, 0.4 mmol), **3a** (14.5 mg, 0.04 mmol), sodium *tert*-butoxide (5.8 mg, 0.06 mmol), and 1,4-dioxane (0.8 mL) were used. After the reaction was complete, all volatiles were removed, and the remaining residue was purified by silica gel flash column chromatography (1% triethylamine in diethyl ether/hexane, 1:9) to afford formamidine **4ka** as an

off-white solid (23.0 mg, 63%). ^{1}H NMR (300 MHz, $CDCl_3$) δ 8.24 (s, 1H), 7.36 – 7.30 (m, 2H), 7.18 (d, *J* = 8.1 Hz, 2H), 7.04 (d, *J* = 8.2 Hz, 2H), 6.40 – 6.33 (m, 2H), 2.36 (s, 3H); 13C NMR (75 MHz, CDCl3) δ 146.4, 144.4, 135.3, 130.0, 121.1, 119.4, 112.5, 21.1; HRMS-ESI (m/z) $[M+H]^+$ calculated for $C_{12}H_{13}N_2$, 185.1073; found: 185.1072.

3.5 References

(1) (a) Bandini, M.; Eichholzer, A. *Angew. Chem., Int. Ed.* **2009**, *48*, 9608. (b) Zhang, M.-Z.; Chen, Q.; Yang, G.-F. *Eur. J. Med. Chem.* **2015**, *89*, 421.

(2) (a) Budylin, V. A.; Ermolenko, M. S.; Kost, A. N. *Chem. Heterocycl. Compd.* **1978**, *14*, 742. (b) Jana, U.; Maiti, S.; Biswas, S. *Tetrahedron Lett.* **2007**, *48*, 7160.

(3) (a) Cardillo, B.; Casnati, G.; Pochini, A.; Ricca, A. *Tetrahedron* **1967**, *23*, 3771. (b) Rubottom, G. M.; Chabala, J. C. *Synthesis* **1972**, 566. (c) Hentz, A.; Retailleau, P.; Gandon, V.; Cariou, K.; Dodd, R. H. *Angew. Chem., Int. Ed.* **2014**, *53*, 8333.

(4) Zhang, Y. *Tetrahedron* **2006**, *62*, 3917.

(5) (a) Yadav, J. S.; Reddy, B. V. S.; Aravind, S.; Kumar, G. G. K. S. N.; Reddy, A. S. *Tetrahedron Lett.* **2007**, *48*, 6117. (b) Stanley, L. M.; Hartwig, J. F. *Angew. Chem., Int. Ed.* **2009**, *48*, 7841. (c) Cui, H. L.; Feng, X.; Peng, J.; Lei, J.; Jiang, K.; Chen, Y. C. *Angew. Chem., Int. Ed.* **2009**, *48*, 5737.

(6) (a) Heller, S. T.; Schultz, E. E.; Sarpong, R. *Angew. Chem., Int. Ed.* **2012**, *51*, 8304. (b) Zhang, Z.-W.; Xue, H.; Li, H.; Kang, H.; Feng, J.; Lin, A.; Liu, S. *Org. Lett.* **2016**, *18*, 3918. (c) Okauchi, T.; Itonaga, M.; Minami, T.; Owa, T.; Kitoh, K.; Yoshino, H. *Org. Lett.* **2000**, *2*, 1485.

(7) (a) Yoo, W. J.; Capdevila, M. G.; Du, X.; Kobayashi, S. *Org. Lett.* **2012**, *14*, 5326. (b) Ueno, A.; Kayaki, Y.; Ikariya, T. *Organometallics* **2014**, *33*, 4479.

(8) (a) Zhu, J. *Eur. J. Org. Chem.* **2003**, 1133. (b) Sadjadi, S.; Heravi, M. M. *Tetrahedron* **2011**, *67*, 2707. (c) Boyarskiy, V. P.; Bokach, N. A.; Luzyanin, K. V.; Kukushkin, V. Y. *Chem. Rev.* **2015**, *115*, 2698.

(9) (a) Tobisu, M.; Chatani, N. *Chem. Lett.* **2011**, *40*, 330. (b) Qiu, G.; Ding, Q.; Wu, J. *Chem. Soc. Rev.* **2013**, *42*, 5257. (c) Vlaar, T.; Ruijter, E.; Maes, B. U.; Orru, R. V.

Angew. Chem., Int. Ed. **2013**, *52*, 7084.

(10) (a) Saegusa, T.; Ito, Y.; Kobayashi, S.; Hirota, K.; Yoshioka, H. *Bull. Chem. Soc. Jpn.* **1969**, *42*, 3310. (b) Oshita, M.; Yamashita, K.; Tobisu, M.; Chatani, N. *J. Am. Chem. Soc.* **2005**, *127*, 761. (c) Fukumoto, Y.; Hagihara, M.; Kinashi, F.; Chatani, N. *J. Am. Chem. Soc.* **2011**, *133*, 10014.

(11) Tobisu, M.; Yamaguchi, S.; Chatani, N. *Org. Lett.* **2007**, *9*, 3351.

(12) (a) Jones, W. D.; Kosar, W. P. *J. Am. Chem. Soc.* **1986**, *108*, 5640. (b) Yavari, I.; Djahaniani, H.; Nasiri, F. *Monatsh. Chem.* **2004**, *135*, 543. (c) Anary-Abbasinejad, M.; Mosslemin, M. H.; Anaraki-Ardakani, H.; Tahan, S. *J. Chem. Res.* **2006**, 306.

(13) (a) Flanigan, D. M.; Romanov-Michailidis, F.; White, N. A.; Rovis, T. *Chem. Rev.* **2015**, *115*, 9307. (b) Hopkinson, M. N.; Richter, C.; Schedler, M.; Glorius, F. *Nature* **2014**, *510*, 485. (c) Enders, D.; Niemeier, O.; Henseler, A. *Chem. Rev.* **2007**, *107*, 5606.

(14) Kim, J.; Hong, S. H. *Chem. Sci.* **2017**, *8*, 2401.

(15) (a) Guo, C.; Fleige, M.; Janssen-Müller, D.; Daniliuc, C. G.; Glorius, F. *J. Am. Chem. Soc.* **2016**, *138*, 7840. (b) Guo, C.; Janssen-Müller, D.; Fleige, M.; Lerchen, A.; Daniliuc, C. G.; Glorius, F. *J. Am. Chem. Soc.* **2017**, *139*, 4443.

(16) (a) Pooi, B.; Lee, J.; Choi, K.; Hirao, H.; Hong, S. H. *J. Org. Chem.* **2014**, *79*, 9231. (b) Kim, S.; Hong, S. H. *Adv. Synth. Catal.* **2015**, *357*, 1004.

(17) César, V.; Labat, S.; Miqueu, K.; Sotiropoulos, J.-M.; Brousses, R.; Lugan, N.; Lavigne, G. *Chem.–Eur. J.* **2013**, *19*, 17113.

(18) (a) Reinecke, M. G.; Sebastian, J. F.; Johnson, H. W.; Pyun, C. *J. Org. Chem.* **1972**, *37*, 3066. (b) Hobbs, C. F.; McMillin, C. K.; Papadopoulos, E. P.; VanderWerf, C. A. *J. Am. Chem. Soc.* **1962**, *84*, 43. (c) Heaney, H.; Ley, S. V. *J.*

Chem. Soc., Perkin Trans. 1 **1973**, 499.

(19) Powers, J. C.; Meyer, W. P.; Parsons, T. G. *J. Am. Chem. Soc.* **1967**, *89*, 5812.

(20) (a) Zhu, X.; Ganesan, A. *J. Org. Chem.* **2002**, *67*, 2705. (b) Ortiz, G. X.; Hemric, B. N.; Wang, Q. *Org. Lett.* **2017**, *19*, 1314.

(21) Nunomoto, S.; Kawakami, Y.; Yamashita, Y.; Takeuchi, H.; Eguchi, S. *J. Chem. Soc., Perkin Trans. 1* **1990**, 111.

(22) Bordwell, F. G.; Drucker, G. E.; Fried, H. E. *J. Org. Chem.* **1981**, *46*, 632.

(23) (a) Cowan, J. A.; Clyburne, J. A. C.; Davidson, M. G.; Harris, R. L. W.; Howard, J. A. K.; Küpper, P.; Leech, M. A.; Richards, S. P. *Angew. Chem., Int. Ed.* **2002**, *41*, 1432. (b) Movassaghi, M.; Schmidt, M. A. *Org. Lett.* **2005**, *7*, 2453. (c) Chen, J.; Meng, S.; Wang, L.; Tang, H.; Huang, Y. *Chem. Sci.* **2015**, *6*, 4184.

(24) Olmstead, W. N.; Margolin, Z.; Bordwell, F. G. *J. Org. Chem.* **1980**, *45*, 3295.

(25) (a) Hudnall, T. W.; Moorhead, E. J.; Gusev, D. G.; Bielawski, C. W. *J. Org. Chem.* **2010**, *75*, 2763. (b) Martin, D.; Canac, Y.; Lavallo, V.; Bertrand, G. *J. Am. Chem. Soc.* **2014**, *136*, 5023.

(26) Nikulin, M. V.; Lebedev, A. Y.; Voskoboinikov, A. Z.; Beletskaya, I. P. *Dokl. Chem.* **2008**, *423*, 326.

(27) Wang, L.; Chen, J.; Huang, Y. *Angew. Chem., Int. Ed.* **2015**, *54*, 15414.

Chapter 4. C(sp^3)–H Bond Functionalizations via Visible Light Photoredox Catalysis

4.1 Introduction

Light has been utilized as an alternative energy source for organic transformations.[1] Inspired by Nature, especially the photosynthesis system in various organics, numerous attempts have been made to harvest light energy using photosensitizer and utilize it as a form of chemical energy.[2] Classical approaches for photochemical reactions usually rely on the use of UV light, which has high energy but has limited practical utilization.[1,3] For past decades, the application of visible light (400-700 nm region) in the organic transformation has been successfully achieved with the aid of efficient visible light photosensitizers (photocatalysts) (Scheme 4.1A).[4] Those species can absorb visible light efficiently, and an intersystem-crossing (ISC) process generates highly reactive triplet-state species. Because of the existence of both high-energy lone-pair electron and a hole, this can act as a transient and robust redox species, either oxidant or reductant, depending on the reaction environment (Scheme 4.1B).[4c-e] This unique property enabled a novel reactivity profile in various organic transformations, and thereby several challenging reactions have been established, including the direct C(sp^3)–H bond functionalizations.[5]

In this chapter, mechanistic aspects of the visible light photoredox catalysis in the C(sp^3)–H bond functionalizations will be discussed, together with

representative examples of each strategy.

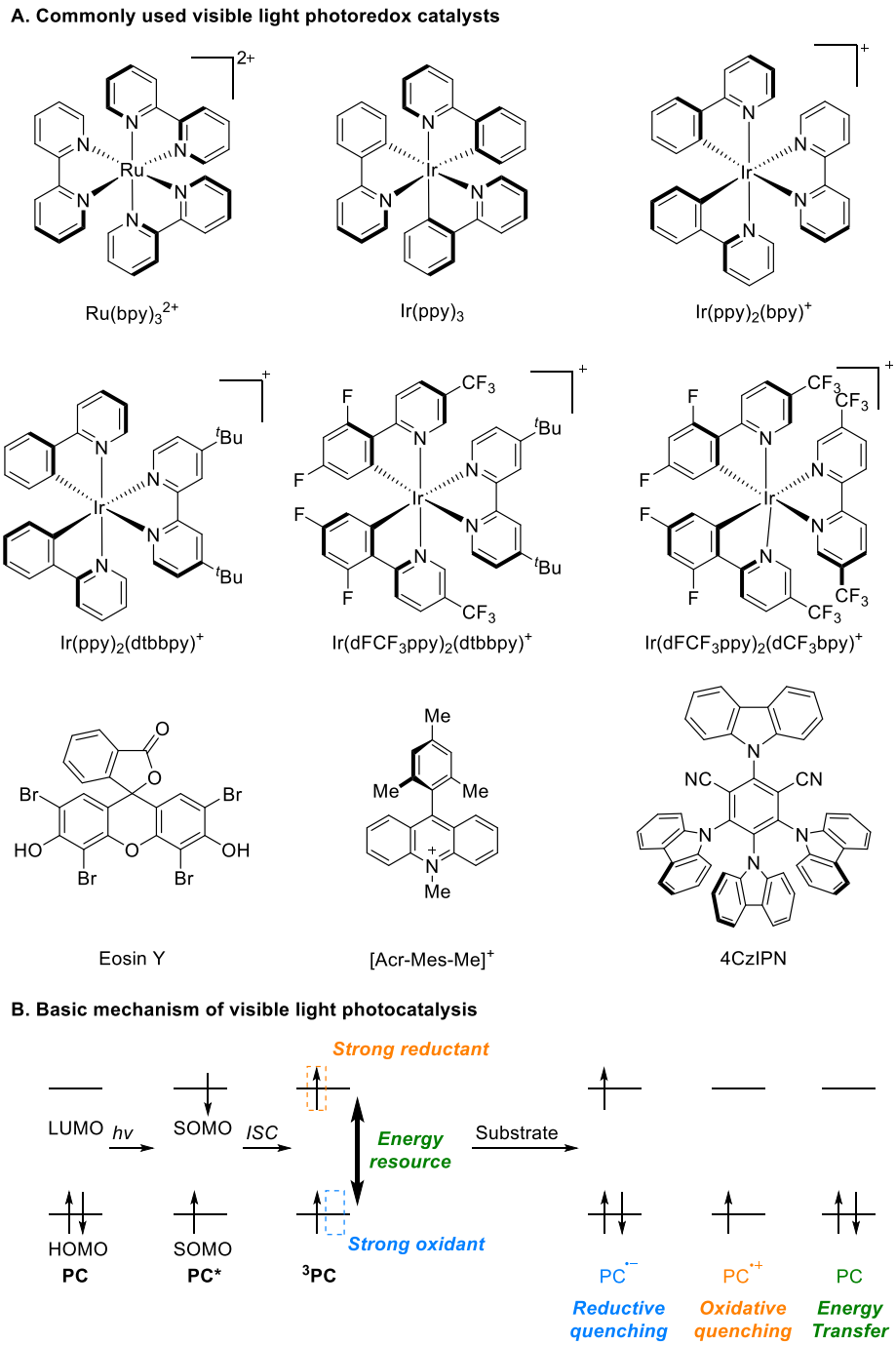

Scheme 4.1 Representative visible light photocatalysts and their working mechanism

4.2 C(sp^3)–H bond activation via single-electron transfer (SET)

The superior ability of visible light photocatalysts as redox mediators can be easily applied to the various types of redox processes, taking advantage of the catalytic formation of reactive species in the reaction media and the transiency of the species under irradiation. Notably, the direct single-electron transfer from the p-electrons of nitrogen atom or the π-bond electrons of the conjugated systems has been performed to activate the functional groups for various organic transformations.[6] One feature of the generated radical cations is that the acidity of an adjacent proton is significantly enhanced (Scheme 4.2).[7] Therefore, relatively facile deprotonation can be accompanied, producing carbon-centered radical intermediate. A combination with various coupling partners provides a new bond-forming process, achieving the direct C(sp^3)–H bond functionalizations.

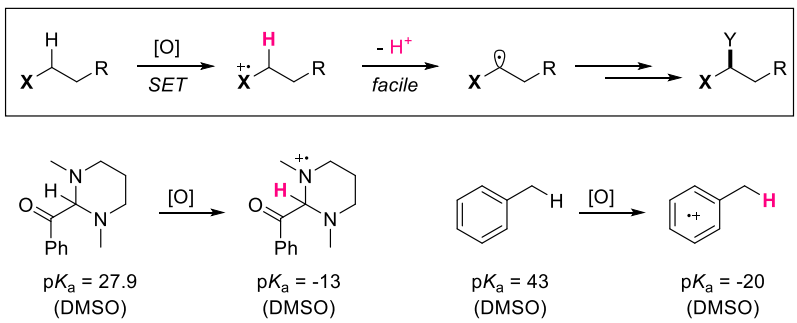

Scheme 4.2 SET of a nitrogen atom and π-system, and the effect of pK_a of an adjacent proton

4.2.1 SET of amines

Early examples of the SET of amines in the visible light photoredox catalysis for the direct C(sp^3)–H bond functionalizations were demonstrated with tetrahydroisoquinoline (THIQ) as a model substrate (Scheme 4.3).[6a] After the SET on the nitrogen atom, THIQ radical cation can undergo either deprotonation or direct hydrogen atom transfer (HAT), producing α-amino radical or iminium species, respectively. In the case of THIQ, the generated α-amino radical readily undergoes further SET to form more-stable iminium species under oxidative conditions. This in situ formed electrophile has an opportunity to react with a variety of nucleophilic coupling partners, providing an array of functionalized THIQ systems. In 2010, Stephenson first demonstrated the aza-Henry reaction with THIQ under visible light irradiation conditions.[8] Since this seminal work, various types of bond formation reactions have been developed including C–C bond formations[9] and C–heteroatom bond formations.[10] Also, several transformations have been achieved by organic photocatalysts, which replace the relatively expensive metal-based photocatalysts.[11] This protocol further provides a new approach toward the construction of ring systems via cycloaddition[12] or intramolecular trapping reaction.[13]

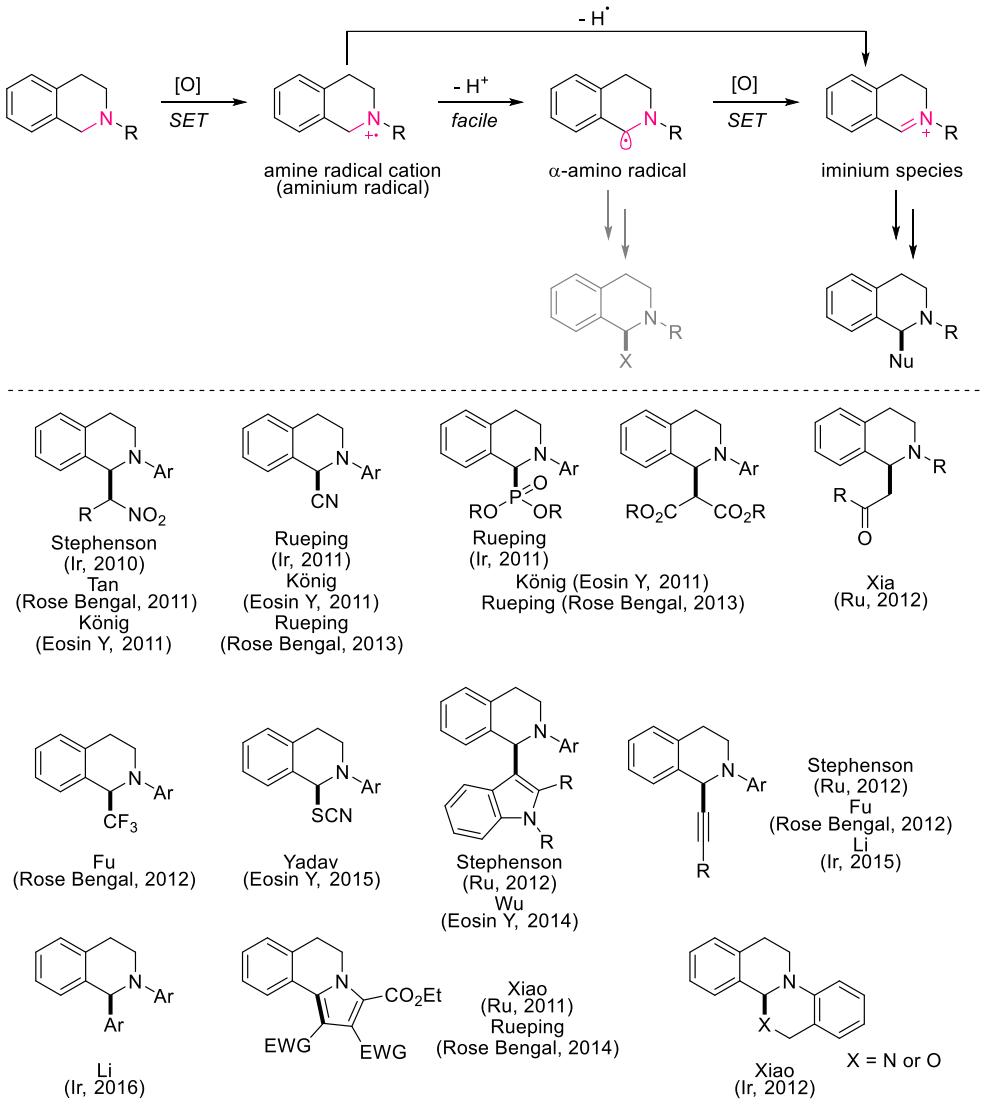

Scheme 4.3 Formation of iminium intermediate via photocatalytic SET of THIQ and its application

The combination of the proposed SET-based C(sp^3)–H bond cleavage of THIQ with previously established catalytic systems enabled novel asymmetric transformations (Scheme 4.4). In 2012, Rovis demonstrated that an introduction of NHC organocatalysis, which generates a chiral Breslow intermediate from aldehyde and chiral NHC organocatalyst, performs asymmetric acylation at the α-nitrogen positions efficiently.[14] Jiang proposed an utilization of β-Isocupreidine as an organocatalyst to provide a chiral enolate in the reaction media, thereby asymmetric Mannich-type transformation could be achieved.[15] Li showed that the combination of a chiral ligand/copper co-catalytic system with the visible light photoredox catalysis could deliver an aryl group asymmetrically.[9f]

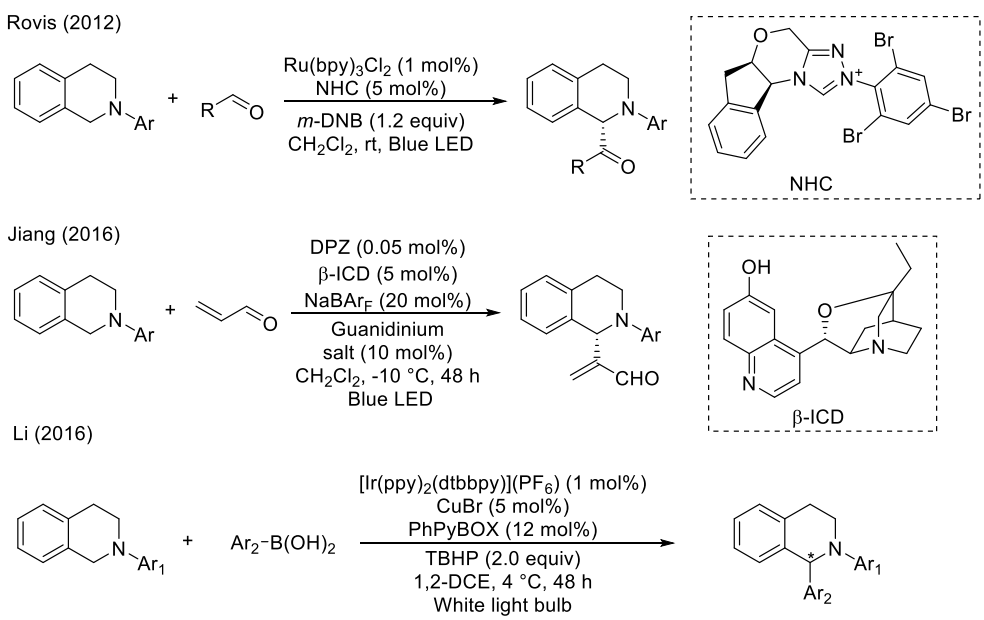

Scheme 4.4 Formation of iminium intermediate via photocatalytic SET of THIQ and in asymmetric transformations

The utilization of α-amino radical generated from the THIQ is less explored, due to the preference toward the formation of iminium species (Scheme 4.5). In 2012, Reiser reported that the trapping of such radical intermediate with Michael acceptors produced a new C–C bond under mild reaction conditions.[16] Later on, Yoon observed that the introduction of Brønsted acid, which activates the carbonyl group of the Michael acceptor, significantly enhanced the reaction efficiency.[17] Ye and Bissember independently applied the radical-trapping approach for the construction of new ring systems. The former case implemented an *ortho*-carbonyl group at the N-phenyl position, thereby an intramolecular radical trapping and a concurrent dehydration could occur.[18] Bissember achieved formal [4+2] cycloaddition with maleimides to synthesize multi-ring-fused skeletons.[19]

Not only Michael acceptors but also other types of coupling partners could participate in the reaction with α-amino radical. In 2015, Xiao proposed the radical-radical coupling process with allyl radical, which is generated from the palladium π-allyl complex, achieving the direct allylation of THIQ under mild reaction conditions.[20]

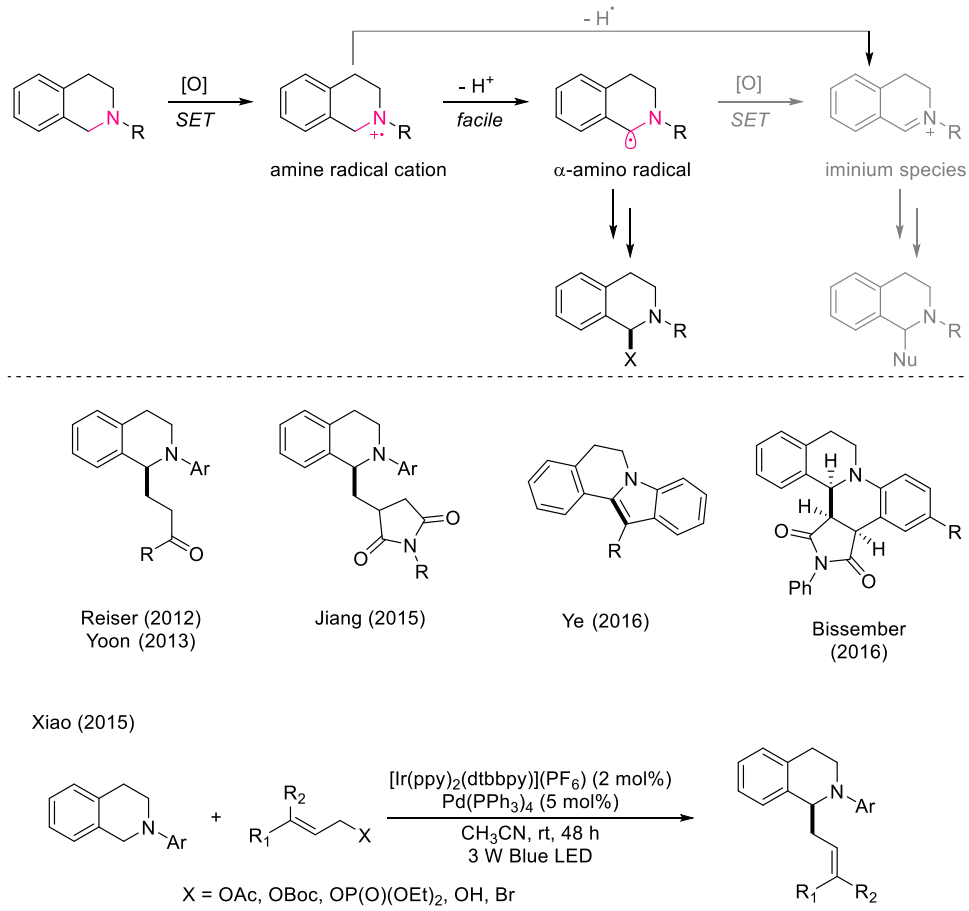

Scheme 4.5 Utilization of α-amino radical generated via photocatalytic SET of THIQ

The chemistry of α-amino radicals generated from SET via visible light photoredox catalysis proved much more prevalent in non-THIQ amine systems. (Scheme 4.6). As previously mentioned, the generated α-amino radical performs either a radical-radical (RR) coupling or a radical-acceptor (RA) coupling, depending on the reaction conditions and the nature of the coupling partner.

MacMillan reported the seminal work for the utilization of amines in the visible light photoredox catalysis in 2011.[21] This reaction was initially discovered by an accelerated serendipity strategy, and the detailed mechanistic scenario suggested the radical-radical coupling between α-amino radical and arene radical anion, which were generated via the SET by the photocatalyst. This RR coupling was expanded toward the alkynyl group by gold(I) photocatalyst by Hashimi.[22] The asymmetric C–C bond formation between an amine and an imine was achieved by Ooi via stabilization of the imine radical anion with a chiral cation species.[23] Xiao further expanded the scope of coupling partner into simple carbonyl compounds using $LiBF_4$ as a key additive.[24]

Much more variations were reported for the use of the RA coupling strategy, taking advantage of the abundant radical acceptors. Starting from conventional Michael acceptors,[25] several radical acceptors, including azodicarboxylate,[26] iso(thio)cyanate,[27] heteroarenes,[28] and vinyl sulfone,[29] provided new bond-forming reactions. Even the use of D_2O or T_2O for isotope-labeling of the organic compounds was possible,[30] and the construction of cyclic skeletons was demonstrated via either a cycloaddition[19,31] or an intramolecular RA coupling.[31a,32]

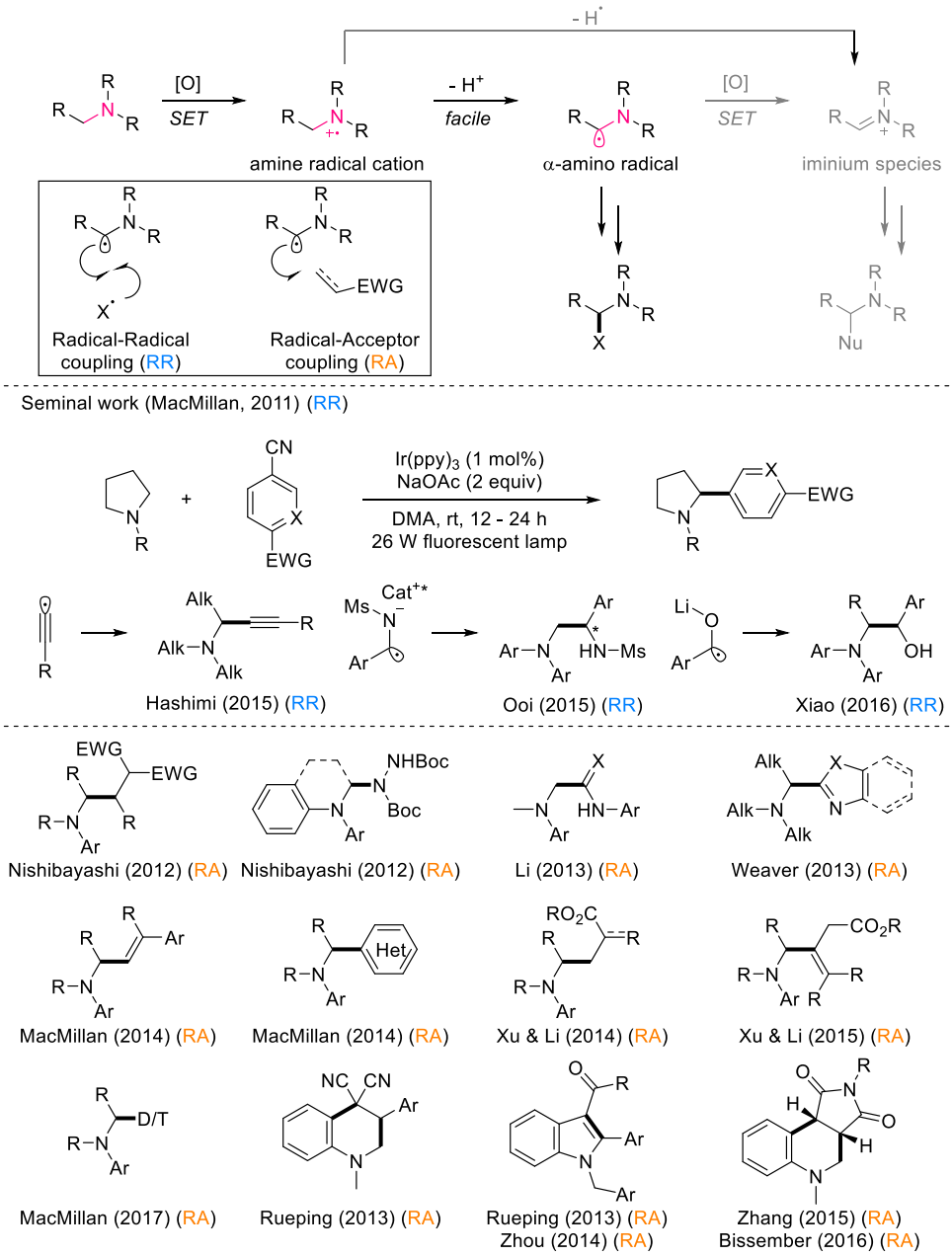

Scheme 4.6 Utilization of α-amino radical generated via photocatalytic SET of amines

The produced α-amino radical can involve in the transition-metal catalysis via the direct coordination to the metal center (Scheme 4.7). For instance, the target coupling partner was initially activated by the transition-metal catalyst via well-established elementary steps (e.g., oxidative addition, migratory insertion). Meanwhile, the visible light photoredox catalysis provides an α-amino radical intermediate in the reaction media, which directly binds to the metal center with the increase of the oxidation state. This process leads to the destabilization of metal-complex, which usually drives a reductive elimination to construct a new bond.

In 2016, Doyle utilized the strategy mentioned above using nickel(0) precatalyst and the anhydride species as the coupling partner.[33] Oxidative addition of Ni(0) into the C–X bond generates Ni(II) acyl complex, which would further react with α-amino radical to form Ni(III) acyl species. Facile reductive elimination achieved the direct acylation of amine at the α-position. A similar approach was demonstrated using aryl iodide as another coupling partner, enabling the direct arylation of amine.[34] In both cases, the choice of the supporting ligand for the nickel catalyst was critical to achieving the high efficiency of the reaction.

In 2017, Rovis combined the cobalt-catalysis with the α-amino radical chemistry, enabling the direct allylation of amines with diene species.[35] Initially formed Co(II) π-allyl complex reacts with the α-amino radical, providing reactive Co(III) species and engages in the facile reductive elimination.

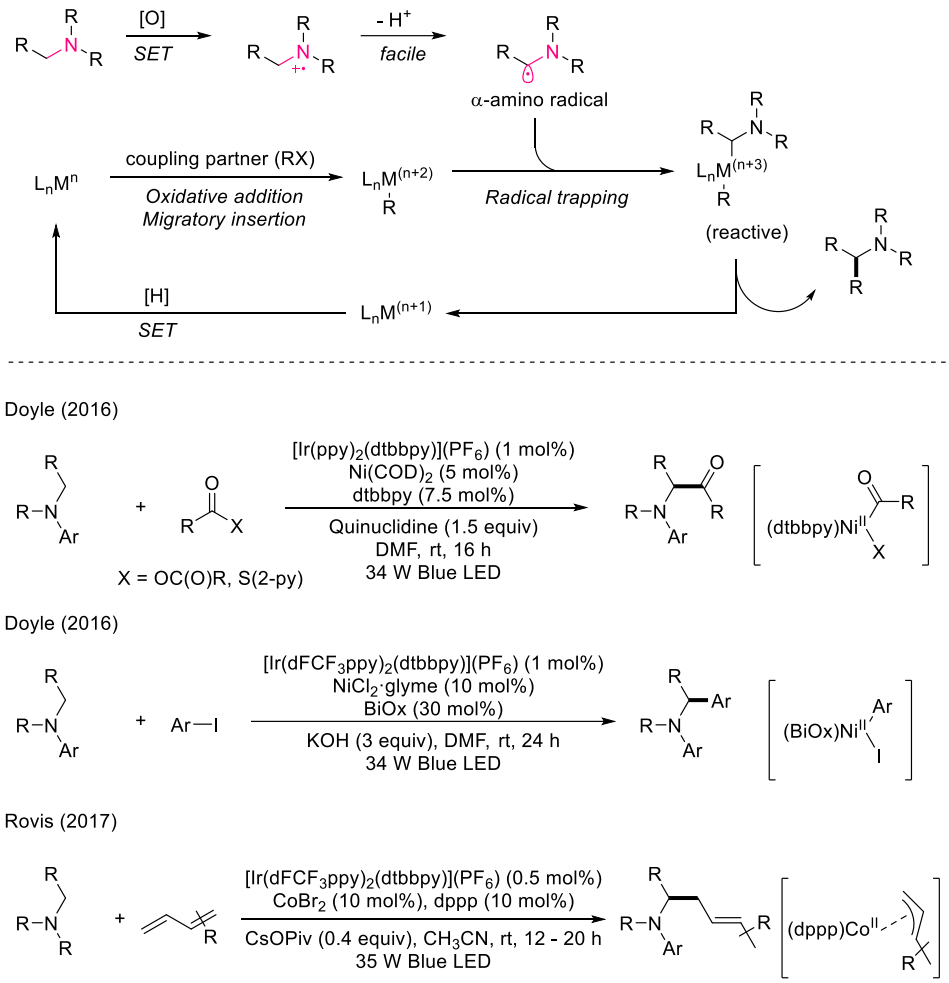

Scheme 4.7 Utilization of α-amino radical in the transition-metal catalysis

The generation of an iminium species from non-THIQ amines in visible light photoredox catalysis are less-developed, presumably because of the low stability of acyclic non-conjugated iminium species. Therefore, only a few examples were reported for this approach (Scheme 4.8). For example, Xiao realized the synthesis of substituted tetrahydroimidazoles via intramolecular trapping of iminium species under visible light irradiation conditions.[36] Rueping[37] and Li[38] independently provided a method to functionalize α-acyl amines with indoles via nucleophilic attack. In those systems, the generated imine is more stable than charged iminium species, so the intermolecular trapping with indole was possible. Very recently, Stodulski demonstrated the direct synthesis of imines from secondary aromatic amines via the visible light photoredox catalysis, suggested a mild and readily available protocol for the preparation of various imine species through an oxidation process.[39]

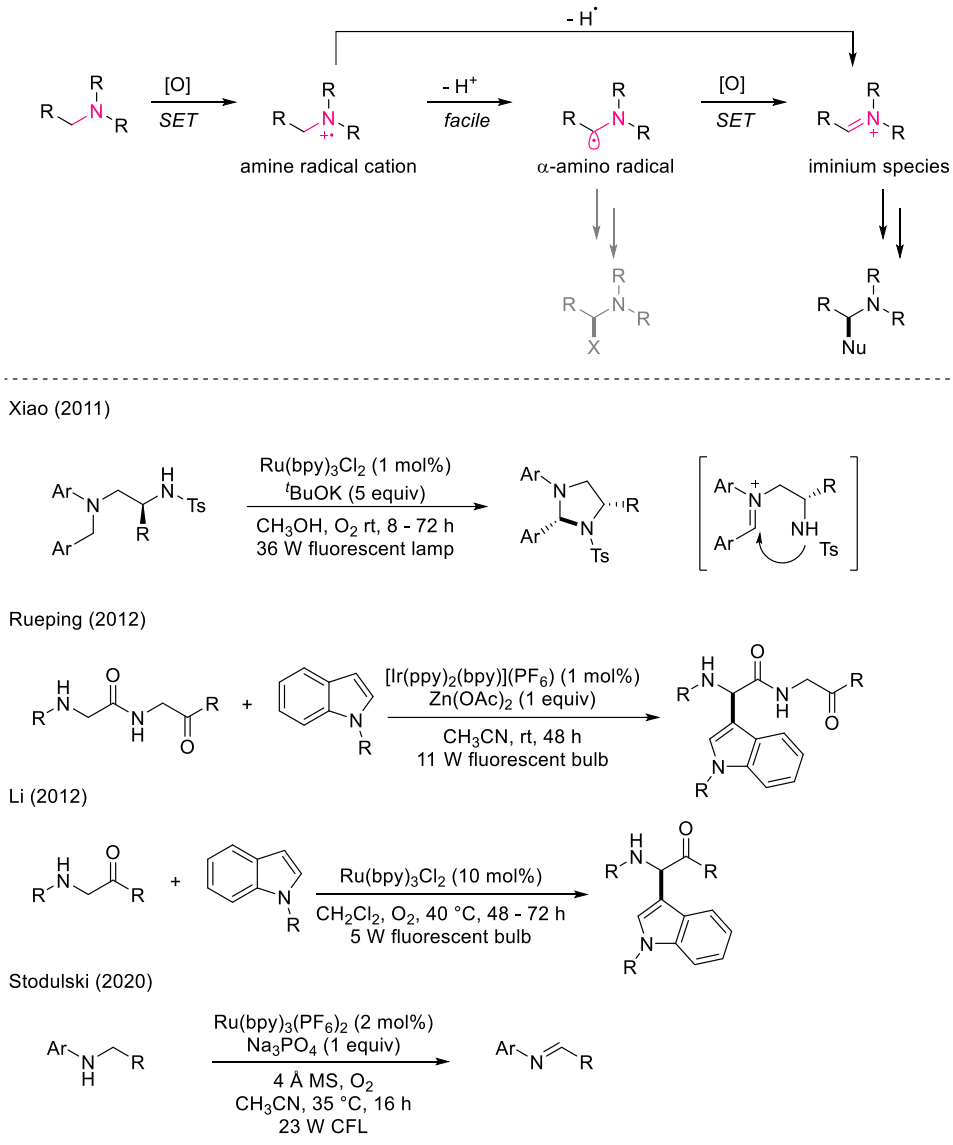

Scheme 4.8 Utilization of iminium species derived from non-THIQ amines

4.2.2 SET of π-systems

The direct single-electron oxidation of the π-system requires higher oxidizing power than amines (E_p^{ox}(toluene) = 2.36 V vs SCE in MeCN)[40]. Therefore, the choice of the photocatalyst is crucial to initiate the desired transformation. Visible light photocatalysts having strong oxidizing power, such as [Ir(dFCF$_3$ppy)$_2$(dtbbpy)](PF$_6$) (E^o(Ir(III)/Ir(II) = 1.69 V vs SCE in MeCN)[4c], Fukuzumi's acridinium-based photocatalyst ([Acr-Mes-Me](ClO$_4$), E^o(PC*/PC$^-$) = 2.18 V vs SCE in MeCN)[4e], and carbazole-based donor-acceptor photocatalyst (4CzIPN, E^o(PC*/PC$^-$) = 1.49 V vs SCE in MeCN)[41] are commonly applied in this type of transformation. Once SET and deprotonation are performed, relatively stable benzyl/allyl radical is generated, which offers a number of opportunities to perform new bond formation reactions.

In 2011, Stephenson firstly applied this strategy to conduct the deprotection of the benzyl group from ethers.[42] Lei introduced a molecular oxygen as a coupling partner, performing the direct oxygenation of the benzylic position.[43] Wu utilized a cobalt catalysis to induce a dehydrogenative C–C bond formation reaction, producing a functionalized isochroman.[44] Pandey accomplished an oxidative transformation using bromotrichloromethane (CCl$_3$Br) as an external oxidant, realizing the benzylic C–N bond formation with benzotriazoles.[45] Wu proposed a general protocol for the allylic/benzylic C–C bond formation with Michael acceptors under the visible light irradiation.[46] Recently, Glorius achieved the NHK-type coupling with simple olefinic compounds via SET strategy,[47] and this protocol was further modified by Kanai to achieve an asymmetric transformation in aid of chiral indane-BOX ligand.[48] Very recently, Xie and Zhu demonstrated a late-stage

trifluomethylthiolation at the benzylic position, which showed a high degree of regioselectivity among several types of activated C(sp^3)–H bonds.[49]

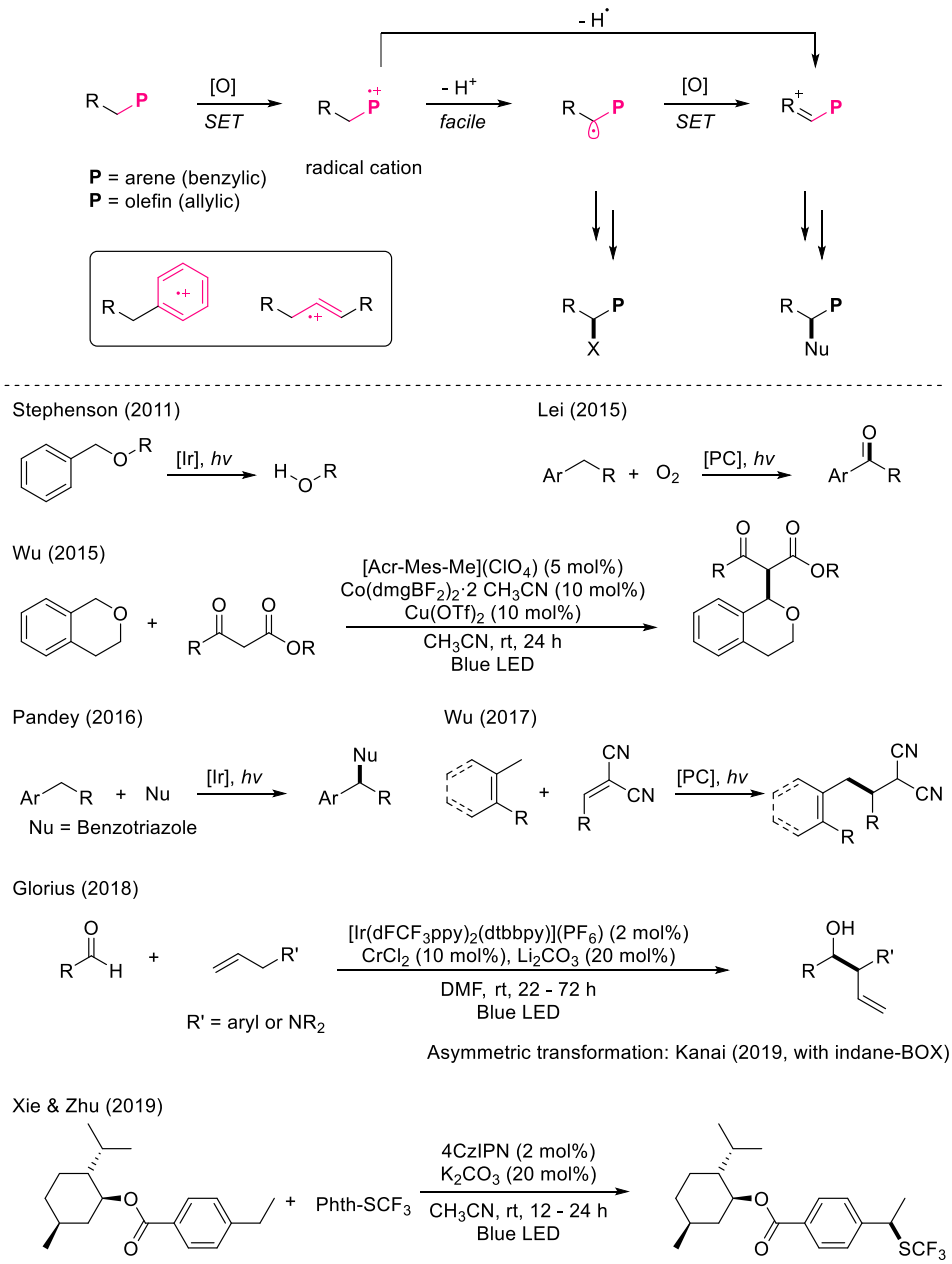

Scheme 4.9 C(sp^3)–H bond activation of allylic/benzylic position via SET

4.2.3 SET of conjugated heteroatoms

The direct single-electron oxidation of heteroatoms adjacent to the π-system leads to the deprotonation of the distal position. For example, SET of an enamine produced a radical cation, which conducts the facile β-deprotonation to generate an allyl radical. This enables the C(sp^3)–H bond cleavage of the distal position from the reaction center. In 2013, MacMillan demonstrated that the in situ generated enamine from carbonyl compound and secondary amine catalysts could be arylated at the β-position.[50] The robustness of the developed protocol enabled the related reactions by simply changing the coupling partners, such as aryl ketones[51], Michael acceptors,[52] and imines.[53] Very recently, Ooi utilized a silyl enol ether as a substrate, which undergoes a similar SET and β-deprotonation to produce a different type of an allyl radical intermediate.[54]

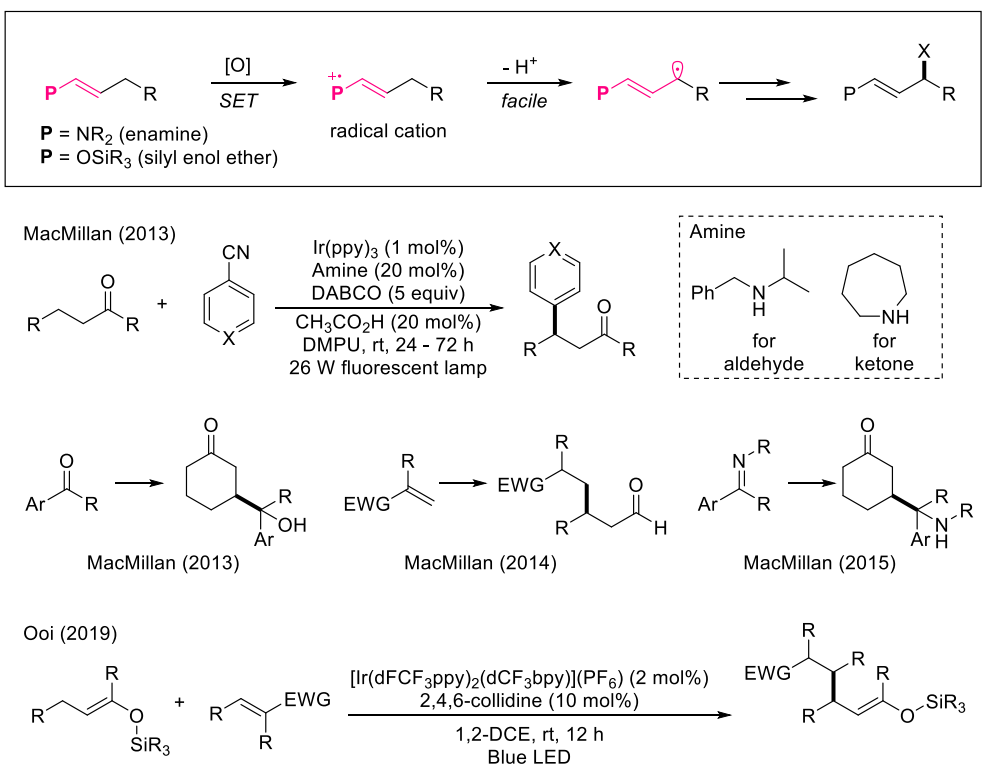

Scheme 4.10 C(sp^3)–H bond activation of via SET and β-deprotonation

4.3 C(sp^3)–H bond activation via hydrogen atom transfer (HAT)

The homolytic cleavage of the C(sp^3)–H bond via an external radical center can be achieved in a concerted manner, providing a carbon-centered radical species. This process, so-called hydrogen atom transfer (HAT), has been widely applied in both free-radical-based transformations[5e,55] and metal-oxo radical transformations.[56] This concept can be implemented into the visible light photoredox catalysis, which offers the formation of reactive radical species in a controlled manner (Scheme 4.11).[5c] The primary driving force of the HAT is the formation of stronger σ-bond than the parent C(sp^3)–H bond.[57] This feature of HAT clearly implies that the relatively activated C(sp^3)–H bonds, such as benzylic, allylic, and α-heteroatom C(sp^3)–H bonds, are much more prone to the direct functionalization under visible light photoredox catalysis. In contrast, the C(sp^3)–H bonds in the non-functionalized hydrocarbons having higher bond dissociation energies are more resistant to the reactions, so the limited examples have been established in those systems (Scheme 4.11).[58]

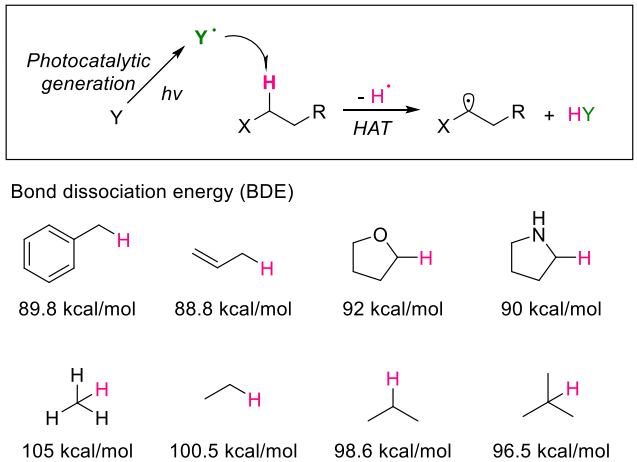

Scheme 4.11 C(sp^3)–H bond cleavage via HAT and typical bond dissociation energies of C(sp^3)–H bonds

4.3.1 HAT with oxygen-centered radicals

Oxygen-centered radical species have been extensively applied in the HAT process, due to the strong O–H bond (BDE of O–H bond in CH_3OH = 104 kcal/mol)[58] provides the sufficient thermodynamic driving force. One of the common oxygen-centered radical sources is the peroxide species, which contains a relatively labile O–O bond (BDE of O–O bond in CH_3OOCH_3 = 37.6 kcal/mol).[58] The cleavage of the peroxide can be achieved in two different pathways in the visible light photoredox catalysis (Scheme 4.12). The classical path involves the triplet-triplet energy transfer (EnT) process to induce the excitation of the peroxide molecule, which subsequently proceeds the homolytic cleavage to produce two equivalence of the radicals (path a). The other pathway follows a heterolytic cleavage from the radical anion state of the peroxide, which is generated via the SET with a photocatalyst (path b).

In 2015, Wang demonstrated the homolytic cleavage of *tert*-butyl hydroperoxide (TBHP) under visible light irradiation conditions.[59] Eosin Y organo-photocatalyst promotes the desired EnT, and the generated *tert*-butoxy radical performs the HAT at the ethereal C(sp^3)–H bond. Trapping of the carbon-centered radical with alkynes and the termination by another substrate provide an alkenylated product. Later on, an identical strategy was applied with the disulfide as a coupling partner, performing C–S bond formation reactions.[60]

Xie reported the use of TBHP as an oxygen-centered radical source via a heterolytic cleavage process.[61] The use of Ru-photocatalyst drives the SET to the TBHP, and the concurrent HAT and trapping with alkynes promotes radical cyclization reactions.

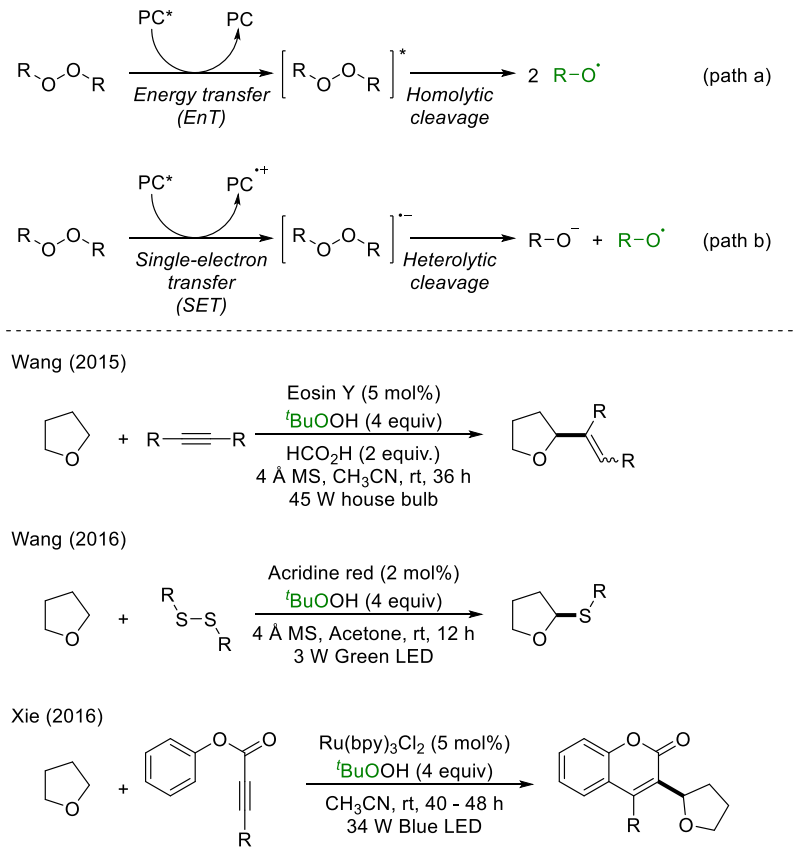

Scheme 4.12 Application of peroxide species in C(sp^3)–H bond cleavage via HAT

A peroxydisulfate ion (persulfate ion) is another class of oxidant, which can involve in the HAT process via the single-electron reduction (Scheme 4.13). This step induces a heterolytic cleavage, generating sulfate dianion and sulfate radical anion. Taking advantage of the ability of the parent peroxydisulfate and the generated sulfate radical anion as strong oxidants, the oxidative processes involving HAT of C(sp^3)–H bond have been reported. In 2012, Stephenson achieved an oxidative coupling of α-C(sp^3)–H bond of the amide with electron-rich aromatic species applying ammonium persulfate as a HAT reagent and an oxidant.[62] This HAT-based protocol was crucial to activate the amide molecule because the direct SET approach with the amide group is relatively challenging. MacMillan applied the strategy to cleave ethereal C(sp^3)–H bonds and achieved the visible light photocatalytic Minisci reaction.[63] Very recently, Wu expanded the scope of C–H bond species into the unactivated hydrocarbons, proving the superior reactivity of sulfate radical anion to cleave the strong C(sp^3)–H bonds.[64]

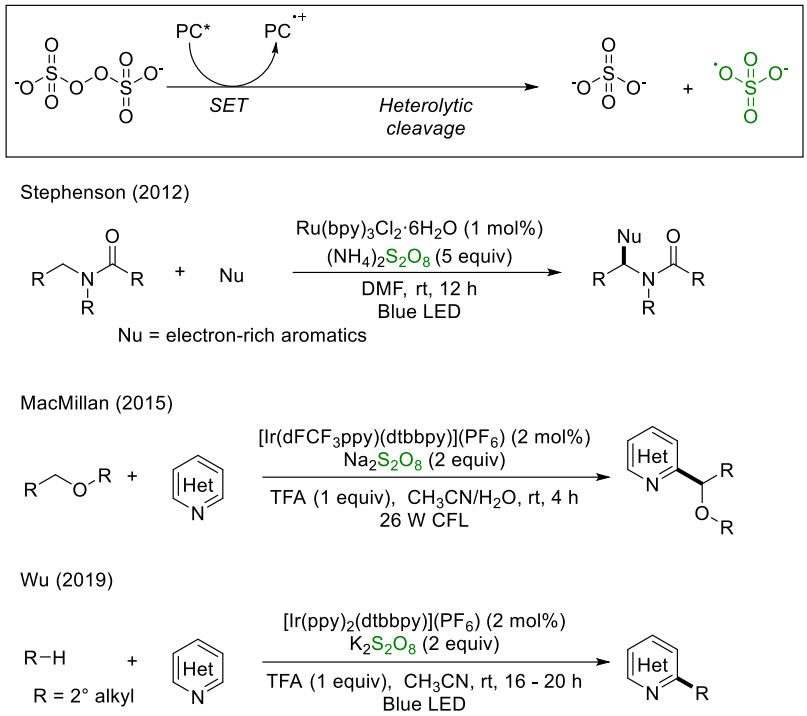

Scheme 4.13 Application of persulfate in C(sp^3)–H bond cleavage via HAT

The utilization of a carbonyl group as the oxygen-centered radical precursor has recently progressed (Scheme 4.14). The concept was initially inspired by the Norrish-Yang cyclization, which demonstrated the Norrish type II reaction via the photochemical excitation of the carbonyl group, an intersystem crossing to form diradical, 1,5-HAT at the distal C(sp^3)–H bond, and the radical-radical coupling to form 4-membered ring system (Scheme 4.14A).[65] From the mechanistic view of the 1,5-HAT by the diradical species, a catalytic utilization of the carbonyl group-containing visible light photocatalysts would induce the intermolecular HAT process, thereby the key carbon-centered radical intermediate would be generated (Scheme 4.14B).

In 2013, Chen firstly realized the proposed activation strategy to achieve the direct benzylic C(sp^3)–H fluorination.[66] In this case, 9-fluorenone was used as a visible light photocatalyst to perform HAT at the benzylic position directly, and further fluorination was accomplished through the reaction with Selectfluor. Wu proposed the possibility of Eosin Y photocatalyst as a direct HAT mediator, and an array of activated and unactivated C(sp^3)–H bond cleavage was performed.[67]

Recent examples introduced the transition-metal catalysis, further widening the scope of the coupling partner. Martin utilized a nickel catalysis to achieve C–C bond formation with aryl/alkyl bromides.[68] Gong showed the asymmetric C–C bond formation reaction using copper catalyst and chiral BOX ligand system, which mediate the coupling between a coordinating imine and the carbon-centered radical generated from the HAT by 5,7,12,14-pentacenetetrone photocatalyst.[69]

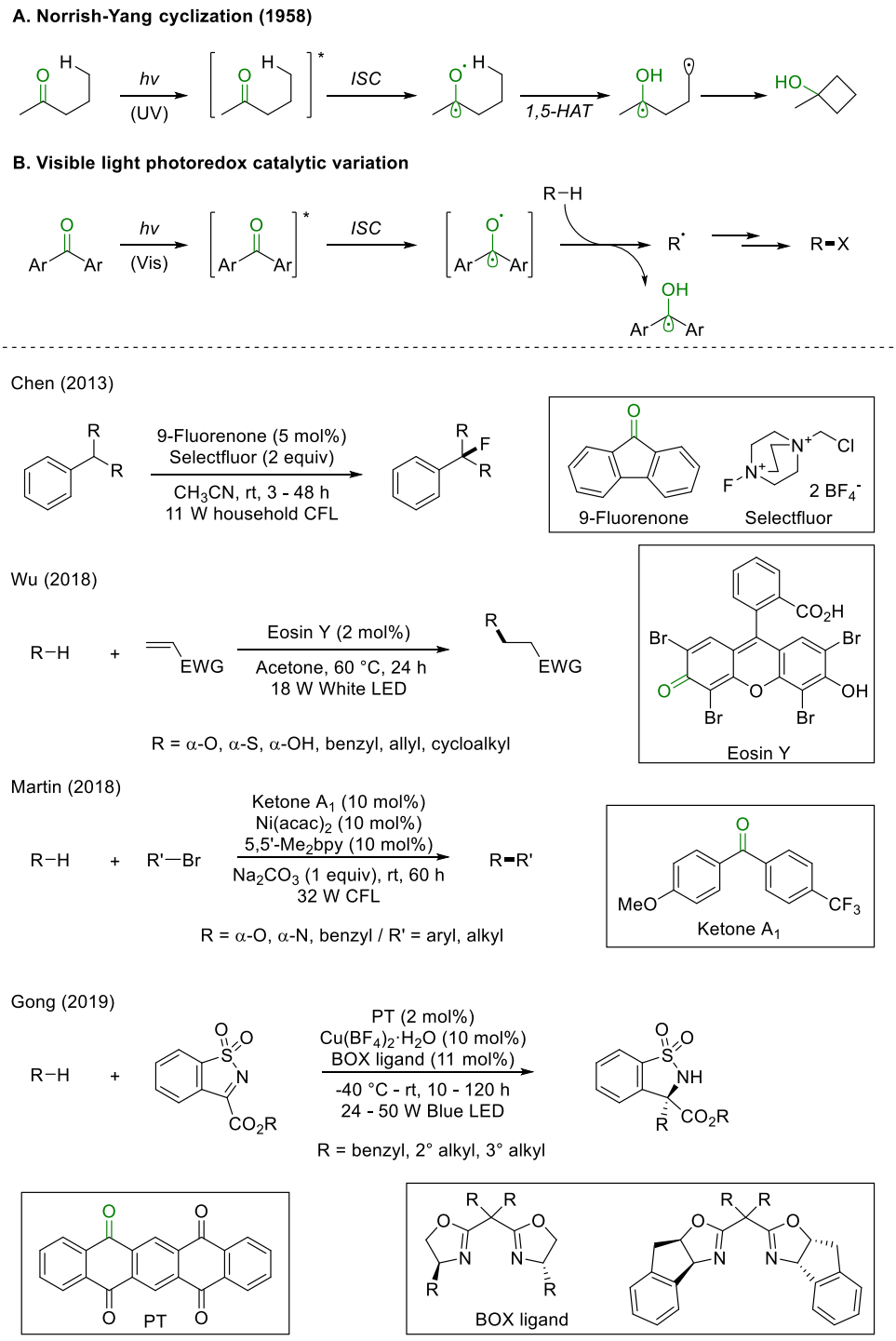

Scheme 4.14 Application of carbonyl group in C(sp^3)–H bond cleavage via HAT

Oxygen-containing molecules that do not have any internal weak bond (O–O bond/π-bond in C=O bond) require different activation strategies to be applied in the HAT process for the C(sp^3)–H bond functionalizations. For instance, the direct single-electron oxidation of anionic species, such as carboxylate and phosphate, can be an alternative pathway to produce the oxygen-centered radicals (Scheme 4.15). However, because of the high electronegativity of the oxygen atom, visible light photocatalysts having strong oxidizing power should be adopted. In 2016, Glorius utilized the benzoate anion as a HAT reagent via SET process, achieving the direct C(sp^3)–H trifluoromethylthiolation of the C–H bonds of various hydrocarbons.[70] Nicewicz and Alexanian developed a general protocol for the direct C(sp^3)–H azidation of unactivated hydrocarbons using a tailored sulfonyl azide.[71] In this case, the direct single-electron oxidation of hydrogen phosphate dianion with a highly reducible acridinium photocatalyst was necessary to generate the reactive phosphate radical anion species. An almost similar strategy was applied in the direct C(sp^3)–H cyanation at an α-heteroatomic position developed by Oisaki and Kanai.[72]

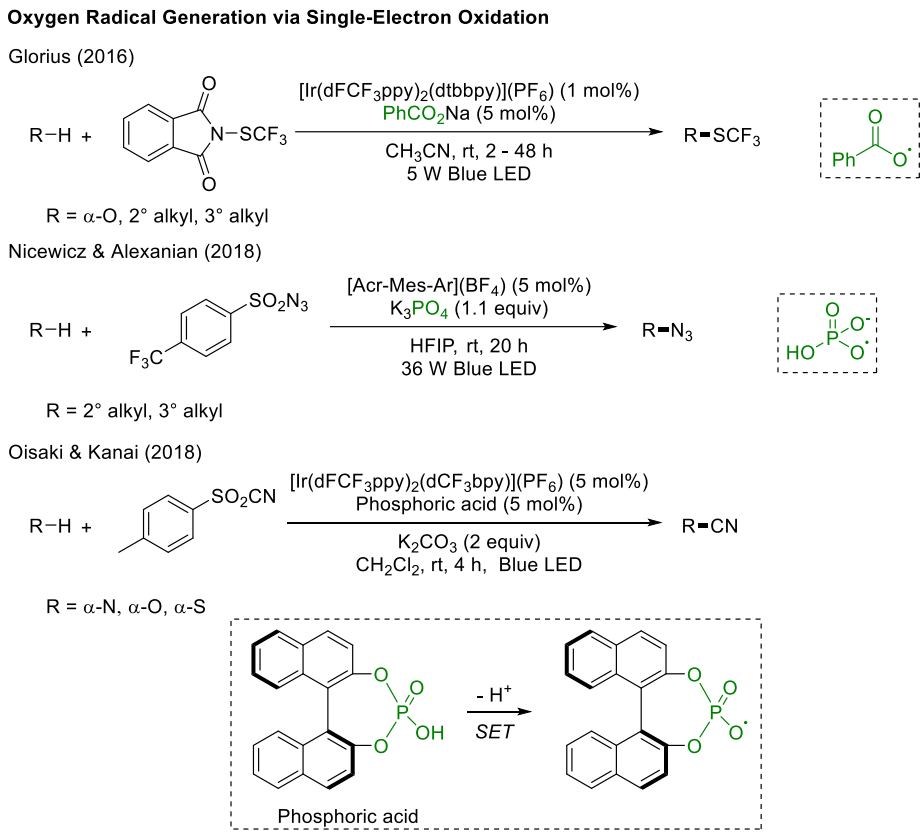

Scheme 4.15 Application of conjugate-bases after single-electron oxidation in C(sp^3)–H bond cleavage

Not only the single-electron oxidation process but also the single-electron reduction of the well-designed precursor induce the photoredox catalytic formation of oxygen-centered radicals. N-alkoxyphthalimide was known to perform the heterolytic fragmentation after the single-electron reduction, producing alkoxy radical and phthalimidate (Scheme 4.16A). This fragmentation process can be utilized in the functionalization of aliphatic alcohols via pre-installation of phthalimide moiety, photocatalytic activation of N–O bond, 1,5-HAT by generated alkoxy radical, and the functionalization of the remote C(sp^3)–H bond. The concept of fragmentation was initially proposed by Sammis in 2011,[73] and Chen first reported the application in the C(sp^3)–H bond functionalization in 2016.[74]

Very recently, Zuo introduced a ligand-to-metal charge transfer (LMCT) between cerium (IV) photocatalyst and alkoxide ligand, generating an alkoxy radical under visible light irradiation conditions (Scheme 4.16B). This strategy enabled the direct access toward the alkoxy radical from simple alcohol species without the use of any strong oxidants.[75] In 2018, this concept was utilized to achieve the challenging C(sp^3)–H bond functionalizations of gaseous hydrocarbon species, producing the corresponding amides.[76] Later on, the scope of the substrate was further expanded to the larger hydrocarbon species and Michael acceptors to perform C–C bond formation reaction, using methanol as a HAT reagent.[77]

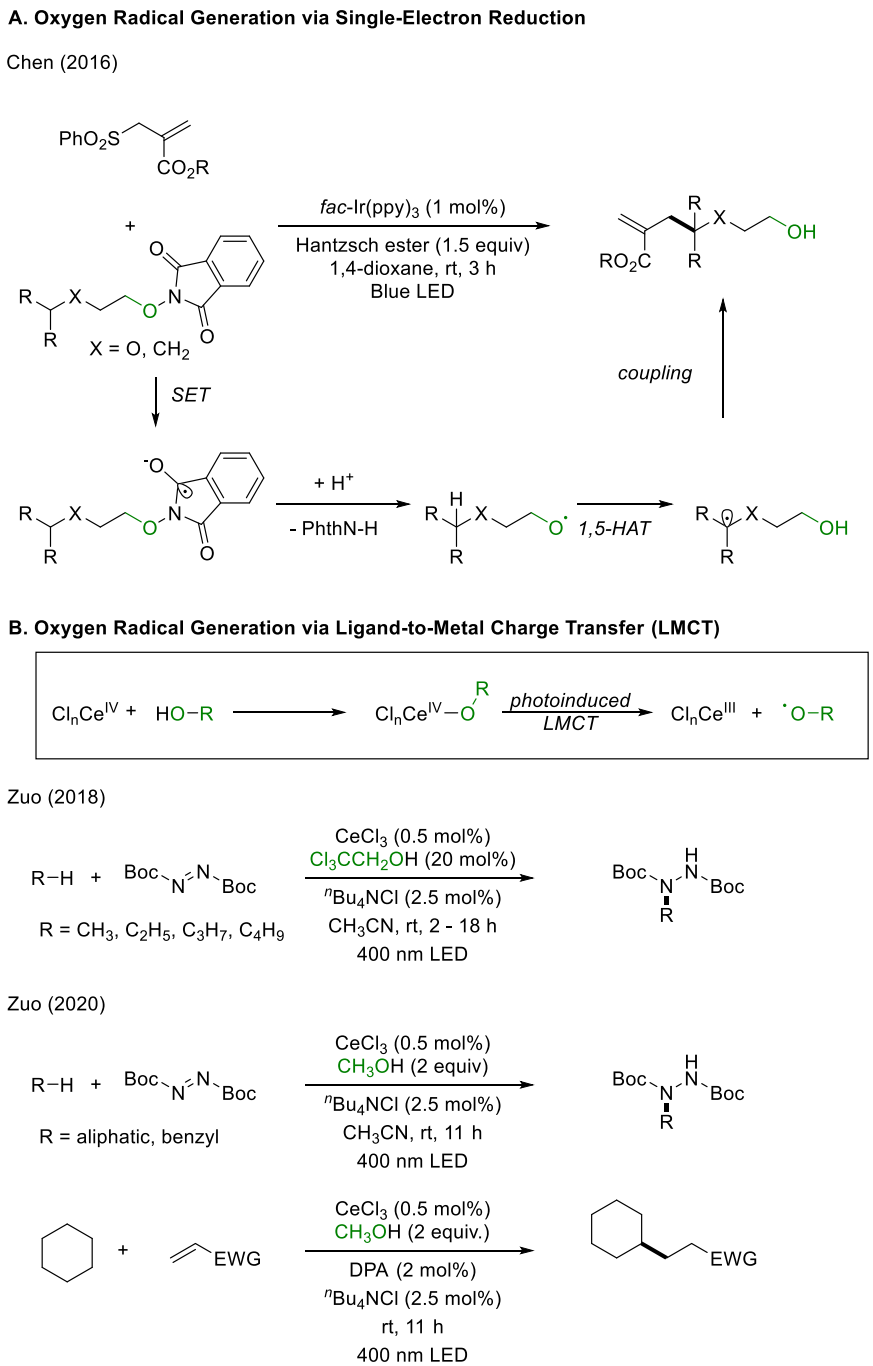

Scheme 4.16 Single-electron reduction and LMCT for the generation of oxygen-centered radicals

Some metal oxides have been known to be activated under the irradiation and provide a reactive site for HAT of the substrates. One of the well-known metal oxide species in the photocatalysis is decatungstate ($W_{10}O_{32}^{4-}$).[78] This metal catalyst can absorb the UV-region light (~324 nm) and becomes an excited state having the ability of either SET or HAT (Scheme 4.17). Although various utilizations of tetra-n-butylammonium salt of the decatungstate (TBADT) have been reported recently,[79] the requirement of the short-wavelength light limited the applications under the mild conditions. In contrast, uranium (VI) oxide (UO_2^{4-}) is reported to absorb the visible light region, which has the potential to be applied in a visible light photoredox catalysis (Scheme 4.17). A number of examples utilizing uranium (VI) oxide demonstrate the direct bond cleavage of either weak or strong C(sp^3)–H bonds. Sorensen reported the first investigation about this aspect of uranium (VI) oxide, choosing fluorination as a model reaction.[80] Very recently, Ravelli achieved the C–C bond-forming process applying Michael acceptor as a coupling partner.[81]

In addition to the use of the simple uranium (VI) oxide, utilization of well-defined ligated uranium complexes has been attempted. For example, Azam successfully synthesized a salen-ligated uranium (VI) oxide and confirmed its reactivity toward the direct cyanation of α-nitrogen C(sp^3)–H bond.[82] Arnold introduced a phenanthroline-type ligand and conducted oxidative process, such as catalytic dehydrogenation and oxygenation via the benzylic C(sp^3)–H bond cleavage.[83]

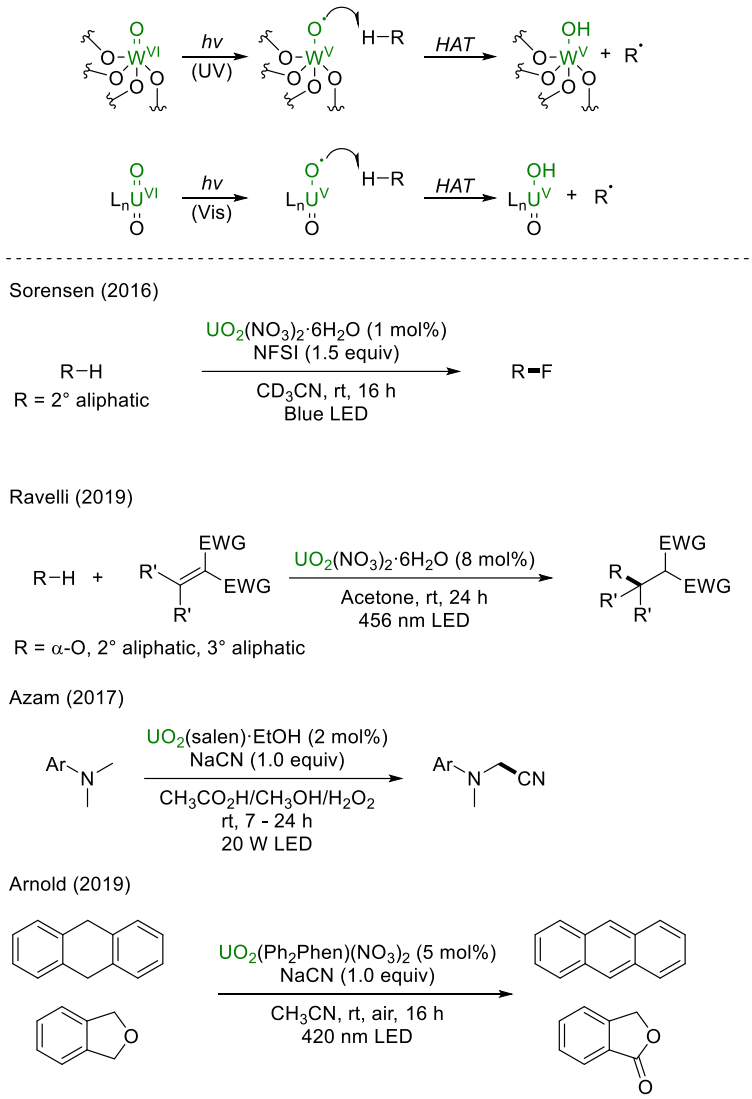

Scheme 4.17 Application of uranium (VI) oxide in C(sp^3)–H bond cleavage via HAT

4.3.2 HAT with nitrogen-centered radicals

A nitrogen-centered radical species serves as the efficient HAT reagent for the C(sp^3)–H bond cleavage, considering the bond dissociation energy of the parent N-H bonds. Both neural aminyl radicals (BDE of N–H bond in CH_3NH_2 = 101.6 kcal/mol)[58] and cationic aminium radicals (BDE of N–H bond in piperidinium cation = 100.8 kcal/mol)[58] provide the sufficient thermodynamic driving force for the HAT process. Several strategies for the utilization of such radical systems have been developed in the visible light photoredox catalysis.

One of the well-established strategies for the HAT by nitrogen-centered radicals is the utilization of Hofmann-Löffler reaction. Especially, the Suarez modification protocol is initiated by the formation of aminium radical intermediate via homolytic cleavage of N–X bond, selective 1,5-HAT via 6-membered cyclic transition state, a further transformation of carbon-centered radical such as halogenation and cyclization (Scheme 4.18).[84] This method was extensively employed in the visible light mediated catalytic transformations by many researchers to achieve much milder and readily available reactions.[85]

In 2016, Rovis[86] and Knowles[87] independently proposed a remote C(sp^3)–H bond functionalization using in situ generated amidyl radical directly from the corresponding NH-amides. Slightly different methods (single-electron oxidation and proton-coupled electron transfer, respectively) were applied for the generation of amidyl radical, but almost identical transformation was achieved in both cases. The modification of the solvent system (DMF/*tert*-AmylOH) enabled the γ-alkylation of amide,[88] and the incorporation of heteroarenes via the Minisci-type approach was also demonstrated[89].

Hofmann-Löffler reaction: Suarez modification

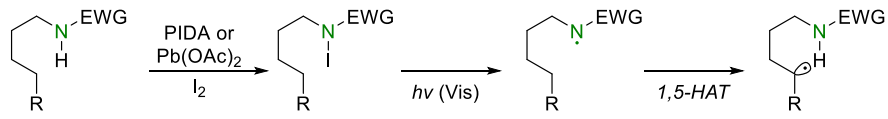

EWG = NO_2, CN, $P(O)(OR)_2$, SO_2R, CBz, Boc

Muñiz (2015) - catalytic I_2, visible light
Yu (2015) - N–Cl, with Ir photocatalyst
Nagib (2016) - catalytic NaI, visible light
Muñiz (2016) - NIS as a sole reagent, visible light

Rovis (2016) / Knowles (2016)

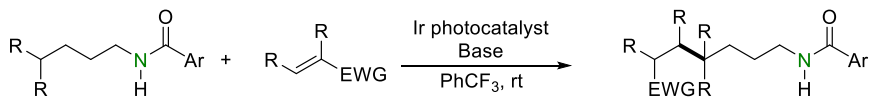

Rovis - $[Ir(dFCF_3ppy)_2(dtbbpy)](PF_6)$, K_3PO_4, Ar = CF_3
Knowles - $[Ir(dFCF_3ppy)_2(dCF_3bpy)](PF_6)$, $NBu_4OP(O)(OBu)_2$, Ar = PMP

Rovis (2017)

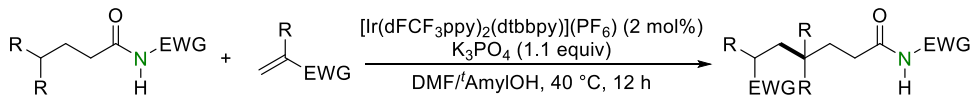

Yuan & Yu (2019)

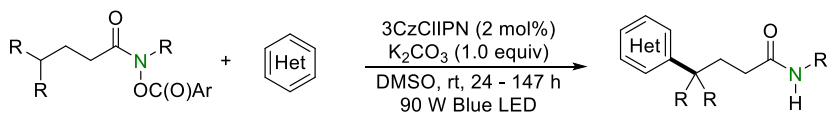

Scheme 4.18 Application of Hofmann-Löffler type strategy in intramolecular C(sp^3)–H bond cleavage via HAT

The intermolecular variation of the strategy mentioned before was also possible (Scheme 4.19). Mechanistically, either the homolytic cleavage of a pre-functionalized N–X bond under visible light irradiation or the single-electron oxidation of a deprotonated amide produces reactive amidyl radical. The intermolecular HAT of the C(sp^3)–H bond generates the desired carbon-centered radical, which undergoes various radical transformations.

Alexanian applied this concept to develop amide-based radical functionalization reagents for unactivated aliphatic compounds. Implementation of the electron-deficient aromatic group promotes the homolytic cleavage of the N–X bond, and the sterically-hindered substituent on the nitrogen enhanced the regioselectivity for the HAT process. With the developed platform, the direct bromination,[90] chlorination,[91] and xanthylation[92] of aliphatic hydrocarbons were accomplished.

The well-designed NH-amides showed the possibility as a HAT catalyst, in combination with the repetitive deprotonation, SET, and HAT. Oisaki and Kanai introduced the sulfonamide group to increase the acidity of NH-proton, so the catalytic utilization of the developed molecule as a HAT catalyst was possible.[93] Very recently, Ooi synthesized a zwitterionic form of amide bearing a triazolium moiety, which provides a relatively stabilized ionic precursor for the single-electron oxidation and HAT.[94]

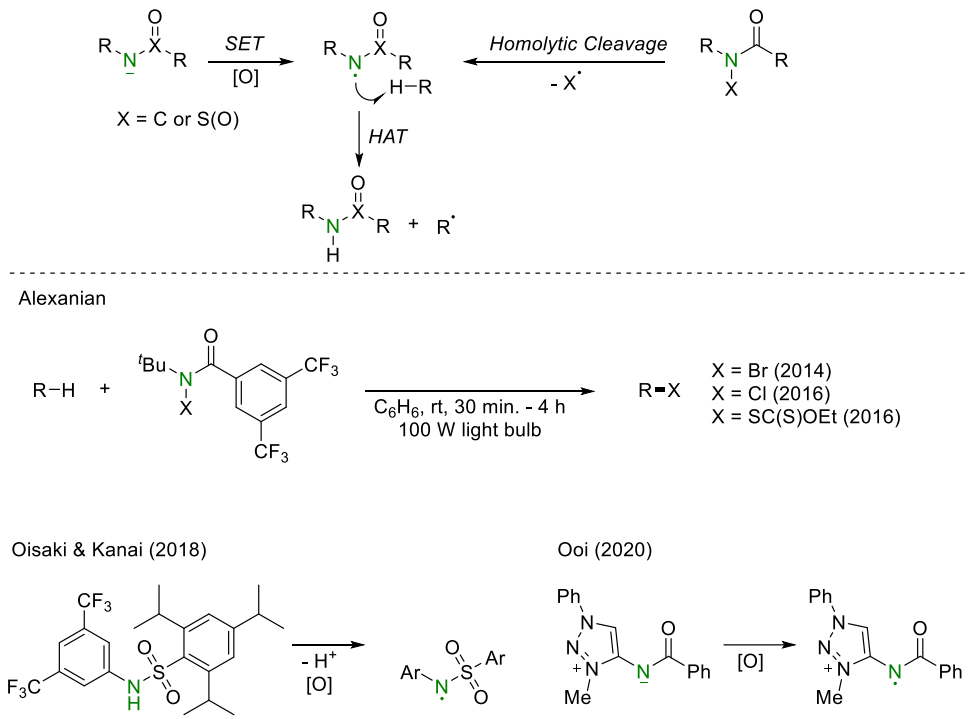

Scheme 4.19 Application of Hofmann-Löffler type strategy in intermolecular C(sp^3)–H bond cleavage via HAT

Other types of nitrogen-centered radicals can achieve the remote-intramolecular 1,5-HAT. For instance, several imine precursors can be transformed into the iminyl radical under visible light photoredox catalysis, which offers an appropriate thermodynamic driving force (BDE of N–H bond in diphenylmethanimine = 117 kcal/mol)[58] (Scheme 4.20). In 2017, Nevado utilized the carbonate-substituted imine precursor in the visible light photoredox catalysis, and the single-electron reduction generates the iminyl radical and carbonate anion.[95] Subsequent 1,5-HAT and radical cyclization were performed to create a cyclic ketone as a product. A similar approach was demonstrated in the formation of new C–C bond at a remote position by Duan.[96] Fu proposed a direct excitation of the substrate by visible light irradiation enabled by donor-acceptor interaction, and the following HAT and ionic coupling provided substituted imidazolines.[97] Nagib developed an interesting protocol for the synthesis of 1,2-amino alcohols via the formation of an NH-imine with an alcohol and an electron-deficient cyanide, the production of N–I bond under the oxidative conditions, and the generation of iminyl radical followed by 1,5-HAT.[98] The hydrolysis of the synthesized oxazolines gives the synthetically useful 1,2-amino alcohols.

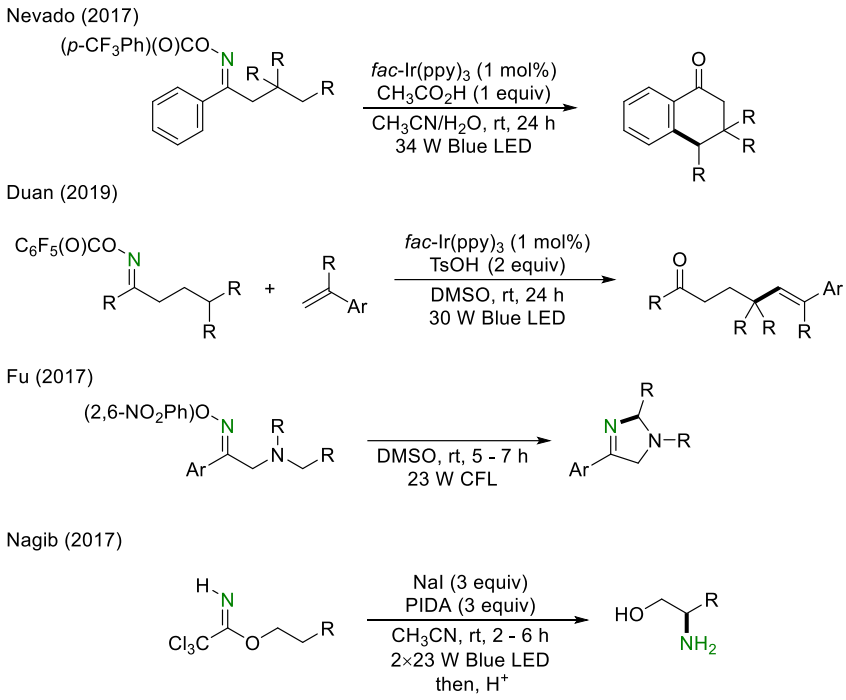

Scheme 4.20 Application of iminyl radical precursors in intramolecular C(sp^3)–H bond cleavage via HAT

Aminium radical (amine radical cation) has a huge potential to act as a HAT reagent, taking advantage of its accessibility via the single-electron oxidation of amines. However, the generated amine radical cation can undergo undesired side-reactions such as the facile deprotonation to generate α-amino radical intermediate (Scheme 4.21).[6a,7a,99] This limitation was overcome by a stereoelectronic modulation of amines to prevent the side reactions. Quinuclidine has been chosen as the optimal structure for the utilization as a HAT reagent. After the formation of aminium radical of quinuclidine, further deprotonation at the α-position was prohibited due to the reduced overlap between p-orbital of nitrogen and the σ-orbital of the C–H bond. Moreover, the generated α-amino radical is structurally unstable, so the transformation itself is thermodynamically unfavored. This aspect of quinuclidine enabled the wide ranges of the C(sp^3)–H bond cleavage and functionalization under visible light photoredox catalysis conditions.

An initial report by MacMillan in 2015 demonstrated the direct alkylation of the primary alcohol at the α-position, in a combination of subsequent cyclization to produce lactone.[100] The scope of the substrate was further extended to electron-deficient amines[101] and primary amines,[102] together with the use of alkyl/aryl bromides,[103] Michael acceptors,[104] and perfluoroarenes[105] as the coupling partners. The significant property of quinuclidine as a HAT catalyst was demonstrated by MacMillan in 2017,[106] showing the high degree of regioselectivity toward the most hydridic hydrogen based on the polarity-match principle in the HAT process.

Selectfluor, which is usually utilized as an electrophilic fluorinating reagent, can be used in the HAT reaction in a similar manner. The direct single-electron reduction provides a corresponding aminium radical and fluoride, and those intermediates underwent either the direct C(sp^3)–H fluorination[107] or another type

of ionic transformation.[108]

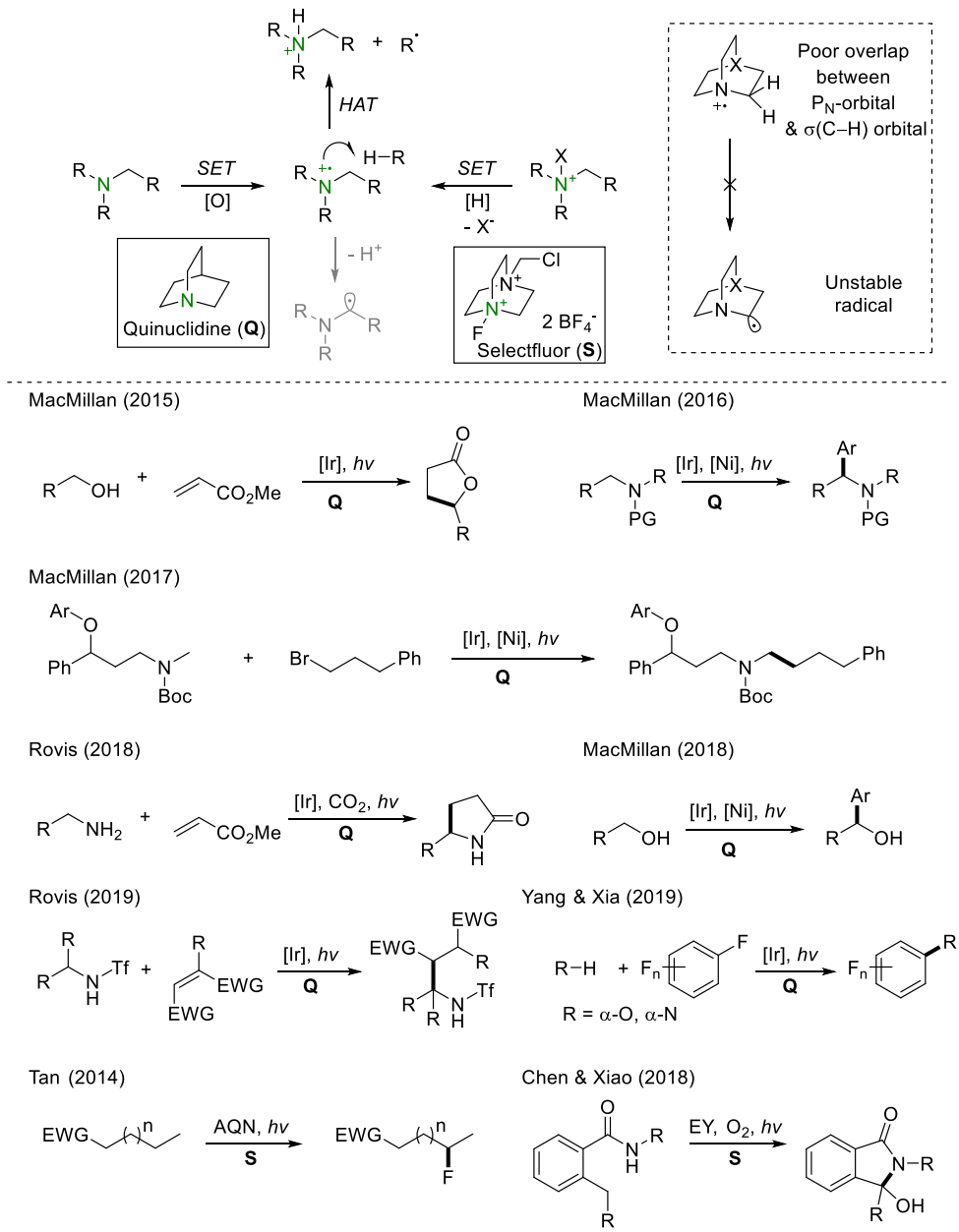

Scheme 4.21 Application of aminium radical in C(sp^3)–H bond cleavage via HAT

4.3.3 HAT with sulfur-centered radicals

Unlike the other types of heteroatom-centered radicals, sulfur-centered radical offers a relatively small thermodynamic driving force, because of the weak S–H bond (BDE of S–H bond in CH_3SH = 87.4 kcal/mol).[58] However, this property provides an opportunity to selectively cleave the weak C(sp^3)–H bond in the C–H bond-rich systems. The reactive thiyl radicals can be generated via the direct single-electron oxidation or the proton-coupled electron transfer of the thiol functionality. Several thiol structures were known to be efficient in the visible light photoredox catalysis (Scheme 4.22).

In 2014, MacMillan firstly demonstrated the potential of the thiyl radical in the C(sp^3)–H bond functionalization of benzylic ethers with electron-deficient arenes.[109] A similar strategy can be applied in the reaction with aromatic imines[110] or the heteroaromatic compounds.[111] Benzylic amines were also reactive under the reactions with the thiol HAT catalyst, providing the substituted pyrrolidines[112] or tetrahydroisoquinolines.[113]

In 2015, MacMillan reported a seminal work in the allylic C(sp^3)–H bond functionalization using thiol as a HAT catalyst.[114] In this case, the use of relatively bulky thiol is required to prevent the facile hydrothiolation reaction with an olefin. Liu later proposed the aromatic ketones as alternative coupling partners, achieving the carbonyl addition reaction with unactivated olefins using other bulky thiol HAT catalysts.[115]

A number of more challenging C(sp^3)–H substrates began to be functionalized by sulfur-centered radicals in recent days. König showed that the simple benzylic substrates could be activated by a thiyl radical, performing the carboxylation with

CO_2.[116] Kanai demonstrated the acceptorless dehydrogenation of tetrahydronaphthalenes[117] and alcohols[118] via the merger of the visible light photoredox catalysis, the transition-metal catalysis, and the HAT catalysis.

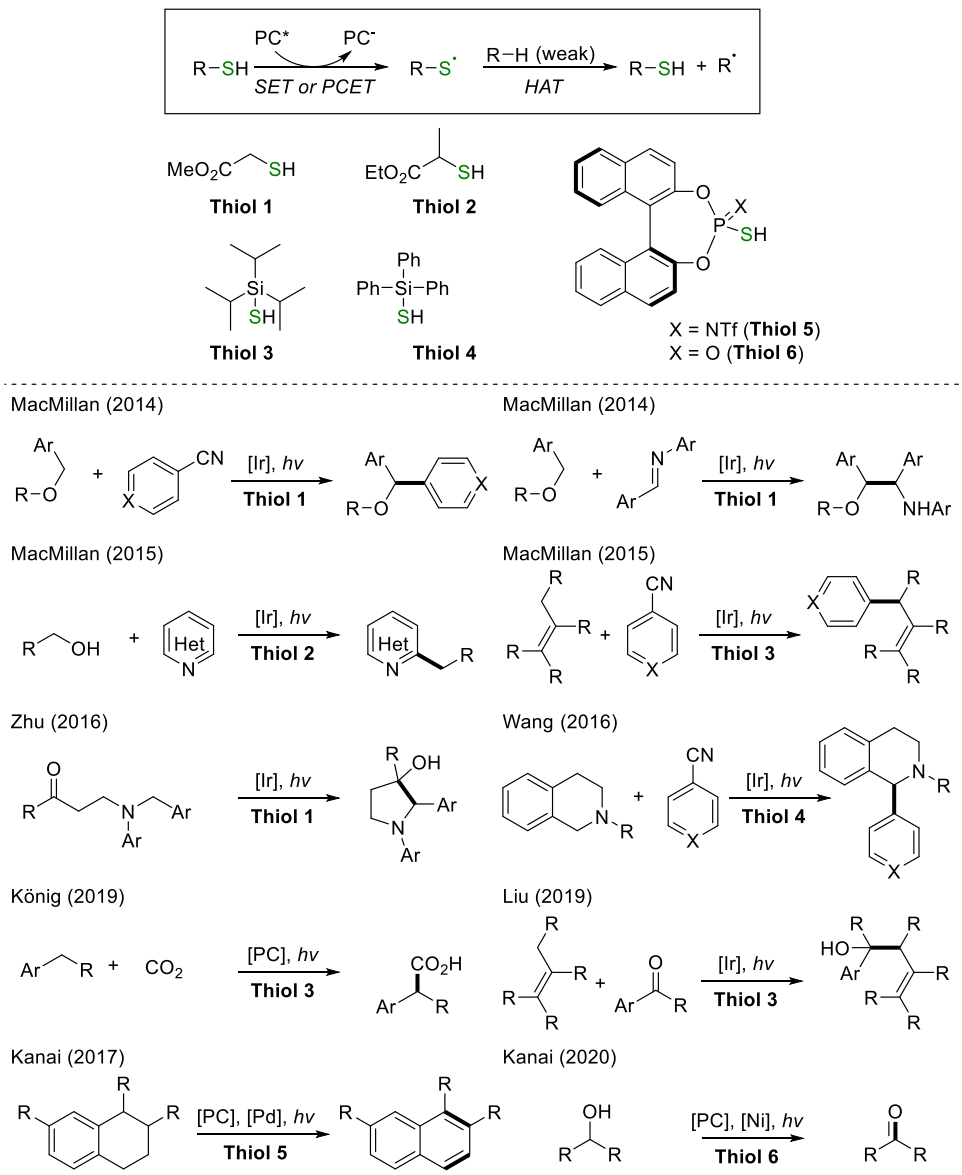

Scheme 4.22 Application of thiyl radical in C(sp^3)–H bond cleavage via HAT

4.3.4 HAT with halogen-centered radicals

The use of halogen-centered radicals in the C(sp^3)–H bond cleavage is a classical protocol to achieve halogenated molecules directly from the hydrocarbon feedstocks and the synthetic intermediates. Especially, free-radical chlorination[55] and bromination[119] have been frequently applied in the organic synthesis, which provides useful synthetic building blocks. However, the control of selectivity is a longstanding challenge, which is directly related to the concentration of reactive radical species. Recent examples in visible light photoredox catalysis suggested that the formation of halogen-centered radical can be controlled under mild reaction conditions.

Chlorine radical has a strong affinity toward the hydrogen atom, considering the BDE of hydrogen chloride (103.2 kcal/mol).[120] The generation of the catalytic amount of chlorine atom under visible light photoredox catalysis has been generally achieved by photoexcitation of a nickel (III) chloride complex, which was pioneered by Nocera[121] (Scheme 4.23). This elementary step was first applied in the catalytic transformation by Doyle, achieving the direct arylation of ethers with aryl chloride.[122] After the oxidative addition, the produced Ni(II) chloride was oxidized by visible light photocatalyst, and further irradiation of the Ni(III) chloride expels the reactive chlorine radical, which can undergo HAT of C(sp^3)–H bond (Scheme 4.23). Doyle further utilized the concept for the synthesis of aldehydes using 1,3-dioxolane as a carbonyl source.[123]

Acyl chloride can participate in the reaction as a coupling partner and a chlorine atom source. Kumagai and Shibasaki developed the direct acylation of ethers with acyl chlorides with nickel (II) precatalyst.[124] Doyle independently

proved that the protocol could be extended to the simple hydrocarbons using nickel (0) precatalyst.[125]

A similar strategy can be operative without using an external chloride-containing coupling partner. Wu devised a catalytic cycle using nickel (II) chloride precatalyst, which enabled the direct alkylation of alkyne with the activated C(sp^3)–H partners only using a catalytic amount of chlorine source.[126] Hong introduced the silyl-protected ynones and ynamides as coupling partners to control the regioselectivity and *E*/*Z*-selectivity of the addition of alkyl radicals.[127]

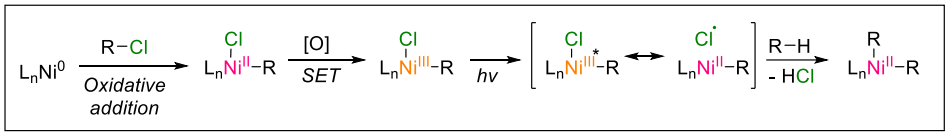

Doyle (2016)

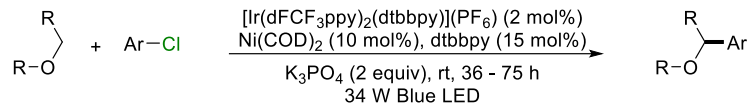

Doyle (2017)

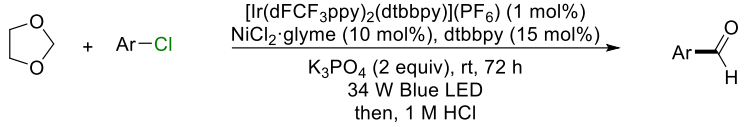

Kumagai & Shibasaki (2017)

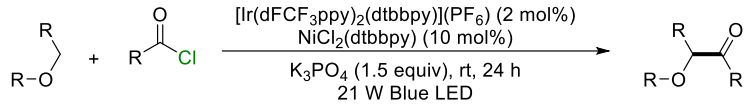

Doyle (2018)

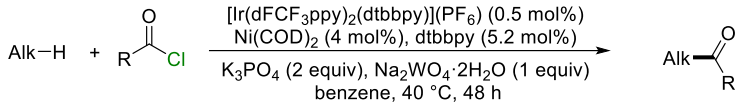

Wu (2017)

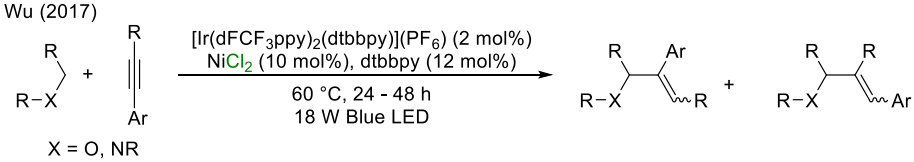

Hong (2018)

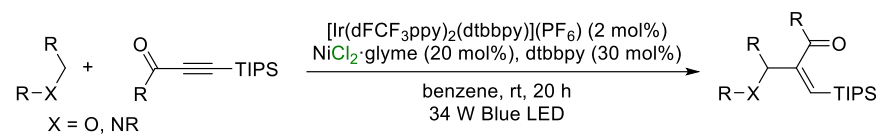

Scheme 4.23 Application of chlorine radical generated from the photoexcited Ni(III) chloride

Attempts to utilize the free chlorine radical generated via the direct single-electron oxidation of a chloride anion have been demonstrated in a few examples (Scheme 4.24). An early example reported by Fukuzumi posed a potential of the suggested strategy by using highly reducible organic photocatalyst, but the efficiency was only moderate in a limited substrate.[128] In 2018, Wu realized a practical application of chlorine radical generated form a catalytic amount of HCl, achieving the C–C bond formation with Michael acceptors.[129] This report applied a flow reactor system to minimize the side reactions derived from the radical species and maximize the irradiation efficiency. Barriaults implemented the chloride anion into the photocatalyst, so the use of highly acidic and gaseous HCl was avoidable.[130]

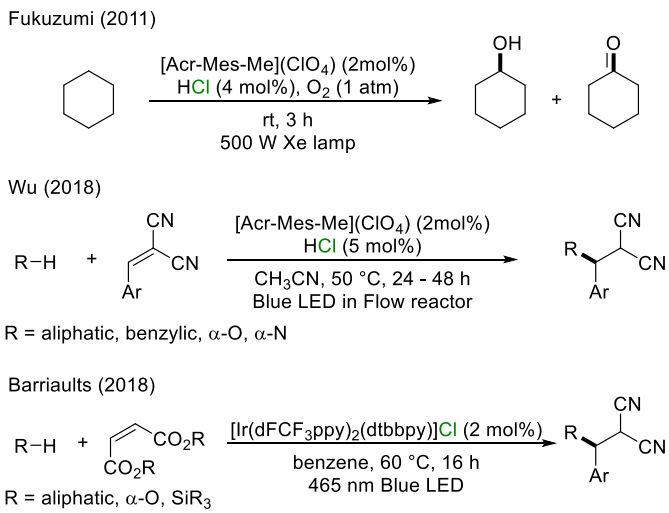

Scheme 4.24 Application of chlorine radical generated from the chloride anion

Bromine atom has a similar thermodynamic driving force to that of S-centered radicals (BDE of HBr = 87.6 kcal/mol)[120], so the selective C(sp^3)–H bond functionalizations have been developed. Although several examples demonstrated the functionalizations of activated C(sp^3)–H bonds, the detailed mechanism for the generation of bromine radical varies, depending on the reaction conditions (Scheme 4.25). In the initial report by Molander, which demonstrated the direct arylation of ethers with aryl bromides, the production of bromine radical proceeded via energy transfer from the excited photocatalyst to nickel (II) bromide complex, producing the excited state of Ni(II) bromide (Scheme 4.25, path a).[131] This species expels the bromine radical, which further undergoes HAT of the weak C(sp^3)–H bond. In this study, the direct HAT by nickel-bound bromine center in a concerted manner is not completely excluded. In the later example demonstrated by Rueping, the direct arylation of allylic C(sp^3)–H bond was performed in a similar mechanism.[132]

In 2019, Lu developed an asymmetric arylation of benzylic C(sp^3)–H with aryl bromides, in a combination of chiral ligand/nickel catalysis system.[133] The mechanism for the bromine radical generation was proposed as the single-electron oxidation of Ni(II) bromide and the facile bromine radical extrusion from Ni(III) bromide (Scheme 4.25, path b).

Very recently, Ishida and Murakami developed a dehydrogenative coupling of aldehyde and benzylic C(sp^3)–H bond using nickel (II) bromide precatalyst.[134] The free bromide anion is generated via single-electron reduction of precatalyst. Further single-electron oxidation of the anion provides bromine radical, which can undergo HAT of both benzylic C(sp^3)–H bond and aldehyde C(sp^2)–H bond (Scheme 4.25, path c).

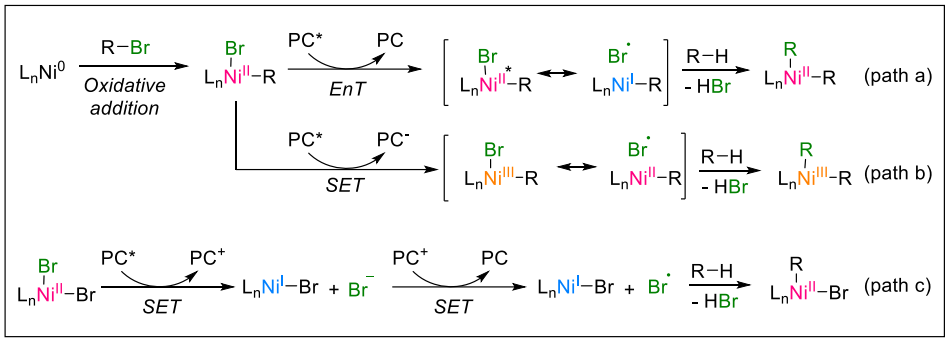

Molander (2016, path a)

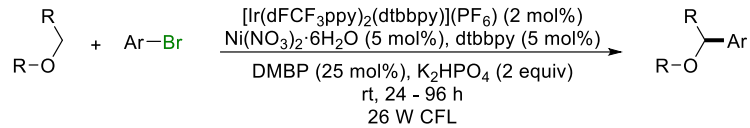

Rueping (2018, path a)

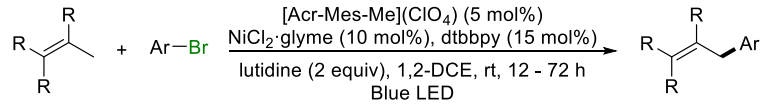

Lu (2019, path b)

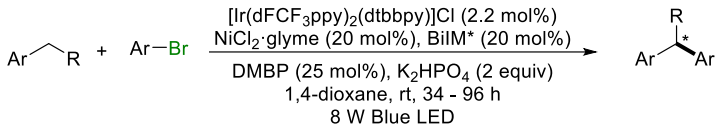

Ishida & Murakami (2020, path c)

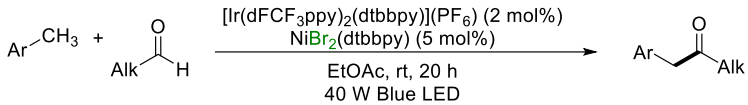

Scheme 4.25 Application of bromine radical generated from the Ni(II) bromide

4.3.5 HAT with carbon-centered radicals

$C(sp^3)$–H bond cleavage via HAT by carbon-centered radicals has been limitedly explored, due to the small thermodynamic driving force and the polarity-mismatch situation. In the reported cases, this problem was generally overcome by the production of an electrophilic carbon-centered radical, which has relatively strong $C(sp^3)$–H bond in the closed-shell form and fulfills the polarity-match principle for the facile HAT steps.[135]

One of the utilized carbon-centered radicals is halogen-substituted carbon-centered radicals. Those species exhibit the high bond strength (BDE of C–H in $CHCl_3$ = 93.8 kcal/mol, BDE of C–H in $CHBr_3$ = 95.4 kcal/mol)[58] and the high electrophilic character at the carbon center by the effect of electronegative halogen atoms. Li demonstrated the generation of this type of carbon-centered radical via single-electron reduction of halomethanes, achieving the deprotection of alcohol[136] and the bromination at the benzylic position.[137]

Aryl radical is also a prominent candidate for the HAT of $C(sp^3)$–H bond, considering the BDE of the $C(sp^2)$–H bond (BDE of C–H in benzene = 112.9 kcal/mol)[58] The major hurdle in the practical use is the generation of the aryl radical in the reaction media, which is relatively challenging due to the instability of the aryl radical. Qi and Zhang applied the in situ formed arene diazonium salt as an aryl radical precursor and conducted the 1,5-HAT to perform alkoxylation.[138] Hong devised a novel strategy to generate the aryl radical from the nickel (II) acyl thiolate species via decarbonylation and fragmentation, achieving the thioesterification of ethereal $C(sp^3)$–H bonds.[139]

A recent example reported by Hong provides an enone system as a promising

carbon-centered radical source for the HAT of weak C(sp^3)–H bonds. The energy transfer from the iridium photocatalyst to the nickel-bound enone generates the triplet diradical, which possesses an electrophilic α-acyl radical position. HAT of weak C(sp^3)–H bonds with the radical and further trapping of radical intermediates by nickel (II) catalyst proceeds the formal Giese addition.[140]

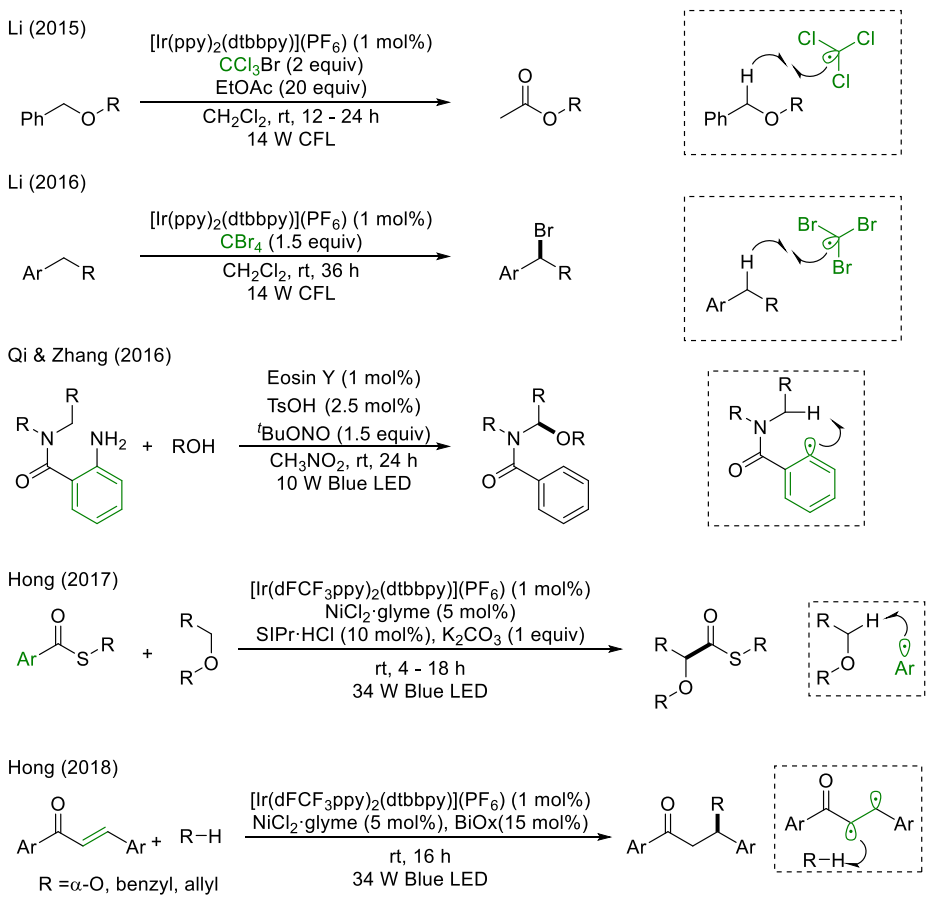

Scheme 4.26 Application of carbon-centered radical in C(sp^3)–H bond cleavage via HAT

4.4 C(sp^3)–H bond activation via proton-coupled electron transfer (PCET)

PCET is the well-established strategy to generate the radical species in a concerted manner, which would be much challenging if the reaction proceeds via the stepwise proton transfer and electron transfer.[141] This mechanism has been implemented in the various areas of organic transformations, including the visible light photoredox catalysis.[142] Although many examples demonstrated the usefulness of the PCET in achieving the challenging transformations,[143] the direct C(sp^3)–H bond cleavage and functionalization via PCET on the carbon center has not been investigated.

In a very recent study reported by Knowles and Alexanian, the first example for the C(sp^3)–H bond cleavage of various aliphatic systems via PCET has been realized.[144] The detailed mechanistic investigations revealed that the pre-complexation of phosphate and Ir photocatalyst via hydrogen bonding exists, and the photoexcitation of the complex induces the multi-site PCET of the aliphatic C(sp^3)–H bond, which is further trapped by the Michael acceptor (Scheme 4.27). The introduction of PCET as an essential elementary step in C(sp^3)–H bond enhances the generality of the developed reaction, which are operative in wide ranges of C(sp^3)–H bonds under mild reaction conditions.

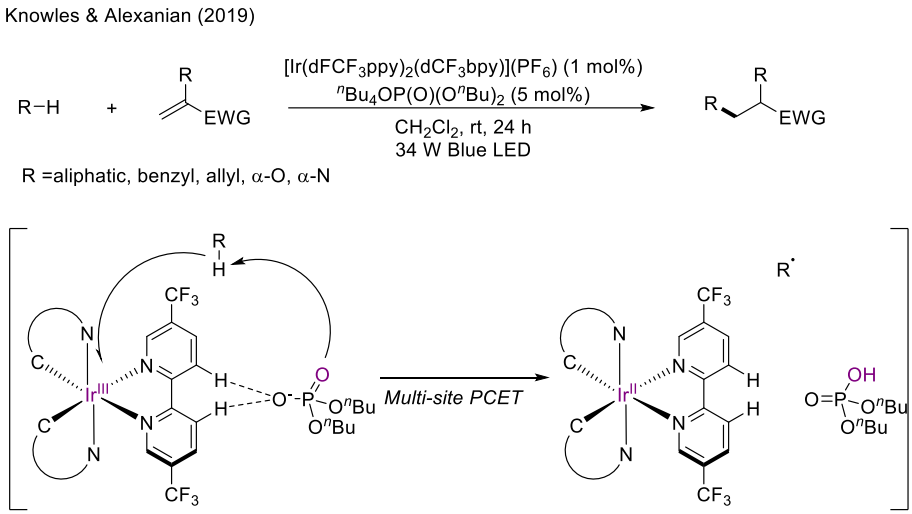

Scheme 4.27 Application of multisite proton-coupled electron transfer for the C(sp^3)–H bond cleavage

4.5 Summary and outlook

The thriving development of visible light photoredox catalysis in the organic transformation has open a new area of synthetic strategy to resolve the remaining challenges. Among several targets, the direct C(sp^3)–H bond functionalization has extensively explored via the new radical-based strategies governed by visible light photoredox catalysis. As a result, a number of traditionally inaccessible categories of the transformations have been realized in a fancy manner without the use of strong reagents or the harsh reaction conditions.

Despite the advantages of the newly developed protocols, a lot of investigations are still required to resolve the common limitations in visible light photoredox catalysis. First, the reaction efficiency should be further improved, since the large excess amount of C(sp^3)–H substrate or the long reaction time is required in usual cases. Much more efforts to accomplish C–heteroatom bond formation reactions are necessary to avoid the limited scopes of transformations, which usually rely on highly reactive Michael acceptors. Lastly, the practicality of the use of visible light photoredox catalysis might be enhanced to obtain the generality of the developed reactions in both academia and industry.

4.6 References

(1) Hoffmann, N. *Chem. Rev.* **2008**, *108*, 1052.

(2) Michelin, C.; Hoffmann, N. *ACS Catal.* **2018**, *8*, 12046.

(3) Pandey, G. In *Photoinduced Electron Transfer V*; Mattay, J., Ed.; Springer Berlin Heidelberg: Berlin, Heidelberg, 1993, pp 175–221.

(4) (a) Zeitler, K. *Angew. Chem., Int. Ed.* **2009**, *48*, 9785. (b) Tucker, J. W.; Stephenson, C. R. *J. Org. Chem.* **2012**, *77*, 1617. (c) Prier, C. K.; Rankic, D. A.; MacMillan, D. W. *Chem. Rev.* **2013**, *113*, 5322. (d) Shaw, M. H.; Twilton, J.; MacMillan, D. W. *J. Org. Chem.* **2016**, *81*, 6898. (e) Romero, N. A.; Nicewicz, D. A. *Chem. Rev.* **2016**, *116*, 10075.

(5) (a) Fabry, D. C.; Rueping, M. *Acc. Chem. Res.* **2016**, *49*, 1969. (b) Wei, G.; Basheer, C.; Tan, C.-H.; Jiang, Z. *Tetrahedron Lett.* **2016**, *57*, 3801. (c) Capaldo, L.; Ravelli, D. *Eur. J. Org. Chem.* **2017**, 2056. (d) Revathi, L.; Ravindar, L.; Fang, W.-Y.; Rakesh, K. P.; Qin, H.-L. *Adv. Synth. Catal.* **2018**, *360*, 4652. (e) Stateman, L. M.; Nakafuku, K. M.; Nagib, D. A. *Synthesis* **2018**, *50*, 1569.

(6) (a) Hu, J.; Wang, J.; Nguyen, T. H.; Zheng, N. *Beilstein J. Org. Chem.* **2013**, *9*, 1977. (b) Nakajima, K.; Miyake, Y.; Nishibayashi, Y. *Acc. Chem. Res.* **2016**, *49*, 1946.

(7) (a) Zhang, X.; Bordwell, F. G. *J. Org. Chem.* **1992**, *57*, 4163. (b) Bordwell, F. G.; Cheng, J. P. *J. Am. Chem. Soc.* **1989**, *111*, 1792.

(8) Condie, A. G.; Gonzalez-Gomez, J. C.; Stephenson, C. R. *J. Am. Chem. Soc.* **2010**, *132*, 1464.

(9) (a) Rueping, M.; Zhu, S.; Koenigs, R. M. *Chem. Commun.* **2011**, *47*, 12709. (b) Zhao, G.; Yang, C.; Guo, L.; Sun, H.; Chen, C.; Xia, W. *Chem. Commun.* **2012**, *48*,

2337. (c) Fu, W.; Guo, W.; Zou, G.; Xu, C. *J. Fluorine Chem.* **2012**, *140*, 88. (d) Freeman, D. B.; Furst, L.; Condie, A. G.; Stephenson, C. R. *Org. Lett.* **2012**, *14*, 94. (e) Perepichka, I.; Kundu, S.; Hearne, Z.; Li, C. J. *Org. Biomol. Chem.* **2015**, *13*, 447. (f) Querard, P.; Perepichka, I.; Zysman-Colman, E.; Li, C. J. *Beilstein J. Org. Chem.* **2016**, *12*, 2636.

(10) (a) Rueping, M.; Zhu, S.; Koenigs, R. M. *Chem. Commun.* **2011**, *47*, 8679. (b) Yadav, A. K.; Yadav, L. D. S. *Tetrahedron Lett.* **2015**, *56*, 6696.

(11) (a) Pan, Y.; Kee, C. W.; Chen, L.; Tan, C.-H. *Green Chem.* **2011**, *13*, 2682. (b) Hari, D. P.; Konig, B. *Org. Lett.* **2011**, *13*, 3852. (c) Rueping, M.; Vila, C.; Bootwicha, T. *ACS Catal.* **2013**, *3*, 1676. (d) Zhong, J. J.; Meng, Q. Y.; Liu, B.; Li, X. B.; Gao, X. W.; Lei, T.; Wu, C. J.; Li, Z. J.; Tung, C. H.; Wu, L. Z. *Org. Lett.* **2014**, *16*, 1988.

(12) (a) Zou, Y. Q.; Lu, L. Q.; Fu, L.; Chang, N. J.; Rong, J.; Chen, J. R.; Xiao, W. J. *Angew. Chem., Int. Ed.* **2011**, *50*, 7171. (b) Vila, C.; Lau, J.; Rueping, M. *Beilstein J. Org. Chem.* **2014**, *10*, 1233.

(13) Xuan, J.; Feng, Z.-J.; Duan, S.-W.; Xiao, W.-J. *RSC Adv.* **2012**, *2*, 4065.

(14) DiRocco, D. A.; Rovis, T. *J. Am. Chem. Soc.* **2012**, *134*, 8094.

(15) Wei, G.; Zhang, C.; Bureš, F.; Ye, X.; Tan, C.-H.; Jiang, Z. *ACS Catal.* **2016**, *6*, 3708.

(16) Kohls, P.; Jadhav, D.; Pandey, G.; Reiser, O. *Org. Lett.* **2012**, *14*, 672.

(17) Ruiz Espelt, L.; Wiensch, E. M.; Yoon, T. P. *J. Org. Chem.* **2013**, *78*, 4107.

(18) Yuan, X.; Wu, X.; Dong, S.; Wu, G.; Ye, J. *Org. Biomol. Chem.* **2016**, *14*, 7447.

(19) Nicholls, T. P.; Constable, G. E.; Robertson, J. C.; Gardiner, M. G.; Bissember, A. C. *ACS Catal.* **2016**, *6*, 451.

(20) Xuan, J.; Zeng, T. T.; Feng, Z. J.; Deng, Q. H.; Chen, J. R.; Lu, L. Q.; Xiao, W.

J.; Alper, H. *Angew. Chem., Int. Ed.* **2015**, *54*, 1625.

(21) McNally, A.; Prier, C. K.; MacMillan, D. W. *Science* **2011**, *334*, 1114.

(22) Xie, J.; Shi, S.; Zhang, T.; Mehrkens, N.; Rudolph, M.; Hashmi, A. S. *Angew. Chem., Int. Ed.* **2015**, *54*, 6046.

(23) Uraguchi, D.; Kinoshita, N.; Kizu, T.; Ooi, T. *J. Am. Chem. Soc.* **2015**, *137*, 13768.

(24) Ding, W.; Lu, L. Q.; Liu, J.; Liu, D.; Song, H. T.; Xiao, W. J. *J. Org. Chem.* **2016**, *81*, 7237.

(25) (a) Miyake, Y.; Nakajima, K.; Nishibayashi, Y. *J. Am. Chem. Soc.* **2012**, *134*, 3338. (b) Dai, X.; Cheng, D.; Guan, B.; Mao, W.; Xu, X.; Li, X. *J. Org. Chem.* **2014**, *79*, 7212. (c) Dai, X.; Mao, R.; Guan, B.; Xu, X.; Li, X. *RSC Adv.* **2015**, *5*, 55290.

(26) Miyake, Y.; Nakajima, K.; Nishibayashi, Y. *Chem.–Eur. J.* **2012**, *18*, 16473.

(27) Zhou, H.; Lu, P.; Gu, X.; Li, P. *Org. Lett.* **2013**, *15*, 5646.

(28) (a) Singh, A.; Arora, A.; Weaver, J. D. *Org. Lett.* **2013**, *15*, 5390. (b) Prier, C. K.; MacMillan, D. W. *Chem. Sci.* **2014**, *5*, 4173.

(29) Noble, A.; MacMillan, D. W. *J. Am. Chem. Soc.* **2014**, *136*, 11602.

(30) Loh, Y. Y.; Nagao, K.; Hoover, A. J.; Hesk, D.; Rivera, N. R.; Colletti, S. L.; Davies, I. W.; MacMillan, D. W. C. *Science* **2017**, *358*, 1182.

(31) (a) Zhu, S.; Das, A.; Bui, L.; Zhou, H.; Curran, D. P.; Rueping, M. *J. Am. Chem. Soc.* **2013**, *135*, 1823. (b) Liang, Z.; Xu, S.; Tian, W.; Zhang, R. *Beilstein J. Org. Chem.* **2015**, *11*, 425.

(32) Zhang, P.; Xiao, T.; Xiong, S.; Dong, X.; Zhou, L. *Org. Lett.* **2014**, *16*, 3264.

(33) Joe, C. L.; Doyle, A. G. *Angew. Chem., Int. Ed.* **2016**, *55*, 4040.

(34) Ahneman, D. T.; Doyle, A. G. *Chem. Sci.* **2016**, *7*, 7002.

(35) Thullen, S. M.; Rovis, T. *J. Am. Chem. Soc.* **2017**, *139*, 15504.

(36) Xuan, J.; Cheng, Y.; An, J.; Lu, L. Q.; Zhang, X. X.; Xiao, W. J. *Chem. Commun.* **2011**, *47*, 8337.

(37) Zhu, S.; Rueping, M. *Chem. Commun.* **2012**, *48*, 11960.

(38) Wang, Z. Q.; Hu, M.; Huang, X. C.; Gong, L. B.; Xie, Y. X.; Li, J. H. *J. Org. Chem.* **2012**, *77*, 8705.

(39) Stanek, F.; Pawlowski, R.; Morawska, P.; Bujok, R.; Stodulski, M. *Org. Biomol. Chem.* **2020**, *18*, 2103.

(40) Roth, H. G.; Romero, N. A.; Nicewicz, D. A. *Synlett* **2016**, *27*, 714.

(41) Speckmeier, E.; Fischer, T. G.; Zeitler, K. *J. Am. Chem. Soc.* **2018**, *140*, 15353.

(42) Tucker, J. W.; Narayanam, J. M.; Shah, P. S.; Stephenson, C. R. *Chem. Commun.* **2011**, *47*, 5040.

(43) Yi, H.; Bian, C.; Hu, X.; Niu, L.; Lei, A. *Chem. Commun.* **2015**, *51*, 14046.

(44) Xiang, M.; Meng, Q. Y.; Li, J. X.; Zheng, Y. W.; Ye, C.; Li, Z. J.; Chen, B.; Tung, C. H.; Wu, L. Z. *Chem.–Eur. J.* **2015**, *21*, 18080.

(45) Pandey, G.; Laha, R.; Singh, D. *J. Org. Chem.* **2016**, *81*, 7161.

(46) Zhou, R.; Liu, H.; Tao, H.; Yu, X.; Wu, J. *Chem. Sci.* **2017**, *8*, 4654.

(47) Schwarz, J. L.; Schafers, F.; Tlahuext-Aca, A.; Luckemeier, L.; Glorius, F. *J. Am. Chem. Soc.* **2018**, *140*, 12705.

(48) Mitsunuma, H.; Tanabe, S.; Fuse, H.; Ohkubo, K.; Kanai, M. *Chem. Sci.* **2019**, *10*, 3459.

(49) Xu, W.; Wang, W.; Liu, T.; Xie, J.; Zhu, C. *Nat. Commun.* **2019**, *10*, 4867.

(50) Pirnot, M. T.; Rankic, D. A.; Martin, D. B.; MacMillan, D. W. *Science* **2013**, *339*, 1593.

(51) Petronijevic, F. R.; Nappi, M.; MacMillan, D. W. *J. Am. Chem. Soc.* **2013**, *135*,

18323.

(52) Terrett, J. A.; Clift, M. D.; MacMillan, D. W. *J. Am. Chem. Soc.* **2014**, *136*, 6858.

(53) Jeffrey, J. L.; Petronijevic, F. R.; MacMillan, D. W. *J. Am. Chem. Soc.* **2015**, *137*, 8404.

(54) Ohmatsu, K.; Nakashima, T.; Sato, M.; Ooi, T. *Nat. Commun.* **2019**, *10*, 2706.

(55) Hendry, D. G.; Mill, T.; Piszkiewicz, L.; Howard, J. A.; Eigenmann, H. K. *J. Phys. Chem. Ref. Data* **1974**, *3*, 937.

(56) Gunay, A.; Theopold, K. H. *Chem. Rev.* **2010**, *110*, 1060.

(57) Mayer, J. M. *Acc. Chem. Res.* **2011**, *44*, 36.

(58) Luo, Y.-R. *Handbook of Bond Dissociation Energies in Organic Compounds*; 1st Edition ed.; CRC Press: Boca Raton, 2002.

(59) Li, J.; Zhang, J.; Tan, H.; Wang, D. Z. *Org. Lett.* **2015**, *17*, 2522.

(60) Zhu, X.; Xie, X.; Li, P.; Guo, J.; Wang, L. *Org. Lett.* **2016**, *18*, 1546.

(61) Feng, S.; Xie, X.; Zhang, W.; Liu, L.; Zhong, Z.; Xu, D.; She, X. *Org. Lett.* **2016**, *18*, 3846.

(62) Dai, C.; Meschini, F.; Narayanam, J. M.; Stephenson, C. R. *J. Org. Chem.* **2012**, *77*, 4425.

(63) Jin, J.; MacMillan, D. W. *Angew. Chem., Int. Ed.* **2015**, *54*, 1565.

(64) Huang, C.; Wang, J. H.; Qiao, J.; Fan, X. W.; Chen, B.; Tung, C. H.; Wu, L. Z. *J. Org. Chem.* **2019**, *84*, 12904.

(65) Yang, N. C.; Yang, D.-D. H. *J. Am. Chem. Soc.* **1958**, *80*, 2913.

(66) Xia, J. B.; Zhu, C.; Chen, C. *J. Am. Chem. Soc.* **2013**, *135*, 17494.

(67) Fan, X. Z.; Rong, J. W.; Wu, H. L.; Zhou, Q.; Deng, H. P.; Tan, J. D.; Xue, C. W.; Wu, L. Z.; Tao, H. R.; Wu, J. *Angew. Chem., Int. Ed.* **2018**, *57*, 8514.

(68) Shen, Y.; Gu, Y.; Martin, R. *J. Am. Chem. Soc.* **2018**, *140*, 12200.

(69) Li, Y.; Lei, M.; Gong, L. *Nat. Catal.* **2019**, *2*, 1016.

(70) Mukherjee, S.; Maji, B.; Tlahuext-Aca, A.; Glorius, F. *J. Am. Chem. Soc.* **2016**, *138*, 16200.

(71) Margrey, K. A.; Czaplyski, W. L.; Nicewicz, D. A.; Alexanian, E. J. *J. Am. Chem. Soc.* **2018**, *140*, 4213.

(72) Wakaki, T.; Sakai, K.; Enomoto, T.; Kondo, M.; Masaoka, S.; Oisaki, K.; Kanai, M. *Chem.–Eur. J.* **2018**, *24*, 8051.

(73) Zlotorzynska, M.; Sammis, G. M. *Org. Lett.* **2011**, *13*, 6264.

(74) Zhang, J.; Li, Y.; Zhang, F.; Hu, C.; Chen, Y. *Angew. Chem., Int. Ed.* **2016**, *55*, 1872.

(75) Zhao, R.; Shi, L. *Org. Chem. Front.* **2018**, *5*, 3018.

(76) Hu, A.; Guo, J. J.; Pan, H.; Zuo, Z. *Science* **2018**, *361*, 668.

(77) An, Q.; Wang, Z.; Chen, Y.; Wang, X.; Zhang, K.; Pan, H.; Liu, W.; Zuo, Z. *J. Am. Chem. Soc.* **2020**, *142*, 6216.

(78) Tzirakis, M. D.; Lykakis, I. N.; Orfanopoulos, M. *Chem. Soc. Rev.* **2009**, *38*, 2609.

(79) (a) Ravelli, D.; Fagnoni, M.; Fukuyama, T.; Nishikawa, T.; Ryu, I. *ACS Catal.* **2018**, *8*, 701. (b) Perry, I. B.; Brewer, T. F.; Sarver, P. J.; Schultz, D. M.; DiRocco, D. A.; MacMillan, D. W. C. *Nature* **2018**, *560*, 70. (c) Laudadio, G.; Govaerts, S.; Wang, Y.; Ravelli, D.; Koolman, H. F.; Fagnoni, M.; Djuric, S. W.; Noël, T. *Angew. Chem., Int. Ed.* **2018**, *57*, 4078. (d) Fukuyama, T.; Nishikawa, T.; Yamada, K.; Ravelli, D.; Fagnoni, M.; Ryu, I. *Org. Lett.* **2017**, *19*, 6436. (e) Sarver, P. J.; Bacauanu, V.; Schultz, D. M.; DiRocco, D. A.; Lam, Y.-h.; Sherer, E. C.; MacMillan, D. W. C. *Nat. Chem.* **2020**, *12*, 459.

(80) West, J. G.; Bedell, T. A.; Sorensen, E. J. *Angew. Chem., Int. Ed.* **2016**, *55*, 8923.

(81) Capaldo, L.; Merli, D.; Fagnoni, M.; Ravelli, D. *ACS Catal.* **2019**, *9*, 3054.

(82) Azam, M.; Al-Resayes, S. I.; Trzesowska-Kruszynska, A.; Kruszynski, R.; Kumar, P.; Jain, S. L. *Polyhedron* **2017**, *124*, 177.

(83) Arnold, P. L.; Purkis, J. M.; Rutkauskaite, R.; Kovacs, D.; Love, J. B.; Austin, J. *ChemCatChem* **2019**, *11*, 3786.

(84) Hernández, R.; Rivera, A.; Salazar, J. A.; Suárez, E. *J. Chem. Soc., Chem. Commun.* **1980**, 958.

(85) (a) Martinez, C.; Muniz, K. *Angew. Chem., Int. Ed.* **2015**, *54*, 8287. (b) Qin, Q.; Yu, S. *Org. Lett.* **2015**, *17*, 1894. (c) Wappes, E. A.; Fosu, S. C.; Chopko, T. C.; Nagib, D. A. *Angew. Chem., Int. Ed.* **2016**, *55*, 9974. (d) O'Broin, C. Q.; Fernandez, P.; Martinez, C.; Muniz, K. *Org. Lett.* **2016**, *18*, 436.

(86) Chu, J. C.; Rovis, T. *Nature* **2016**, *539*, 272.

(87) Choi, G. J.; Zhu, Q.; Miller, D. C.; Gu, C. J.; Knowles, R. R. *Nature* **2016**, *539*, 268.

(88) Chen, D. F.; Chu, J. C. K.; Rovis, T. *J. Am. Chem. Soc.* **2017**, *139*, 14897.

(89) Chen, H.; Fan, W.; Yuan, X. A.; Yu, S. *Nat. Commun.* **2019**, *10*, 4743.

(90) Schmidt, V. A.; Quinn, R. K.; Brusoe, A. T.; Alexanian, E. J. *J. Am. Chem. Soc.* **2014**, *136*, 14389.

(91) Quinn, R. K.; Konst, Z. A.; Michalak, S. E.; Schmidt, Y.; Szklarski, A. R.; Flores, A. R.; Nam, S.; Horne, D. A.; Vanderwal, C. D.; Alexanian, E. J. *J. Am. Chem. Soc.* **2016**, *138*, 696.

(92) Czaplyski, W. L.; Na, C. G.; Alexanian, E. J. *J. Am. Chem. Soc.* **2016**, *138*, 13854.

(93) Tanaka, H.; Sakai, K.; Kawamura, A.; Oisaki, K.; Kanai, M. *Chem. Commun.* **2018**, *54*, 3215.

(94) Ohmatsu, K.; Suzuki, R.; Furukawa, Y.; Sato, M.; Ooi, T. *ACS Catal.* **2020**, *10*, 2627.

(95) Shu, W.; Nevado, C. *Angew. Chem., Int. Ed.* **2017**, *56*, 1881.

(96) Chen, L.; Guo, L. N.; Ma, Z. Y.; Gu, Y. R.; Zhang, J.; Duan, X. H. *J. Org. Chem.* **2019**, *84*, 6475.

(97) Li, J.; Zhang, P.; Jiang, M.; Yang, H.; Zhao, Y.; Fu, H. *Org. Lett.* **2017**, *19*, 1994.

(98) Wappes, E. A.; Nakafuku, K. M.; Nagib, D. A. *J. Am. Chem. Soc.* **2017**, *139*, 10204.

(99) Dinnocenzo, J. P.; Banach, T. E. *J. Am. Chem. Soc.* **1989**, *111*, 8646.

(100) Jeffrey, J. L.; Terrett, J. A.; MacMillan, D. W. *Science* **2015**, *349*, 1532.

(101) Shaw, M. H.; Shurtleff, V. W.; Terrett, J. A.; Cuthbertson, J. D.; MacMillan, D. W. *Science* **2016**, *352*, 1304.

(102) Ye, J.; Kalvet, I.; Schoenebeck, F.; Rovis, T. *Nat. Chem.* **2018**, *10*, 1037.

(103) Twilton, J.; Christensen, M.; DiRocco, D. A.; Ruck, R. T.; Davies, I. W.; MacMillan, D. W. C. *Angew. Chem., Int. Ed.* **2018**, *57*, 5369.

(104) Ashley, M. A.; Yamauchi, C.; Chu, J. C. K.; Otsuka, S.; Yorimitsu, H.; Rovis, T. *Angew. Chem., Int. Ed.* **2019**, *58*, 4002.

(105) Wang, J.; Huang, B.; Gao, Y.; Yang, C.; Xia, W. *J. Org. Chem.* **2019**, *84*, 6895.

(106) Le, C.; Liang, Y.; Evans, R. W.; Li, X.; MacMillan, D. W. C. *Nature* **2017**, *547*, 79.

(107) Kee, C. W.; Chin, K. F.; Wong, M. W.; Tan, C. H. *Chem. Commun.* **2014**, *50*,

8211.

(108) Yan, D. M.; Zhao, Q. Q.; Rao, L.; Chen, J. R.; Xiao, W. J. *Chem.–Eur. J.* **2018**, *24*, 16895.

(109) Qvortrup, K.; Rankic, D. A.; MacMillan, D. W. *J. Am. Chem. Soc.* **2014**, *136*, 626.

(110) Hager, D.; MacMillan, D. W. *J. Am. Chem. Soc.* **2014**, *136*, 16986.

(111) Jin, J.; MacMillan, D. W. *Nature* **2015**, *525*, 87.

(112) Li, W.; Duan, Y.; Zhang, M.; Cheng, J.; Zhu, C. *Chem. Commun.* **2016**, *52*, 7596.

(113) Yan, C.; Li, L.; Liu, Y.; Wang, Q. *Org. Lett.* **2016**, *18*, 4686.

(114) Cuthbertson, J. D.; MacMillan, D. W. *Nature* **2015**, *519*, 74.

(115) Vu, M. D.; Das, M.; Guo, A.; Ang, Z.-E.; Đokić, M.; Soo, H. S.; Liu, X.-W. *ACS Catal.* **2019**, *9*, 9009.

(116) Meng, Q. Y.; Schirmer, T. E.; Berger, A. L.; Donabauer, K.; Konig, B. *J. Am. Chem. Soc.* **2019**, *141*, 11393.

(117) Kato, S.; Saga, Y.; Kojima, M.; Fuse, H.; Matsunaga, S.; Fukatsu, A.; Kondo, M.; Masaoka, S.; Kanai, M. *J. Am. Chem. Soc.* **2017**, *139*, 2204.

(118) Fuse, H.; Mitsunuma, H.; Kanai, M. *J. Am. Chem. Soc.* **2020**, *142*, 4493.

(119) Wohl, A. *Ber. Dtsch. Chem. Ges.* **1919**, *52*, 51.

(120) Luo, Y. R. *Comprehensive Handbook of Chemical Bond Energies*; CRC Press: Boca Raton, FL, 2007.

(121) Hwang, S. J.; Powers, D. C.; Maher, A. G.; Anderson, B. L.; Hadt, R. G.; Zheng, S. L.; Chen, Y. S.; Nocera, D. G. *J. Am. Chem. Soc.* **2015**, *137*, 6472.

(122) Shields, B. J.; Doyle, A. G. *J. Am. Chem. Soc.* **2016**, *138*, 12719.

(123) Nielsen, M. K.; Shields, B. J.; Liu, J.; Williams, M. J.; Zacuto, M. J.; Doyle,

A. G. *Angew. Chem., Int. Ed.* **2017**, *56*, 7191.

(124) Sun, Z.; Kumagai, N.; Shibasaki, M. *Org. Lett.* **2017**, *19*, 3727.

(125) Ackerman, L. K. G.; Martinez Alvarado, J. I.; Doyle, A. G. *J. Am. Chem. Soc.* **2018**, *140*, 14059.

(126) Deng, H. P.; Fan, X. Z.; Chen, Z. H.; Xu, Q. H.; Wu, J. *J. Am. Chem. Soc.* **2017**, *139*, 13579.

(127) Go, S. Y.; Lee, G. S.; Hong, S. H. *Org. Lett.* **2018**, *20*, 4691.

(128) Ohkubo, K.; Fujimoto, A.; Fukuzumi, S. *Chem. Commun.* **2011**, *47*, 8515.

(129) Deng, H. P.; Zhou, Q.; Wu, J. *Angew. Chem., Int. Ed.* **2018**, *57*, 12661.

(130) Rohe, S.; Morris, A. O.; McCallum, T.; Barriault, L. *Angew. Chem., Int. Ed.* **2018**, *57*, 15664.

(131) Heitz, D. R.; Tellis, J. C.; Molander, G. A. *J. Am. Chem. Soc.* **2016**, *138*, 12715.

(132) Huang, L.; Rueping, M. *Angew. Chem., Int. Ed.* **2018**, *57*, 10333.

(133) Cheng, X.; Lu, H.; Lu, Z. *Nat. Commun.* **2019**, *10*, 3549.

(134) Kawasaki, T.; Ishida, N.; Murakami, M. *J. Am. Chem. Soc.* **2020**, *142*, 3366.

(135) Minisci, F.; Galli, R.; Galli, A.; Bernardi, R. *Tetrahedron Lett.* **1967**, *8*, 2207.

(136) Lu, P.; Hou, T.; Gu, X.; Li, P. *Org. Lett.* **2015**, *17*, 1954.

(137) Hou, T.; Lu, P.; Li, P. *Tetrahedron Lett.* **2016**, *57*, 2273.

(138) Huang, F.-Q.; Dong, X.; Qi, L.-W.; Zhang, B. *Tetrahedron Lett.* **2016**, *57*, 1600.

(139) Kang, B.; Hong, S. H. *Chem. Sci.* **2017**, *8*, 6613.

(140) Lee, G. S.; Hong, S. H. *Chem. Sci.* **2018**, *9*, 5810.

(141) Weinberg, D. R.; Gagliardi, C. J.; Hull, J. F.; Murphy, C. F.; Kent, C. A.; Westlake, B. C.; Paul, A.; Ess, D. H.; McCafferty, D. G.; Meyer, T. J. *Chem. Rev.*

2012, *112*, 4016.

(142) (a) Miller, D. C.; Tarantino, K. T.; Knowles, R. R. *Top. Curr. Chem.* **2016**, *374*, 30. (b) Gentry, E. C.; Knowles, R. R. *Acc. Chem. Res.* **2016**, *49*, 1546.

(143) (a) Rono, L. J.; Yayla, H. G.; Wang, D. Y.; Armstrong, M. F.; Knowles, R. R. *J. Am. Chem. Soc.* **2013**, *135*, 17735. (b) Miller, D. C.; Choi, G. J.; Orbe, H. S.; Knowles, R. R. *J. Am. Chem. Soc.* **2015**, *137*, 13492. (c) Zhu, Q.; Graff, D. E.; Knowles, R. R. *J. Am. Chem. Soc.* **2018**, *140*, 741. (d) Gentry, E. C.; Rono, L. J.; Hale, M. E.; Matsuura, R.; Knowles, R. R. *J. Am. Chem. Soc.* **2018**, *140*, 3394. (e) Ota, E.; Wang, H.; Frye, N. L.; Knowles, R. R. *J. Am. Chem. Soc.* **2019**, *141*, 1457. (f) Zhao, K.; Yamashita, K.; Carpenter, J. E.; Sherwood, T. C.; Ewing, W. R.; Cheng, P. T. W.; Knowles, R. R. *J. Am. Chem. Soc.* **2019**, *141*, 8752.

(144) Morton, C. M.; Zhu, Q.; Ripberger, H.; Troian-Gautier, L.; Toa, Z. S. D.; Knowles, R. R.; Alexanian, E. J. *J. Am. Chem. Soc.* **2019**, *141*, 13253.

Chapter 5. Direct Allylic C(sp^3)–H Thiolation with Disulfides via Visible Light Photoredox Catalysis*

5.1 Introduction

Allyl thioethers not only serve as an open platform for the diverse sulfur functionality (thioester, sulfoxide, sulfone, and so forth)[1] but also occupy a pivotal position in the biological and pharmaceutical fields because of their high bioactivity, including potent anticancer activity.[2] To fulfill such a high demand for the allyl thioether surrogate, various synthetic approaches, such as S-allylation with allyl (pseudo)halide,[3] [3,3]-sigmatropic rearrangement,[4] and hydrothiolation of allenes[5] or 1,3-dienes,[6] have been developed via transition-metal catalysis (Scheme 5.1A). However, the direct introduction of a sulfur functionality to an allylic position of simple olefins via C(sp^3)–H bond activation has not been demonstrated, although a wide range of allylic C(sp^3)–H bond functionalizations have been developed.[7] This is mainly because of strong interactions between sulfur and transition metal complexes, resulting in deactivation of the catalytic cycle[8] or facile oxidation of the sulfur atom under oxidative conditions,[9] which drives the need for a different catalytic system.

Recently, a visible light photoredox catalysis approach for direct allylic C(sp^3)–H bond functionalization has emerged as a powerful tool. After MacMillan

* The majority of this work has been published: Jungwon Kim, Byungjoon Kang, and Soon Hyeok Hong*, *ACS Catal.* **2020**, *10*, 6013.

and co-workers demonstrated an elegant protocol for direct allylic C(sp^3)–H arylation using a thiol organocatalyst,[10] a number of examples of photocatalytic C–C bond formation reactions at the allylic position have been reported.[7d,7e,11] Inspired by these studies, along with the reported photocatalytic activation of disulfides,[12] we envisioned the utilization of visible light photoredox catalysis for the activation of disulfide and selective allylic C(sp^3)–H bond cleavage by hydrogen atom transfer (HAT) with the generated thiyl radical (Scheme 5.1B, blue arrow).[10,13] In this approach, highly versatile hydrothiolation between the olefin and the sulfur surrogate should be avoided (Scheme 5.1B, orange arrow).[14] Many examples using visible light photoredox catalysis for the initiation of hydrothiolation have been reported.[15] Very recently, Glorius and co-workers reported the utilization of a disulfide under photoredox catalysis for a versatile disulfide-ene reaction.[12c] To prevent the facile and reactive addition process, an introduction of basic conditions was proposed, which would aid the removal of the hydrogen source (mainly thiol); thus, the reversible thiyl radical addition could be shifted backward in order to proceed the desired allylic thiolation (Scheme 5.1C). This mechanism-based suppression of the well-established hydrothiolation enabled us to develop the first direct allylic C(sp^3)–H thiolation under visible light irradiation conditions (Scheme 5.1D). Experimental and computational studies revealed that the reaction proceeded predominately via ionic coupling between the allyl cation and the thiolate with the aid of a photocatalyst as a redox mediator.

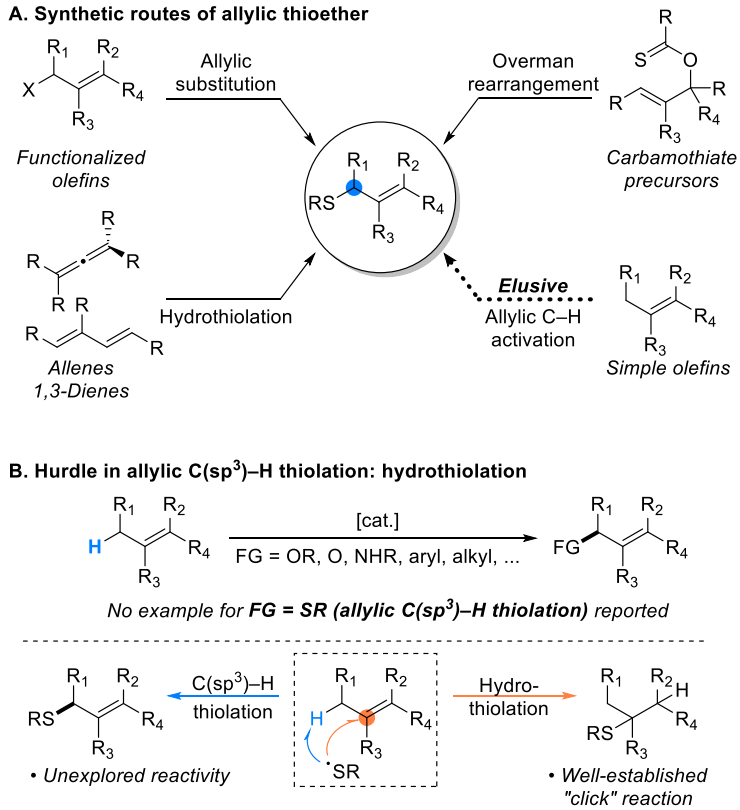

Scheme 5.1 Synthesis of allyl thioethers

5.2 Result and discussion

5.2.1 Optimization

The initial optimization of reaction conditions was done using diphenyl disulfide (**1a**) and 2,3-dimethyl-2-butene (**2a**) as the model substrates. It was revealed that the desired allyl thioether **3aa** can be synthesized in high yields (91%) under visible light irradiation (40 W blue LED) of $Ir(CF_3ppy)_3$ (2.0 mol%) and NaOH (1.0 equiv) (Scheme 5.2A). However, unfortunately, relatively high equivalence of olefin (20 equiv) was required to obtain the full conversion of **1a** and high yields of **3aa**. Sensitivity assessment of the developed reaction showed that the reaction was moderately sensitive to the variation of the reaction conditions (Scheme 5.2A).[16] Notably, the hydrothiolation product was not observed under standard reaction conditions. When cyclohexene (**2h**), which rapidly undergoes the hydrothiolation reaction, was used as a substrate, a noticeable base effect was observed (Scheme 5.2B). The choice of the base (NaOH) was critical to achieving high efficiency and selectivity toward allyl thioether **3ah**. Under the base-free conditions, a significant amount of the addition product **3ah'** was formed (32%), supporting the hypothesis on the role of the base in inhibiting the hydrothiolation (Scheme 5.2B).

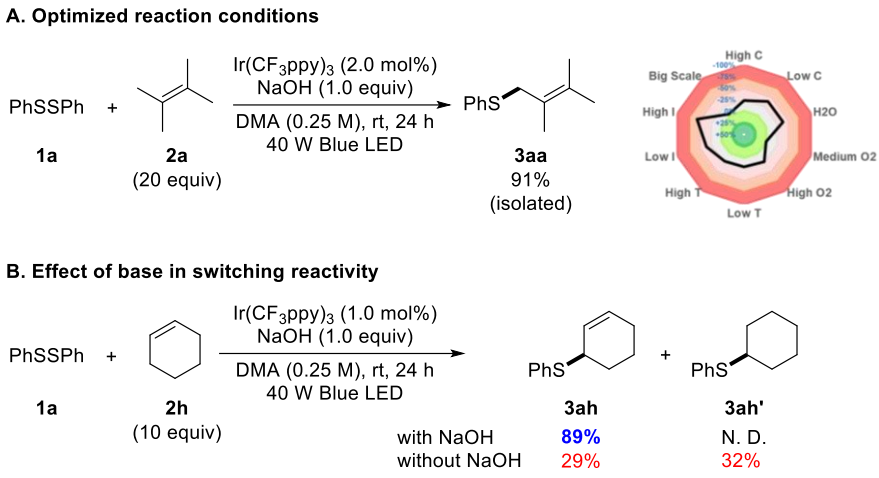

Scheme 5.2 Optimized reaction conditions and the effect of the base

5.2.2 Substrate scope evaluation

With the optimal conditions in hand, we investigated the scope of the reaction (Table 5.1). Initially, a variety of diaryl disulfides were tested. Diaryl disulfides bearing electron-withdrawing (**1b**, **1c**, **1d**, **1e**, **1f**, **1i**, and **1l**) or electron-donating (**1g**, **1h**, **1j**, **1k**, **1m**, and **1n**) substituents provided the desired allyl thioethers in moderate to good yields. Trifluoromethyl (**1e**) and trifluoromethoxy (**1f**) groups were well tolerated, producing the desired allyl thioethers in excellent yields. The *meta*-(**1i**–**1l**) or *ortho*-substituted (**1m** and **1n**) diaryl disulfides could also be used in this reaction. Notably, the reactions with bis(2-benzothiazolyl) disulfides (**1o** and **1p**) smoothly proceeded to functionalize the allylic position. A scaled-up reaction (5 mmol (1.1 g) of **1a**) with more light sources (4 × 40 W Blue LEDs) produced **3aa** in a synthetically useful yield (69%). Unfortunately, dialkyl disulfides, such as dibenzyl disulfide (**1q**), were not reactive under the reaction conditions, and only the corresponding thiols were obtained.

Next, different olefins bearing allylic C(sp^3)–H bonds were applied in the reaction. In addition to 2,3-dimethyl-2-butene (**2a**), other tetra-/tri-substituted linear (**2b** and **2c**) or cyclic (**2f** and **2g**) olefins were successfully functionalized with disulfide **1a**. In those cases, a regioselectivity preference (secondary > primary ≫ tertiary) was observed, presumably due to the combinatorial effect of HAT efficiency and the steric effect. To our delight, (+)-α-pinene (**2g**) was also reactive, providing the corresponding allyl thioether (**3ag**) as a single stereoisomer. The reaction of **2g** demonstrated that the developed reaction can serve as a complementary method to a conventional two-step approach—allylic bromination, which gives a mixture of regioisomers,[17] and a nucleophilic substitution with

thiolate. Not only multisubstituted olefins but also di-substituted olefins, which are more susceptible to the competitive hydrothiolation reaction, selectively generated allyl thioethers in moderate to good yields. Cyclic olefins with different ring sizes (**2h**–**2l**), substituted cyclohexene (**2m**), a heteroatom-bearing cyclic olefin (**2n**), and even simple linear internal olefins (**2d** and **2e**) were selectively functionalized at the allylic C(sp^3)–H position without the generation of any hydrothiolation byproducts. In some olefin substrates, migration of the double bond in the product was observed. When 3-methylcyclohexene (**2o**) or *trans*-4-methyl-2-pentene (**2p**) was used in the reaction, allyl thioethers bearing migrated double bonds (**3af** and **3ap**, respectively) were observed exclusively, showing a preference toward the secondary allylic position in the coupling step.

Table 5.1 Substrate scope[a]

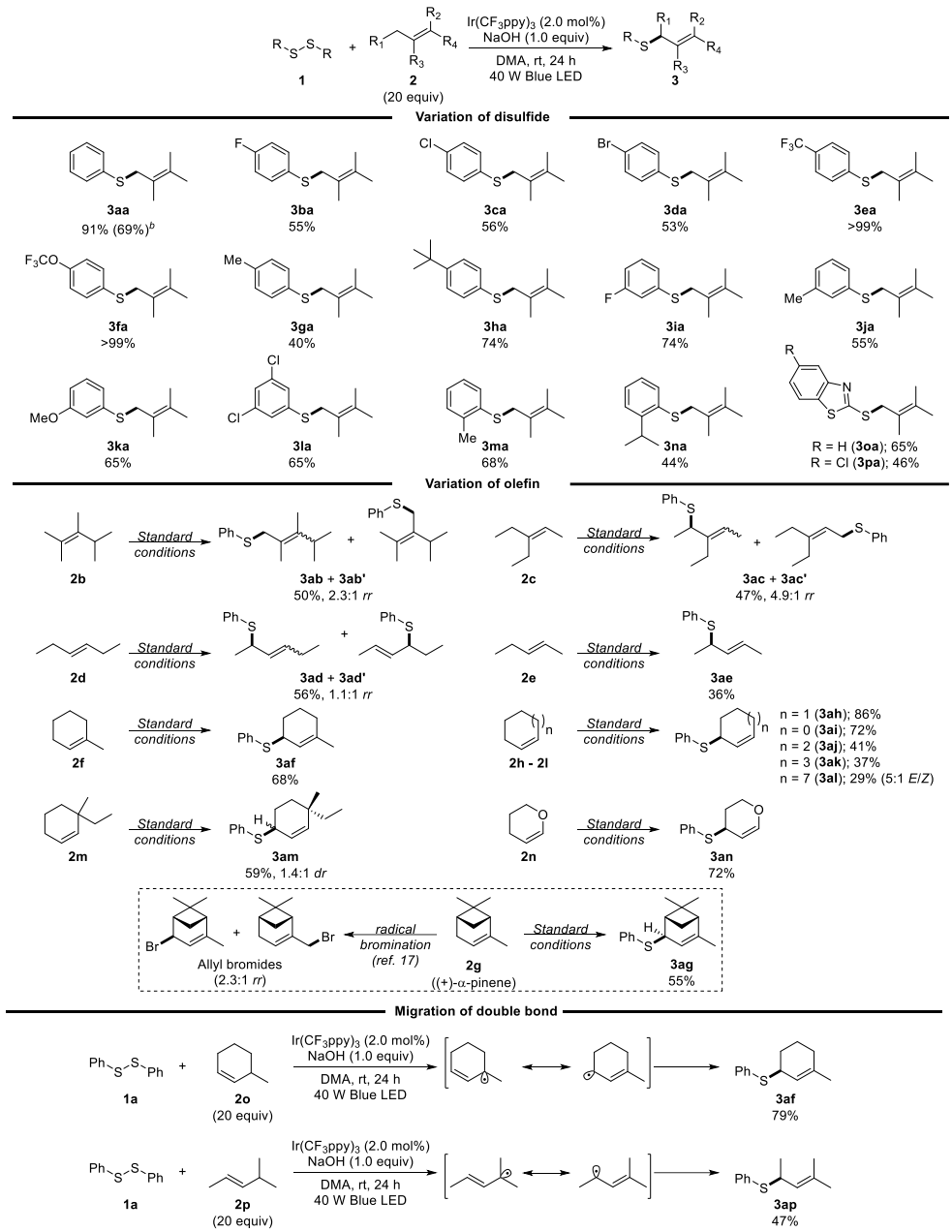

[a]Reaction conditions: **1** (0.25 mmol), **2** (5.0 mmol), $Ir(CF_3ppy)_3$ (0.0050 mmol), NaOH (0.25 mmol), and DMA (1 mL) in a 4 mL reaction vial irradiated with a 40 W Blue LED under fan cooling. [b]Reaction conditions: **1** (5.0 mmol), **2** (100 mmol), $Ir(CF_3ppy)_3$ (0.10 mmol), NaOH (5.0 mmol), and DMA (20 mL) in a 100 mL quartz round-bottom flask irradiated with 4 × 40 W Blue LEDs under fan cooling. All yields are isolated yields.

5.2.3 Further utilization of allyl thioethers

The synthesized allyl thioethers could be further functionalized (Scheme 5.3). Synthesis of sulfoxide or sulfone was performed under appropriate oxidation conditions, giving **3ah**$_{\textbf{sulfoxide}}$ and **3oa**$_{\textbf{sulfone}}$ from **3ah** and **3oa**, respectively.[18] It is noteworthy that the selective oxidations to sulfoxide or sulfone could be accomplished while the olefin functional group remained intact. The synthesized **3ah**$_{\textbf{sulfoxide}}$ was further utilized in an interrupted Pummerer coupling/[3,3]-sigmatropic rearrangement with *N*-methylindole to produce 2,3-disubstituted indole **4**.[19] In the case of **3oa**$_{\textbf{sulfone}}$, modified Julia olefination was done with hydrocinnamaldehyde to produce 1,3-diene **6**.[20] The result suggested that our reaction can serve as a useful synthetic tool for various conjugated dienes from simple olefins. The utility of allyl thioether itself was also demonstrated by the Doyle-Kirmse reaction with carbenoid, generating functionalized hydrocarbon skeleton **5** with good efficiency.[21]

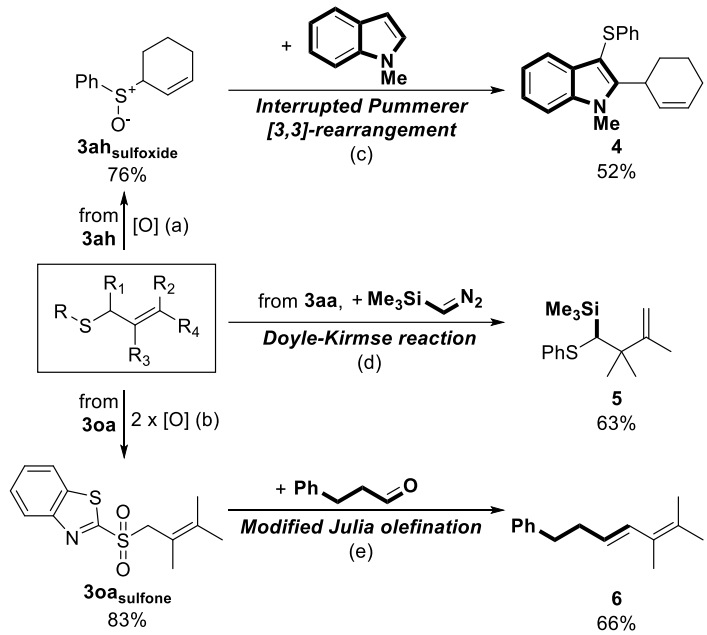

Scheme 5.3 Utilization of allyl thioethers. (a) **3ah** (0.50 mmol, 1.0 equiv), H_2O_2 (1.5 mmol, 3.0 equiv), acetic acid (3 mL), rt, 24 h. (b) **3oa** (0.34 mmol, 1.0 equiv), $(NH_4)_6Mo_7O_{24}\cdot 4H_2O$ (0.085 mmol, 25 mol%), H_2O_2 (3.4 mmol, 10 equiv), MeOH (4 mL), rt, 1 h (c) $\mathbf{3ah_{sulfoxide}}$ (0.15 mmol, 1.0 equiv), *N*-methylindole (0.15 mmol, 1.0 equiv), trifluoroacetic anhydride (0.165 mmol, 1.1 equiv), $NaHCO_3$ (0.33 mmol, 2.2 equiv), CH_2Cl_2 (1.5 mL), -78 °C to rt, 3 h. (d) **3aa** (0.20 mmol, 1.0 equiv), (trimethylsilyl)diazomethane (0.40 mmol, 2.0 equiv), $FeBr_2$ (0.020 mmol, 10 mol%), dppe (0.020 mmol, 10 mol%), 1,2-dichloroethane (2 mL), reflux, 12 h. (e) $\mathbf{3oa_{sulfone}}$ (0.25 mmol, 1.0 equiv), 3-phenylpropionaldehyde (0.275 mmol, 1.1 equiv), potassium bis(trimethylsilyl)amide (0.325 mmol, 1.3 equiv), THF (2.5 mL), -78 °C to rt, 7 h.

5.2.4 Mechanistic investigations

When the reaction was designed, it was hypothesized that the Ir photocatalyst can aid the generation of thiyl radicals, and a further allylic C(sp^3)–H bond cleavage and a coupling reaction were expected to proceed via a radical pathway without any involvement of the photocatalyst (Scheme 5.1C). However, only a trace amount of desired product was observed under photocatalyst-free conditions (Scheme 5.4A, entry 2), although a homolytic cleavage of diaryl disulfide under irradiation of blue LED has been utilized in various radical cyclization processes.[22] Even the use of the Ir photocatalyst having a larger triplet-state energy (entry 3)[23] or the use of a 370 nm LED light source (entry 4), which can further facilitate the homolytic cleavage of diaryl disulfide, gave a trace amount of the coupled product **3aa** (<2%).[24] Hypothetically, the generated thiyl radical could induce the HAT from the allylic C(sp^3)–H bond. Then, a further coupling reaction between the allylic radical and disulfide would be able to form the C–S bond with the regeneration of the thiyl radical without the aid of a photocatalyst (radical pathway in Scheme 5.4B). However, based on the observed necessity of the appropriate Ir photocatalyst for high efficiency, an additional redox process mediated by the photocatalyst was proposed involving the allyl cation as the other intermediate to perform an ionic coupling between the allyl cation and aryl thiolate (ionic pathway in Scheme 5.4B).[25]

A. Effect of Ir photocatalyst

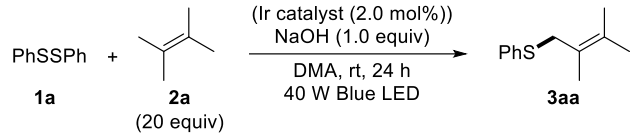

Entry	Variation	Yield **3aa**
1	with $Ir(CF_3ppy)_3$ (E_T = 56.4 kcal/mol)	91%
2	without Ir catalyst	<2%
3	with $[Ir(dFCF_3ppy)_2(dtbbpy)](PF_6)$ (E_T = 60.4 kcal/mol)	<2%
4	without Ir catalyst, 370 nm LED	<1%

B. Proposed reaction mechanism - possible role of Ir photocatalyst

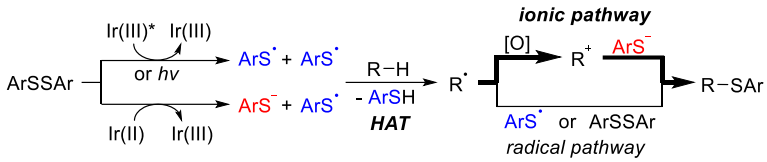

Scheme 5.4 Possible role of a photocatalyst

To determine whether the allyl cation is involved in the reaction, reactions with single-electron oxidants under photocatalyst-free conditions were conducted using olefin **2a** or **2h** as a substrate (Table 5.2). Interestingly, various types of single-electron oxidants, such as Ce^{4+} (entry 2), tris(4-bromophenyl)ammoniumyl ($TBPA^{+}$) (entry 3), and (2,2,6,6-tetramethylpiperidin-1-yl)oxyl (TEMPO) (entry 4), can promote the coupling reactions in the absence of a photocatalyst, proving that the separated approaches (HAT by the thiyl radical from light irradiation and further generation of the allyl cation by a single-electron oxidant) can promote the same reaction. In addition, no desired product was observed when the oxidant has an oxidizing power below a certain threshold. For example, ferrocenium (Fc^{+}) (entry 6) cannot participate in the thiolation reaction with olefins **2a** or **2h**, and 2,3-dichloro-5,6-dicyano-*p*-benzoquinone (DDQ) (entry 5) produces very little allyl thioether (**3aa**) or almost no product (**3ah**). These trends suggest that an oxidant with a certain level of oxidizing power (0.51–0.65 V) is required to induce oxidation of the allyl radical. In addition, the reaction with $TBPA^{+}$ under dark conditions did not produce the desired thioether (entry 7), further demonstrating that the thiyl radical is necessary for the reaction.

Table 5.2 Reaction without photocatalyst: effect of single-electron oxidants[a]

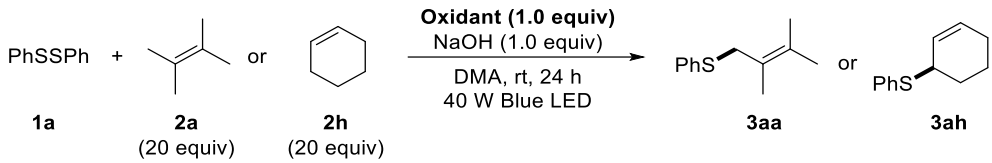

1a **2a** (20 equiv) **2h** (20 equiv) **3aa** **3ah**

entry	Oxidant	E^{ob}	Yield 3aa (%)[c]	Yield 3ah (%)[c]
1	None	-	<2	N. D.
2	$Ce(NH_4)_2(NO_3)_6$	1.06 V[d]	17	19[e]
3	$(TBPA)(SbCl_6)$	1.05 V[f]	36	6
4	TEMPO	0.65 V[g]	13	23
5	DDQ	0.51 V[h]	3	<1
6	$(Fc)(BF_4)$	0.4 V[i]	N. D.	N. D.
7[j]	$(TBPA)(SbCl_6)$	1.05 V[f]	N. D.	N. D.

[a]Reaction conditions: **1a** (0.25 mmol), **2a** or **2h** (5.0 mmol), oxidant (0.25 mmol), NaOH (0.25 mmol), and DMA (1 mL) in 4 mL reaction vial irradiated with a 40 W Blue LED under fan cooling. [b]Versus SCE in MeCN. [c]Yields determined by GC using dodecane as the internal standard. [d]ref.26. [e]$Ce(SO_4)_2$ was used as an oxidant. [f]ref.27. [g]ref.28. [h]ref.29. [i]ref.30. [j]Dark conditions. N. D. = not detected.

To verify the involvement of the allyl cation in the reaction, DFT calculations of redox potentials for allyl radicals were conducted following Liu and Guo's protocol (Scheme 5.5).[31] First, the allyl radical (**2a-rad**) derived from olefin **1a** showed E^o (calc., **2a-cat**/**2a-rad**) = 0.54 V (vs SCE in MeCN), which matched the experimentally observed oxidation potential threshold (~0.51 V) (Scheme 5.5A). Next, in the case of olefin **2h**, both the allyl radical (**2h-rad**) and the thiyl radical adduct (**3ah-rad**) were considered (Scheme 5.5B). Because the phenyl thiyl radical (**1a-rad**) is known to readily attack 1,2-disubstituted olefin systems, we wonder whether this thiol-ene type mechanism can be a part of the reaction pathway via sequential single-electron oxidation by the Ir photocatalyst and deprotonation of a sulfonium intermediate (**3ah-cat**).[32] The results clearly suggest that the redox potential of **2h-rad** (E_1^o (calc., **2h-cat**/**2h-rad**) = 0.61 V vs SCE in MeCN) is well-matched with the experimentally determined oxidation threshold (0.51 V–0.65 V), whereas **3ah-rad** is much more easily oxidizable (E_2^o (calc., **3ah-cat**/**3ah-rad**) = 0.04 V vs SCE in MeCN) and does not match the observed threshold in Table 5.2. In addition, the observed chemoselectivity in the reactions with olefin **2f** or **2n** further supports the allylic C(sp^3)–H cleavage pathway (Scheme 5.5C).[14d,15a] Based on these analyses, we concluded that a mechanism involving HAT by the thiyl radical operates in the developed reactions, together with the oxidation of the allyl radical to the allyl cation prior to the coupling process as a major pathway.

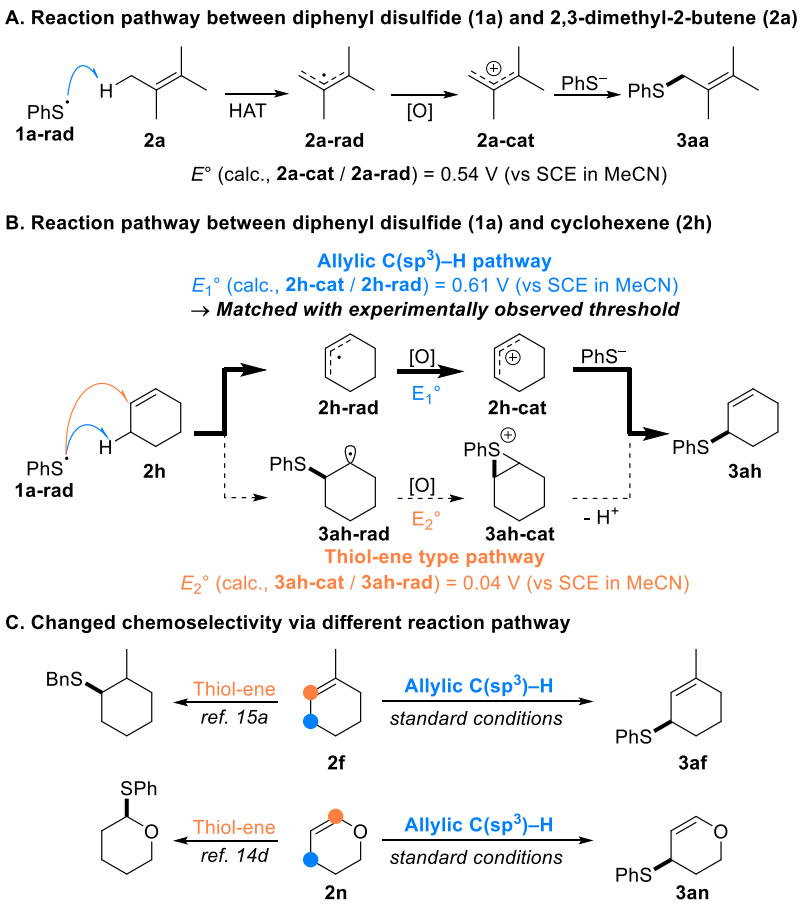

Scheme 5.5 Involvement of allyl cation intermediate

To further check the viability of the proposed reaction strategy, two possible reaction pathways (hydrothiolation and allylic thiolation) were analyzed via DFT calculation (Figure 5.1). In the reaction pathway, olefin **2h** can be involved in both allylic C(sp^3)–H bond cleavage via HAT by the phenyl thiyl radical ($\Delta G^{\ddagger}$=18.1 kcal/mol) and thiol-ene addition ($\Delta G^{\ddagger}$=12.1 kcal/mol).[33] In the case of thiol-ene pathway, hydrogen transfer by thiophenol (PhSH) exhibited an energy barrier of 18.8 kcal/mol, which is very similar to the energy barrier of the HAT process. This clearly indicates that control of reaction pathways relying on the innate reactivity of the thiyl radical and olefin is highly challenging, which is consistent with the result of the reaction between disulfide **1a** and olefin **2h** under base-free conditions (Scheme 5.2B). However, under basic conditions, the appropriate hydrogen source (PhSH) was removed, so that the completion of hydrothiolation was prohibited. Besides, the basic conditions prevent the reverse HAT of thiol to **2h-rad**, making the allylic C(sp^3)–H bond cleavage pathway irreversible. This clearly suggests that the application of basic conditions is crucial to derive the desired allylic C(sp^3)–H thiolation while preventing the facile hydrothiolation.

Next, three different pathways for the formation of allyl thioether (**3ah**) from the allyl radical (**2h-rad**) were considered. Coupling between two radical species would not be favorable, because of the low effective concentration of **1a-rad** in consumption through the HAT process and the reversible thiol-ene addition between **1a-rad** and **2h**. The reaction between **1a** and **2h-rad** is also possible (21.7 kcal/mol of activation barrier), but only as the minor pathway, considering the experimental support of the observed primary KIE (k_H/k_D = 3.99 with **2h**), low quantum yield (Φ = 0.029), and the control experiment under the Ir-free conditions (Scheme 5.4A). Therefore, after the conversion of **2h-rad** into **2h-cat** via oxidation

by Ir(III)*, relatively long-lived and less-reactive intermediates (**2h-cat** and PhS^-) can undergo the ionic coupling to produce the desired product. In summary, removal of free thiol from the reaction conditions and introduction of the redox-active Ir photocatalyst are keys to achieving the allylic C(sp^3)–H thiolation selectively.

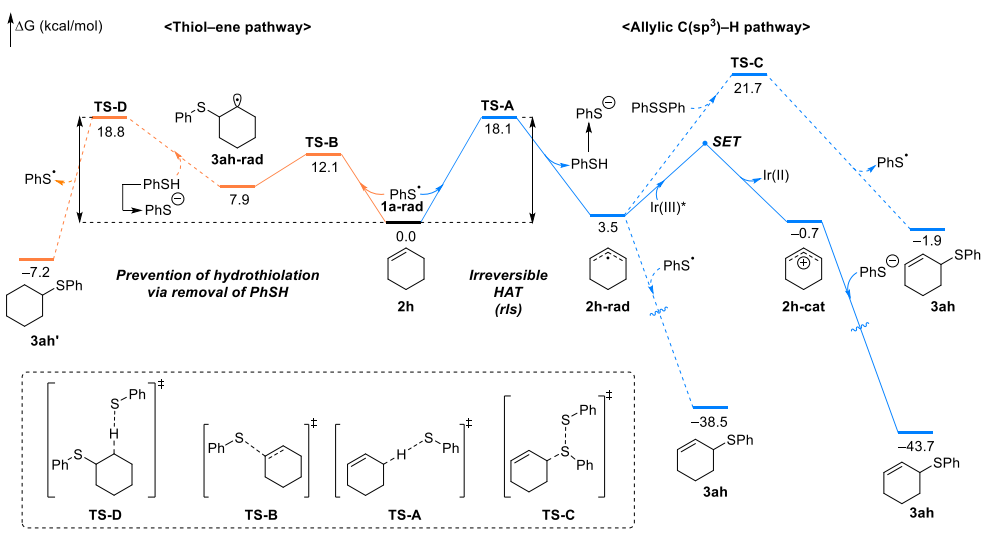

Figure 5.1 Computed energy profile for the reaction pathway. Free energies in solution (DMA) at the (U)M06-2X(PCM)/SDD/6-311+G**//(U)B3LYP/LANL2DZ/6-31G** level are displayed.

Based on the experimental and theoretical studies, a plausible reaction mechanism was proposed (Figure 5.2). At first, the S–S bond can be homolytically cleaved by irradiation of the blue LED, and this step can be accelerated by the energy transfer process by the photoexcited Ir photocatalyst (Ir(III)*)[12c] or the complexation between disulfide and olefin.[34] The generated thiyl radical can participate in either HAT from the allylic position to produce an ally radical (**Int-1**) or addition to olefin (R–H) to form a thiol-ene radical adduct (**Int-2**). The resulting thiophenol is immediately deprotonated by hydroxide, which prevents further hydrogen transfer to **Int-2**, driving the irreversible HAT process. **Int-1** undergoes single-electron oxidation (E^o (calc., **2a-cat**/**2a-rad**) = 0.54 V vs SCE in MeCN) by the photoexcited Ir photocatalyst (Ir(III)*, E^o (Ir(III)*/Ir(II) = 0.63 V vs SCE in MeCN)[23] to the allyl cation (**Int-3**), which can further react with the thiolate. The reduced photocatalyst (Ir(II), E^o (Ir(III)/Ir(II) = –2.13 V vs SCE in MeCN)[23] is re-oxidized by diaryl disulfide (E_p^{red} (PhSSPh) = –1.65 V vs SCE in DMF),[35] producing Ir(III) species, the thiyl radical, and thiolate at the same time. Meanwhile, **Int-1** can directly react with disulfide in the minor pathway, producing the desired product and the thiyl radical. Throughout the reaction, quenching of Ir(III)* by thiolate (E^o ($PhS^{\cdot}/PhS^{-}$) = 0.40 V vs SCE in MeCN)[36] is also possible, and this process could facilitate the HAT from olefin via the production of the reactive thiyl radical.

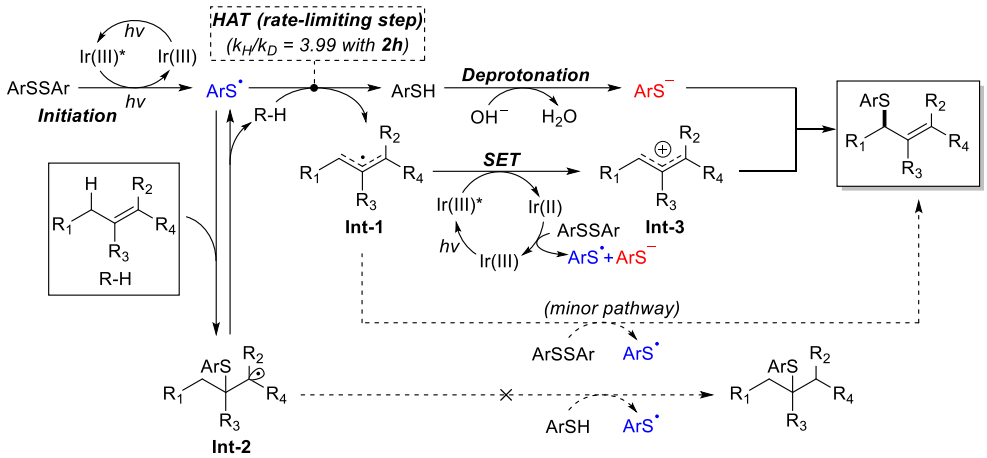

Figure 5.2 Proposed mechanism

5.2.5 Expansion of the substrate scope toward alkyl allyl sulfides

In the substrate scope evaluation, more electron-rich dialkyl disulfides were not active under the developed conditions (Table 5.1). In all attempts, the corresponding thiol was isolated, indicating that S–S bond cleavage and HAT are still operative under the reaction conditions. However, re-oxidation of the Ir(II) intermediate (E^{o} (Ir(III)/Ir(II) = –2.13 V vs SCE in MeCN)[23] would be problematic with dialkyl disulfide (E_{p}^{red} (MeSSMe) = –2.43 V vs SCE in DMF)[35], because of its higher reduction barrier compared to that of diaryl disulfide (E_{p}^{red} (PhSSPh) = –1.65 V vs SCE in DMF).[35] The higher reduction barrier makes the catalytic cycle not viable (Scheme 5.6A), so that the ionic coupling between the allyl cation and thiolate cannot be performed. To overcome this innate limitation on the utilization of dialkyl disulfide, we envisaged designing unsymmetrical disulfides to realize the direct synthesis of alkyl allyl sulfides (Scheme 5.6B). By introducing an electron-deficient aromatic motif in disulfides, the reduction barrier of disulfide can be lowered for the disulfides to interact with the Ir(II) intermediate. Then, the selective coupling of the resulting alkyl thiolate with the allyl cation is expected to occur, because of higher nucleophilicity of alkyl thiolate than that of aryl thiolate.

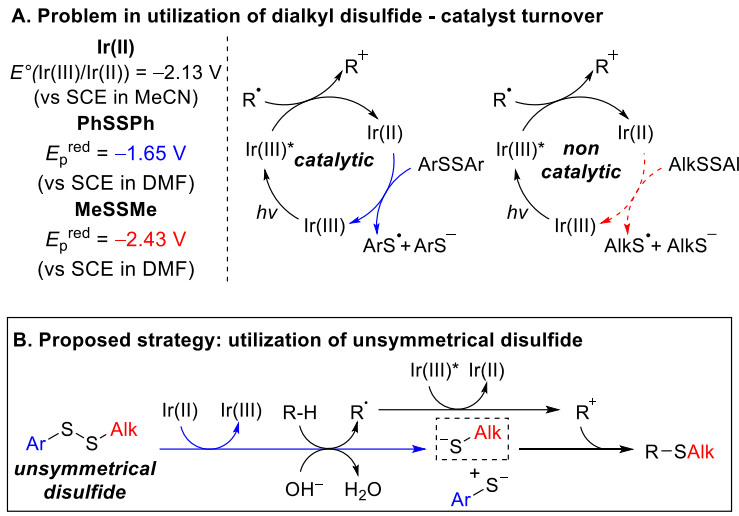

Scheme 5.6 Problems and a proposed strategy for the synthesis of alkyl allyl sulfides

With the hypothesis, unsymmetrical disulfides bearing an aryl moiety were prepared and evaluated in the reaction with olefin **2a** (Table 5.3). To our delight, the desired allyl thioether **3qa** began to appear when individually prepared unsymmetrical disulfides, which exhibit lower reduction barriers, were subjected to the reaction conditions (entries 2–4). Especially, disulfide bearing 2-benzothiazole moiety (**1q**$_{\mathbf{Bzt}}$) gave the highest yields of **3qa** among the tested disulfides. Alkyl 2-benzothiazolyl disulfides can be easily prepared by a substitution reaction between disulfide **1o** and alkyl mercaptan, which could allow the unsymmetrical disulfide as a practical and versatile reagent.[37] Further optimization of the reaction conditions was conducted. Interestingly, the addition of a catalytic amount of diphenyl disulfide **1a** significantly boosts the yield of **3qa** (entry 5), presumably because of the acceleration of initial HAT by the phenyl thiyl radical through the facile S–S bond cleavage under irradiation. However, increased amount of **1a** (10 mol%) rather decreased the overall reactivity (entry 6). Additional elaboration of catalyst loading and concentration gave a good yield of **3qa** (70%, entry 8).

Table 5.3 Survey of unsymmetrical disulfides[a]

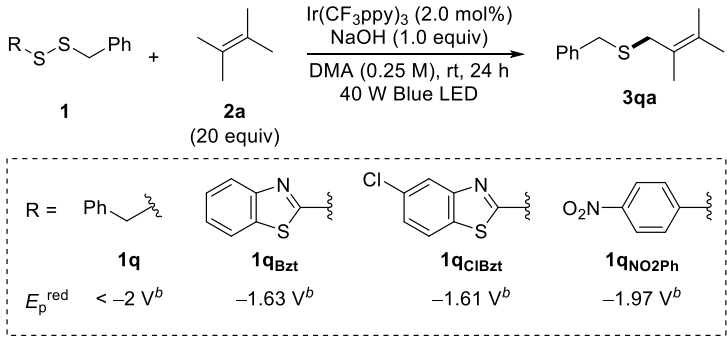

entry	Disulfide	Changes in conditions	Yield 3qa (%)[c]
1	**1q**	None	N. D.
2	**1q$_{Bzt}$**	None	26
3	**1q$_{ClBzt}$**	None	23
4	**1q$_{NO2Ph}$**	None	5
5	**1q$_{Bzt}$**	+ 5.0 mol% **1a**	48
6	**1q$_{Bzt}$**	+ 10.0 mol% **1a**	26
7	**1q$_{Bzt}$**	+ 5.0 mol% **1a**, 3.0 mol% Ir(CF$_3$ppy)$_3$	57
8	**1q$_{Bzt}$**	+ 5.0 mol% **1a**, 3.0 mol% Ir(CF$_3$ppy)$_3$, 0.17 M	70 (69)[d]

[a]Reaction conditions: **1** (0.25 mmol), **2a** (5.0 mmol), Ir(CF$_3$ppy)$_3$ (0.0050 mmol), NaOH (0.25 mmol), and DMA (1 mL) in a 4 mL reaction vial irradiated with a 40 W Blue LED under fan cooling. [b]Versus SCE in MeCN. [c]Yields determined by GC using dodecane as the internal standard. [d]Isolated yield. N. D. = not detected.

The optimized reaction conditions were further evaluated with various alkyl 2-benzothiazolyl disulfides taking advantage of the excellent availability of the unsymmetrical disulfides (Table 5.4). Benzyl (**3qa**), phenethyl (**3ra**), linear alkyl (**3sa**), and branched alkyl (**3ta**) containing allyl thioethers were accessible with the developed reaction. Notably, no hydrothiolation product was obtained even with cyclic olefins (**2h**–**2j**) in clear contrast with the recently reported photoredox thiol-ene reactions with alkyl mercaptans or dialkyl disulfides.[12c,15b] To our delight, the ability to utilize the alkyl mercaptan motif enabled us to apply biorelated thiols to the reaction. For example, a thiol-containing cysteine derivative can be functionalized with olefin **2a**, producing the corresponding allyl thioether (**3ua**). In addition, β-$_D$-glucopyranose (**3va**) and Captopril (**3wa**) derivatives were able to be synthesized under the developed reaction conditions, demonstrating the utility of the reaction for the functionalization of thiol-containing molecules with simple allyl sources.

Table 5.4 Synthesis of alkyl allyl sulfides[a]

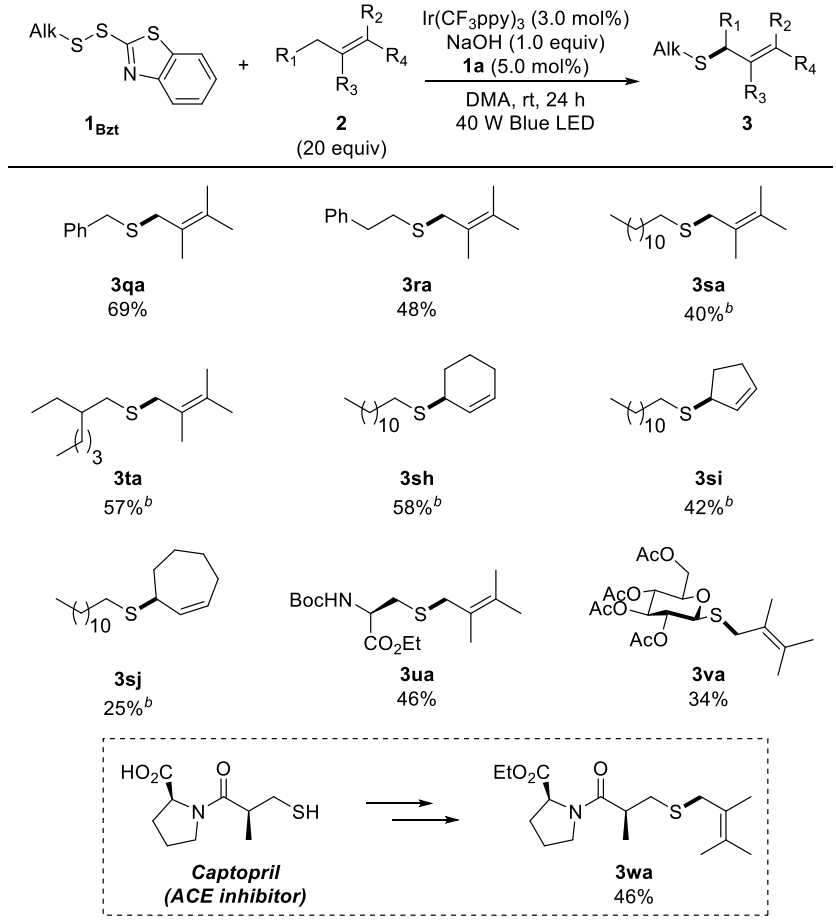

[a]Reaction conditions: **1**$_{\mathbf{Bzt}}$ (0.25 mmol), **2** (5.0 mmol), $Ir(CF_3ppy)_3$ (0.0075 mmol), NaOH (0.25 mmol), **1a** (0.0125 mmol) and DMA (1.5 mL) in a 4 mL reaction vial irradiated with a 40 W Blue LED under fan cooling. All yields are isolated yields. [b]2.0 equivalence of NaOH (0.50 mmol).

5.3 Conclusion

The first direct allylic C(sp^3)–H thiolation with disulfides using visible light photoredox catalysis was achieved. To overcome the previous limitations in transition-metal catalysis for the direct allylic C(sp^3)–H thiolation, visible light photoredox catalysis was introduced to induce selective hydrogen atom transfer at the allylic position, together with a deprotonation strategy to prevent the unwanted hydrothiolation reaction. As a result, a wide range of olefins and diaryl disulfides were successfully transformed into the corresponding allyl thioethers with high efficiency. Based on the mechanistic investigation, readily accessible unsymmetrical alkyl 2-benzothiazolyl disulfides were designed to realize the synthesis of challenging alkyl allyl sulfides. The developed strategy could serve as a new synthetic method to construct diverse allyl thioethers directly from unactivated allyl compounds.

5.4 Experimental section

5.4.1 General information

Unless otherwise noted, all reactions were performed under inert conditions. All reagents and solvents, unless otherwise noted, were purchased from commercial suppliers and used as received without further purification. All anhydrous solvents were purchased from commercial suppliers and degassed with dry argon before usage. All photocatalytic reactions were conducted under irradiation by 40 W blue LED lamps purchased from Kessil (Kessil A160WE) using a maximum light intensity and shortest wavelength setup. In the case of the reaction with 370 nm light source, Kessil PR160-370 was used. Reactions were monitored by thin-layer chromatography (TLC) on EMD Silica Gel 60 F254 plates and visualized using either UV light (254 nm) or by staining with potassium permanganate and heating. Gas chromatography (GC) was carried out using a 7980A GC system (Agilent Technologies) equipped with an HP-5 column and a flame ionization detector (FID). Nuclear magnetic resonance (NMR) spectra were recorded in $CDCl_3$ or DMSO-d_6 on a Bruker DPX-300 (300 MHz), Bruker AVANCE 300 (300 MHz), Bruker AVANCE 400 (400 MHz), Bruker AVANCE III HD (400 MHz), Varian 400 (400 MHz) and Varian 500 (500 MHz), and the residue solvent signal was used as a reference. Chemical shifts were reported in ppm and coupling constants in Hz. Multiplicity was indicated by one or more of the following: s (singlet); brs (broad singlet); d (doublet); t (triplet); q (quartet); quin (quintet); sex (sexet); sep (septet); m (multiplet). Stern-Volmer quenching experiment and quantum yield measurement were conducted via a Photon Technology International (PTI) QM-400 spectrofluorometer with FelixGX software and Perkin Elmer Lambda 1050

UV-Vis/NIR spectrophotometer. Cyclic voltammetry was measured using an ElectraSyn 2.0 pro. We thank Organic Chemistry Research Center of Sogang University for HRMS-ESI analysis, Korea Basic Science Institute (KBSI) for HRMS-EI analysis, and KAIST Analysis Center for Research Advancement (KARA) for quantum yield measurement.

5.4.2 Substrate preparation

Photocatalysts ($[Ir(ppy)_2(dtbbpy)](PF_6)$[23], $[Ir(dFCF_3ppy)_2(dtbbpy)](PF_6)$[23], $Ir(ppy)_3$[23], $Ir(dFppy)_3$[23], $Ir(CF_3ppy)_3$[23], 4CzIPN[38]) were synthesized following the literature procedures.

Disulfides **1a**, **1o**, and **1q** were purchased from commercial sources, and the rest of the diaryl disulfides were synthesized following the procedure reported by M. Kirihara and co-workers.[39]

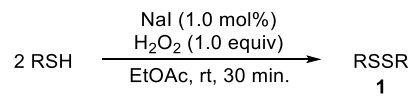

To a stirred solution of a thiol (2.0 mmol) in EtOAc (6 mL) were added NaI (3.0 mg, 0.020 mmol, 0.010 equiv) and 30% aqueous H_2O_2 solution (0.23 mL, 2.0 mmol, 1.0 equiv), and the mixture was stirred at room temperature for 30 min. Saturated aqueous $Na_2S_2O_3$ solution (15 mL) was added, and the resulting mixture was extracted with EtOAc (3 × 15 mL). The combined organic phase was washed with brine (15 mL), dried ($MgSO_4$), filtered, and concentrated in vacuo. The crude mixture was purified by silica gel flash column chromatography (Hexane) to acquire the desired disulfide **1**. In the case of disulfide **1p**, which has poor solubility toward most of the organic solvents, the resulting solid was washed with 10% aqueous NaOH (3 × 10 mL) and dried to afford the desired product.

1,2-Bis(4-fluorophenyl)disulfane (**1b**)

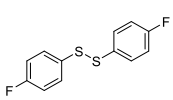

White solid. ^1H NMR (300 MHz, $CDCl_3$) δ 7.46 (dd, J = 8.9, 5.1 Hz, 4H), 7.02 (t, J = 8.7 Hz, 4H). The compound was identified by spectral comparison with literature data.[40]

1,2-Bis(4-chlorophenyl)disulfane (**1c**)

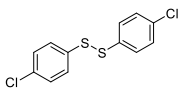

Beige solid. ^{1}H NMR (300 MHz, $CDCl_3$) δ 7.28 (d, *J* = 8.5 Hz, 4H), 7.15 (d, *J* = 8.7 Hz, 4H). The compound was identified by spectral comparison with literature data.[41]

1,2-Bis(4-bromophenyl(disulfane) (**1d**)

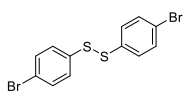

White solid. ^{1}H NMR (400 MHz, $CDCl_3$) δ 7.45 – 7.39 (m, 4H), 7.36 – 7.30 (m, 4H). The compound was identified by spectral comparison with literature data.[42]

1,2-Bis(4-(trifluoromethyl)phenyl)disulfane (**1e)**

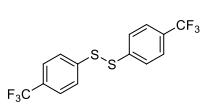

White solid. ^{1}H NMR (400 MHz, $CDCl_3$) δ 7.60 – 7.55 (m, 8H). The compound was identified by spectral comparison with literature data.[43]

1,2-Bis(4-(trifluoromethoxy)phenyl)disulfane (**1f**)

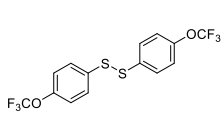

Yellow oil. ^{1}H NMR (400 MHz, $CDCl_3$) δ 7.54 – 7.45 (m, 4H), 7.22 – 7.12 (m, 4H). The compound was identified by spectral comparison with literature data.[44]

1,2-Di-*p*-tolyldisulfane (**1g**)

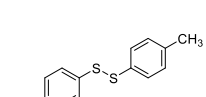

Pale yellow solid. ^{1}H NMR (300 MHz, $CDCl_3$) δ 7.29 (d, *J* = 8.0 Hz, 4H), 7.00 (d, *J* = 7.9 Hz, 4H), 2.21 (s, 6H). The compound was identified by spectral comparison with literature data.[45]

1,2-Bis(4-(*tert*-butyl)phenyl)disulfane (**1h**)

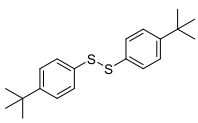

White solid. ^{1}H NMR (300 MHz, $CDCl_3$) δ 7.36 (d, *J* = 8.3 Hz, 4H), 7.24 (d, *J* = 8.5 Hz, 4H), 1.21 (s, 18H). The compound was identified by spectral comparison with literature data.[40]

1,2-Bis(3-fluorophenyl)disulfane (**1i**)

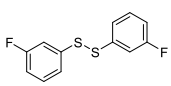

Yellow oil. ^{1}H NMR (300 MHz, $CDCl_3$) δ 7.34 – 7.24 (m, 6H), 6.98 – 6.92 (m, 2H). The compound was identified by spectral comparison with literature data.[46]

1,2-Di-*m*-tolyldisulfane (**1j**)

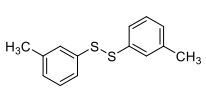

Yellow oil. ^{1}H NMR (400MHz, $CDCl_3$) δ 7.36 (s, 2H), 7.35 (d, *J* = 7.4 Hz, 2H), 7.22 (t, *J* = 8.0 Hz, 2H), 7.06 (d, *J* = 7.4 Hz, 2H), 2.35 (s, 6H). The compound was identified by spectral comparison with literature data.[41]

1,2-Bis(3-methoxyphenyl)disulfane (**1k**)

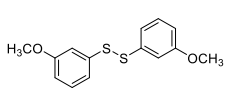

Colorless oil. ^{1}H NMR (300 MHz, $CDCl_3$) δ 7.06 (t, *J* = 8.2 Hz, 2H), 7.00 – 6.91 (m, 4H), 6.62 (d, *J* = 8.1 Hz, 2H), 3.60 (s, 6H). The compound was identified by spectral comparison with literature data.[46]

1,2-Bis(3,5-dichlorophenyl)disulfane (**1l**)

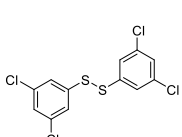

Yellow solid. ^{1}H NMR (400 MHz, $CDCl_3$) δ 7.33 (d, *J* = 1.8 Hz, 4H), 7.23 (t, *J* = 1.8 Hz, 2H). The compound was identified by spectral comparison with literature data.[47]

1,2-Di-*o*-tolyldisulfane (**1m**)

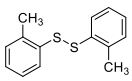

White solid. ^{1}H NMR (300 MHz, $CDCl_3$) δ 7.59 – 7.50 (m, 2H), 7.22 – 7.11 (m, 6H), 2.45 (s, 6H). The compound was identified by spectral comparison with literature data.[41]

1,2-Bis(2-isopropylphenyl)disulfane (**1n**)

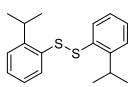

Light-green oil. ^{1}H NMR (300 MHz, $CDCl_3$) δ 7.47 (d, *J* = 7.8 Hz, 2H), 7.20 – 7.09 (m, 4H), 7.03 (ddd, *J* = 7.9, 6.9, 2.0 Hz, 2H), 3.42 (sep, *J* = 6.8 Hz, 2H), 1.14 (d, *J* = 6.8 Hz, 12H); ^{13}C NMR (75 MHz, $CDCl_3$) δ 148.3, 134.8, 129.7, 128.0, 126.7, 125.7, 30.4, 23.5; HRMS-EI (m/z) $[M]^+$ calculated for $C_{18}H_{22}S_2$, 302.1163; found: 302.1165.

1,2-Bis(5-chlorobenzo[*d*]thiazol-2-yl)disulfane (**1p**)

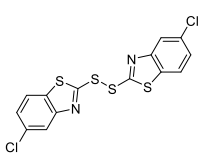

White solid. ^{1}H NMR (400 MHz, DMSO-d_6) δ 7.65 (d, *J* = 8.5 Hz, 2H), 7.28 (dd, *J* = 8.5, 2.0 Hz, 2H), 7.22 (d, *J* = 1.9 Hz, 2H); ^{13}C NMR (101 MHz, DMSO-d_6) δ 190.9, 142.3, 131.9, 127.6, 124.2, 123.3, 112.0; HRMS-EI (m/z) $[M]^+$ calculated for $C_{14}H_{10}Cl_2N_2S_4$, 399.8791; found: 399.8794.

Unsymmetrical disulfides were synthesized following the procedure reported by Y. S. Choe and co-workers.[37]

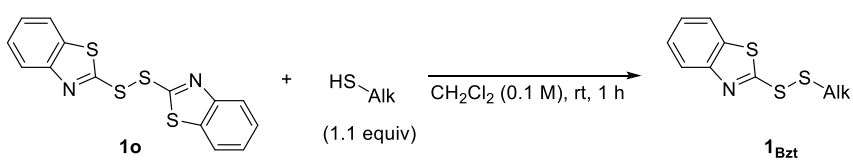

To a stirred solution of a 2,2'-dibenzothiazolyl disulfide (**1o**, 2.0 mmol, 665

mg, 1.0 equiv) in CH_2Cl_2 (18 mL) was added a solution of thiol (2.2 mmol, 1.1 equiv) in CH_2Cl_2 (2 mL) dropwise, and the mixture was stirred at room temperature for 1 h. After the reaction was finished, the reaction mixture was washed with 5% aqueous NaOH solution (2 × 20 mL) and brine (20 mL), dried ($MgSO_4$), filtered, and concentrated in vacuo. The crude mixture was purified by silica gel flash column chromatography (Hexane) to afford the desired unsymmetrical disulfide **1$_{Bzt}$**. For the synthesis of **1q$_{ClBzt}$** and **1q$_{NO2Ph}$**, 1,2-bis(5-chlorobenzo[*d*]thiazol-2-yl)disulfane (**1p**, 803 mg, 2.0 mmol, 1.0 equiv) and 1,2-bis(4-nitrophenyl)disulfane (617 mg, 2.0 mmol, 1.0 equiv) were used instead of **1o**, respectively.

2-(Benzyldisulfaneyl)benzo[*d*]thiazole (**1q$_{Bzt}$**)

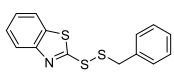

White solid. ^{1}H NMR (499 MHz, $CDCl_3$) δ 7.89 (d, *J* = 8.2 Hz, 1H), 7.80 (d, *J* = 8.0 Hz, 1H), 7.45 (t, *J* = 8.0 Hz, 1H), 7.39 – 7.28 (m, 6H), 4.19 (s, 2H). The compound was identified by spectral comparison with literature data.[37]

2-(Benzyldisulfaneyl)-5-chlorobenzo[*d*]thiazole (**1q$_{ClBzt}$**)

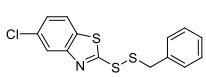

White solid. ^{1}H NMR (400 MHz, $CDCl_3$) δ 7.82 (d, *J* = 1.7 Hz, 1H), 7.67 (d, *J* = 8.5 Hz, 1H), 7.35 – 7.22 (m, 6H), 4.16 (s, 2H); ^{13}C NMR (101 MHz, $CDCl_3$) δ 175.1, 155.8, 135.4, 134.2, 132.4, 129.6, 128.9, 128.3, 125.1, 122.0, 121.9, 44.1; HRMS-ESI (m/z) $[M+Na]^+$ calculated for $C_{14}H_{10}ClNS_3Na$, 345.9556; found: 345.9555.

1-Benzyl-2-(4-nitrophenyl)disulfane (**1q$_{NO2Ph}$**)

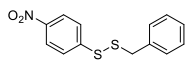

Light yellow solid. ^{1}H NMR (400 MHz, $CDCl_3$) δ 7.97 – 7.89 (m, 2H), 7.37 – 7.29 (m, 2H), 7.16 – 7.08 (m, 5H), 3.85 (s, 2H); ^{13}C NMR (101 MHz, $CDCl_3$) δ 146.6, 146.0, 136.0, 129.4, 128.7, 127.9, 125.8, 123.8, 43.6; HRMS-ESI (m/z) $[M+Na]^+$ calculated for $C_{13}H_{11}NO_2S_2Na$, 300.0123; found: 300.0122.

2-(Phenethyldisulfaneyl)benzo[*d*]thiazole (**1r$_{Bzt}$**)

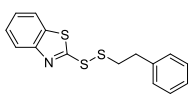

Beige solid. ^{1}H NMR (400 MHz, $CDCl_3$) δ 7.87 (d, *J* = 7.8 Hz, 1H), 7.79 (d, *J* = 8.0 Hz, 1H), 7.43 (ddd, *J* = 8.3, 7.3, 1.3 Hz, 1H), 7.37 – 7.15 (m, 6H), 3.20 (dd, *J* = 9.0, 6.3 Hz, 1H), 3.07 (dd, *J* = 9.1, 6.2 Hz, 1H); ^{13}C NMR (101 MHz, $CDCl_3$) δ 172.7, 155.1, 139.1, 135.9, 128.6, 128.6, 126.7, 126.3, 124.6, 122.2, 121.2, 40.6, 35.5; HRMS-ESI (m/z) $[M+Na]^+$ calculated for $C_{15}H_{13}NS_3Na$, 326.0102; found: 326.0103.

2-(Dodecyldisulfaneyl)benzo[*d*]thiazole (**1s$_{Bzt}$**)

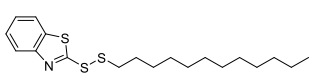

Colorless oil. ^{1}H NMR (400 MHz, $CDCl_3$) δ 7.88 (dd, *J* = 8.3, 3.1 Hz, 1H), 7.81 (dd, J = 8.0, 1.3 Hz, 1H), 7.44 (ddd, *J* = 8.2, 6.5, 1.3 Hz, 1H), 7.34 (ddd, *J* = 7.9, 6.7, 1.2 Hz, 1H), 2.97 (t, *J* = 7.4 Hz, 2H), 1.76 (quin, *J* = 7.4 Hz, 2H), 1.41 (quin, *J* = 7.1 Hz, 2H), 1.33 – 1.19 (m, 16H), 0.88 (t, *J* = 6.7 Hz, 3H); ^{13}C NMR (101 MHz, $CDCl_3$) δ 173.5, 155.2, 136.0, 126.3, 124.6, 122.2, 121.2, 39.7, 32.0, 29.7, 29.7, 29.6, 29.5, 29.3, 29.1, 28.6, 27.4, 22.8, 14.3; HRMS-ESI (m/z) $[M+H]^+$ calculated for $C_{19}H_{30}NS_3$, 368.1535; found: 368.1538.

2-((2-Ethylhexyl)disulfaneyl)benzo[*d*]thiazole (**1t$_{Bzt}$**)

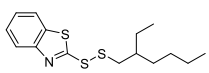

Colorless oil. ^{1}H NMR (400 MHz, $CDCl_3$) δ 7.87 (d, *J* = 8.1 Hz, 1H), 7.81 (d, *J* = 8.0 Hz, 1H), 7.44 (t, *J* = 7.7 Hz, 1H), 7.34 (t, *J* = 7.6 Hz, 1H), 3.00 (d, *J* = 6.3 Hz, 2H), 1.70 (sep, *J* = 6.3 Hz, 1H), 1.52 – 1.37 (m, 4H), 1.36 – 1.22 (m, 4H), 0.90 (t, *J* = 7.4 Hz, 3H), 0.89 (t, *J* = 6.9 Hz, 3H); ^{13}C NMR (101 MHz, $CDCl_3$) δ 173.3, 155.2, 135.8, 126.2, 124.5, 122.1, 121.1, 44.8, 39.1, 32.0, 28.7, 25.3, 22.9, 14.1, 10.7; HRMS-ESI (m/z) $[M+H]^+$ calculated for $C_{15}H_{22}NS_3$, 312.0909; found: 312.0910.

Ethyl *S*-(benzo[*d*]thiazol-2-ylthio)-*N*-(*tert*-butoxycarbonyl)-L-cysteinate (**1u$_{Bzt}$**)

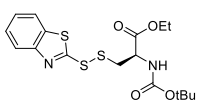

White solid. ^{1}H NMR (400 MHz, $CDCl_3$) δ 7.90 (d, *J* = 8.1 Hz, 1H), 7.79 (d, *J* = 8.0 Hz, 1H), 7.43 (t, *J* = 7.7 Hz, 1H), 7.33 (t, *J* = 7.6 Hz, 1H), 5.79 (s, 1H), 4.63 (s, 1H), 4.20 (q, *J* = 7.1 Hz, 2H), 3.48 (d, *J* = 4.0 Hz, 2H), 1.42 (s, 9H), 1.24 (t, *J* = 7.1 Hz, 3H); ^{13}C NMR (101 MHz, $CDCl_3$) δ 171.0, 170.2, 155.1, 154.6, 135.8, 126.3, 124.8, 122.2, 121.2, 80.3, 62.1, 53.1, 42.1, 28.3, 14.1; HRMS-ESI (m/z) $[M+Na]^+$ calculated for $C_{17}H_{22}N_2O_4S_3Na$, 437.0634; found: 437.0636.

(2*R*,3*R*,4*S*,5*R*,6*S*)-2-(acetoxymethyl)-6-(benzo[*d*]thiazol-2-yldisulfaneyl)tetrahydro-2*H*-pyran-3,4,5-triyl triacetate (**1v$_{Bzt}$**)

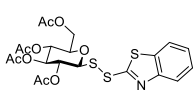

White solid. ^{1}H NMR (400 MHz, $CDCl_3$) δ 7.88 (d, *J* = 8.1 Hz, 1H), 7.78 (d, *J* = 8.0 Hz, 1H), 7.44 (t, *J* = 7.7 Hz, 1H), 7.35 (t, *J* = 7.6 Hz, 1H), 5.31 – 5.21 (m, 2H), 5.09 (tt, *J* = 9.4, 6.7 Hz, 1H), 4.80 – 4.70 (m, 1H), 4.14 – 4.01 (m, 2H), 3.74 (ddd, *J* = 10.1, 4.5, 2.7 Hz, 1H), 2.10 (s, 3H), 2.01 (s, 3H), 2.00 (s, 3H), 1.76 (s, 3H); ^{13}C NMR (101 MHz, $CDCl_3$) δ 171.0, 170.6,

170.2, 169.4, 169.4, 154.1, 136.0, 126.5, 125.2, 122.3, 121.2, 87.6, 76.3, 73.6, 69.6, 68.0, 61.7, 20.8, 20.7, 20.7, 20.4; HRMS-ESI (m/z) $[M+Na]^+$ calculated for $C_{21}H_{23}NO_9S_3Na$, 552.0427; found: 552.0427.

Ethyl ((*S*)-3-(benzo[*d*]thiazol-2-yldisulfaneyl)-2-methylpropanoyl)-L-prolinate (**1w$_{bzt}$**)

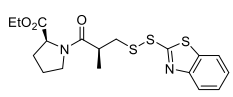

Colorless sticky oil. Rotameric mixture. ^{1}H NMR (400 MHz, $CDCl_3$) δ 7.67 (d, *J* = 8.1 Hz, 1H), 7.65 – 7.58 (m, 1H), 7.29 – 7.19 (m, 1H), 7.17 – 7.11 (m, 1H), 4.30 (dd, *J* = 8.5, 3.8 Hz, 0.9H), 4.26 (dd, *J* = 8.5, 2.4 Hz, 0.1H), 4.04 – 3.92 (m, 2H), 3.51 (ddd, *J* = 11.8, 8.0, 3.8 Hz, 0.1H), 3.41 – 3.34 (m, 1H), 3.34 – 3.25 (m, 0.1H), 3.25 – 3.11 (m, 1.9H), 2.89 (ddt, *J* = 12.1, 9.1, 6.0 Hz, 0.9H), 2.75 (dd, *J* = 13.4, 5.2 Hz, 0.9H), 2.60 (sex, *J* = 7.0 Hz, 0.1H), 2.14 – 2.05 (m, 0.1H), 2.05 – 1.95 (m, 0.1H), 1.94 – 1.84 (m, 0.9H), 1.82 – 1.71 (m, 2H), 1.67 – 1.55 (m, 0.9H), 1.11 – 0.98 (m, 6H); ^{13}C NMR (101 MHz, $CDCl_3$) δ 172.8, 172.2, 172.1, 171.6, 171.6, 154.7, 154.5, 135.5, 135.4, 126.0, 125.9, 124.4, 124.2, 121.7, 121.6, 120.9, 120.8, 61.5, 60.6, 58.8, 58.5, 46.4, 46.1, 42.3, 41.9, 37.7, 37.3, 31.1, 28.6, 24.3, 22.0, 16.7, 16.4, 13.8; HRMS-ESI (m/z) $[M+Na]^+$ calculated for $C_{18}H_{22}N_2O_3S_3Na$, 433.0685; found: 433.0687.

All olefins except **2o** were purchased from commercial sources. **2o** was synthesized following a reported procedure.[48] Oxidants except $(Fc)(BF_4)$ were purchased from commercial sources. $(Fc)(BF_4)$ was synthesized following a reported procedure.[30]

5.4.3 Screening experiments

A 4 mL reaction vial equipped with a PTFE-coated stir bar was charged with diphenyl disulfide **1a** (54.6 mg, 0.25 mmol, 1.0 equiv), photocatalyst, and NaOH (10 mg, 0.25 mmol, 1.0 equiv) in a glovebox. The vial was closed with a Teflon-lined septum cap and taken out of the glovebox. 2,3-Dimethyl-2-butene **2a** (594 μL, 5.0 mmol, 20 equiv) and solvent (1 mL) were added via syringe, and the solution was stirred for 24 h under 40 W blue LED irradiation with fan cooling, located on the 2.5 cm away from the LED. After the reaction was complete, dodecane (56.8 μL, 0.25 mmol, 1.0 equiv) was added, and the result was analyzed by GC.

Table 5.5 Optimization of the reaction with **1a** and **2a**

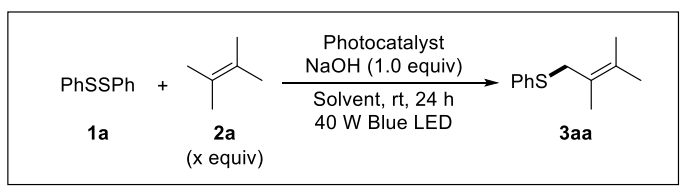

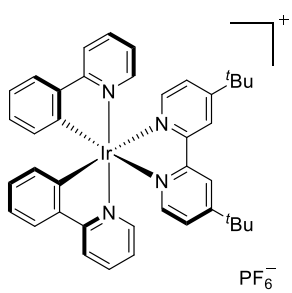

[Ir(ppy)$_2$(dtbbpy)](PF$_6$)

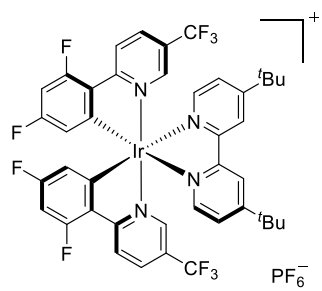

[Ir(dFCF$_3$ppy)$_2$(dtbbpy)](PF$_6$)

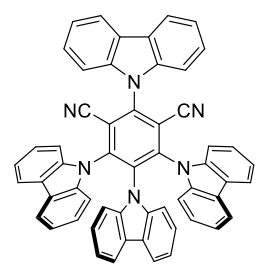

4CzIPN

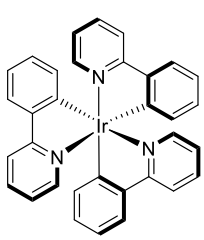

Ir(ppy)$_3$

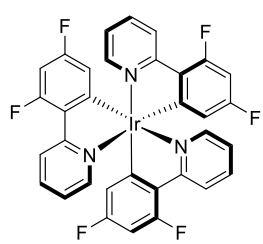

Ir(dFppy)$_3$

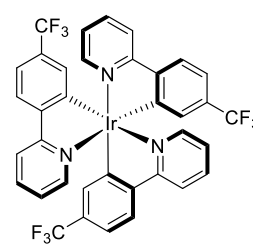

Ir(CF$_3$ppy)$_3$

entry	Photocatalyst (mol%)	x	Solvent (M)	Yield 3aa (%)
1	$[Ir(ppy)_2(dtbbpy)](PF_6)$ (1.0)	10	DMA (0.25 M)	6
2	$[Ir(dFCF_3ppy)_2(dtbbpy)](PF_6)$ (1.0)	10	DMA (0.25 M)	<2
3	4CzIPN (1.0)	10	DMA (0.25 M)	16
4	$Ir(ppy)_3$ (1.0)	10	DMA (0.25 M)	18
5	$Ir(dFppy)_3$ (1.0)	10	DMA (0.25 M)	24
6	$Ir(CF_3ppy)_3$ (1.0)	10	DMA (0.25 M)	50
7	$Ir(CF_3ppy)_3$ (1.0)	10	DMF (0.25 M)	35
8	$Ir(CF_3ppy)_3$ (1.0)	10	CH_3CN (0.25 M)	44
9	$Ir(CF_3ppy)_3$ (1.0)	10	THF (0.25 M)	17
10	$Ir(CF_3ppy)_3$ (1.0)	10	Benzene (0.25 M)	18
11	$Ir(CF_3ppy)_3$ (1.0)	10	DMA (0.5 M)	51
12[a]	$Ir(CF_3ppy)_3$ (1.0)	10	DMF (0.25 M)	6
13[b]	$Ir(CF_3ppy)_3$ (1.0)	10	DMF (0.25 M)	50
14	$Ir(CF_3ppy)_3$ (0.5)	10	DMF (0.25 M)	26
15	$Ir(CF_3ppy)_3$ (2.0)	10	DMA (0.25 M)	60
16	$Ir(CF_3ppy)_3$ (2.0)	5	DMA (0.25 M)	31
17	$Ir(CF_3ppy)_3$ (1.0)	20	DMA (0.25 M)	69
18	$Ir(CF_3ppy)_3$ (2.0)	20	DMA (0.25 M)	91[d]
19[c]	$Ir(CF_3ppy)_3$ (2.0)	20	DMA (0.25 M)	18
20	None	20	DMA (0.25 M)	<2

[a]0.5 equivalence of NaOH. [b]1.5 equivalence of NaOH [c]Without NaOH. [d]Isolated yield. DMA = *N*,*N*-dimethylacetamide; DMF = *N*,*N*-dimethylformamide; THF = tetrahydrofuran.

Scheme 5.7 Effect of base in the reaction between **1a** and **2h**

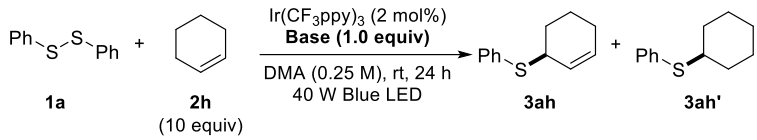

Base	None	Na_2CO_3	K_2CO_3	Cs_2CO_3	$NaHCO_3$	Na_2SO_4
3ah	29%	83%	60%	Messy	55%	33%
3ah'	32%	16%	N. D.	Messy	29%	31%

KOAc	HCO_2Na	K_3PO_4	K_2HPO_4	KH_2PO_4	NaOH	KOH
85%	74%	78%	55%	33%	89%	89%
15%	22%	N. D.	27%	28%	N. D.	N. D.

5.4.4 Sensitivity assessment of the reaction

Following the protocol reported by Glorius and co-workers,[16] the sensitivity assessment of the reaction was performed under the optimized reaction conditions. The detailed variations and the results were listed below. In the case of the entry 10, 4 × 40 W Blue LED were applied, and further isolation process was performed.

Table 5.6 Sensitivity assessment of the reaction

entry	Experiment	Variation from the optimized reaction conditions	Yield 3aa (%)	Deviation
1	High c	0.9 mL DMA	68	-23
2	Low c	1.1 mL DMA	53	-38
3	High H_2O	+ 100 uL H_2O	53	-38
4	Medium O_2 (control)	Inert atmosphere (optimized conditions)	91	0
5	High O_2	Aerobic conditions (with 8 mL reaction vial)	68	-23
6	Low T	T ~ 20 °C	71	-20
7	High T	T ~ 40 °C	70	-21
8	Low I	*d* = 10 cm (I/16)	56	-35
9	High I	*d* = 0.5 cm (16·I)	35	-56
10	Big scale	5 mmol scale	86 (69)*	-5

*Isolated yield

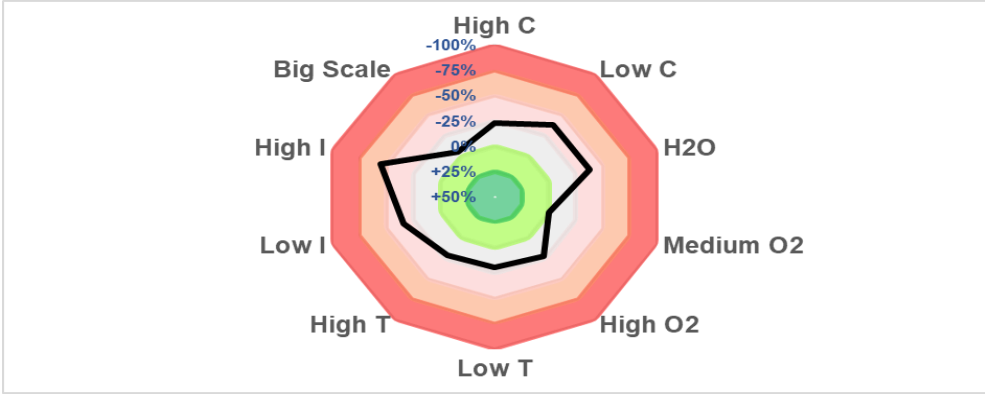

Figure 5.3 Radar diagram

5.4.5 General procedure for the synthesis of allyl thioethers (3)

5.4.5.1 Synthesis of allyl thioethers from symmetric disulfides

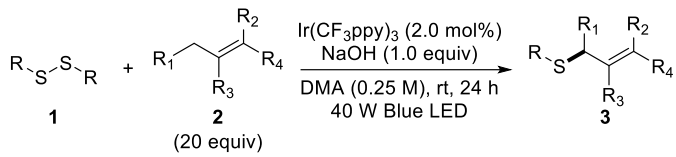

A 4 mL reaction vial equipped with a PTFE-coated stir bar was charged with disulfide **1** (0.25 mmol, 1.0 equiv), $Ir(CF_3ppy)_3$ (4.3 mg, 0.0050 mmol, 0.020 equiv), and NaOH (10 mg, 0.25 mmol, 1.0 equiv) in a glovebox. The vial was closed with a Teflon-lined septum cap and taken out of the glovebox. Olefin **2** (5.0 mmol, 20 equiv) and DMA (1 mL) were added via syringe, and the solution was stirred for 24 h under 40 W blue LED irradiation with fan cooling, located on the 2.5 cm away from the LED. After the reaction was complete, the reaction mixture was diluted with diethyl ether (10 mL) and quenched with a saturated aqueous sodium bicarbonate solution (10 mL). The organic layer was collected, and the aqueous layer was further extracted with diethyl ether (5 × 10 mL). The combined organic layer was dried ($MgSO_4$), filtered, and concentrated in vacuo. The crude mixture was purified by silica gel flash column chromatography (Hexane) to afford the corresponding allyl thioether **3**.

5.4.5.2 Synthesis of allyl thioethers from unsymmetrical disulfides

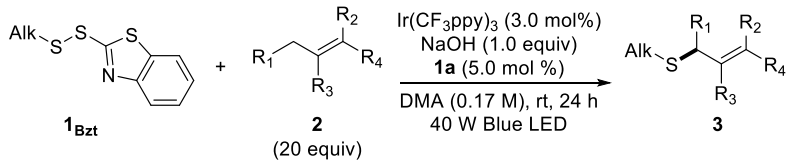

A 4 mL reaction vial equipped with a PTFE-coated stir bar was charged with disulfide $\mathbf{1_{Bzt}}$ (0.25 mmol, 1.0 equiv), $Ir(CF_3ppy)_3$ (6.4 mg, 0.0075 mmol, 0.030 equiv), NaOH (10–20 mg, 0.25–0.50 mmol, 1.0–2.0 equiv), and **1a** (2.7 mg, 0.0125 mmol, 0.050 equiv) in a glovebox. The vial was closed with a Teflon-lined septum cap and taken out of the glovebox. Olefin **2** (5.0 mmol, 20 equiv) and DMA (1.5 mL) were added via syringe, and the solution was stirred for 24 h under 40 W blue LED irradiation with fan cooling, located on the 2.5 cm away from the LED. After the reaction was complete, the reaction mixture was diluted with diethyl ether (10 mL) and quenched with a saturated aqueous sodium bicarbonate solution (10 mL). The organic layer was collected, and the aqueous layer was further extracted with diethyl ether (5 × 10 mL). The combined organic layer was dried ($MgSO_4$), filtered, and concentrated in vacuo. The crude mixture was purified by silica gel flash column chromatography (Hexane) to afford the corresponding allyl thioether **3**.

5.4.5.3 Scaled-up reaction for the synthesis of allyl thioether 3aa

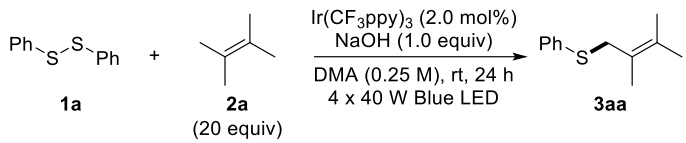

A 100 mL quartz round-bottom flask equipped with a PTFE-coated stir bar was charged with diphenyl disulfide **1a** (1.1 g, 5.0 mmol, 1.0 equiv), $Ir(CF_3ppy)_3$ (86 mg, 0.1 mmol, 0.020 equiv), and NaOH (200 mg, 5.0 mmol, 1.0 equiv) in a glovebox. The RBF was closed with a rubber septum and taken out of the glovebox. 2,3-Dimethyl-2-butene 2 (12 mL, 100 mmol, 20 equiv) and DMA (20 mL) were added via syringe, and the solution was stirred for 24 h under 4 × 40 W blue LED irradiation with fan cooling, located on the 2.5 cm away from each LEDs. After the reaction was complete, the reaction mixture was diluted with diethyl ether (30 mL) and quenched with a saturated aqueous sodium bicarbonate solution (50 mL). The GC yield of the allyl thioether **3aa** was measured using dodecane as the internal standard (86%). After that, the organic layer was collected, and the aqueous layer was further extracted with diethyl ether (5 × 100 mL). The combined organic layer was dried ($MgSO_4$), filtered, and concentrated in vacuo. The crude mixture was purified by silica gel flash column chromatography (hexane) to afford the corresponding allyl thioether **3aa**.

5.4.6 Characterization of allyl thioethers (3)

(2,3-Dimethylbut-2-en-1-yl)(phenyl)sulfane (**3aa**)

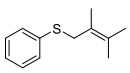

Yellow oil (44.0 mg, 0.23 mmol, 91%; 666.2 mg, 3.45 mmol, 69% for scaled-up reaction); ^{1}H NMR (300 MHz, $CDCl_3$) δ 7.26 (d, *J* = 7.8 Hz, 2H), 7.18 (t, *J* = 7.4 Hz, 2H), 7.14 – 7.06 (m, 1H), 3.50 (s, 2H), 1.71 (s, 3H), 1.58 (s, 3H), 1.48 (s, 3H); ^{13}C NMR (75 MHz, $CDCl_3$) δ 137.4, 130.5, 129.9, 128.7, 126.3, 122.8, 39.3, 21.0, 20.4, 18.3; HRMS-EI (m/z) $[M]^+$ calculated for $C_{12}H_{16}S$, 192.0973; found: 192.0972.

(2,3-Dimethylbut-2-en-1-yl)(4-fluorophenyl)sulfane (**3ba**)

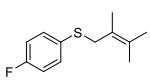

Yellow oil (29.0 mg, 0.14 mmol, 55%); ^{1}H NMR (300 MHz, $CDCl_3$) δ 7.41 – 7.30 (m, 2H), 6.99 – 6.93 (m, 2H), 3.50 (s, 2H), 1.77 (s, 3H), 1.63 (s, 3H), 1.44 (s, 3H); ^{13}C NMR (75 MHz, $CDCl_3$) δ 162.3 (d, *J* = 246.5 Hz), 134.2 (d, *J* = 8.1 Hz), 131.6 (d, *J* = 3.3 Hz), 130.0, 122.9, 115.8 (d, *J* = 21.7 Hz), 40.6, 20.9, 20.2, 18.1; ^{19}F NMR (376 MHz, $CDCl_3$) δ −115.3 (ddd, *J* = 8.6, 5.2, 3.3 Hz); HRMS-EI (m/z) $[M]^+$ calculated for $C_{12}H_{15}FS$, 210.0879; found: 210.0876.

(4-Chlorophenyl)(2,3-dimethylbut-2-en-1-yl)sulfane (**3ca**)

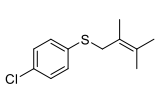

Yellow oil (28.3 mg, 0.13 mmol, 50%); ^{1}H NMR (499 MHz, $CDCl_3$) δ 7.28 (d, *J* = 8.6 Hz, 2H), 7.24 (d, *J* = 8.5 Hz, 2H), 3.56 (s, 2H), 1.78 (s, 3H), 1.67 (s, 3H), 1.56 (s, 3H); ^{13}C NMR (126 MHz, $CDCl_3$) δ 135.8, 132.5, 132.1, 130.2, 128.9, 122.7, 39.7, 21.0, 20.4, 18.2; HRMS-EI (m/z) $[M]^+$ calculated for $C_{12}H_{15}ClS$, 226.0583; found: 226.0585.

(4-Bromophenyl)(2,3-dimethylbut-2-en-1-yl)sulfane (**3da**)

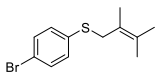

Colorless oil (35.9 mg, 0.13 mmol, 53%); ^{1}H NMR (400 MHz, $CDCl_3$) δ 7.40 – 7.35 (m, 2H), 7.22 – 7.17 (m, 2H), 3.56 (s, 2H), 1.77 (s, 3H), 1.66 (s, 3H), 1.57 (s, 3H); ^{13}C NMR (101 MHz, $CDCl_3$) δ 136.5, 132.1, 131.8, 130.3, 122.6, 120.2, 39.4, 21.0, 20.4, 18.2; HRMS-EI (m/z) $[M]^+$ calculated for $C_{12}H_{15}BrS$, 270.0078; found: 270.0079.

(2,3-Dimethylbut-2-en-1-yl)(4-(trifluoromethyl)phenyl)sulfane (**3ea**)

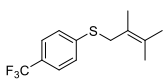

White solid (65.3 mg, 0.25 mmol, >99%); ^{1}H NMR (400 MHz, $CDCl_3$) δ 7.50 (d, *J* = 8.3 Hz, 2H), 7.36 (d, *J* = 8.3 Hz, 2H), 3.65 (s, 2H), 1.79 (s, 3H), 1.69 (s, 2H), 1.67 (s, 2H); ^{13}C NMR (101 MHz, $CDCl_3$) δ 143.4, 130.8, 128.4, 127.6 (q, *J* = 32.6 Hz), 125.55 (q, *J* = 3.8 Hz)., 124.4 (q, *J* = 272 Hz), 122.0, 38.2, 21.1, 20.5, 18.3.; ^{19}F NMR (376 MHz, $CDCl_3$) δ -62.4; HRMS-EI (m/z) $[M]^+$ calculated for $C_{13}H_{15}F_3S$, 260.0847; found: 260.0844.

(2,3-Dimethylbut-2-en-1-yl)(4-(trifluoromethoxy)phenyl)sulfane (**3fa**)

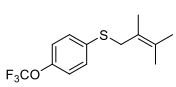

Colorless oil (69.2 mg, 0.25 mmol, >99%) ^{1}H NMR (400 MHz, $CDCl_3$) δ 7.35 (d, *J* = 8.6 Hz, 2H), 7.11 (d, *J* = 8.3 Hz, 2H), 3.56 (s, 2H), 1.78 (s, 3H), 1.65 (s, 3H), 1.53 (s, 3H); ^{13}C NMR (101 MHz, $CDCl_3$) δ 148.0, 136.0, 132.2, 130.4, 122.5, 121.3, 120.6 (q, *J* = 257.0 Hz), 39.7, 20.9, 20.3, 18.1; ^{19}F NMR (376 MHz, $CDCl_3$) δ -58.0; HRMS-EI (m/z) $[M]^+$ calculated for $C_{13}H_{15}F_3OS$, 276.0796; found: 276.0792.

(2,3-Dimethylbut-2-en-1-yl)(*p*-tolyl)sulfane (**3ga**)

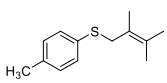

Yellow oil (20.7 mg, 0.10 mmol, 40%); ^{1}H NMR (300 MHz, $CDCl_3$) δ 7.23 – 7.15 (m, 2H), 7.00 (d, *J* = 8.2 Hz, 2H), 3.47 (s, 2H), 2.25 (s, 3H), 1.70 (s, 3H), 1.57 (s, 3H), 1.46 (s, 3H); ^{13}C NMR (75 MHz, $CDCl_3$) δ 136.5, 133.4, 131.4, 129.7, 129.5, 123.2, 40.1, 21.2, 21.0, 20.4, 18.2; HRMS-EI (m/z) $[M]^+$ calculated for $C_{13}H_{18}S$, 206.1129; found: 206.1127.

(4-(*tert*-Butyl)phenyl)(2,3-dimethylbut-2-en-1-yl)sulfane (**3ha**)

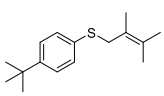

Yellow oil (46.1 mg, 0.19 mmol, 74%); ^{1}H NMR (300 MHz, $CDCl_3$) δ 7.21 (brs, 4H), 3.48 (s, 2H), 1.71 (s, 3H), 1.57 (s, 3H), 1.46 (s, 3H), 1.22 (s, 9H); ^{13}C NMR (75 MHz, $CDCl_3$) δ 149.5, 133.7, 130.5, 129.6, 125.7, 122.9, 39.6, 34.5, 31.3, 20.9, 20.2, 18.2; HRMS-EI (m/z) $[M]^+$ calculated for $C_{16}H_{24}S$, 248.1599; found: 248.1602.

(2,3-Dimethylbut-2-en-1-yl)(3-fluorophenyl)sulfane (**3ia**)

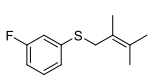

Yellow oil (39.0 mg, 0.19 mmol, 74%); ^{1}H NMR (300 MHz, $CDCl_3$) δ 7.19 – 7.08 (m, 1H), 7.06 – 6.90 (m, 2H), 6.83 – 6.73 (m, 1H), 3.52 (s, 2H), 1.71 (s, 3H), 1.60 (s, 3H), 1.55 (s, 3H); ^{13}C NMR (126 MHz, $CDCl_3$) δ 162.9 (d, *J* = 247.9 Hz), 140.2 (d, *J* = 8.0 Hz), 130.4, 129.9 (d, *J* = 8.5 Hz), 125.4, 122.43, 116.5 (d, *J* = 22.2 Hz), 112.9 (d, *J* = 21.2 Hz), 39.0, 21.0, 20.5, 18.3; ^{19}F NMR (376 MHz, $CDCl_3$) δ -112.89 (td, *J* = 9.0, 6.3 Hz); HRMS-EI (m/z) $[M]^+$ calculated for $C_{12}H_{15}FS$, 210.0879; found: 210.0876.

(2,3-Dimethylbut-2-en-1-yl)(*m*-tolyl)sulfane (**3ja**)

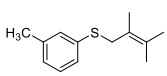

Yellow oil (28.6 mg, 0.14 mmol, 55%); ^{1}H NMR (300 MHz, $CDCl_3$) δ 7.19 – 7.11 (m, 3H), 7.03 – 6.96 (m, 1H), 3.58 (s, 2H), 2.32 (s, 3H), 1.79 (s, 3H), 1.66 (s, 3H), 1.59 (s, 3H); ^{13}C NMR (101 MHz, $CDCl_3$) δ 138.5, 137.2, 130.9, 129.9, 128.6, 127.3, 127.0, 122.9, 39.3, 21.5, 21.0, 20.4, 18.3; HRMS-EI (m/z) $[M]^+$ calculated for $C_{13}H_{18}S$, 206.1129; found: 206.1131.

(2,3-Dimethylbut-2-en-1-yl)(3-methoxyphenyl)sulfane (**3ka**)

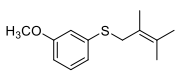

Yellow oil (36.0 mg, 0.16 mmol, 65%); ^{1}H NMR (499 MHz, $CDCl_3$) δ 7.17 (t, *J* = 8.0 Hz, 1H), 6.92 (d, *J* = 7.7 Hz, 1H), 6.90 – 6.87 (m, 1H), 6.72 (dd, *J* = 8.3, 2.5 Hz, 1H), 3.79 (s, 3H), 3.60 (s, 2H), 1.79 (s, 3H), 1.67 (s, 3H), 1.62 (s, 3H); ^{13}C NMR (75 MHz, $CDCl_3$) δ 159.8, 139.0, 130.0, 129.6, 122.8, 122.2, 115.2, 111.9, 55.4, 39.1, 21.0, 20.5, 18.3; HRMS-EI (m/z) $[M]^+$ calculated for $C_{13}H_{18}OS$, 222.1078; found: 222.1075.

(3,5-Dichlorophenyl)(2,3-dimethylbut-2-en-1-yl)sulfane (**3la**)

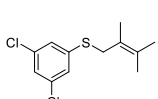

White solid (42.3 mg, 0.16 mmol, 65%); ^{1}H NMR (400 MHz, $CDCl_3$) δ 7.18 – 7.11 (m, 3H), 3.60 (s, 2H), 1.78 (s, 3H), 1.69 (s, 3H), 1.65 (s, 3H); ^{13}C NMR (101 MHz, $CDCl_3$) δ 141.6, 134.9, 131.1, 127.1, 125.9, 121.8, 38.7, 21.1, 20.5, 18.2; HRMS-EI (m/z) $[M]^+$ calculated for $C_{12}H_{14}Cl_2S$, 260.0193; found: 260.0194.

(2,3-Dimethylbut-2-en-1-yl)(*o*-tolyl)sulfane (**3ma**)

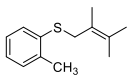

Yellow oil (35.0 mg, 0.17 mmol, 68%); ^{1}H NMR (400 MHz, $CDCl_3$) δ 7.30 – 7.24 (m, 1H), 7.15 – 6.97 (m, 3H), 3.53 (s, 2H), 2.38 (s, 3H), 1.79 (s, 3H), 1.66 (s, 3H), 1.58 (s, 3H); ^{13}C NMR (126 MHz, $CDCl_3$) δ 136.5, 133.5, 131.4, 131.2, 130.1, 130.0, 129.5, 123.2, 40.1, 21.2, 21.0, 20.3, 18.2; HRMS-EI (m/z) $[M]^+$ calculated for $C_{13}H_{18}S$, 206.1129; found: 206.1131.

(2,3-Dimethylbut-2-en-1-yl)(2-isopropylphenyl)sulfane (**3na**)

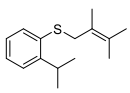

Yellow oil (25.4 mg, 0.11 mmol, 44%); ^{1}H NMR (300 MHz, $CDCl_3$) δ 7.25 (dd, *J* = 7.6, 1.3 Hz, 1H), 7.17 (dd, *J* = 7.3, 1.9 Hz, 1H), 7.11 (td, *J* = 7.4, 1.4 Hz, 1H), 7.04 (td, *J* = 7.3, 1.7 Hz, 1H), 3.58 – 3.47 (m, 1H), 3.46 (s, 2H), 1.72 (s, 3H), 1.59 (s, 3H), 1.49 (s, 3H), 1.16 (d, *J* = 6.9 Hz, 6H); ^{13}C NMR (75 MHz, $CDCl_3$) δ 149.2, 135.6, 130.9, 130.0, 126.7, 126.1, 125.4, 122.9, 39.8, 30.4, 23.6, 21.0, 20.4, 18.5; HRMS-EI (m/z) $[M]^+$ calculated for $C_{15}H_{22}S$, 234.1442; found: 234.1441.

2-((2,3-Dimethylbut-2-en-1-yl)thio)benzo[*d*]thiazole (**3oa**)

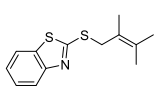

Light yellow oil (40.5 mg, 0.16 mmol, 65%); ^{1}H NMR (499 MHz, $CDCl_3$) δ 7.87 (d, *J* = 8.1 Hz, 1H), 7.75 (d, *J* = 7.9 Hz, 1H), 7.41 (t, *J* = 7.7 Hz, 1H), 7.28 (t, *J* = 7.6 Hz, 1H), 4.10 (s, 2H), 1.82 (s, 3H), 1.81 (s, 3H), 1.72 (s, 3H); ^{13}C NMR (101 MHz, $CDCl_3$) δ 167.8, 153.4, 135.4, 131.9, 126.1, 124.2, 121.6, 121.5, 121.0, 38.6, 21.2, 20.8, 18.4; HRMS-ESI (m/z) $[M+Na]^+$ calculated for $C_{13}H_{15}NNaS_2$, 272.0544; found: 272.0543.

5-Chloro-2-((2,3-dimethylbut-2-en-1-yl)thio)benzo[*d*]thiazole (**3pa**)

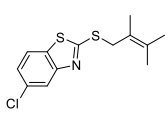

White solid (34.1 mg, 0.12 mmol, 46%); ^{1}H NMR (400 MHz, $CDCl_3$) δ 7.82 (d, *J* = 1.9 Hz, 1H), 7.62 (d, *J* = 8.5 Hz, 1H), 7.24 (dd, *J* = 8.4, 2.0 Hz, 1H), 4.08 (s, 2H), 1.79 (s, 6H), 1.70 (s, 3H); ^{13}C NMR (101 MHz, $CDCl_3$) δ 170.1, 154.2, 133.7, 132.2, 124.5, 121.6, 121.4, 121.4, 38.6, 21.2, 20.8, 18.3; HRMS-ESI (m/z) $[M+H]^+$ calculated for $C_{13}H_{15}ClNS_2$, 284.0329; found: 284.0328.

Benzyl(2,3-dimethylbut-2-en-1-yl)sulfane (**3qa**)

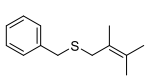

Colorless oil (35.1 mg, 0.17 mmol, 69%); ^{1}H NMR (400 MHz, $CDCl_3$) δ 7.37 – 7.19 (m, 5H), 3.66 (s, 2H), 3.16 (s, 2H), 1.72 (s, 3H), 1.67 (s, 3H), 1.62 (s, 3H); ^{13}C NMR (101 MHz, $CDCl_3$) δ 138.9, 128.9, 128.9, 128.5, 126.9, 123.6, 36.3, 36.1, 21.0, 20.5, 18.0; HRMS-EI (m/z) $[M]^+$ calculated for $C_{13}H_{18}S$, 206.1129; found: 206.1128.

(2,3-Dimethylbut-2-en-1-yl)(phenethyl)sulfane (**3ra**)

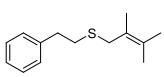

Yellow oil (26.4 mg, 0.12 mmol, 48%); ^{1}H NMR (400 MHz, $CDCl_3$) δ 7.32 – 7.29 (m, 2H), 7.24 – 7.19 (m, 3H), 3.25 (s, 2H), 2.89 (dd, *J* = 9.5, 6.3 Hz, 2H), 2.70 (dd, *J* = 9.5, 6.3 Hz, 2H), 1.76 (s, 3H), 1.74 (s, 3H), 1.70 (s, 3H); ^{13}C NMR (101 MHz, $CDCl_3$) δ 141.0, 128.6, 128.6, 128.5, 126.4, 124.1, 36.8, 36.3, 33.1, 21.0, 20.7, 17.9; HRMS-EI (m/z) $[M]^+$ calculated for $C_{14}H_{20}S$, 220.1286; found: 220.1287.

(2,3-Dimethylbut-2-en-1-yl)(dodecyl)sulfane (**3sa**)

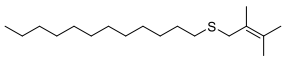

Yellow oil (28.4 mg, 0.10 mmol, 40%); ^{1}H NMR (400 MHz, $CDCl_3$) δ 3.20 (s, 2H), 2.42 (t, *J* = 7.4 Hz, 2H), 1.74 (s, 3H), 1.71 (s, 3H), 1.68 (s, 3H), 1.56 (quin, *J* = 7.3 Hz, 2H), 1.39 – 1.29 (m, 2H), 1.25 (brs, 16H), 0.88 (t, *J* = 6.7 Hz, 3H); ^{13}C NMR (101 MHz, $CDCl_3$) δ 128.2, 124.2, 36.1, 32.1, 31.7, 30.1, 29.8, 29.8, 29.8, 29.7, 29.5, 29.4, 29.2, 22.8, 21.0, 20.6, 18.0, 14.3; HRMS-EI (m/z) $[M]^+$ calculated for $C_{18}H_{36}S$, 284.2538; found: 284.2541.

Cyclohex-2-en-1-yl(dodecyl)sulfane (**3sh**)

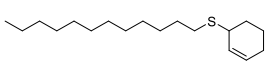

Light yellow oil (41.0 mg, 0.15 mmol, 58%); ^{1}H NMR (400 MHz, $CDCl_3$) δ 5.77 (dtd, *J* = 8.8, 3.5, 1.6 Hz, 1H), 5.70 (ddt, *J* = 10.0, 3.9, 2.0 Hz, 1H), 3.35 (tdq, *J* = 5.7, 3.9, 2.1 Hz, 1H), 2.54 (td, *J* = 7.3, 2.4 Hz, 2H), 2.05 – 1.90 (m, 3H), 1.84 (dddd, *J* = 15.5, 12.6, 6.2, 2.6 Hz, 1H), 1.74 (dddd, *J* = 13.0, 8.1, 5.7, 2.6 Hz, 1H), 1.65 – 1.52 (m, 3H), 1.37 (quin, *J* = 6.7 Hz, 2H), 1.32 – 1.22 (m, 16H), 0.88 (t, *J* = 6.8 Hz, 3H); ^{13}C NMR (101 MHz, $CDCl_3$) δ 129.6, 128.2, 40.8, 32.1, 31.1, 30.2, 29.8, 29.8, 29.8, 29.7, 29.6, 29.5, 29.4, 29.2, 25.1, 22.8, 20.1, 14.3; HRMS-EI (m/z) $[M]^+$ calculated for $C_{18}H_{34}S$, 282.2381; found: 282.2383.

Cyclopent-2-en-1-yl(dodecyl)sulfane (**3si**)

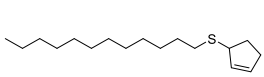

Colorless oil (28.2 mg, 0.11 mmol, 42%); ^{1}H NMR (400 MHz, $CDCl_3$) δ 5.85 (dq, *J* = 6.0, 2.0 Hz, 1H), 5.72 (dq, *J* = 4.4, 2.2 Hz, 1H), 3.88 – 3.82 (m, 1H), 2.53 – 2.49 (m, 2H), 2.49 – 2.41 (m, 1H), 2.41 – 2.24 (m, 2H), 1.94 – 1.84 (m, 1H), 1.59 (quin, *J* = 7.3 Hz, 2H), 1.37 (quin, *J*

= 6.9, 6.3 Hz, 2H), 1.26 (s, 16H), 0.90 – 0.86 (m, 3H); ^{13}C NMR (101 MHz, $CDCl_3$) δ 132.6, 132.0, 50.0, 32.1, 32.0, 31.8, 30.8, 30.1, 29.8, 29.8, 29.8, 29.7, 29.5, 29.4, 29.3, 22.8, 14.3; HRMS-EI (m/z) $[M]^+$ calculated for $C_{17}H_{32}S$, 268.2225; found: 268.2226.

Cyclohept-2-en-1-yl(dodecyl)sulfane (**3sj**)

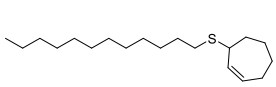

Yellow oil (18.6 mg, 0.063 mmol, 25%); ^{1}H NMR (400 MHz, $CDCl_3$) δ 5.83 – 5.66 (m, 2H), 3.56 – 3.47 (m, 1H), 2.56 – 2.48 (m, 2H), 2.26 – 1.46 (m, 10H), 1.41 – 1.34 (m, 2H), 1.34 – 1.21 (m, 16H), 0.88 (t, *J* = 6.7 Hz, 3H); ^{13}C NMR (101 MHz, $CDCl_3$) δ 133.8, 132.9, 44.9, 33.0, 32.1, 31.4, 29.9, 29.8, 29.8, 29.7, 29.7, 29.5, 29.4, 29.2, 28.4, 27.8, 27.1, 22.8, 14.3; HRMS-EI (m/z) $[M]^+$ calculated for $C_{19}H_{36}S$, 296.2538; found: 296.2536.

(2,3-Dimethylbut-2-en-1-yl)(2-ethylhexyl)sulfane (**3ta**)

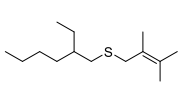

Yellow oil (32.6 mg, 0.14 mmol, 57%); ^{1}H NMR (400 MHz, $CDCl_3$) δ 3.18 (s, 2H), 2.41 (d, *J* = 5.9 Hz, 2H), 1.74 (s, 3H), 1.71 (s, 3H), 1.68 (s, 3H), 1.48 – 1.18 (m, 9H), 0.93 – 0.81 (m, 6H); ^{13}C NMR (101 MHz, $CDCl_3$) δ 128.2, 124.3, 39.5, 36.7, 36.1, 32.6, 29.1, 25.8, 23.2, 21.0, 20.6, 17.9, 14.3, 10.9; HRMS-EI (m/z) $[M]^+$ calculated for $C_{14}H_{28}S$, 228.1912; found: 228.1908.

Ethyl *N*-(*tert*-butoxycarbonyl)-*S*-(2,3-dimethylbut-2-en-1-yl)-L-cysteinate (**3ua**)

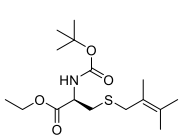

Yellow oil (38.2 mg, 0.12 mmol, 46%); ^{1}H NMR (400 MHz, $CDCl_3$) δ 5.30 (d, *J* = 7.6 Hz, 1H), 4.50 – 4.45 (m, 1H), 4.20 (q, *J* = 7.1 Hz, 2H), 3.27 (d, *J* = 12.2 Hz, 1H), 3.18 (d, *J* = 12.2 Hz, 1H), 2.92 – 2.76 (m,

2H), 1.71 (s, 6H), 1.67 (s, 3H), 1.44 (s, 9H), 1.27 (t, *J* = 7.1 Hz, 3H); ^{13}C NMR (101 MHz, $CDCl_3$) δ 171.3, 155.3, 129.5, 123.4, 80.1, 61.7, 53.5, 36.9, 34.3, 28.4, 21.0, 20.6, 17.8, 14.3; HRMS-ESI (m/z) $[M+Na]^+$ calculated for $C_{16}H_{29}NO_4SNa$, 354.1710; found: 354.1711.

(2*S*,3*S*,4*S*,5*R*,6*S*)-6-((2,3-dimethylbut-2-en-1-yl)thio)tetrahydro-2*H*-pyran-2,3,4,5-tetrayl tetraacetate (**3va**)

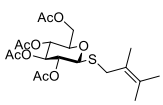

Sticky yellow oil (37.9 mg, 0.09 mmol, 34%); ^{1}H NMR (400 MHz, $CDCl_3$) δ 5.19 (t, *J* = 9.4 Hz, 1H), 5.09 – 5.04 (m, 1H), 5.06 – 4.97 (m, 1H), 4.33 (d, *J* = 10.1 Hz, 1H), 4.20 (dd, *J* = 12.4, 5.2 Hz, 1H), 4.13 (dd, *J* = 12.1, 2.2 Hz, 1H), 3.69 (d, *J* = 12.7 Hz, 1H), 3.60 (ddd, *J* = 10.2, 5.2, 2.3 Hz, 1H), 3.01 (d, *J* = 12.7 Hz, 1H), 2.06 (s, 3H), 2.03 (s, 3H), 2.01 (s, 3H), 1.99 (s, 3H), 1.71 (s, 3H), 1.70 (s, 3H), 1.69 (s, 3H); ^{13}C NMR (101 MHz, $CDCl_3$) δ 170.7, 170.4, 169.5, 169.5, 130.2, 122.6, 82.2, 75.8, 74.0, 69.8, 68.5, 62.4, 33.9, 21.1, 20.8, 20.8, 20.7, 20.7, 20.3, 17.4; HRMS-ESI (m/z) $[M+Na]^+$ calculated for $C_{20}H_{30}O_9SNa$, 469.1503; found: 469.1506.

Ethyl ((*S*)-3-((2,3-dimethylbut-2-en-1-yl)thio)-2-methylpropanoyl)-L-prolinate (**3wa**)

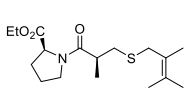

Yellow oil (37.6 mg, 0.12 mmol, 46%); Rotameric mixture. ^{1}H NMR (400 MHz, $CDCl_3$) δ 4.53 – 4.45 (m, 0.9H), 4.38 (dd, *J* = 8.5, 2.4 Hz, 0.1H), 4.14 (qd, *J* = 7.1, 1.6 Hz, 2H), 3.63 (t, *J* = 6.8 Hz, 2H), 3.19 (s, 2H), 2.85 – 2.67 (m, 2H), 2.43 (dd, *J* = 11.8, 4.8 Hz, 1H), 2.24 – 2.10 (m, 1H), 2.09 – 1.86 (m, 3H), 1.70 (s, 3H), 1.68 (s, 3H), 1.65 (s, 3H), 1.29 – 1.15 (m, 6H); ^{13}C NMR (101 MHz, $CDCl_3$) δ 174.5, 174.2, 172.4, 172.4, 128.9, 128.5, 124.0, 123.9,

61.8, 61.1, 59.4, 58.8, 47.1, 46.5, 39.2, 39.1, 36.9, 36.9, 35.2, 35.1, 31.5, 29.8, 29.2, 24.9, 22.5, 21.0, 20.9, 20.5, 17.9, 17.9, 17.4, 17.4, 14.2, 14.2; HRMS-ESI (m/z) $[M+Na]^+$ calculated for $C_{17}H_{29}NO_3SNa$, 350.1760; found: 350.1763.

Phenyl(2,3,4-trimethylpent-2-en-1-yl)sulfane (**3ab**) + (2-isopropyl-3-methylbut-2-en-1-yl)(phenyl)sulfane (**3ab'**)

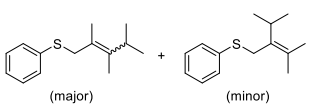

Light yellow oil (27.5 mg, 0.13 mmol, 50%, 2.3:1 ratio, containing diphenyl disulfide (**1a**) and diphenyl sulfide as impurities. Yield was determined by ^{1}H NMR via subtraction of the impurities); ^{1}H NMR (499 MHz, $CDCl_3$) δ 7.38 – 7.13 (m, 16.5H, major + minor), 3.62 (s, 2H, minor), 3.59 (s, 2.63H, major), 3.55 (s, 1.97H, major), 2.92 (sep, *J* = 6.9 Hz, 1.32H, major), 2.87 – 2.77 (m, 2.06H, major + minor), 1.80 (dd, *J* = 2.7, 1.3 Hz, 3H, major), 1.78 (d, *J* = 0.8 Hz, 3H, minor), 1.77 (s, 4H, major), 1.74 (s, 4H, major), 1.54 (d, *J* = 0.6 Hz, 3H, minor), 1.39 (d, *J* = 1.3 Hz, 3H, major), 1.06 (d, *J* = 6.9 Hz, 8.02H, major), 0.89 (d, *J* = 6.9 Hz, 6.35H), 0.87 (d, *J* = 6.8 Hz, 6.35H); ^{13}C NMR (75 MHz, $CDCl_3$) δ 139.4, 139.1, 137.7, 131.8, 131.1, 130.6, 130.0, 129.2, 128.9, 128.8, 128.7, 128.5, 126.5, 126.1, 125.7, 125.5, 121.6, 121.5, 39.9, 38.5, 34.4, 32.0, 30.5, 30.3, 30.1, 21.5, 21.0, 20.5, 20.3, 18.9, 17.5, 12.6, 11.9; HRMS-EI (m/z) $[M]^+$ calculated for $C_{14}H_{20}S$, 220.1286; found: 220.1288.

(3-Ethylpent-3-en-2-yl)(phenyl)sulfane (**3ac**) + (3-ethylpent-2-en-1-yl)(phenyl)sulfane (**3ac'**)

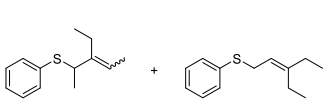

Light yellow oil (24.2 mg, 0.12 mmol, 47%, 4.9:1 ratio, containing diphenyl disulfide (**1a**) as an impurity. Yield was determined by ^{1}H NMR via subtraction of the impurity); ^{1}H

NMR (499 MHz, $CDCl_3$) δ 7.41 – 7.15 (m, 28.8H, major + minor), 5.26 (q, *J* = 6.8 Hz, 5.9H, major + minor), 4.37 (q, *J* = 7.1 Hz, 1.37H, major), 3.75 (q, *J* = 7.0 Hz, 3.53H, major), 3.58 (d, *J* = 7.7 Hz, 2H, minor), 2.27 – 2.08 (m, 9.8H, major), 2.05 – 2.00 (m, 4H, minor), 1.57 (d, *J* = 6.8 Hz, 10.6H, major), 1.43 (d, *J* = 5.9 Hz, 4.51 H, major), 1.39 (d, *J* = 7.0 Hz, 9.97H, major), 1.37 (d, *J* = 7.1 Hz, 3.41H, major), 1.03 (t, *J* = 7.6 Hz, 13.6H, major), 0.98 (t, *J* = 7.4 Hz, 3H, minor), 0.94 (t, *J* = 7.6 Hz, 3H, minor); ^{13}C NMR (101 MHz, $CDCl_3$) δ 147.7, 141.8, 141.2, 136.0, 132.8, 132.6, 129.9, 129.2, 128.8, 128.7, 128.6, 127.7, 127.1, 126.9, 126.1, 125.7, 121.5, 121.4, 50.8, 44.5, 34.4, 32.0, 30.5, 29.2, 23.5, 23.3, 21.5, 20.5, 19.4, 13.9, 13.3, 13.1, 12.8; HRMS-EI (m/z) $[M]^+$ calculated for $C_{13}H_{18}S$, 206.1129; found: 206.1130.

Hex-3-en-2-yl(phenyl)sulfane (**3ad**) + hex-4-en-3-yl(phenyl)sulfane (**3ad'**)

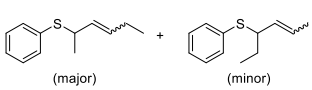

Light yellow oil (26.9 mg, 0.14 mmol, 56%, 1.1:1 ratio); ^1H NMR (400 MHz, $CDCl_3$) δ 7.46 – 7.33 (m, 4.1H, major + minor), 7.31 – 7.16 (m, 6.4H, major + minor), 5.54 – 5.19 (m, 4.2H, major + minor),4.08 (dq, *J* = 9.4, 6.9 Hz, 0.11H, major), 3.88 (td, *J* = 9.5, 5.1 Hz, 0.2H, minor), 3.72 (dq, *J* = 8.3, 6.8 Hz, 0.98H, major), 3.47 (td, *J* = 8.0, 5.4 Hz, 0.8H, minor), 1.99 – 1.88 (m, 2.1H, major + minor),1.84 – 1.64 (m, 1.5H, major + minor), 1.66 – 1.49 (m, 1.1H, major + minor), 1.60 (d, *J* = 4.7 Hz, 3H, minor), 1.45 – 1.37 (m, 1.6H, major + minor), 1.35 (d, *J* = 6.8 Hz, 2.94H, major), 1.33 (d, *J* = 7.1 Hz, 0.33H, major), 0.97 (t, *J* = 7.4 Hz, 3H, minor), 0.87 (t, *J* = 7.4 Hz, 2.97H, major), 0.78 (t, *J* = 7.5 Hz, 0.33H, major); ^{13}C NMR (101 MHz, $CDCl_3$) δ 135.3, 135.2, 133.5, 133.4, 133.2, 133.1, 132.9, 132.6, 131.6, 131.5, 130.7, 129.3, 128.7, 128.7, 128.7, 128.6, 127.4, 127.3, 127.2, 127.1, 126.9, 126.1, 125.6, 53.4, 47.6,

46.1, 41.2, 30.5, 28.4, 28.0, 25.4, 21.5, 20.9, 17.8, 13.7, 13.0, 12.0; HRMS-EI (m/z) $[M]^+$ calculated for $C_{12}H_{16}S$, 192.0973; found: 192.0972.

(*E*)-Pent-3-en-2-yl(phenyl)sulfane (**3ae**)

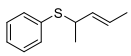

Yellow oil (16.2 mg, 0.09 mmol, 36%); ^{1}H NMR (300 MHz, $CDCl_3$) δ 7.44 – 7.37 (m, 2H), 7.35 – 7.23 (m, 3H), 5.52 – 5.34 (m, 2H), 3.76 (quin, *J* = 7.0 Hz, 1H), 1.63 (d, *J* = 5.2 Hz, 3H), 1.38 (d, *J* = 6.8 Hz, 3H). The compound was identified by spectral comparison with literature data.[48]

(3-Methylcyclohex-2-en-1-yl)(phenyl)sulfane (**3af**)

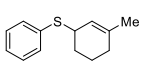

Yellow oil (35.2 mg, 0.17 mmol, 68% from **2d**; 40.9 mg, 0.20 mmol, 79% from **2m**); ^{1}H NMR (300 MHz, $CDCl_3$) δ 7.33 (d, *J* = 6.9 Hz, 2H), 7.21 (t, *J* = 7.6 Hz, 2H), 7.17 – 7.09 (m, 1H), 5.44 (s, 1H), 3.80 (s, 1H), 1.94 – 1.66 (m, 5H), 1.62 (s, 3H), 1.57 – 1.49 (m, 1H); ^{13}C NMR (75 MHz, $CDCl_3$) δ 138.5, 136.4, 131.2, 129.0, 126.6, 121.2, 44.6, 30.1, 28.6, 24.0, 19.7; HRMS-EI (m/z) $[M]^+$ calculated for $C_{13}H_{16}S$, 204.0973; found: 204.0971.

Phenyl((1*S*,2*R*,5*S*)-4,6,6-trimethylbicyclo[3.1.1]hept-3-en-2-yl)sulfane (**3ag**)

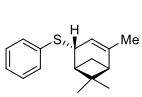

Yellow oil (33.6 mg, 0.14 mmol, 55%); ^{1}H NMR (499 MHz, $CDCl_3$) δ 7.40 (d, *J* = 8.0 Hz, 2H), 7.29 (t, *J* = 7.7 Hz, 2H), 7.21 (t, *J* = 7.4 Hz, 1H), 5.34 (s, 1H), 4.01 (s, 1H), 2.33 (dt, *J* = 9.1, 5.6 Hz, 1H), 2.25 (s, 1H), 2.05 (t, *J* = 5.5 Hz, 1H), 1.73 (s, 3H), 1.48 (d, *J* = 9.1 Hz, 1H), 1.31 (s, 3H), 0.90 (s, 3H); ^{13}C NMR (126 MHz, $CDCl_3$) δ 147.8, 136.5, 131.2, 129.0, 126.5, 116.7, 50.8, 47.7, 45.9, 42.6, 29.2, 26.7, 23.0, 20.7; HRMS-EI (m/z) $[M]^+$ calculated for $C_{16}H_{20}S$, 244.1286; found: 244.1288.

Cyclohex-2-en-1-yl(phenyl)sulfane (**3ah**)

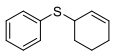

Yellow oil (40.9 mg, 0.22 mmol, 86%); ^{1}H NMR (499 MHz, $CDCl_3$) δ 7.42 (d, *J* = 7.3 Hz, 2H), 7.29 (t, *J* = 7.5 Hz, 2H), 7.22 (t, *J* = 7.3 Hz, 1H), 5.84 (d, *J* = 10.0 Hz, 1H), 5.78 (d, *J* = 10.0 Hz, 1H), 3.87 (s, 1H), 2.06 – 1.88 (m, 4H), 1.83 – 1.76 (m, 1H), 1.65 – 1.57 (m, 1H). The compound was identified by spectral comparison with literature data.[49]

Cyclopent-2-en-1-yl(phenyl)sulfane (**3ai**)

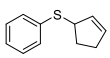

Yellow oil (32.0 mg, 0.18 mmol, 72%); ^{1}H NMR (300 MHz, $CDCl_3$) δ 7.42 (d, *J* = 8.1 Hz, 2H), 7.35 – 7.27 (m, 2H), 7.27 – 7.19 (m, 1H), 5.92 (d, *J* = 5.5 Hz, 1H), 5.81 (d, *J* = 5.5 Hz, 1H), 4.32 (dd, *J* = 3.7, 2.1 Hz, 1H), 2.50 – 2.27 (m, 3H), 2.11 – 1.94 (m, 1H); ^{13}C NMR (75 MHz, $CDCl_3$) δ 134.0, 131.2, 131.1, 128.9, 126.5, 121.7, 52.8, 31.7, 31.4; HRMS-EI (m/z) $[M]^+$ calculated for $C_{11}H_{12}S$, 176.0660; found: 176.0661.

Cyclohept-2-en-1-yl(phenyl)sulfane (**3aj**)

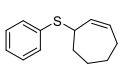

Light yellow oil (20.9 mg, 0.10 mmol, 41%); ^{1}H NMR (400 MHz, $CDCl_3$) δ 7.40 (d, *J* = 8.1 Hz, 2H), 7.29 (t, *J* = 7.6 Hz, 2H), 7.21 (t, *J* = 7.3 Hz, 1H), 5.86 – 5.77 (m, 2H), 4.02 (t, *J* = 5.2 Hz, 1H), 2.25 – 2.13 (m, 2H), 2.10 – 2.01 (m, 1H), 1.94 – 1.84 (m, 1H), 1.85 – 1.75 (m, 1H), 1.70 – 1.56 (m, 3H); ^{13}C NMR (75 MHz, $CDCl_3$) δ 136.2, 133.6, 132.8, 131.4, 129.0, 126.7, 48.2, 32.7, 28.6, 27.8, 27.0; HRMS-EI (m/z) $[M]^+$ calculated for $C_{13}H_{16}S$, 204.0973; found: 204.0970.

(*Z*)-Cyclooct-2-en-1-yl(phenyl)sulfane (**3ak**)

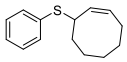

Yellow oil (20.6 mg, 0.09 mmol, 37%); ^{1}H NMR (300 MHz, $CDCl_3$) δ 7.34 (dd, *J* = 7.3, 1.2 Hz, 2H), 7.31 – 7.22 (m, 2H), 7.17 (ddd, *J* = 7.6, 3.8, 1.4 Hz, 1H), 5.73 (dd, *J* = 18.6, 8.2 Hz, 1H), 5.54 – 5.43 (m, 1H), 4.26 – 4.11 (m, 1H), 2.30 – 2.07 (m, 2H), 1.96 (td, *J* = 10.1, 6.6 Hz, 1H), 1.74 (dd, *J* = 9.1, 6.2 Hz, 2H), 1.65 – 1.55 (m, 3H). 1.48 – 1.24 (m, 2H). The compound was identified by spectral comparison with literature data.[50]

Cyclododec-2-en-1-yl(phenyl)sulfane (**3al**)

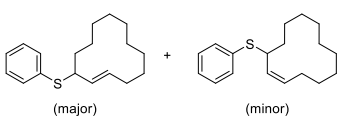

Colorless oil (19.9 mg, 0.07 mmol, 29%, 5:1 *E*/*Z* ratio); ^{1}H NMR (400 MHz, $CDCl_3$) δ 7.44 – 7.32 (m, 12H, major + minor), 7.29 – 7.14 (m, 18H, major + minor), 5.36 (ddd, *J* = 14.4, 9.8, 4.4 Hz, 6H, major + minor), 5.26 (dd, *J* = 15.7, 9.4 Hz, 6H, major + minor), 4.09 (td, *J* = 9.2, 5.8 Hz, 1H, minor), 3.63 (td, *J* = 10.3, 3.8 Hz, 5H, major), 2.13 – 2.05 (m, 7H, major + minor), 1.97 – 1.80 (m, 11H, major + minor), 1.70 – 1.62 (m, 2H, major + minor), 1.60 – 1.46 (m, 17H, major + minor), 1.34 – 1.17 (m, 80H, major + minor); ^{13}C NMR (101 MHz, $CDCl_3$) δ 135.5, 135.1, 133.6, 132.4, 131.7, 131.3, 128.7, 128.7, 127.3, 126.8, 51.6, 44.3, 33.2, 33.1, 32.0, 26.7, 26.2, 26.2, 25.3, 25.1, 24.9, 24.8, 24.6, 24.4, 24.4, 24.3, 24.2, 24.1, 22.3, 22.0; HRMS-EI (m/z) $[M]^+$ calculated for $C_{18}H_{26}S$, 274.1755; found: 274.1757.

(4-Ethyl-4-methylcyclohex-2-en-1-yl)(phenyl)sulfane (**3am**)

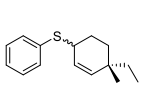

Colorless oil (34.4 mg, 0.15 mmol, 59%, 1.4:1 unisolable diastereomeric mixture); ^{1}H NMR (400 MHz, $CDCl_3$) δ 7.43 – 7.38 (m, 4.8H), 7.29 – 7.24 (m, 4.8H), 7.22 – 7.18 (m, 2.4H), 5.70 – 5.63 (m, 2.4H),

5.54 (brs, 1.4H), 5.50 (brs, 1H), 3.80 – 3.73 (m, 2.4H), 2.03 – 1.91 (m, 3.2H), 1.77 – 1.70 (m, 3.2H), 1.56 – 1.49 (m, 3.2 H), 1.31 – 1.24 (m, 4.8H), 0.91 (s, 3H), 0.90 (s, 4.2H), 0.84 – 0.79 (m, 7.2H); ^{13}C NMR (75 MHz, $CDCl_3$) δ 140.0, 139.7, 136.2, 135.7, 131.6, 131.4, 129.0, 128.9, 126.8, 126.7, 125.5, 124.9, 44.2, 44.0, 34.9, 34.8, 34.6, 34.5, 32.0, 30.5, 26.4, 26.2, 25.6, 8.5, 8.5; HRMS-EI (m/z) $[M]^+$ calculated for $C_{15}H_{20}S$, 232.1286; found: 232.1289.

4-(Phenylthio)-3,4-dihydro-2*H*-pyran (**3an**)

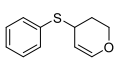

Yellow oil (38.7 mg, 0.18 mmol, 72%); ^{1}H NMR (300 MHz, $CDCl_3$) δ 7.41 (d, *J* = 6.9 Hz, 2H), 7.30 – 7.28 (m, 2H), 7.25 – 7.19 (m, 1H), 6.48 (d, *J* = 6.1 Hz, 1H), 4.94 – 4.81 (m, 1H), 4.27 – 4.15 (m, 1H), 4.09 (dd, *J* = 5.1, 2.7 Hz, 1H), 3.90 – 3.80 (m, 1H), 2.26 – 2.08 (m, 1H), 1.91 (d, *J* = 14.3 Hz, 1H). The compound was identified by spectral comparison with literature data.[51]

(4-Methylpent-3-en-2-yl)(phenyl)sulfane (**3ap**)

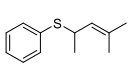

Light yellow oil (22.6 mg, 0.12 mmol, 47%); ^{1}H NMR (400 MHz, $CDCl_3$) δ 7.39 (dd, *J* = 7.7, 1.6 Hz, 2H), 7.26 – 7.21 (m, 3H), 5.06 (d, *J* = 9.9 Hz, 1H), 3.98 (dq, *J* = 9.8, 6.7 Hz, 1H), 1.64 (s, 3H), 1.40 (s, 3H), 1.30 (d, *J* = 6.7 Hz, 3H); ^{13}C NMR (101 MHz, $CDCl_3$) δ 135.3, 133.8, 133.6, 128.6, 127.2, 127.1, 42.4, 25.6, 21.6, 17.9; HRMS-EI (m/z) $[M]^+$ calculated for $C_{12}H_{16}S$, 192.0973; found: 192.0971.

5.4.7 Post modifications of allyl thioethers

5.4.7.1 Synthesis of allyl sulfoxide (3ah$_{sulfoxide}$)

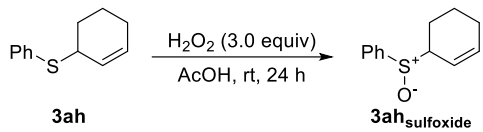

3ah **3ah$_{sulfoxide}$**

A reported procedure by S. Koo and co-workers was applied.[18] To a 25 mL round-bottom flask equipped with a PTFE-coated stir bar were added allyl thioether **3ah** (95.2 mg, 0.50 mmol, 1.0 equiv), H_2O_2 (34 wt% in water, 136 μL, 1.5 mmol, 3.0 equiv), and acetic acid (3 mL). The reaction mixture was stirred at room temperature for 24 h. After the reaction was finished, the reaction mixture was diluted with diethyl ether (6 mL) and water (3 mL), and the resulting mixture was washed with 1 M aqueous NaOH solution (3 × 10 mL), dried ($MgSO_4$), and concentrated in vacuo. The crude mixture was purified by silica gel flash column chromatography (EtOAc:hexane = 1:1) to afford the corresponding allyl sulfoxide **3ah$_{sulfoxide}$** (78.7 mg, 76%) as a colorless liquid.

(Cyclohex-2-en-1-ylsulfinyl)benzene (**3ah$_{sulfoxide}$**)

Inseparable diastereomeric mixture (1.2:1). ^{1}H NMR (400 MHz, $CDCl_3$) δ 7.66 (ddd, *J* = 6.0, 2.4, 1.5 Hz, 2H), 7.63 (ddd, *J* = 7.0, 3.1, 1.5 Hz, 2.4H), 7.55 – 7.47 (m, 6.6H), 6.14 (dtd, *J* = 9.9, 3.8, 1.9 Hz, 1H), 6.02 (dtd, *J* = 9.4, 3.7, 1.5 Hz, 1.2H), 5.63 (dq, *J* = 10.2, 2.2 Hz, 1H), 5.20 – 5.11 (m, 1.2H), 3.37 (qt, J = 5.9, 2.4 Hz, 1H), 3.32 – 3.27 (m, 1.2H), 2.38 – 2.30 (m, 1.2H), 2.15 – 1.64 (m, 11H), 1.60 – 1.48 (m, 1H). The compound was identified by spectral comparison with literature data.[52]

5.4.7.2 Synthesis of allyl sulfone (3oa$_{sulfone}$)

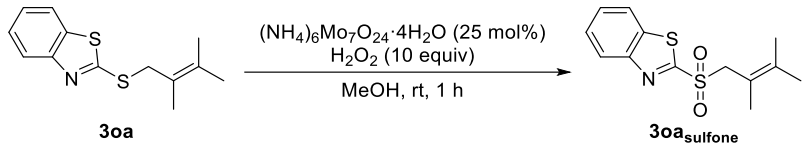

A reported procedure by D. K. Chand and co-workers was applied.[53] To a 25 mL round-bottom flask equipped with a PTFE-coated stir bar were added allyl thioether **3oa** (84.7 mg, 0.34 mmol, 1.0 equiv), ammonium molybdate tetraacetate (105 mg, 0.085 mmol, 0.25 equiv), and methanol (4 mL). H_2O_2 (34 wt% in water, 309 μL, 10 mmol, 10.0 equiv) was added dropwise, and the reaction mixture was further stirred at room temperature for 1 h. After the reaction was finished, the reaction mixture was diluted with ethyl acetate (20 mL) and washed with saturated aqueous $NaHCO_3$ solution (20 mL). The aqueous layer was further extracted with EtOAc (3 × 20 mL), and the combined organic layer was dried ($MgSO_4$), filtered, and concentrated in vacuo. The desired product was purified by silica gel flash column chromatography (EtOAc:hexane = 1:3) to afford the corresponding sulfone **3oa$_{sulfone}$** (79.5 mg, 83%) as a white solid.

2-((2,3-Dimethylbut-2-en-1-yl)sulfonyl)benzo[*d*]thiazole (**3oa$_{sulfone}$**)

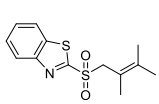

^{1}H NMR (400 MHz, $CDCl_3$) δ 8.28 – 8.23 (m, 1H), 8.05 – 8.00 (m, 1H), 7.66 (ddd, *J* = 8.2, 7.2, 1.5 Hz, 1H), 7.64 – 7.59 (m, 1H), 4.31 (s, 2H), 1.87 (s, 3H), 1.72 (s, 3H), 1.63 (s, 3H); ^{13}C NMR (101 MHz, $CDCl_3$) δ 166.5, 152.9, 138.2, 137.2, 128.0, 127.7, 125.5, 122.4, 114.4, 60.5, 21.4, 21.3, 19.8; HRMS-ESI (m/z) $[M+Na]^+$ calculated for $C_{13}H_{15}NO_2S_2Na$, 304.0436; found: 304.0438.

5.4.7.3 Interrupted Pummerer coupling/[3,3]-sigmatropic rearrangement with *N*-methylindole

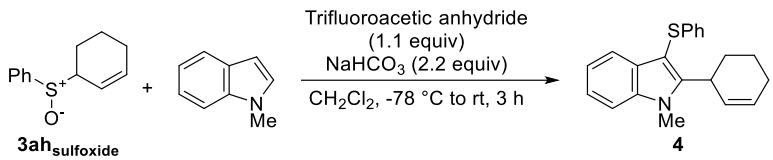

A reported procedure by D. J. Procter and co-workers was applied.[19] To a 10 mL Schlenk tube equipped with a PTFE-coated stir bar were added allyl sulfoxide **3ah**$_{\textbf{sulfoxide}}$ (31 mg, 0.15 mmol, 1.0 equiv), *N*-methylindole (18.7 μL, 0.15 mmol, 1.0 equiv), sodium bicarbonate (27.7 mg, 0.33 mmol, 2.2 equiv) and dichloromethane (1.5 mL) under argon atmosphere, and the reaction mixture was cooled to -78 °C. Trifluoroacetic anhydride (23 μL, 0.275 mmol, 2.2 equiv) was added to the reaction mixture dropwise, and the resulting mixture was further stirred at -78 °C for 30 min. and at room temperature for 3 h. After the reaction was finished, the reaction mixture was directly purified by silica gel flash column chromatography (CH_2Cl_2:hexane = 1:9) to afford the corresponding indole **4** (24.9 mg, 52%) as a yellow oil.

2-(Cyclohex-2-en-1-yl)-1-methyl-3-(phenylthio)-1*H*-indole (**4**)

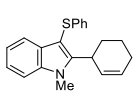

^{1}H NMR (400 MHz, $CDCl_3$) δ 7.60 (d, J = 7.7 Hz, 1H), 7.37 (d, *J* = 8.0 Hz, 1H), 7.27 (t, *J* = 7.5 Hz, 1H), 7.19 – 7.13 (m, 3H), 7.09 – 7.01 (m, 3H), 5.97 – 5.88 (m, 1H), 5.71 (d, *J* = 10.0 Hz, 1H), 4.43 – 4.37 (m, 1H), 3.87 (d, *J* = 1.4 Hz, 3H), 2.18 – 2.15 (m, 2H), 1.95 – 1.90 (m, 2H), 1.85 – 1.68 (m, 2H); ^{13}C NMR (101 MHz, $CDCl_3$) δ 148.7, 140.2, 137.9, 129.6, 128.7, 128.7, 128.6, 125.5, 124.5, 122.2, 120.7, 119.4, 109.2, 98.5, 34.5, 31.4, 29.2, 24.8, 22.7; HRMS-EI (m/z) $[M]^+$ calculated for $C_{21}H_{21}NS$, 319.1395; found: 319.1395.

5.4.7.4 Doyle-Kirmse reaction with allyl thioether 3aa

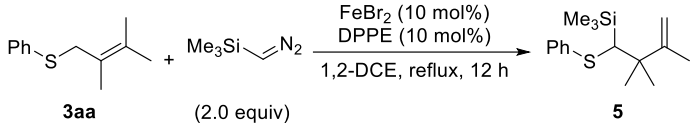

A reported procedure by D. L. Van Vranken and co-workers was applied.[21] To a flame-dried 10 mL Schlenk tube equipped with a PTFE-coated stir bar were added iron(II) bromide (4.3 mg, 0.020 mmol, 0.010 equiv) and 1,2-bis(diphenylphosphino)ethane (dppe, 8 mg, 0.020 mmol, 0.010 equiv) under argon atmosphere. Allyl thioether **3aa** (38.5 mg, 0.20 mmol, 1.0 equiv) was dissolved in 1,2-dichloroethane (2.5 mL) and injected to the tube via syringe. After the reaction mixture was stirred for 10 min., (trimethylsilyl)diazomethane (2.0 M in diethyl ether, 200 μL, 0.40 mmol, 2.0 equiv) was added and stirred at reflux temperature for 12 h. After the reaction was finished, the reaction mixture was cooled to room temperature, filtered through Celite, dried ($MgSO_4$) and concentrated in vacuo. The resulting crude mixture was purified by silica gel flash column chromatography (Hexane) to afford the corresponding thioether **5** (34.6 mg, 62%) as a colorless liquid.

Trimethyl(2,2,3-trimethyl-1-(phenylthio)but-3-en-1-yl)silane (**5**)

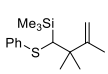

^{1}H NMR (400 MHz, $CDCl_3$) δ 7.39 (d, *J* = 7.4 Hz, 2H), 7.25 (t, *J* = 7.6 Hz, 2H), 7.13 (t, *J* = 7.3 Hz, 1H), 4.84 (s, 1H), 4.75 (s, 1H), 2.77 (s, 1H), 1.67 (s, 3H), 1.20 (s, 3H), 1.10 (s, 3H), 0.18 (s, 9H); ^{13}C NMR (101 MHz, $CDCl_3$) δ 152.0, 140.8, 129.3, 128.8, 125.6, 110.9, 45.1, 44.5, 28.7, 25.6, 20.1, 0.6; HRMS-EI (m/z) $[M]^+$ calculated for $C_{16}H_{26}SSi$, 278.1525; found: 278.1525.

5.4.7.5 Modified Julia olefination with hydrocinnamaldehyde

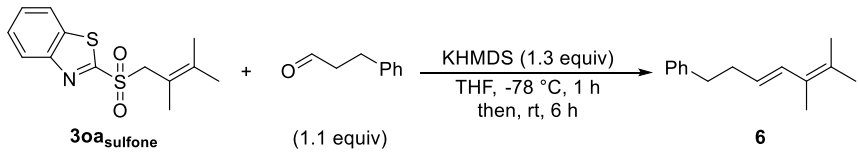

3oa$_{sulfone}$ (1.1 equiv) **6**

A reported procedure by J. Pospisil and co-workers was applied.[20] To a flame-dried 10 mL Schlenk tube equipped with a PTFE-coated stir bar were added **3oa$_{sulfone}$** (70.3 mg, 0.25 mmol, 1.0 equiv), 3-phenylpropionaldehyde (36.2 µL, 0.275 mmol, 1.1 equiv) and tetrahydrofuran (2.5 mL) under argon atmosphere. The reaction mixture was cooled to -78 °C, and potassium bis(trimethylsilyl)amide (0.50 M in toluene, 650 µL, 0.325 mmol, 1.3 equiv) was added dropwise. The resulting mixture was stirred for 1 h at -78 °C and 6 h at room temperature. After the reaction was finished, the reaction mixture was quenched with saturated aqueous NH_4Cl solution (10 mL) and further extracted with EtOAc (3 × 20 mL). The combined organic layer was dried ($MgSO_4$), filtered, and concentrated in vacuo. The resulting crude mixture was purified by silica gel flash column chromatography (EtOAc:hexane = 1:9) to afford the corresponding olefin **6** (32.9 mg, 66%) as a colorless liquid.

(*E*)-(5,6-dimethylhepta-3,5-dien-1-yl)benzene (**6**)

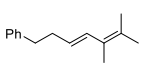

^{1}H NMR (400 MHz, $CDCl_3$) δ 7.29 (t, *J* = 7.4 Hz, 2H), 7.24 – 7.15 (m, 3H), 6.55 (d, *J* = 15.5 Hz, 1H), 5.63 (dt, *J* = 14.8, 6.9 Hz, 1H), 2.73 (dd, *J* = 9.2, 6.6 Hz, 2H), 2.46 (q, *J* = 7.3 Hz, 2H), 1.81 (s, 3H), 1.78 (s, 3H), 1.76 (s, 3H). The compound was identified by spectral comparison with literature data.[54]

5.4.8 General procedures for single-electron oxidant additive studies

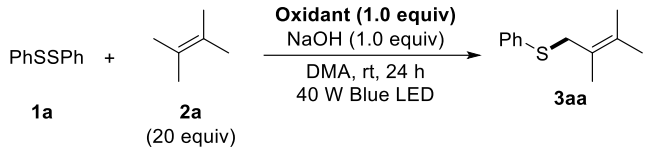

A 4 mL reaction vial equipped with a PTFE-coated stir bar was charged with diphenyl disulfide **1a** (54.6 mg, 0.25 mmol, 1.0 equiv), oxidant (0.25 mmol, 1.0 equiv) and NaOH (10 mg, 0.25 mmol, 1.0 equiv) in a glovebox. The vial was closed with a Teflon-lined septum cap and taken out of the glovebox. 2,3-dimethyl-2-butene **2a** (594 μL, 5.0 mmol, 20 equiv) and DMA (1 mL) were added via syringe, and the solution was stirred for 24 h under 40 W blue LED irradiation with fan cooling, located on the 2.5 cm away from the LED. After the reaction was complete, dodecane (56.8 μL, 0.25 mmol, 1.0 equiv) was added, and the result was analyzed by GC.

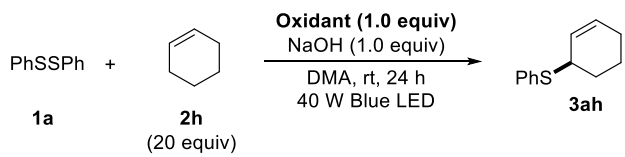

A 4 mL reaction vial equipped with a PTFE-coated stir bar was charged with diphenyl disulfide **1a** (54.6 mg, 0.25 mmol, 1.0 equiv), oxidant (0.25 mmol, 1.0 equiv) and NaOH (10 mg, 0.25 mmol, 1.0 equiv) in a glovebox. The vial was closed with a Teflon-lined septum cap and taken out of the glovebox. Cyclohexene **2h** (506 μL, 5.0 mmol, 20 equiv) and DMA (1 mL) were added via syringe, and the solution was stirred for 24 h under 40 W blue LED irradiation with fan cooling, located on the 2.5 cm away from the LED. After the reaction was complete,

dodecane (56.8 μL, 0.25 mmol, 1.0 equiv) was added, and the result was analyzed by GC.

In the case of the reaction with TEMPO (entry 4, Table 5.2), TEMPO adduct derived from thiyl radical (**1a-TEMPO**) was detected in HRMS-ESI analysis of the reaction mixture, proving the homolytic cleavage of **1a** under Blue LED irradiation without the photocatalyst.

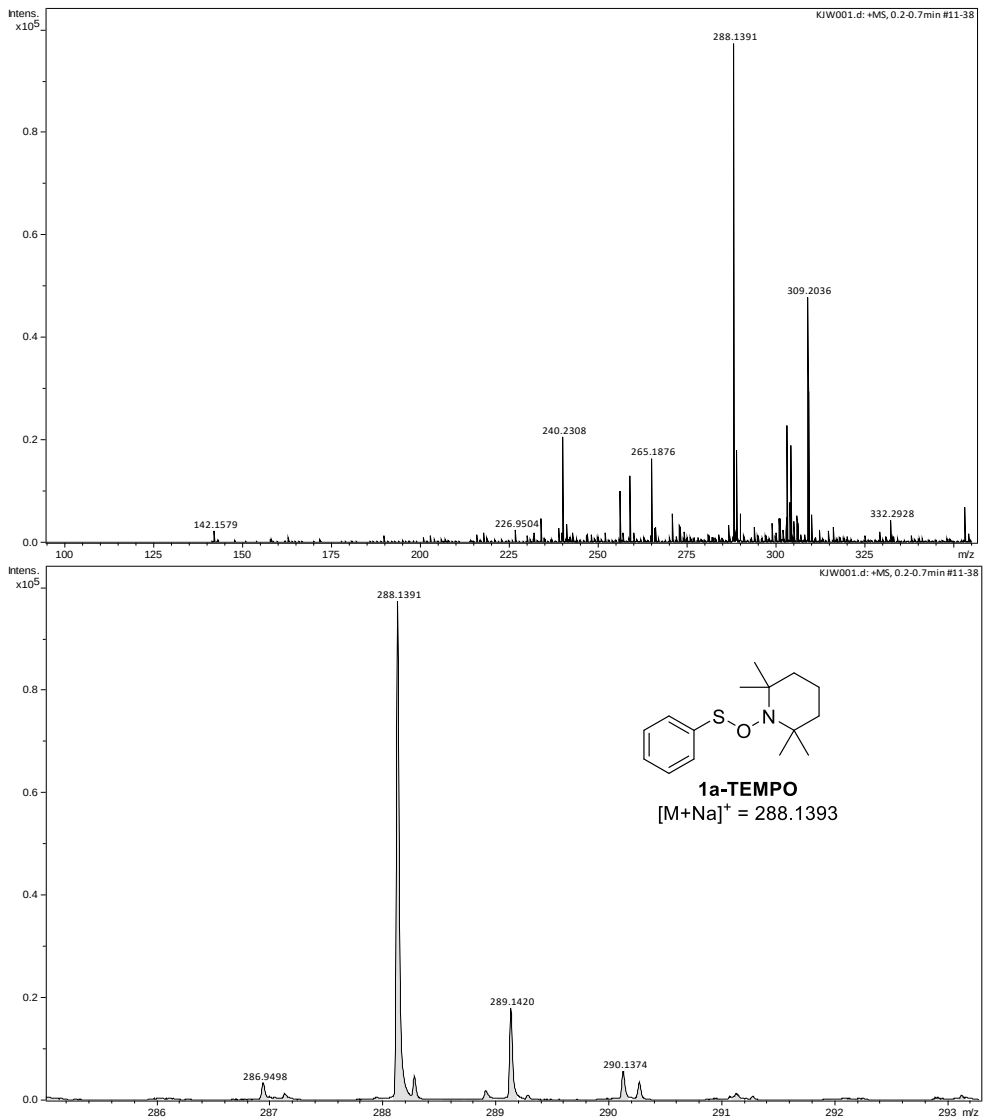

Figure 5.4 HRMS-ESI data for the detection of TEMPO adduct

5.4.9 DFT calculation

5.4.9.1 DFT calculation of redox potentials

The redox potentials (E^o) of radical species were calculated using the protocol reported by Liu and Guo.[31] Computation was conducted to obtain values described in the thermodynamic cycles. All DFT calculations were carried out using Gaussian 09W.[55] Specifically, the (U)B3LYP functional and 6-31+G(d) basis set were used to conduct geometry optimization and frequency calculation in the gas phase. Single-point energy calculations were carried out on the optimized geometries using the 6-311++G(2df,2p) basis set. The solvation free energies in acetonitrile were calculated with 6-311++G(2df,2p) using D-PCM, including additional keywords (Icomp=4, TSNUM=60, TSARE=0.4, radii=bondi, alpha=1.20). All structures were confirmed to be local minima by the absence of imaginary frequencies. The lowest-energy conformers were used in the final calculations.

5.4.9.1.1 The redox potential of 2a-rad

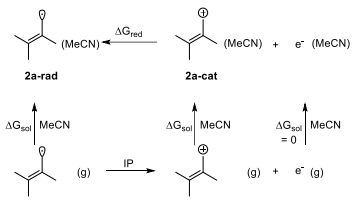

Structure	2a-rad	2a-cat
H_{corr}	0.160166	0.161611
G_{corr}	0.116506	0.119044
E [Hartree]	−235.2444052	−234.9951938
H [kcal/mol]	−147517.4758	−147360.1867
G [kcal/mol]	−147544.8729	−147386.8979
E [Hartree] (MeCN)	−235.2462083	−235.0750079
ΔG_{solv} [kcal/mol]	−1.131489088	−50.08411251

IP (ionization potential) = H (**2a-cat**) – H (**2a-rad**)

= (−147360.1867) − (−147517.4758) = 157.2891 kcal/mol = 6.82 eV

IP (corrected) = 6.82 eV + 0.28 eV = 7.10 eV

TΔS (ionization) = H (**2a-cat**) – H (**2a-rad**) – G (**2a-cat**) + G (**2a-rad**)

= (−147360.1867) – (−147517.4758) – (−147386.8979) + (−147544.8729)

= −0.6859 kcal/mol

TΔS (ionization, corrected for the electron spin degeneracy)

= (−0.6859) + 0.82 = 0.1341 kcal/mol

E^o (calc, **2a-cat**/**2a-rad**) = IP (corrected) + (1/23.06)[−TΔS (ionization, corrected)

+ ΔG_{solv} (**2a-cat**) – ΔG_{solv} (**2a-rad**)] – 4.43[56]

= 7.10 + (1/23.06)((−0.1341) + (−50.08411251) – (−1.131489088)) – 4.43

= 0.54 V

5.4.9.1.2 The redox potential of 2h-rad

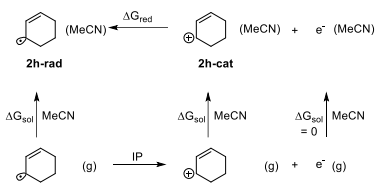

Structure	2h-rad	2h-cat
H_{corr}	0.139106	0.140551
G_{corr}	0.103464	0.105463
E [Hartree]	−234.0865256	−233.8317608
H [kcal/mol]	−146804.1113	−146643.3374
G [kcal/mol]	−146826.4770	−146665.3554
E [Hartree] (MeCN)	−234.0881717	−233.9140493
ΔG_{solv} [kcal/mol]	−1.032999041	−51.63677811

IP (ionization potential) = H (**2h-cat**) – H (**2h-rad**)

= (–146643.3374) – (–146804.1113) = 160.7739 kcal/mol = 6.97 eV

IP (corrected) = 6.97 eV + 0.28 eV = 7.25 eV

TΔS (ionization) = H (**2h-cat**) – H (**2h-rad**) – G (**2h-cat**) + G (**2h-rad**)

= (–146643.3374) – (–146804.1113) – (–146665.3554) + (–146826.4770)

= –0.3477 kcal/mol

TΔS (ionization, corrected for the electron spin degeneracy)

= (–0.3477) + 0.82 = 0.4723 kcal/mol

E^o (calc, **2h-cat**/**2h-rad**) = IP (corrected) + (1/23.06)[–TΔS (ionization, corrected)

+ ΔG_{solv} (**2h-cat**) – ΔG_{solv} (**2h-rad**)] – 4.43[56]

= 7.25 + (1/23.06)((–0.4723) + (–51.63677811) – (–1.032999041)) – 4.43

= 0.61 V

5.4.9.1.3 The redox potential of 3ah-rad

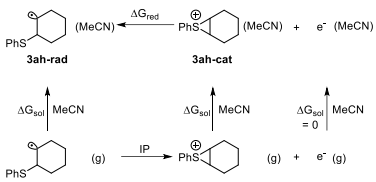

Structure	3ah-rad	3ah-cat
H_{corr}	0.251396	0.254145
G_{corr}	0.196788	0.202526
E [Hartree]	−864.6325818	−864.4200790
H [kcal/mol]	−542406.9735	−542271.9011
G [kcal/mol]	−542441.2405	−542304.2925
E [Hartree] (MeCN)	−864.6372876	−864.4879073
ΔG_{solv} [kcal/mol]	−2.952993976	−42.56284486

IP (ionization potential) = H (**3ah-cat**) – H (**3ah-rad**)

= (–542271.9011) – (–542406.9735) = 135.0724 kcal/mol = 5.86 eV

IP (corrected) = 5.86 eV + 0.28 eV = 6.14 eV

TΔS (ionization) = H (**3ah-cat**) – H (**3ah-rad**) – G (**3ah-cat**) + G (**3ah-rad**)

= (–542271.9011) – (–542406.9735) – (–542304.2925) + (–542441.2405)

= –1.8756 kcal/mol

TΔS (ionization, corrected for the electron spin degeneracy)

= (–1.8756) + 0.82 = –1.0556 kcal/mol

E^o (calc, **3ah-cat**/**3ah-rad**) = IP (corrected) + (1/23.06)[–TΔS (ionization, corrected) + ΔG_{solv} (**3ah-cat**) – ΔG_{solv} (**3ah-rad**)] – 4.43[56]

= 6.14 + (1/23.06)((1.0556) + (–42.56284486) – (–2.952993976)) – 4.43

= 0.04 V

5.4.9.2 DFT calculation of the reaction pathway

All DFT calculations were carried out using Gaussian 09W.[55] Specifically, the (U)B3LYP functional and LANL2DZ basis set for Ir and 6-31G(d,p) basis set for other atoms were used to conduct geometry optimization and frequency calculation in the gas phase. A scaling factor of 0.961 for frequency analysis was applied.[57] Single-point energy calculations were carried out on the optimized geometries using the (U)M06-2X functional and SDD basis set for Ir and 6-311+G(d,p) basis set for other atoms. The solvation effect was considered using the polarization continuum model (PCM) for *N*,*N*-dimethylacetamide (ε = 37.781). All structures were confirmed to be local minima (ground state) by the absence of imaginary frequencies or to be a transition state by the existence of a single imaginary frequency. The lowest-energy conformers were used in the final calculations.

Table 5.7 Computed energy component for optimized structures

Species	**E(SCF) (Hartree)** (U)B3LYP 6-31G(d,p) /LANL2DZ	**G_{corr} (Hartree)** (U)B3LYP 6-31G(d,p) /LANL2DZ	**E(SCF) (Hartree)** (U)M06-2X 6-311+G(d,p) /SDD	**G (solvated) (Hartree)**
PhSH	-630.445230476	0.064758	-630.38802610	-630.3232681
PhS^-	-629.88591653	0.056229	-629.93058690	-629.8743579
$PhS^{\cdot}$	-629.817838888	0.056573	-629.75695769	-629.7003847
PhSSPh	-1259.69402022	0.133768	-1259.58730041	-1259.453532
Ir(III)*	-2552.05792752	0.389982	-2551.40955830	-2551.019576
Ir(II)	-2552.17713560	0.388676	-2551.59602776	-2551.207352
2h	-234.66268160	0.112033	-234.59159288	-234.4795599
TS-A	-864.45774752	0.179163	-864.33027122	-864.1511082
2h-rad	-234.02136623	0.098155	-233.94925642	-233.8511014
2h-cat	-233.77393688	0.099822	-233.76983622	-233.6700142
TS-C	-1493.69980555	0.251863	-1493.52752953	-1493.275667
3ah-rad	-864.47382207	0.187243	-864.35452468	-864.1672817
TS-B	-864.47082938	0.186677	-864.34726228	-864.1605853
3ah	-863.90518757	0.179858	-863.79274034	-863.6128823
TS-D	-1494.91901091	0.269368	-1494.74289122	-1494.473523
3ah'	-865.13694787	0.202602	-865.01721209	-864.8146101

5.4.10 Stern-Volmer quenching experiment

A solution of $Ir(CF_3ppy)_3$ in degassed DMA (100 μM) was prepared in a cuvette. Diphenyl disulfide (**1a**), 2,3-dimethyl-2-butene (**2a**), and sodium thiophenolate (**1a'**) were used as quenchers. The prepared sample was excited at 460 nm and peak emissions were measured at 513 nm. The fluorescence spectra and the Stern-Volmer regression data for each quencher are presented as follows.

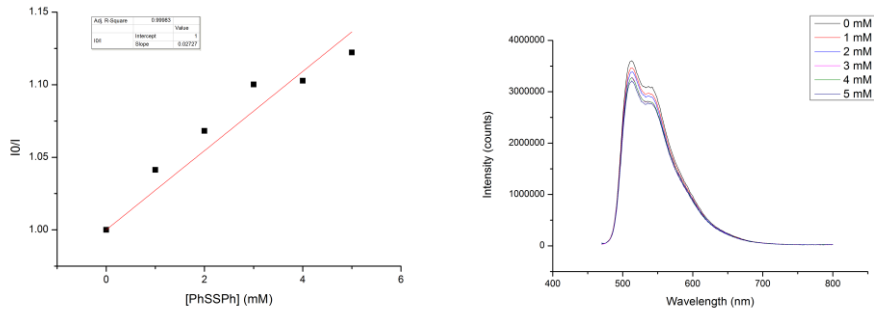

Figure 5.5 Stern-Volmer quenching study with diphenyl disulfide (**1a**)

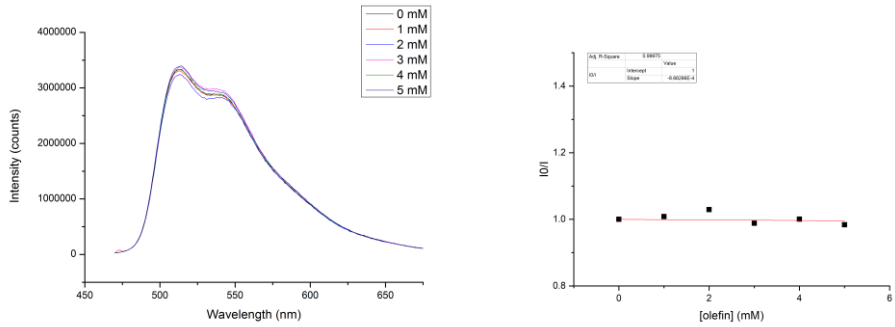

Figure 5.6 Stern-Volmer quenching study with 2,3-dimethyl-2-butene **(2a)**

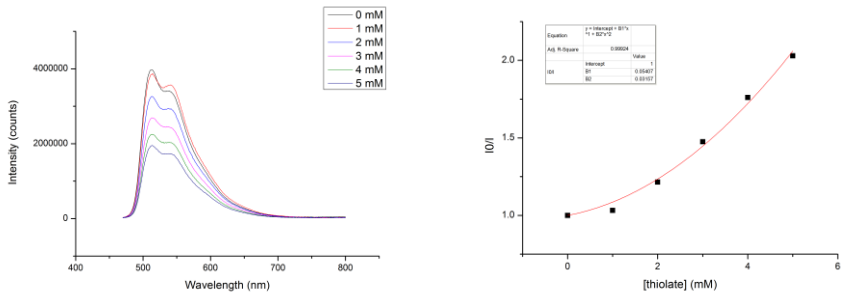

Figure 5.7 Stern-Volmer quenching study with sodium thiophenolate **(1a')**

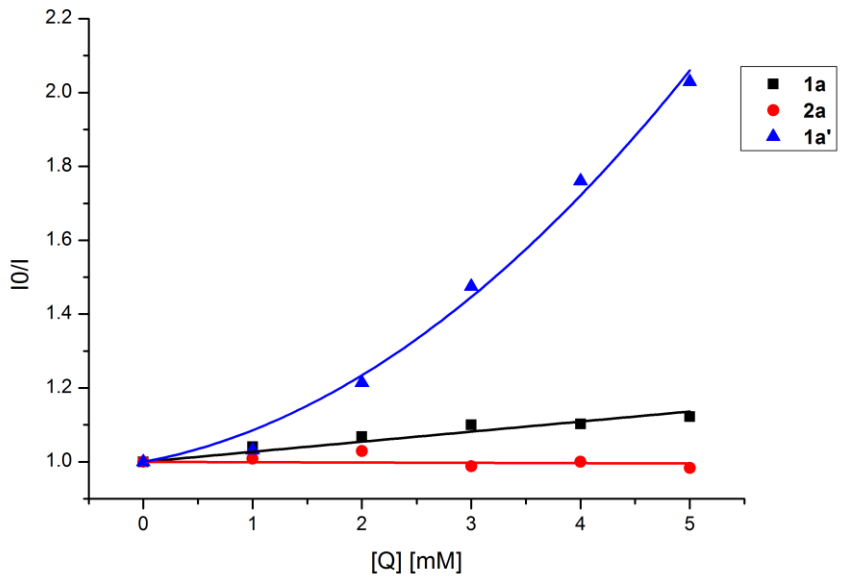

Figure 5.8 Combined plot of Stern-Volmer quenching studies

The degree of quenching increases in the order of sodium thiophenolate (**1a'**) >> diphenyl disulfide (**1a**) > 2,3-dimethyl-2-butene (**2a**). The non-linear quadratic relation between I_0/I and [Q] in the case of **1a'** can be explained by the involvement of both static and dynamic quenching processes.[58]

5.4.11 Quantum yield measurement

Quantum yield was measured following a procedure reported by Yoon and co-workers.[59]

5.4.11.1 Actinometry

The photon flux was measured following standard actinometry with potassium ferrioxalate. All solutions were handled under dark condition. Potassium ferrioxalate solution was prepared by dissolving 1.105 g of potassium ferrioxalate trihydrate in 15 mL of 0.05 M sulfuric acid, followed by vigorous mixing to make solution homogeneous. Separately, 25 mg of 1,10-phenanthroline and 5.63 g of sodium acetate was dissolved in 25 mL of 0.5 M sulfuric acid, making buffered solution.

2.0 mL of the ferrioxalate solution was transferred to a cuvette and irradiated for 90.0 seconds at 436 nm with a slit size of 10.0 nm. After irradiation, 0.35 mL of the phenanthroline solution was added to the irradiated solution. Separately, 2.0 mL of the ferrioxalate solution was taken and mixed with 0.35 mL of the phenanthroline solution for comparison. After 1 h, the absorbance of the solutions was measured at 510 nm.

Conversion of the ferrioxalate solution could be calculated using the equation:

$$\text{mol } Fe^{2+} = (V \cdot \Delta A) / (l \cdot \varepsilon)$$

Here, V is the volume of the solution (0.00235 L), ΔA is the difference in absorbance in 510 nm, l is the cuvette dimension (1.00 cm), and ε is the molar absorption coefficient (11100 L mol^{-1} cm^{-1}).[60]

The photon flux could be calculated using the equation:

$$\text{photon flux} = (\text{mol } Fe^{2+}) / (\Phi \cdot t \cdot f)$$

Here, Φ is the quantum yield of the ferrioxalate actinometer (1.01 for a 0.15 M solution at λ = 436 nm),[32] t is the time (90 s), and f is the fraction of light absorbed at λ = 436 nm (0.99835).

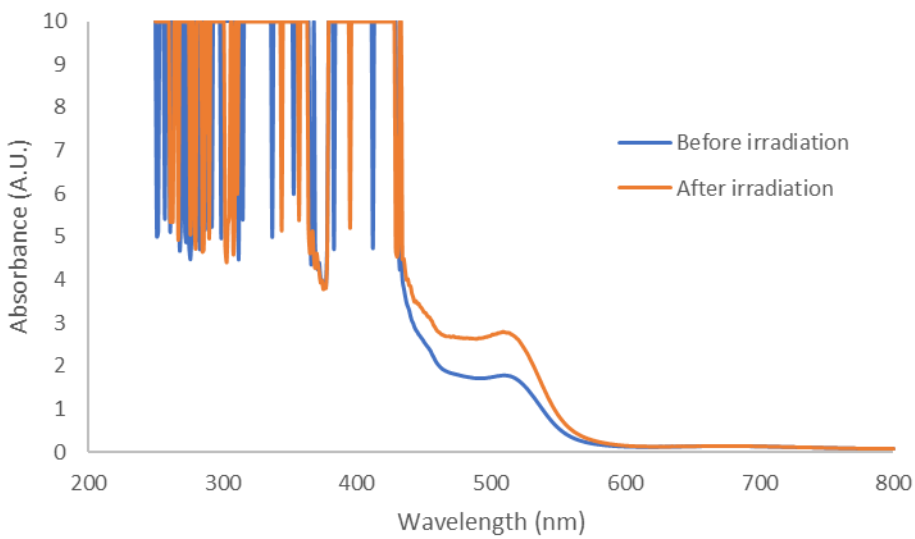

Figure 5.9 Absorbance of the ferrioxalate solutions

From the above absorption spectrum, ΔA = 1.0074. Therefore,

$$\text{mol } Fe^{2+} = (V \cdot \Delta A) / (l \cdot \varepsilon) = (0.00235 \cdot 1.0074) / (1 \cdot 11000) = 2.13278 \times 10^{-6} \text{ mol}$$

Then,

$$\text{photon flux} = (\text{mol } Fe^{2+}) / (\Phi \cdot t \cdot f) = (2.13278 \times 10^{-6}) / (1.01 \cdot 90 \cdot 0.99835)$$

$$= 2.35017 \times 10^{-8} \text{ einstein/s}$$

5.4.11.2 Absorption spectrum of $Ir(CF_3ppy)_3$ in DMA/olefin 2a

Absorption spectrum of $Ir(CF_3ppy)_3$ was measured by preparing a solution of $Ir(CF_3ppy)_3$ (8.6 mg) in DMA (2 mL) and olefin **2a** (1.2 mL), which has concentration to that of the standard reaction conditions.

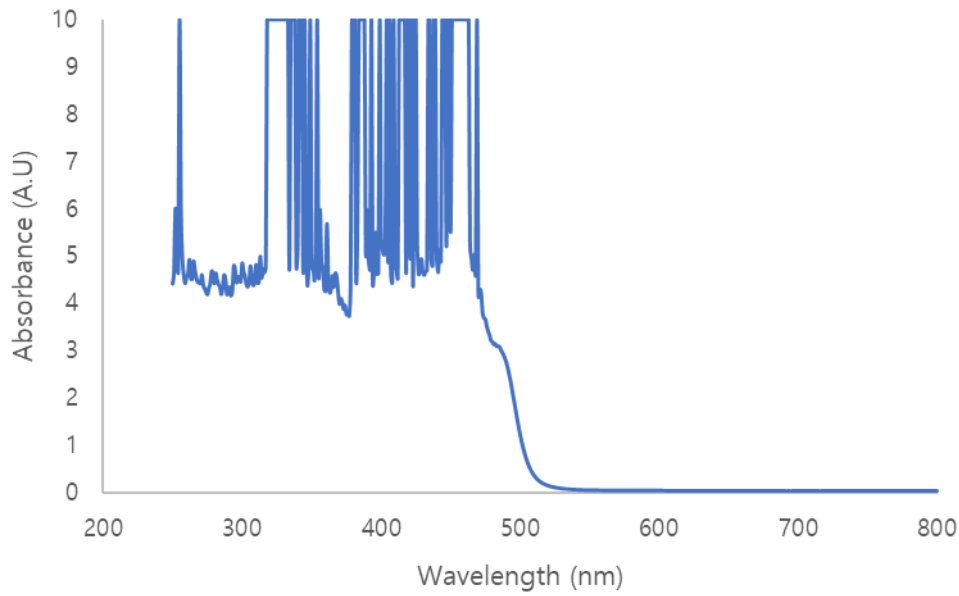

Figure 5.10 Absorbance of $Ir(CF_3ppy)_3$ in DMF/olefin **2a**

The absorbance of $Ir(CF_3ppy)_3$ at 436 nm is >3 indicating the fraction of light absorbed (f) is >0.999.

5.4.11.3 Quantum yield measurement

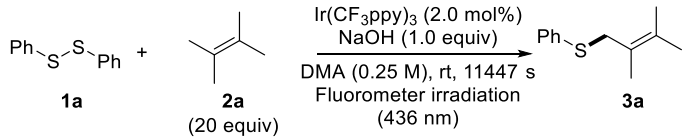

To a sealable cuvette equipped with a PTFE-coated stir bar were added disulfide **1a** (54.6 mg, 0.25 mmol, 1.0 equiv), $Ir(CF_3ppy)_3$ (4.3 mg, 0.0050 mmol, 0.020 equiv), and NaOH (10 mg, 0.25 mmol, 1.0 equiv) in a glovebox. The cuvette was closed with a Teflon-lined septum cap and taken out of the glovebox. Olefin **2a** (594 μL, 5.0 mmol, 20 equiv) and DMA (1 mL) were added via syringe, and the resulting solution was irradiated for 11447 s with stirring under the identical conditions with the actinometry. After the irradiation was finished, the resulting mixture was analyzed by GC using dodecane (56.8 μL, 0.25 mmol, 1.0 equiv) as an internal standard to give 2.969% yield of the desired product.

$$\text{mol product} = 2.969\% \cdot 0.25\ \text{mmol} = 7.421 \times 10^{-6}\ \text{mol}$$

$$\text{Quantum yield } (\Phi) = (\text{mol product}) / (\text{flux} \cdot t \cdot f)$$

$$= (7.421 \times 10^{-6}) / (2.35017 \times 10^{-8} \cdot 11447 \cdot 1) = 0.029$$

5.4.12 Kinetic isotope effect

The kinetic isotope effect was measured using commercially available cyclohexene-d_{10} (**2h-d_{10}**), according to the following procedure.

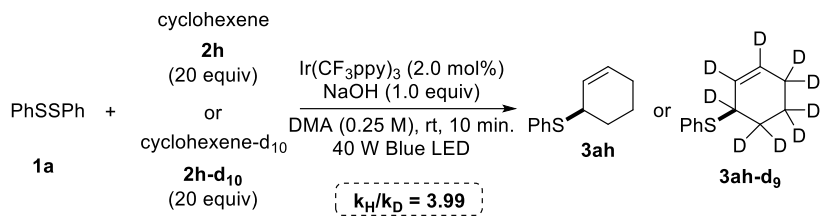

A 4 mL reaction vial equipped with a PTFE-coated stir bar was charged with diphenyl disulfide **1a** (54.6 mg. 0.25 mmol, 1.0 equiv), $Ir(CF_3ppy)_3$ (4.3 mg, 0.0050 mmol, 0.020 equiv), and NaOH (10 mg, 0.25 mmol, 1.0 equiv) in a glovebox. The vial was closed with a Teflon-lined septum cap and taken out of the glovebox. Dodecane (56.8 μL, 0.25 mmol, 1.0 equiv) and DMA (1 mL) were added via syringe, and a nitrogen balloon was attached to the septum with a needle. Cyclohexene **2h** (506 μL, 5.0 mmol, 20.0 equiv) was added, and the mixture was stirred under 40 W blue LED irradiation with fan cooling, located on the 2.5 cm away from the LED. Aliquots (10 μL) of the reaction mixture were taken every 2 min. and analyzed by GC to check the yield of **3ah**. The same experiment was repeated two more times, and the yields of **3ah** across the three experiments were averaged to check the initial rate.

The same procedure was extended to cyclohexene-d_{10} **2h-d_{10}** (508 μL, 5.0 mmol, 20.0 equiv) for measuring the initial rate.

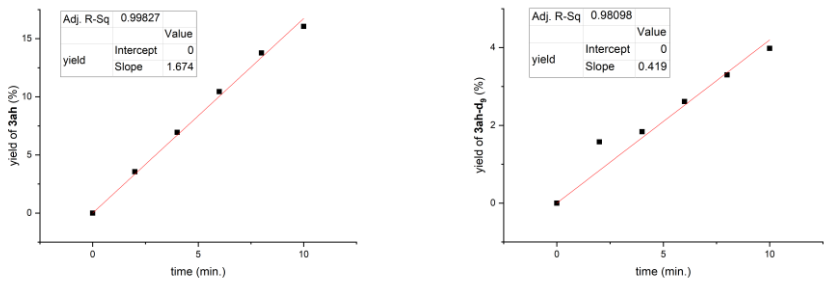

Figure 5.11 Initial rate measurement with **2h** and **2h-d_{10}**

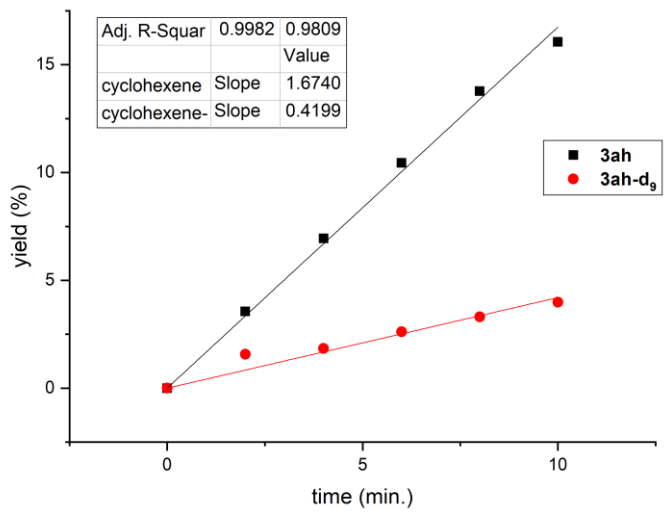

Figure 5.12 KIE measurement with **2h** and **2h-d_{10}** (k_H/k_D = 3.99)

5.4.13 CV experiments

5.4.13.1 Calibration of the reference electrode

<Electrode composition>

Working electrode: glassy carbon

Reference electrode: Ag/AgCl in KCl (aq)

Counter electrode: Pt sheet

<Procedure>

A solution of Ferrocene (**Fc**, 0.0010 M) and tetra-n-butylammonium perchlorate (0.10 M) in acetonitrile (10 mL) was transferred to an electrochemical cell equipped with the above three-electrode systems. The cyclic voltammogram was obtained using ElectraSyn CV measurement experiment with a scan rate 0.2 V/s and a scan range of -1.0 to 1.0 V.

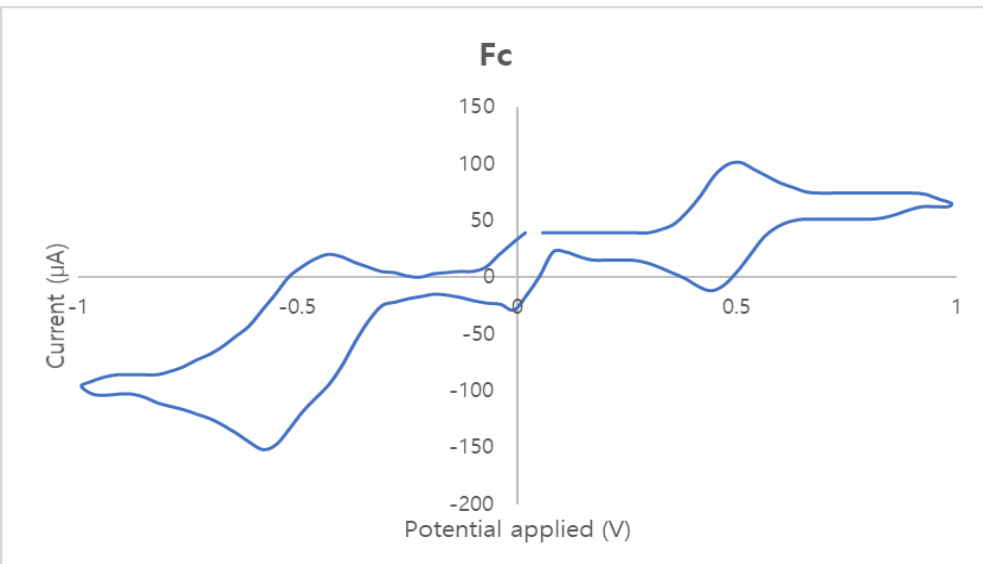

Measured: $E_{1/2}$[**Fc**/**Fc**$^+$] = 0.475 V vs Ag/AgCl

Reference: $E_{1/2}$[**Fc**/**Fc**$^+$] = 0.380 V vs SCE (Saturated Calomel Electrode)

Conversion constant: -0.095 V

5.4.13.2 Disulfide 1q

<Electrode composition>

Working electrode: glassy carbon

Reference electrode: Ag/AgCl in KCl (aq)

Counter electrode: Pt sheet

<Procedure>

A solution of **1q** (0.0020 M) and tetra-n-butylammonium perchlorate (0.10 M) in acetonitrile (10 mL) was transferred to an electrochemical cell equipped with the above three-electrode systems. The cyclic voltammogram was obtained using ElectraSyn CV measurement experiment with a scan rate of 0.2 V/s and a scan range of -2.5 to 1.0 V.

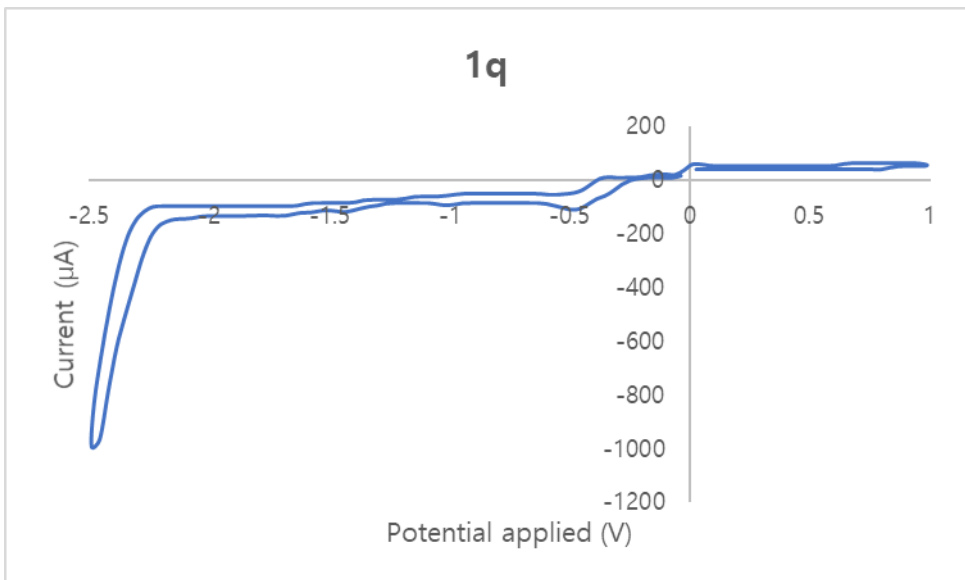

The cyclic voltammogram indicates that no irreversible reduction occurred in a range of >-2.0 V.

5.4.13.3 Disulfide $1q_{Bzt}$

<Electrode composition>

Working electrode: glassy carbon

Reference electrode: Ag/AgCl in KCl (aq)

Counter electrode: Pt sheet

<Procedure>

A solution of **$1q_{Bzt}$** (0.0020 M) and tetra-n-butylammonium perchlorate (0.10 M) in acetonitrile (10 mL) was transferred to an electrochemical cell equipped with the above three-electrode systems. The cyclic voltammogram was obtained using ElectraSyn CV measurement experiment with a scan rate of 0.2 V/s and a scan range of -2.5 to 1.0 V.

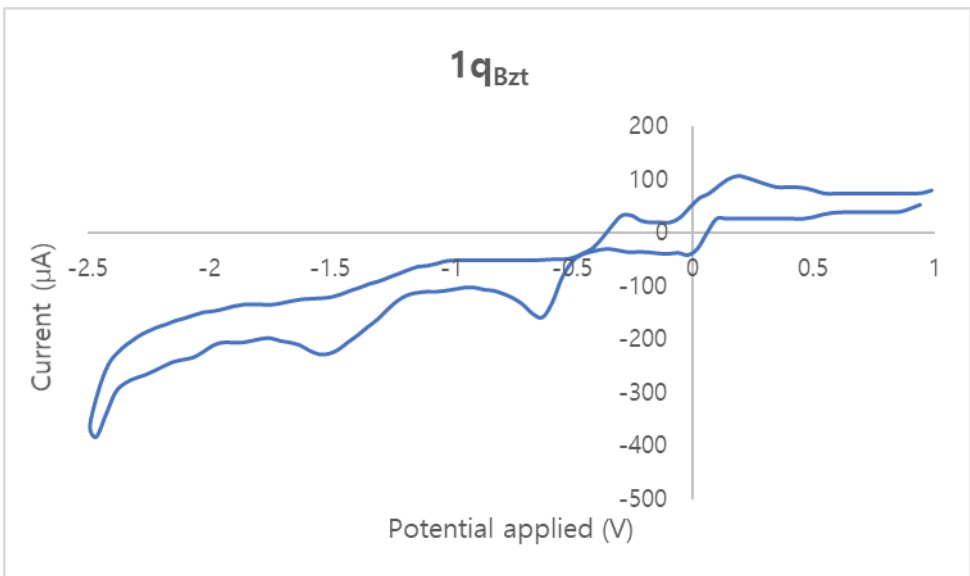

The cyclic voltammogram indicates that an irreversible reduction occurred at -1.544 V (-1.639 V vs SCE).

5.4.13.4 Disulfide $1q_{ClBzt}$

<Electrode composition>

Working electrode: glassy carbon

Reference electrode: Ag/AgCl in KCl (aq)

Counter electrode: Pt sheet

<Procedure>

A solution of $\mathbf{1q_{ClBzt}}$ (0.0010 M) and tetra-n-butylammonium perchlorate (0.10 M) in acetonitrile (10 mL) was transferred to an electrochemical cell equipped with the above three-electrode systems. The cyclic voltammogram was obtained using ElectraSyn CV measurement experiment with a scan rate of 0.2 V/s and a scan range of -2.5 to 1.0 V.

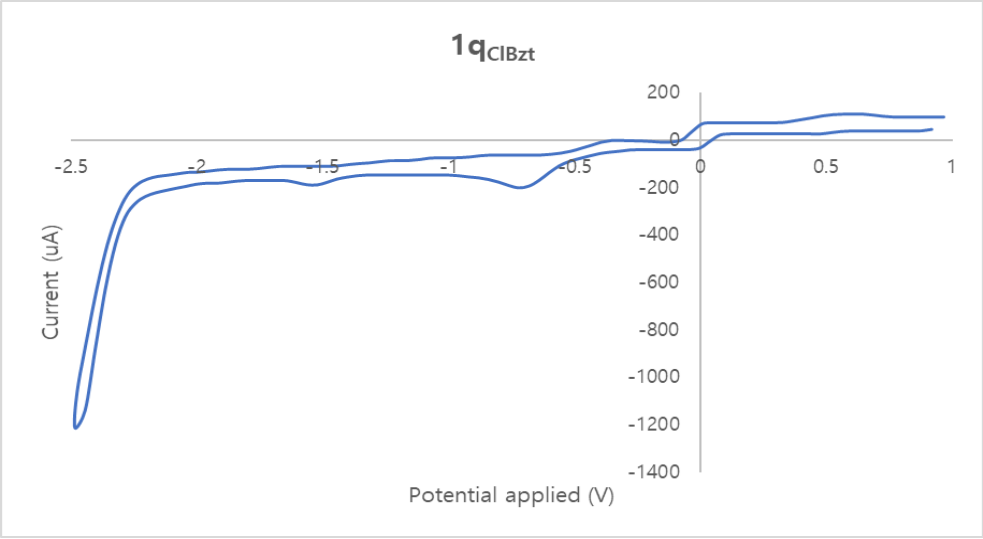

The cyclic voltammogram indicates that an irreversible reduction occurred at -1.524 V (-1.619 V vs SCE).

5.4.13.5 Disulfide $1q_{NO2Ph}$

<Electrode composition>

Working electrode: glassy carbon

Reference electrode: Ag/AgCl in KCl (aq)

Counter electrode: Pt sheet

<Procedure>

A solution of **$1q_{NO2Ph}$** (0.0020 M) and tetra-n-butylammonium perchlorate (0.10 M) in acetonitrile (10 mL) was transferred to an electrochemical cell equipped with the above three-electrode systems. The cyclic voltammogram was obtained using ElectraSyn CV measurement experiment with a scan rate of 0.2 V/s and a scan range of -2.5 to 1.0 V.

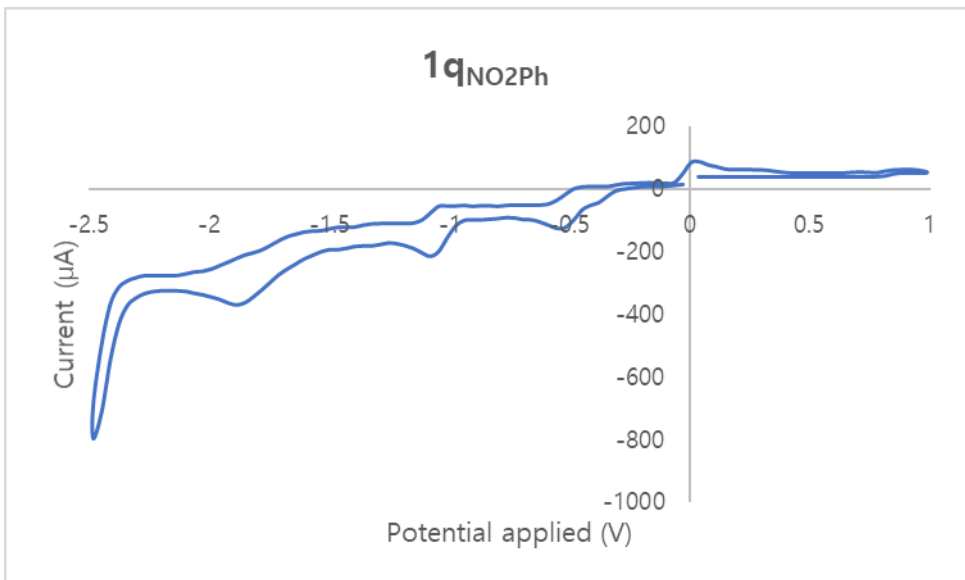

The cyclic voltammogram indicates that an irreversible reduction occurred at -1.886 V (-1.981 V vs SCE).

5.5 References

(1) (a) Rayner, C. M. *Contemp. Org. Synth.* **1995**, *2*, 409. (b) Evans, D. A.; Andrews, G. C. *Acc. Chem. Res.* **1974**, *7*, 147.

(2) (a) Arora, A.; Siddiqui, I. A.; Shukla, Y. *Mol. Cancer Ther.* **2004**, *3*, 1459. (b) Arunkumar, A.; Vijayababu, M. R.; Venkataraman, P.; Senthilkumar, K.; Arunakaran, J. *Bio. Pharm. Bull.* **2006**, *29*, 375. (c) Wargovich, M. J. *J. Nutr.* **2006**, *136*, 832S. (d) Rao, P. ; Midde, N.; Miller, D.; Chauhan, S.; Kumar, A.; Kumar, S. *Curr. Drug Metab.* **2015**, *16*, 486. (e) Malki, A.; Issa, D. A. E.; Elbayaa, R. Y.; Ashour, H. M. A. *Lett. Drug Des. Discov.* **2019**, *16*, 200.

(3) (a) Rong, M.; Li, D.; Huang, R.; Huang, Y.; Han, X.; Weng, Z. *Eur. J. Org. Chem.* **2014**, 5010. (b) Herkert, L.; Green, S. L. J.; Barker, G.; Johnson, D. G.; Young, P. C.; Macgregor, S. A.; Lee, A.-L. *Chem.—Eur. J.* **2014**, *20*, 11540. (c) Gao, N.; Zhao, X. *Eur. J. Org. Chem.* **2013**, 2708. (d) Roggen, M.; Carreira, E. M. *Angew. Chem., Int. Ed.* **2012**, *51*, 8652. (e) Gao, N.; Zheng, S.; Yang, W.; Zhao, X. *Org. Lett.* **2011**, *13*, 1514. (f) Zheng, S.; Gao, N.; Liu, W.; Liu, D.; Zhao, X.; Cohen, T. *Org. Lett.* **2010**, *12*, 4454. (g) Tanaka, S.; Pradhan, P. K.; Maegawa, Y.; Kitamura, M. *Chem. Commun.* **2010**, *46*, 3996. (h) Saha, A.; Ranu, B. C. *Tetrahedron Lett.* **2010**, *51*, 1902. (i) Zaitsev, A. B.; Caldwell, H. F.; Pregosin, P. S.; Veiros, L. F. *Chem.—Eur. J.* **2009**, *15*, 6468. (j) Yatsumonji, Y.; Ishida, Y.; Tsubouchi, A.; Takeda, T. *Org. Lett.* **2007**, *9*, 4603. (k) Kondo, T.; Morisaki, Y.; Uenoyama, S.-y.; Wada, K.; Mitsudo, T.-a. *J. Am. Chem. Soc.* **1999**, *121*, 8657. (l) Frank, M.; Gais, H.-J. *Tetrahedron: Asymmetry* **1998**, *9*, 3353. (m) Goux, C.; Lhoste, P.; Sinou, D. *Tetrahedron* **1994**, *50*, 10321. (n) Goux, C.; Lhoste, P.; Sinou, D. *Tetrahedron Lett.* **1992**, *33*, 8099.

(4) (a) Overman, L. E.; Roberts, S. W.; Sneddon, H. F. *Org. Lett.* **2008**, *10*, 1485. (b) Gais, H.-J.; Böhme, A. *J. Org. Chem.* **2002**, *67*, 1153.

(5) (a) Pritzius, A. B.; Breit, B. *Angew. Chem., Int. Ed.* **2015**, *54*, 3121. (b) Pritzius, A. B.; Breit, B. *Angew. Chem., Int. Ed.* **2015**, *54*, 15818.

(6) (a) Yang, X.-H.; Davison, R. T.; Dong, V. M. *J. Am. Chem. Soc.* **2018**. (b) Yang, X.-H.; Davison, R. T.; Nie, S.-Z.; Cruz, F. A.; McGinnis, T. M.; Dong, V. M. *J. Am. Chem. Soc.* **2019**, *141*, 3006. (c) He, C.; Brouwer, C.; Rahaman, R. *Synlett* **2007**, 1785.

(7) (a) Liron, F.; Oble, J.; Lorion, M. M.; Poli, G. *Eur. J. Org. Chem.* **2014**, 5863. (b) Young, A. J.; White, M. C. *J. Am. Chem. Soc.* **2008**, *130*, 14090. (c) Li, Z.; Li, C.-J. *J. Am. Chem. Soc.* **2006**, *128*, 56. (d) Zhou, R.; Liu, H.; Tao, H.; Yu, X.; Wu, J. *Chem. Sci.* **2017**, *8*, 4654. (e) Schwarz, J. L.; Schäfers, F.; Tlahuext-Aca, A.; Lückemeier, L.; Glorius, F. *J. Am. Chem. Soc.* **2018**, *140*, 12705. (f) Wang, G.-W.; Zhou, A.-X.; Li, S.-X.; Yang, S.-D. *Org. Lett.* **2014**, *16*, 3118. (g) Yamaguchi, T.; Kommagalla, Y.; Aihara, Y.; Chatani, N. *Chem. Commun.* **2016**, *52*, 10129. (h) Maity, S.; Dolui, P.; Kancherla, R.; Maiti, D. *Chem. Sci.* **2017**, *8*, 5181. (i) Lerchen, A.; Knecht, T.; Koy, M.; Ernst, J. B.; Bergander, K.; Daniliuc, C. G.; Glorius, F. *Angew. Chem., Int. Ed.* **2018**, *57*, 15248. (j) Chen, M. S.; White, M. C. *J. Am. Chem. Soc.* **2004**, *126*, 1346. (k) Campbell, A. N.; White, P. B.; Guzei, I. A.; Stahl, S. S. *J. Am. Chem. Soc.* **2010**, *132*, 15116. (l) Alam, R.; Pilarski, L. T.; Pershagen, E.; Szabó, K. J. *J. Am. Chem. Soc.* **2012**, *134*, 8778. (m) Fraunhoffer, K. J.; White, M. C. *J. Am. Chem. Soc.* **2007**, *129*, 7274. (n) Reed, S. A.; White, M. C. *J. Am. Chem. Soc.* **2008**, *130*, 3316. (o) Liu, G.; Yin, G.; Wu, L. *Angew. Chem., Int. Ed.* **2008**, *47*, 4733. (p) Harvey, M. E.; Musaev, D. G.; Du Bois, J. *J. Am. Chem. Soc.* **2011**, *133*, 17207. (q) Paradine, S. M.; White, M. C. *J. Am. Chem. Soc.* **2012**, *134*,

2036. (r) Pattillo, C. C.; Strambeanu, l. i.; Calleja, P.; Vermeulen, N. A.; Mizuno, T.; White, M. C. *J. Am. Chem. Soc.* **2016**, *138*, 1265. (s) Ma, R.; White, M. C. *J. Am. Chem. Soc.* **2018**, *140*, 3202. (t) Yang, W.; Chen, H.; Li, J.; Li, C.; Wu, W.; Jiang, H. *Chem. Commun.* **2015**, *51*, 9575. (u) Horn, E. J.; Rosen, B. R.; Chen, Y.; Tang, J.; Chen, K.; Eastgate, M. D.; Baran, P. S. *Nature* **2016**, *533*, 77. (v) Li, C.; Chen, H.; Li, J.; Li, M.; Liao, J.; Wu, W.; Jiang, H. *Adv. Synth. Catal.* **2018**, *360*, 1600. (w) Larsson, J. M.; Zhao, T. S. N.; Szabó, K. J. *Org. Lett.* **2011**, *13*, 1888. (x) Braun, M.-G.; Doyle, A. G. *J. Am. Chem. Soc.* **2013**, *135*, 12990. (y) Mao, L.; Bertermann, R.; Rachor, S. G.; Szabó, K. J.; Marder, T. B. *Org. Lett.* **2017**, *19*, 6590.

(8) Kondo, T.; Mitsudo, T.-a. *Chem. Rev.* **2000**, *100*, 3205.

(9) (a) Aldea, R.; Alper, H. *J. Org. Chem.* **1995**, *60*, 8365. (b) Martín, S. E.; Rossi, L. I. *Tetrahedron Lett.* **2001**, *42*, 7147. (c) O'Mahony, G. E.; Ford, A.; Maguire, A. R. *J. Org. Chem.* **2012**, *77*, 3288.

(10) Cuthbertson, J. D.; MacMillan, D. W. C. *Nature* **2015**, *519*, 74.

(11) (a) Huang, L.; Rueping, M. *Angew. Chem., Int. Ed.* **2018**, *57*, 10333. (b) Fan, X.-Z.; Rong, J.-W.; Wu, H.-L.; Zhou, Q.; Deng, H.-P.; Tan, J. D.; Xue, C.-W.; Wu, L.-Z.; Tao, H.-R.; Wu, J. *Angew. Chem., Int. Ed.* **2018**, *57*, 8514. (c) Mitsunuma, H.; Tanabe, S.; Fuse, H.; Ohkubo, K.; Kanai, M. *Chem. Sci.* **2019**, *10*, 3459. (d) Ohmatsu, K.; Nakashima, T.; Sato, M.; Ooi, T. *Nat. Commun.* **2019**, *10*, 2706.

(12) (a) Majek, M.; von Wangelin, A. J. *Chem. Commun.* **2013**, *49*, 5507. (b) Zhu, X.; Xie, X.; Li, P.; Guo, J.; Wang, L. *Org. Lett.* **2016**, *18*, 1546. (c) Teders, M.; Henkel, C.; Anhäuser, L.; Strieth-Kalthoff, F.; Gómez-Suárez, A.; Kleinmans, R.; Kahnt, A.; Rentmeister, A.; Guldi, D.; Glorius, F. *Nat. Chem.* **2018**, *10*, 981.

(13) (a) Hager, D.; MacMillan, D. W. C. *J. Am. Chem. Soc.* **2014**, *136*, 16986. (b) Capacci, A. G.; Malinowski, J. T.; McAlpine, N. J.; Kuhne, J.; MacMillan, D. W. C.

Nat. Chem. **2017**, *9*, 1073. (c) Loh, Y. Y.; Nagao, K.; Hoover, A. J.; Hesk, D.; Rivera, N. R.; Colletti, S. L.; Davies, I. W.; MacMillan, D. W. C. *Science* **2017**, *358*, 1182. (d) Zhao, G.; Wang, T. *Angew. Chem., Int. Ed.* **2018**, *57*, 6120.

(14) (a) Hoyle, C. E.; Bowman, C. N. *Angew. Chem., Int. Ed.* **2010**, *49*, 1540. (b) Hoyle, C. E.; Lowe, A. B.; Bowman, C. N. *Chem. Soc. Rev.* **2010**, *39*, 1355. (c) Lowe, A. B. *Polym. Chem.* **2014**, *5*, 4820. (d) Silveira, C.; Mendes, S.; Líbero, F. *Synlett* **2010**, 790.

(15) (a) Tyson, E. L.; Ament, M. S.; Yoon, T. P. *J. Org. Chem.* **2013**, *78*, 2046. (b) Tyson, E. L.; Niemeyer, Z. L.; Yoon, T. P. *J. Org. Chem.* **2014**, *79*, 1427. (c) Keylor, M. H.; Park, J. E.; Wallentin, C.-J.; Stephenson, C. R. J. *Tetrahedron* **2014**, *70*, 4264. (d) Bhat, V. T.; Duspara, P. A.; Seo, S.; Abu Bakar, N. S. B.; Greaney, M. F. *Chem. Commun.* **2015**, *51*, 4383. (e) Bordoni, A. V.; Lombardo, M. V.; Wolosiuk, A. *RSC Adv.* **2016**, *6*, 77410. (f) Limnios, D.; Kokotos, C. G. *Adv. Synth. Catal* **2017**, *359*, 323. (g) Zhao, G.; Kaur, S.; Wang, T. *Org. Lett.* **2017**, *19*, 3291.

(16) Pitzer, L.; Schäfers, F.; Glorius, F. *Angew. Chem., Int. Ed.* **2019**, *58*, 8572.

(17) Zweifel, G.; Whitney, C. C. *J. Org. Chem.* **1966**, *31*, 4178.

(18) Choi, S.; Yang, J.-D.; Ji, M.; Choi, H.; Kee, M.; Ahn, K.-H.; Byeon, S.-H.; Baik, W.; Koo, S. *J. Org. Chem.* **2001**, *66*, 8192.

(19) Šiaučiulis, M.; Sapmaz, S.; Pulis, A. P.; Procter, D. J. *Chem. Sci.* **2018**, *9*, 754.

(20) Billard, F.; Robiette, R.; Pospíšil, J. *J. Org. Chem.* **2012**, *77*, 6358.

(21) Carter, D. S.; Van Vranken, D. L. *Org. Lett.* **2000**, *2*, 1303.

(22) (a) Xie, X.; Li, P.; Shi, Q.; Wang, L. *Org. Biomol. Chem.* **2017**, *15*, 7678. (b) Ye, L.-m.; Chen, J.; Mao, P.; Zhang, X.-j.; Yan, M. *Tetrahedron Lett.* **2017**, *58*, 2743. (c) Czyz, M. L.; Weragoda, G. K.; Monaghan, R.; Connell, T. U.; Brzozowski, M.; Scully, A. D.; Burton, J.; Lupton, D. W.; Polyzos, A. *Org. Biomol. Chem.* **2018**,

16, 1543.

(23) Singh, A.; Teegardin, K.; Kelly, M.; Prasad, K. S.; Krishnan, S.; Weaver, J. D. *J. Organomet. Chem.* **2015**, *776*, 51.

(24) The reaction without any photocatalyst was affected by the setups for irradiation, especially by the intensity of the light. If the distance between the reaction vial and LED was increased (~6 cm), the yield of **3aa** was increased up to 14%. This might be related to the concentration of disulfide, which can be cleaved under irradiation of blue light. If the concentration of disulfide **1a** becomes relatively higher, presumably due to decreased homolytic cleavage under low light intensity, the radical coupling between allyl radical and disulfide could happen, exhibiting the reactivity under the photocatalyst-free conditions. Although it is, the results indicated that the product cannot be efficiently formed without the Ir photocatalyst suggesting the radical mechanism could be only a minor product forming pathway even if it would be operative under certain conditions.

(25) (a) Li, G.-X.; Morales-Rivera, C. A.; Gao, F.; Wang, Y.; He, G.; Liu, P.; Chen, G. *Chem. Sci.* **2017**, *8*, 7180. (b) Pagire, S. K.; Paria, S.; Reiser, O. *Org. Lett.* **2016**, *18*, 2106. (c) Yasu, Y.; Koike, T.; Akita, M. *Angew. Chem., Int. Ed.* **2012**, *51*, 9567.

(26) Rao, G. P.; Murthy, A. R. V. *J. Phys. Chem.* **1964**, *68*, 1573.

(27) Reynolds, R.; Line, L. L.; Nelson, R. F. *J. Am. Chem. Soc.* **1974**, *96*, 1087.

(28) Gerken, J. B.; Stahl, S. S. *ACS Cent. Sci.* **2015**, *1*, 234.

(29) Peover, M. E. *J. Chem. Soc.* **1962**, 4540.

(30) Connelly, N. G.; Geiger, W. E. *Chem. Rev.* **1996**, *96*, 877.

(31) Fu, Y.; Liu, L.; Yu, H.-Z.; Wang, Y.-M.; Guo, Q.-X. *J. Am. Chem. Soc.* **2005**, *127*, 7227.

(32) Laali, K. K.; Borosky, G. L. *J. Fluorine Chem.* **2013**, *151*, 26.

(33) Northrop, B. H.; Coffey, R. N. *J. Am. Chem. Soc.* **2012**, *134*, 13804.

(34) Deng, Y.; Wei, X.-J.; Wang, H.; Sun, Y.; Noël, T.; Wang, X. *Angew. Chem., Int. Ed.* **2017**, *56*, 832.

(35) Antonello, S.; Benassi, R.; Gavioli, G.; Taddei, F.; Maran, F. *J. Am. Chem. Soc.* **2002**, *124*, 7529.

(36) Schmidt am Busch, M.; Knapp, E.-W. *J. Am. Chem. Soc.* **2005**, *127*, 15730.

(37) Ryu, E. K.; Choe, Y. S.; Byun, S. S.; Lee, K.-H.; Chi, D. Y.; Choi, Y.; Kim, B.-T. *Bioorg. Med. Chem.* **2004**, *12*, 859.

(38) Luo, J.; Zhang, J. *ACS Catal.* **2016**, *6*, 873.

(39) Kirihara, M.; Asai, Y.; Ogawa, S.; Noguchi, T.; Hatano, A.; Hirai, Y. *Synthesis* **2007**, 3286.

(40) Carbonnel, E.; Besset, T.; Poisson, T.; Labar, D.; Pannecoucke, X.; Jubault, P. *Chem. Commun.* **2017**, *53*, 5706.

(41) Dou, Y.; Huang, X.; Wang, H.; Yang, L.; Li, H.; Yuan, B.; Yang, G. *Green Chem.* **2017**, *19*, 2491.

(42) Rathore, V.; Upadhyay, A.; Kumar, S. *Org. Lett.* **2018**, *20*, 6274.

(43) Mampuys, P.; Zhu, Y.; Sergeyev, S.; Ruijter, E.; Orru, R. V.; Van Doorslaer, S.; Maes, B. U. *Org. Lett.* **2016**, *18*, 2808.

(44) Zhu, F.; Miller, E.; Zhang, S. Q.; Yi, D.; O'Neill, S.; Hong, X.; Walczak, M. A. *J. Am. Chem. Soc.* **2018**, *140*, 18140.

(45) Sun, Y.; Jiang, H.; Wu, W.; Zeng, W.; Wu, X. *Org. Lett.* **2013**, *15*, 1598.

(46) Howard, J. L.; Schotten, C.; Alston, S. T.; Browne, D. L. *Chem. Commun.* **2016**, *52*, 8448.

(47) Habibi, A.; Baghersad, M. H.; Bilabary, M.; Valizadeh, Y. *Tetrahedron Lett.* **2016**, *57*, 559.

(48) Lysenko, I. L.; Kim, K.; Lee, H. G.; Cha, J. K. *J. Am. Chem. Soc.* **2008**, *130*, 15997.

(49) Croft, R. A.; Mousseau, J. J.; Choi, C.; Bull, J. A. *Chem.—Eur. J.* **2018**, *24*, 818.

(50) Hardinger, S. A.; Fuchs, P. L. *J. Org. Chem.* **1987**, *52*, 2739.

(51) Brichacek, M. P.; Carlson, R. M. *Synth. Commun.* **2007**, *37*, 3541.

(52) Linden, A. A.; Kruger, L.; Backvall, J. E. *J. Org. Chem.* **2003**, *68*, 5890.

(53) Jeyakumar, K.; Chakravarthy, R. D.; Chand, D. K. *Catal. Commun.* **2009**, *10*, 1948.

(54) Molander, G. A.; Felix, L. A. *J. Org. Chem.* **2005**, *70*, 3950.

(55) Gaussian 09, Revision D.01, M. J. Frisch, G. W. Trucks, H. B. Schlegel, G. E. Scuseria, M. A. Robb, J. R. Cheeseman, G. Scalmani, V. Barone, B. Mennucci, G. A. Petersson, H. Nakatsuji, M. Caricato, X. Li, H. P. Hratchian, A. F. Izmaylov, J. Bloino, G. Zheng, J. L. Sonnenberg, M. Hada, M. Ehara, K. Toyota, R. Fukuda, J. Hasegawa, M. Ishida, T. Nakajima, Y. Honda, O. Kitao, H. Nakai, T. Vreven, J. A. Montgomery, Jr., J. E. Peralta, F. Ogliaro, M. Bearpark, J. J. Heyd, E. Brothers, K. N. Kudin, V. N. Staroverov, T. Keith, R. Kobayashi, J. Normand, K. Raghavachari, A. Rendell, J. C. Burant, S. S. Iyengar, J. Tomasi, M. Cossi, N. Rega, J. M. Millam, M. Klene, J. E. Knox, J. B. Cross, V. Bakken, C. Adamo, J. Jaramillo, R. Gomperts, R. E. Stratmann, O. Yazyev, A. J. Austin, R. Cammi, C. Pomelli, J. W. Ochterski, R. L. Martin, K. Morokuma, V. G. Zakrzewski, G. A. Voth, P. Salvador, J. J. Dannenberg, S. Dapprich, A. D. Daniels, O. Farkas, J. B. Foresman, J. V. Ortiz, J. Cioslowski, and D. J. Fox, Gaussian, Inc., Wallingford CT, 2013.

(56) Isse, A. A.; Gennaro, A. *J. Phys. Chem. B* **2010**, *114*, 7894.

(57) Johnson III, R. D. *NIST Standard Reference Database Number 101* **2019**,

Release 20.

(58) Arias-Rotondo, D. M.; McCusker, J. K. *Chem. Soc. Rev.* **2016**, *45*, 5803.

(59) Cismesia, M. A.; Yoon, T. P. *Chem. Sci.* **2015**, *6*, 5426.

(60) Hatchard, C. G.; Parker, C. A. *Proc. Royal Soc. A* **1956**, *235*, 518.

Appendix – NMR spectra

Chapter 2

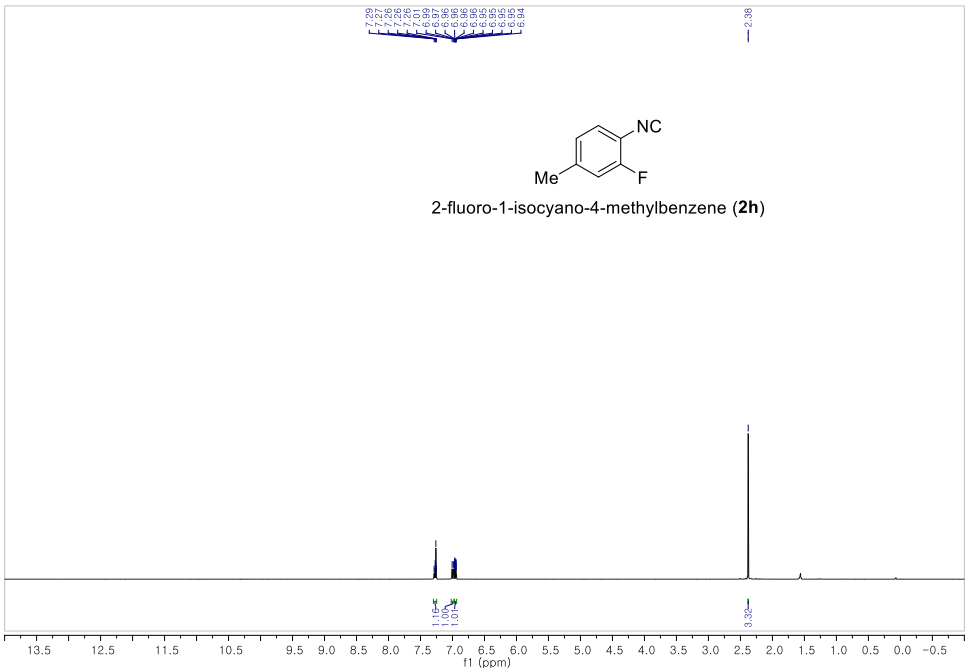

^{1}H NMR ($CDCl_3$, 499 MHz)

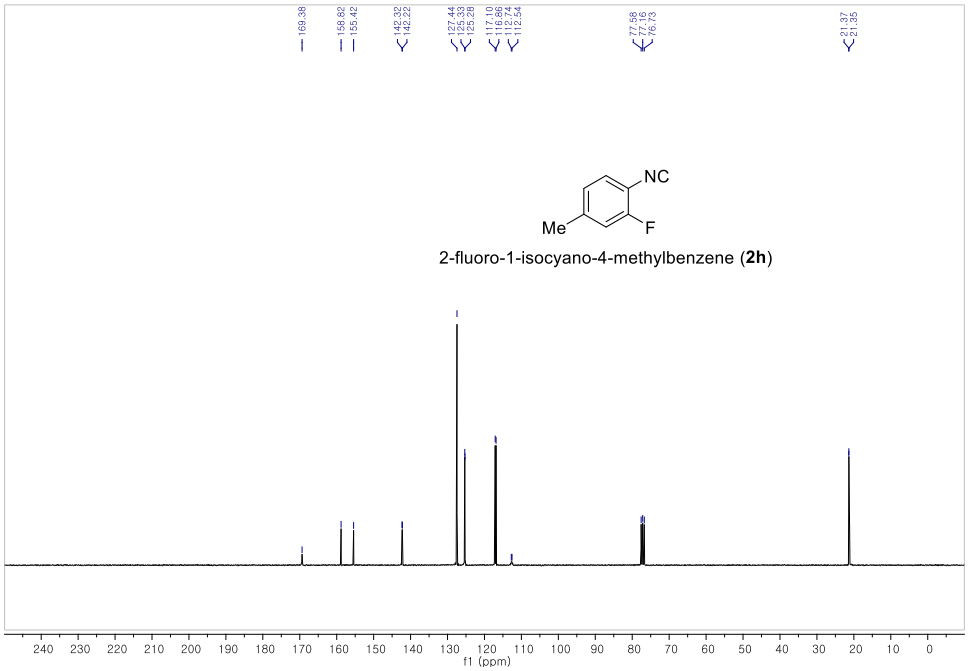

^{13}C NMR ($CDCl_3$, 75 MHz)

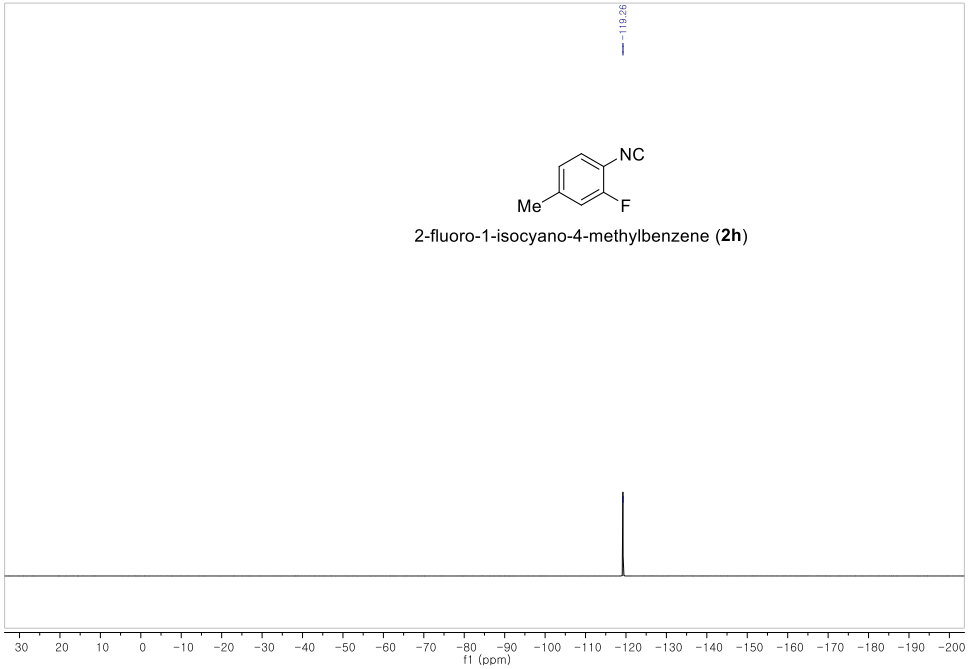

^{19}F NMR ($CDCl_3$, 376 MHz)

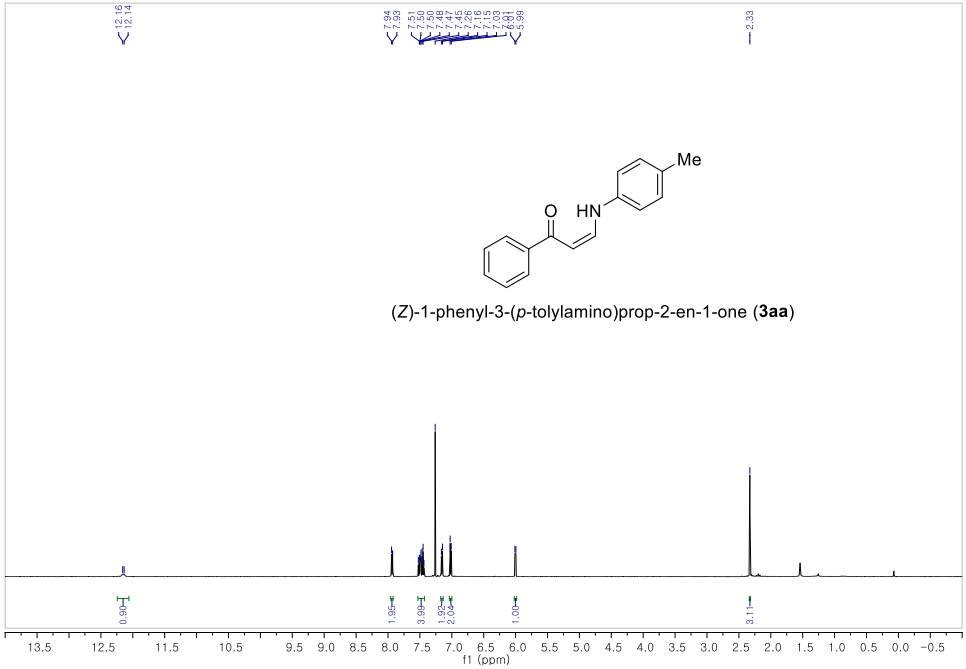

^{1}H NMR ($CDCl_3$, 499 MHz)

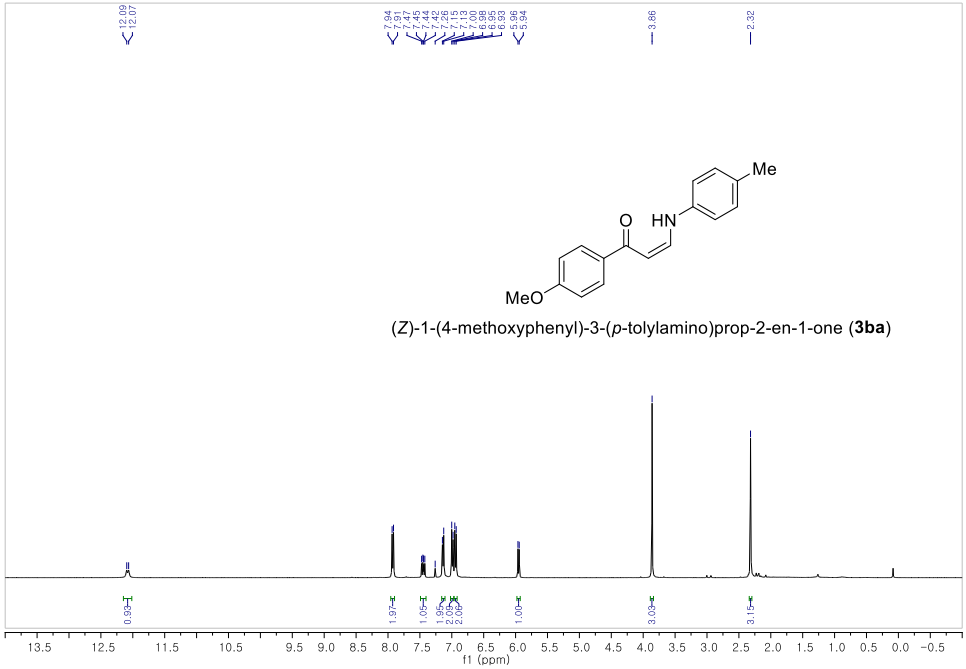

(*Z*)-1-(4-methoxyphenyl)-3-(*p*-tolylamino)prop-2-en-1-one (**3ba**)

^{1}H NMR ($CDCl_3$, 400 MHz)

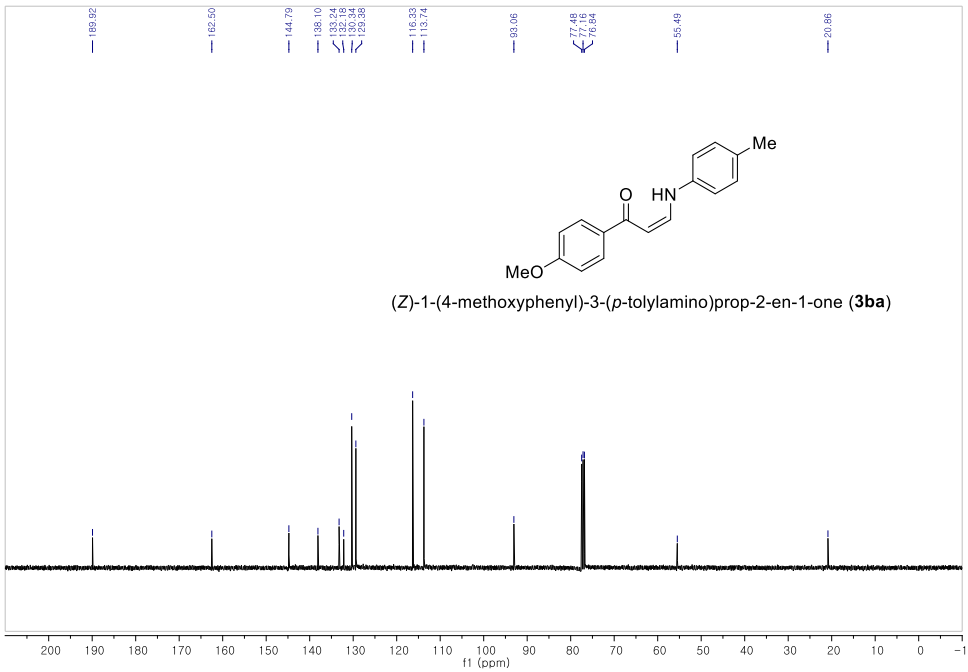

(*Z*)-1-(4-methoxyphenyl)-3-(*p*-tolylamino)prop-2-en-1-one (**3ba**)

^{13}C NMR ($CDCl_3$, 101 MHz)

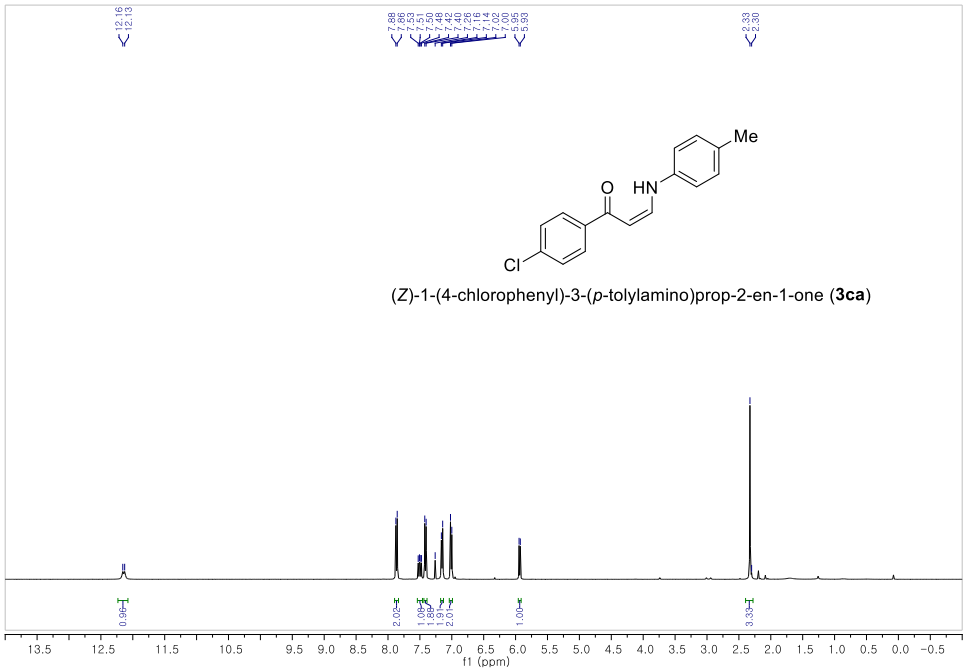

(*Z*)-1-(4-chlorophenyl)-3-(*p*-tolylamino)prop-2-en-1-one (**3ca**)

^{1}H NMR ($CDCl_3$, 400 MHz)

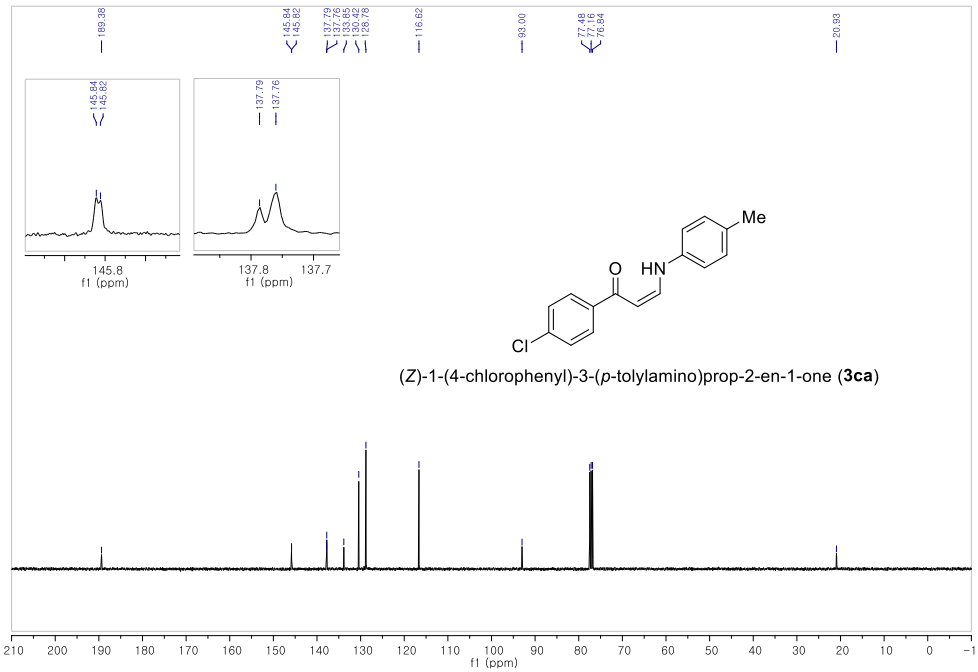

(*Z*)-1-(4-chlorophenyl)-3-(*p*-tolylamino)prop-2-en-1-one (**3ca**)

^{13}C NMR ($CDCl_3$, 101 MHz)

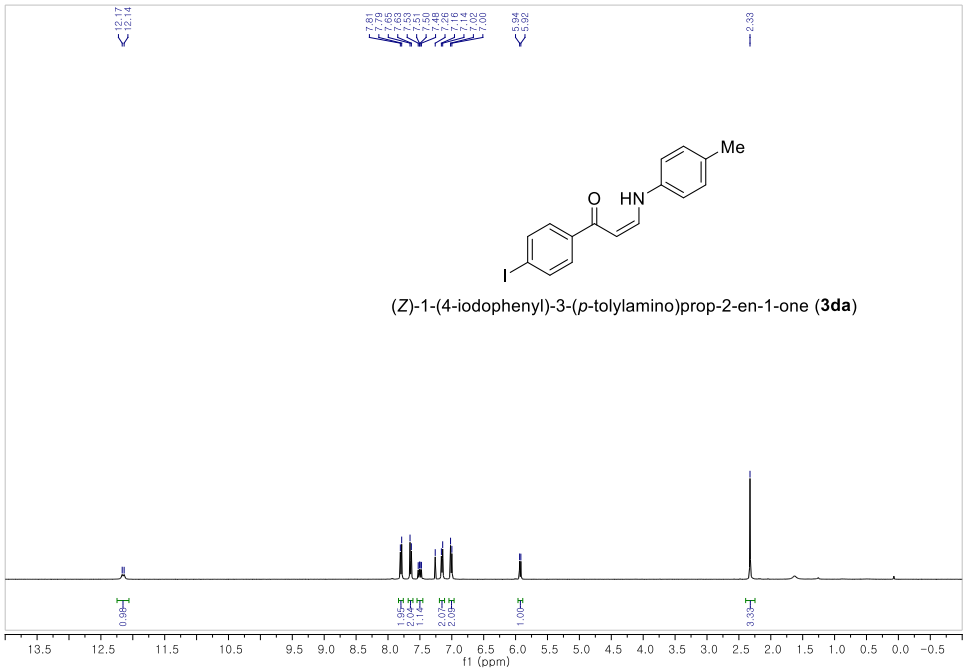

(*Z*)-1-(4-iodophenyl)-3-(*p*-tolylamino)prop-2-en-1-one (**3da**)

^{1}H NMR ($CDCl_3$, 400 MHz)

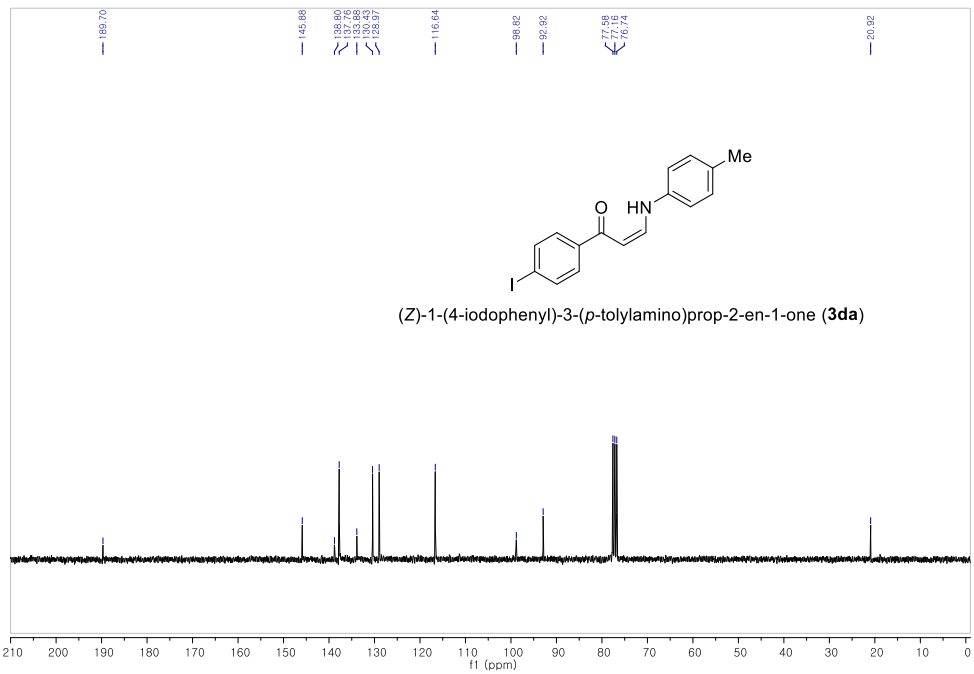

(*Z*)-1-(4-iodophenyl)-3-(*p*-tolylamino)prop-2-en-1-one (**3da**)

^{13}C NMR ($CDCl_3$, 75 MHz)

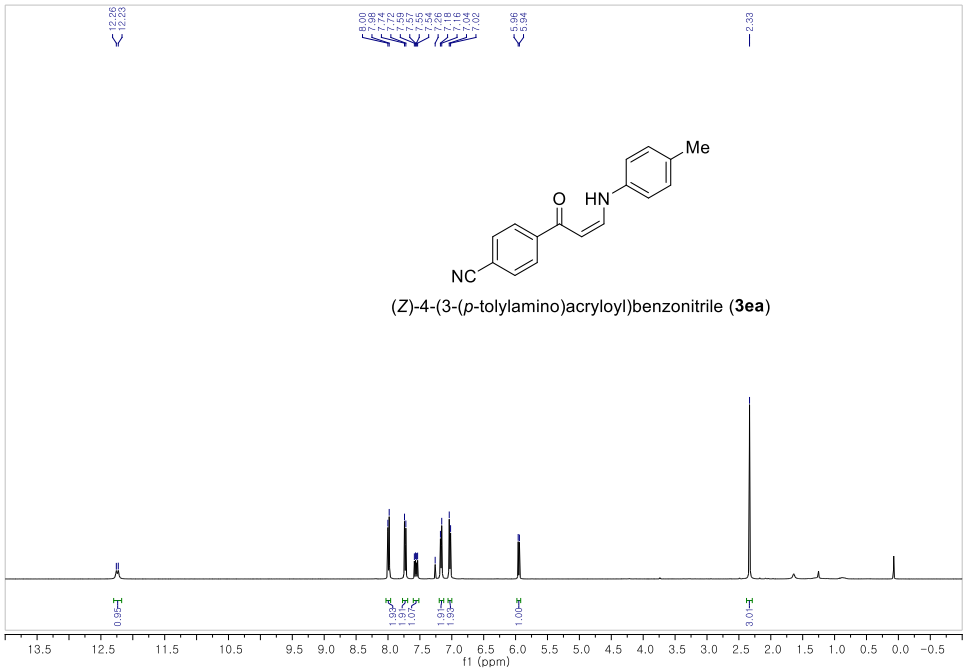

(*Z*)-4-(3-(*p*-tolylamino)acryloyl)benzonitrile (**3ea**)

^{1}H NMR ($CDCl_3$, 400 MHz)

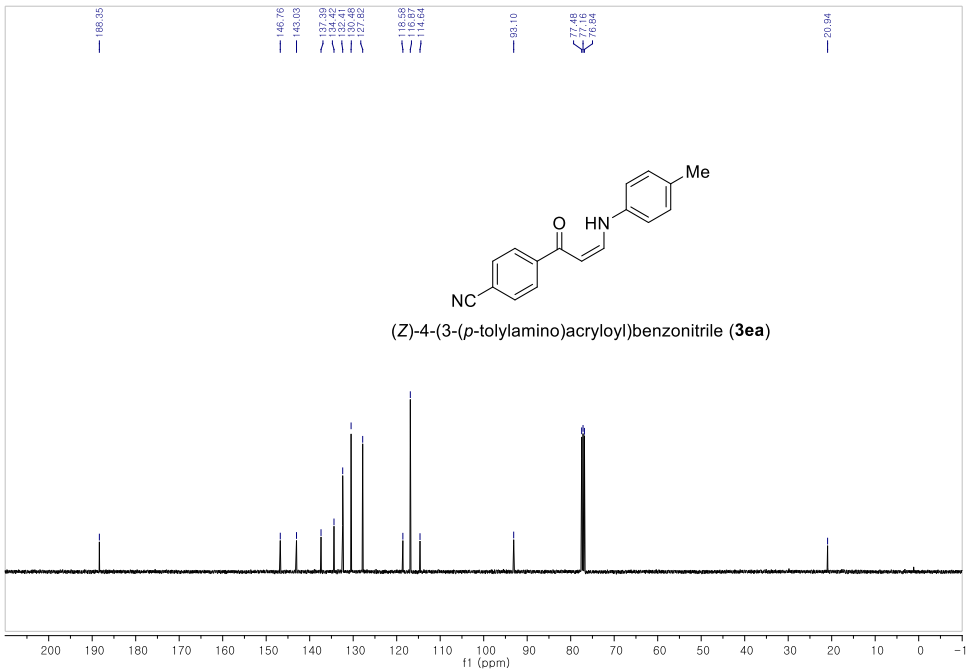

(*Z*)-4-(3-(*p*-tolylamino)acryloyl)benzonitrile (**3ea**)

^{13}C NMR ($CDCl_3$, 101 MHz)

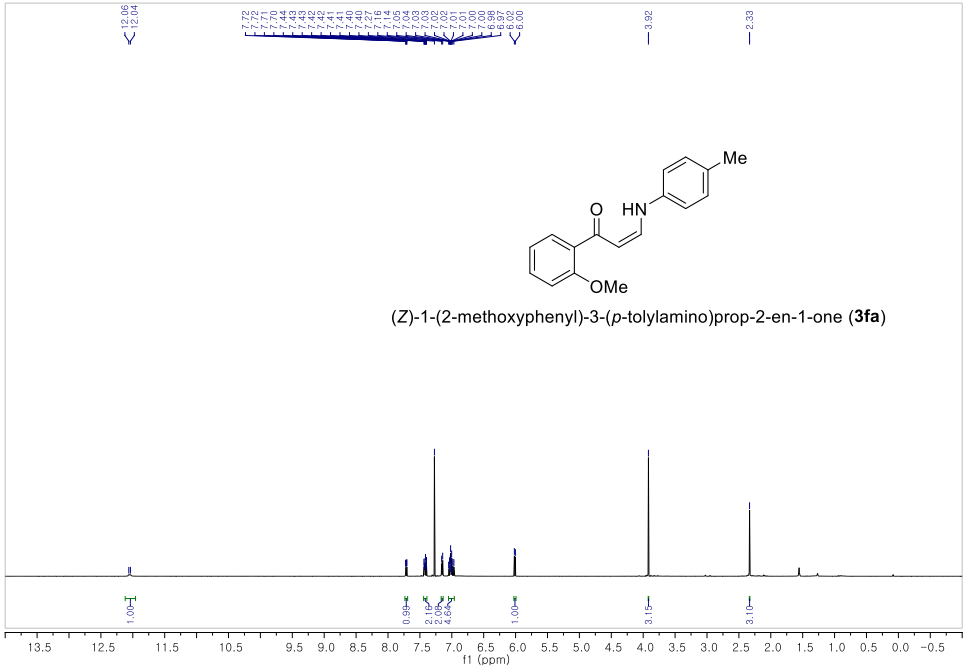

(*Z*)-1-(2-methoxyphenyl)-3-(*p*-tolylamino)prop-2-en-1-one (**3fa**)

^{1}H NMR ($CDCl_3$, 400 MHz)

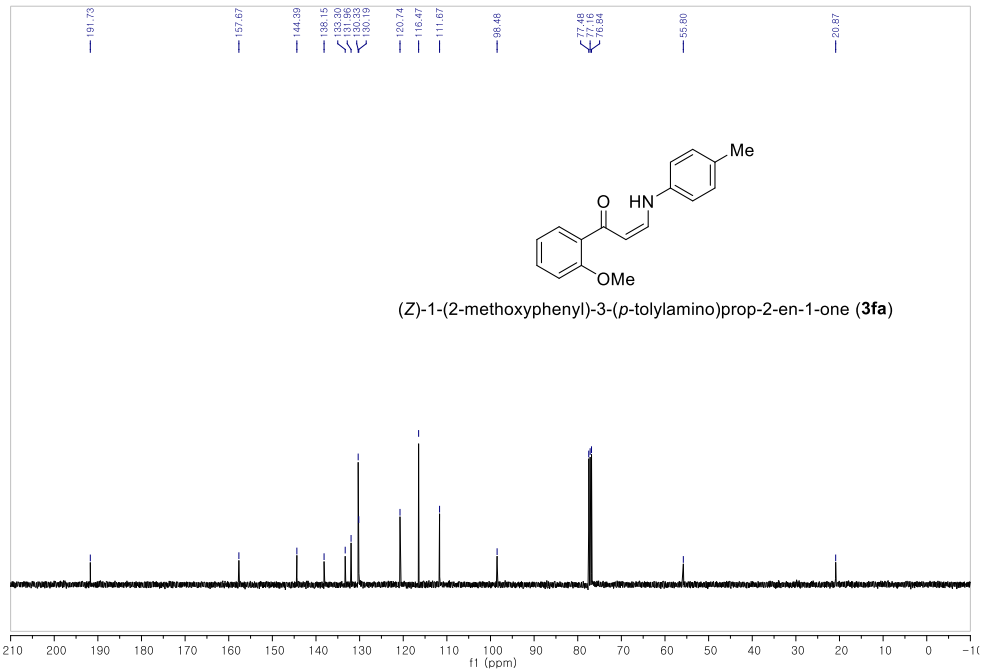

(*Z*)-1-(2-methoxyphenyl)-3-(*p*-tolylamino)prop-2-en-1-one (**3fa**)

^{13}C NMR ($CDCl_3$, 101 MHz)

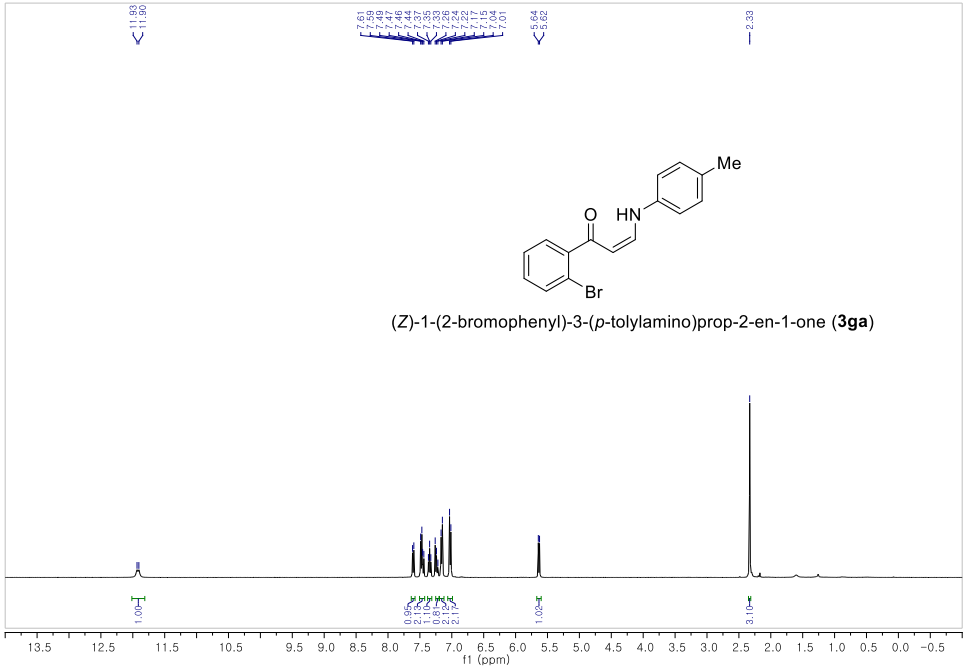

^{1}H NMR ($CDCl_3$, 400 MHz)

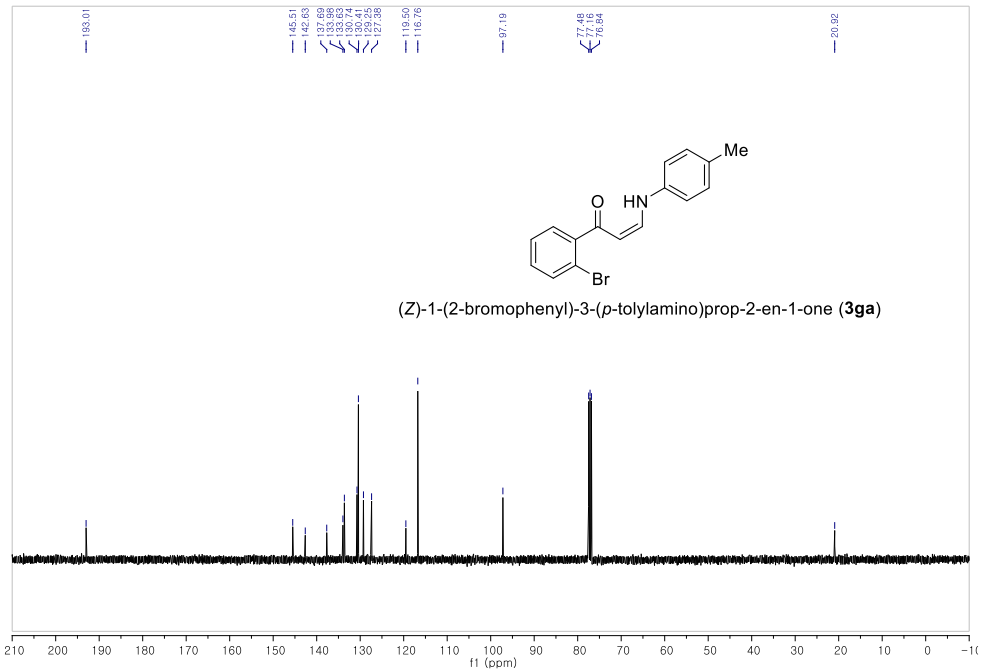

^{13}C NMR ($CDCl_3$, 101 MHz)

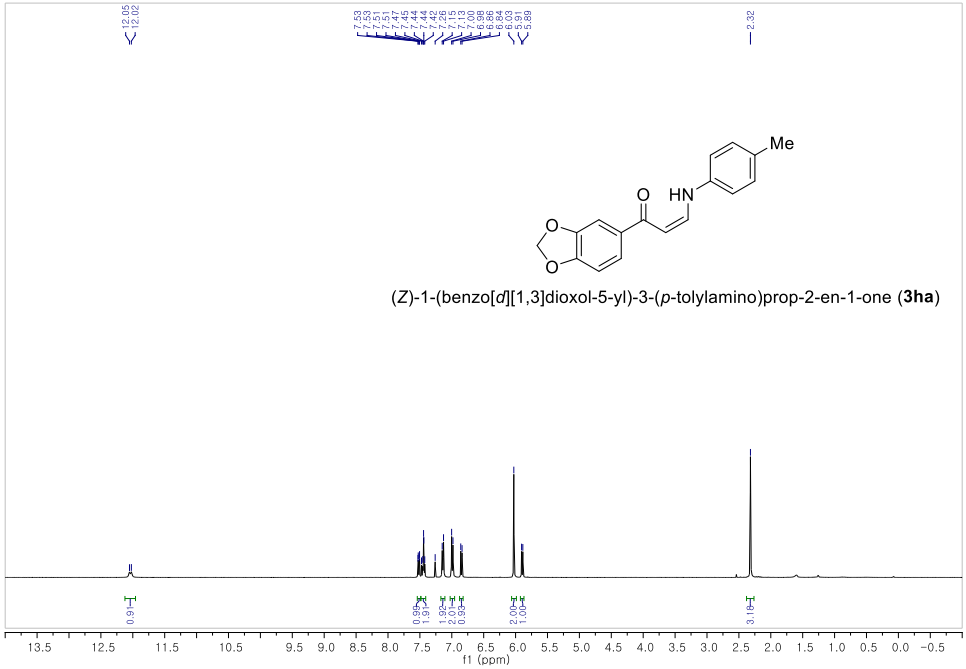

(*Z*)-1-(benzo[*d*][1,3]dioxol-5-yl)-3-(*p*-tolylamino)prop-2-en-1-one (**3ha**)

^{1}H NMR ($CDCl_3$, 400 MHz)

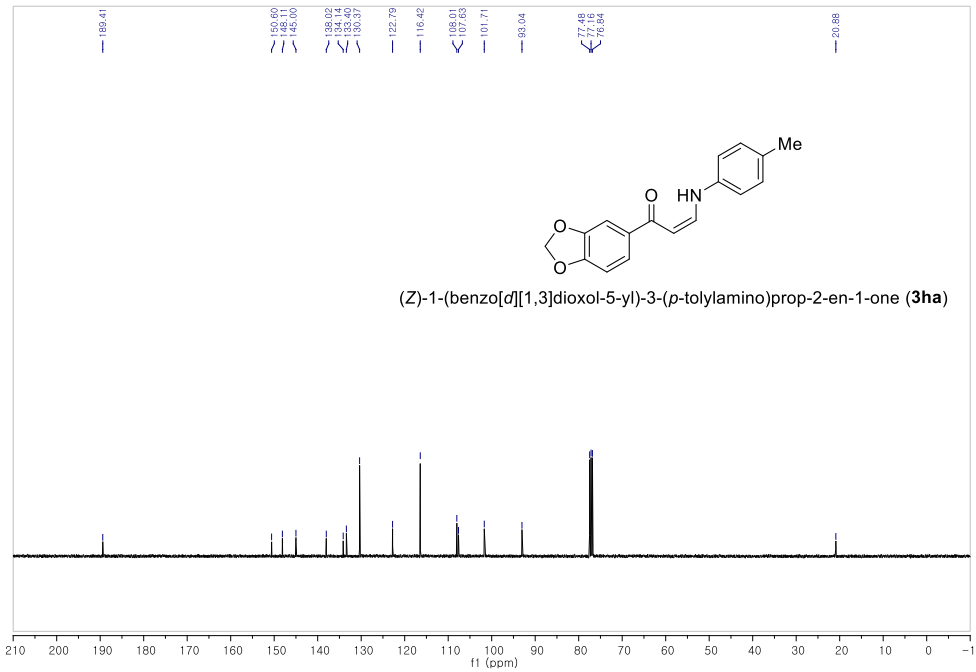

(*Z*)-1-(benzo[*d*][1,3]dioxol-5-yl)-3-(*p*-tolylamino)prop-2-en-1-one (**3ha**)

^{13}C NMR ($CDCl_3$, 101 MHz)

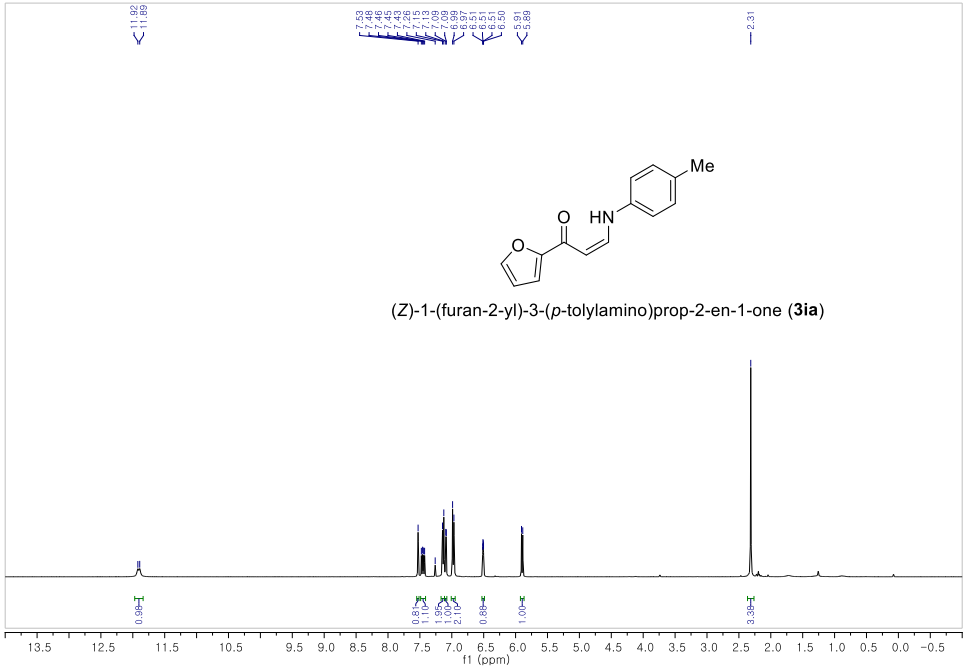

^{1}H NMR ($CDCl_3$, 400 MHz)

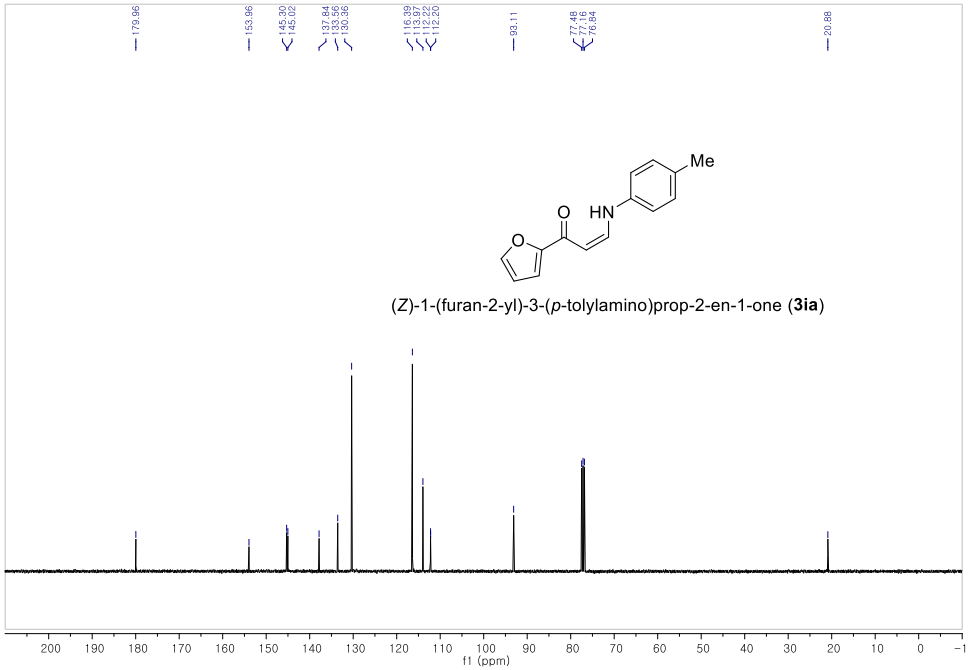

^{13}C NMR ($CDCl_3$, 101 MHz)

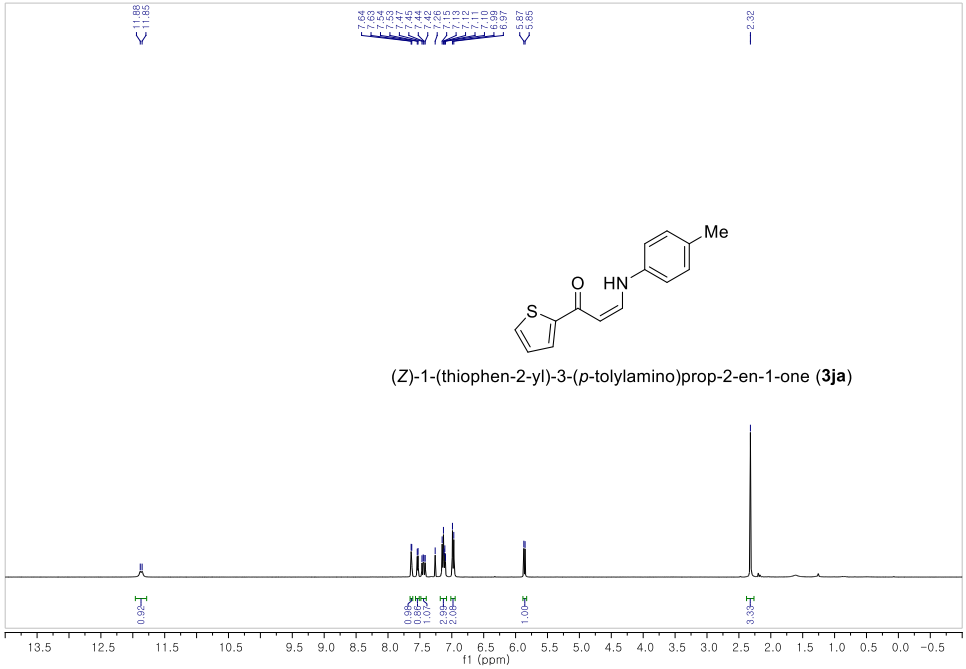

(*Z*)-1-(thiophen-2-yl)-3-(*p*-tolylamino)prop-2-en-1-one (**3ja**)

^{1}H NMR ($CDCl_3$, 400 MHz)

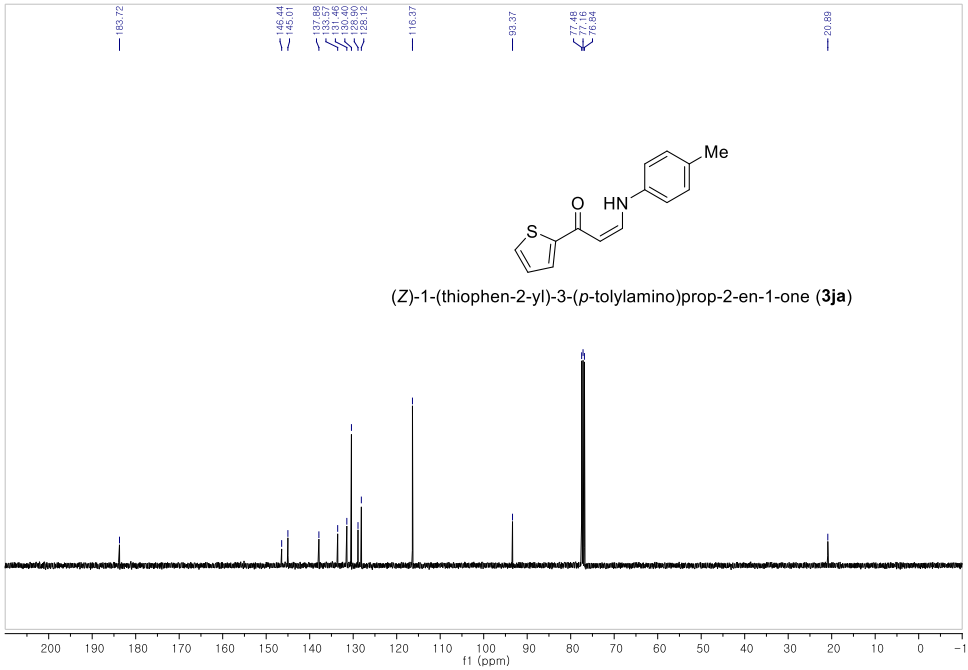

(*Z*)-1-(thiophen-2-yl)-3-(*p*-tolylamino)prop-2-en-1-one (**3ja**)

^{13}C NMR ($CDCl_3$, 101 MHz)

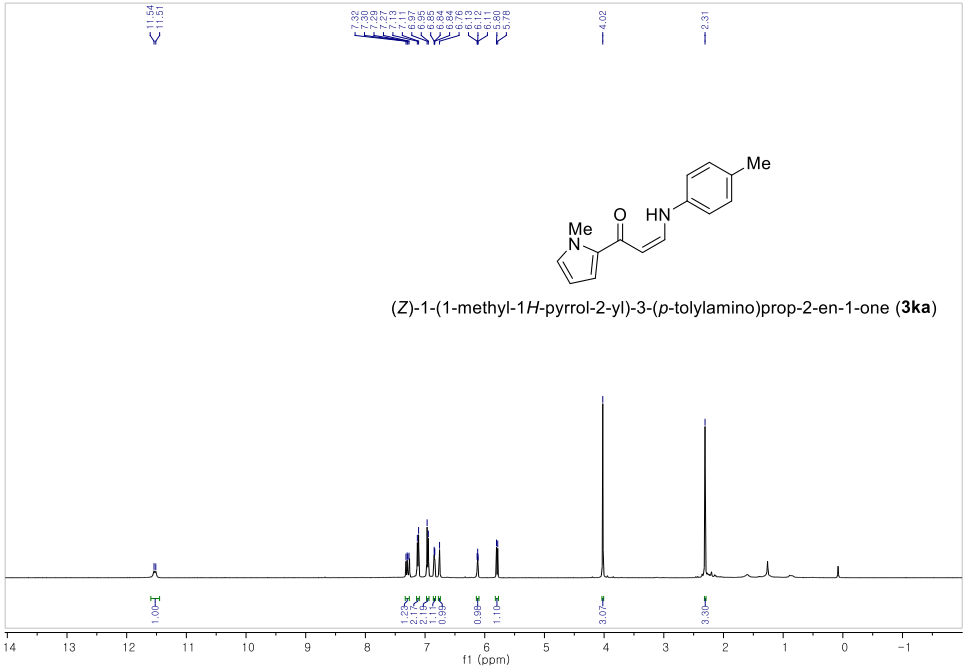

(*Z*)-1-(1-methyl-1*H*-pyrrol-2-yl)-3-(*p*-tolylamino)prop-2-en-1-one (**3ka**)

^{1}H NMR ($CDCl_3$, 400 MHz)

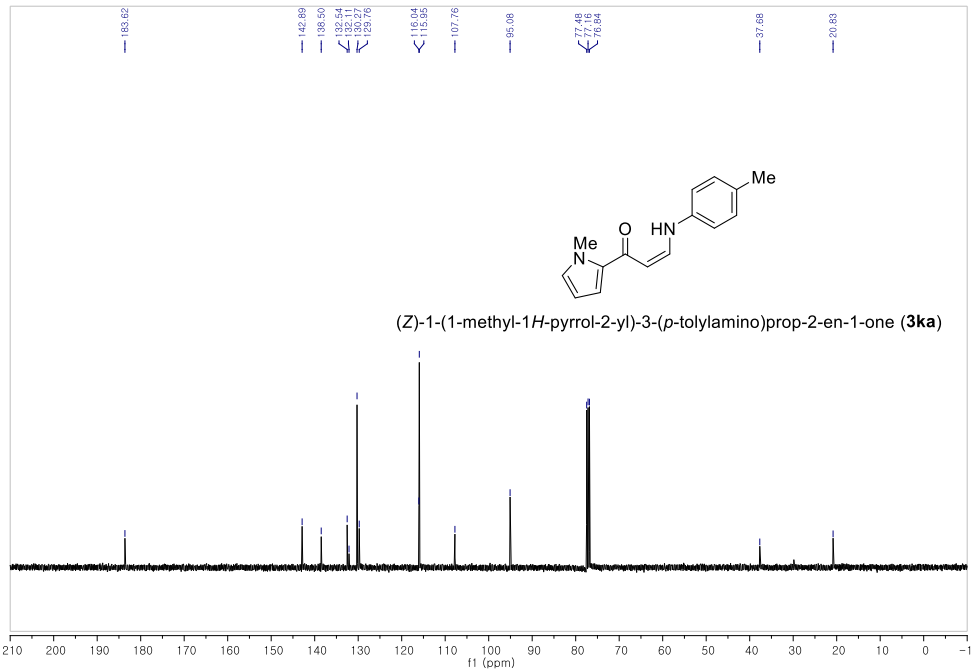

(*Z*)-1-(1-methyl-1*H*-pyrrol-2-yl)-3-(*p*-tolylamino)prop-2-en-1-one (**3ka**)

^{13}C NMR ($CDCl_3$, 101 MHz)

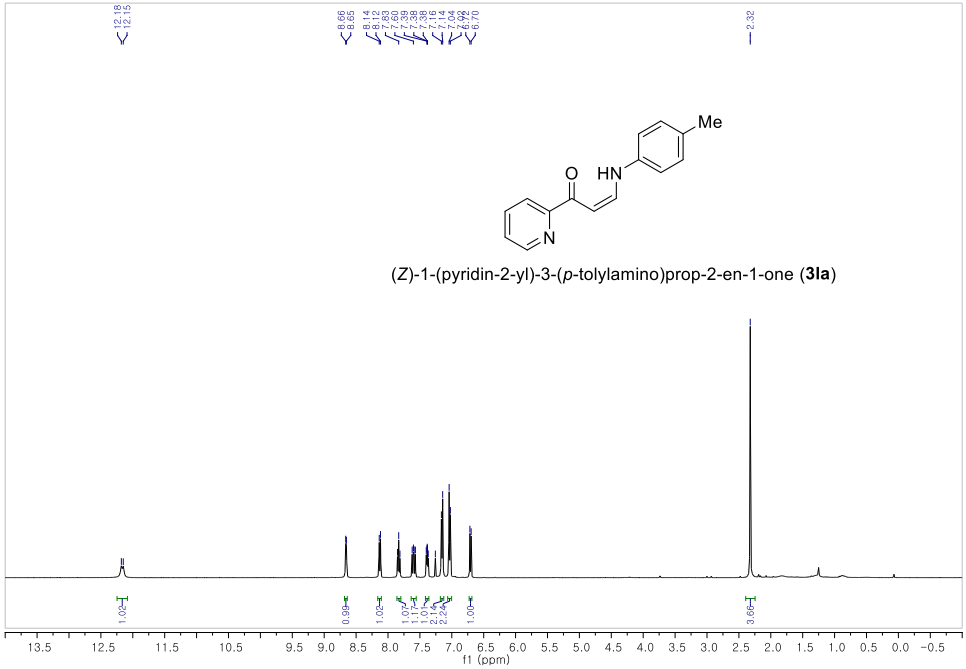

(*Z*)-1-(pyridin-2-yl)-3-(*p*-tolylamino)prop-2-en-1-one (**3la**)

^{1}H NMR ($CDCl_3$, 400 MHz)

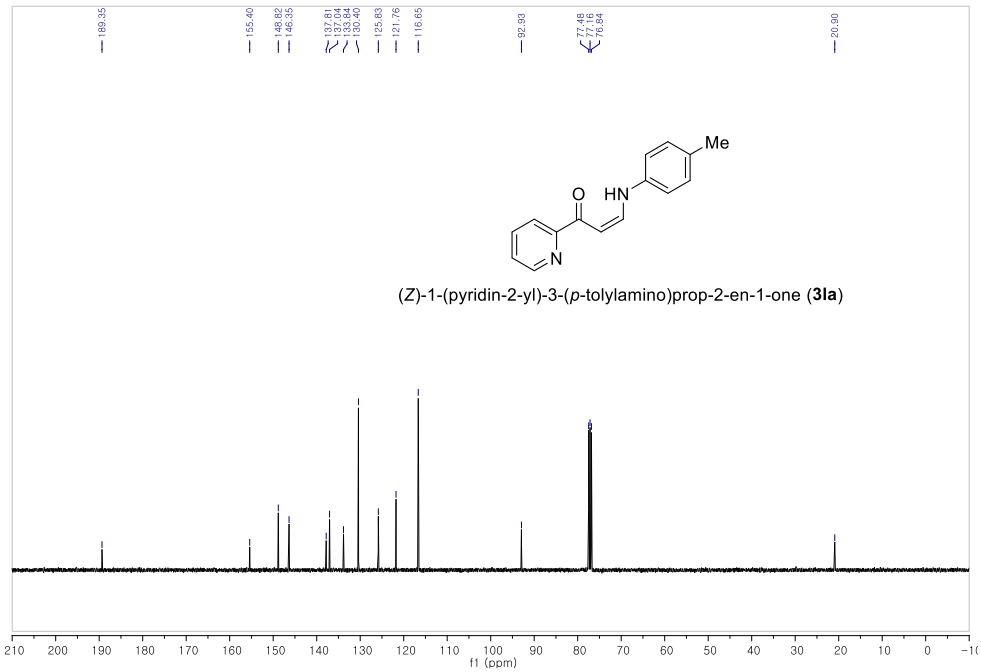

(*Z*)-1-(pyridin-2-yl)-3-(*p*-tolylamino)prop-2-en-1-one (**3la**)

^{13}C NMR ($CDCl_3$, 101 MHz)

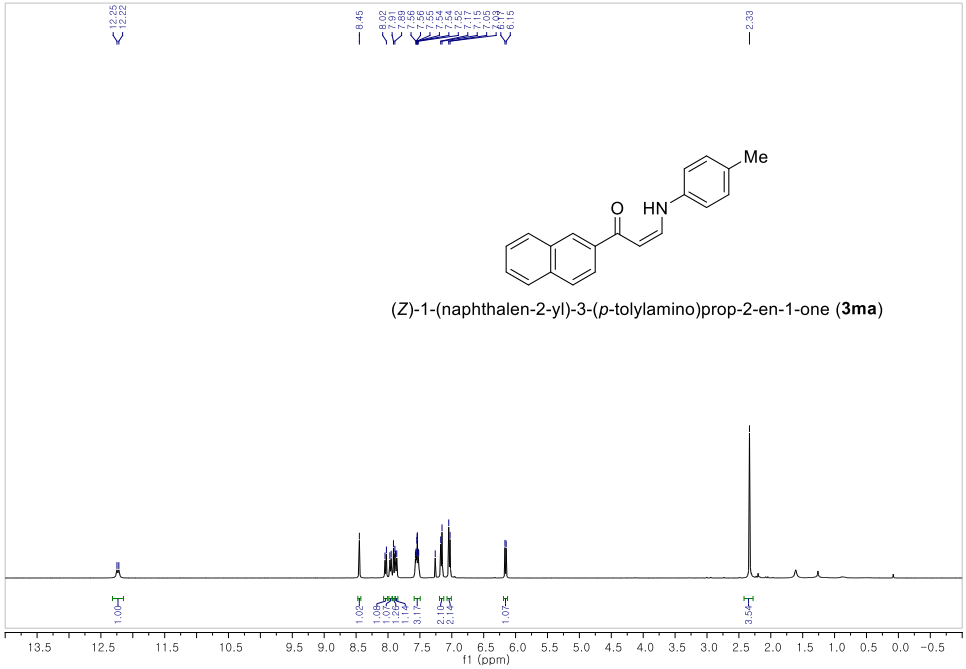

(*Z*)-1-(naphthalen-2-yl)-3-(*p*-tolylamino)prop-2-en-1-one (**3ma**)

^{1}H NMR ($CDCl_3$, 400 MHz)

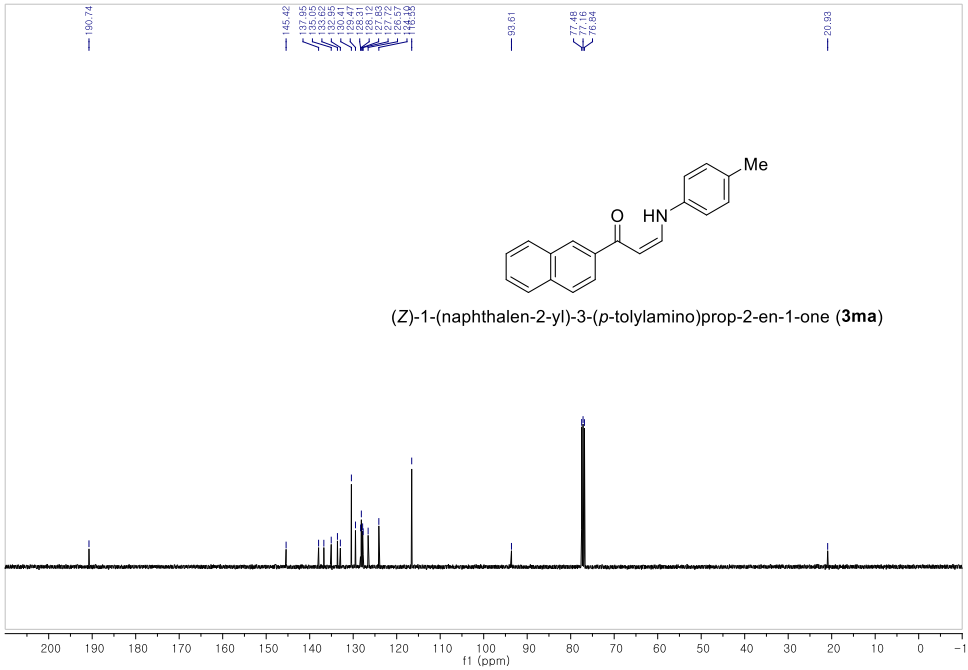

(*Z*)-1-(naphthalen-2-yl)-3-(*p*-tolylamino)prop-2-en-1-one (**3ma**)

^{13}C NMR ($CDCl_3$, 101 MHz)

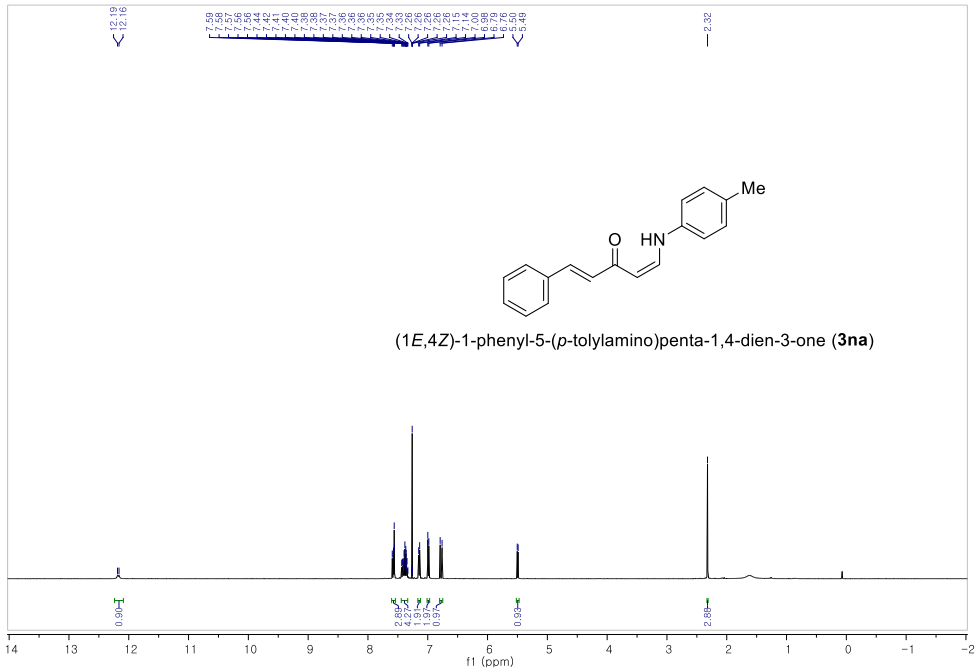

^{1}H NMR ($CDCl_3$, 499 MHz)

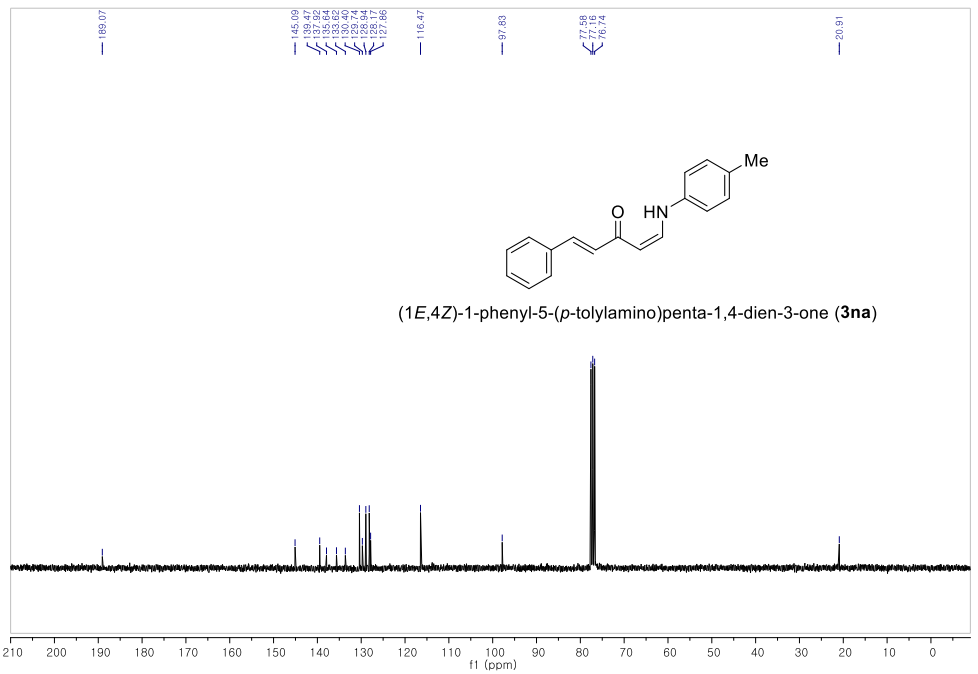

^{13}C NMR ($CDCl_3$, 75 MHz)

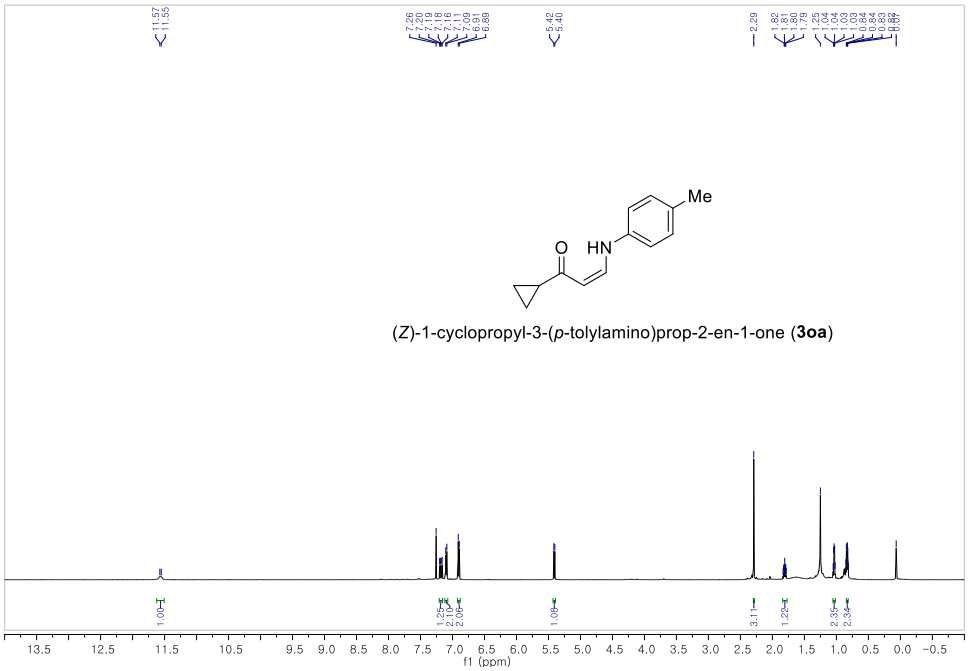

(*Z*)-1-cyclopropyl-3-(*p*-tolylamino)prop-2-en-1-one (**3oa**)

^{1}H NMR ($CDCl_3$, 499 MHz)

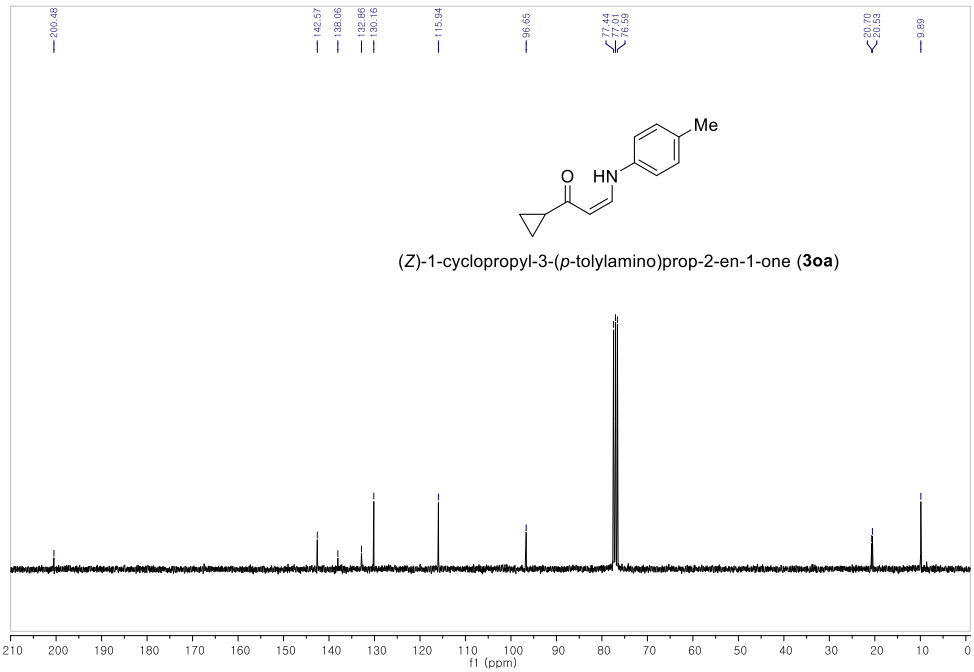

(*Z*)-1-cyclopropyl-3-(*p*-tolylamino)prop-2-en-1-one (**3oa**)

^{13}C NMR ($CDCl_3$, 75 MHz)

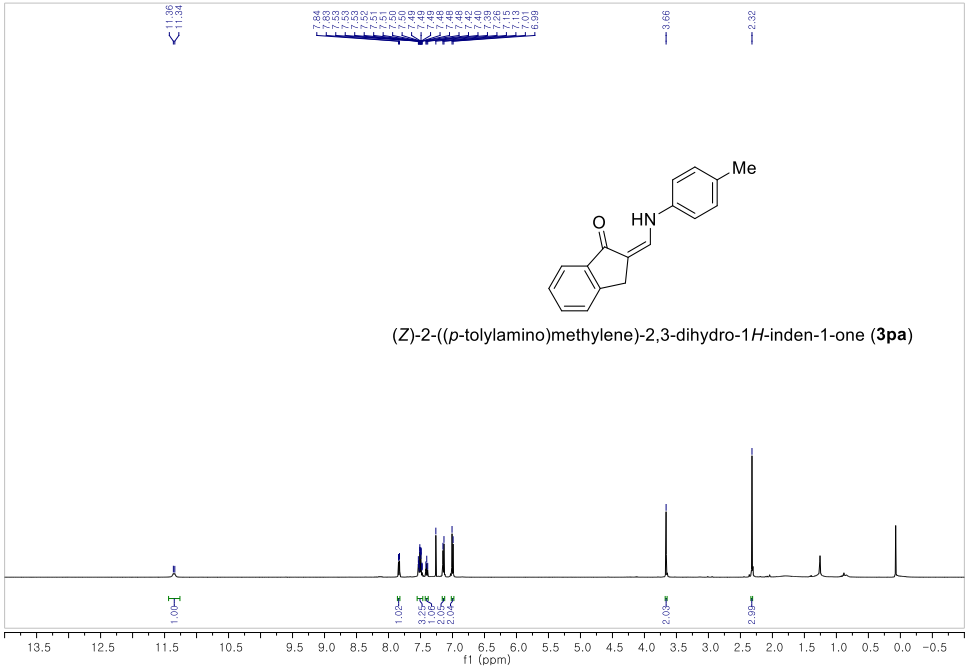

^{1}H NMR ($CDCl_3$, 499 MHz)

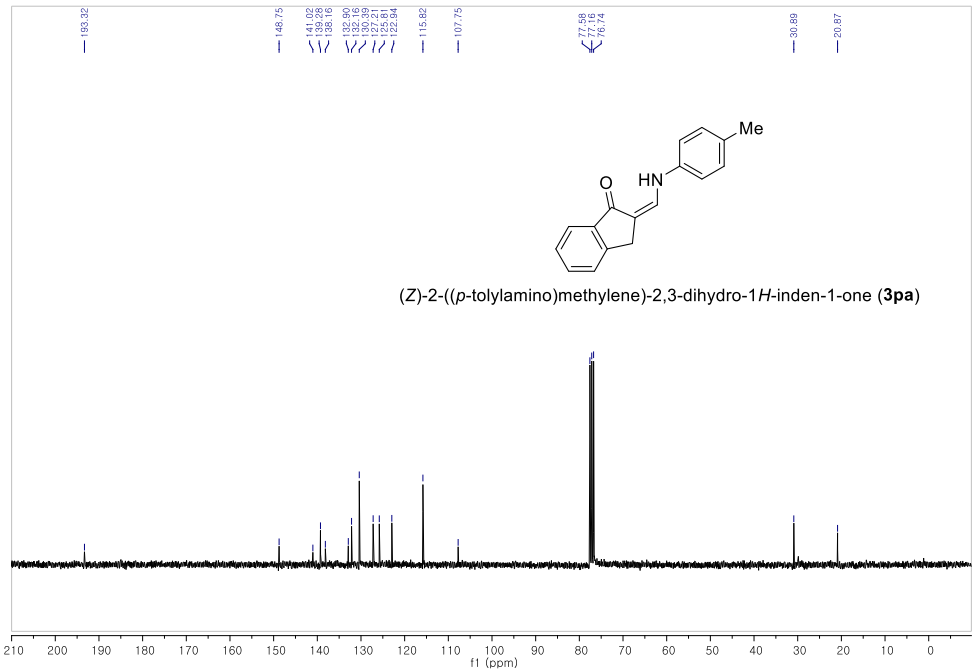

^{13}C NMR ($CDCl_3$, 75 MHz)

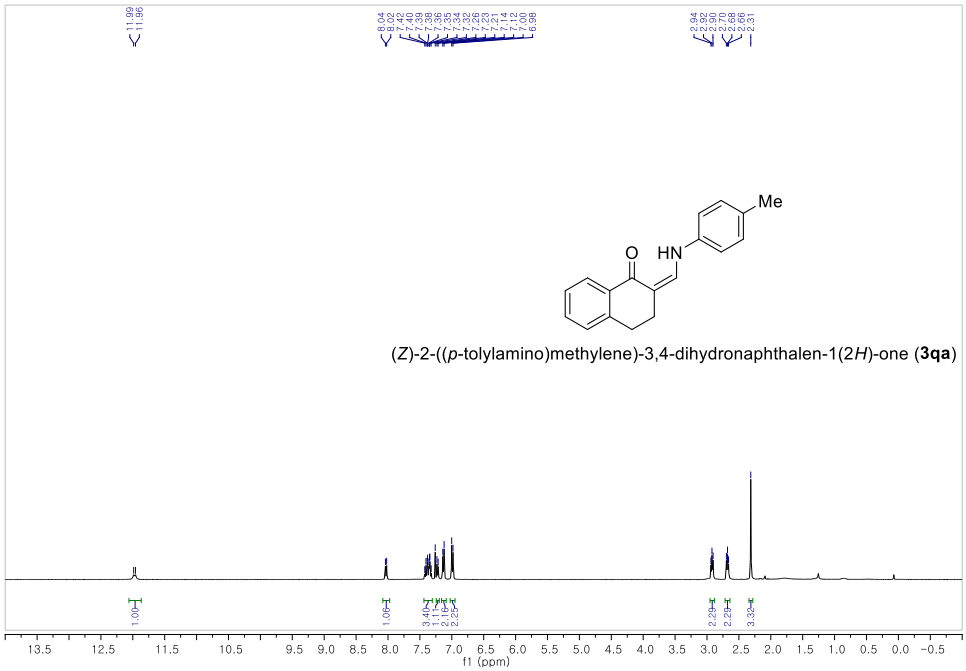

^{1}H NMR ($CDCl_3$, 400 MHz)

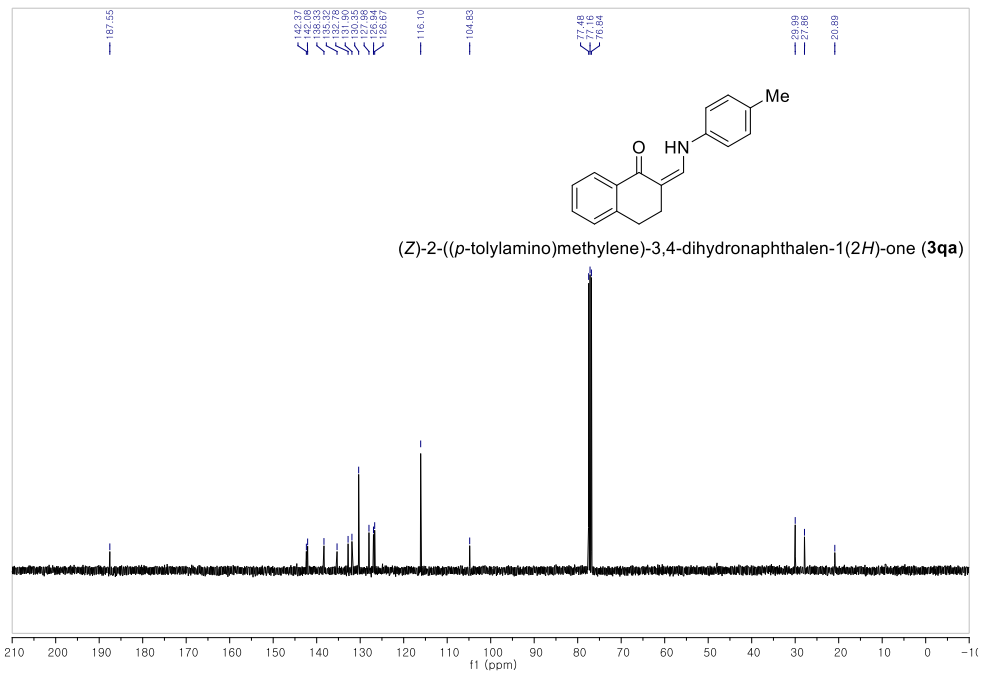

^{13}C NMR ($CDCl_3$, 101 MHz)

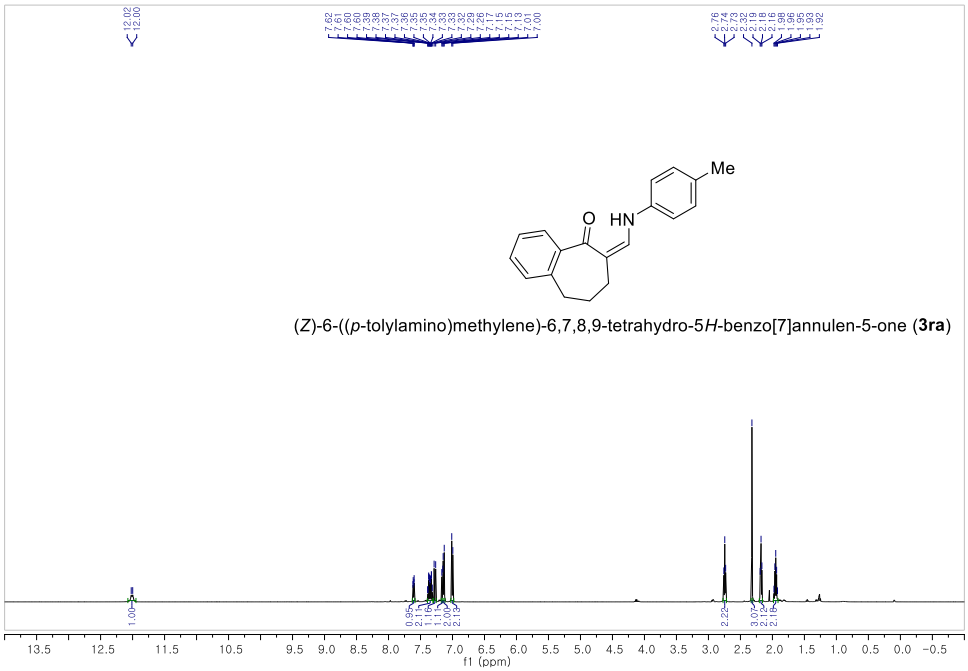

^{1}H NMR ($CDCl_3$, 499 MHz)

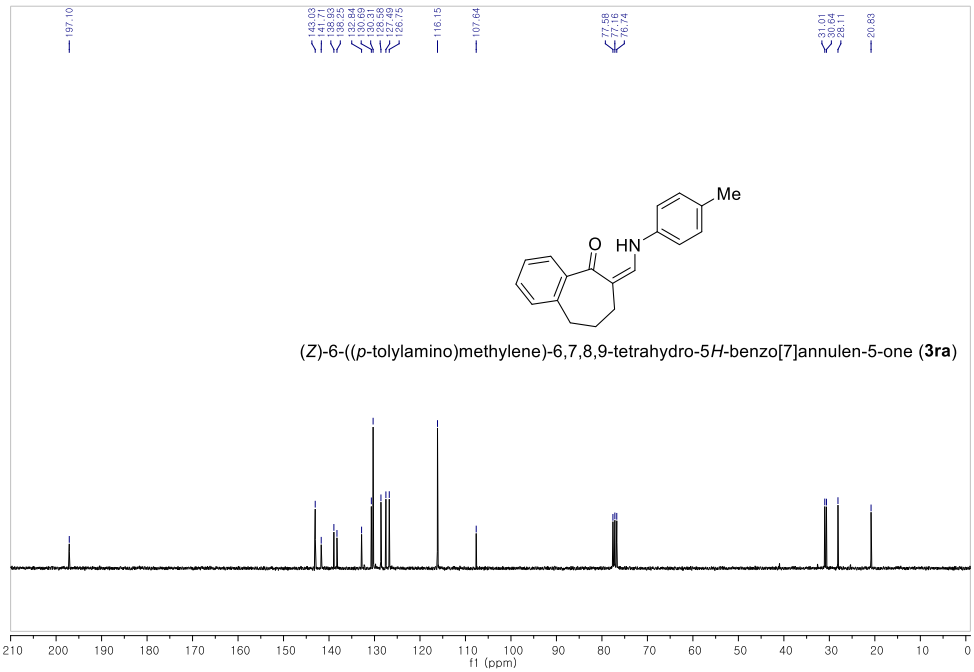

^{13}C NMR ($CDCl_3$, 101 MHz)

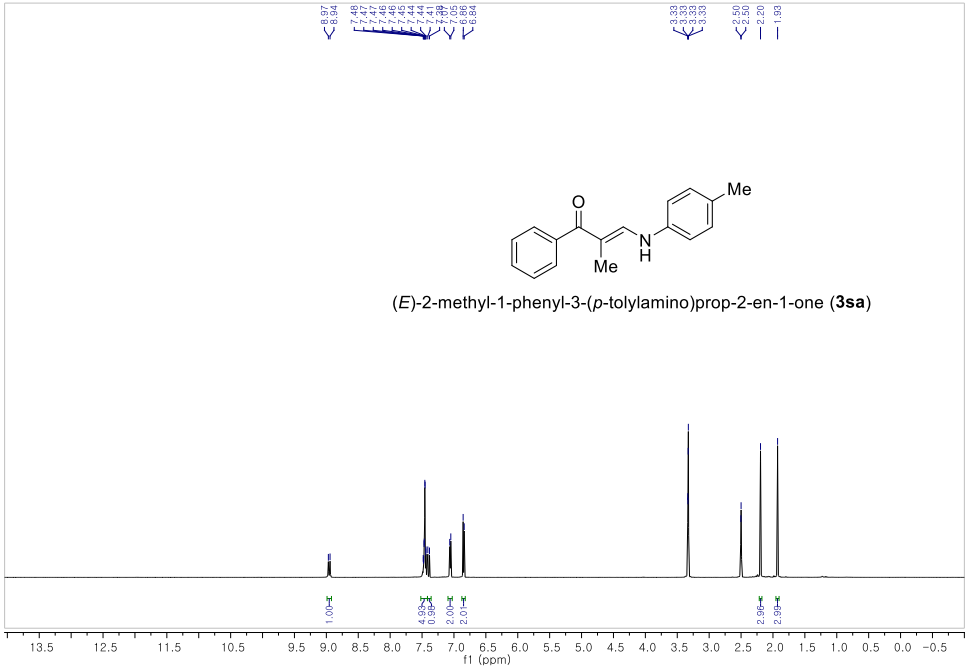

(*E*)-2-methyl-1-phenyl-3-(*p*-tolylamino)prop-2-en-1-one (**3sa**)

^{1}H NMR (DMSO-d_6, 499 MHz)

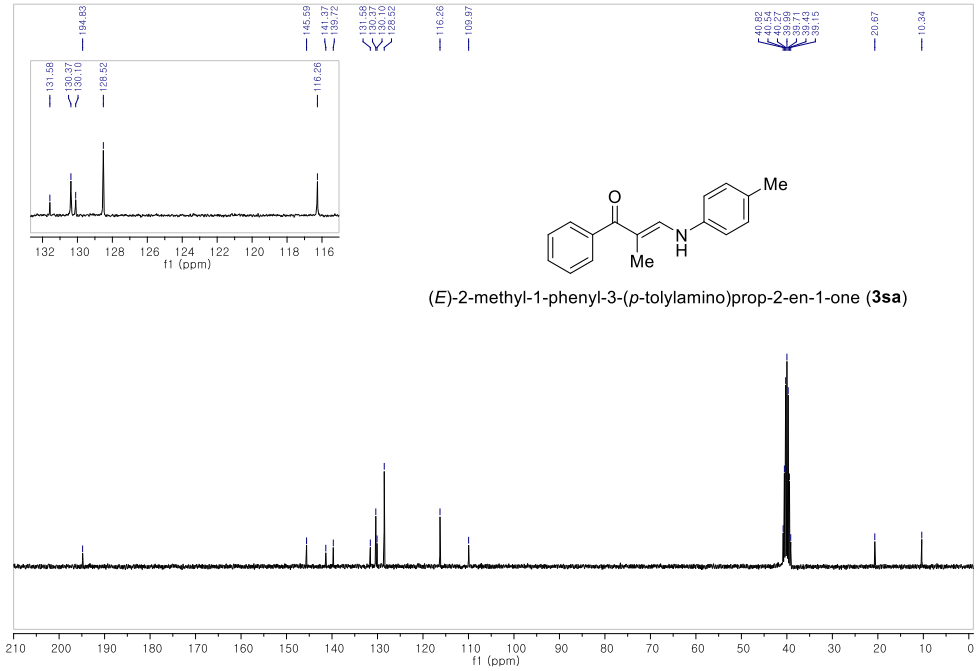

(*E*)-2-methyl-1-phenyl-3-(*p*-tolylamino)prop-2-en-1-one (**3sa**)

^{13}C NMR (DMSO-d_6, 75 MHz)

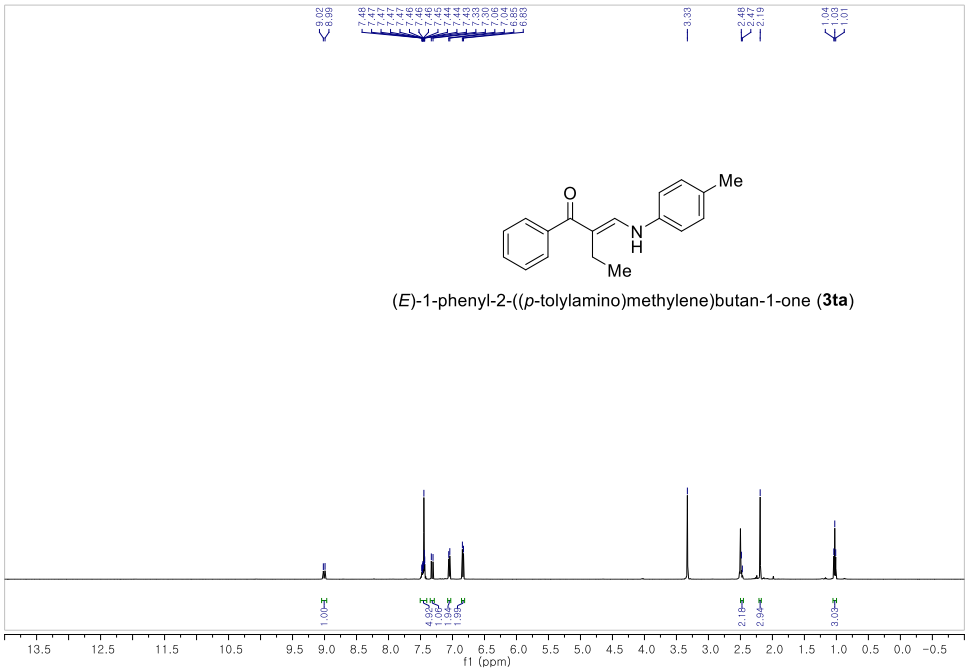

^{1}H NMR (DMSO-d_6, 499 MHz)

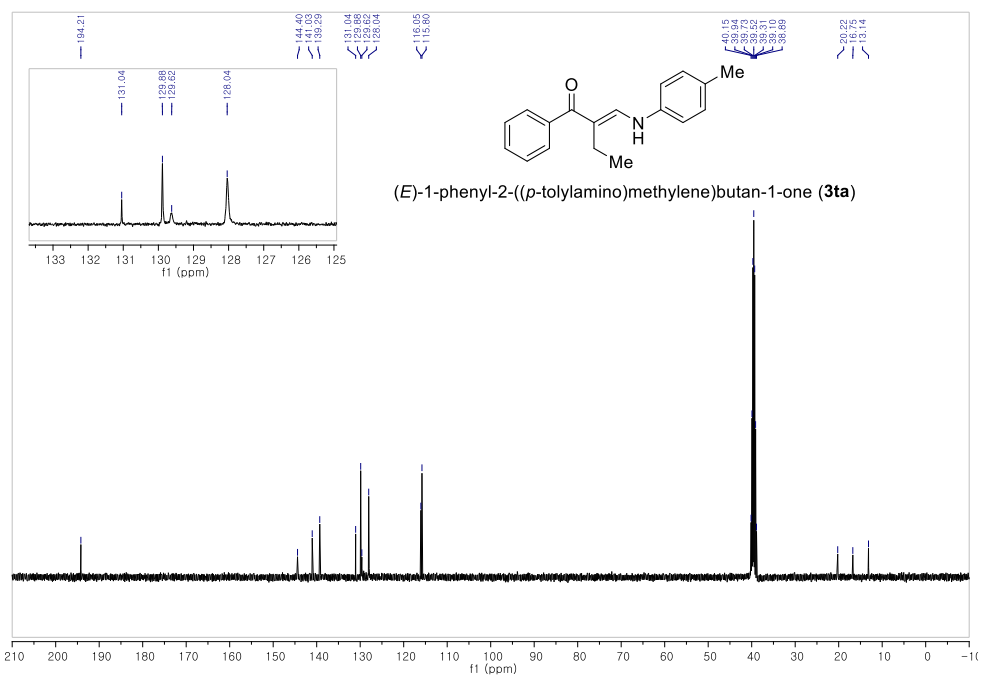

^{13}C NMR (DMSO-d_6, 101 MHz)

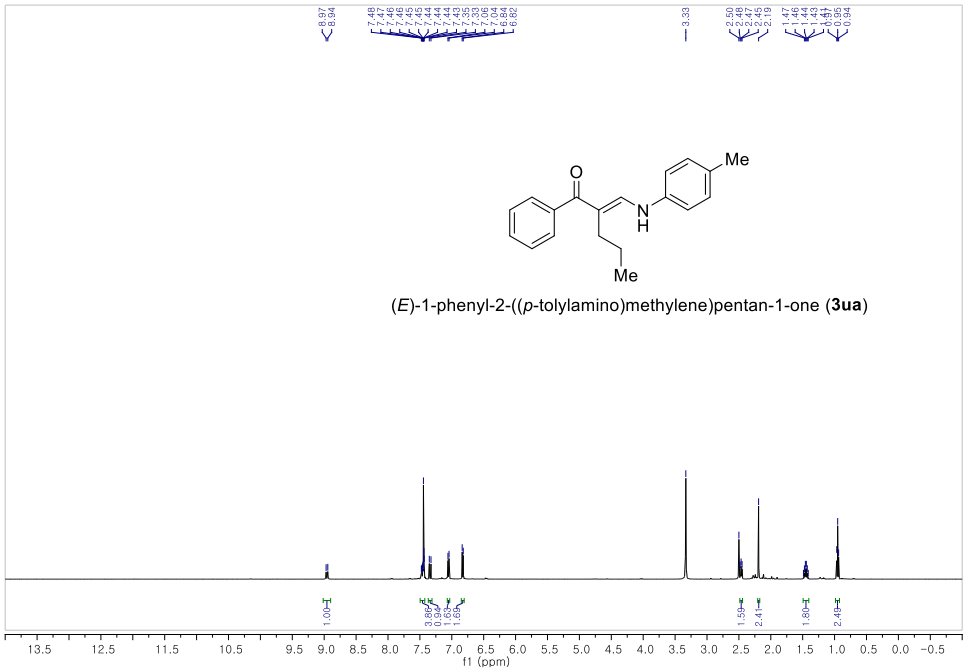

(*E*)-1-phenyl-2-((*p*-tolylamino)methylene)pentan-1-one (**3ua**)

^{1}H NMR (DMSO-d_6, 499 MHz)

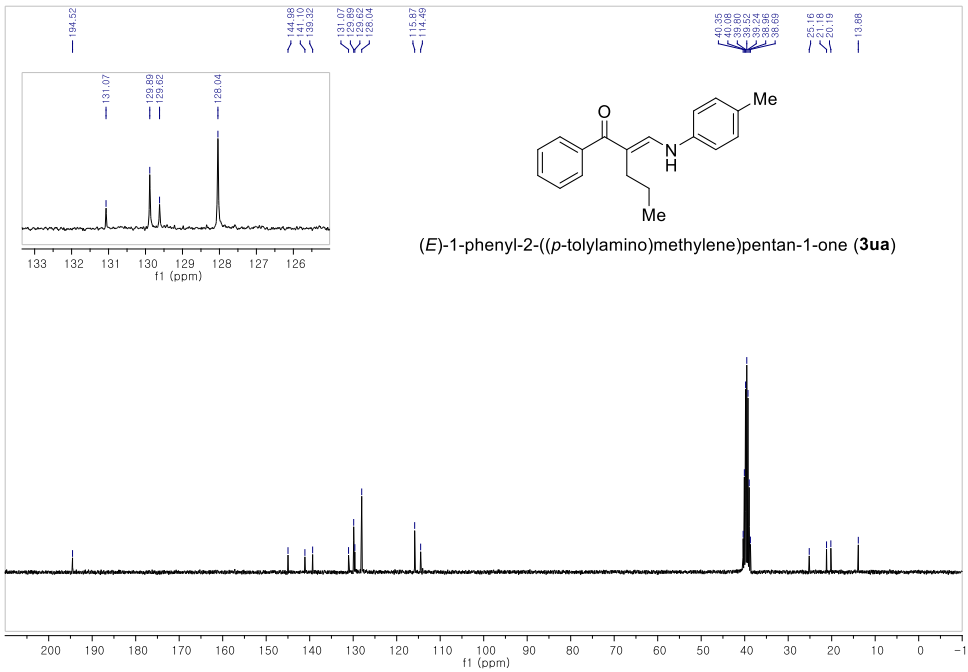

(*E*)-1-phenyl-2-((*p*-tolylamino)methylene)pentan-1-one (**3ua**)

^{13}C NMR (DMSO-d_6, 75 MHz)

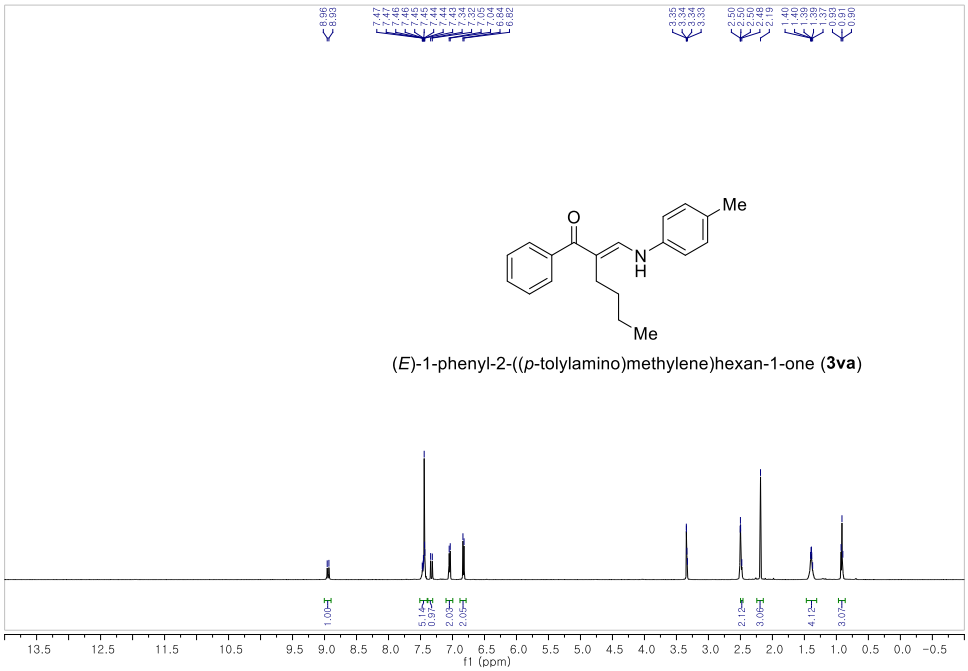

(*E*)-1-phenyl-2-((*p*-tolylamino)methylene)hexan-1-one (**3va**)

^{1}H NMR (DMSO-d_6, 499 MHz)

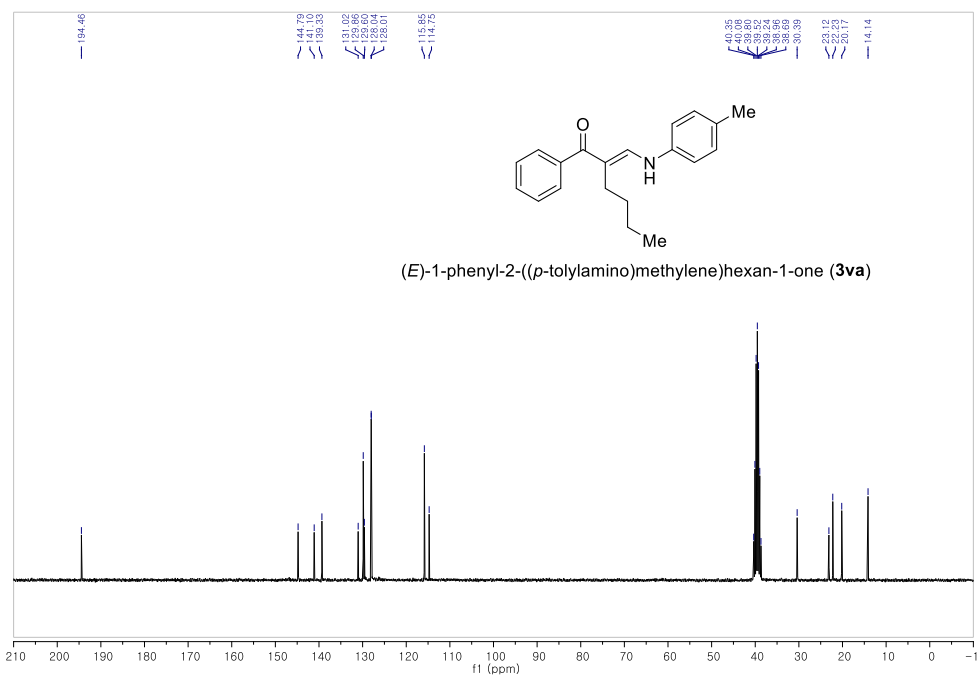

(*E*)-1-phenyl-2-((*p*-tolylamino)methylene)hexan-1-one (**3va**)

^{13}C NMR (DMSO-d_6, 75 MHz)

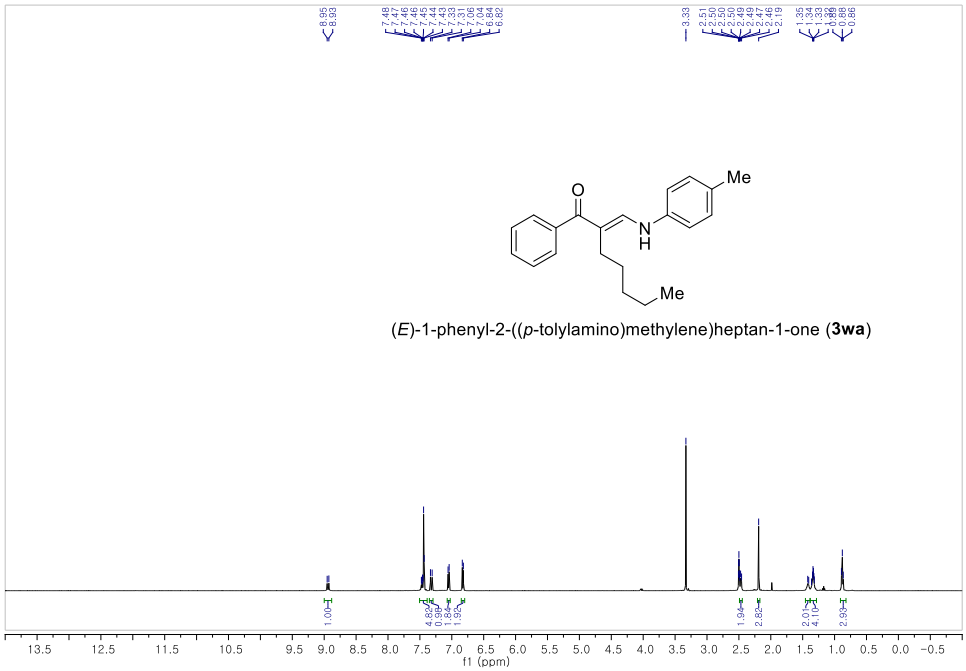

^{1}H NMR (DMSO-d_6, 499 MHz)

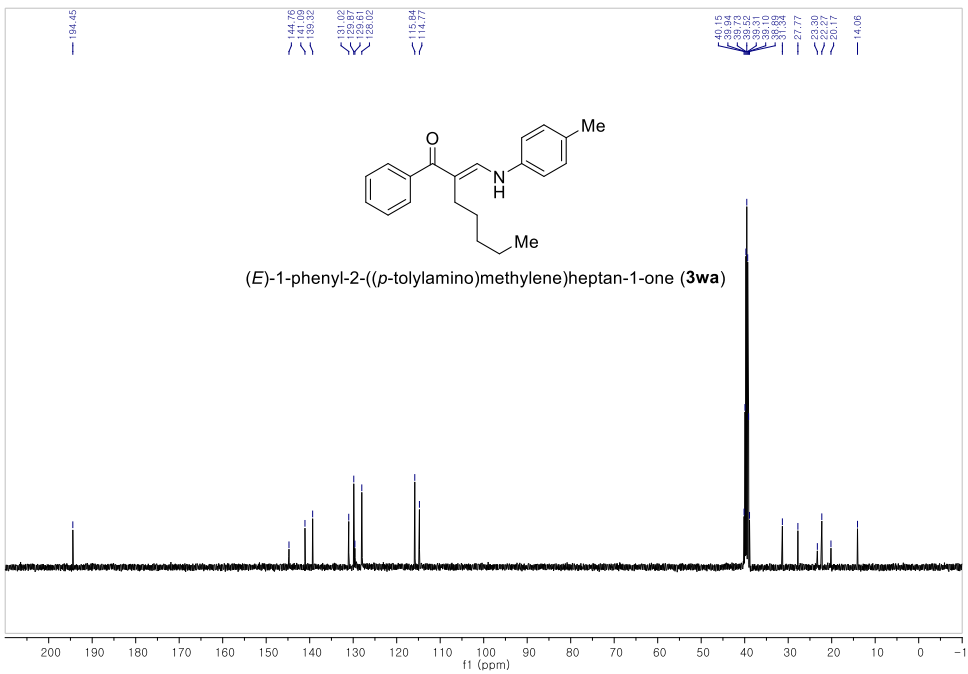

^{13}C NMR (DMSO-d_6, 101 MHz)

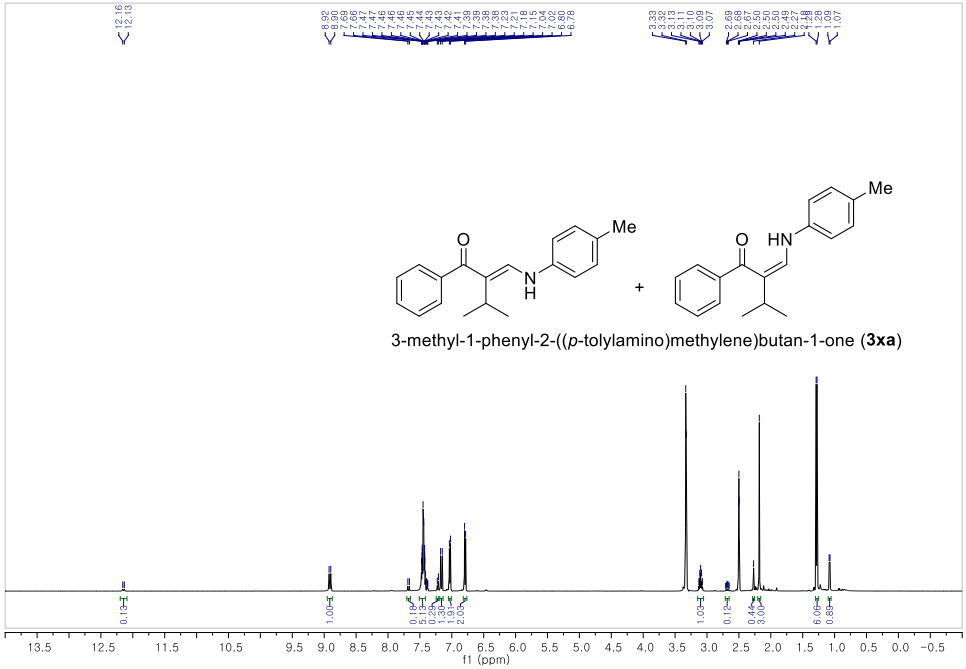

^{1}H NMR (DMSO-d_6, 499 MHz)

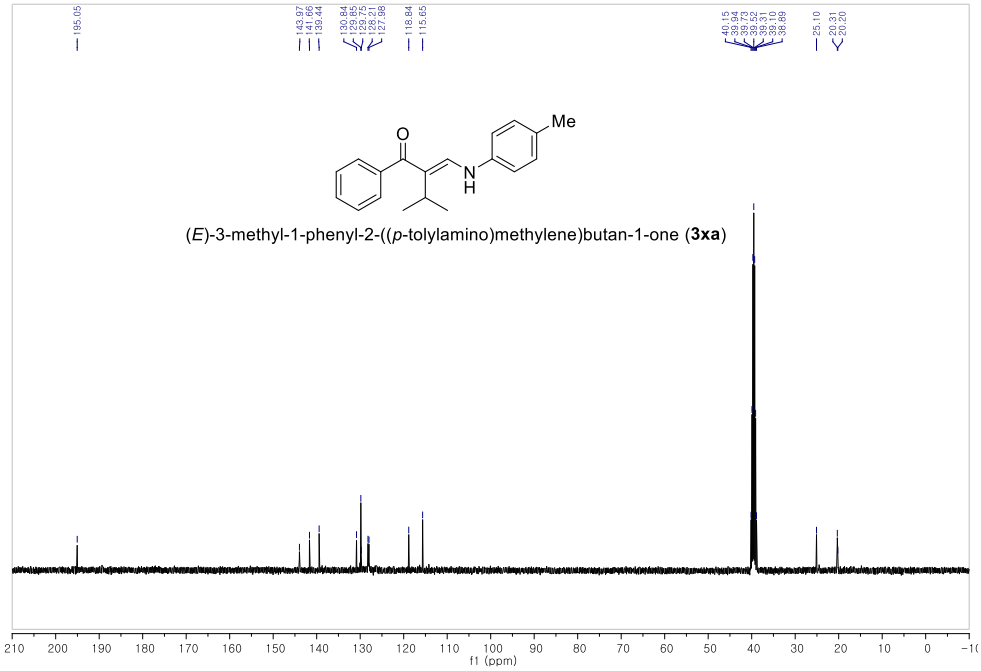

^{13}C NMR (DMSO-d_6, 101 MHz)

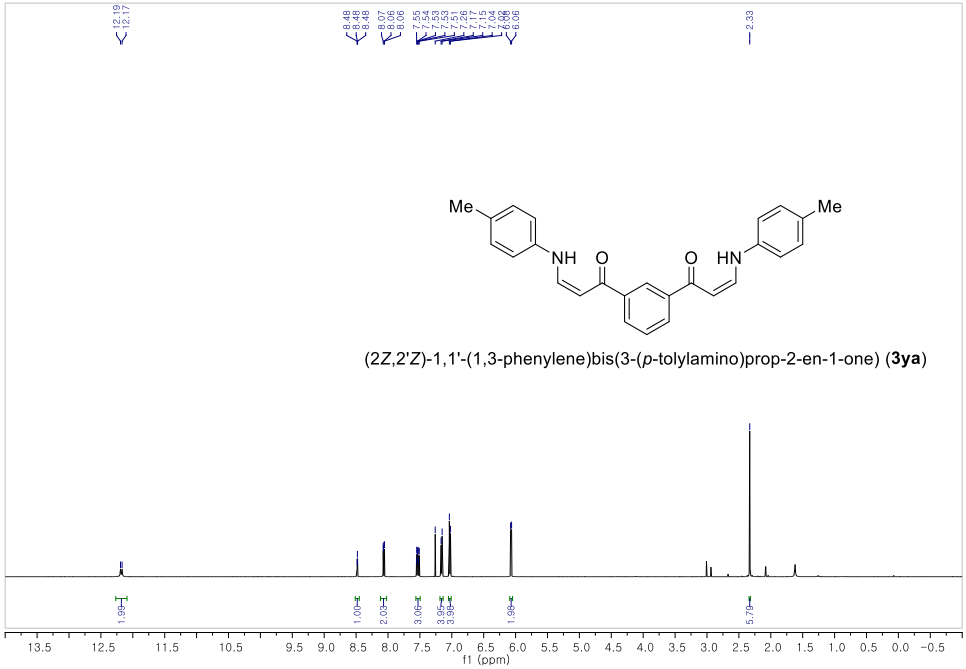

(2*Z*,2'*Z*)-1,1'-(1,3-phenylene)bis(3-(*p*-tolylamino)prop-2-en-1-one) (**3ya**)

^{1}H NMR ($CDCl_3$, 499 MHz)

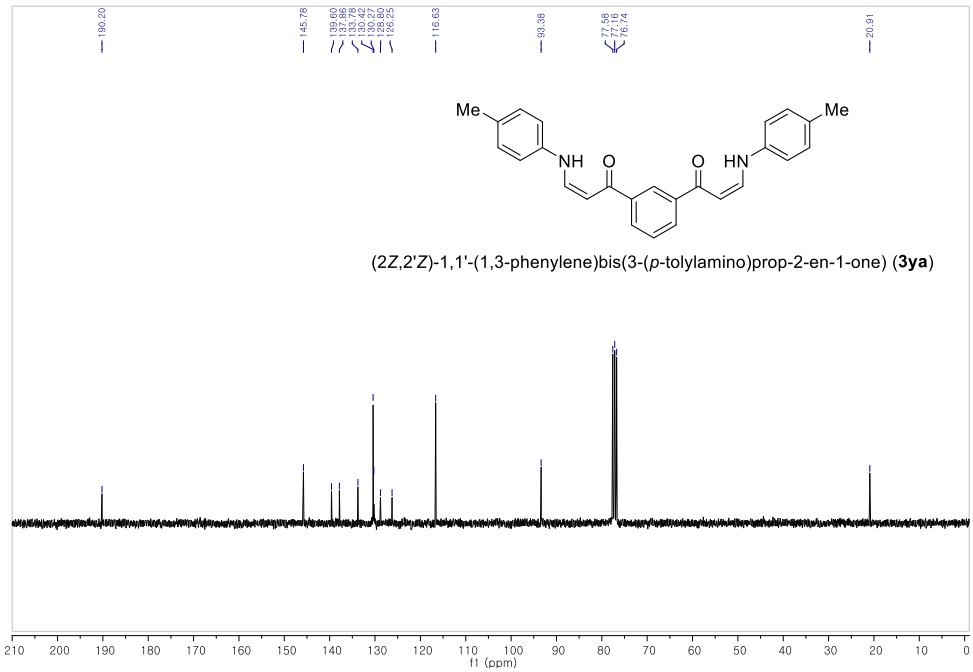

(2*Z*,2'*Z*)-1,1'-(1,3-phenylene)bis(3-(*p*-tolylamino)prop-2-en-1-one) (**3ya**)

^{13}C NMR ($CDCl_3$, 75 MHz)

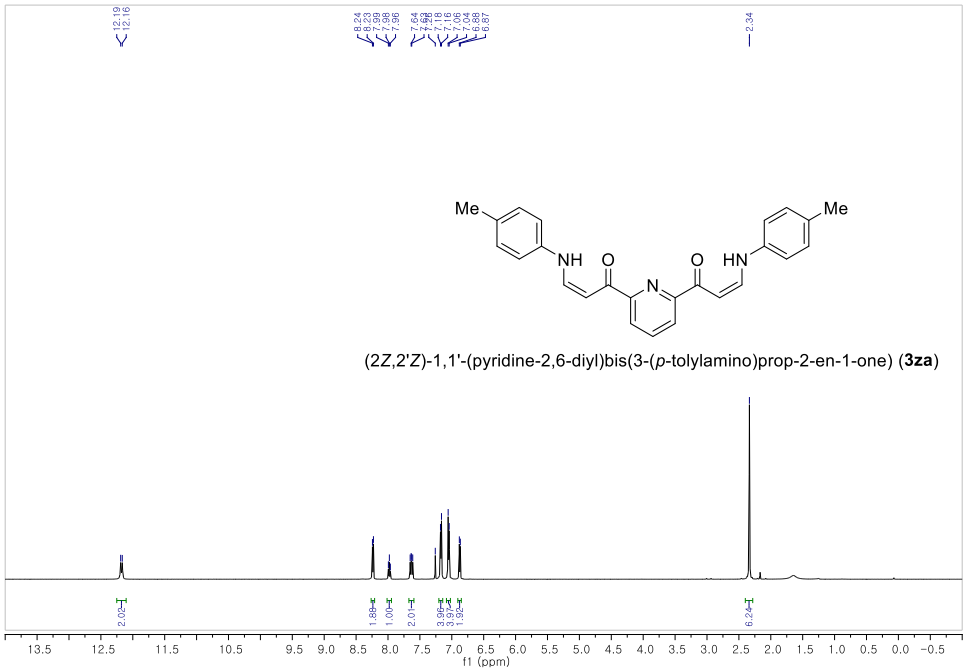

(2*Z*,2'*Z*)-1,1'-(pyridine-2,6-diyl)bis(3-(*p*-tolylamino)prop-2-en-1-one) (**3za**)

^{1}H NMR ($CDCl_3$, 499 MHz)

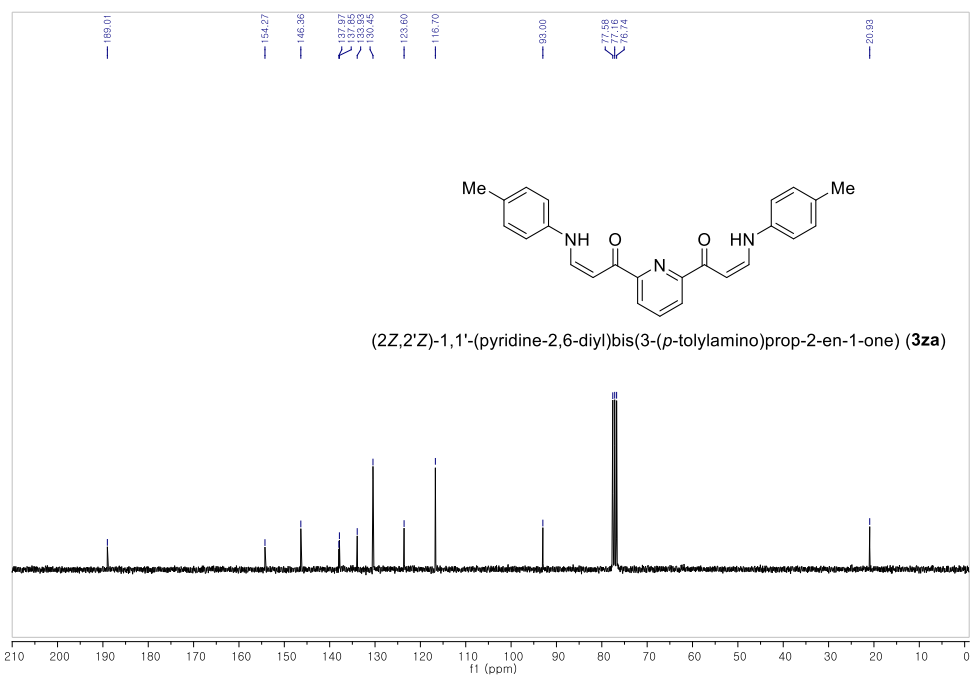

(2*Z*,2'*Z*)-1,1'-(pyridine-2,6-diyl)bis(3-(*p*-tolylamino)prop-2-en-1-one) (**3za**)

^{13}C NMR ($CDCl_3$, 75 MHz)

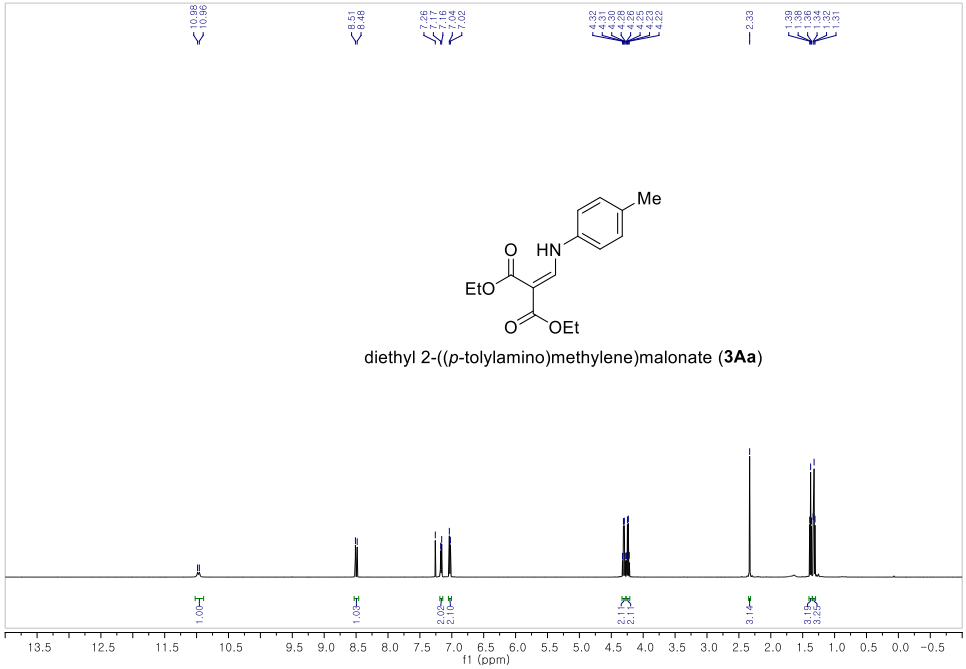

diethyl 2-((*p*-tolylamino)methylene)malonate (**3Aa**)

^{1}H NMR ($CDCl_3$, 499 MHz)

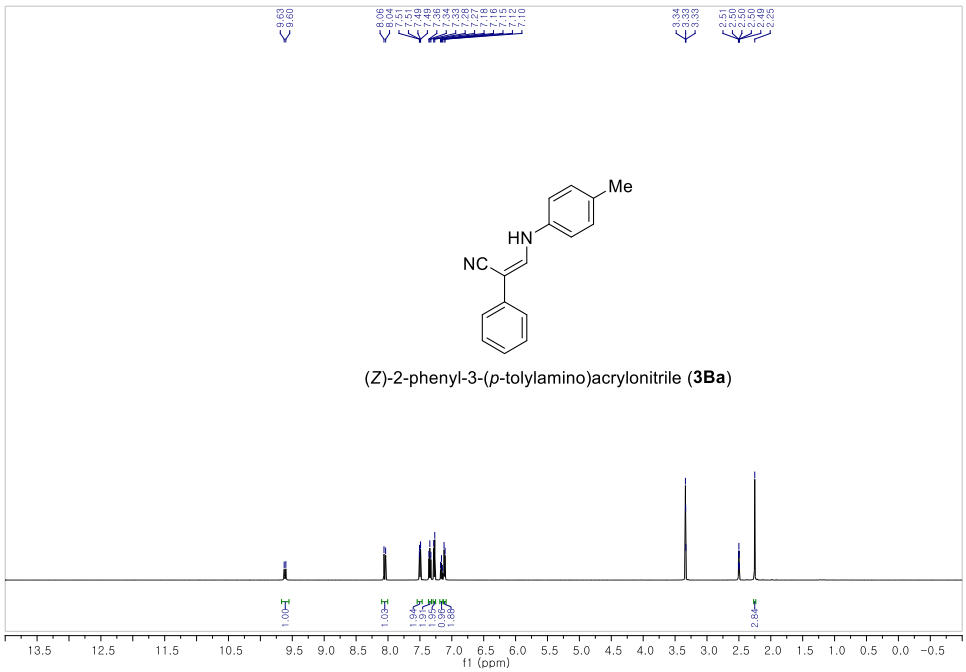

(*Z*)-2-phenyl-3-(*p*-tolylamino)acrylonitrile (**3Ba**)

^{1}H NMR (DMSO-d_6, 499 MHz)

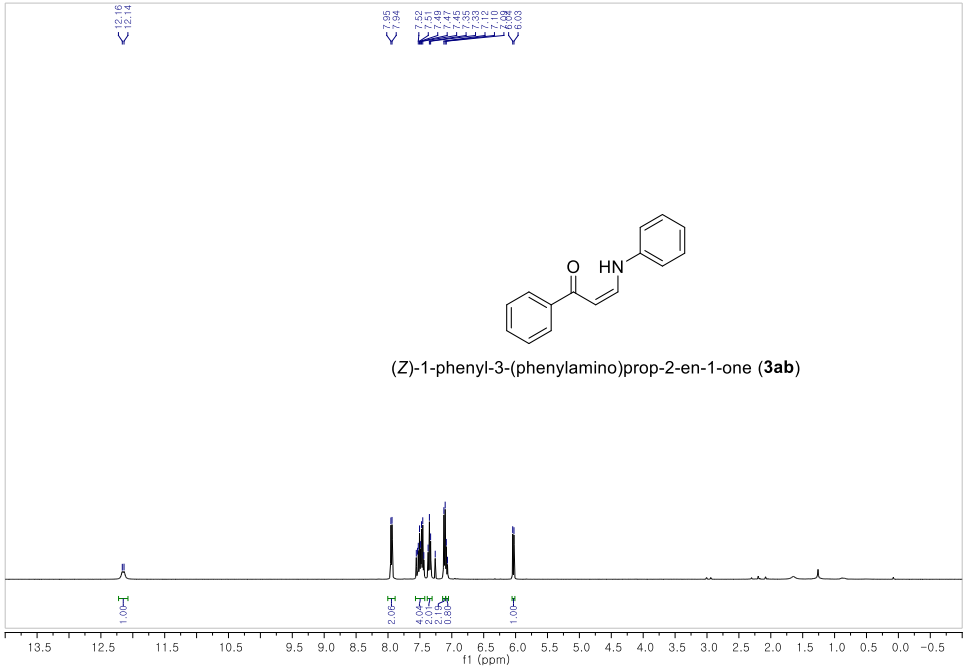

(*Z*)-1-phenyl-3-(phenylamino)prop-2-en-1-one (**3ab**)

^{1}H NMR ($CDCl_3$, 400 MHz)

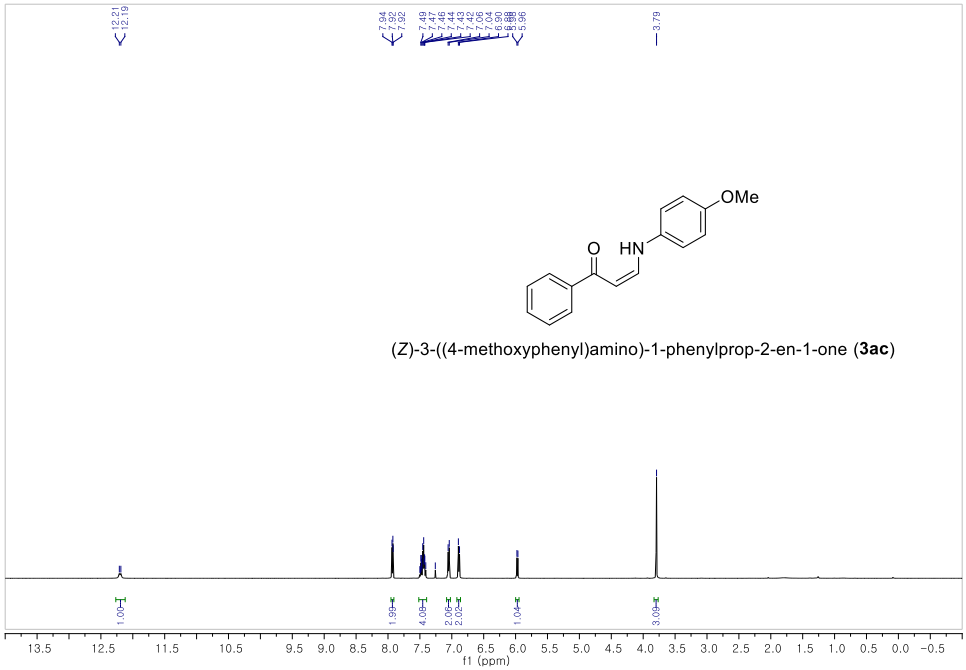

(*Z*)-3-((4-methoxyphenyl)amino)-1-phenylprop-2-en-1-one (**3ac**)

^{1}H NMR ($CDCl_3$, 499 MHz)

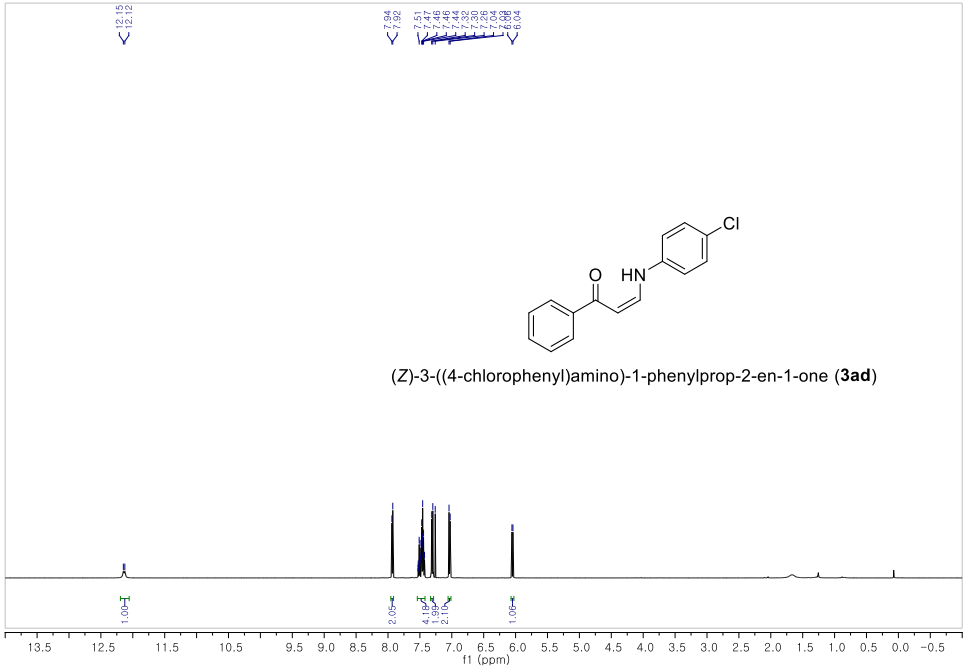

(*Z*)-3-((4-chlorophenyl)amino)-1-phenylprop-2-en-1-one (**3ad**)

^{1}H NMR ($CDCl_3$, 499 MHz)

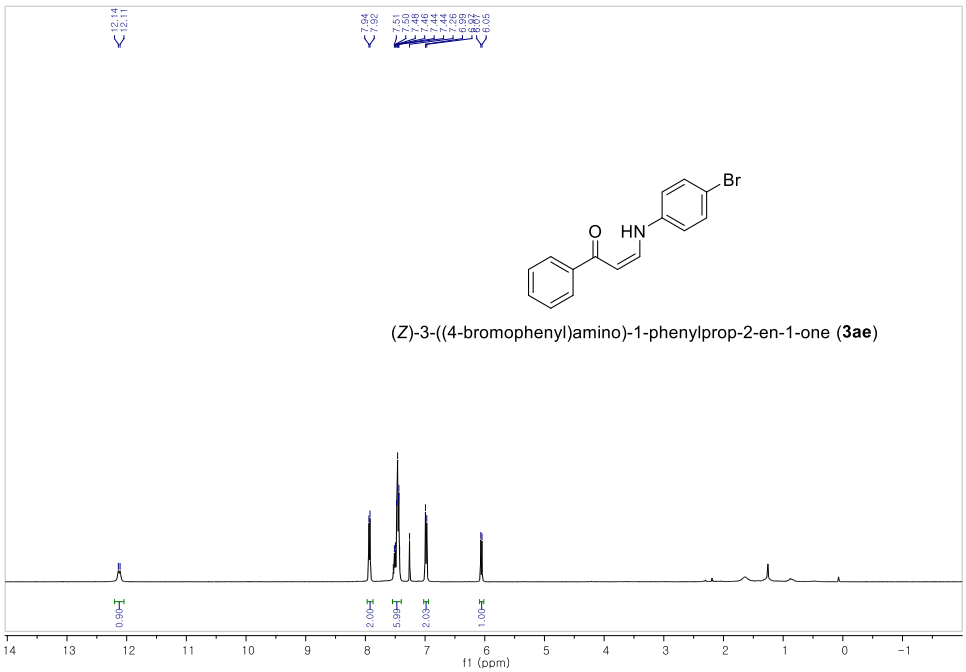

(*Z*)-3-((4-bromophenyl)amino)-1-phenylprop-2-en-1-one (**3ae**)

^{1}H NMR ($CDCl_3$, 400 MHz)

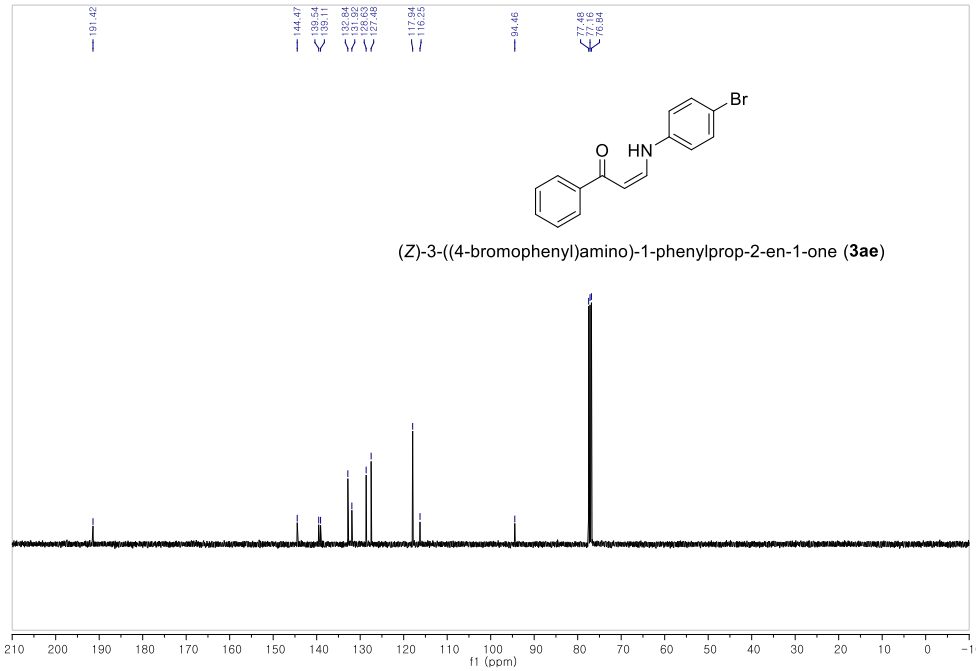

(*Z*)-3-((4-bromophenyl)amino)-1-phenylprop-2-en-1-one (**3ae**)

^{13}C NMR ($CDCl_3$, 101 MHz)

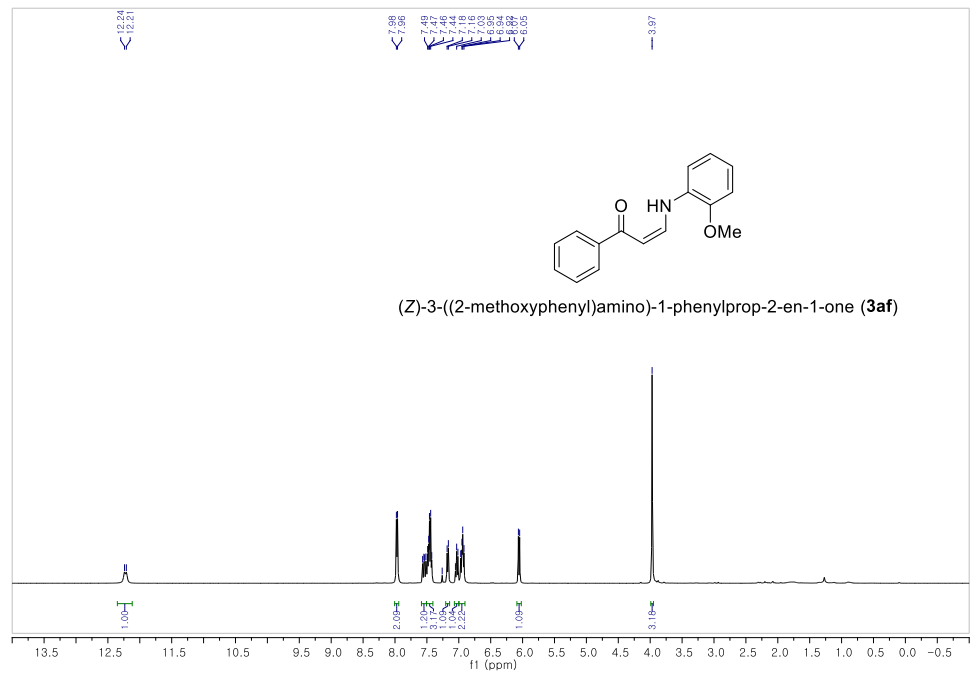

(*Z*)-3-((2-methoxyphenyl)amino)-1-phenylprop-2-en-1-one (**3af**)

^{1}H NMR ($CDCl_3$, 400 MHz)

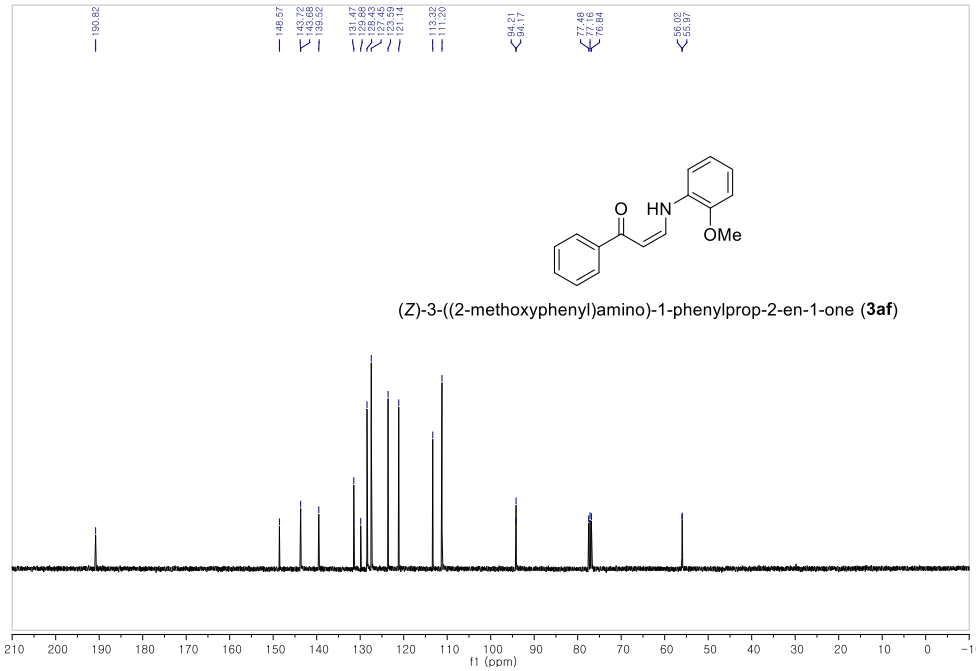

(*Z*)-3-((2-methoxyphenyl)amino)-1-phenylprop-2-en-1-one (**3af**)

^{13}C NMR ($CDCl_3$, 101 MHz)

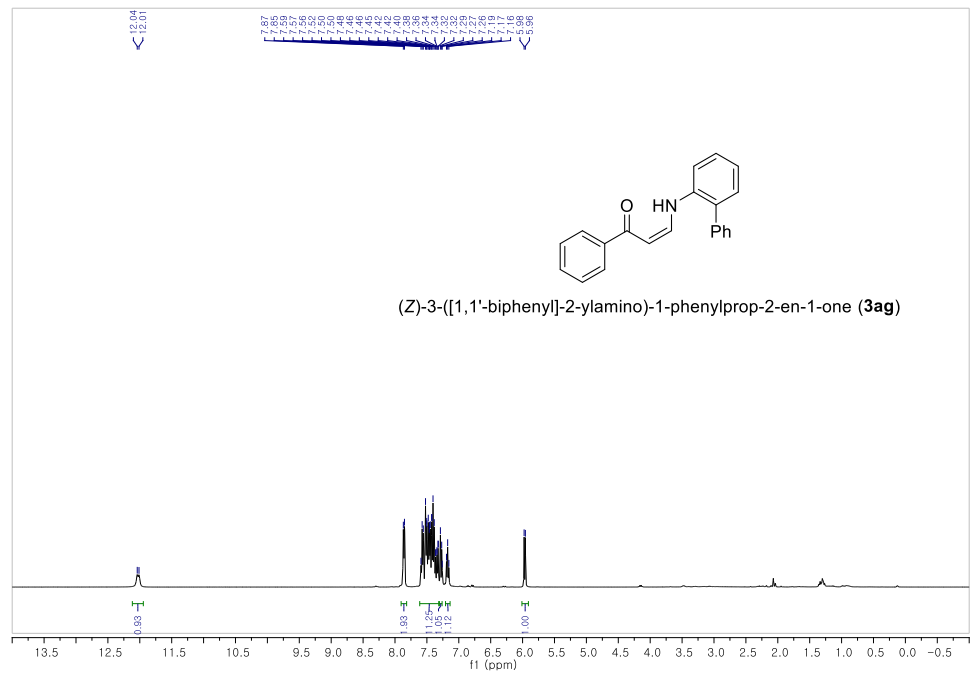

(*Z*)-3-([1,1'-biphenyl]-2-ylamino)-1-phenylprop-2-en-1-one (**3ag**)

^{1}H NMR ($CDCl_3$, 400 MHz)

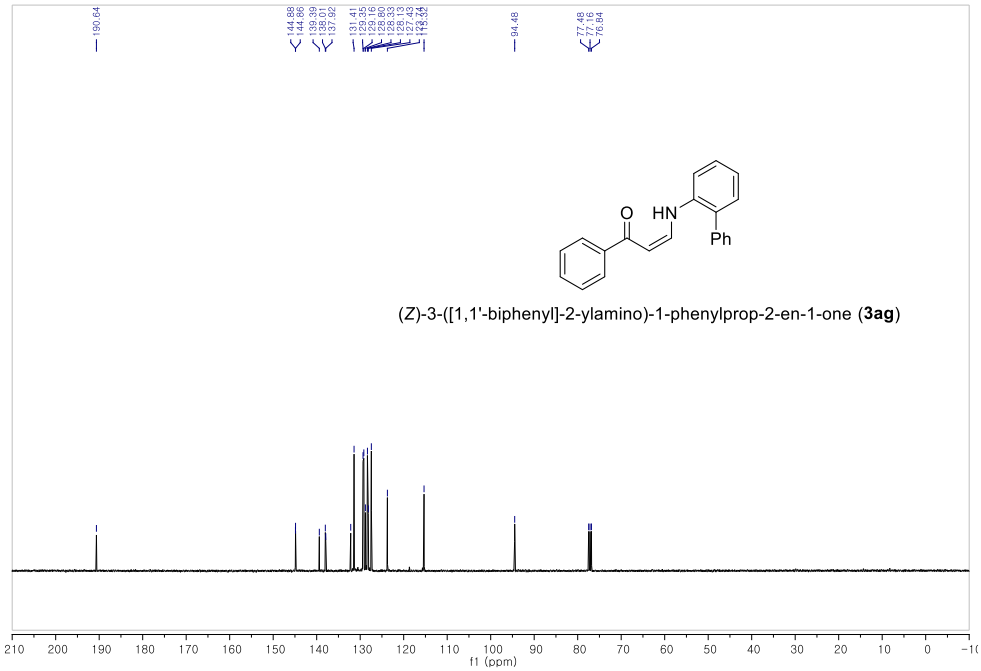

^{13}C NMR ($CDCl_3$, 101 MHz)

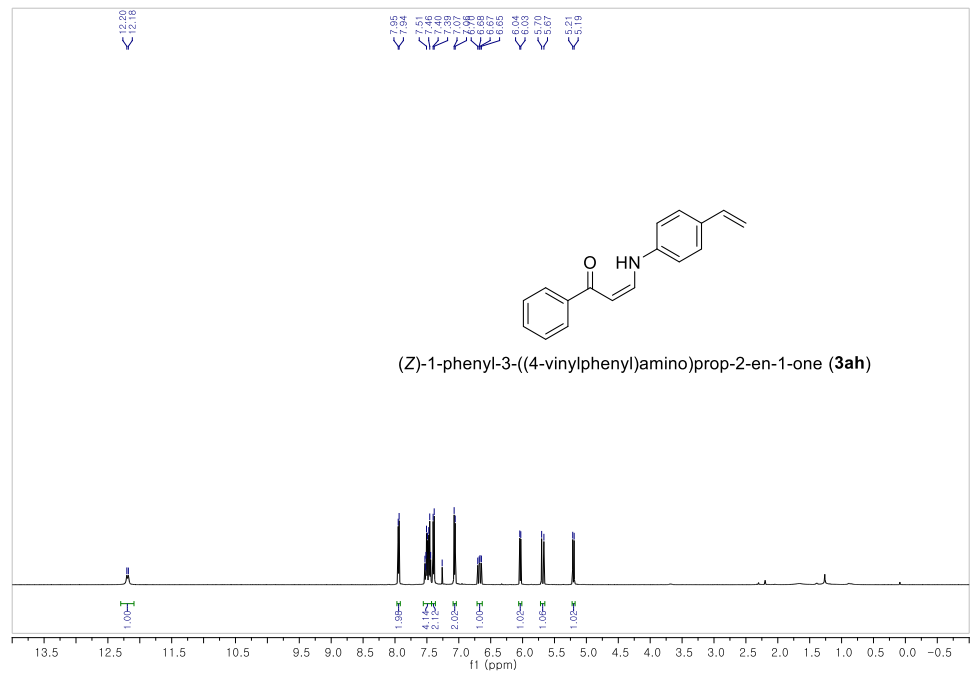

^{1}H NMR ($CDCl_3$, 499 MHz)

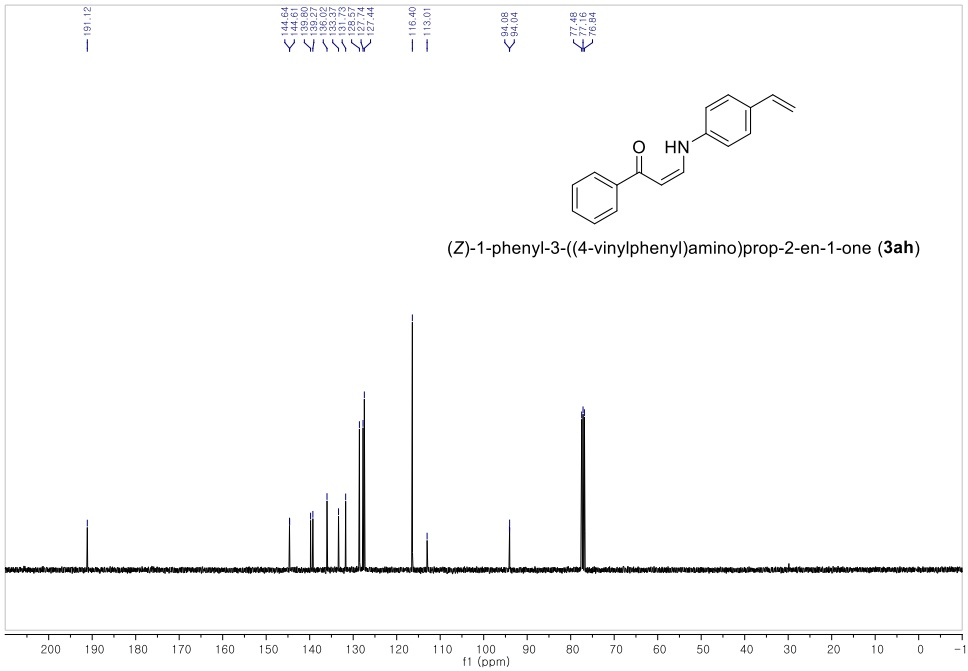

^{13}C NMR ($CDCl_3$, 101 MHz)

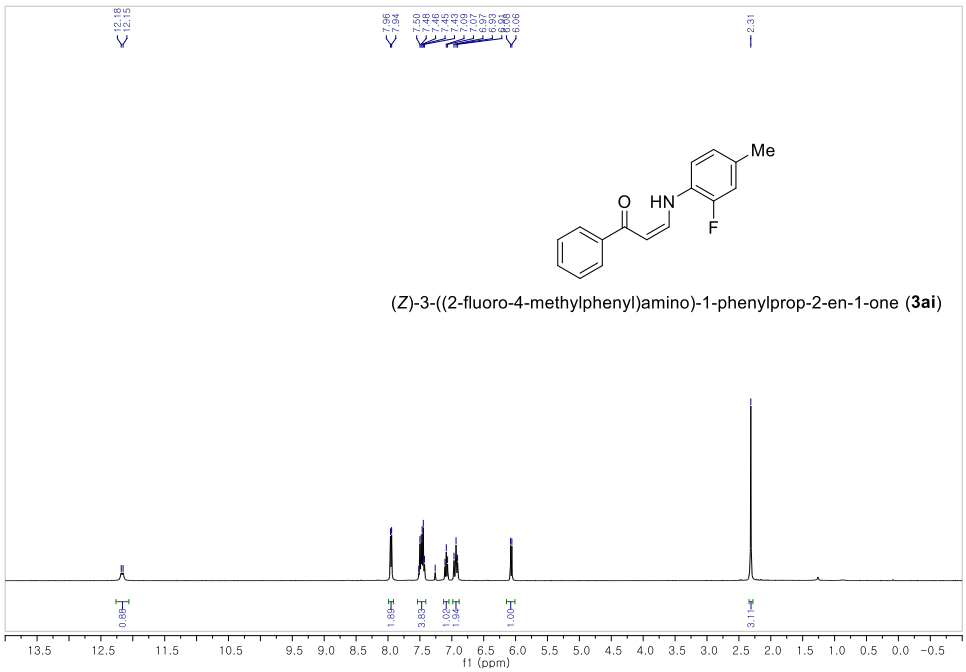

^{1}H NMR ($CDCl_3$, 400 MHz)

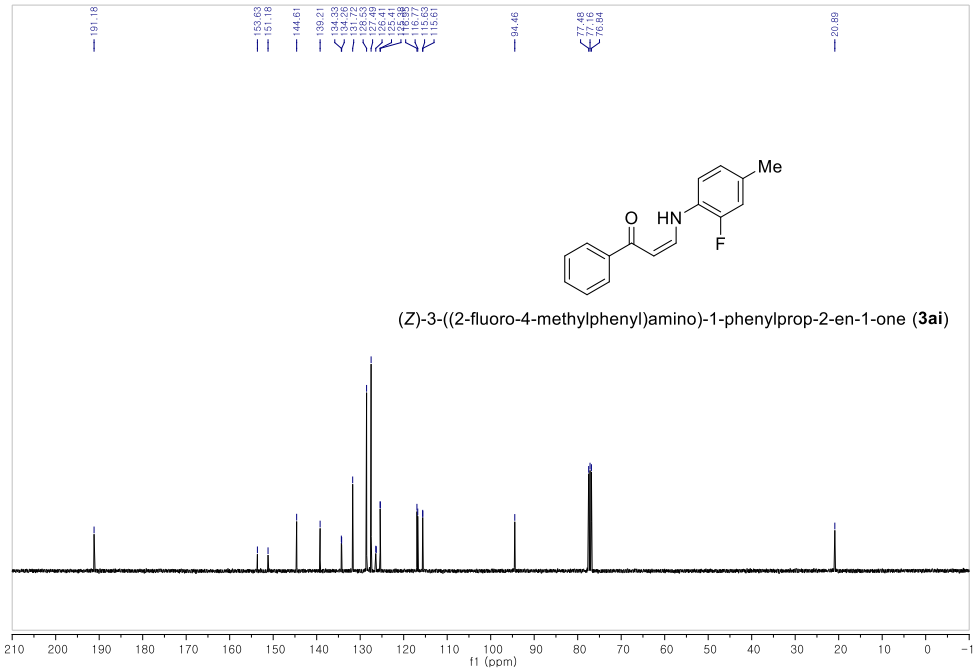

^{13}C NMR ($CDCl_3$, 101 MHz)

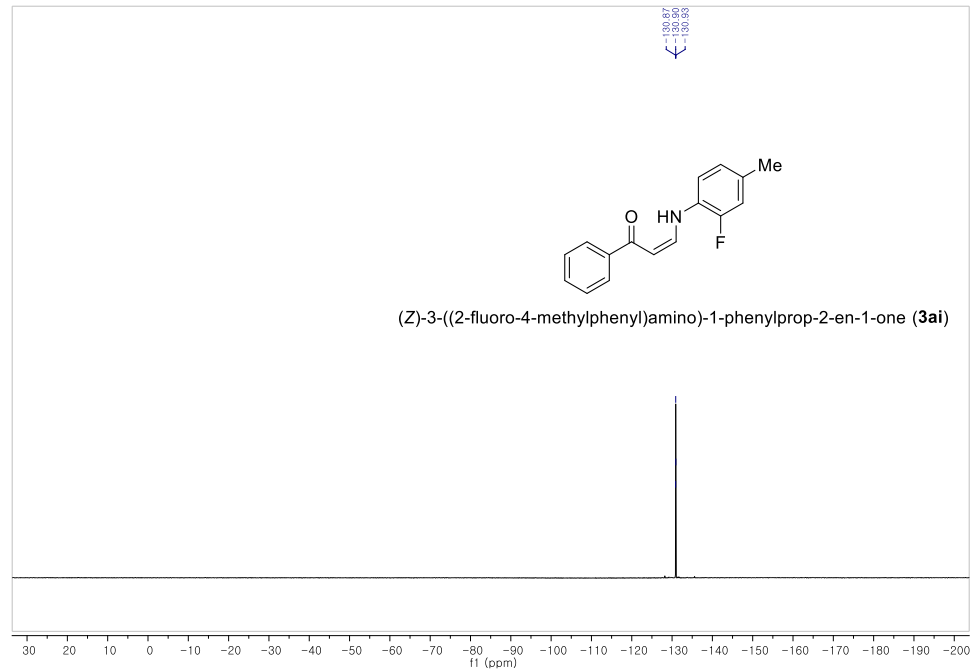

^{19}F NMR ($CDCl_3$, 376 MHz)

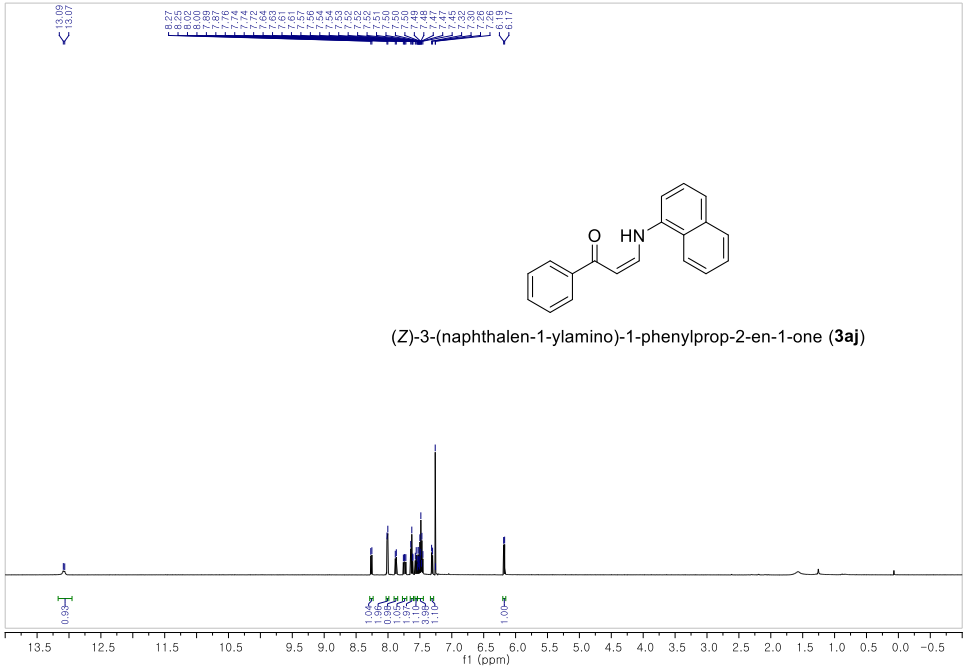

^{1}H NMR ($CDCl_3$, 499 MHz)

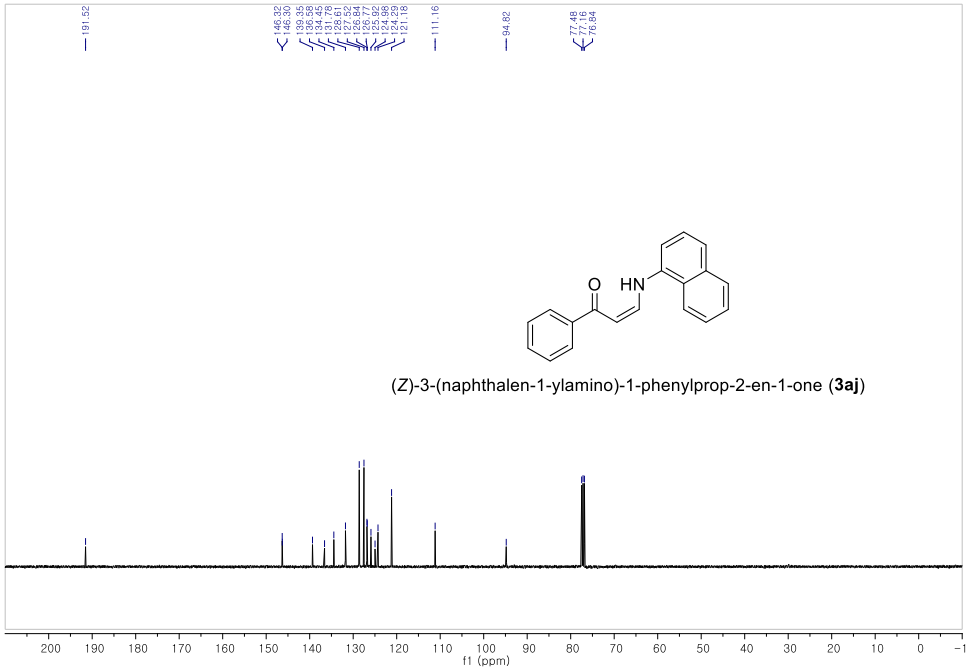

^{13}C NMR ($CDCl_3$, 101 MHz)

Chapter 3

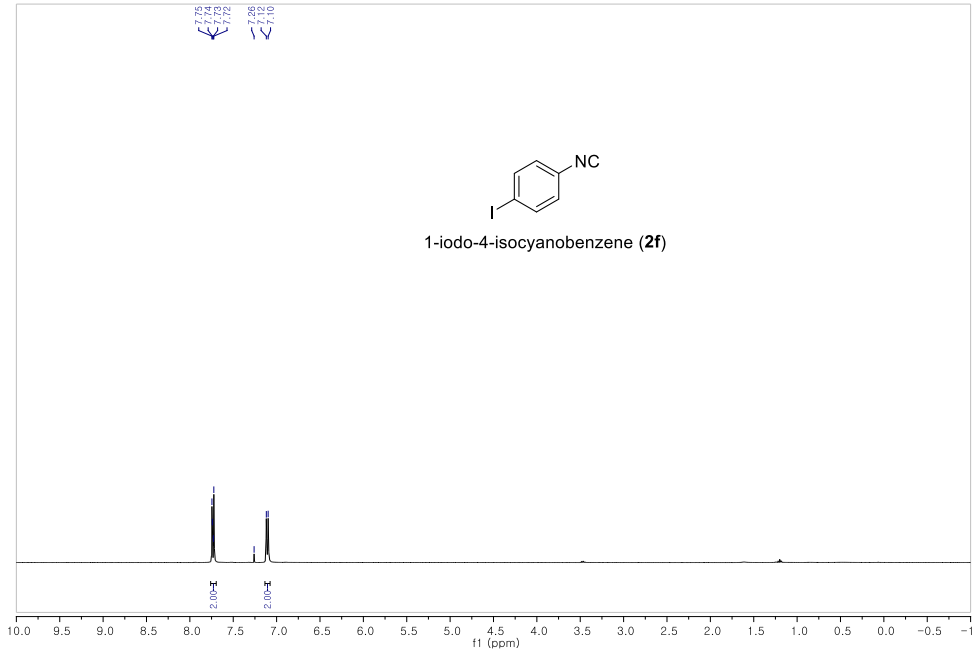

H NMR ($CDCl_3$, 400 MHz)

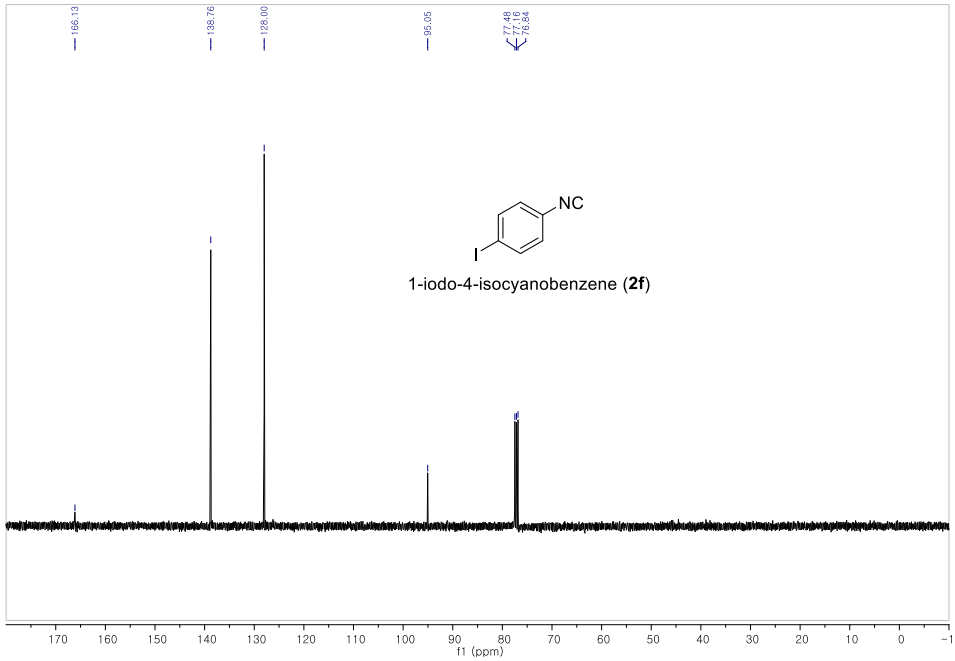

^{13}C NMR ($CDCl_3$, 100 MHz)

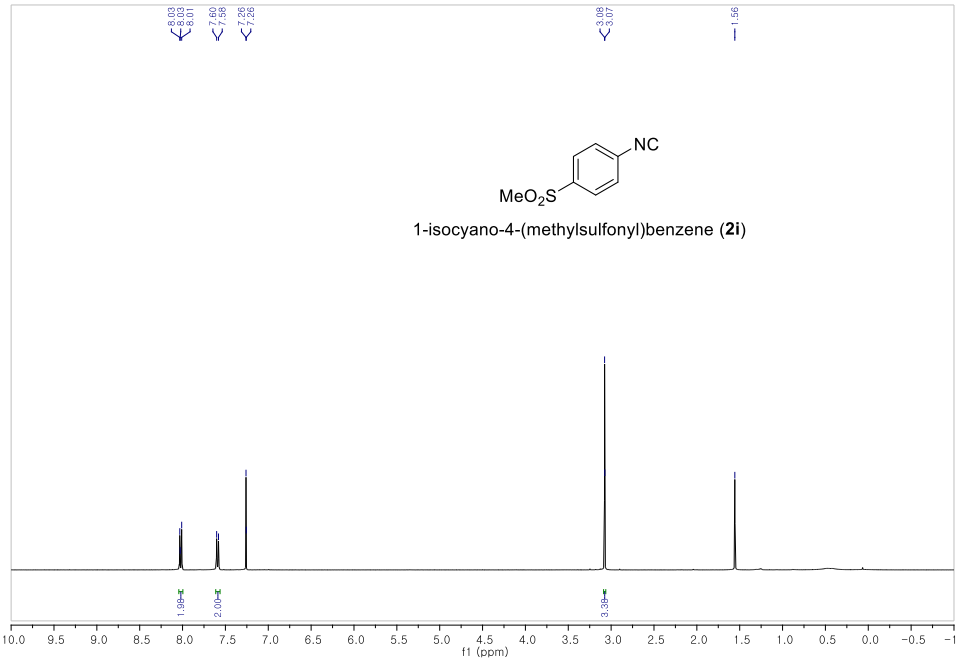

^{1}H NMR ($CDCl_3$, 400 MHz)

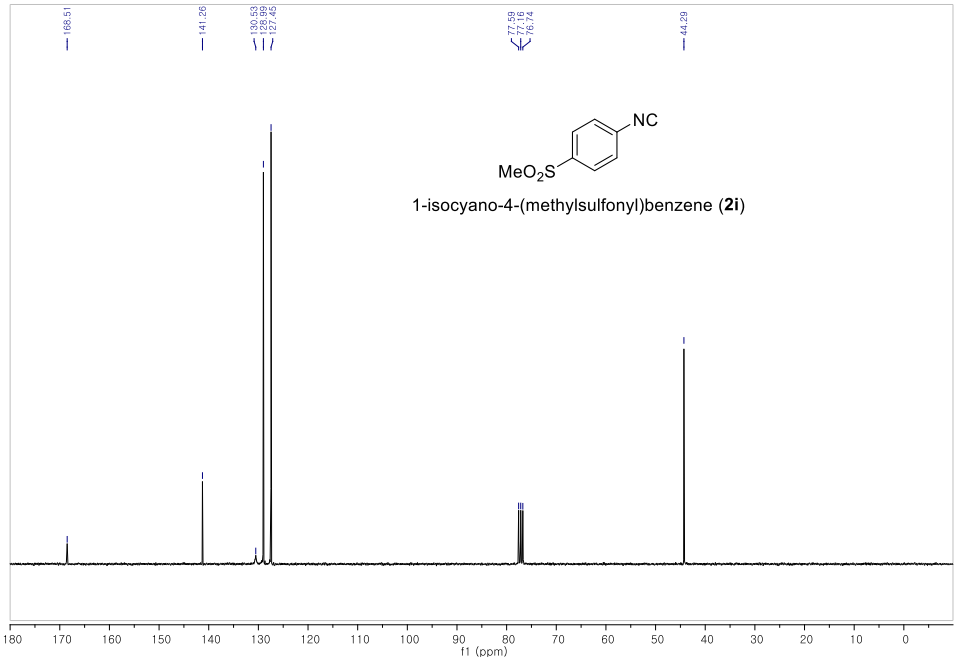

^{13}C NMR ($CDCl_3$, 75 MHz)

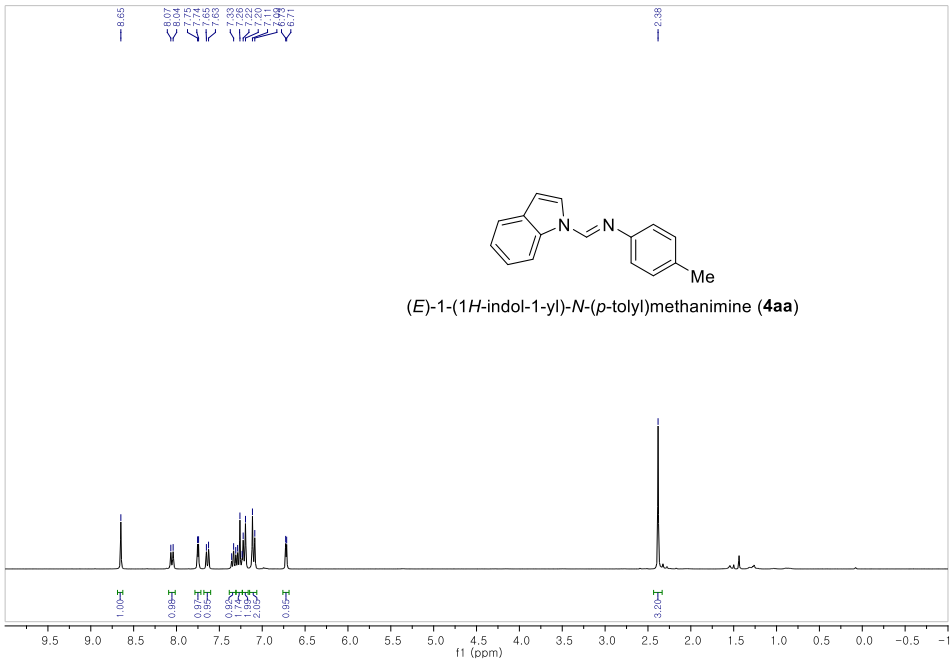

(*E*)-1-(1*H*-indol-1-yl)-*N*-(*p*-tolyl)methanimine (**4aa**)

^{1}H NMR ($CDCl_3$, 300 MHz)

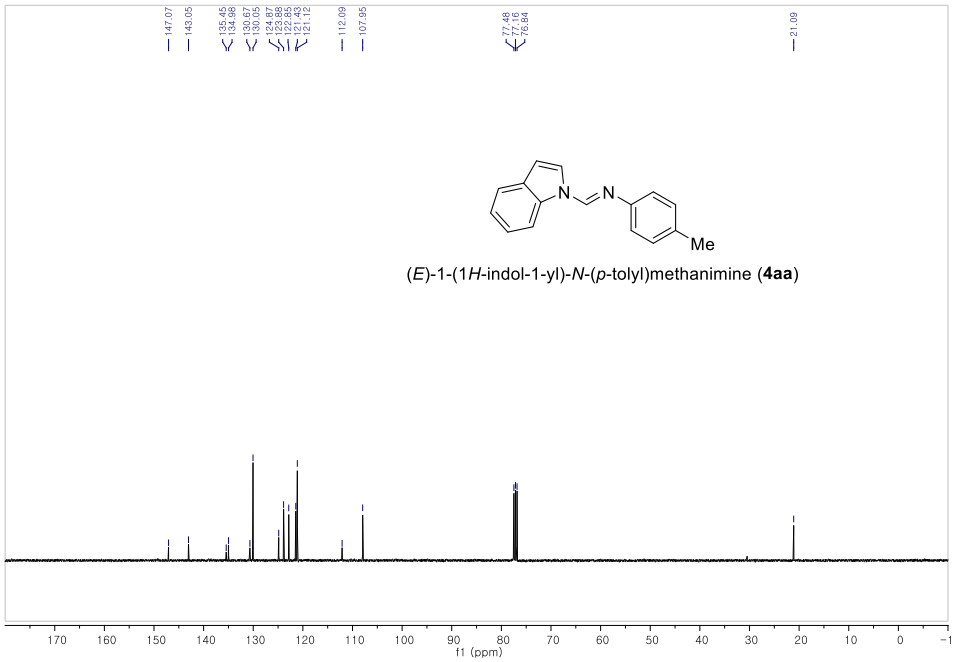

(*E*)-1-(1*H*-indol-1-yl)-*N*-(*p*-tolyl)methanimine (**4aa**)

^{13}C NMR ($CDCl_3$, 100 MHz)

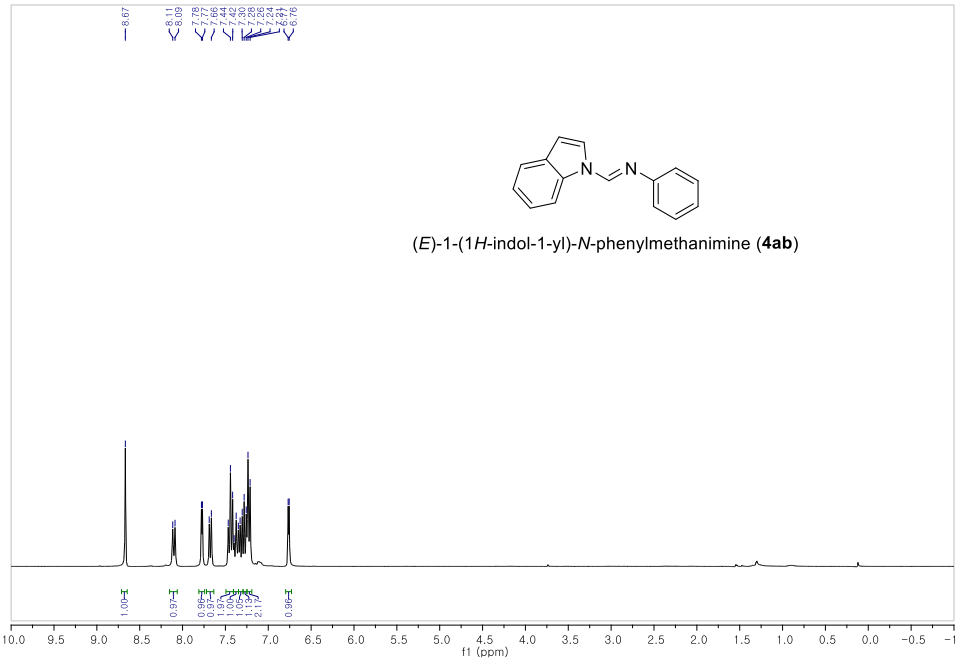

(*E*)-1-(1*H*-indol-1-yl)-*N*-phenylmethanimine (**4ab**)

^{1}H NMR ($CDCl_3$, 300 MHz)

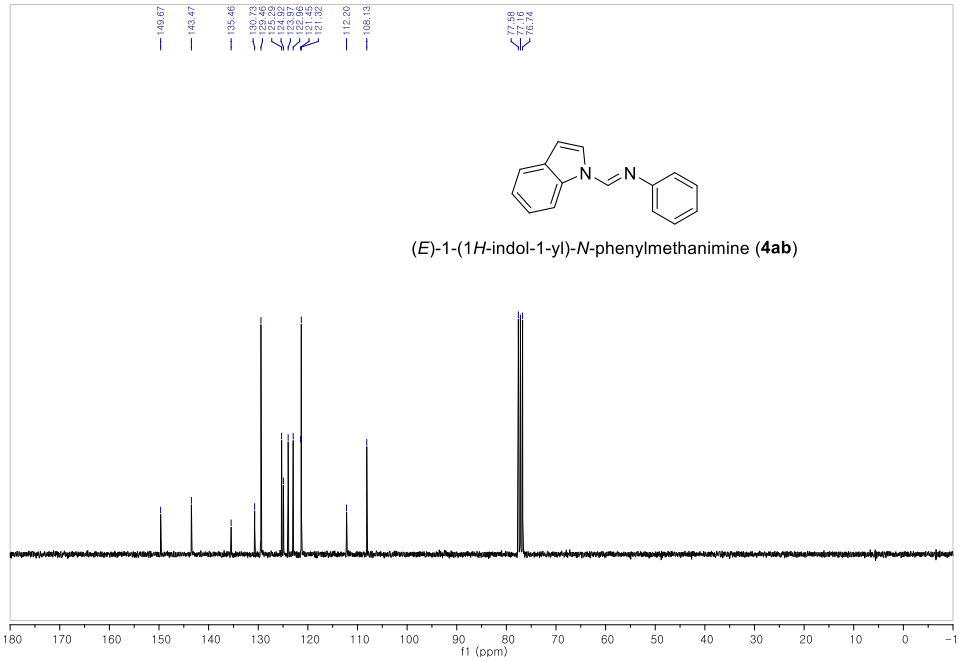

(*E*)-1-(1*H*-indol-1-yl)-*N*-phenylmethanimine (**4ab**)

^{13}C NMR ($CDCl_3$, 75 MHz)

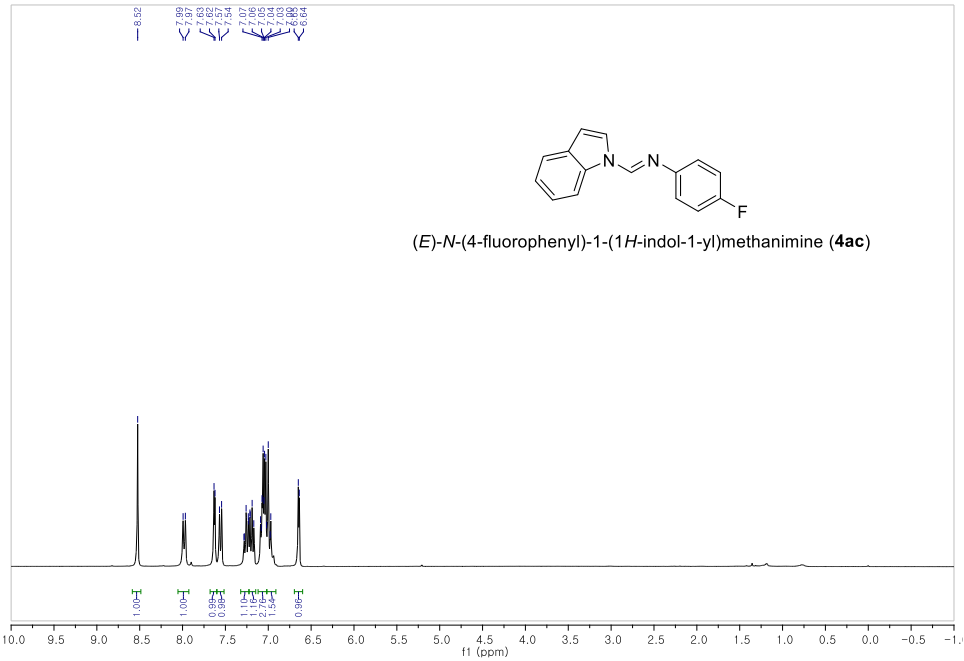

^{1}H NMR ($CDCl_3$, 300 MHz)

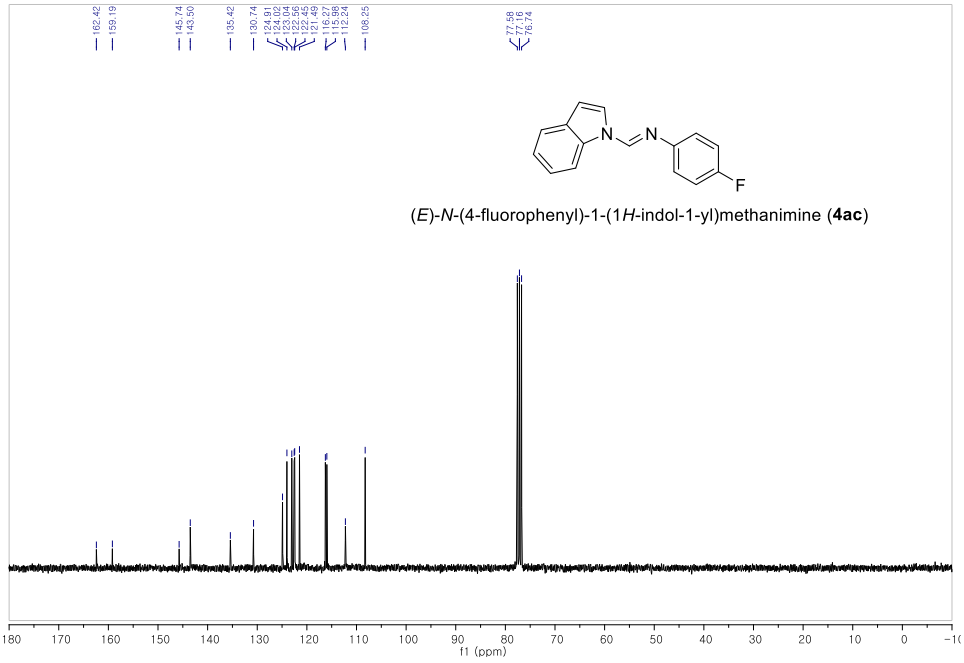

^{13}C NMR ($CDCl_3$, 75 MHz)

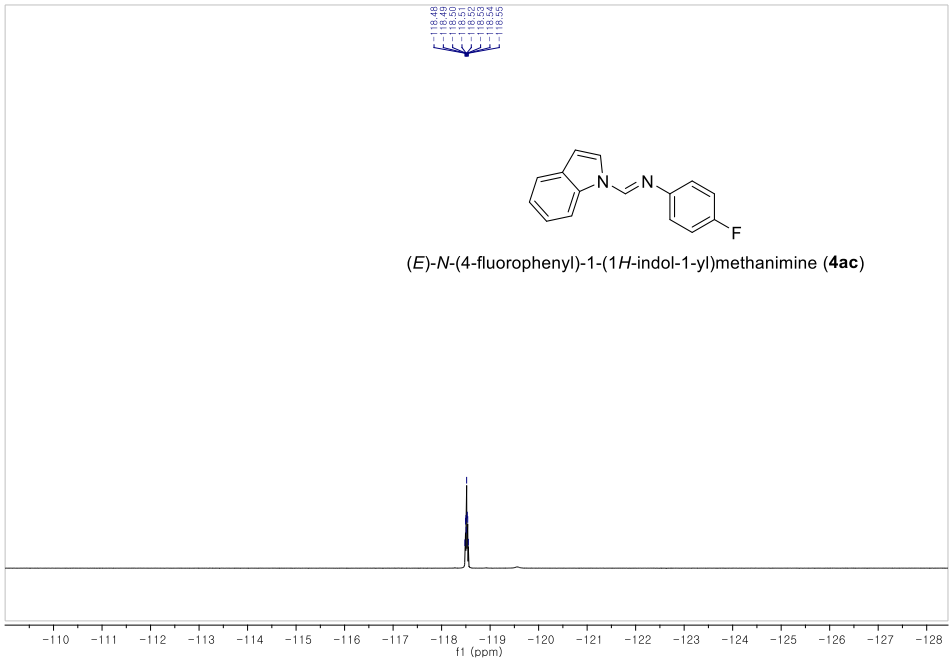

^{19}F NMR ($CDCl_3$, 376 MHz)

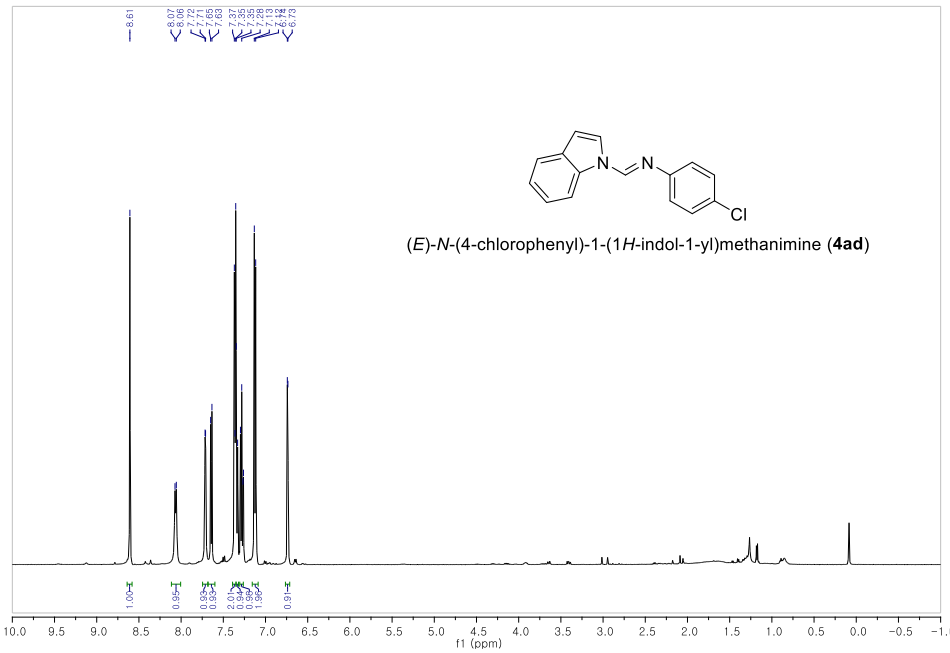

^{1}H NMR ($CDCl_3$, 499 MHz)

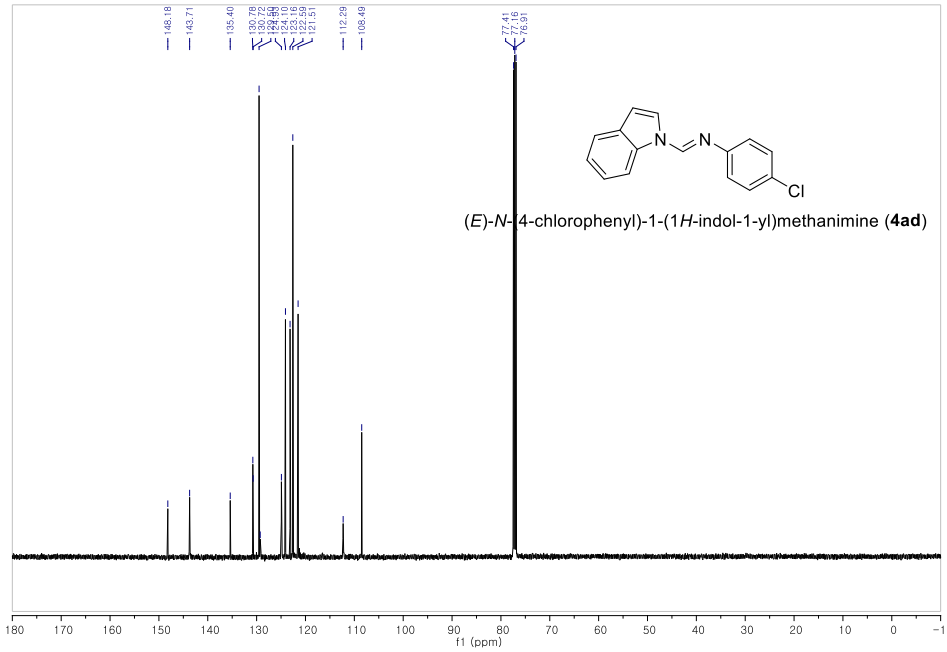

^{13}C NMR ($CDCl_3$, 126 MHz)

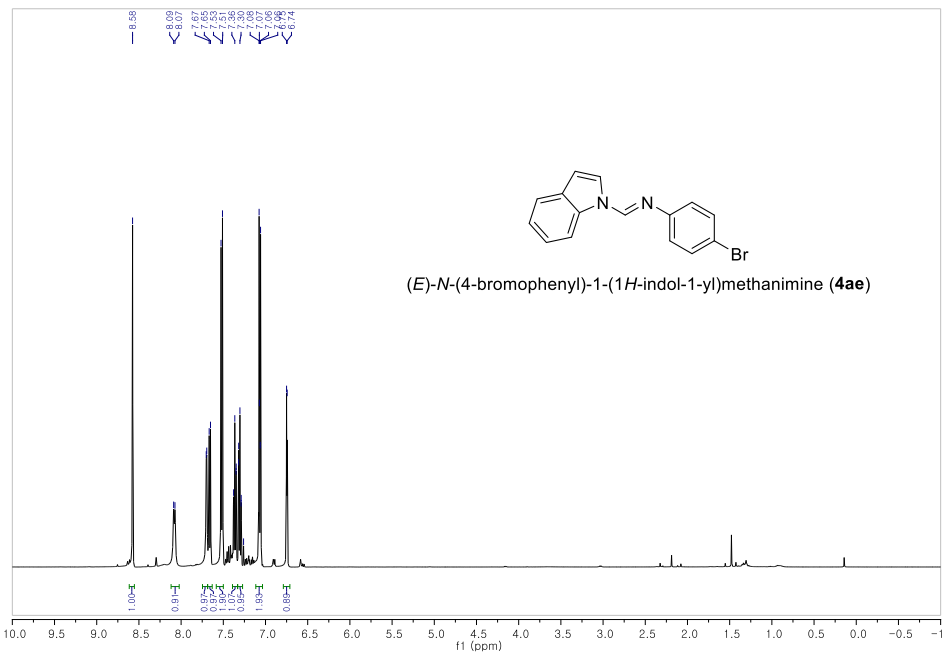

^{1}H NMR ($CDCl_3$, 499 MHz)

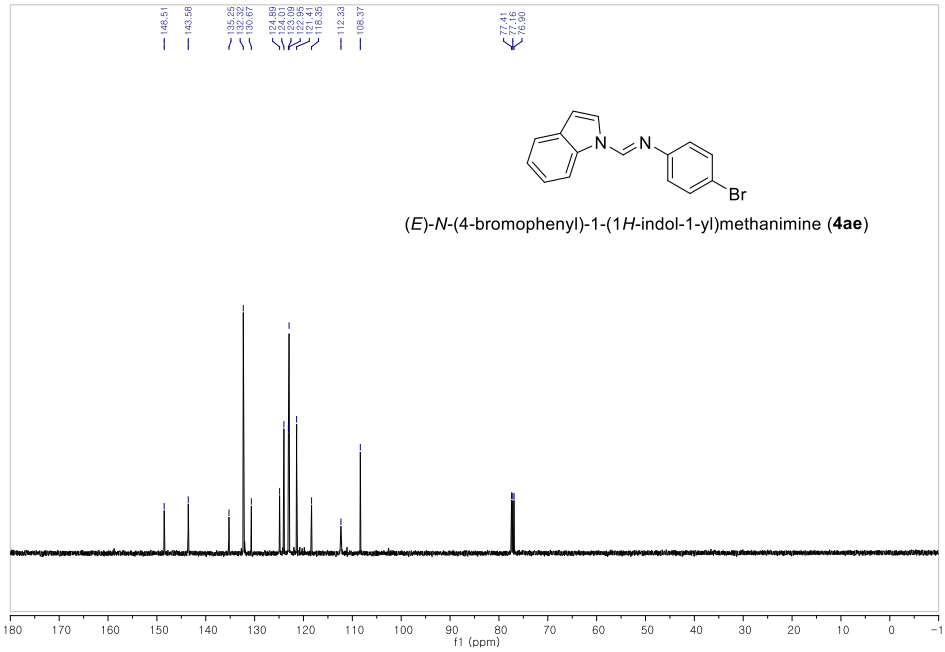

^{13}C NMR ($CDCl_3$, 126 MHz)

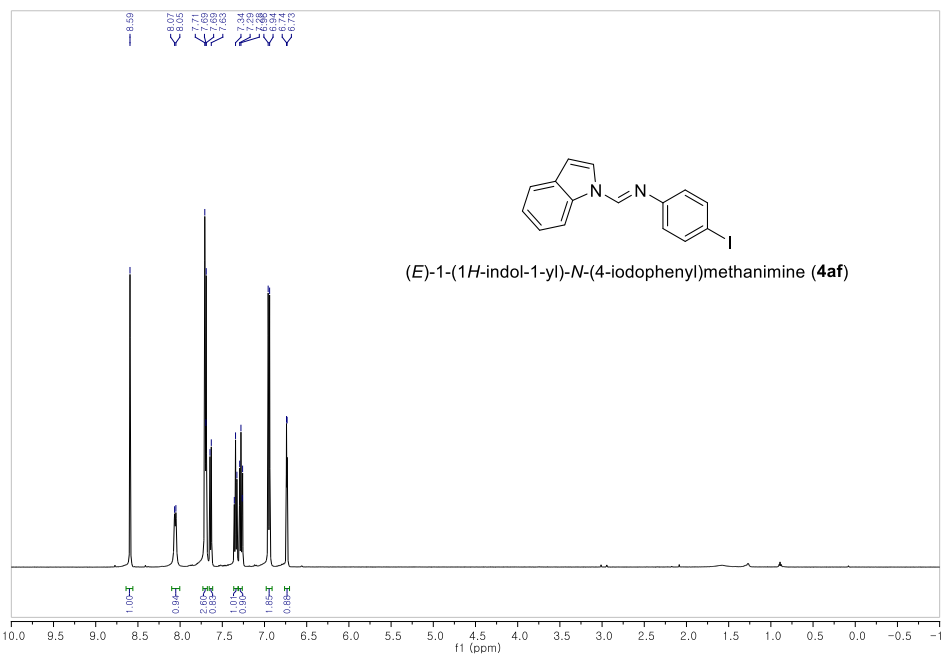

^{1}H NMR ($CDCl_3$, 499 MHz)

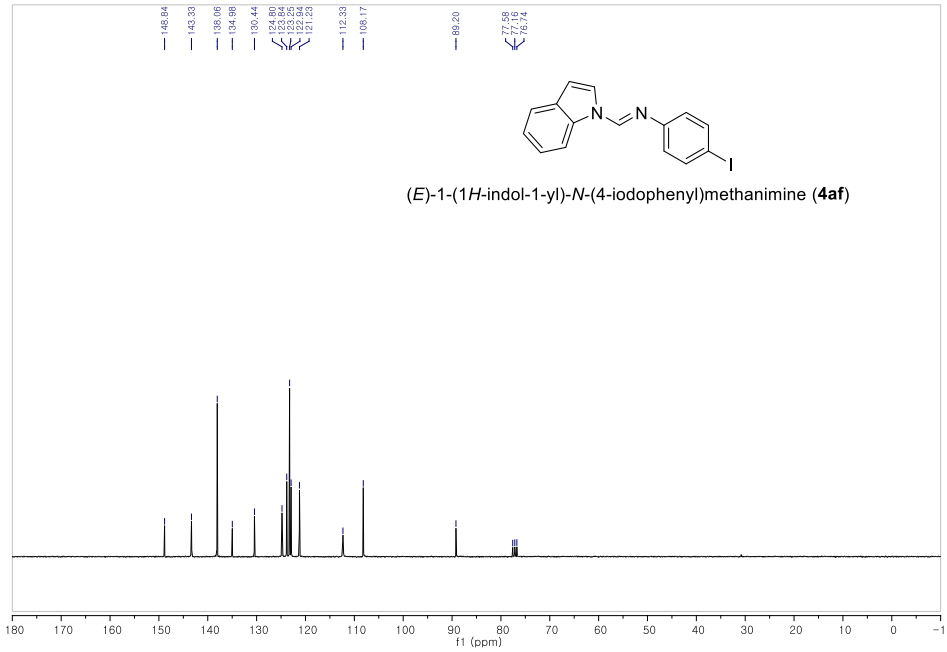

^{13}C NMR ($CDCl_3$, 75 MHz)

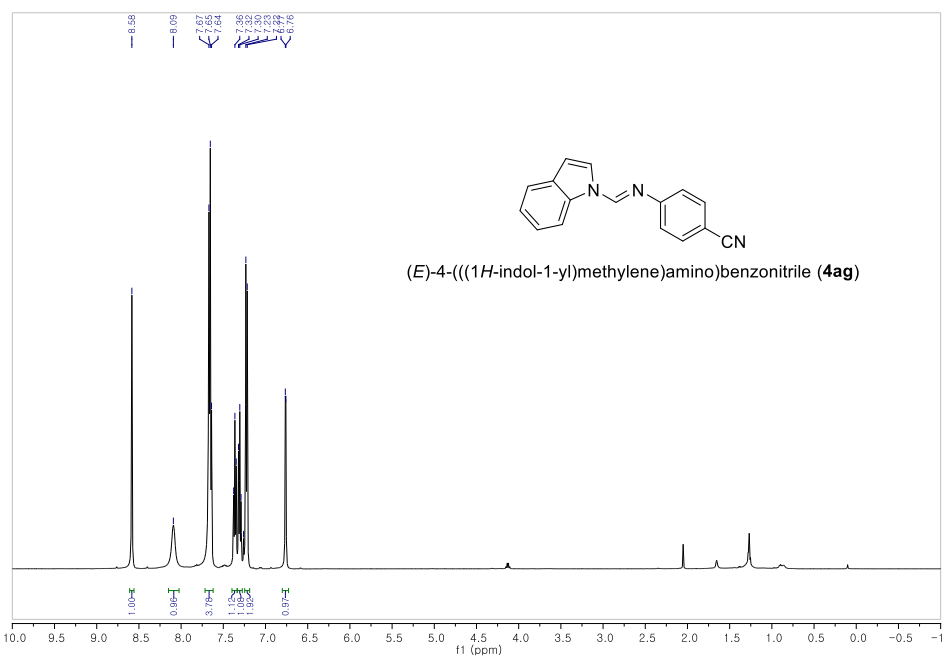

^{1}H NMR ($CDCl_3$, 499 MHz)

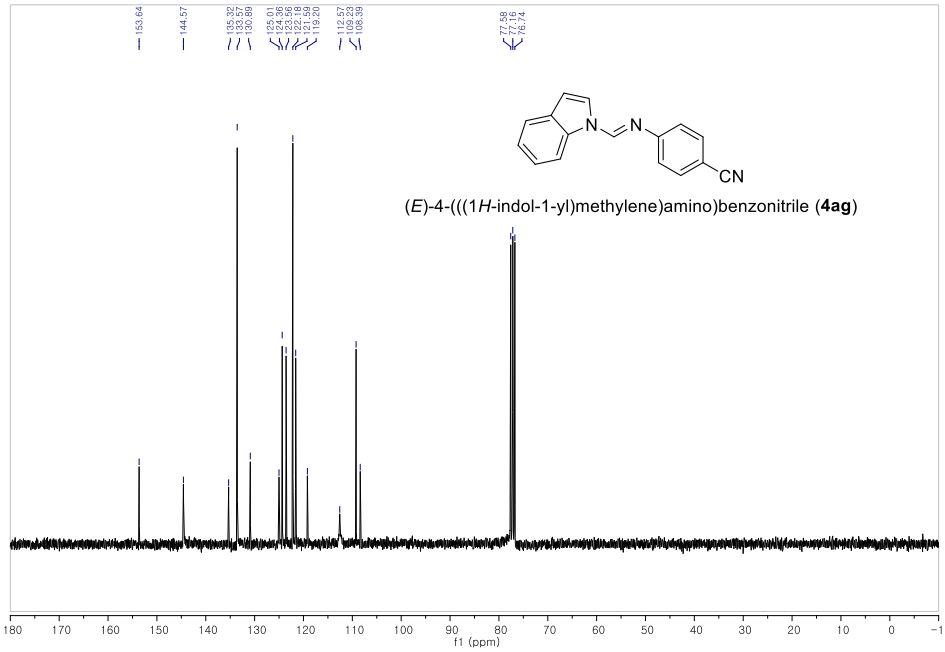

^{13}C NMR ($CDCl_3$, 75 MHz)

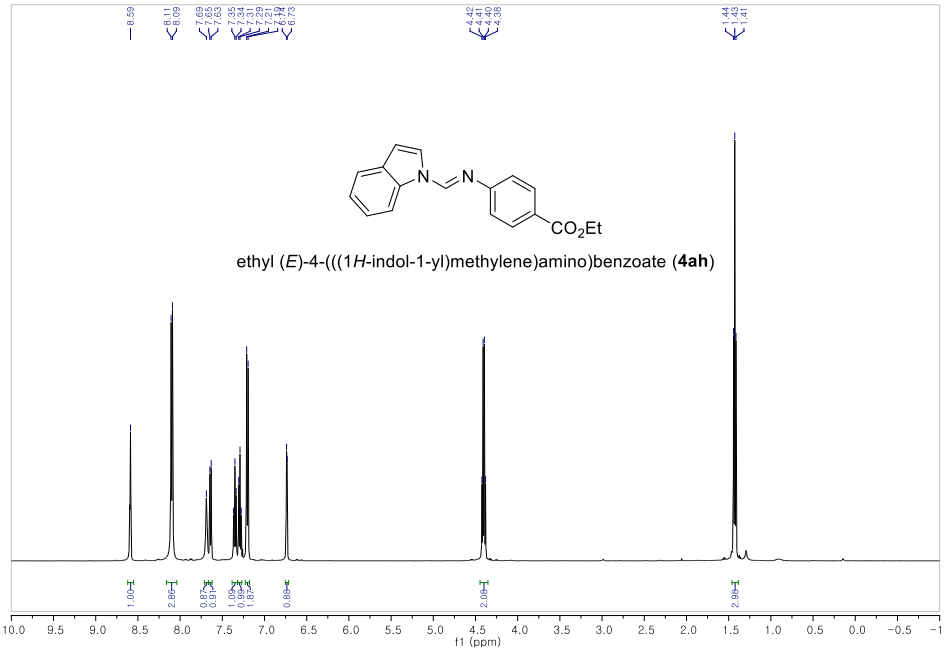

^{1}H NMR ($CDCl_3$, 499 MHz)

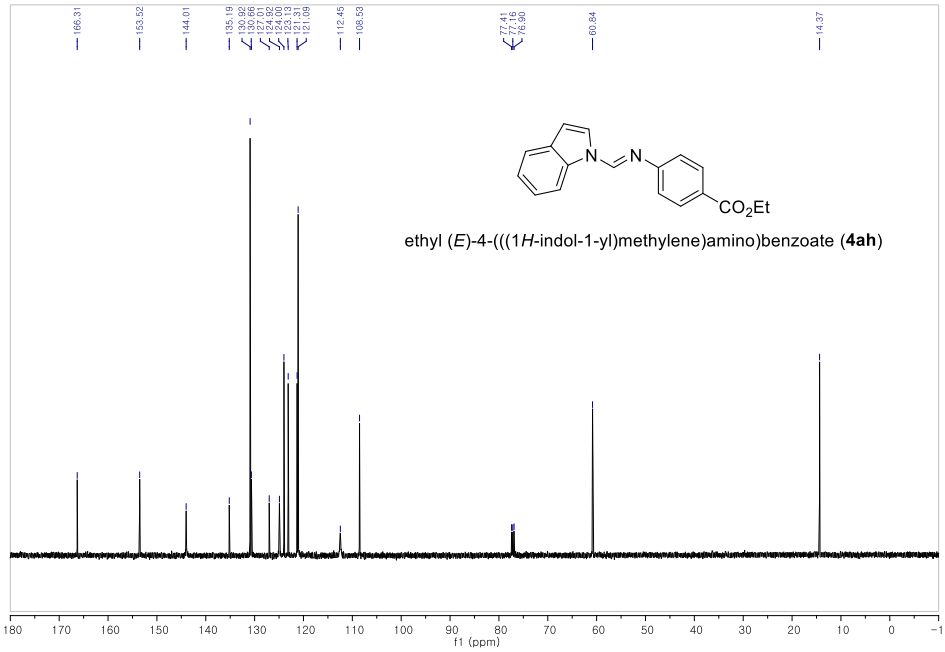

^{13}C NMR ($CDCl_3$, 126 MHz)

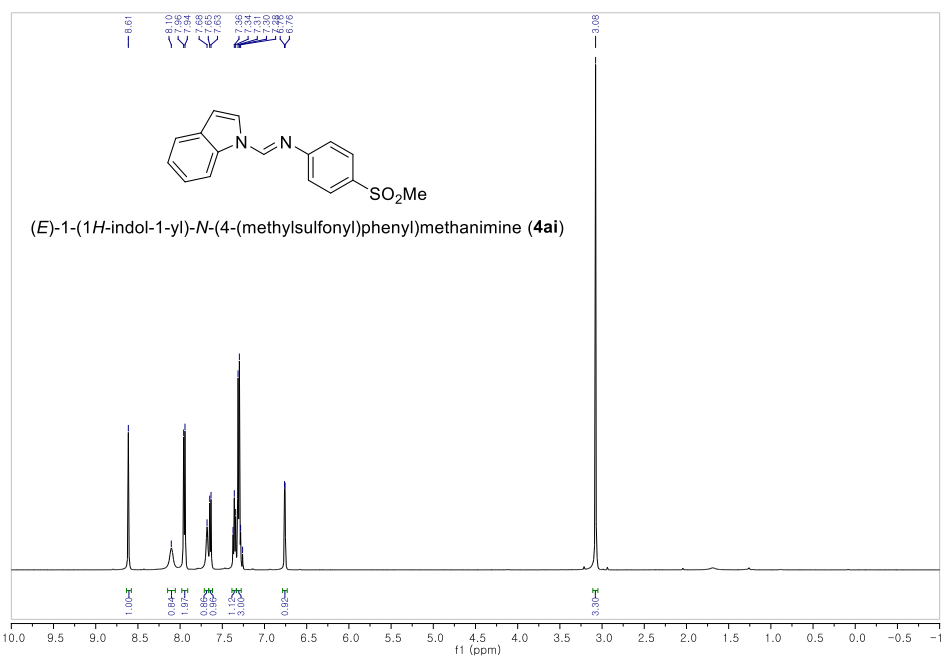

^{1}H NMR ($CDCl_3$, 499 MHz)

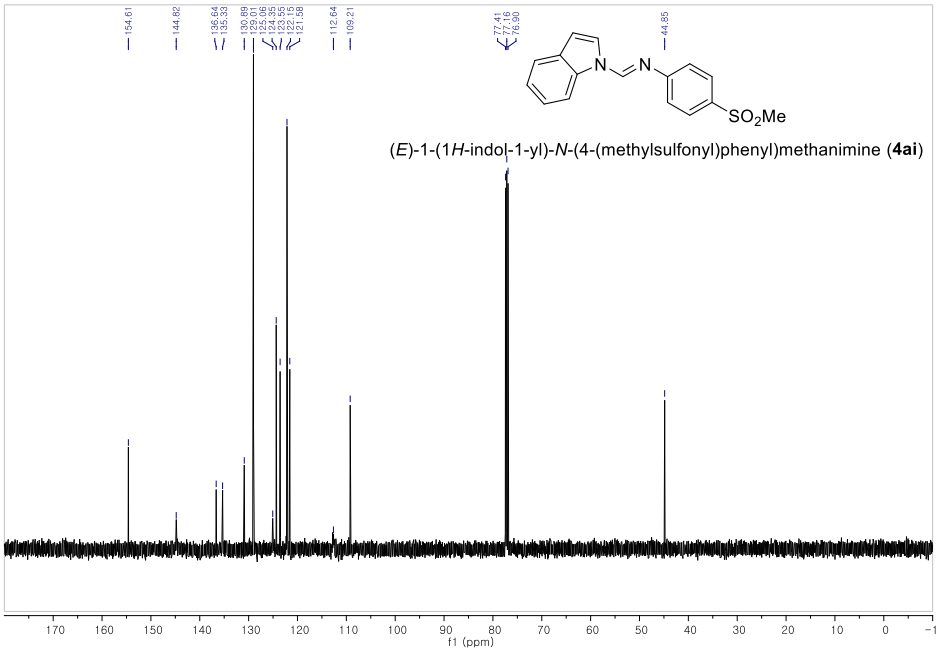

^{13}C NMR ($CDCl_3$, 126 MHz)

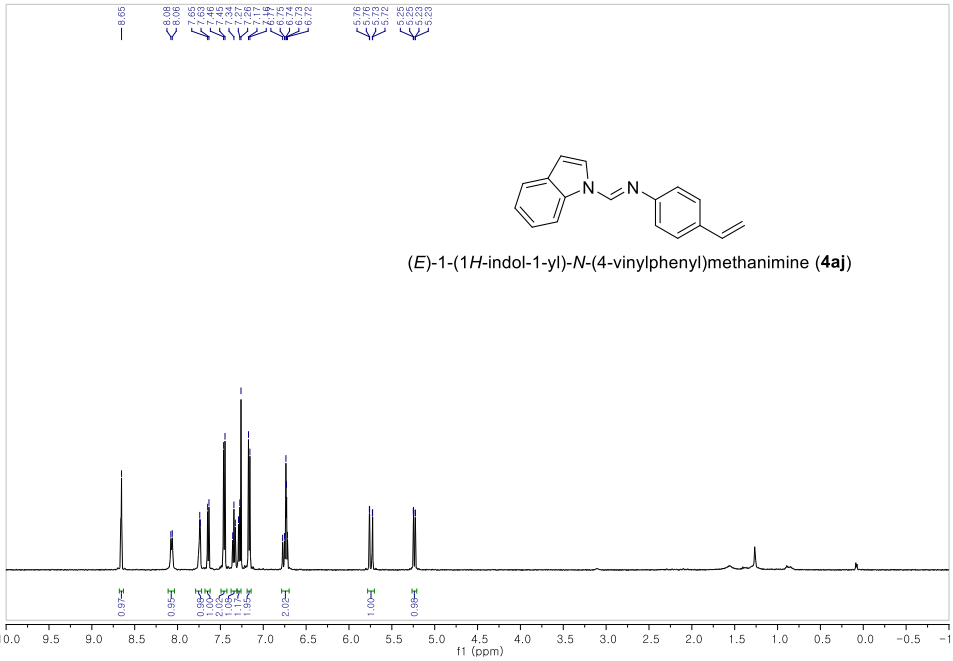

^{1}H NMR ($CDCl_3$, 499 MHz)

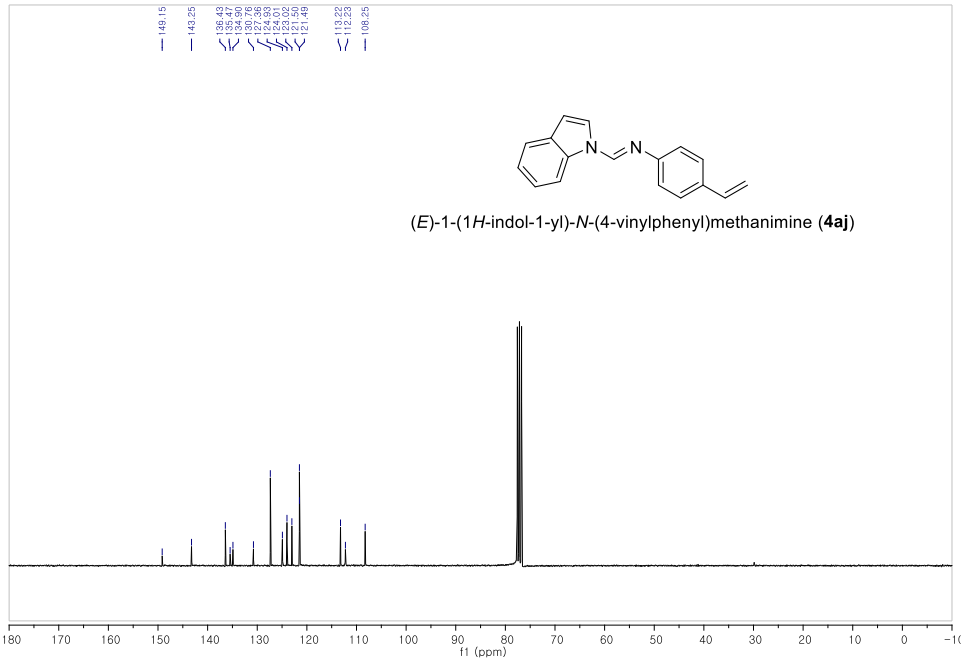

^{13}C NMR ($CDCl_3$, 75 MHz)

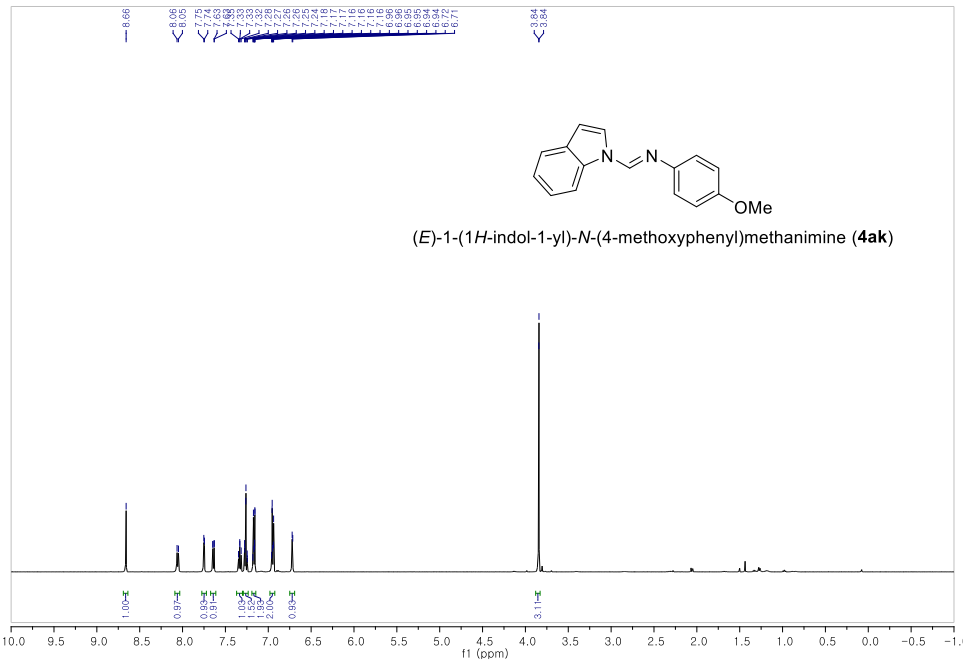

^{1}H NMR ($CDCl_3$, 499 MHz)

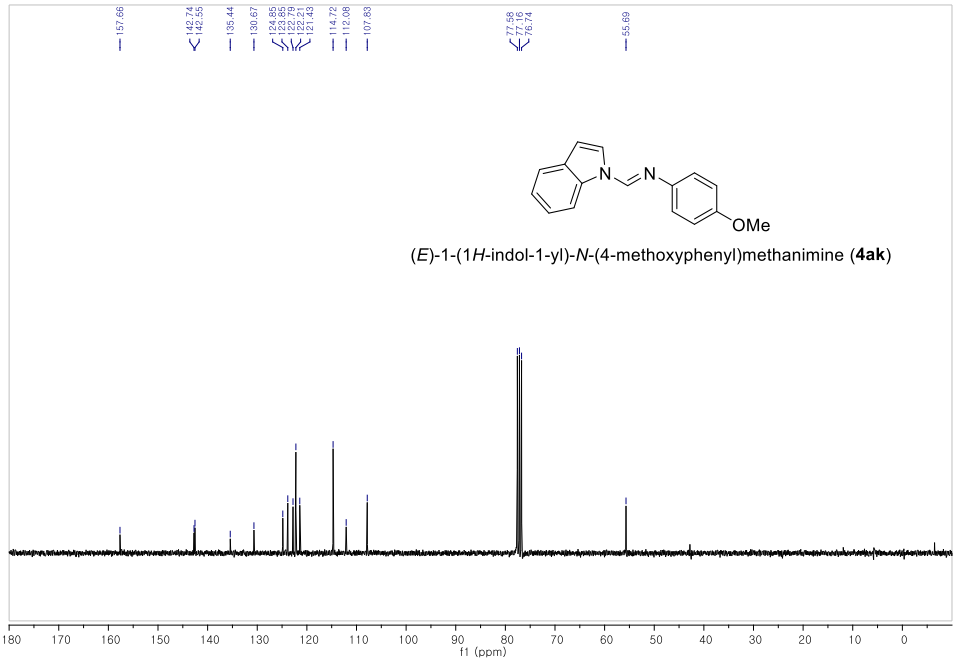

(*E*)-1-(1*H*-indol-1-yl)-*N*-(4-methoxyphenyl)methanimine (**4ak**)

^{13}C NMR ($CDCl_3$, 75 MHz)

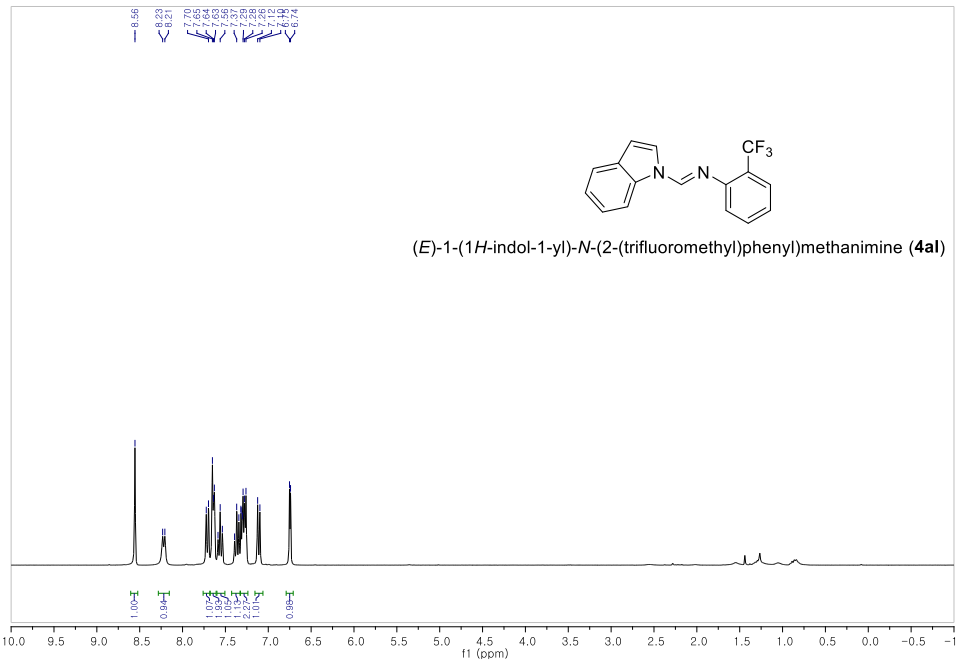

(*E*)-1-(1*H*-indol-1-yl)-*N*-(2-(trifluoromethyl)phenyl)methanimine (**4al**)

^{1}H NMR ($CDCl_3$, 300 MHz)

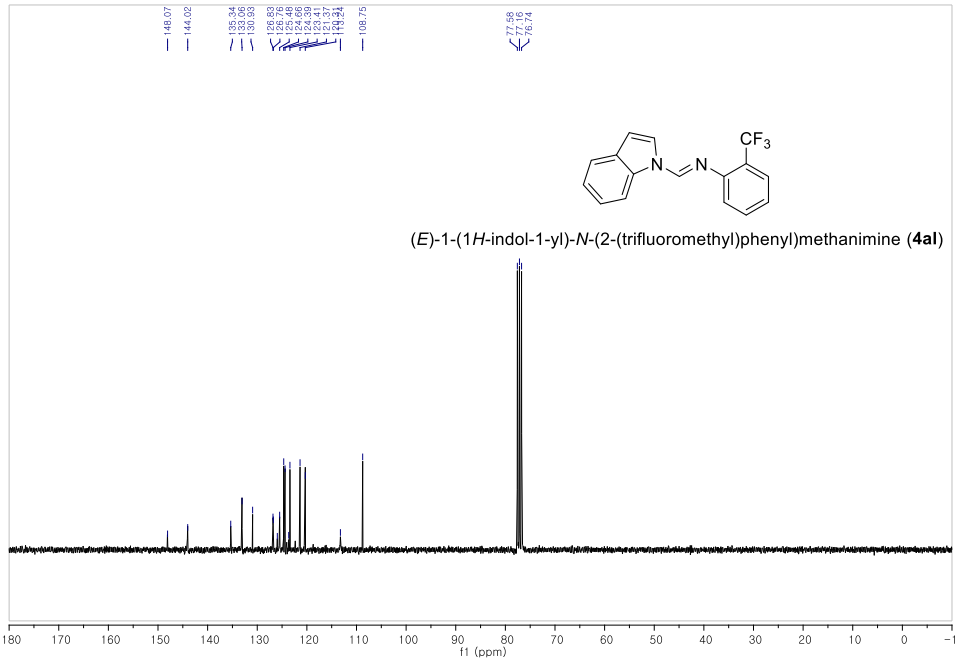

^{13}C NMR ($CDCl_3$, 75 MHz)

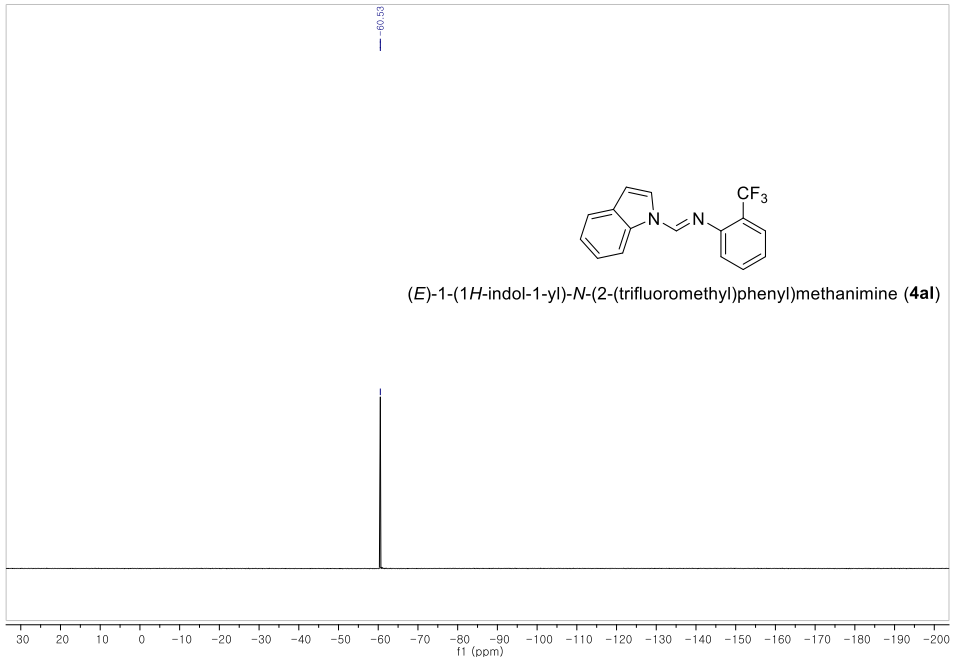

^{19}F NMR ($CDCl_3$, 376 MHz)

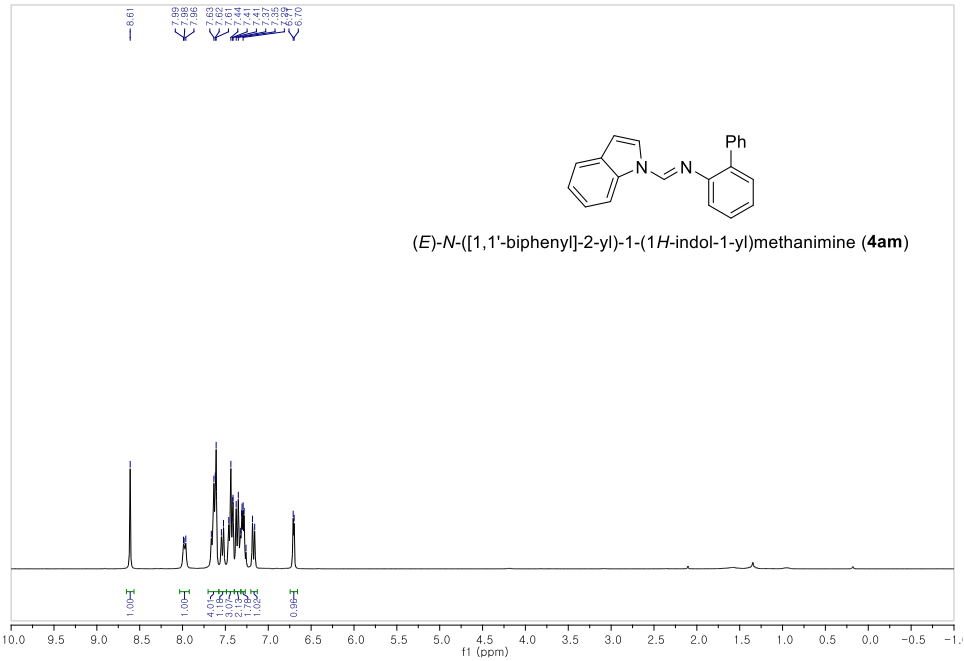

^{1}H NMR ($CDCl_3$, 300 MHz)

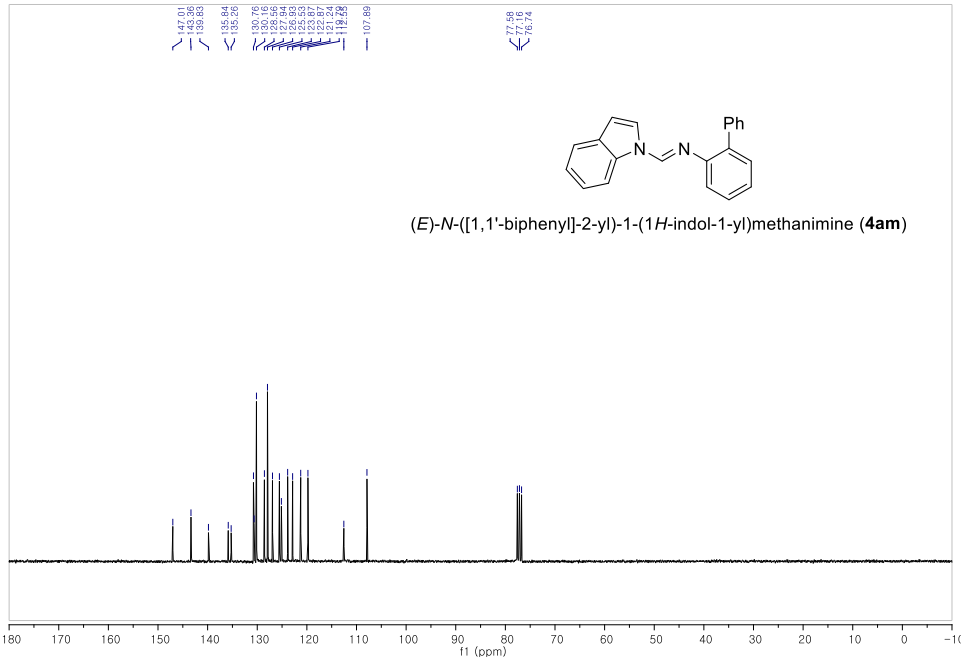

^{13}C NMR ($CDCl_3$, 75 MHz)

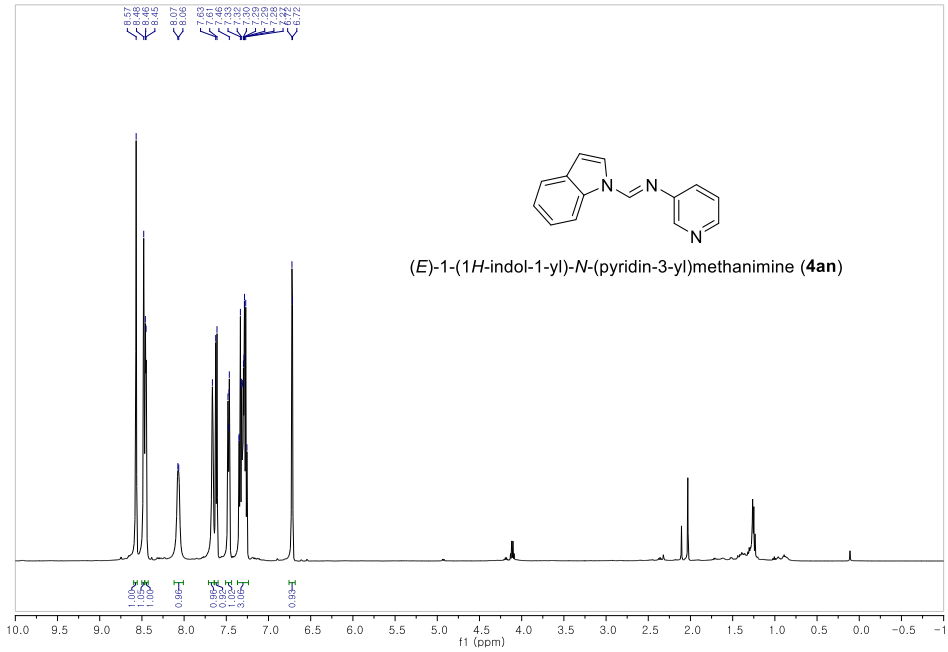

(*E*)-1-(1*H*-indol-1-yl)-*N*-(pyridin-3-yl)methanimine (**4an**)

^{1}H NMR ($CDCl_3$, 499 MHz)

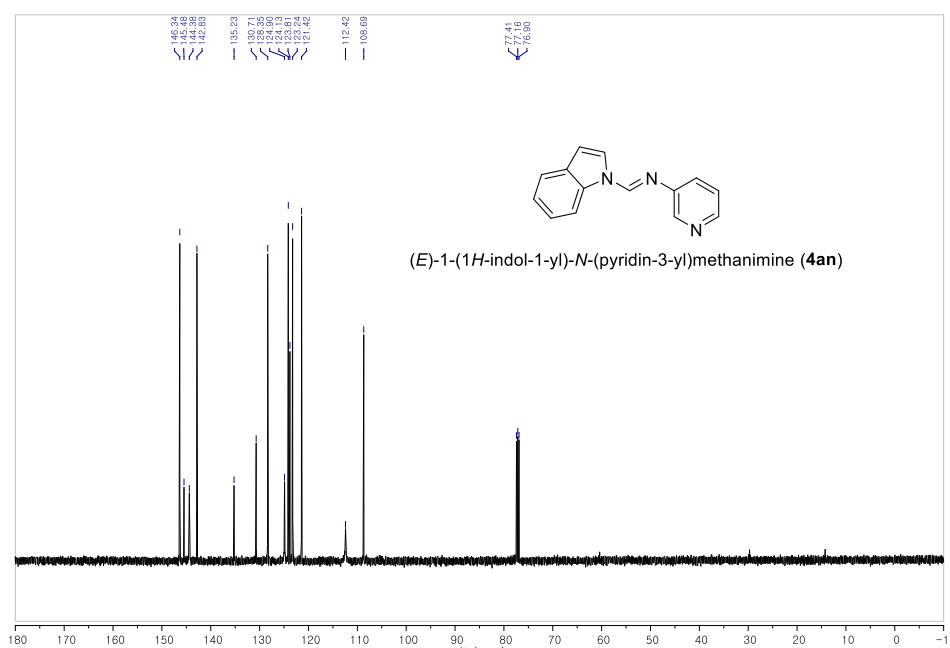

(*E*)-1-(1*H*-indol-1-yl)-*N*-(pyridin-3-yl)methanimine (**4an**)

^{13}C NMR ($CDCl_3$, 126 MHz)

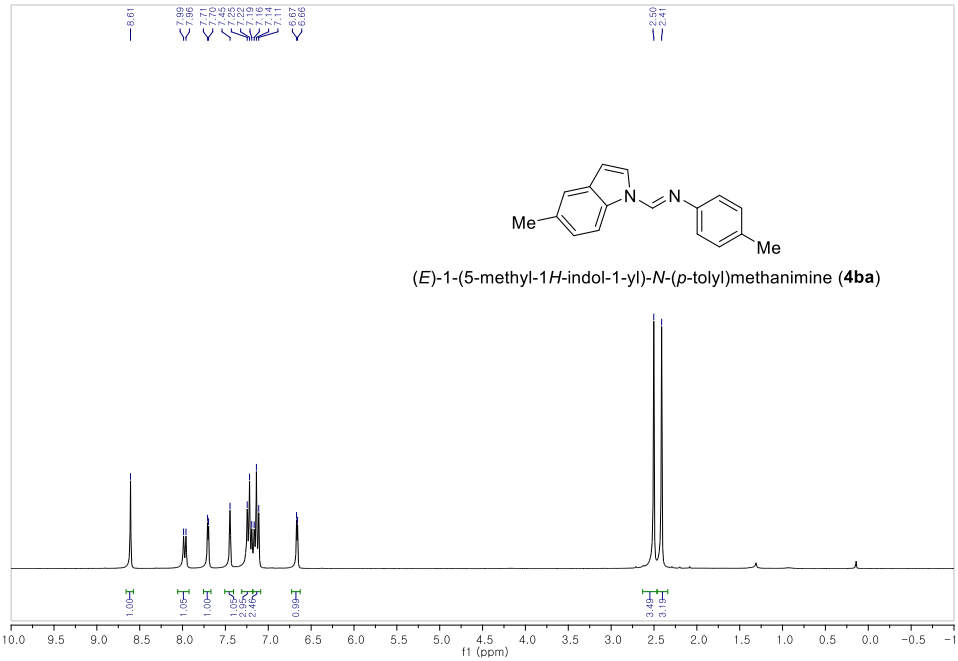

^{1}H NMR ($CDCl_3$, 300 MHz)

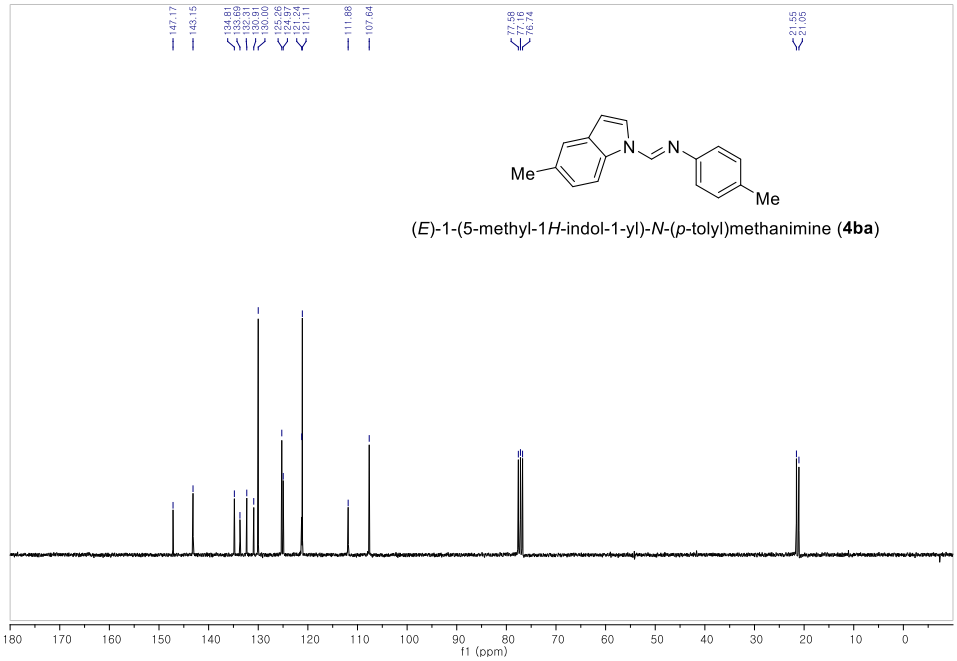

^{13}C NMR ($CDCl_3$, 75 MHz)

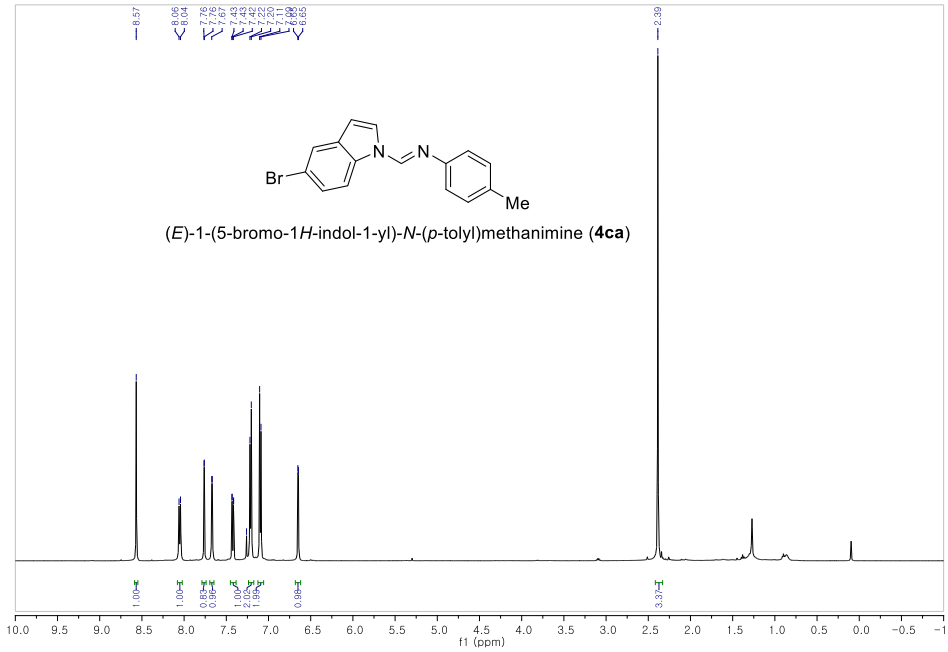

^{1}H NMR ($CDCl_3$, 499 MHz)

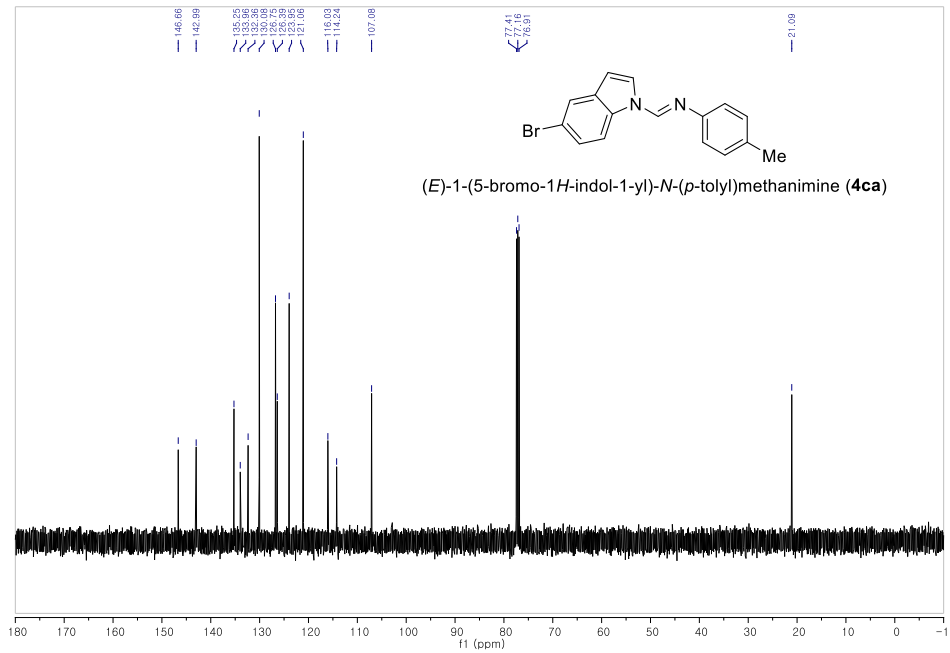

^{13}C NMR ($CDCl_3$, 126 MHz)

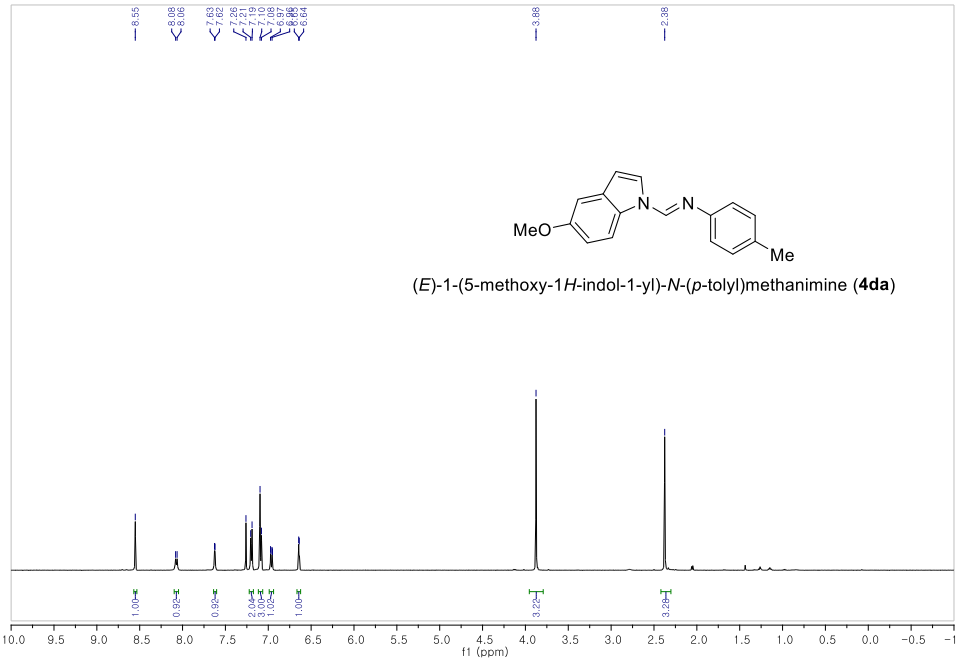

(*E*)-1-(5-methoxy-1*H*-indol-1-yl)-*N*-(*p*-tolyl)methanimine (**4da**)

^{1}H NMR ($CDCl_3$, 499 MHz)

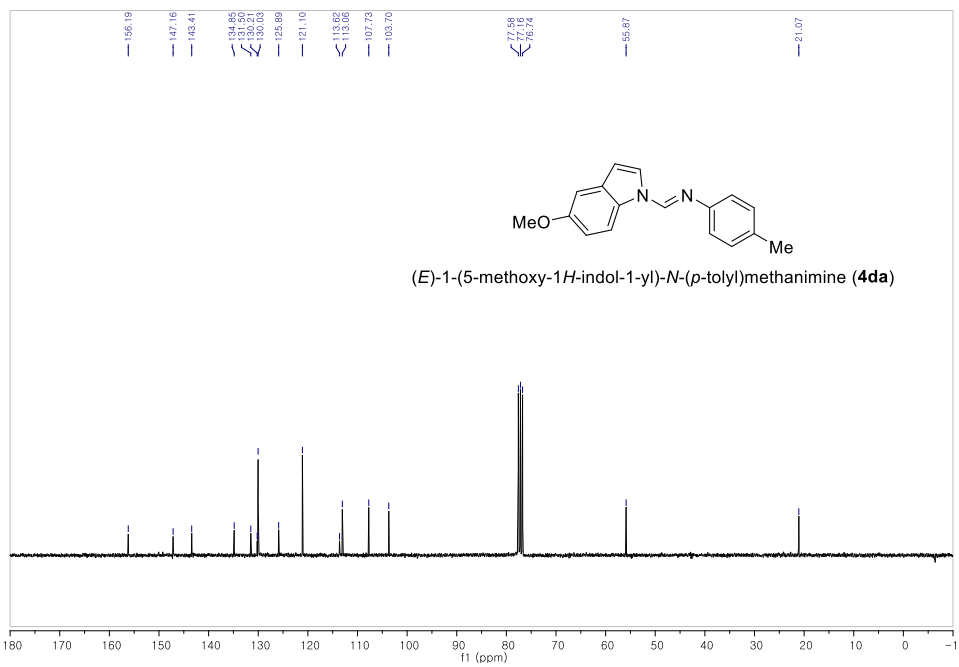

(*E*)-1-(5-methoxy-1*H*-indol-1-yl)-*N*-(*p*-tolyl)methanimine (**4da**)

^{13}C NMR ($CDCl_3$, 75 MHz)

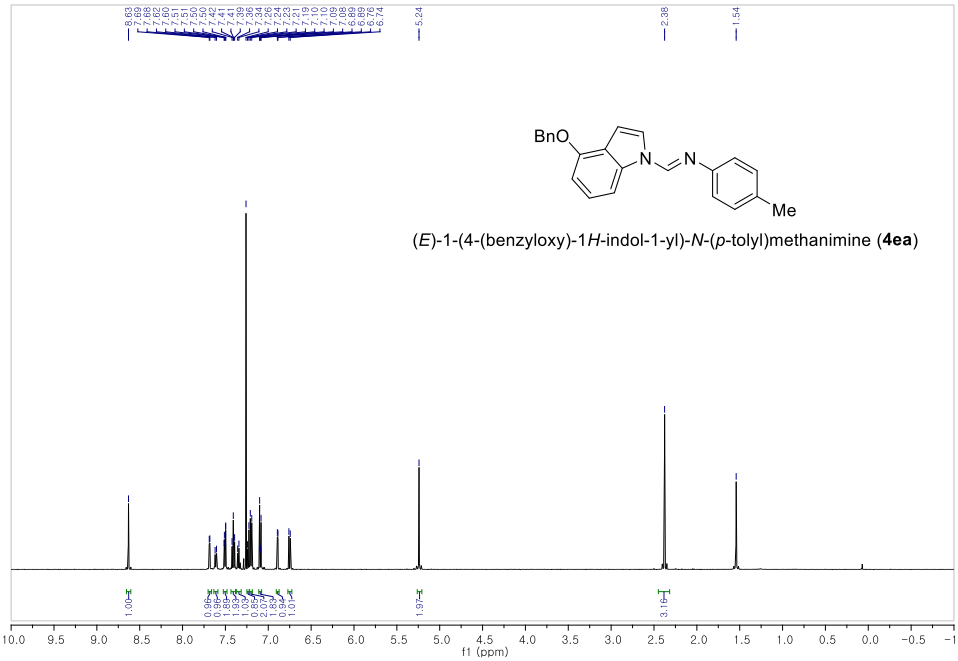

^{1}H NMR ($CDCl_3$, 499 MHz)

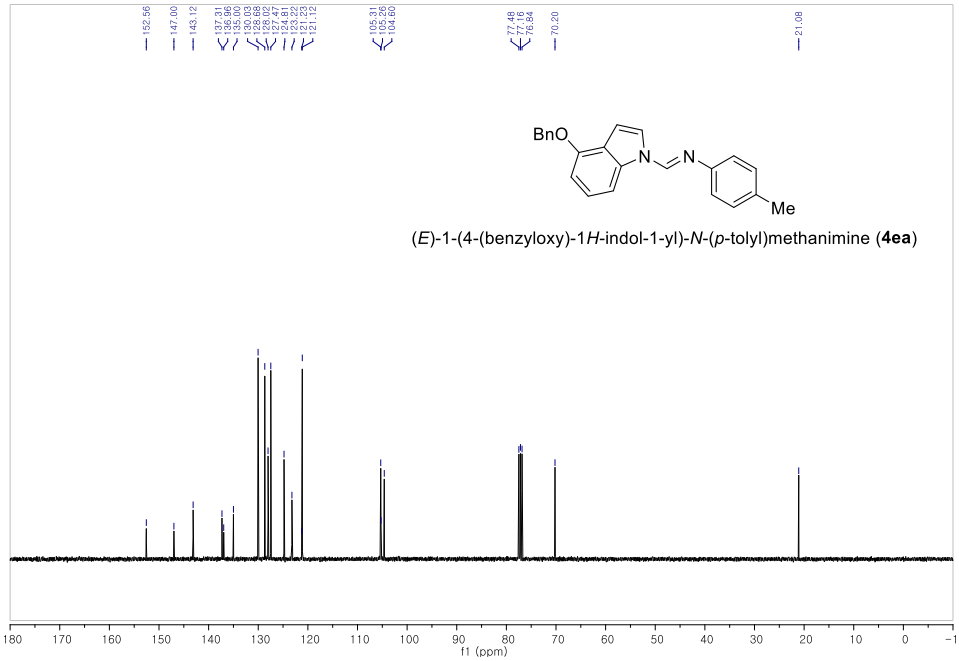

^{13}C NMR ($CDCl_3$, 100 MHz)

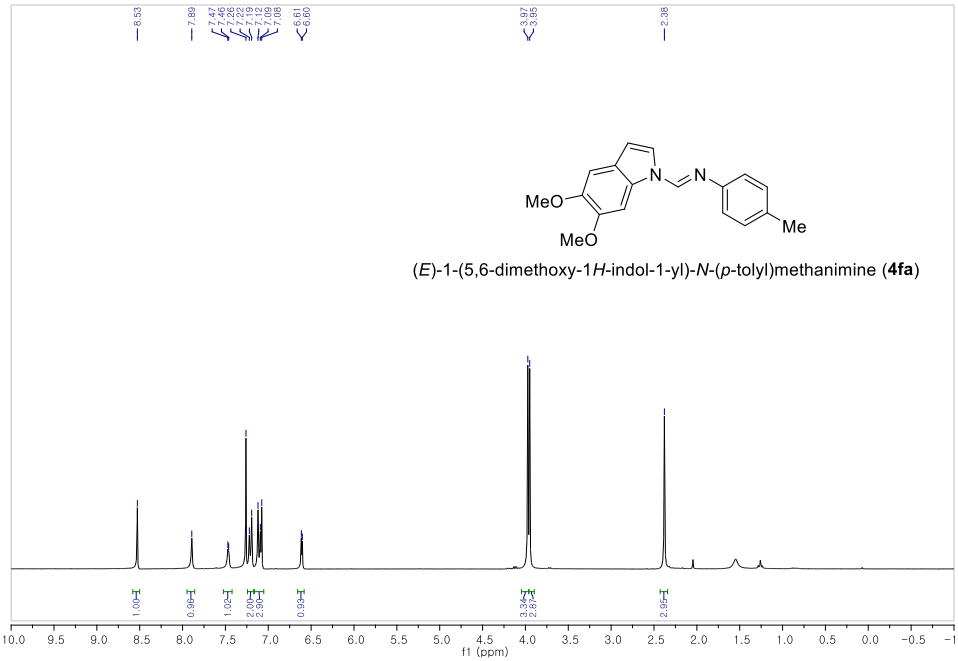

(*E*)-1-(5,6-dimethoxy-1*H*-indol-1-yl)-*N*-(*p*-tolyl)methanimine (**4fa**)

^{1}H NMR ($CDCl_3$, 300 MHz)

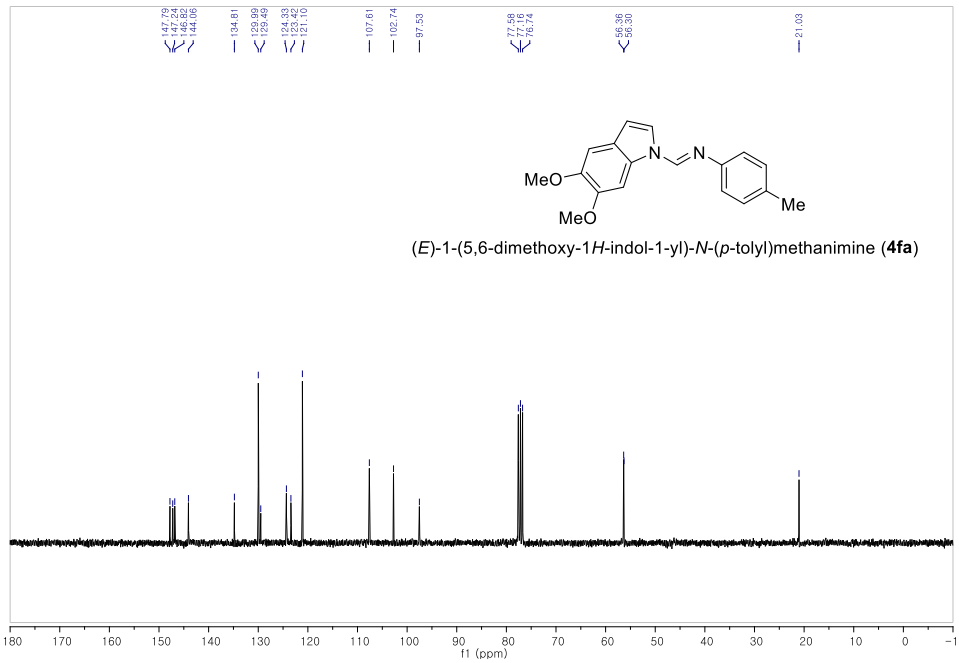

(*E*)-1-(5,6-dimethoxy-1*H*-indol-1-yl)-*N*-(*p*-tolyl)methanimine (**4fa**)

^{13}C NMR ($CDCl_3$, 75 MHz)

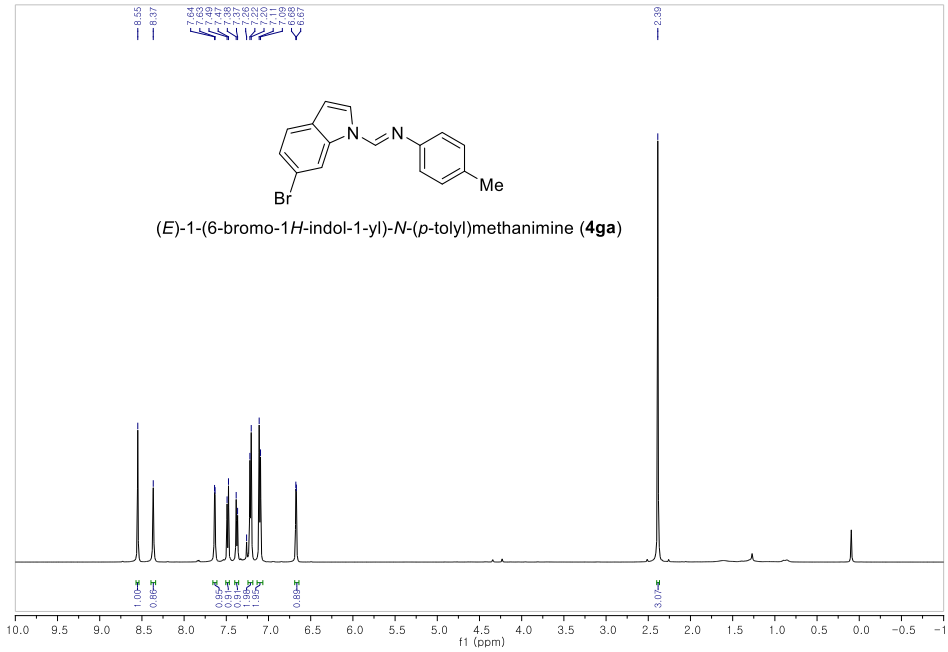

^{1}H NMR ($CDCl_3$, 499 MHz)

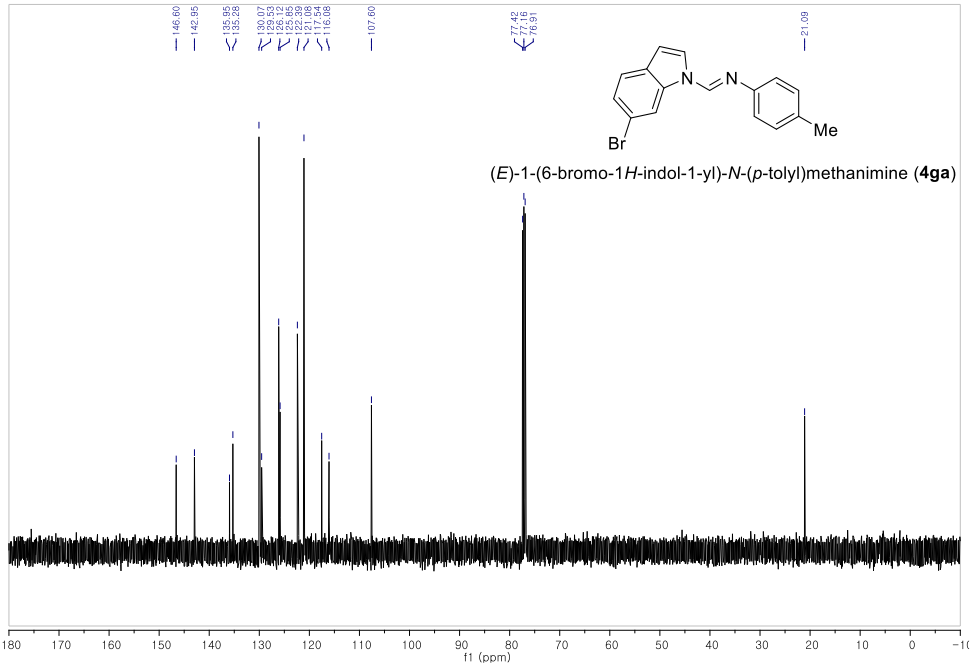

^{13}C NMR ($CDCl_3$, 126 MHz)

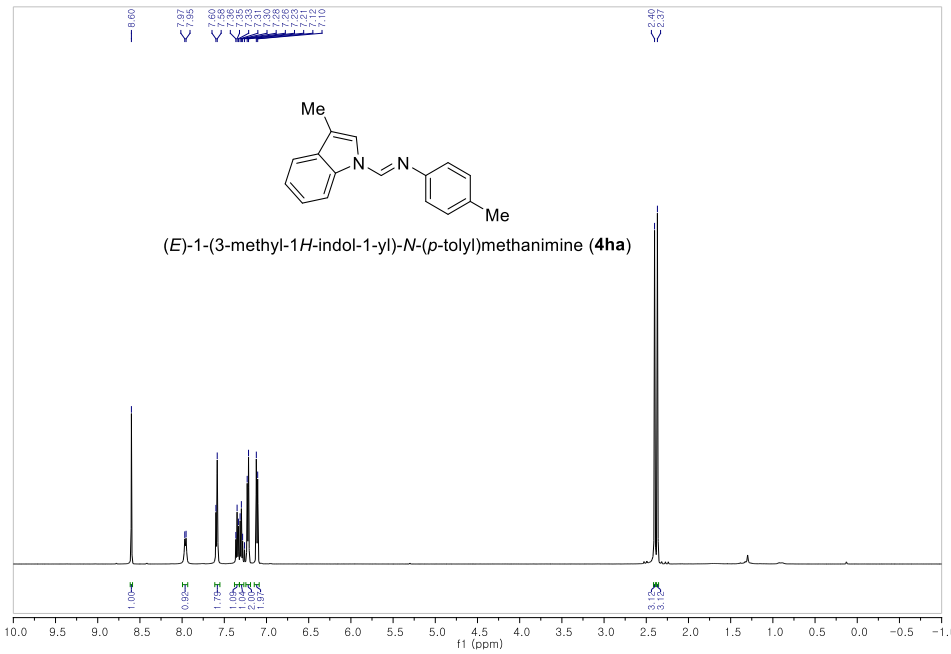

^{1}H NMR ($CDCl_3$, 499 MHz)

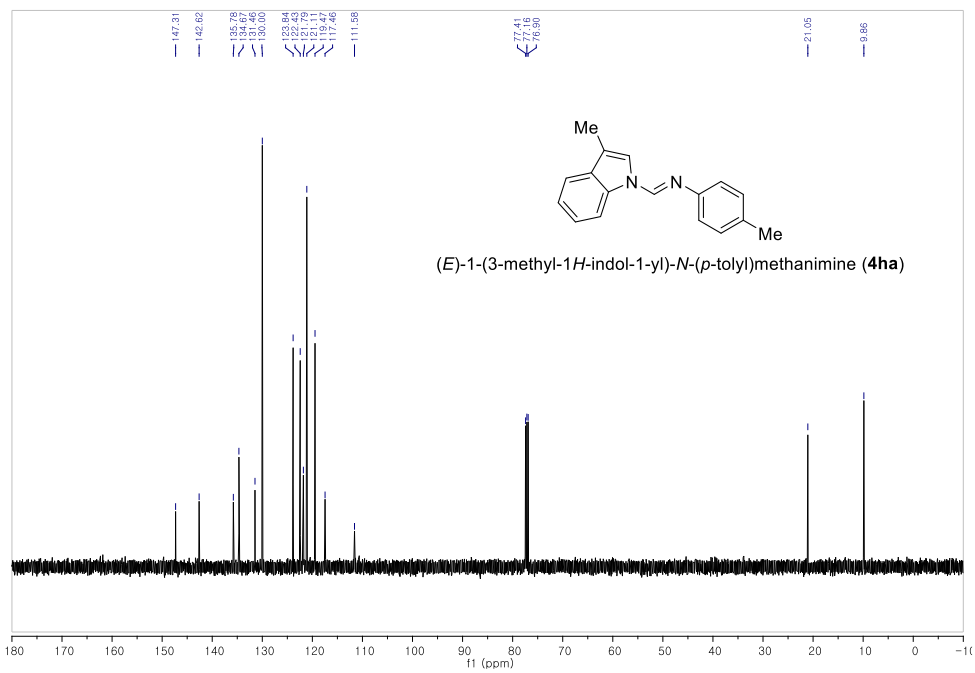

^{13}C NMR ($CDCl_3$, 126 MHz)

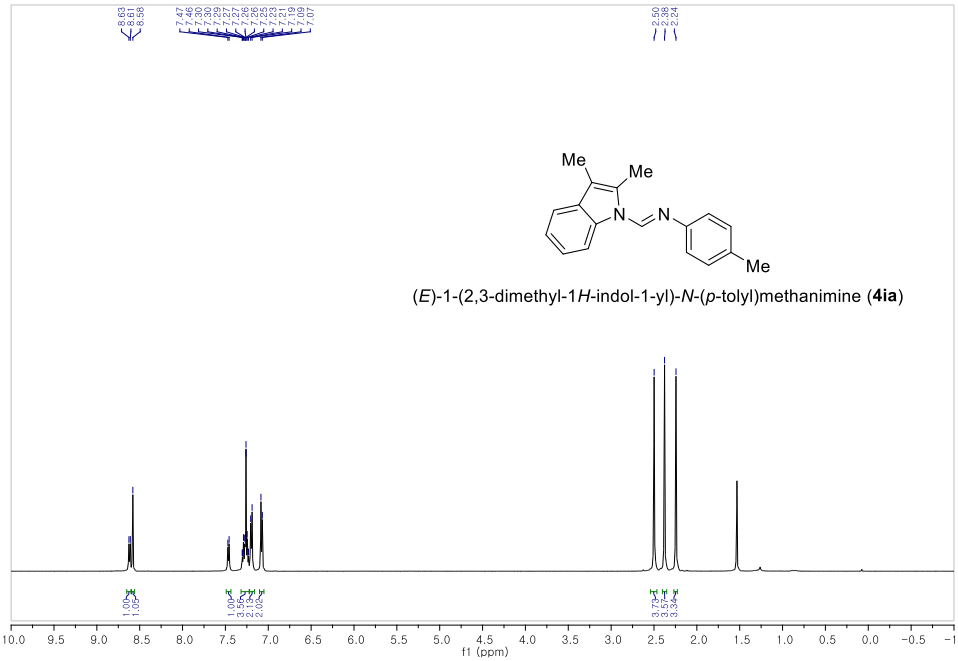

^{1}H NMR ($CDCl_3$, 499 MHz)

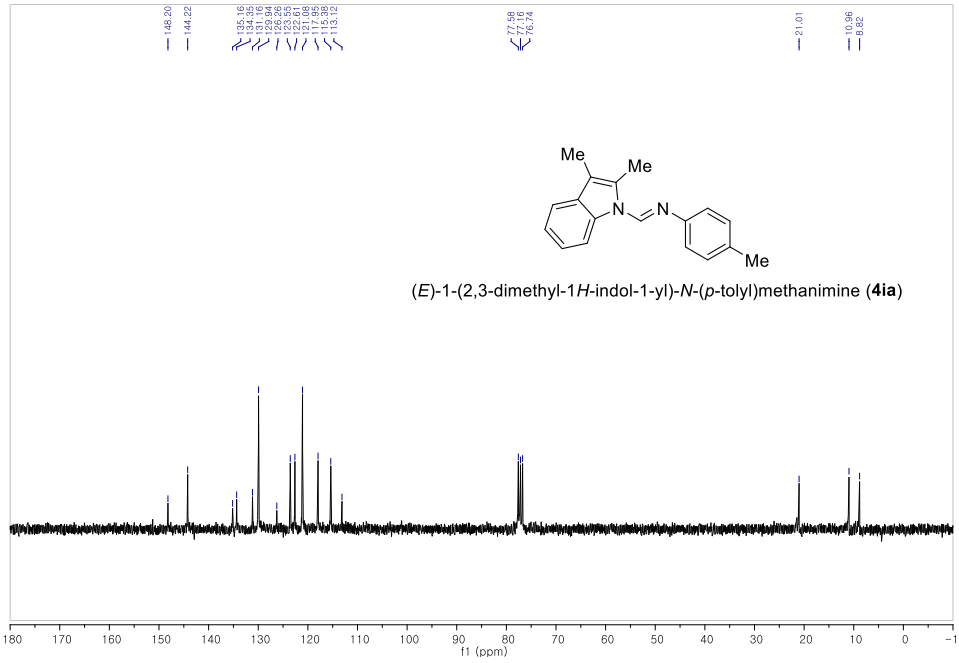

^{13}C NMR ($CDCl_3$, 75 MHz)

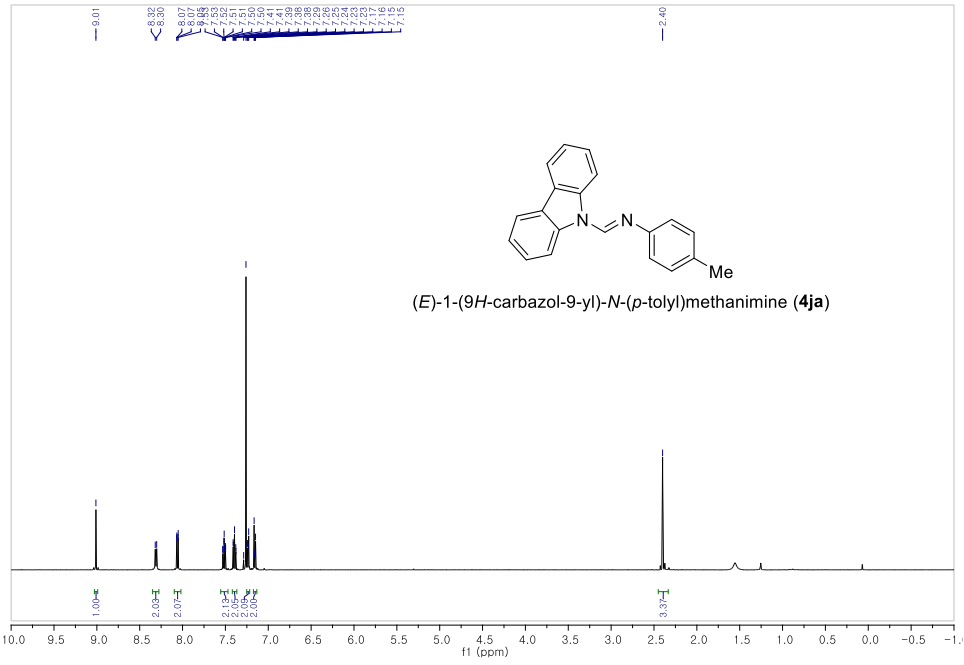

^{1}H NMR ($CDCl_3$, 499 MHz)

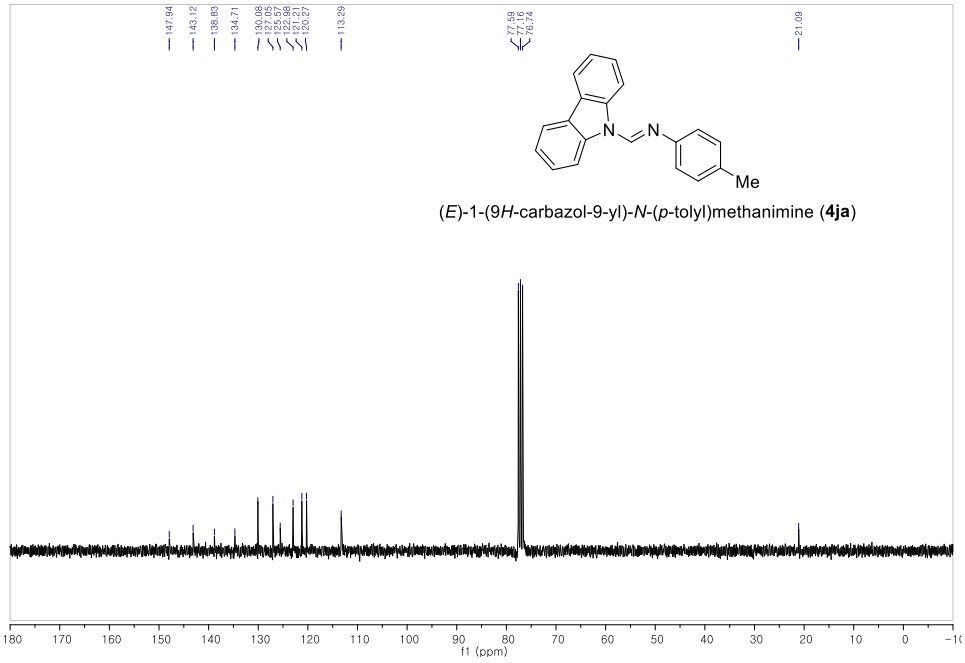

^{13}C NMR ($CDCl_3$, 75 MHz)

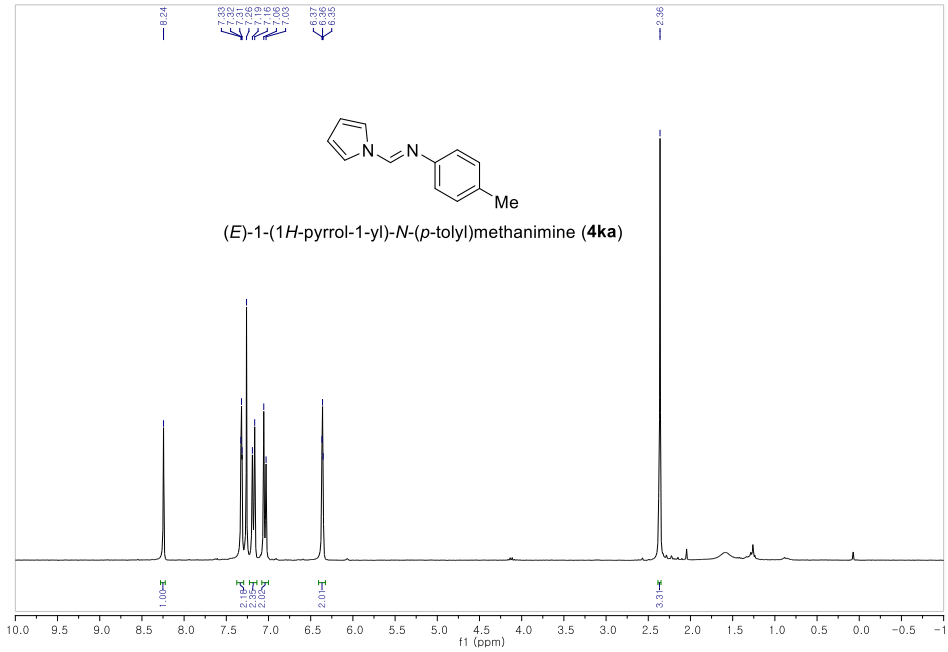

^{1}H NMR ($CDCl_3$, 300 MHz)

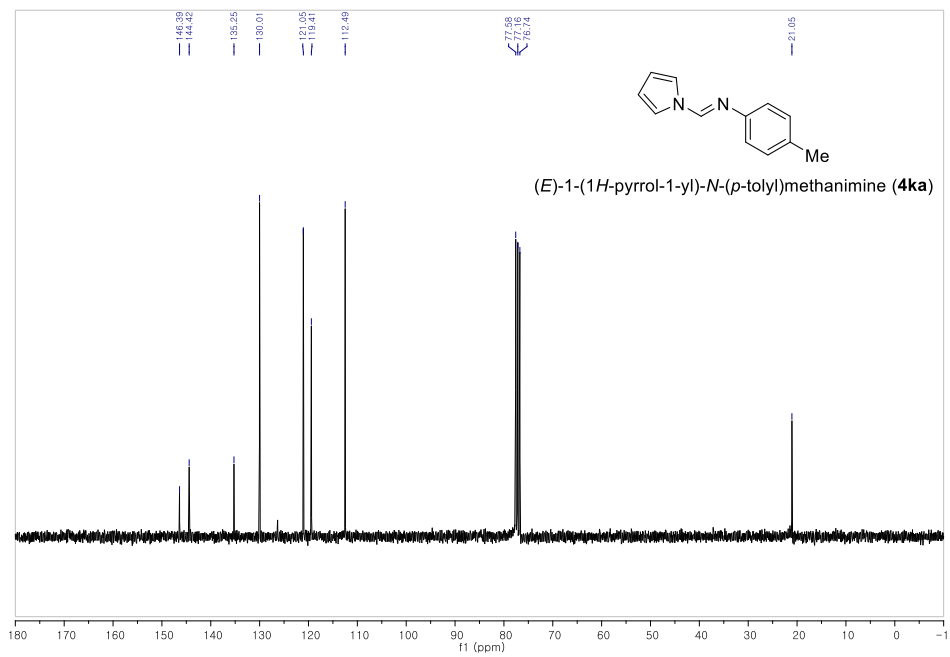

^{13}C NMR ($CDCl_3$, 75 MHz)

Chapter 5

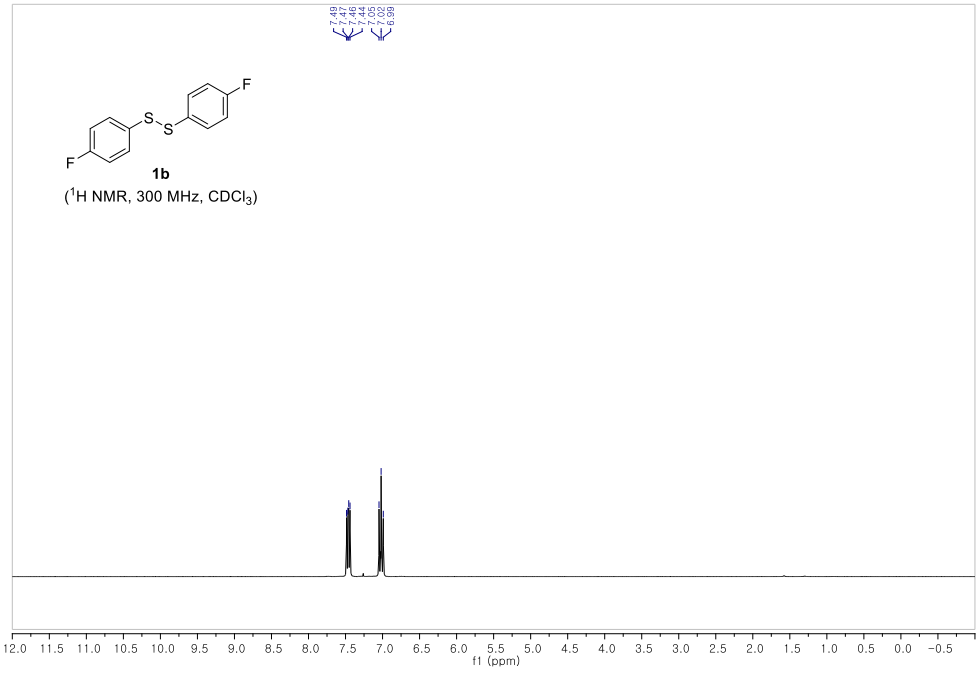
7.49
7.47
7.46
7.44
7.05
7.02
6.99
F
S
S
F
1b
(1H NMR, 300 MHz, CDCl3)
12.0 11.5 11.0 10.5 10.0 9.5 9.0 8.5 8.0 7.5 7.0 6.5 6.0 5.5 5.0 4.5 4.0 3.5 3.0 2.5 2.0 1.5 1.0 0.5 0.0 -0.5
f1 (ppm)

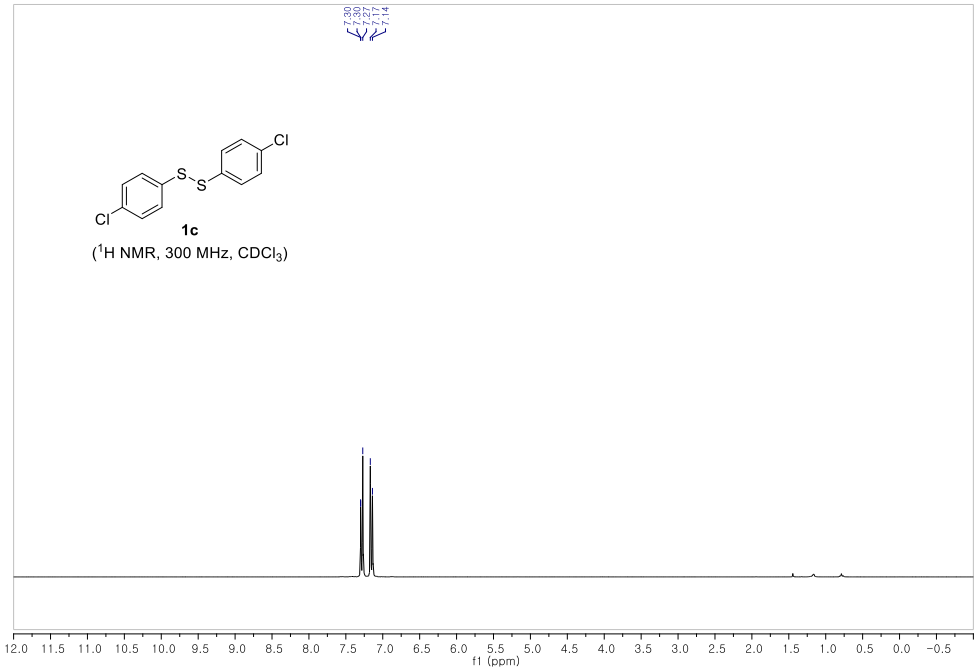
7.30
7.30
7.27
7.17
7.14
Cl
S
S
Cl
1c
(1H NMR, 300 MHz, CDCl3)
12.0 11.5 11.0 10.5 10.0 9.5 9.0 8.5 8.0 7.5 7.0 6.5 6.0 5.5 5.0 4.5 4.0 3.5 3.0 2.5 2.0 1.5 1.0 0.5 0.0 -0.5
f1 (ppm)

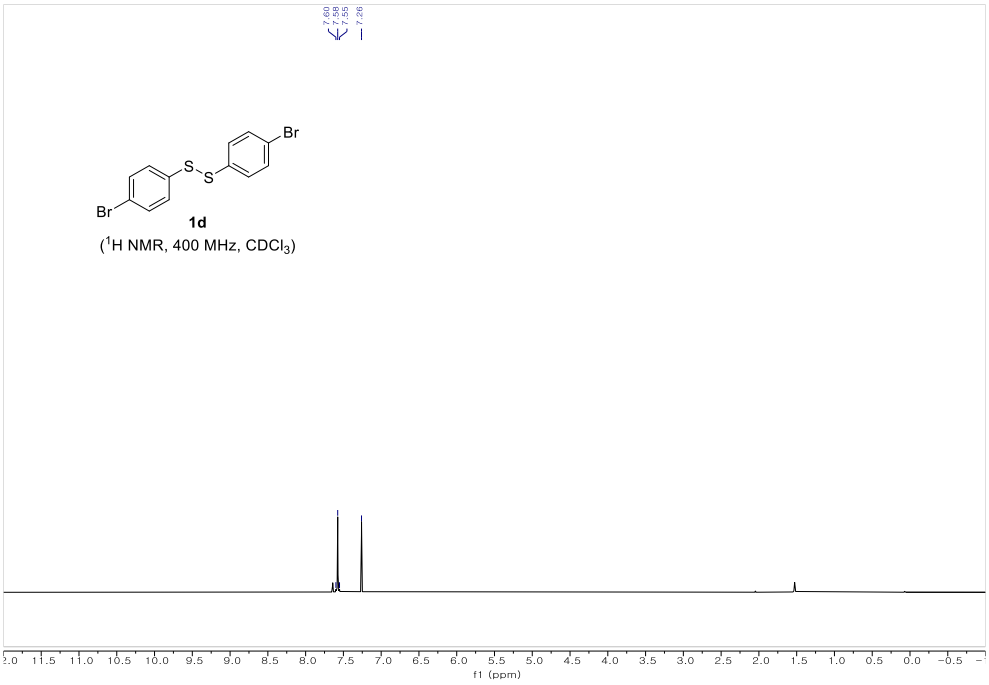
7.69
7.68
7.55
7.26
Br
S
S
Br
1d
(^{1}H NMR, 400 MHz, $CDCl_3$)
f1 (ppm)

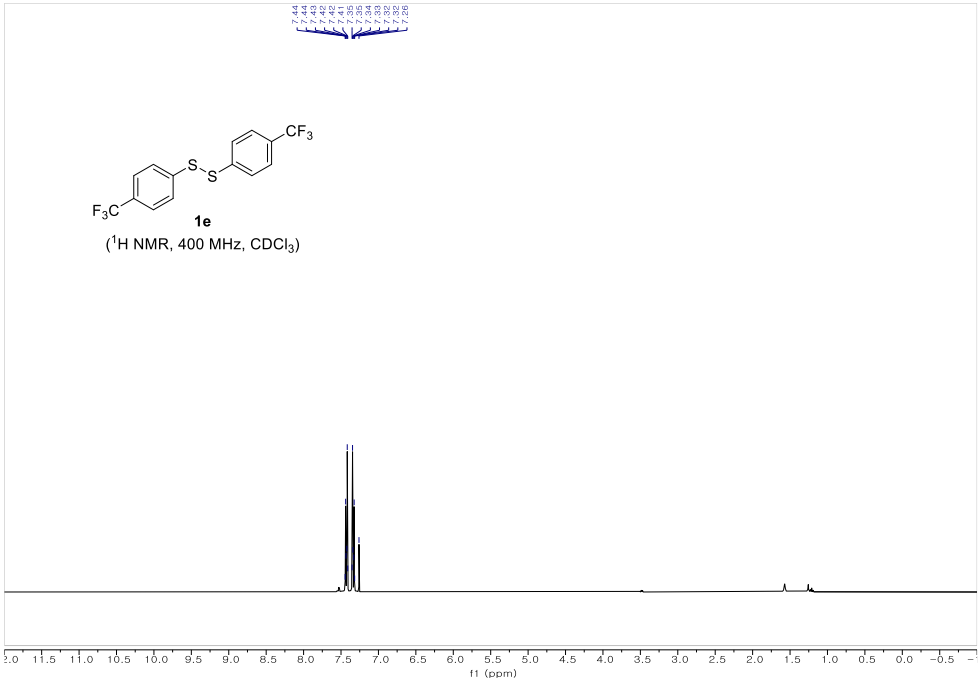
7.44
7.44
7.43
7.42
7.42
7.41
7.35
7.35
7.34
7.33
7.32
7.32
7.26
CF3
S
S
F3C
1e
(^{1}H NMR, 400 MHz, $CDCl_3$)
f1 (ppm)

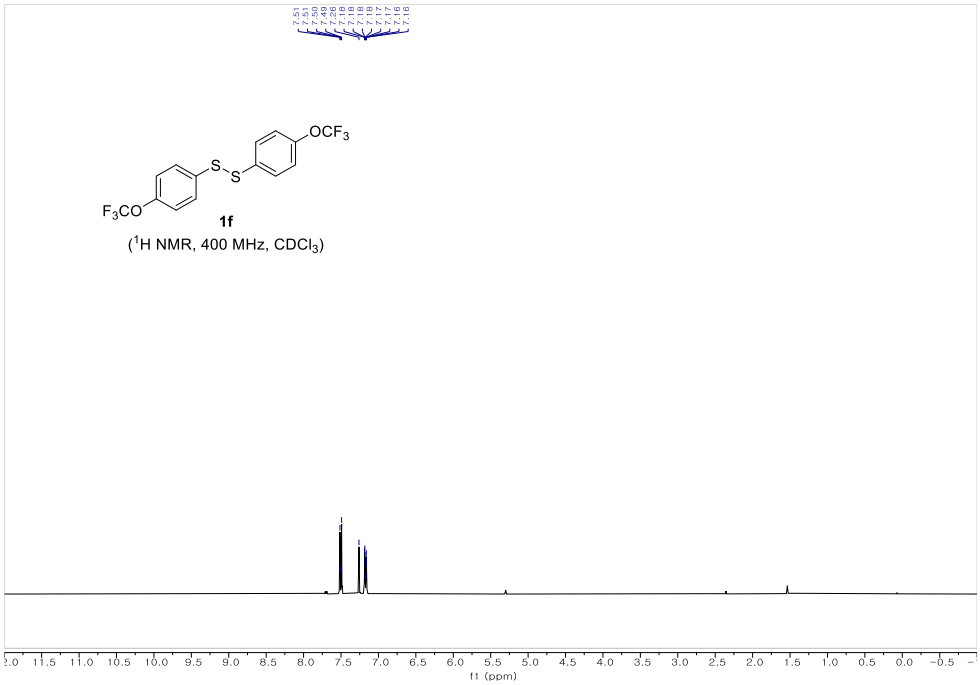
7.51
7.51
7.50
7.49
7.18
7.18
7.18
7.18
7.17
7.17
7.16
7.16
OCF3
S
S
F3CO
1f
(1H NMR, 400 MHz, CDCl3)
f1 (ppm)

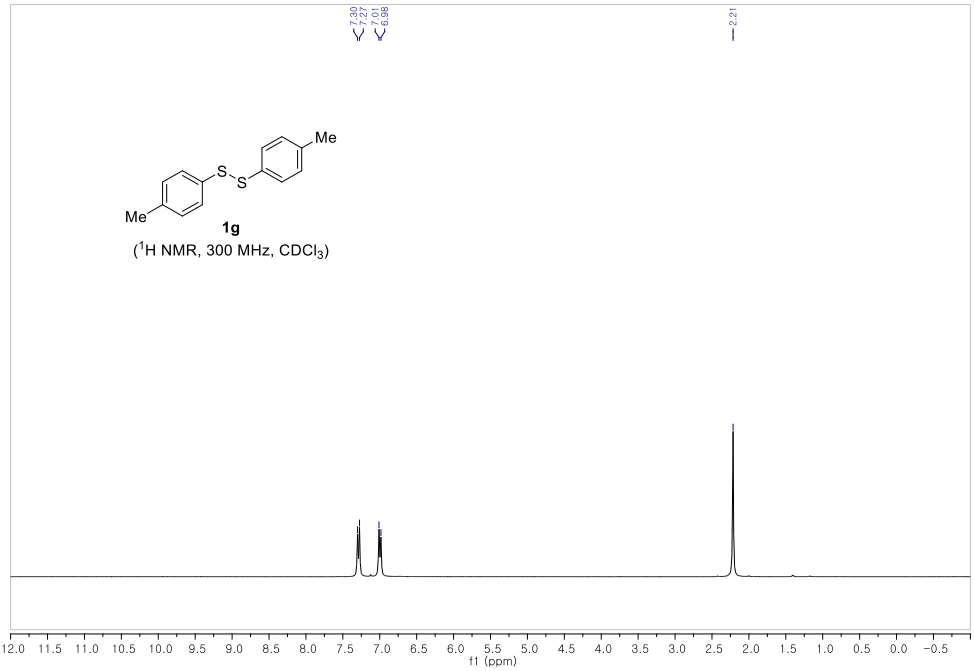
7.30
7.27
7.01
6.98
2.21
Me
S
S
Me
1g
(1H NMR, 300 MHz, CDCl3)
f1 (ppm)

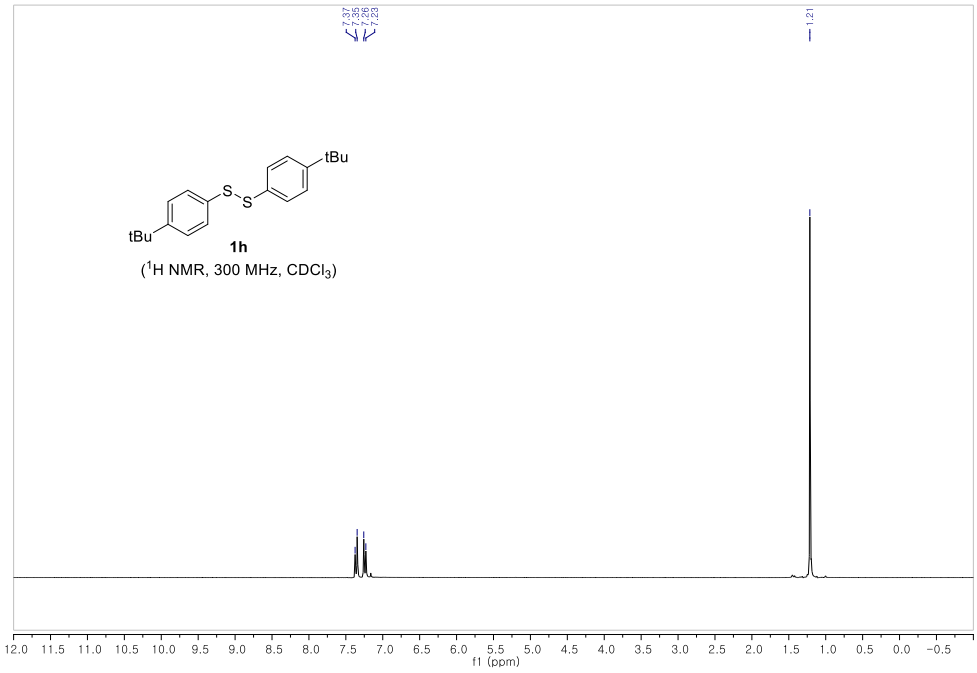

1h

(^{1}H NMR, 300 MHz, $CDCl_3$)

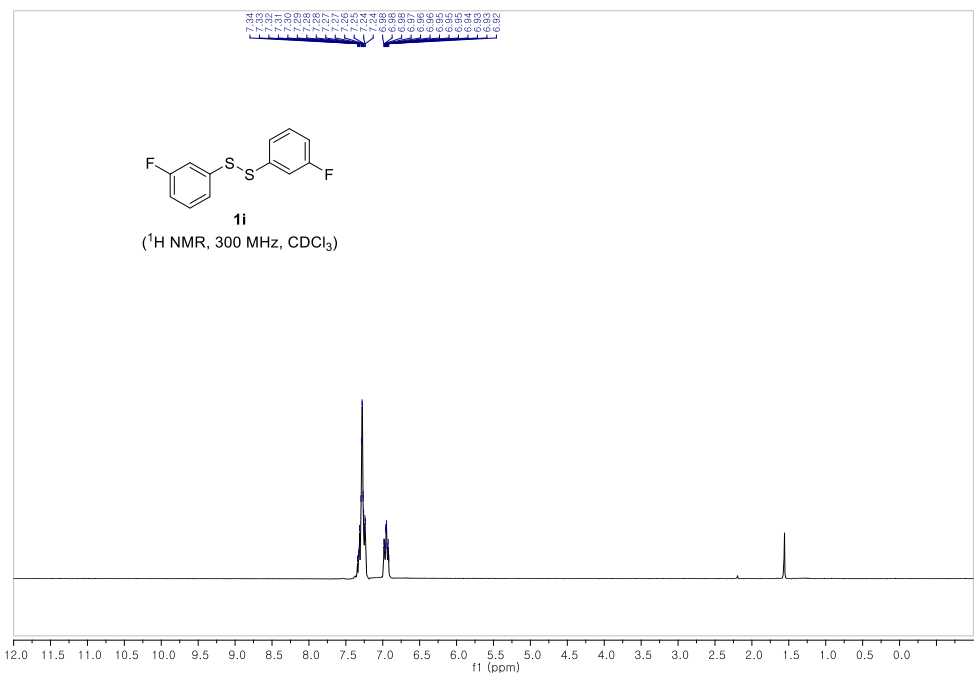

1i

(^{1}H NMR, 300 MHz, $CDCl_3$)

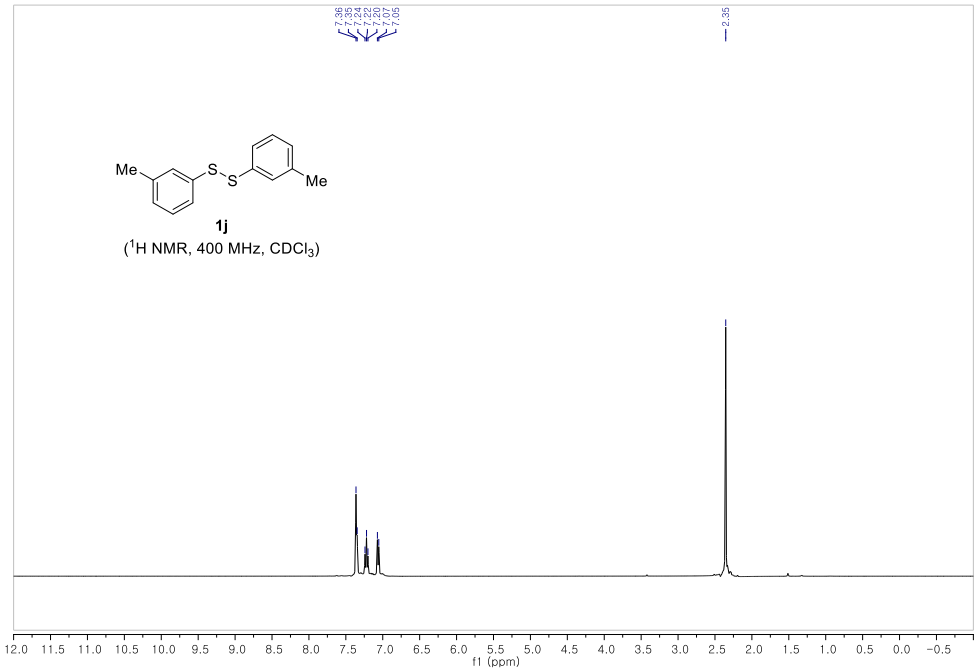
7.36
7.35
7.24
7.22
7.20
7.07
7.05
2.35
Me
S
S
Me
1j
(1H NMR, 400 MHz, CDCl3)
12.0 11.5 11.0 10.5 10.0 9.5 9.0 8.5 8.0 7.5 7.0 6.5 6.0 5.5 5.0 4.5 4.0 3.5 3.0 2.5 2.0 1.5 1.0 0.5 0.0 −0.5
f1 (ppm)

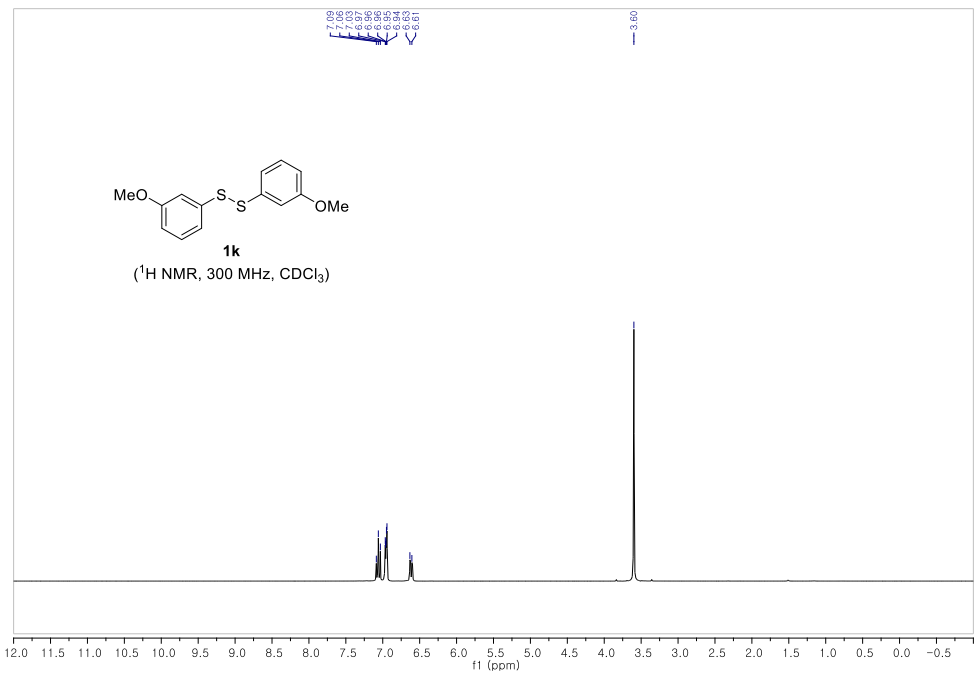
7.09
7.06
7.03
6.97
6.96
6.95
6.95
6.94
6.63
6.61
3.60
MeO
S
S
OMe
1k
(1H NMR, 300 MHz, CDCl3)
12.0 11.5 11.0 10.5 10.0 9.5 9.0 8.5 8.0 7.5 7.0 6.5 6.0 5.5 5.0 4.5 4.0 3.5 3.0 2.5 2.0 1.5 1.0 0.5 0.0 −0.5
f1 (ppm)

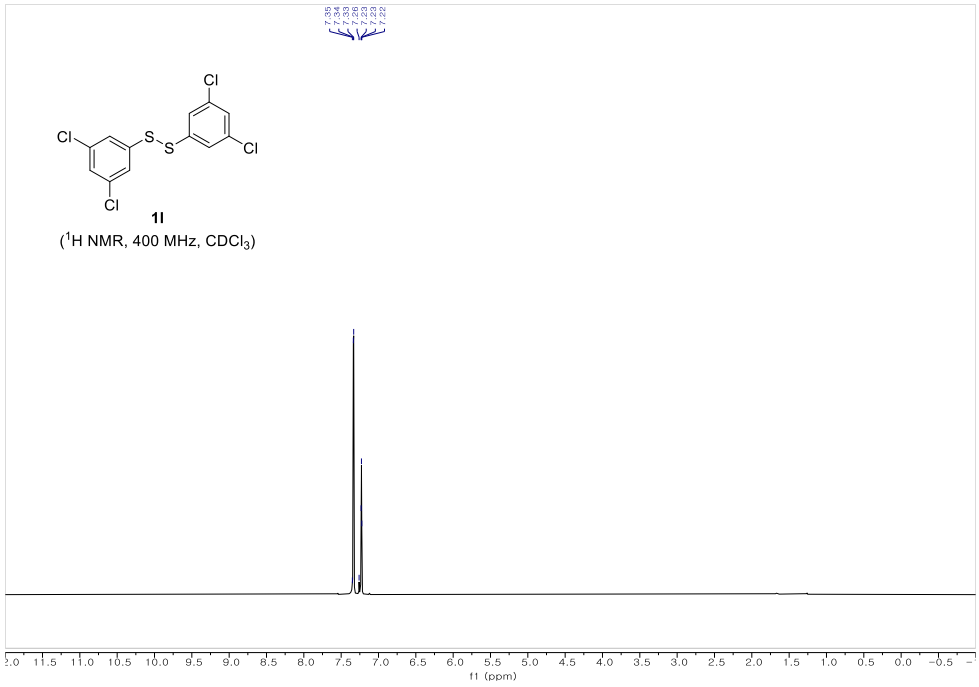
7.35
7.34
7.28
7.23
7.23
7.22
Cl
Cl
S
S
Cl
Cl
1l
(1H NMR, 400 MHz, CDCl3)
f1 (ppm)

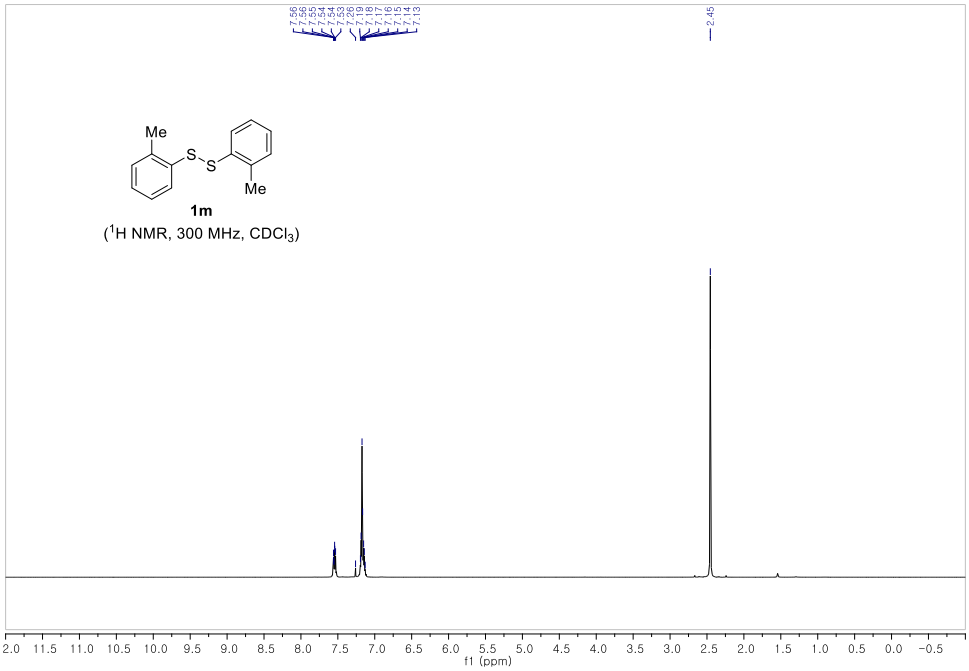
7.56
7.56
7.55
7.55
7.54
7.54
7.53
7.26
7.19
7.18
7.17
7.16
7.15
7.14
7.13
2.45
Me
S
S
Me
1m
(1H NMR, 300 MHz, CDCl3)
f1 (ppm)

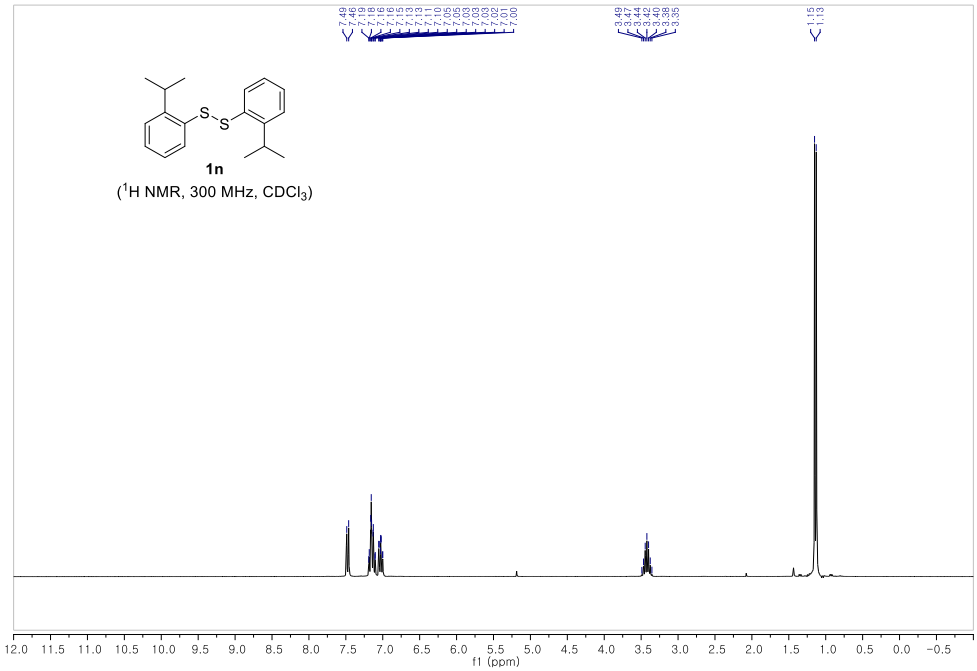
7.49
7.46
7.19
7.18
7.16
7.15
7.13
7.13
7.11
7.10
7.05
7.03
7.03
7.02
7.01
7.00
3.49
3.47
3.44
3.42
3.40
3.38
3.35
1.15
1.13
S
S
1n
(1H NMR, 300 MHz, CDCl3)
12.0 11.5 11.0 10.5 10.0 9.5 9.0 8.5 8.0 7.5 7.0 6.5 6.0 5.5 5.0 4.5 4.0 3.5 3.0 2.5 2.0 1.5 1.0 0.5 0.0 -0.5
f1 (ppm)

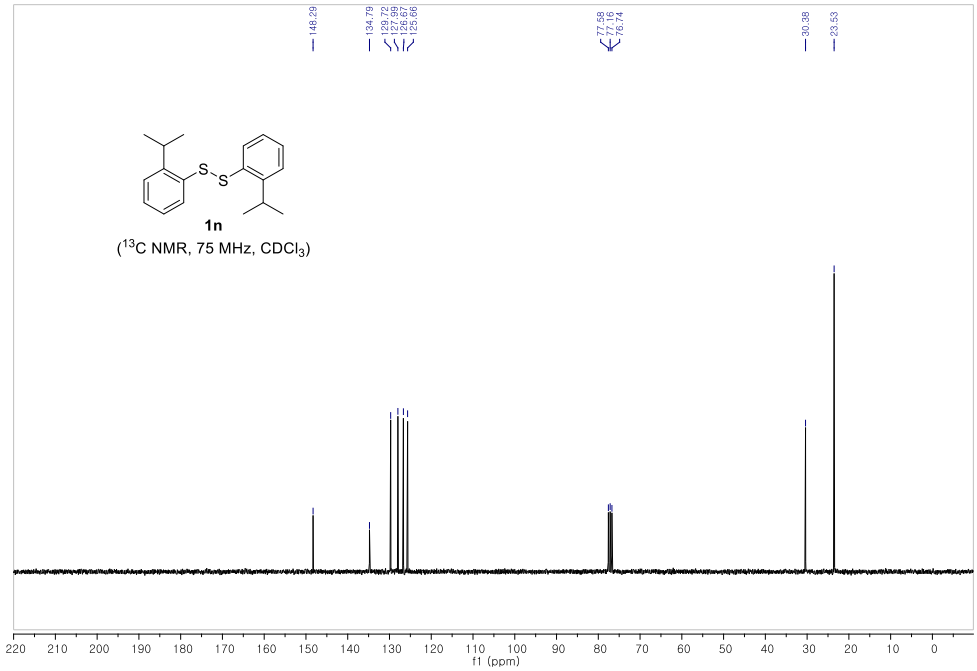
148.29
134.79
129.72
127.99
126.67
125.66
77.58
77.16
76.74
30.38
23.53
S
S
1n
(13C NMR, 75 MHz, CDCl3)
220 210 200 190 180 170 160 150 140 130 120 110 100 90 80 70 60 50 40 30 20 10 0
f1 (ppm)

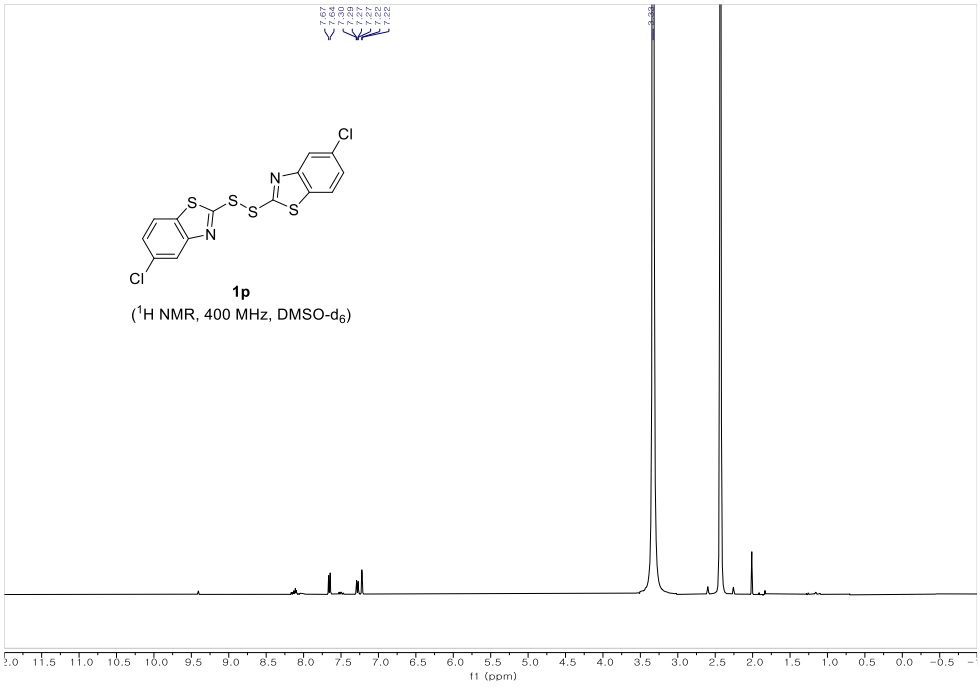

1p

(^{1}H NMR, 400 MHz, DMSO-d_6)

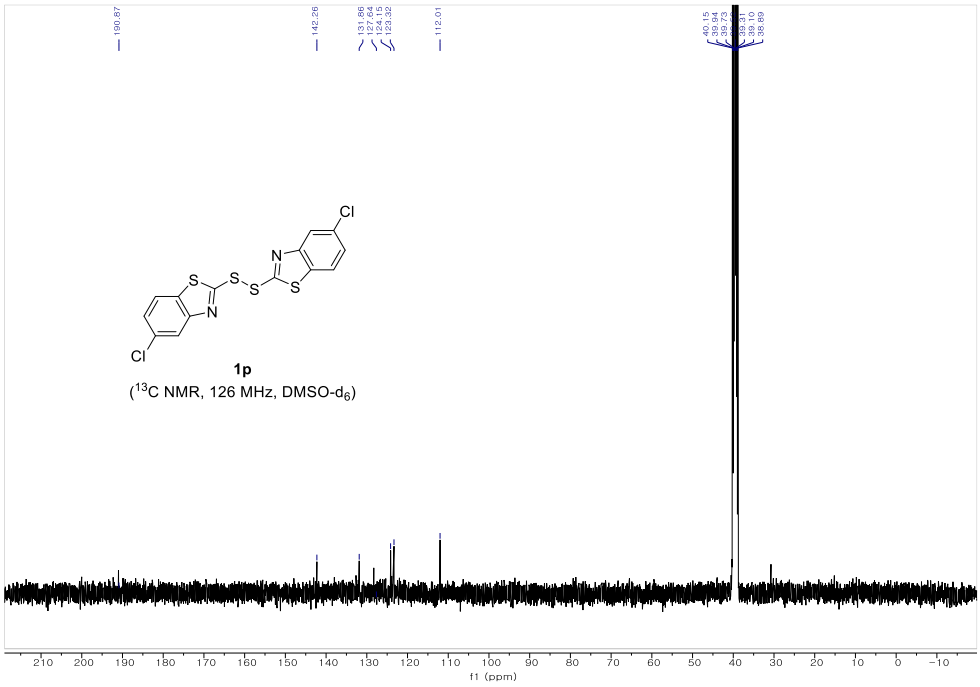

1p

(^{13}C NMR, 126 MHz, DMSO-d_6)

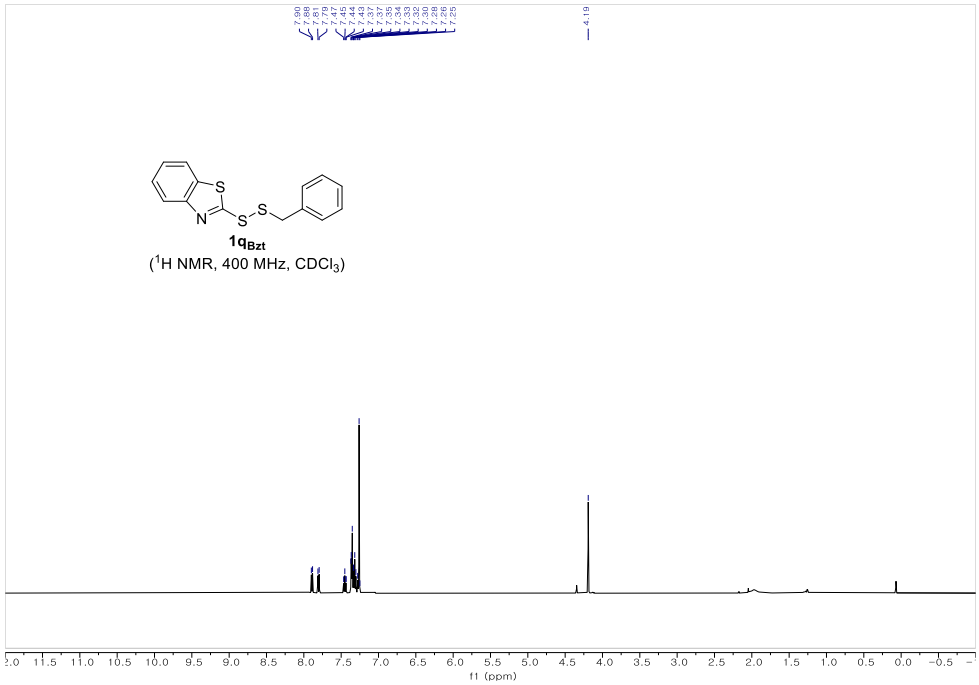

1q$_{Bzt}$
(^{1}H NMR, 400 MHz, $CDCl_3$)

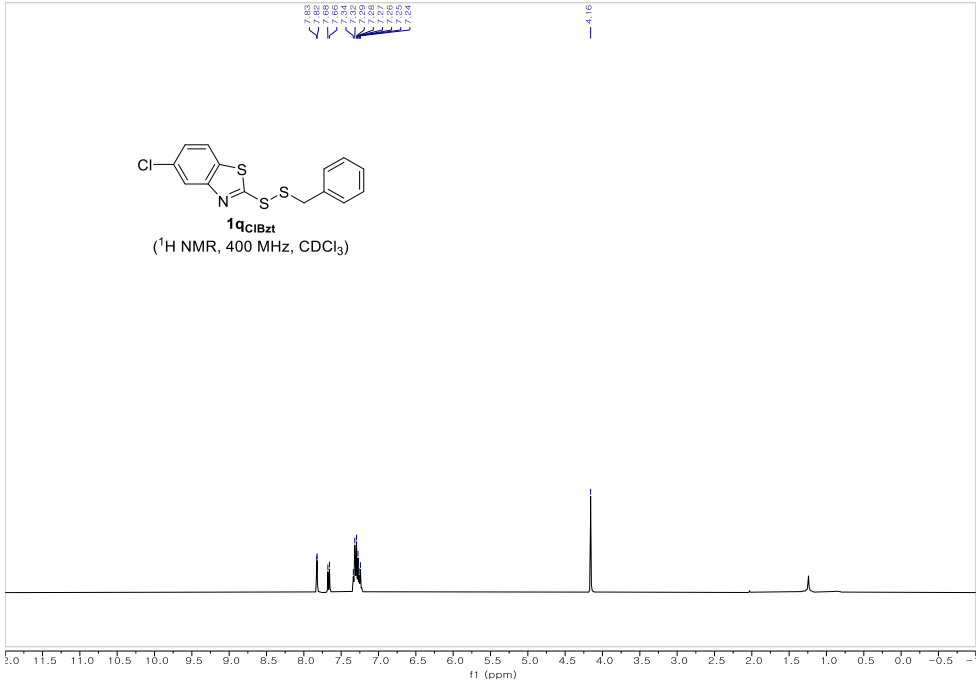

1q$_{ClBzt}$
(^{1}H NMR, 400 MHz, $CDCl_3$)

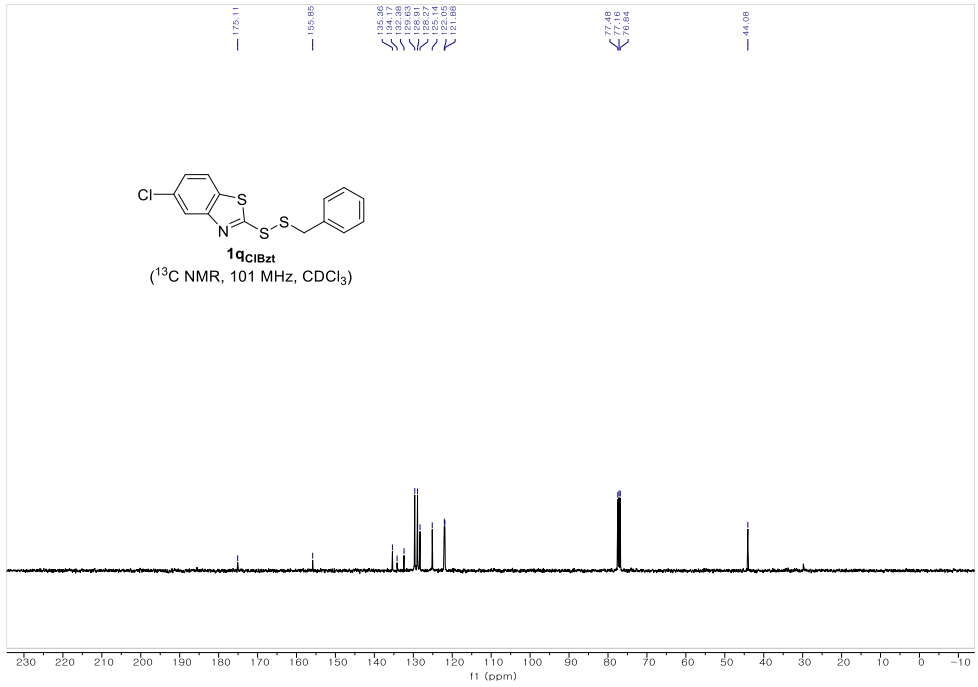
175.11
155.85
135.36
134.77
134.38
129.63
128.91
128.27
125.14
122.65
121.88
77.48
77.16
76.84
44.08
Cl
S
N
S
S
1q$_{ClBzt}$
(^{13}C NMR, 101 MHz, CDCl$_3$)
230 220 210 200 190 180 170 160 150 140 130 120 110 100 90 80 70 60 50 40 30 20 10 0 −10
f1 (ppm)

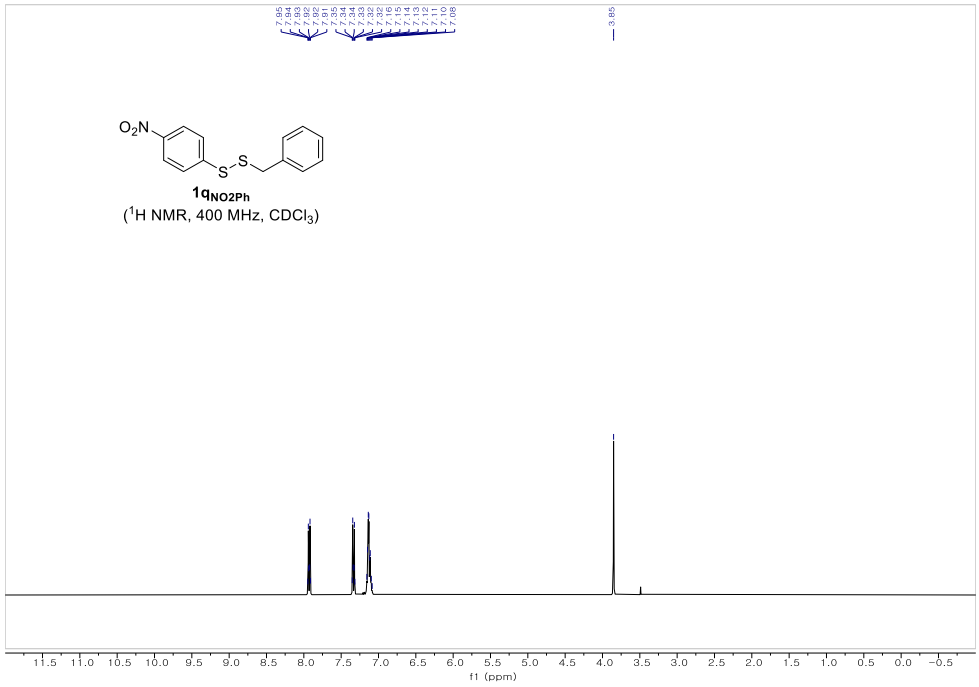
7.95
7.94
7.93
7.92
7.92
7.91
7.35
7.34
7.33
7.32
7.16
7.15
7.14
7.13
7.12
7.11
7.10
7.09
3.85
O$_2$N
S
S
1q$_{NO2Ph}$
(^{1}H NMR, 400 MHz, CDCl$_3$)
11.5 11.0 10.5 10.0 9.5 9.0 8.5 8.0 7.5 7.0 6.5 6.0 5.5 5.0 4.5 4.0 3.5 3.0 2.5 2.0 1.5 1.0 0.5 0.0 −0.5
f1 (ppm)

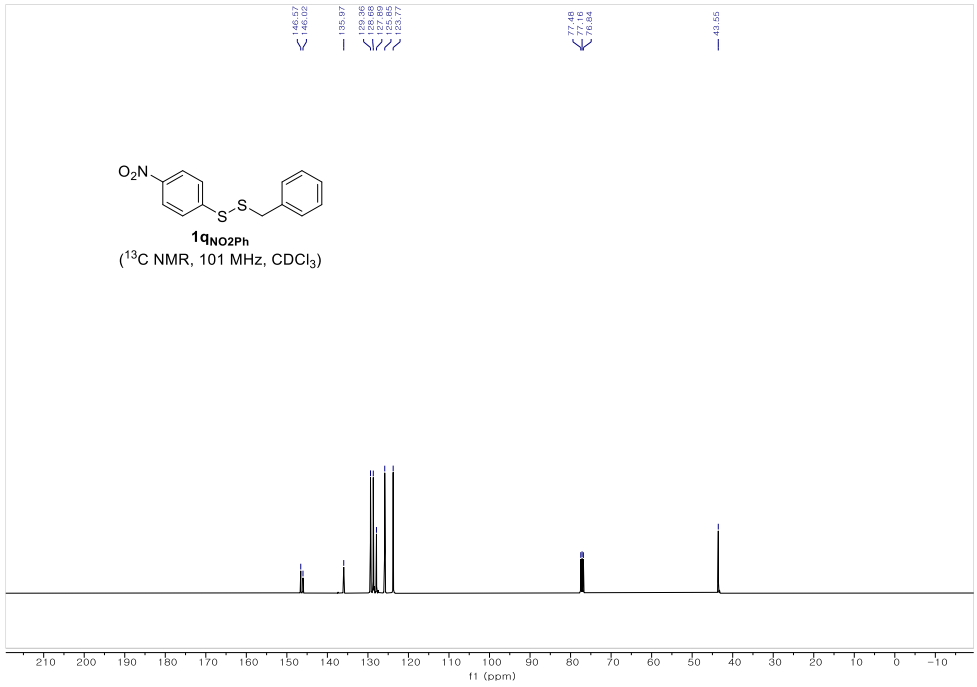

1q$_{NO2Ph}$
(^{13}C NMR, 101 MHz, $CDCl_3$)

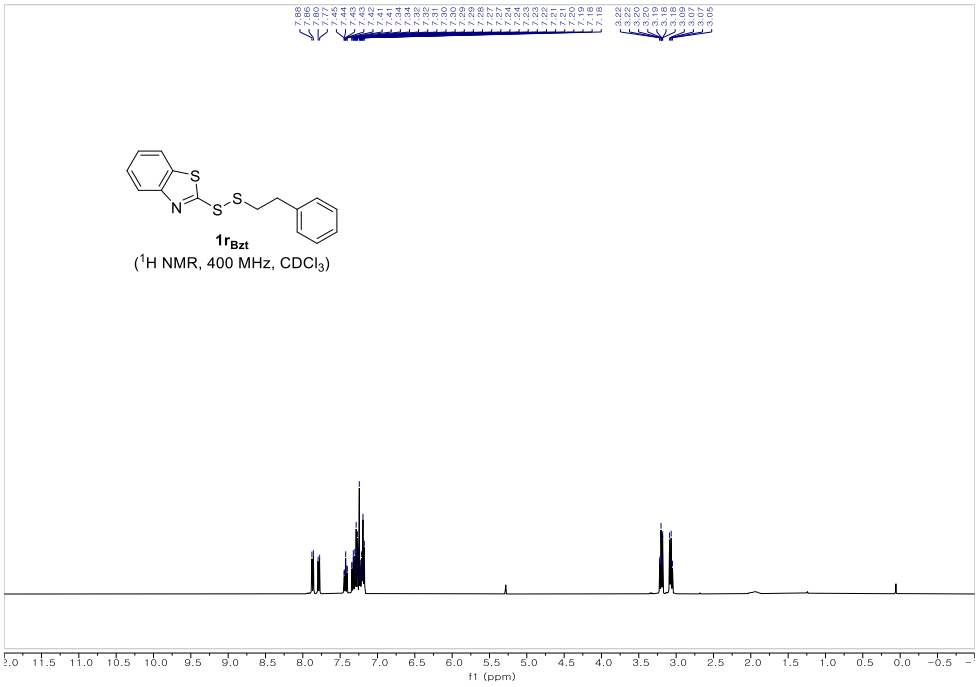

1r$_{Bzt}$
(^{1}H NMR, 400 MHz, $CDCl_3$)

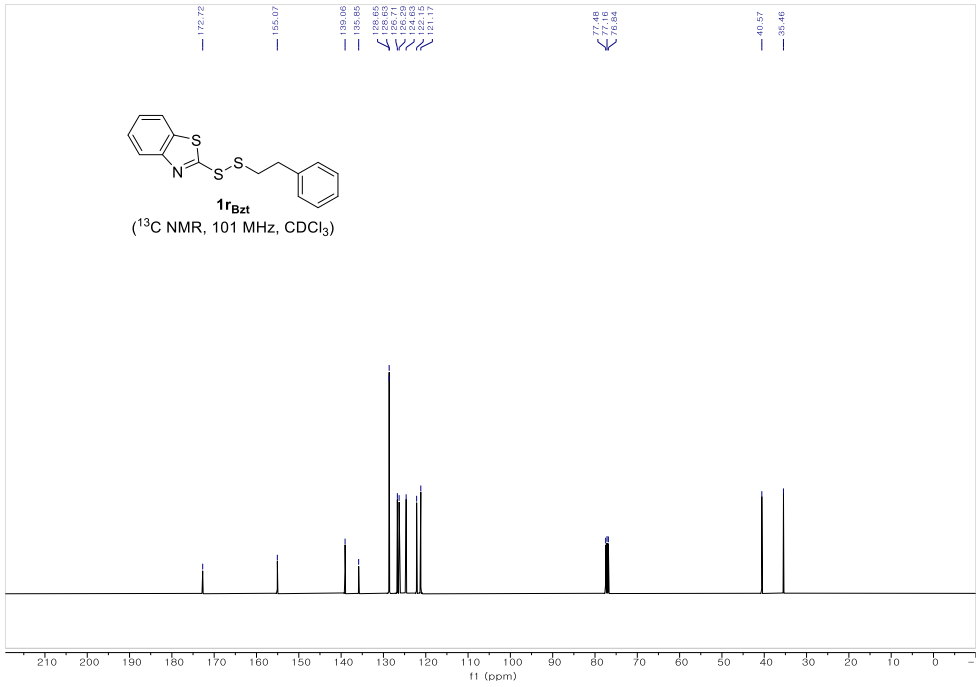
172.72
155.07
139.06
135.85
128.65
128.50
126.71
124.89
122.15
121.17
77.48
77.16
76.84
40.57
35.46
1r$_{Bzt}$
(^{13}C NMR, 101 MHz, CDCl$_3$)
f1 (ppm)

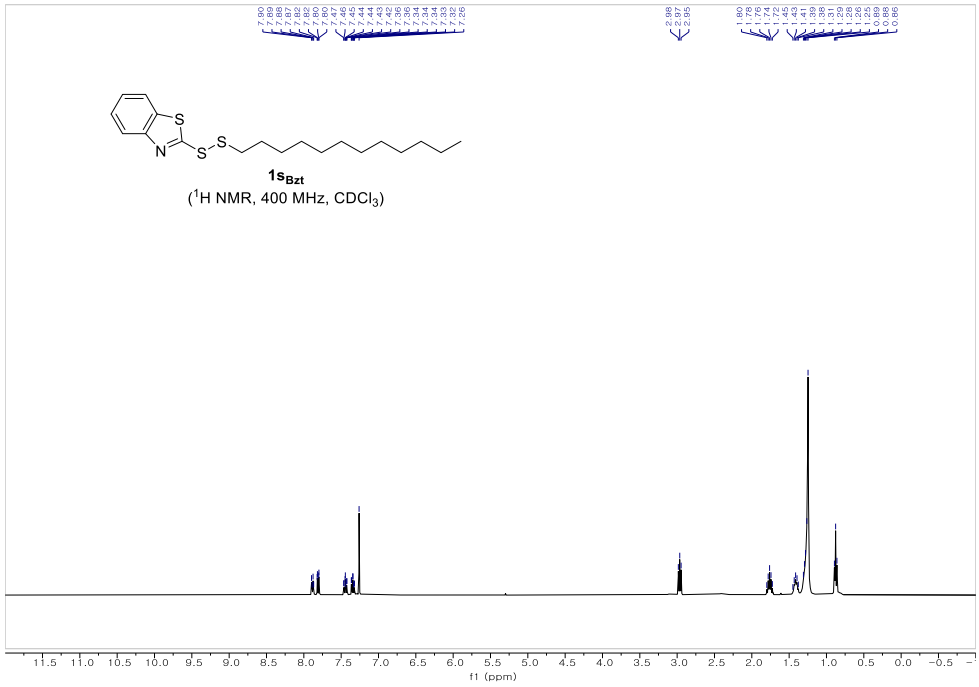
7.90
7.89
7.88
7.87
7.82
7.82
7.80
7.80
7.47
7.46
7.45
7.44
7.43
7.42
7.36
7.36
7.34
7.34
7.33
7.33
7.26
2.98
2.97
2.95
1.80
1.78
1.76
1.74
1.72
1.45
1.43
1.41
1.39
1.38
1.31
1.29
1.28
1.26
1.25
0.89
0.88
0.86
1s$_{Bzt}$
(^{1}H NMR, 400 MHz, CDCl$_3$)
f1 (ppm)

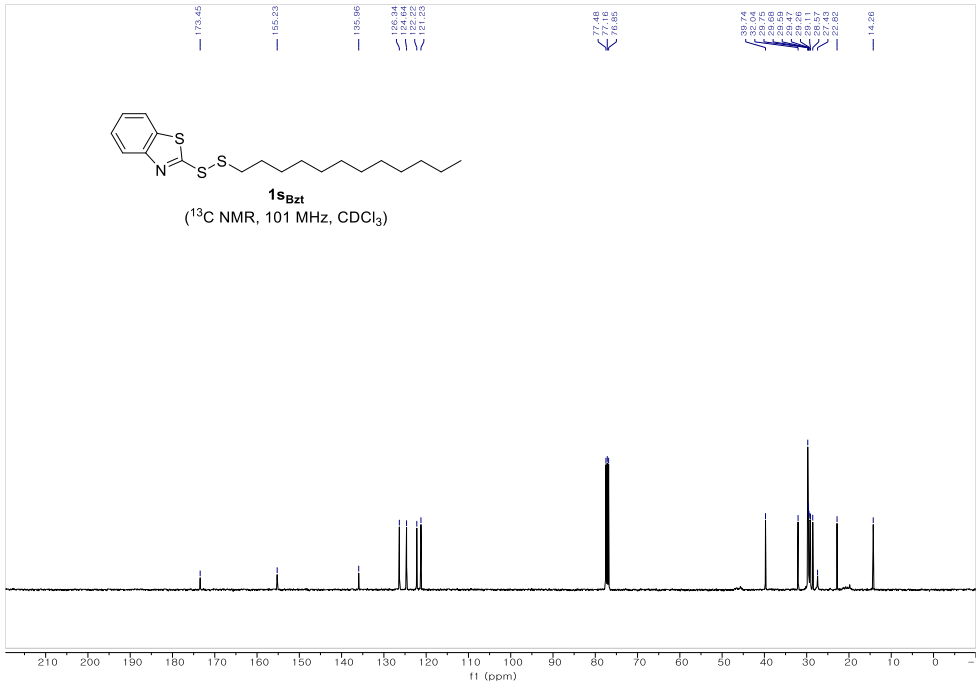
173.45
155.23
135.96
126.34
124.64
122.52
121.23
77.48
77.16
76.85
39.74
37.74
29.75
29.68
29.59
29.47
29.26
29.11
28.57
27.43
22.82
14.26
S
N
S
S
1s$_{Bzt}$
(^{13}C NMR, 101 MHz, CDCl$_3$)
f1 (ppm)

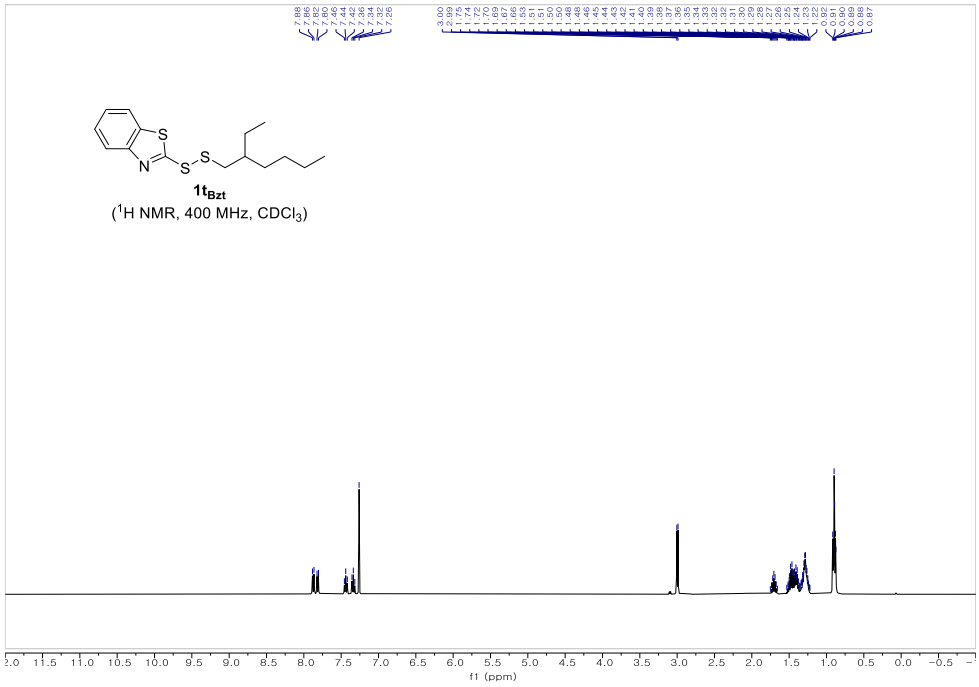
7.88
7.86
7.82
7.80
7.46
7.44
7.42
7.38
7.34
7.32
7.26
3.00
2.99
1.75
1.74
1.72
1.70
1.69
1.67
1.66
1.53
1.51
1.51
1.50
1.50
1.49
1.48
1.46
1.45
1.44
1.43
1.42
1.41
1.40
1.39
1.38
1.37
1.36
1.35
1.34
1.33
1.32
1.31
1.30
1.29
1.28
1.27
1.26
1.25
1.24
1.23
1.22
0.92
0.91
0.90
0.89
0.88
0.87
S
N
S
S
1t$_{Bzt}$
(^{1}H NMR, 400 MHz, CDCl$_3$)
f1 (ppm)

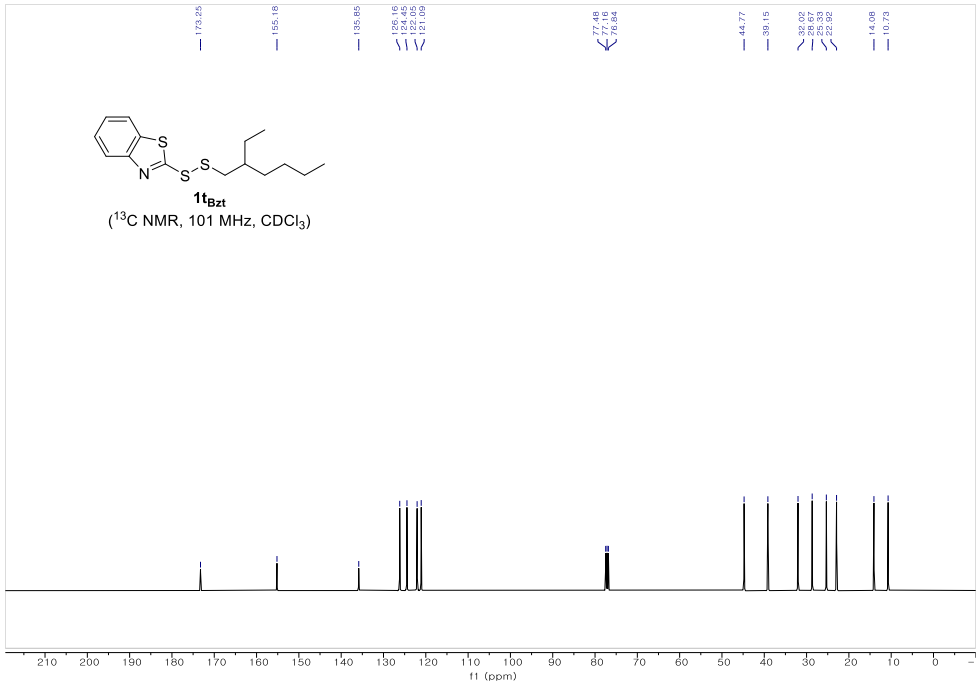

1t$_{Bzt}$
(^{13}C NMR, 101 MHz, $CDCl_3$)

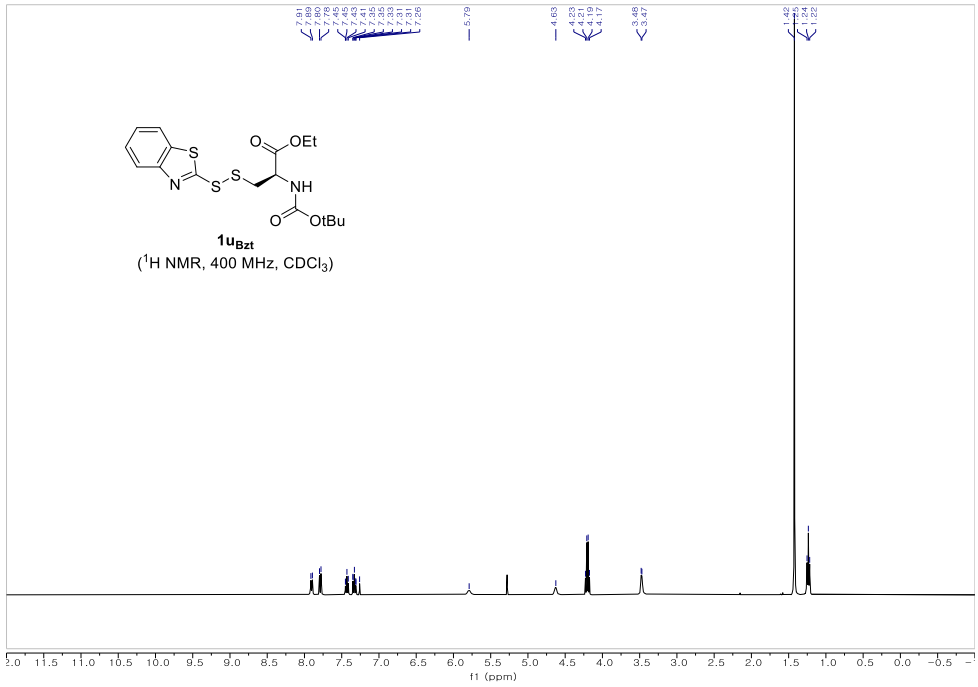

1u$_{Bzt}$
(^{1}H NMR, 400 MHz, $CDCl_3$)

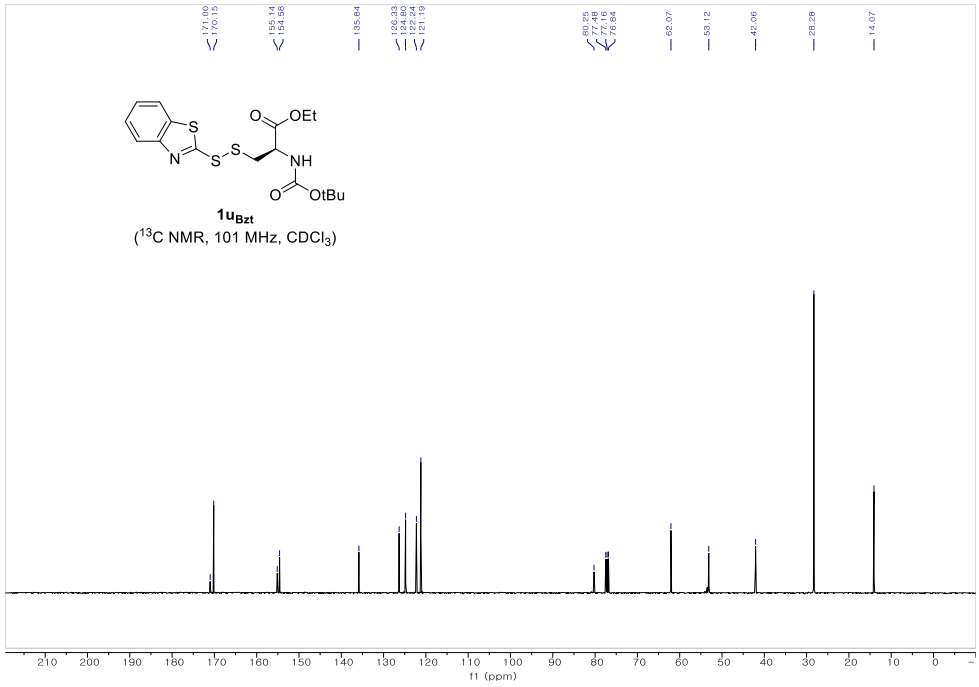

1u$_{Bzt}$

(^{13}C NMR, 101 MHz, CDCl$_3$)

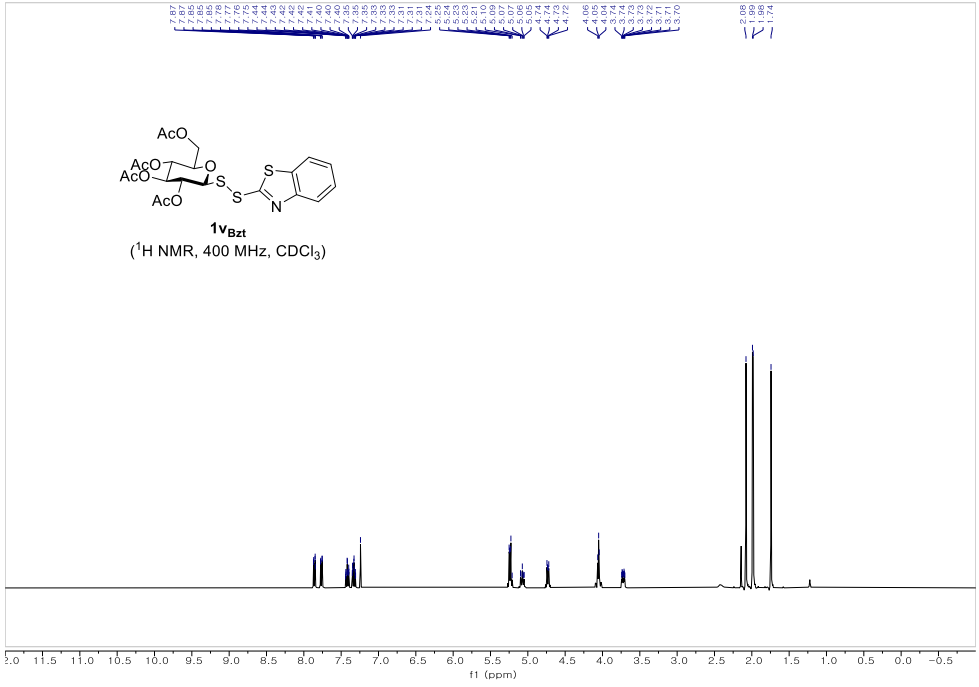

1v$_{Bzt}$

(^{1}H NMR, 400 MHz, CDCl$_3$)

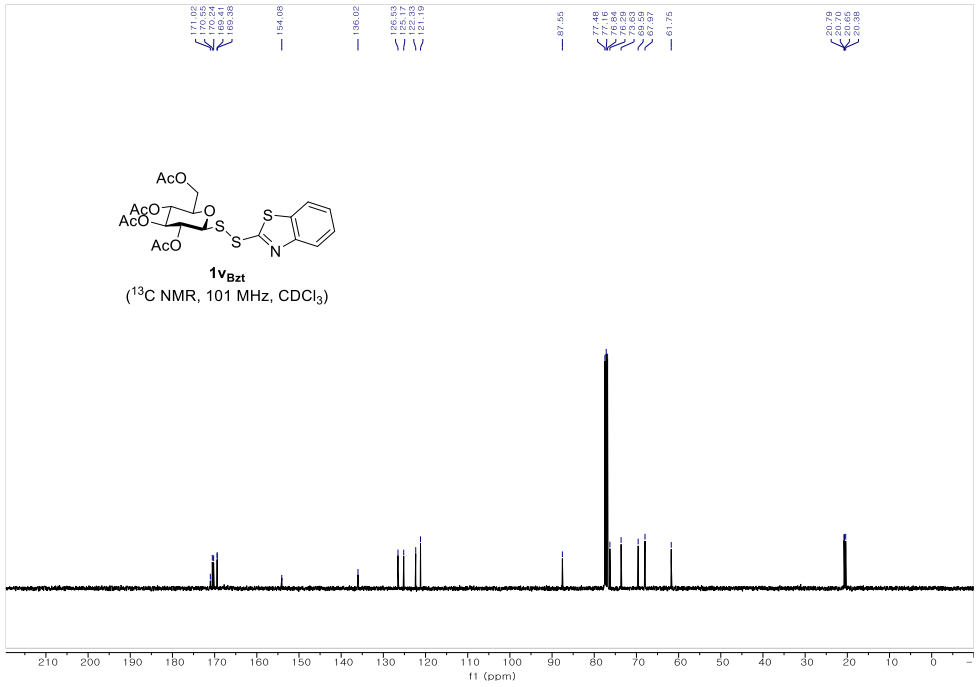
AcO
AcO
AcO
AcO
O
S
S
S
N
1v$_{Bzt}$
(^{13}C NMR, 101 MHz, CDCl$_3$)
f1 (ppm)

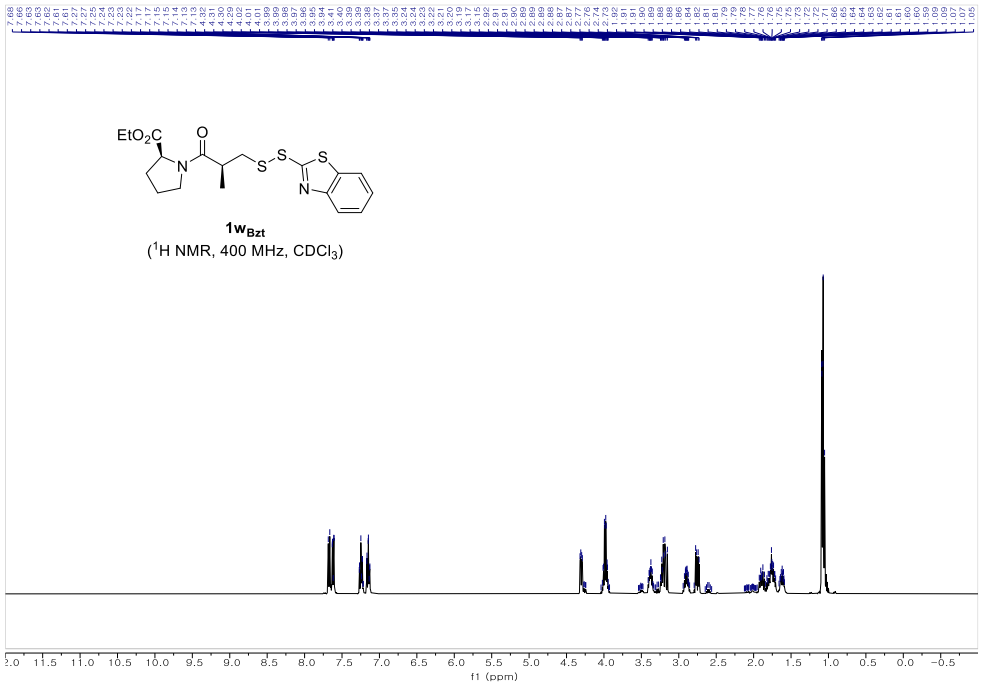
EtO$_2$C
O
N
S
S
S
N
1w$_{Bzt}$
(^{1}H NMR, 400 MHz, CDCl$_3$)
f1 (ppm)

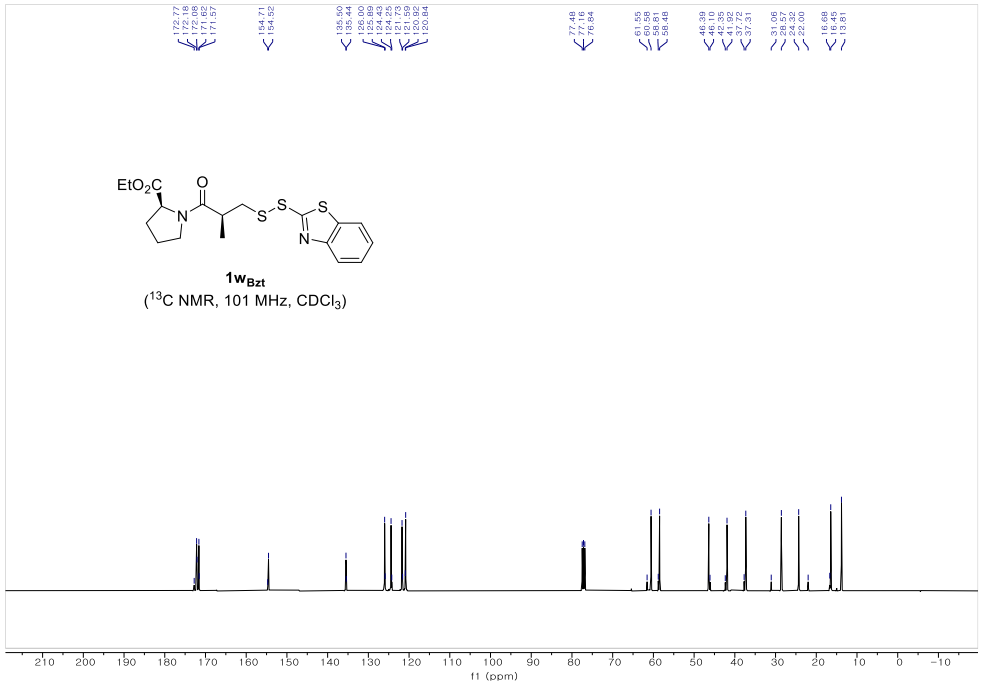

1w$_{Bzt}$

(^{13}C NMR, 101 MHz, $CDCl_3$)

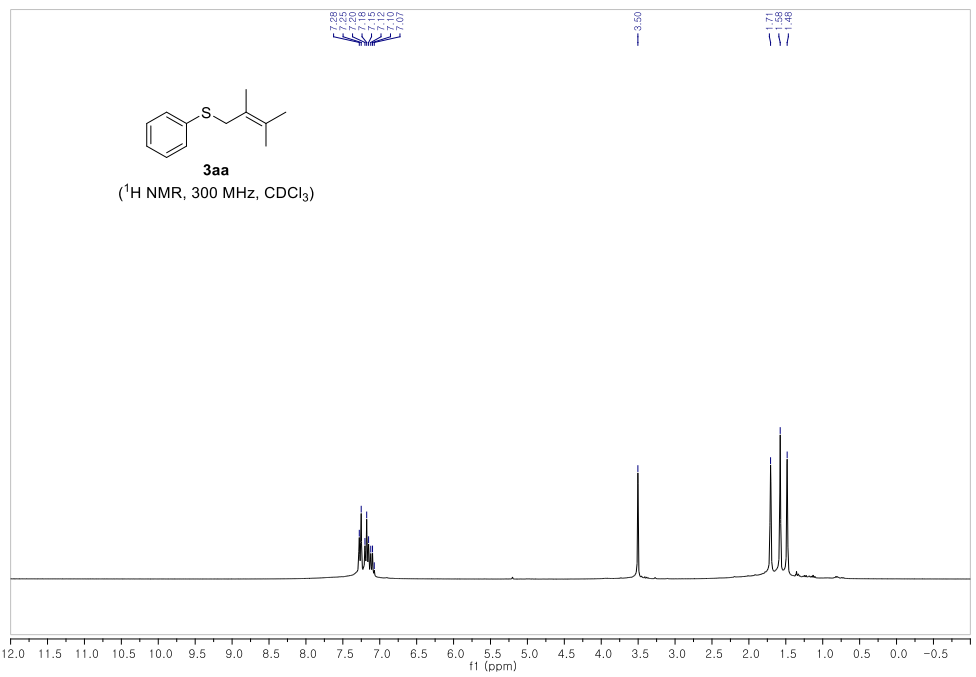

3aa

(^{1}H NMR, 300 MHz, $CDCl_3$)

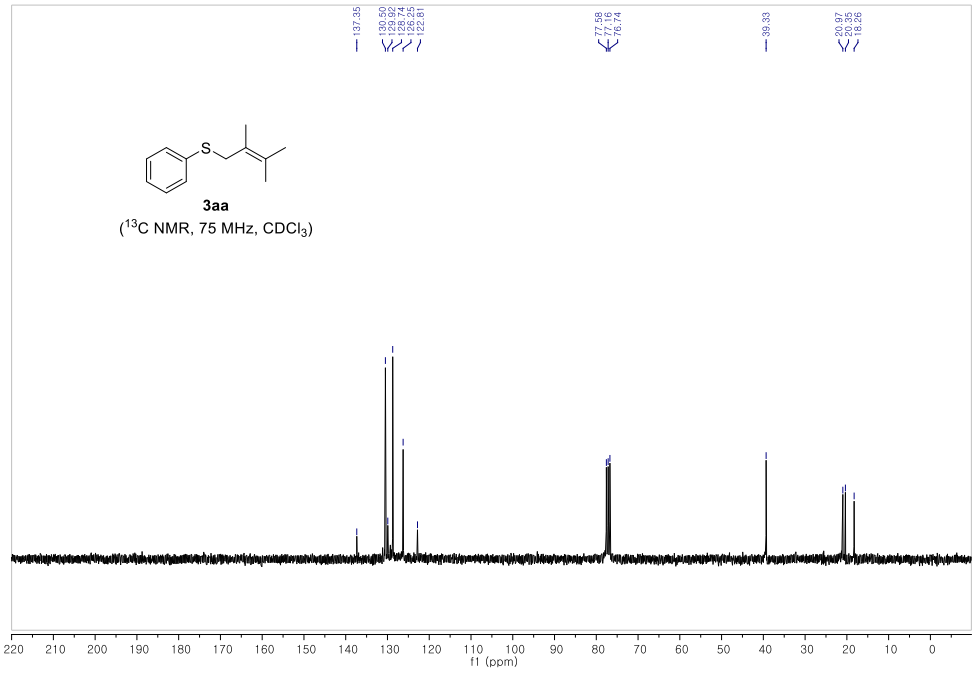
137.35
130.50
129.92
127.44
126.25
122.81
77.58
77.16
76.74
39.33
20.97
20.35
18.26
S
3aa
(^{13}C NMR, 75 MHz, $CDCl_3$)
220 210 200 190 180 170 160 150 140 130 120 110 100 90 80 70 60 50 40 30 20 10 0
f1 (ppm)

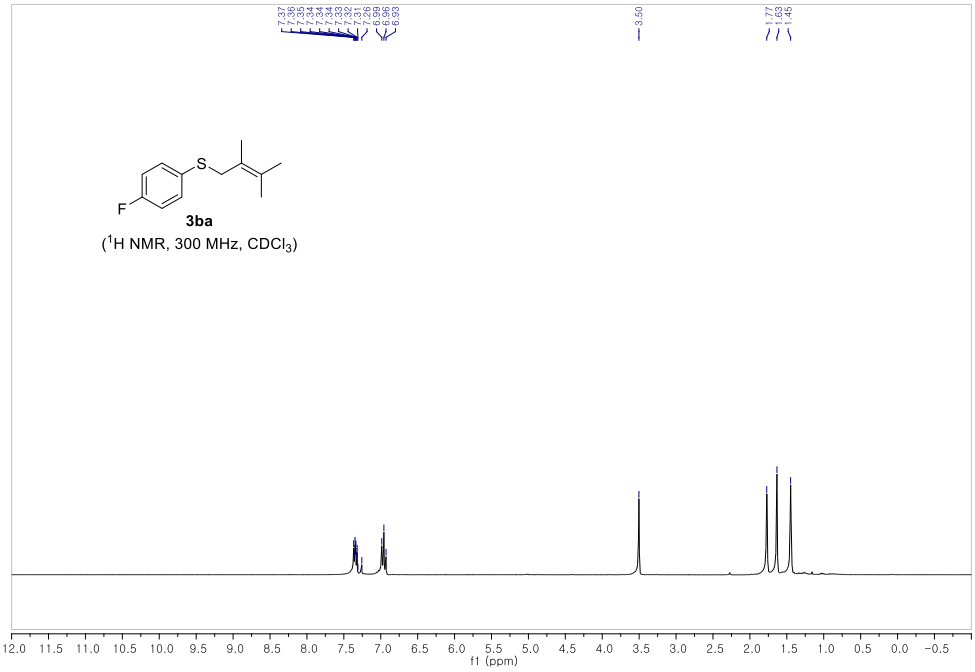
7.37
7.36
7.35
7.34
7.34
7.34
7.33
7.32
7.31
7.26
6.99
6.98
6.93
3.50
1.77
1.63
1.45
S
F
3ba
(^{1}H NMR, 300 MHz, $CDCl_3$)
12.0 11.5 11.0 10.5 10.0 9.5 9.0 8.5 8.0 7.5 7.0 6.5 6.0 5.5 5.0 4.5 4.0 3.5 3.0 2.5 2.0 1.5 1.0 0.5 0.0 -0.5
f1 (ppm)

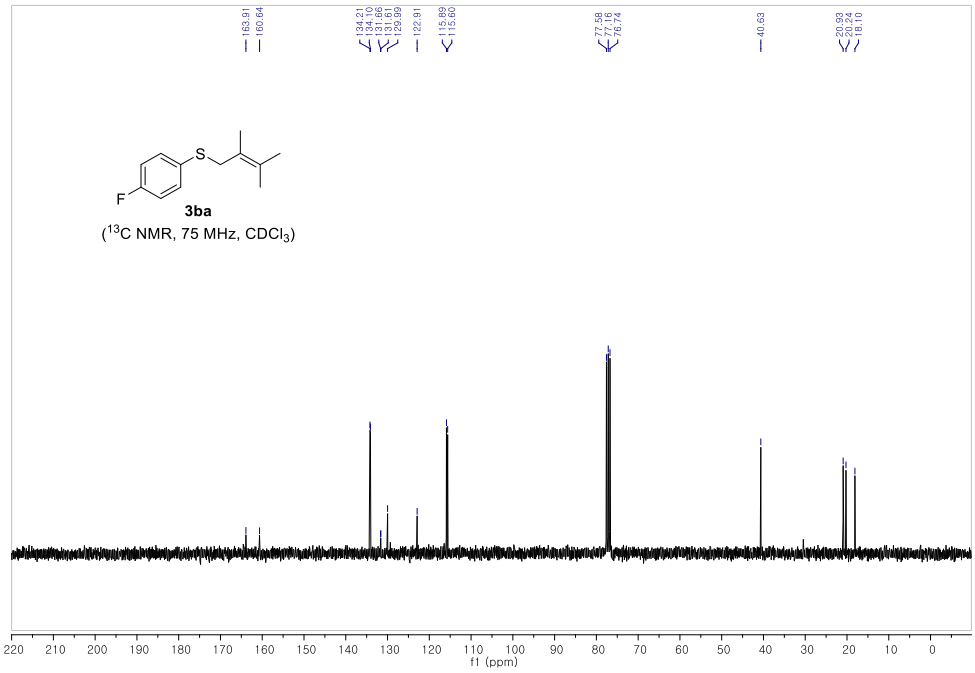
163.91
160.64
134.21
134.10
131.66
131.61
129.99
122.91
115.89
115.60
77.58
77.16
76.74
40.63
20.93
20.24
18.10
S
F
3ba
(^{13}C NMR, 75 MHz, $CDCl_3$)
220 210 200 190 180 170 160 150 140 130 120 110 100 90 80 70 60 50 40 30 20 10 0
f1 (ppm)

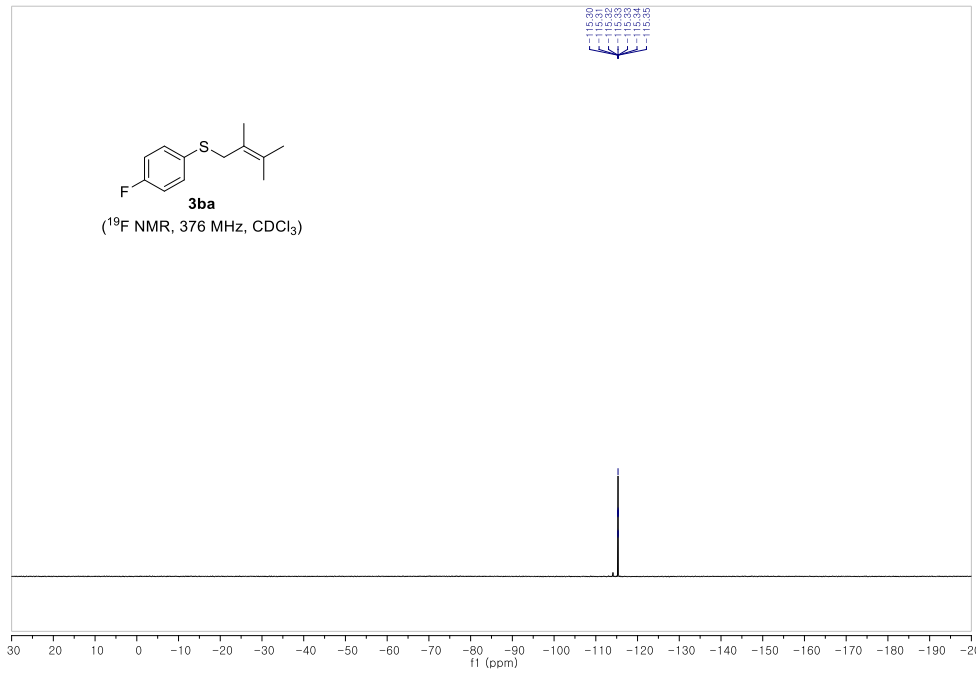
-115.30
-115.31
-115.32
-115.33
-115.33
-115.34
-115.35
S
F
3ba
(^{19}F NMR, 376 MHz, $CDCl_3$)
30 20 10 0 -10 -20 -30 -40 -50 -60 -70 -80 -90 -100 -110 -120 -130 -140 -150 -160 -170 -180 -190 -20
f1 (ppm)

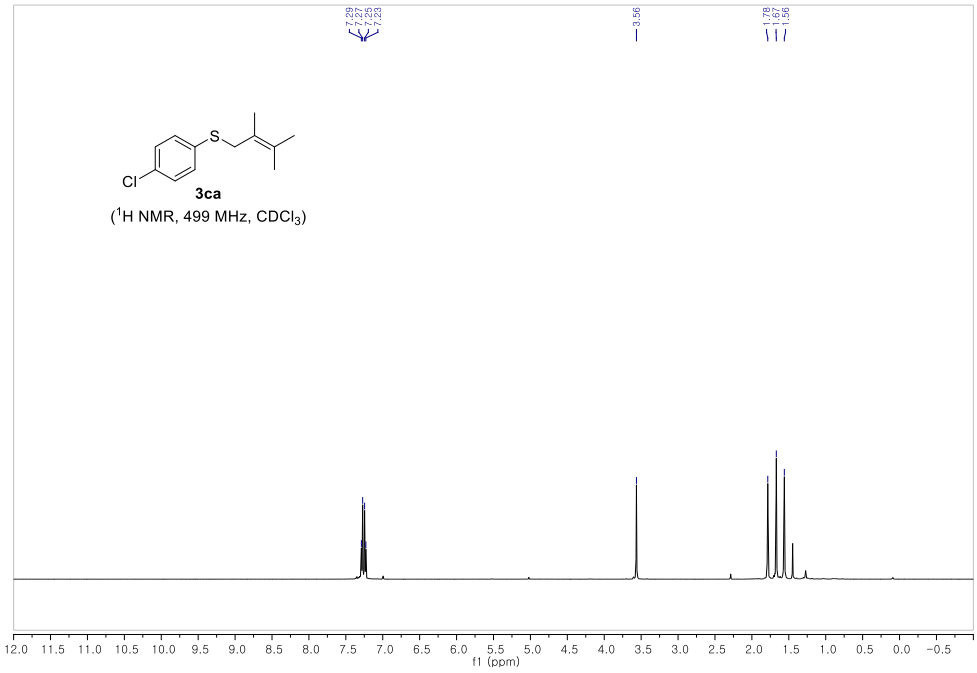
7.29
7.27
7.25
7.23
3.56
1.78
1.67
1.56
S
Cl
3ca
(1H NMR, 499 MHz, CDCl3)
f1 (ppm)

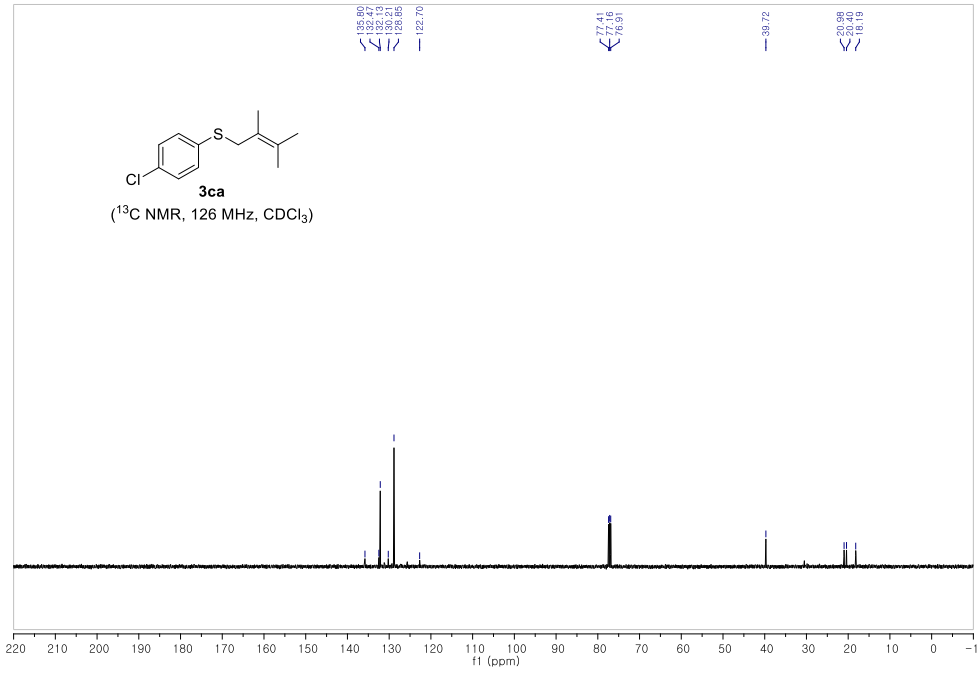
135.90
132.47
132.13
130.21
128.85
122.70
77.41
77.16
76.91
39.72
20.98
20.40
18.19
S
Cl
3ca
(13C NMR, 126 MHz, CDCl3)
f1 (ppm)

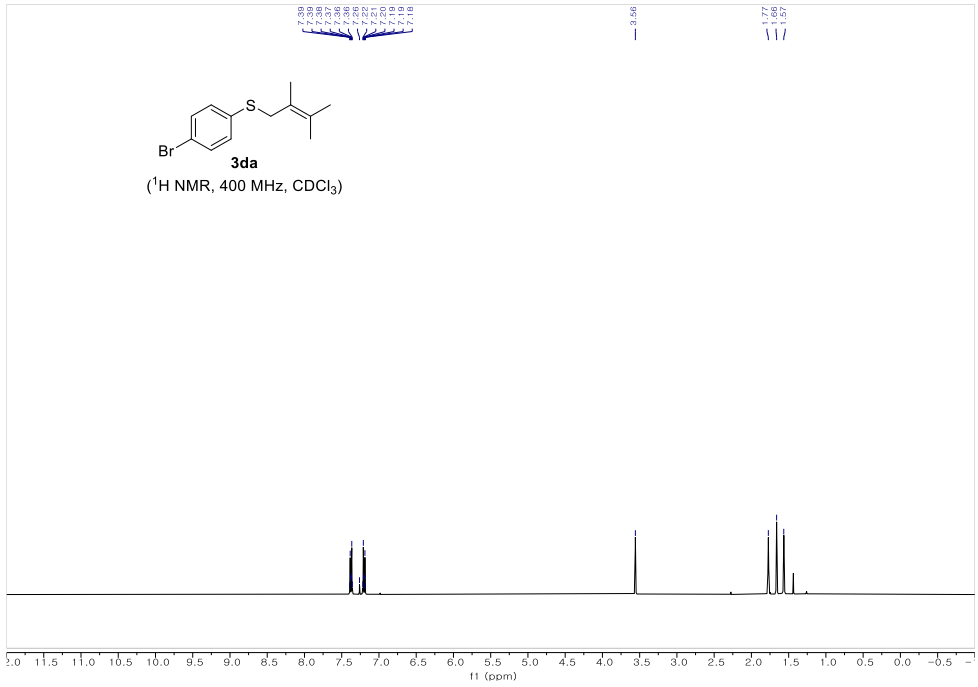

3da

(^{1}H NMR, 400 MHz, $CDCl_3$)

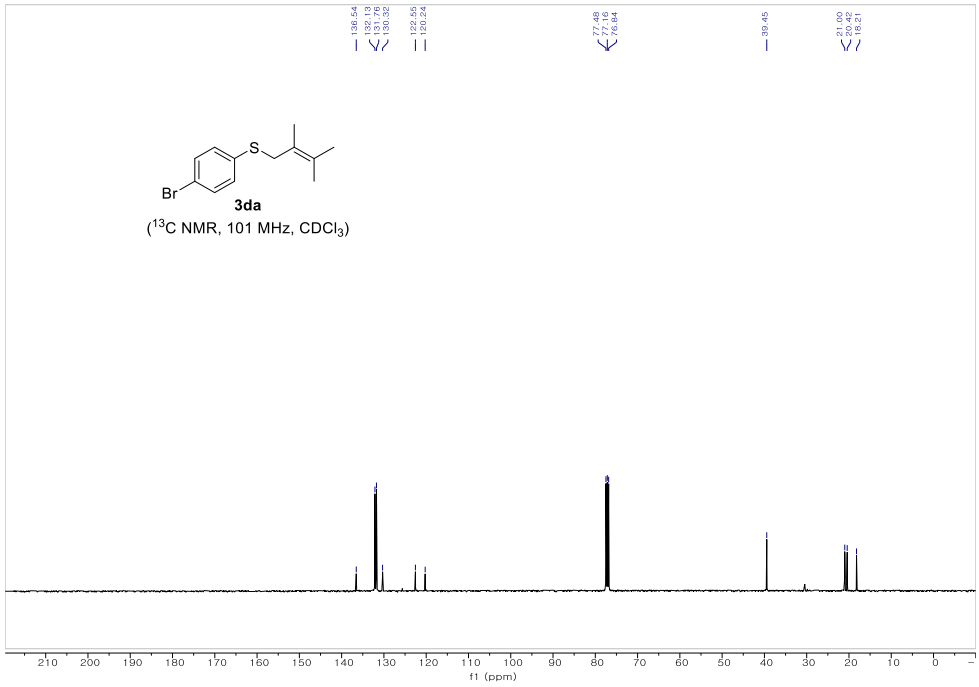

3da

(^{13}C NMR, 101 MHz, $CDCl_3$)

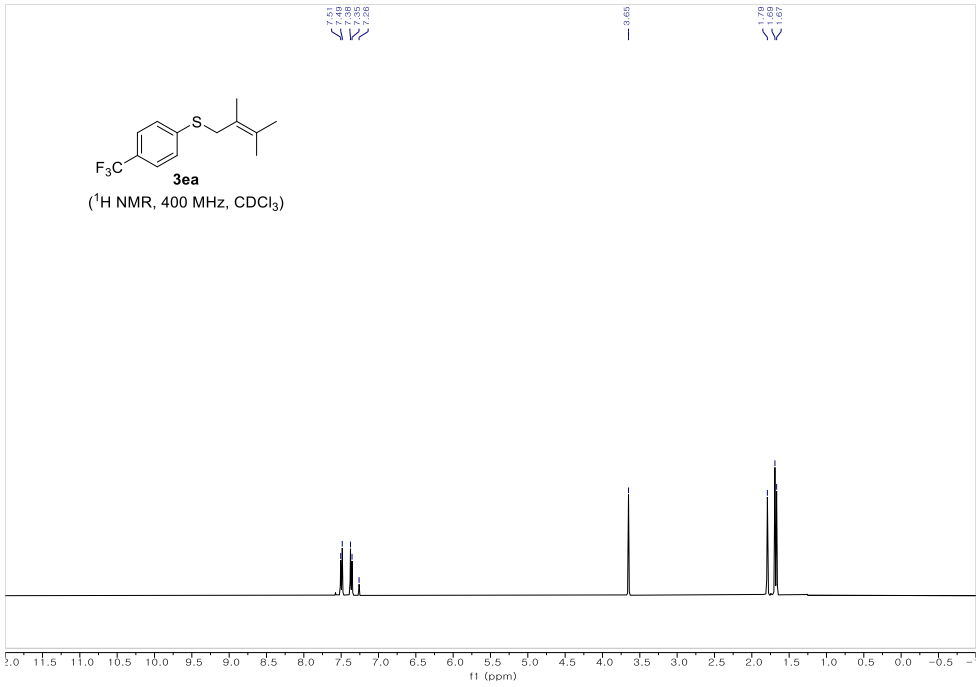
7.51
7.49
7.38
7.36
7.26
3.65
1.79
1.69
1.67
S
F3C
3ea
(1H NMR, 400 MHz, CDCl3)
f1 (ppm)

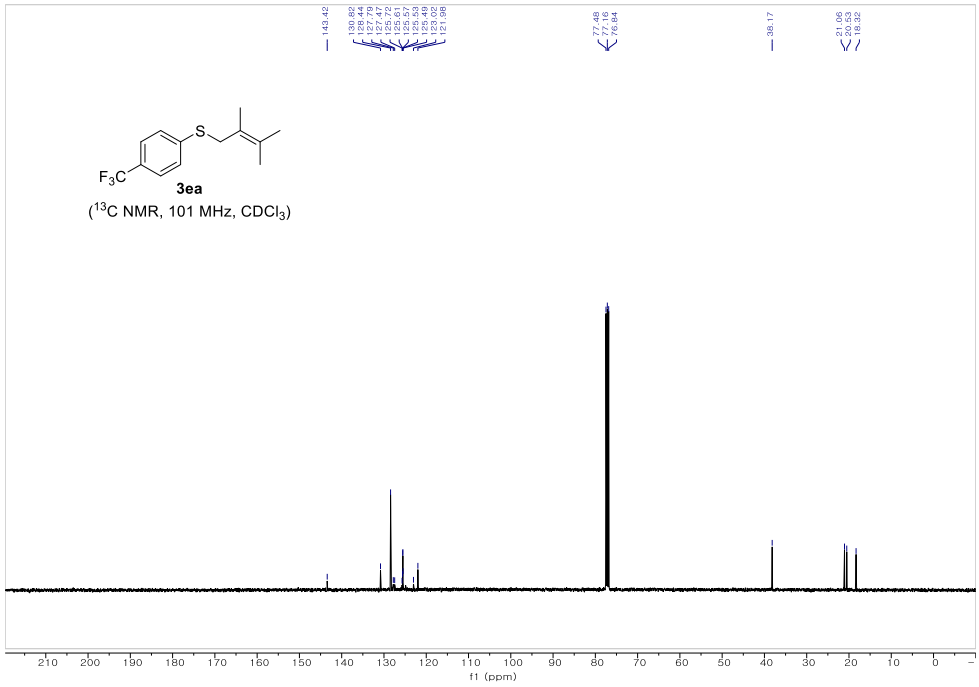
143.42
130.82
129.44
127.79
127.47
125.72
125.61
125.57
125.53
125.49
123.02
121.98
77.48
77.16
76.84
38.17
21.05
20.53
18.32
S
F3C
3ea
(13C NMR, 101 MHz, CDCl3)
f1 (ppm)

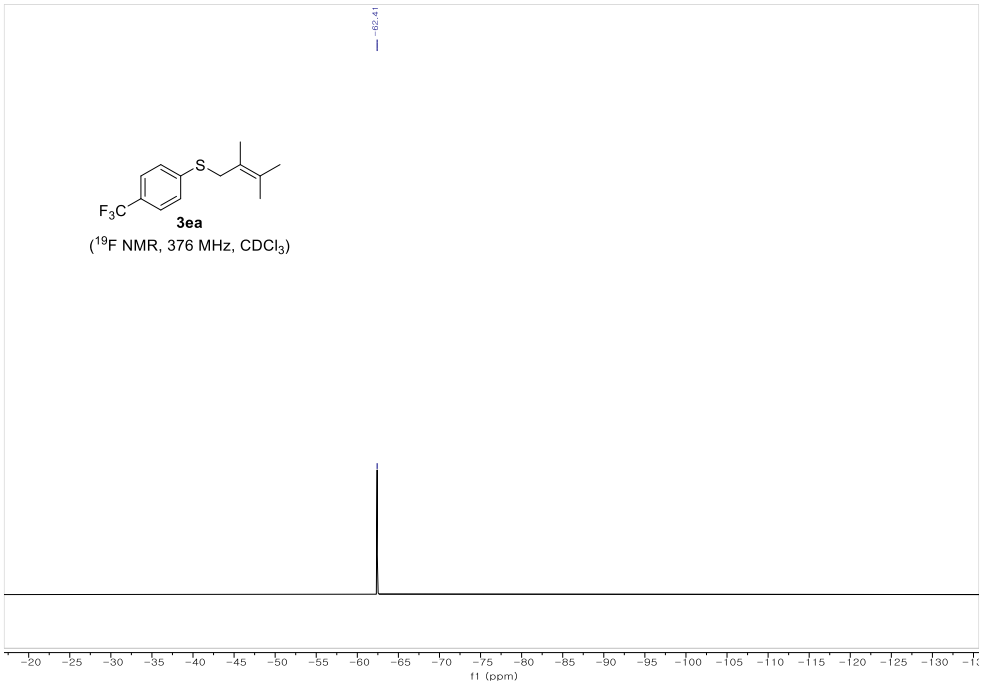
-62.41
S
F3C
3ea
(19F NMR, 376 MHz, CDCl3)
f1 (ppm)

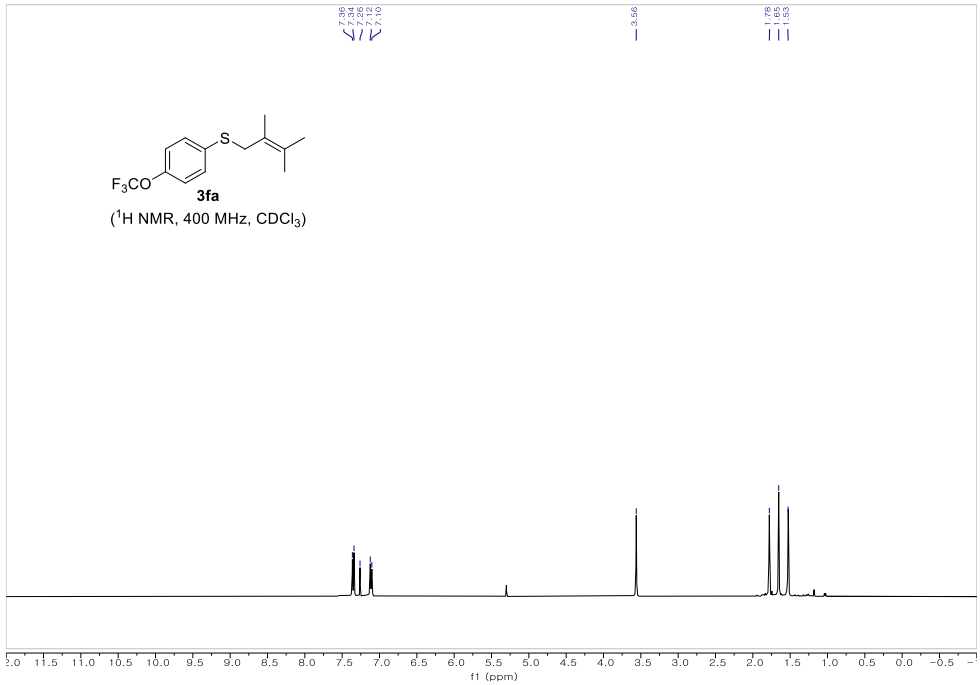
7.36
7.34
7.16
7.12
7.10
3.56
1.78
1.65
1.53
S
F3CO
3fa
(1H NMR, 400 MHz, CDCl3)
f1 (ppm)

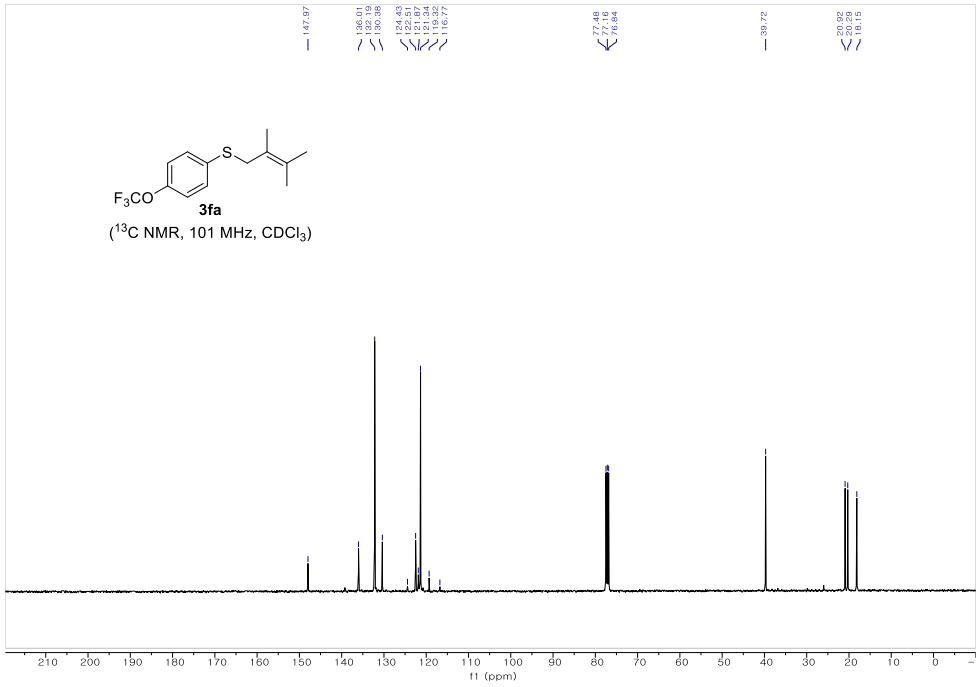
147.97
136.01
132.19
130.38
124.43
122.51
121.97
121.84
119.32
116.77
77.48
77.16
76.84
39.72
20.92
20.89
18.15
S
F3CO
3fa
(13C NMR, 101 MHz, CDCl3)
f1 (ppm)

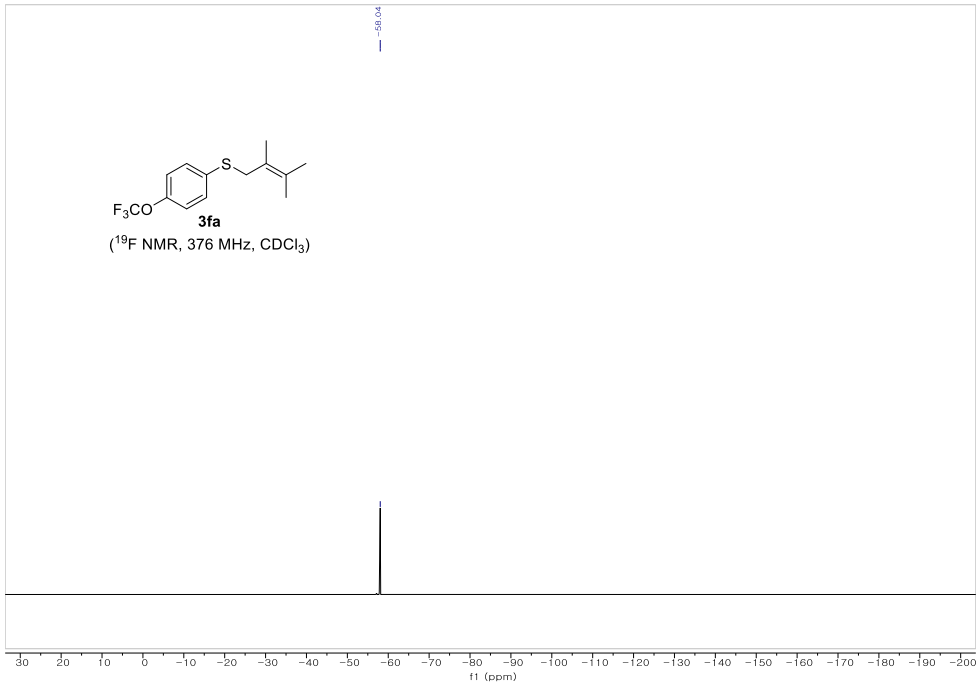
-58.04
S
F3CO
3fa
(19F NMR, 376 MHz, CDCl3)
f1 (ppm)

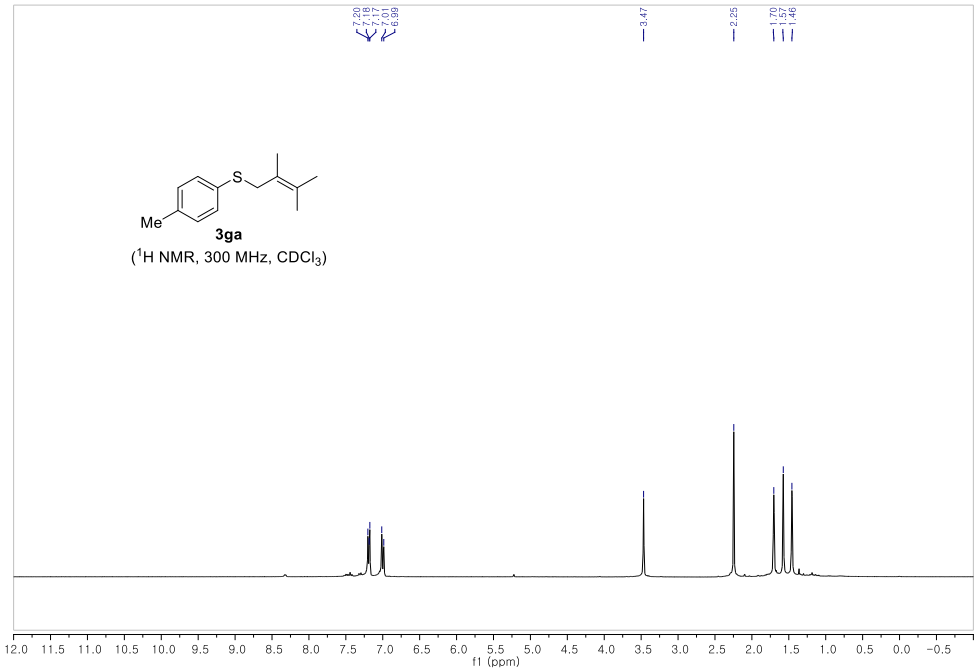
7.20
7.18
7.17
7.01
6.99
3.47
2.25
1.70
1.57
1.46
S
Me
3ga
(1H NMR, 300 MHz, CDCl3)
f1 (ppm)

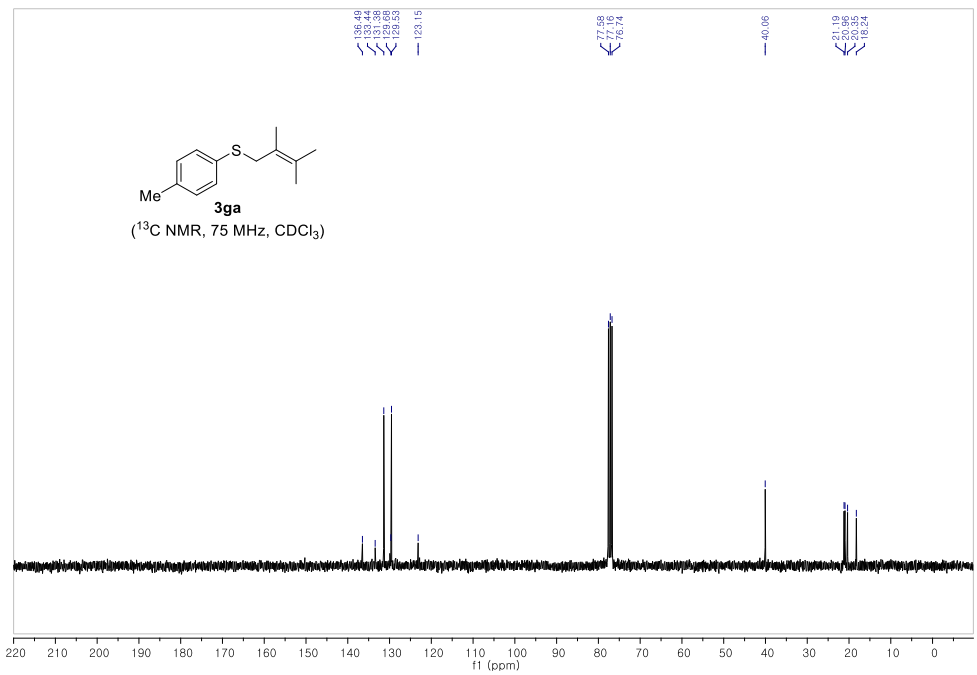
136.49
133.44
131.38
129.68
129.53
123.15
77.58
77.16
76.74
40.06
21.19
20.96
20.35
16.24
S
Me
3ga
(13C NMR, 75 MHz, CDCl3)
f1 (ppm)

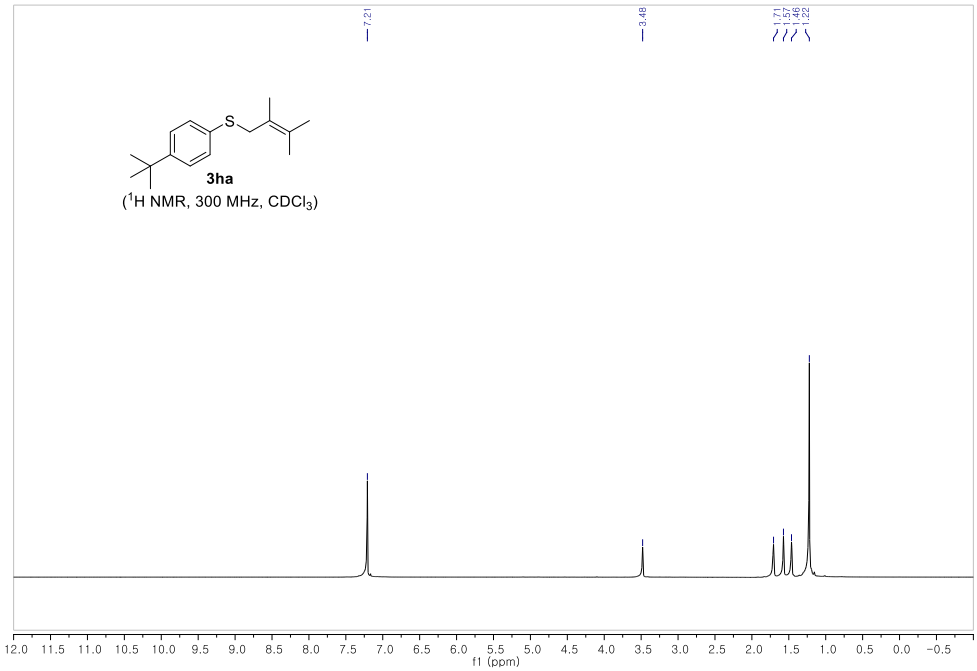
7.21
3.48
1.71
1.57
1.45
1.22
S
3ha
(1H NMR, 300 MHz, CDCl3)
f1 (ppm)

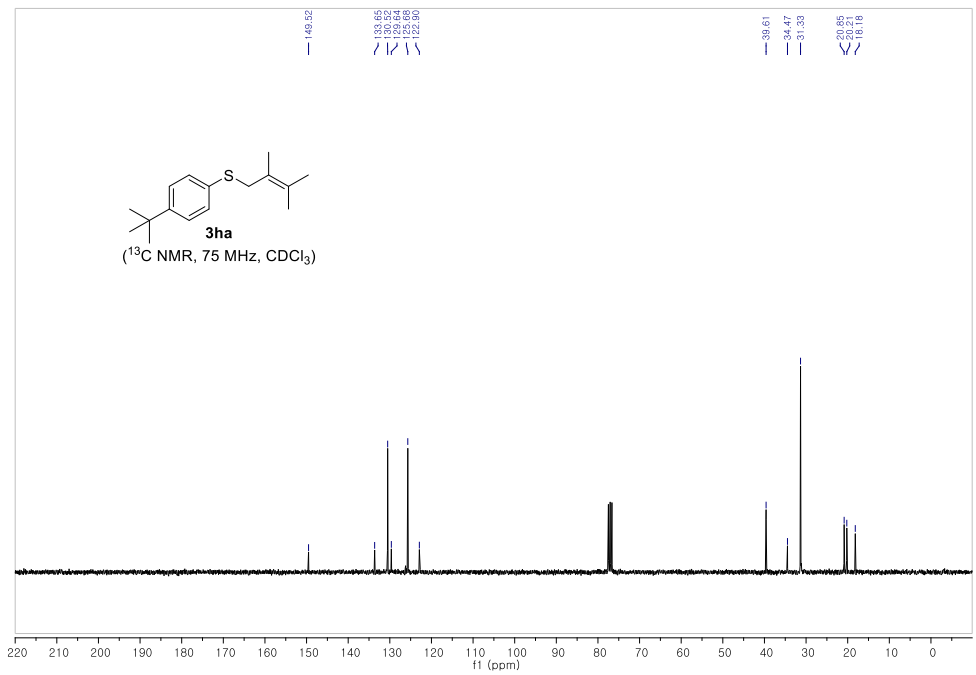
149.52
130.85
130.52
129.64
125.68
122.90
39.61
34.47
31.33
20.85
20.21
18.18
S
3ha
(13C NMR, 75 MHz, CDCl3)
f1 (ppm)

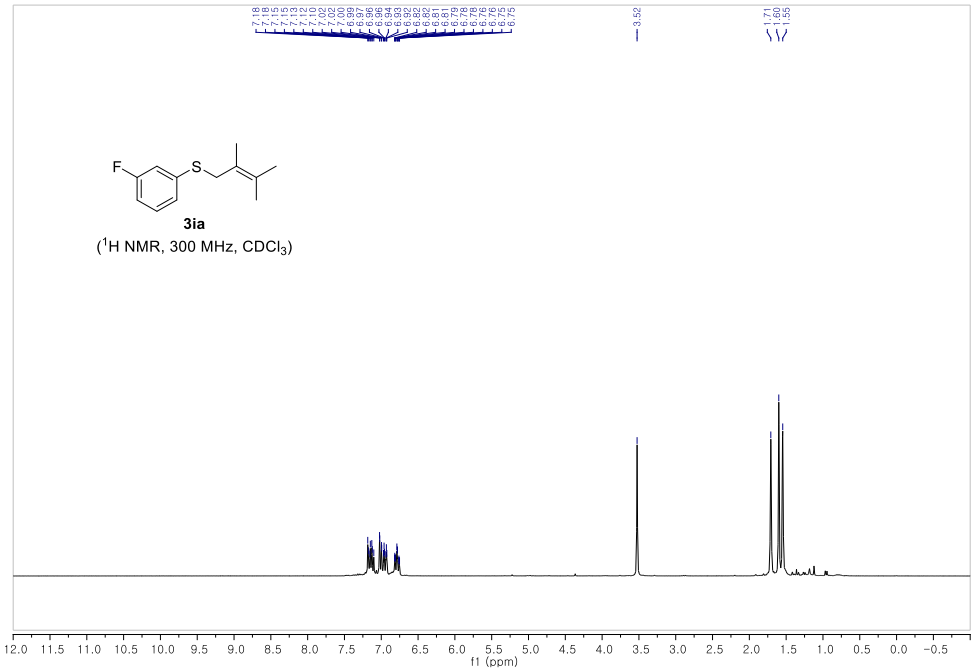
7.18
7.18
7.15
7.15
7.13
7.12
7.10
7.02
7.02
7.00
6.99
6.97
6.96
6.94
6.93
6.92
6.92
6.82
6.81
6.81
6.79
6.78
6.78
6.76
6.76
6.75
6.75
3.52
1.71
1.60
1.55
F
S
3ia
(1H NMR, 300 MHz, CDCl3)
12.0 11.5 11.0 10.5 10.0 9.5 9.0 8.5 8.0 7.5 7.0 6.5 6.0 5.5 5.0 4.5 4.0 3.5 3.0 2.5 2.0 1.5 1.0 0.5 0.0 −0.5
f1 (ppm)

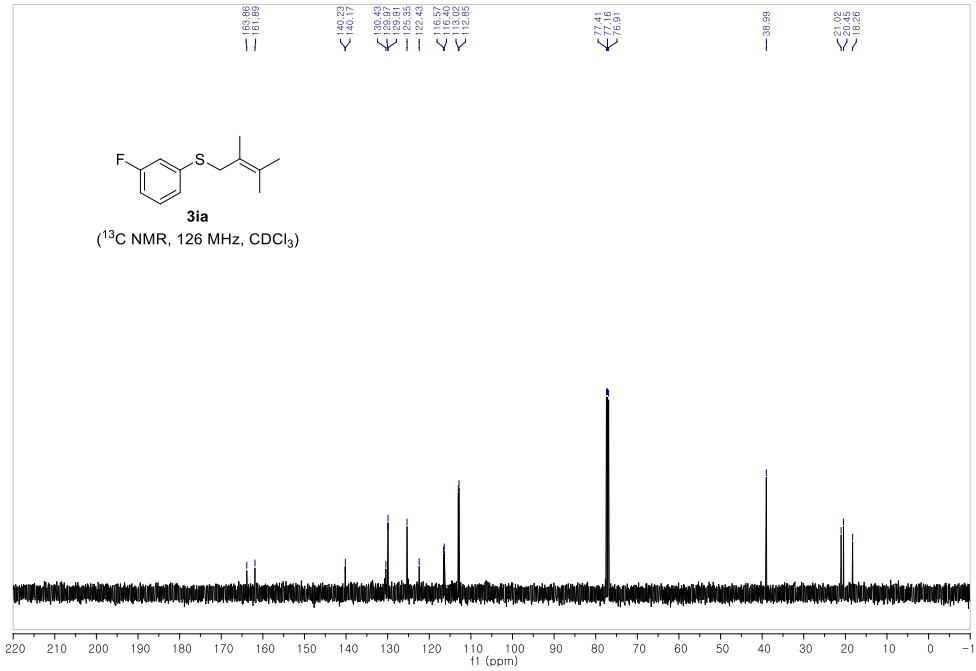
163.86
161.89
140.23
140.17
130.43
129.97
129.91
125.35
122.43
116.57
116.40
112.90
112.85
77.41
77.16
76.91
38.99
21.02
20.45
18.26
F
S
3ia
(13C NMR, 126 MHz, CDCl3)
220 210 200 190 180 170 160 150 140 130 120 110 100 90 80 70 60 50 40 30 20 10 0 −10
f1 (ppm)

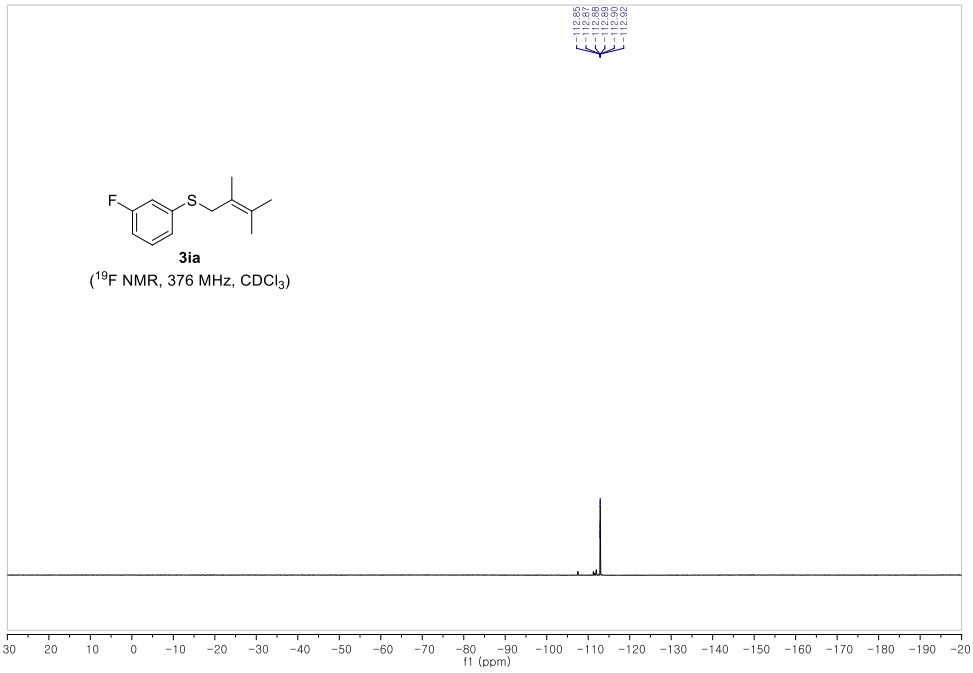

3ia

(^{19}F NMR, 376 MHz, $CDCl_3$)

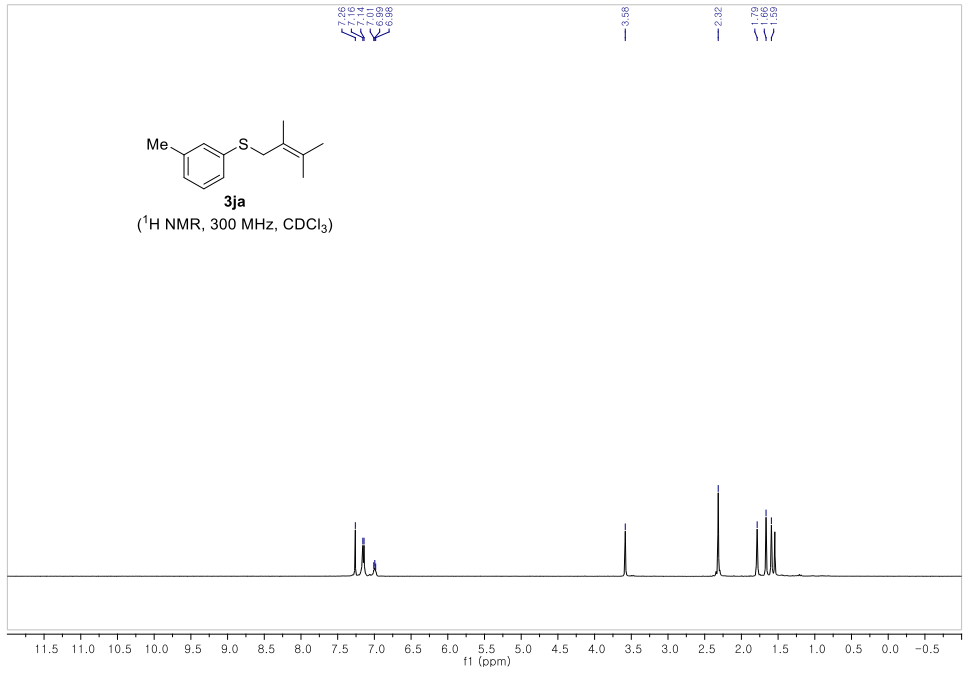

3ja

(^{1}H NMR, 300 MHz, $CDCl_3$)

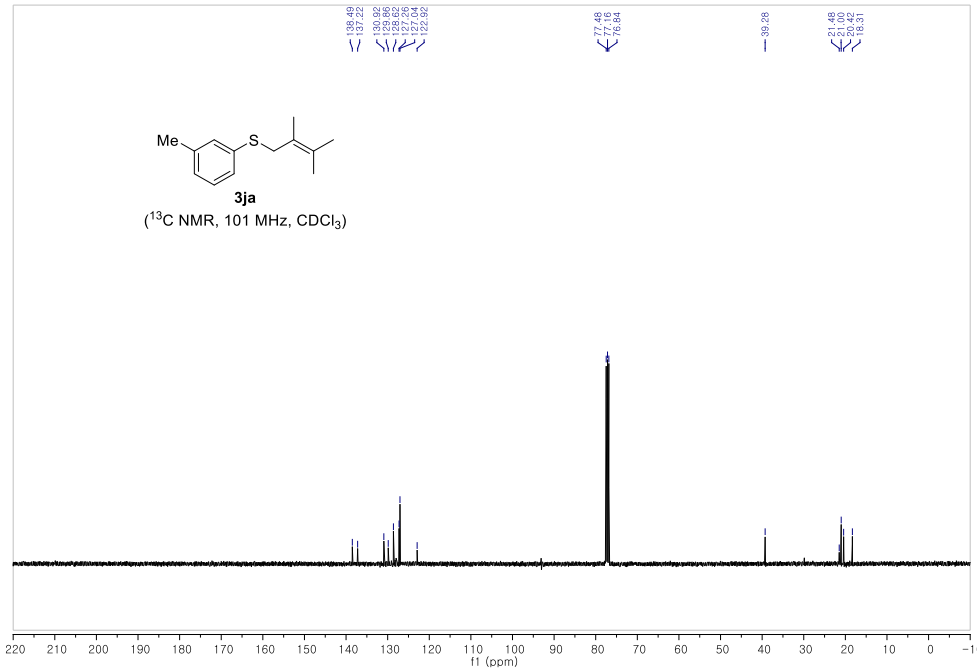
139.49
137.22
129.92
129.66
128.62
127.26
125.04
122.92
77.48
77.16
76.84
39.28
21.48
21.00
20.42
18.31
Me
S
3ja
(^{13}C NMR, 101 MHz, $CDCl_3$)
f1 (ppm)

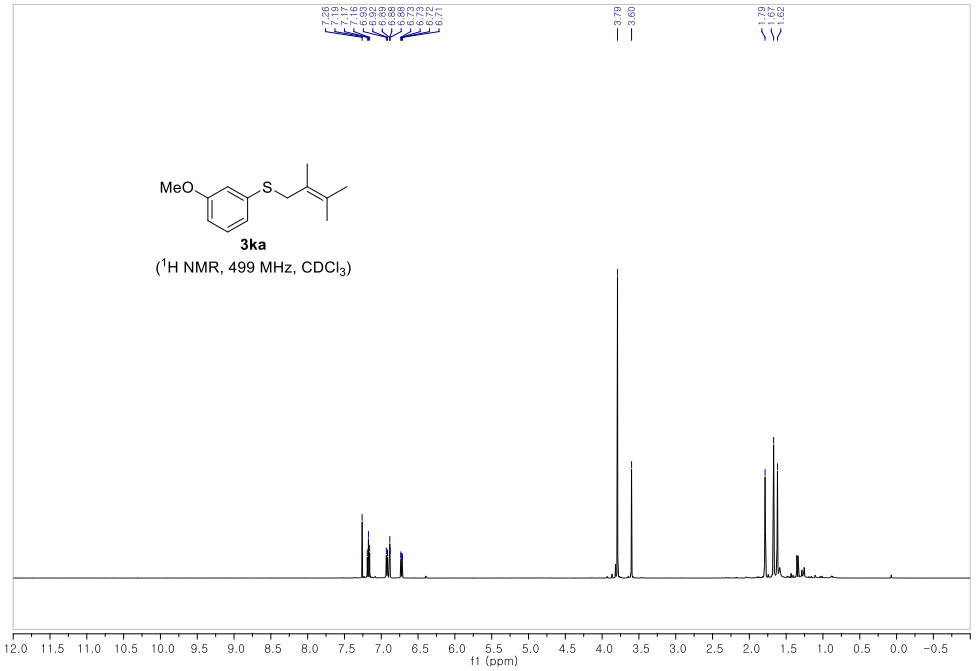
7.26
7.19
7.17
7.16
6.93
6.92
6.89
6.88
6.88
6.73
6.73
6.72
6.71
3.79
3.60
1.79
1.67
1.62
MeO
S
3ka
(^{1}H NMR, 499 MHz, $CDCl_3$)
f1 (ppm)

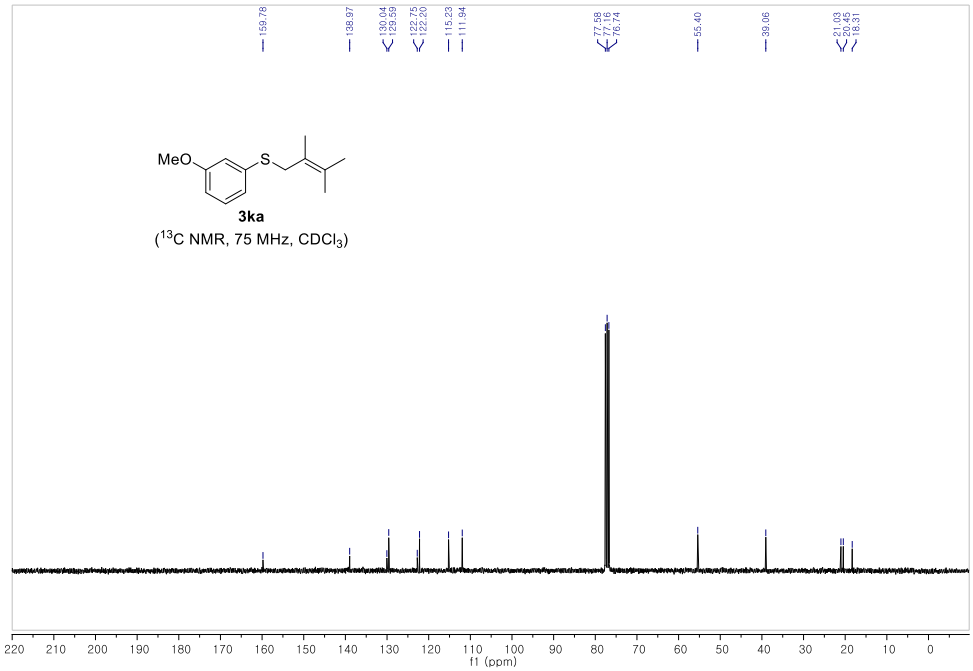

3ka

(^{13}C NMR, 75 MHz, $CDCl_3$)

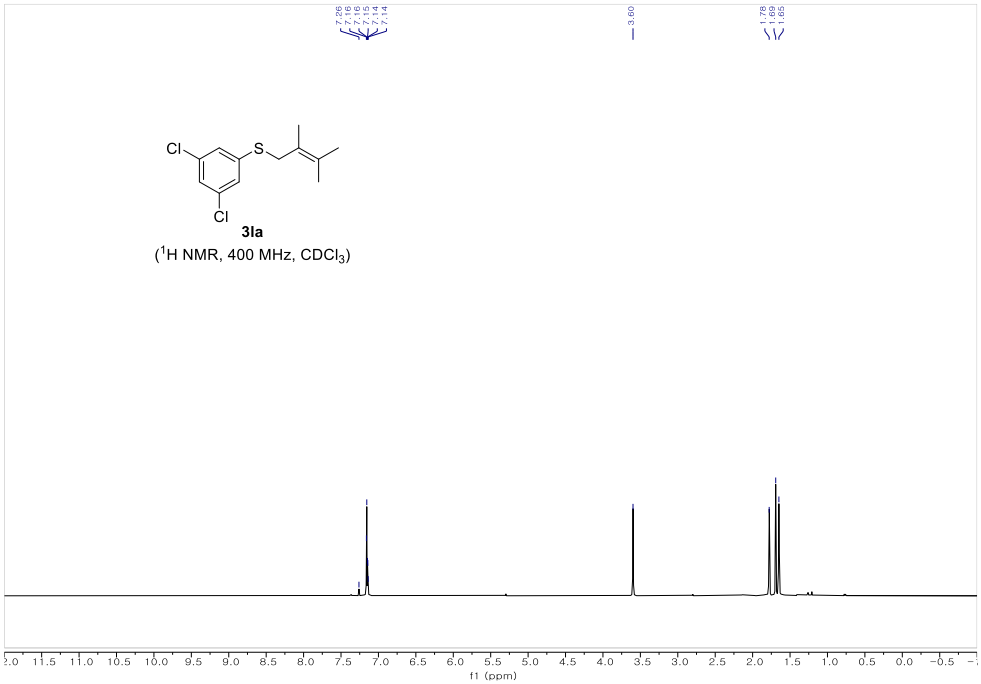

3la

(^{1}H NMR, 400 MHz, $CDCl_3$)

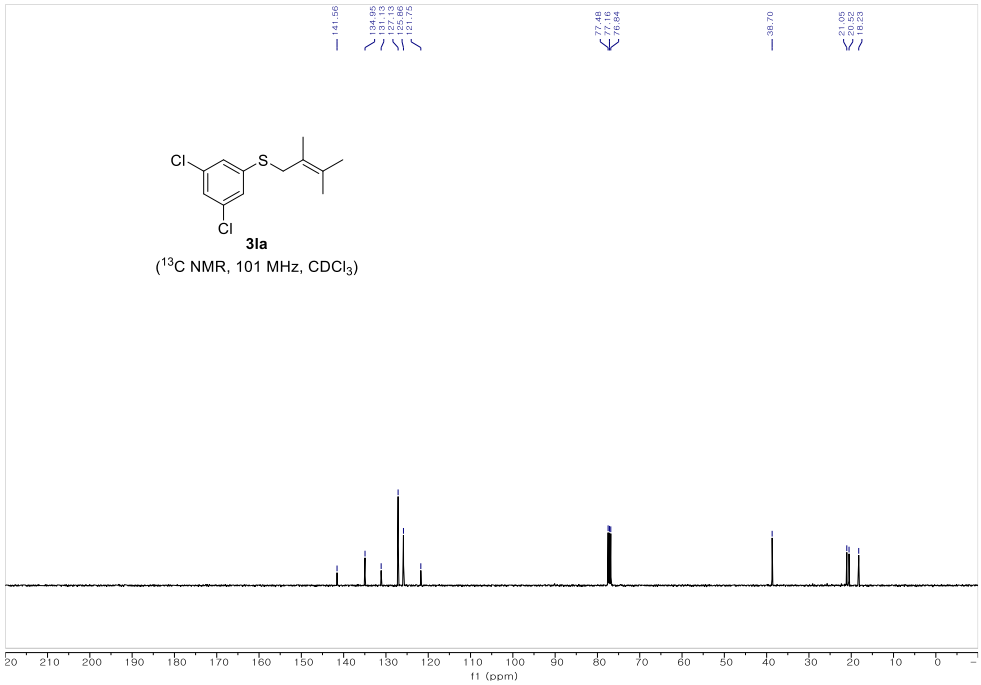

3la

(^{13}C NMR, 101 MHz, $CDCl_3$)

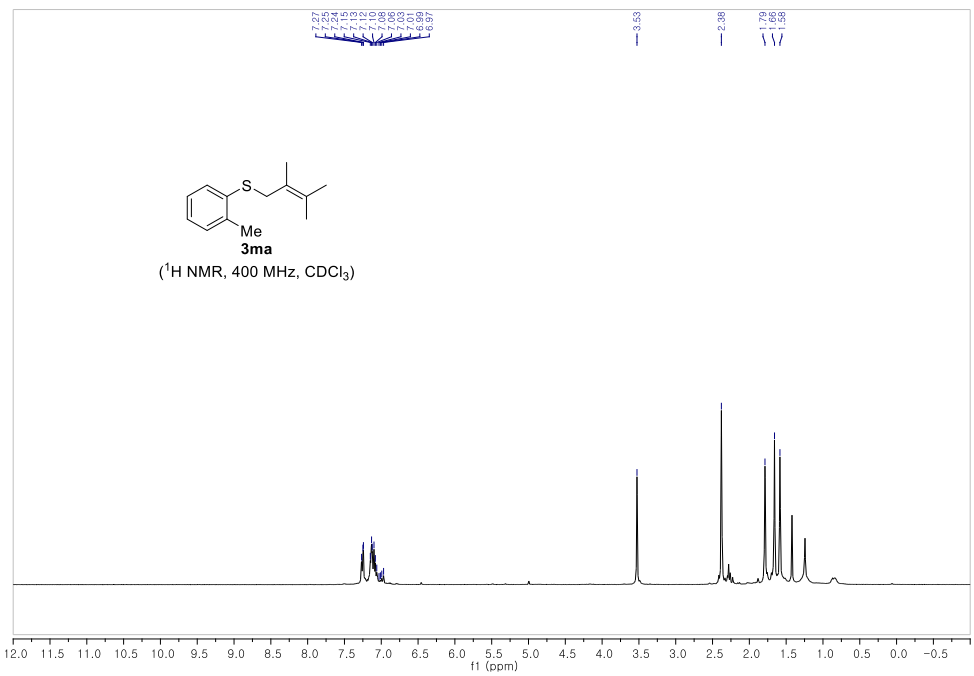

3ma

(^{1}H NMR, 400 MHz, $CDCl_3$)

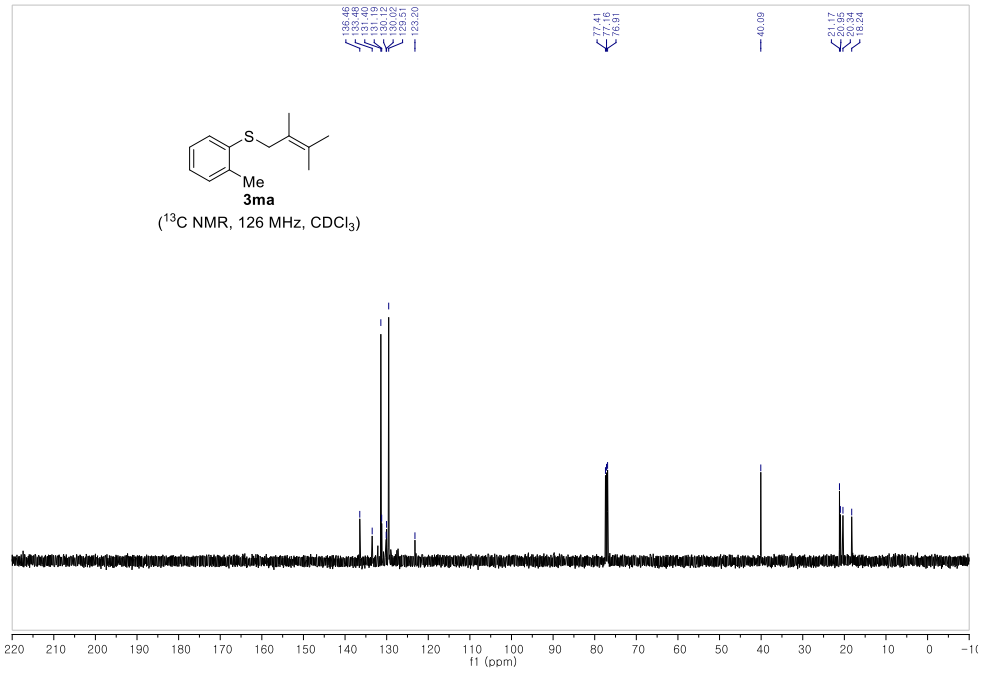
136.46
133.48
131.40
131.19
130.12
130.02
125.51
123.20
77.41
77.16
76.91
40.09
21.17
20.95
20.44
18.24
S
Me
3ma
(^{13}C NMR, 126 MHz, $CDCl_3$)
f1 (ppm)

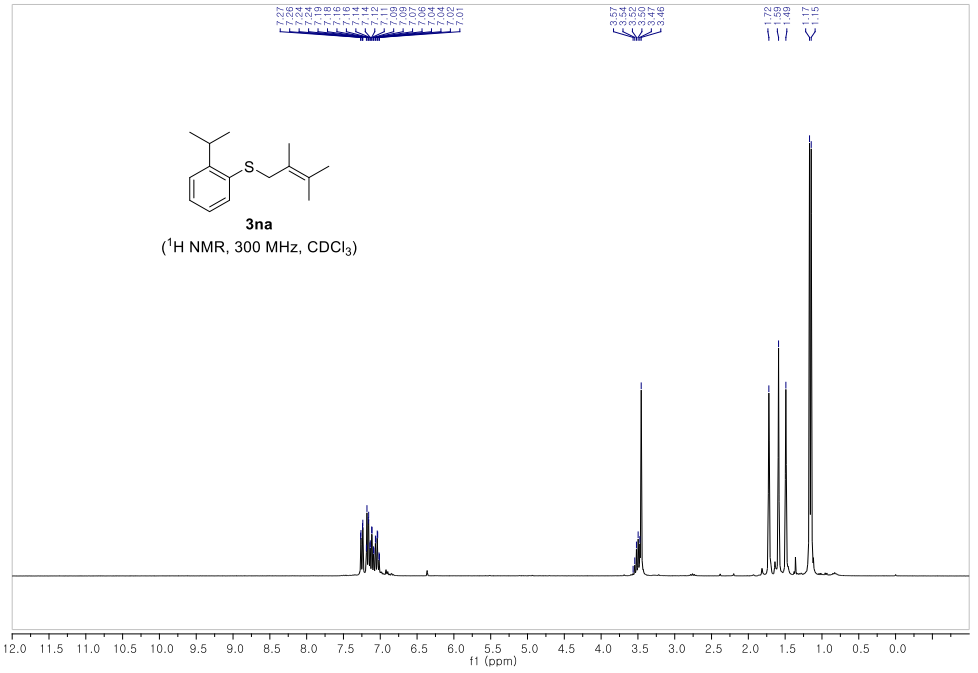
7.27
7.26
7.24
7.24
7.19
7.18
7.16
7.15
7.14
7.12
7.11
7.09
7.07
7.06
7.04
7.04
7.02
7.01
3.57
3.54
3.52
3.50
3.47
3.46
1.72
1.51
1.50
1.49
1.17
1.15
S
3na
(^{1}H NMR, 300 MHz, $CDCl_3$)
f1 (ppm)

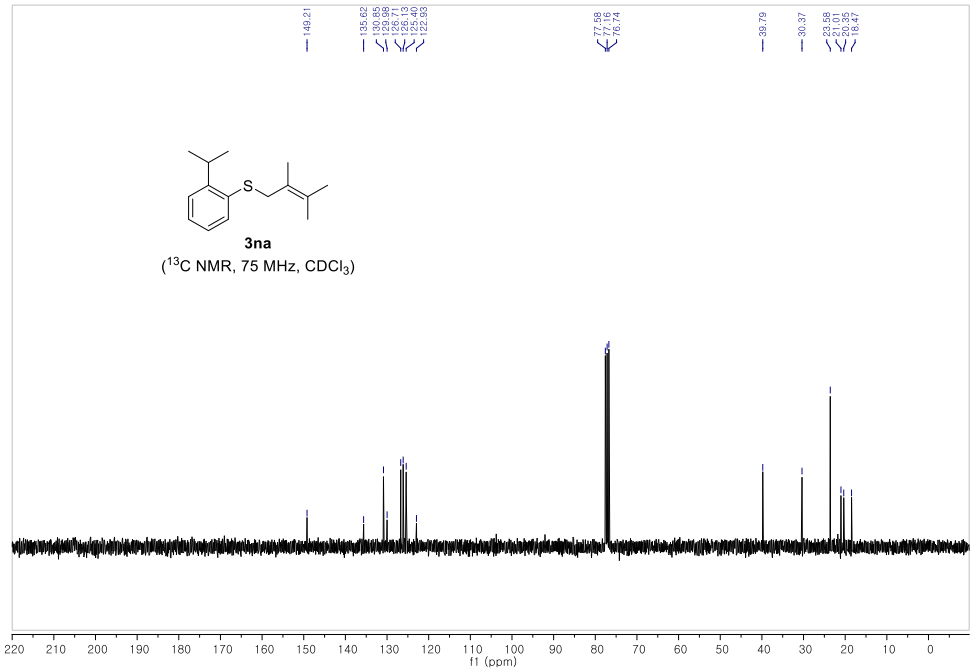
149.21
135.62
130.85
129.98
126.71
126.13
124.40
122.93
77.58
77.16
76.74
39.79
30.37
23.58
21.10
20.35
18.47
S
3na
(^{13}C NMR, 75 MHz, $CDCl_3$)
220 210 200 190 180 170 160 150 140 130 120 110 100 90 80 70 60 50 40 30 20 10 0
f1 (ppm)

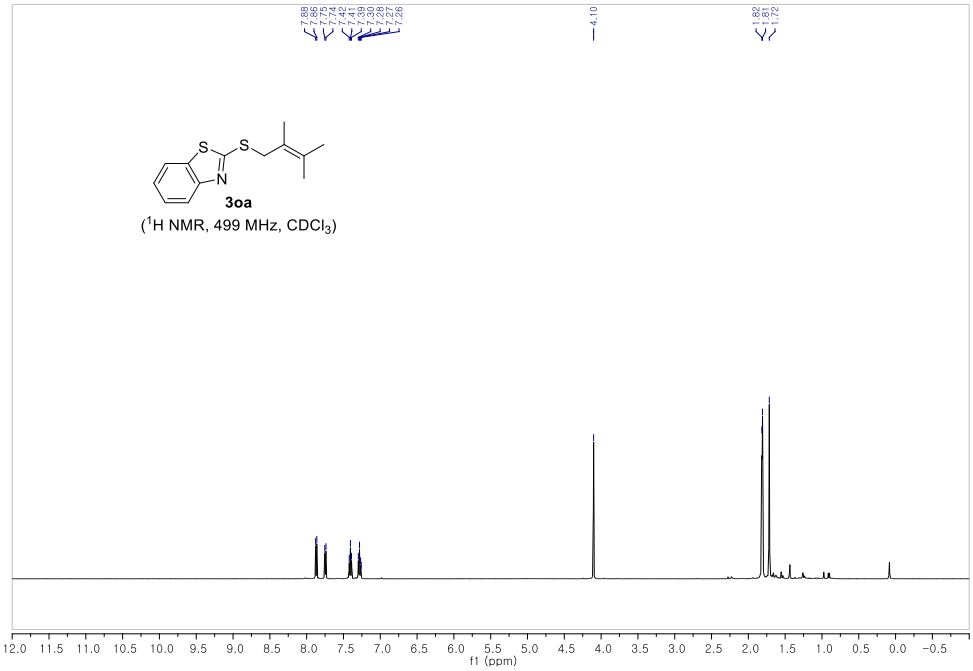
7.88
7.86
7.75
7.74
7.42
7.41
7.39
7.39
7.28
7.27
7.26
4.10
1.82
1.81
1.72
S
S
N
3oa
(^{1}H NMR, 499 MHz, $CDCl_3$)
12.0 11.5 11.0 10.5 10.0 9.5 9.0 8.5 8.0 7.5 7.0 6.5 6.0 5.5 5.0 4.5 4.0 3.5 3.0 2.5 2.0 1.5 1.0 0.5 0.0 −0.5
f1 (ppm)

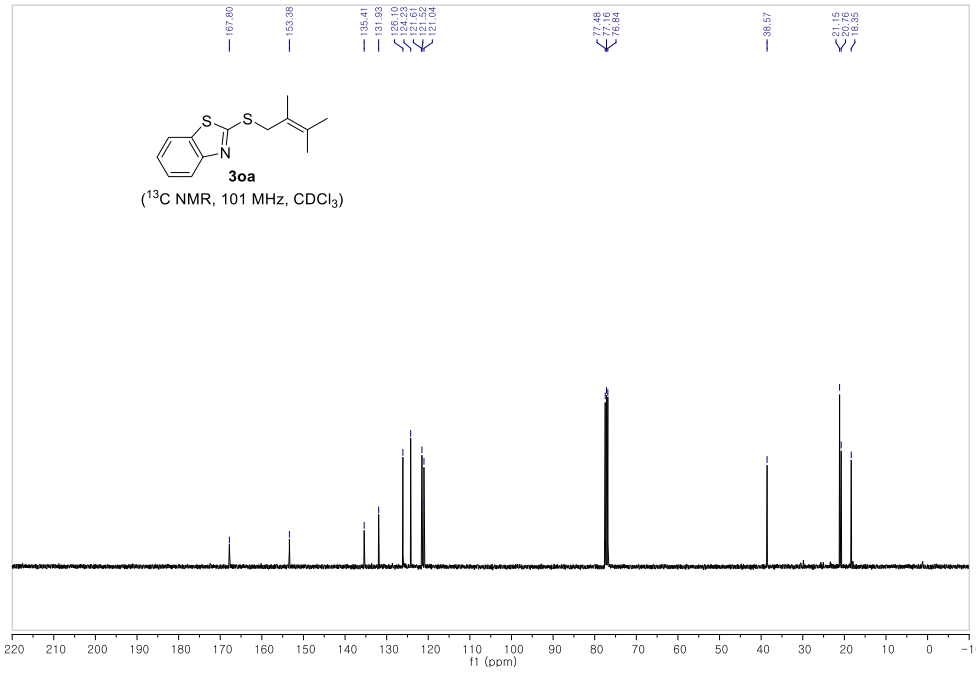

3oa

(^{13}C NMR, 101 MHz, $CDCl_3$)

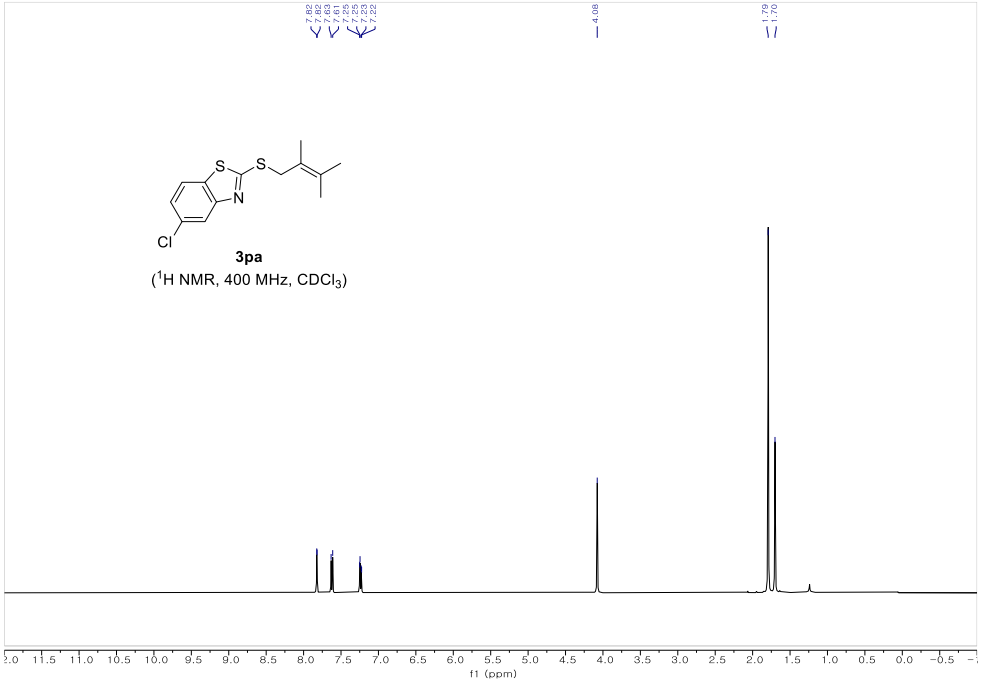

3pa

(^{1}H NMR, 400 MHz, $CDCl_3$)

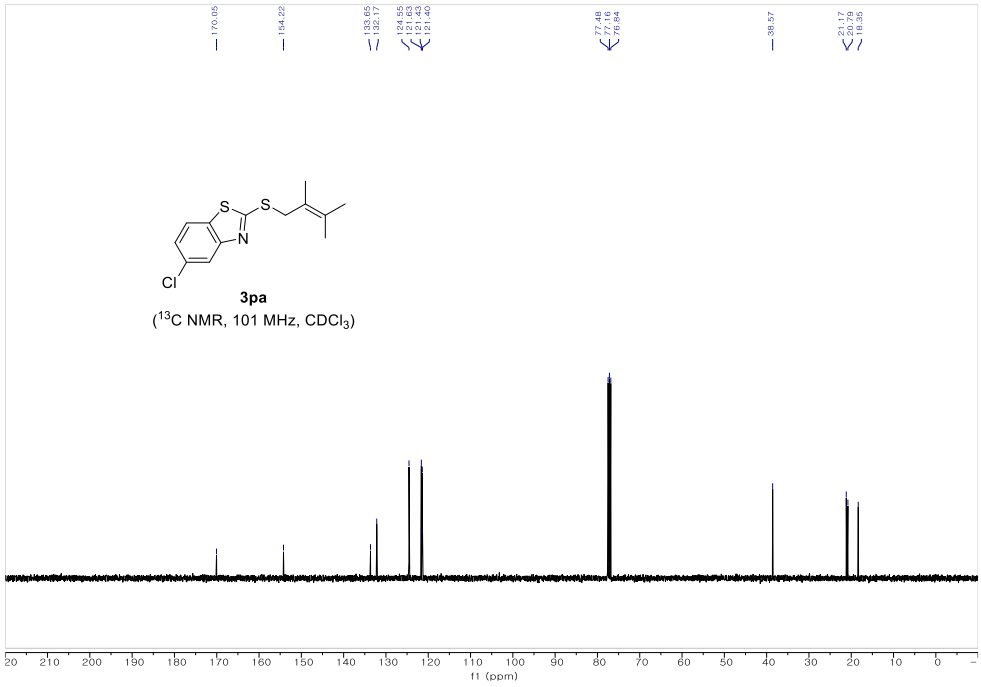

3pa

(^{13}C NMR, 101 MHz, $CDCl_3$)

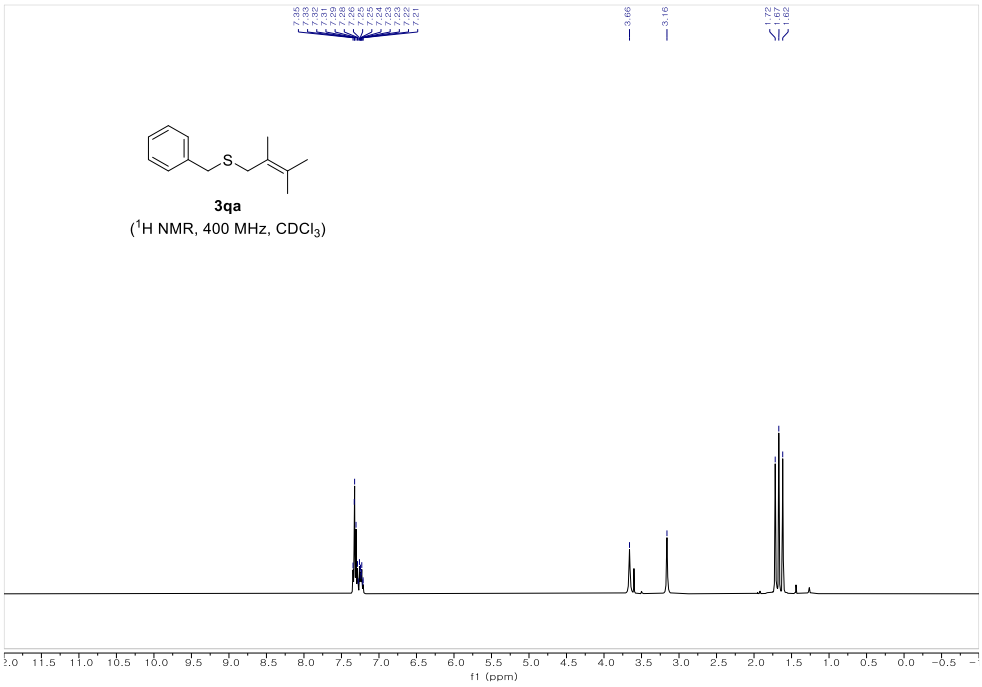

3qa

(^{1}H NMR, 400 MHz, $CDCl_3$)

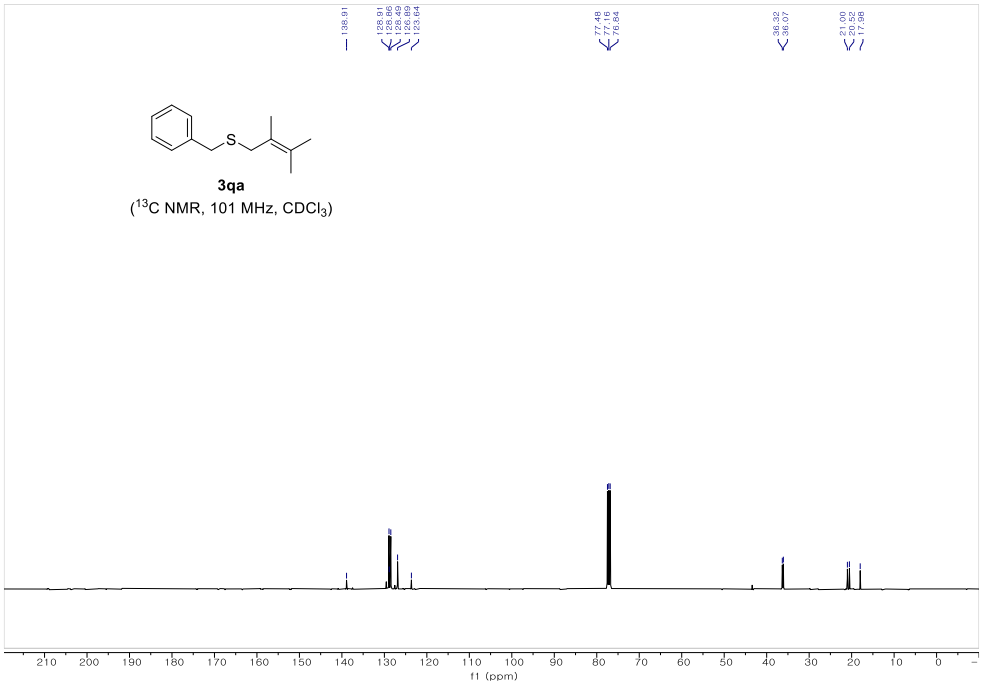

3qa

(^{13}C NMR, 101 MHz, $CDCl_3$)

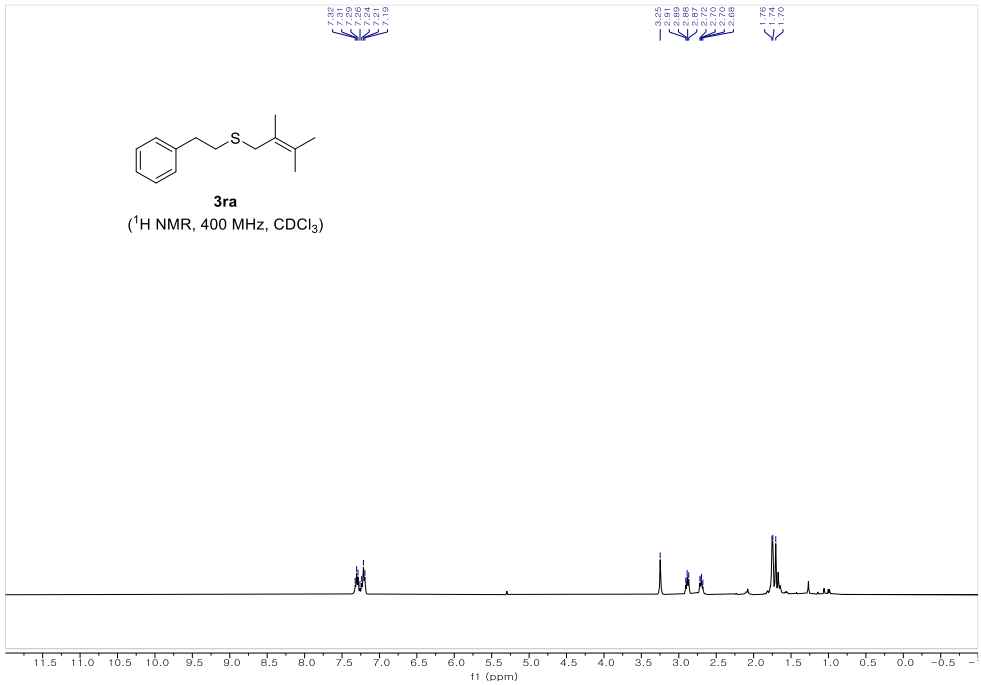

3ra

(^{1}H NMR, 400 MHz, $CDCl_3$)

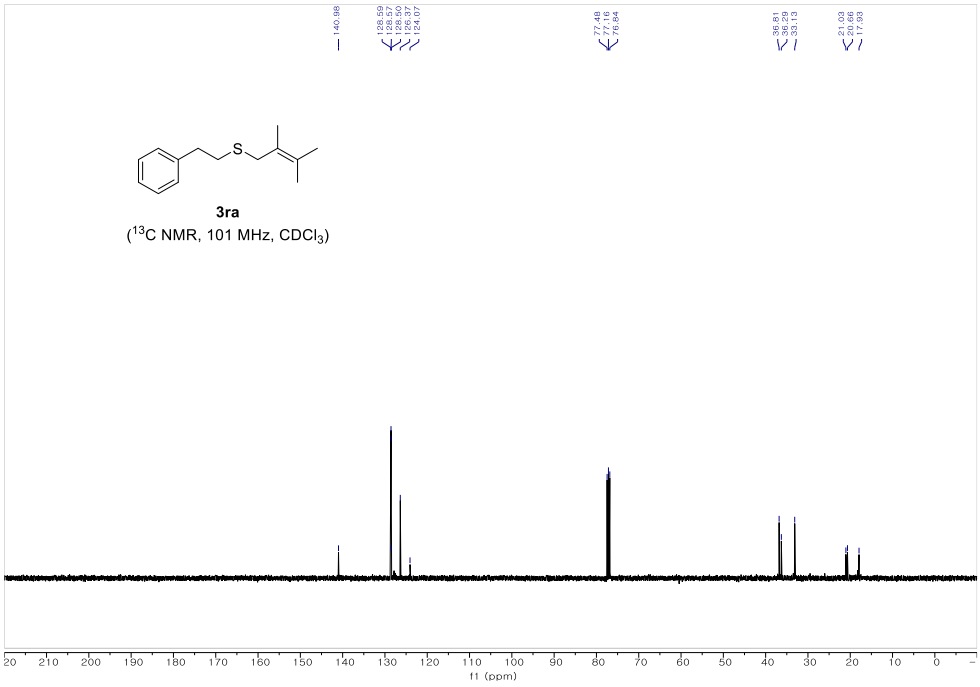

3ra

(^{13}C NMR, 101 MHz, $CDCl_3$)

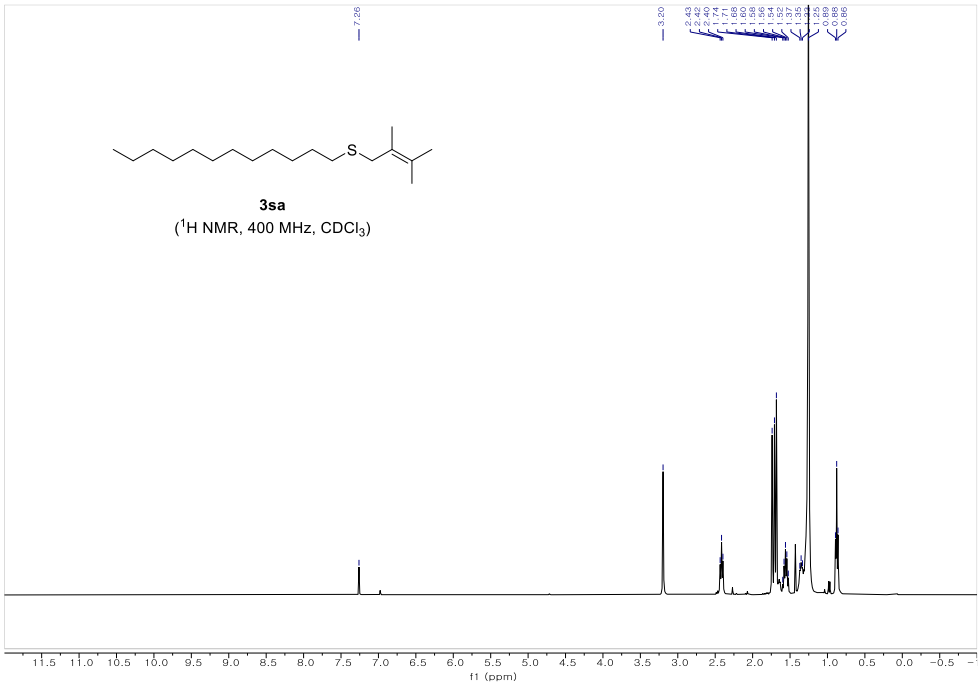

3sa

(^{1}H NMR, 400 MHz, $CDCl_3$)

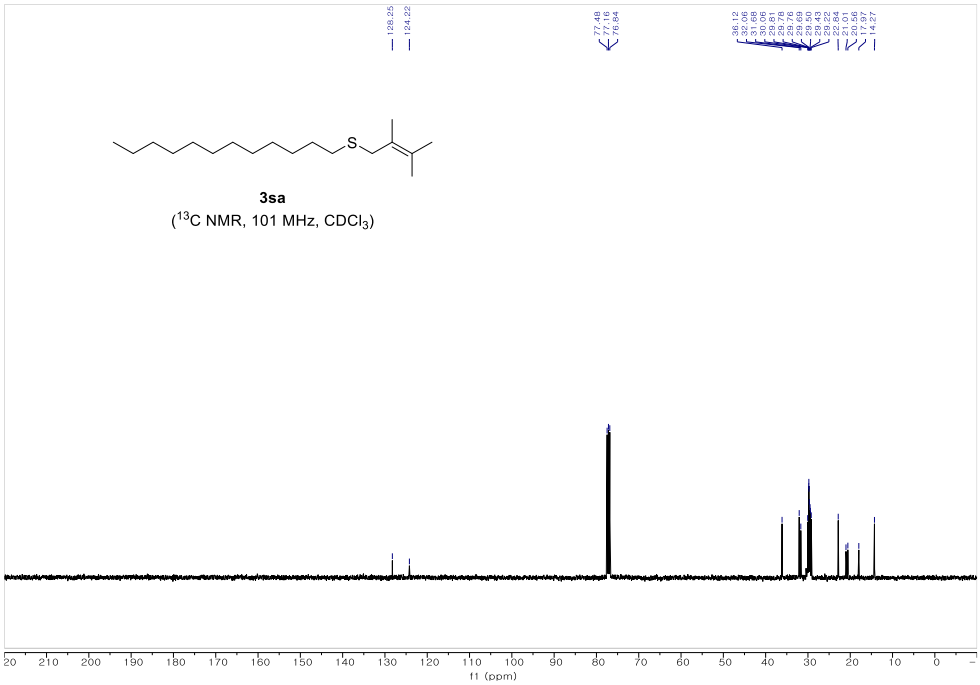

3sa

(^{13}C NMR, 101 MHz, $CDCl_3$)

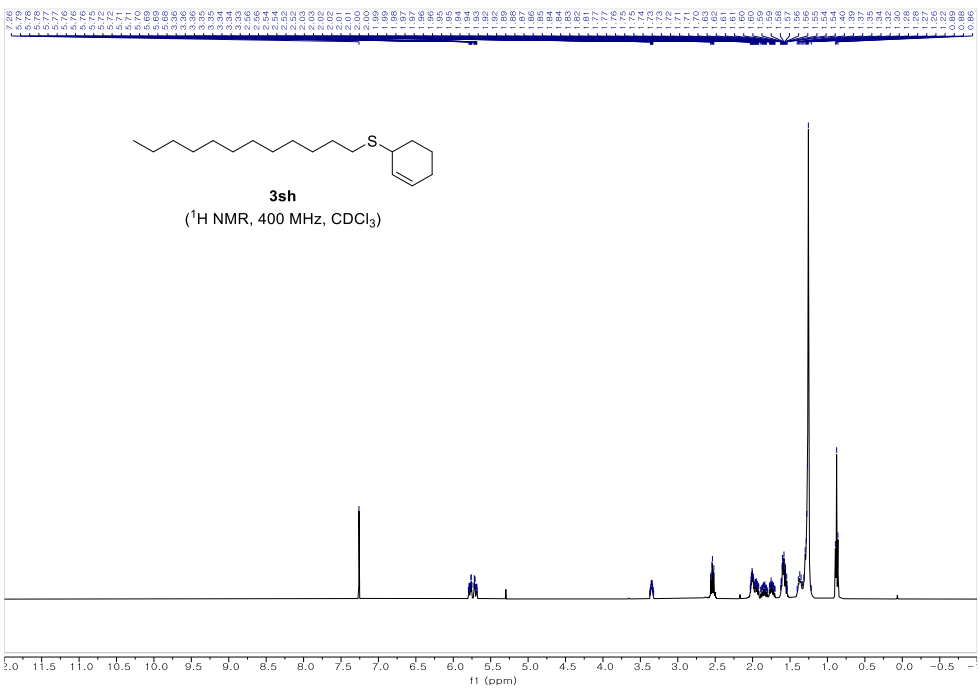

3sh

(^{1}H NMR, 400 MHz, $CDCl_3$)

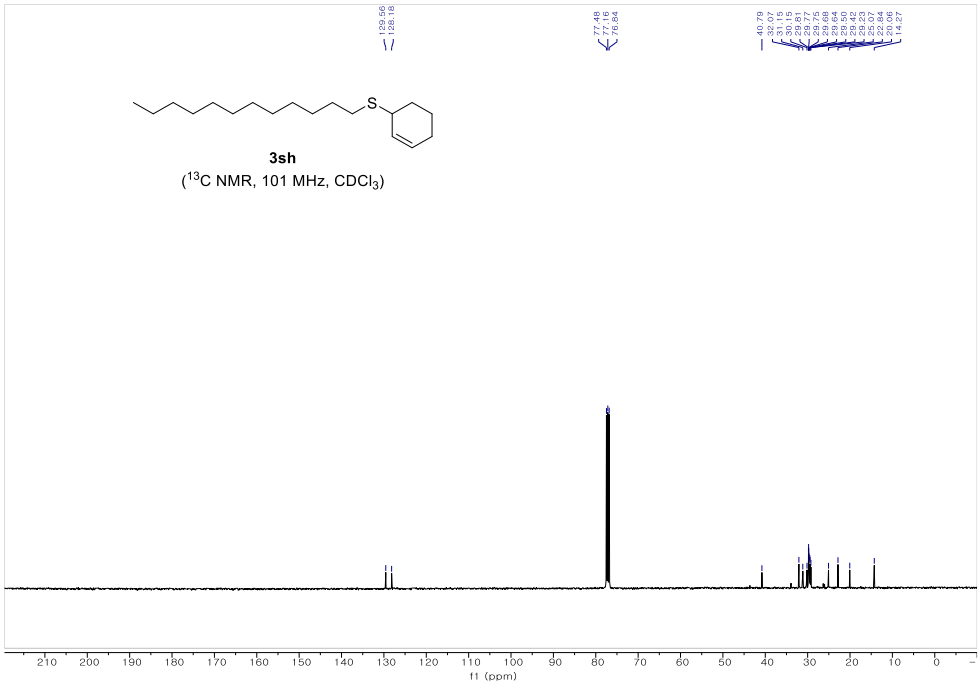

3sh

(^{13}C NMR, 101 MHz, $CDCl_3$)

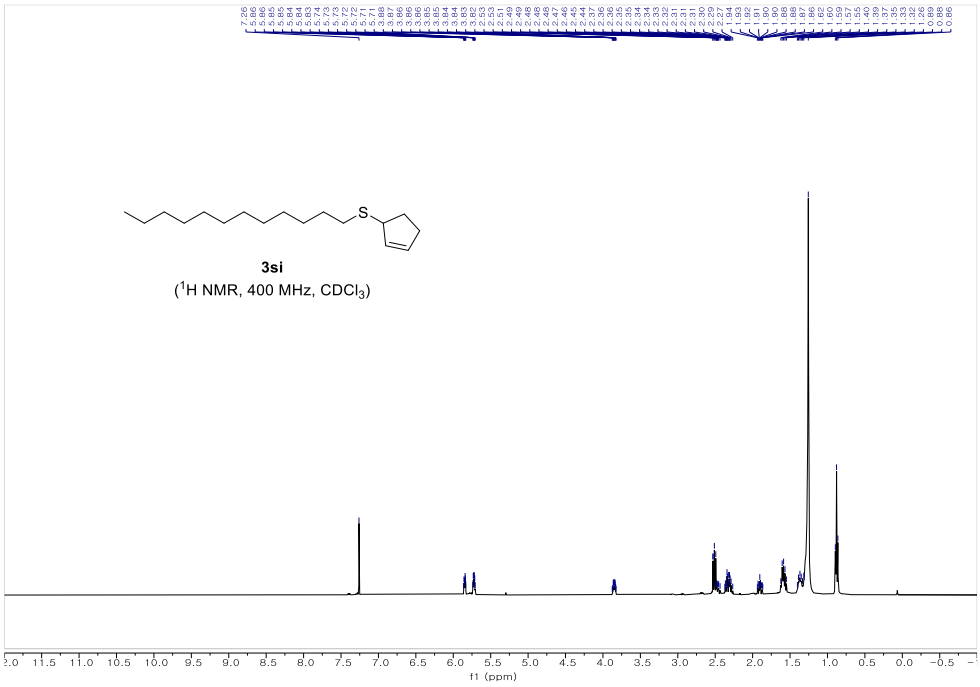

3si

(^{1}H NMR, 400 MHz, $CDCl_3$)

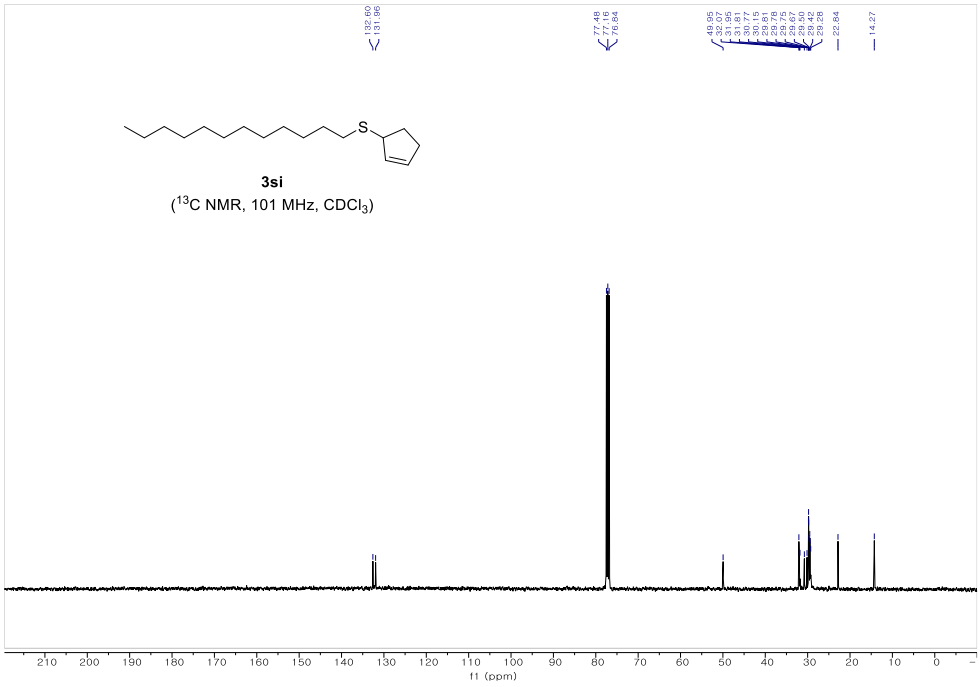

3si

(^{13}C NMR, 101 MHz, $CDCl_3$)

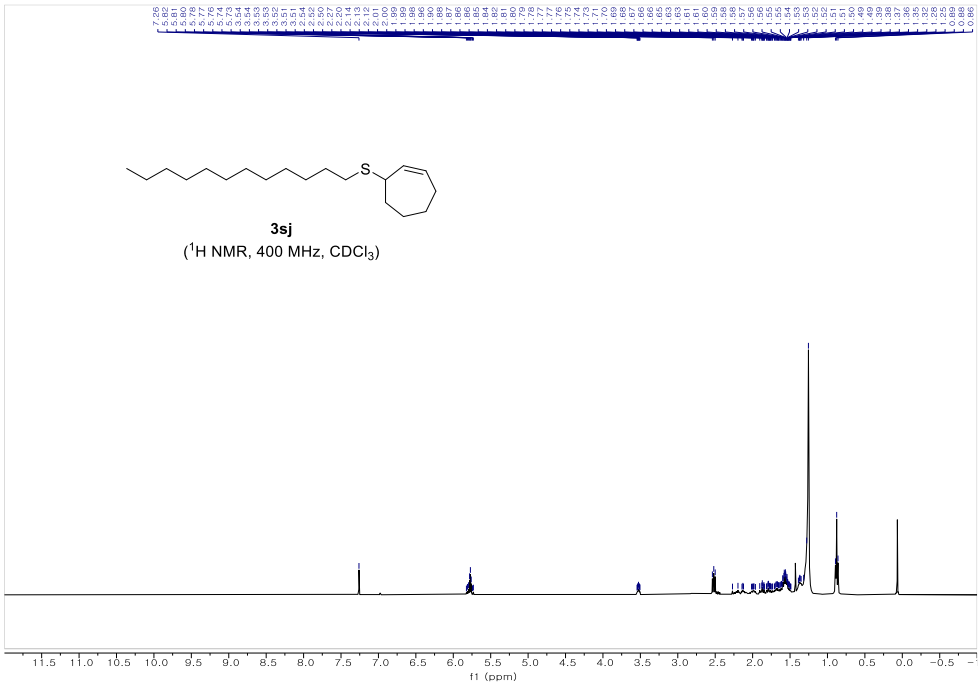

3sj

(^{1}H NMR, 400 MHz, $CDCl_3$)

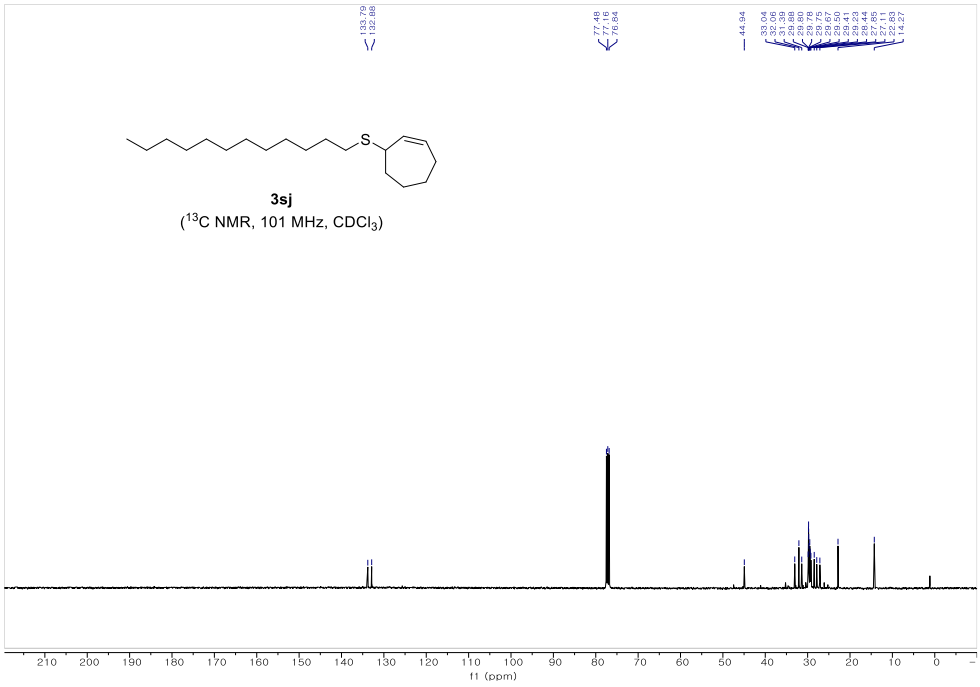

3sj

(^{13}C NMR, 101 MHz, $CDCl_3$)

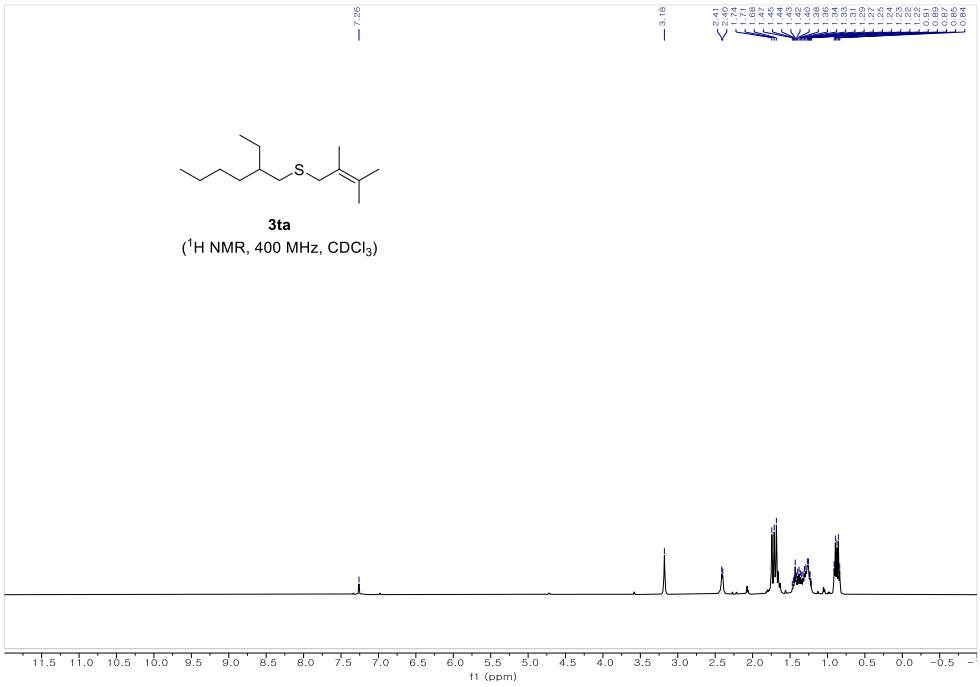

3ta

(^{1}H NMR, 400 MHz, $CDCl_3$)

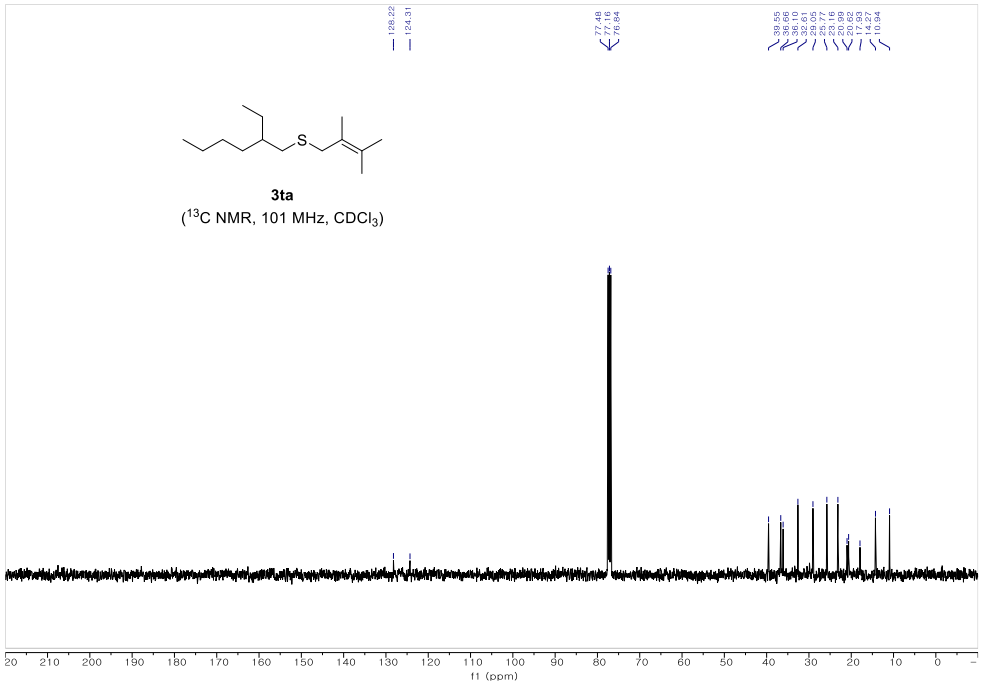

3ta

(^{13}C NMR, 101 MHz, $CDCl_3$)

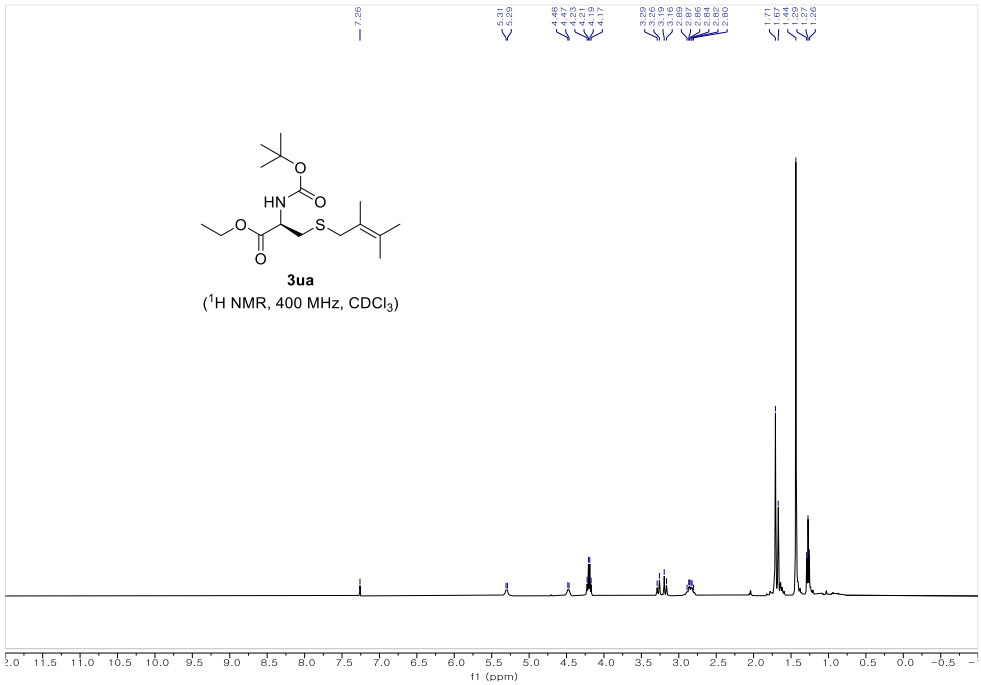

3ua

(^{1}H NMR, 400 MHz, $CDCl_3$)

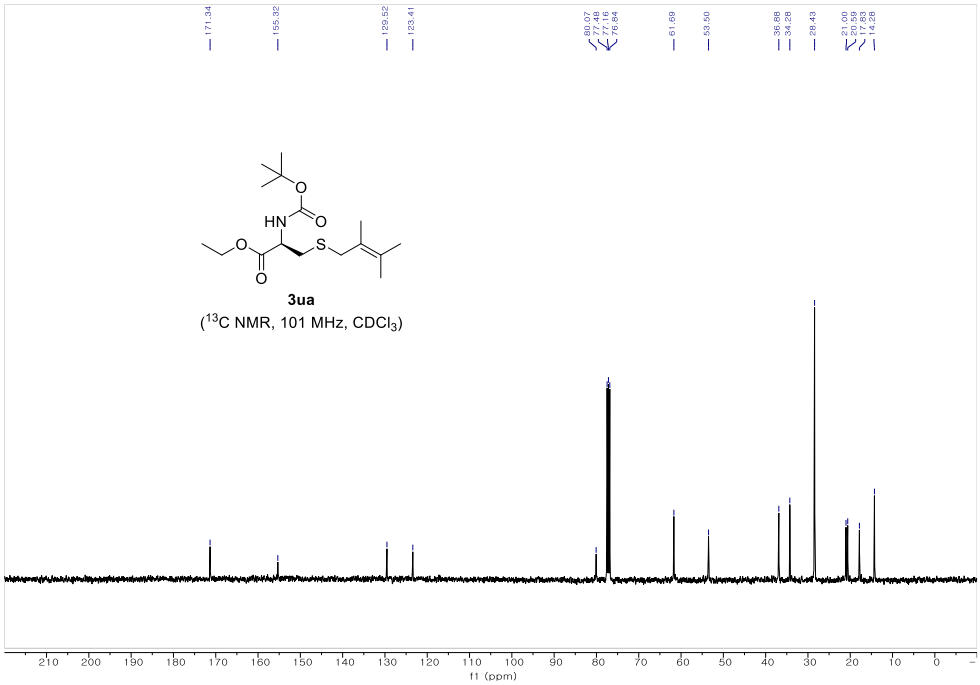

3ua

(^{13}C NMR, 101 MHz, $CDCl_3$)

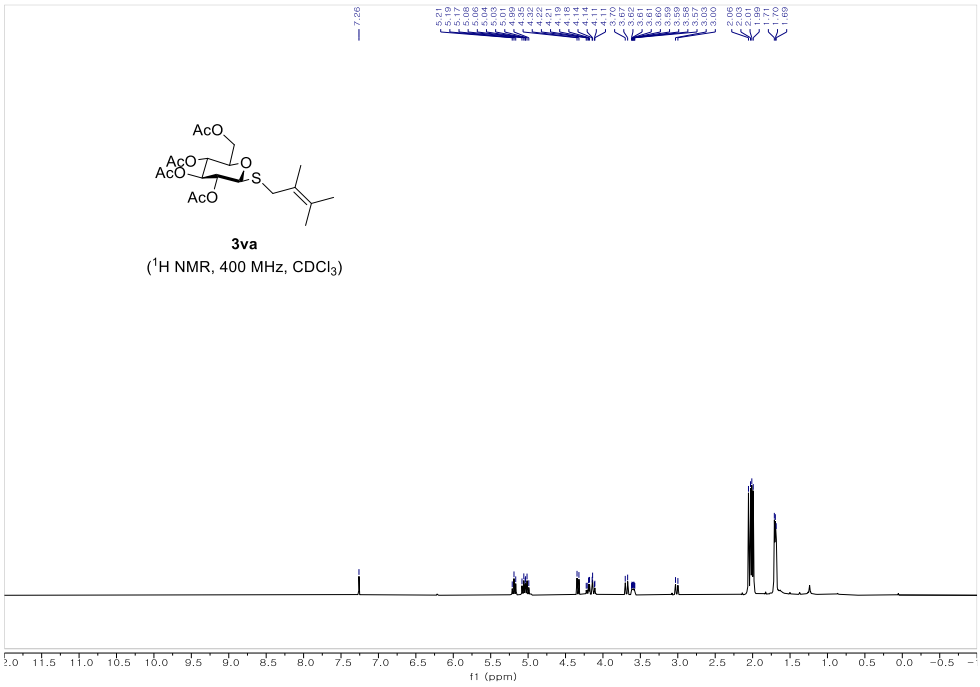

3va

(^{1}H NMR, 400 MHz, $CDCl_3$)

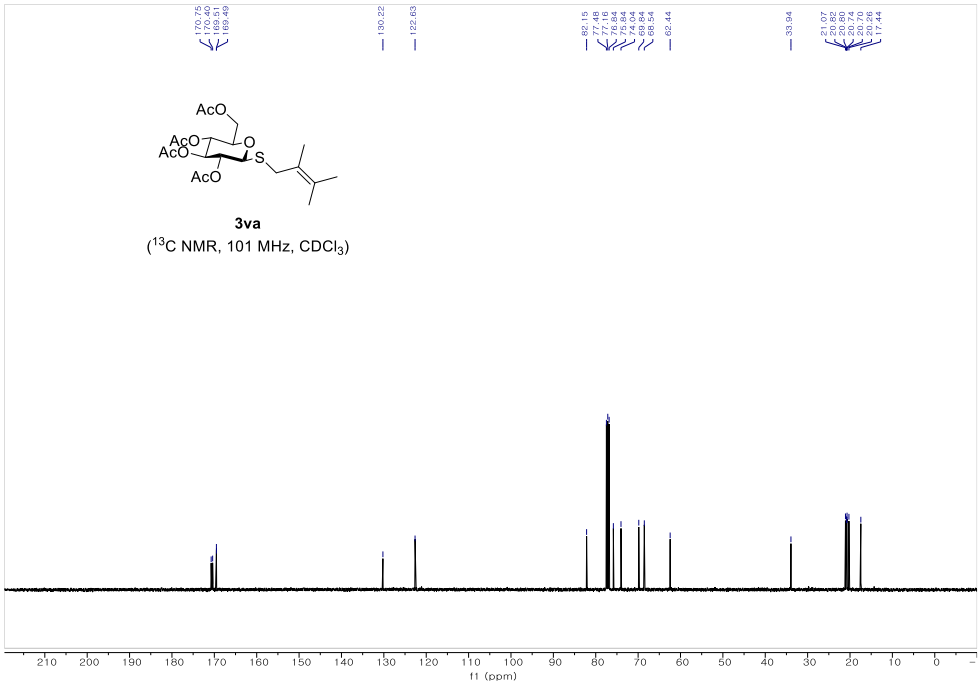

3va

(^{13}C NMR, 101 MHz, $CDCl_3$)

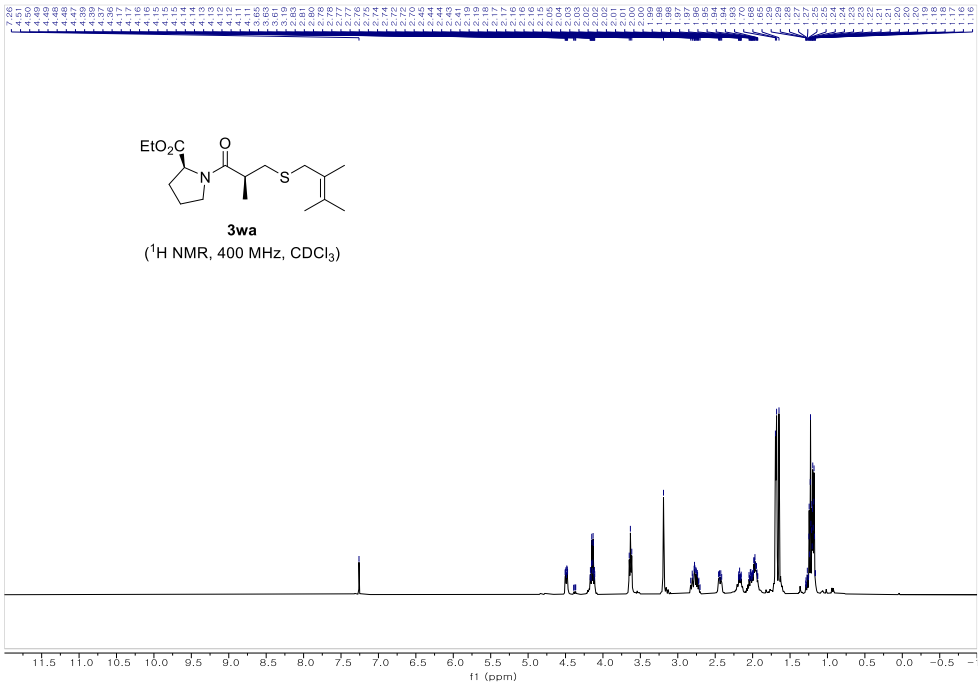

3wa

(^{1}H NMR, 400 MHz, $CDCl_3$)

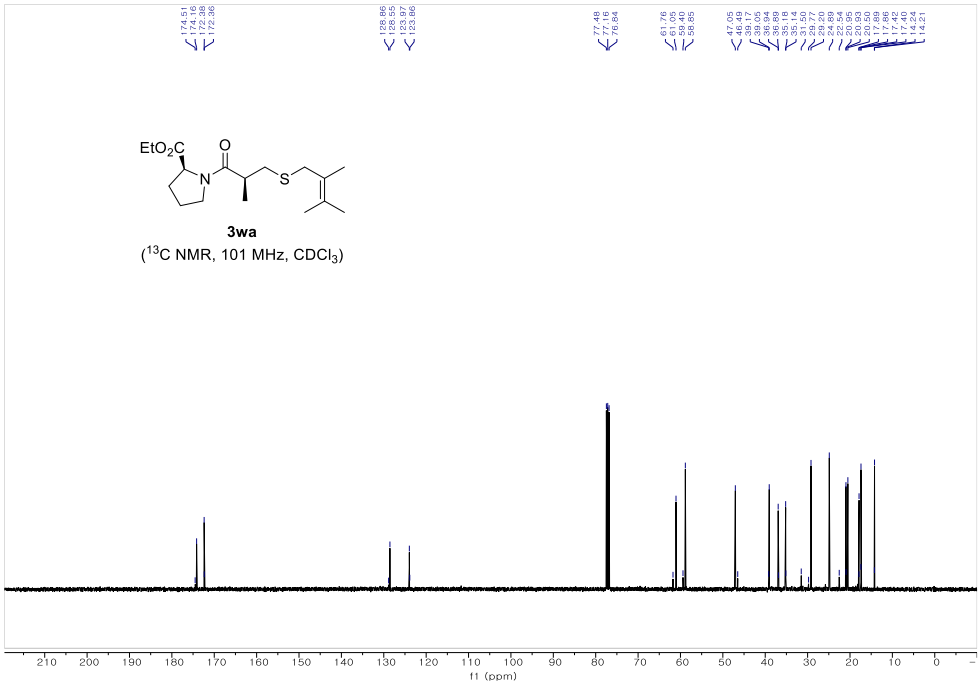
EtO2C
O
N
S
3wa
(13C NMR, 101 MHz, CDCl3)
f1 (ppm)

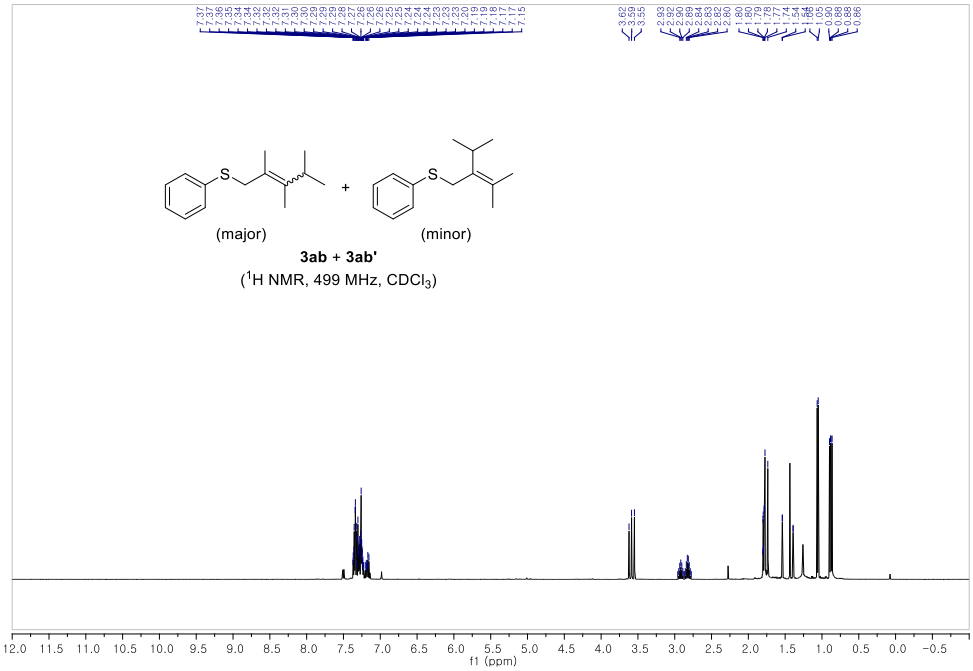
S
+
S
(major)
(minor)
3ab + 3ab'
(1H NMR, 499 MHz, CDCl3)
f1 (ppm)

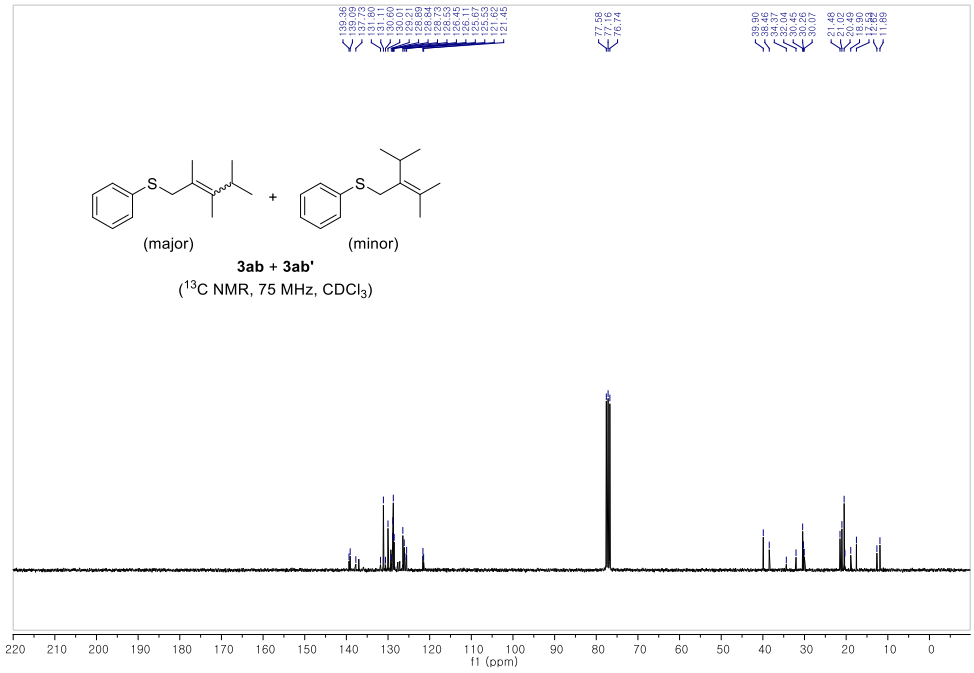
(major)
(minor)
3ab + 3ab'
(13C NMR, 75 MHz, CDCl3)
f1 (ppm)

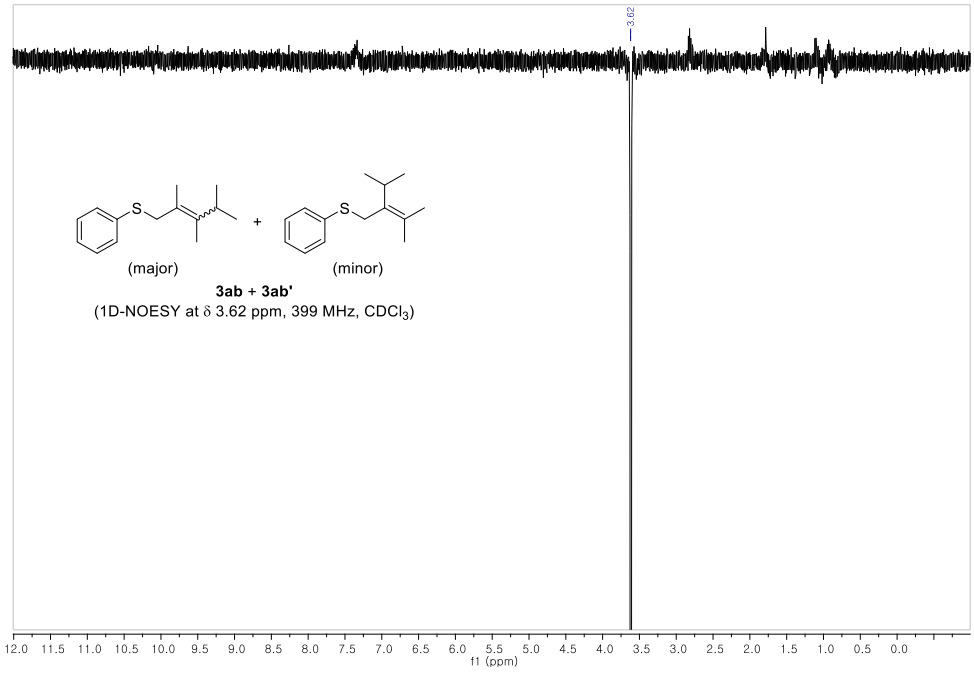
3.62
(major)
(minor)
3ab + 3ab'
(1D-NOESY at δ 3.62 ppm, 399 MHz, CDCl3)
f1 (ppm)

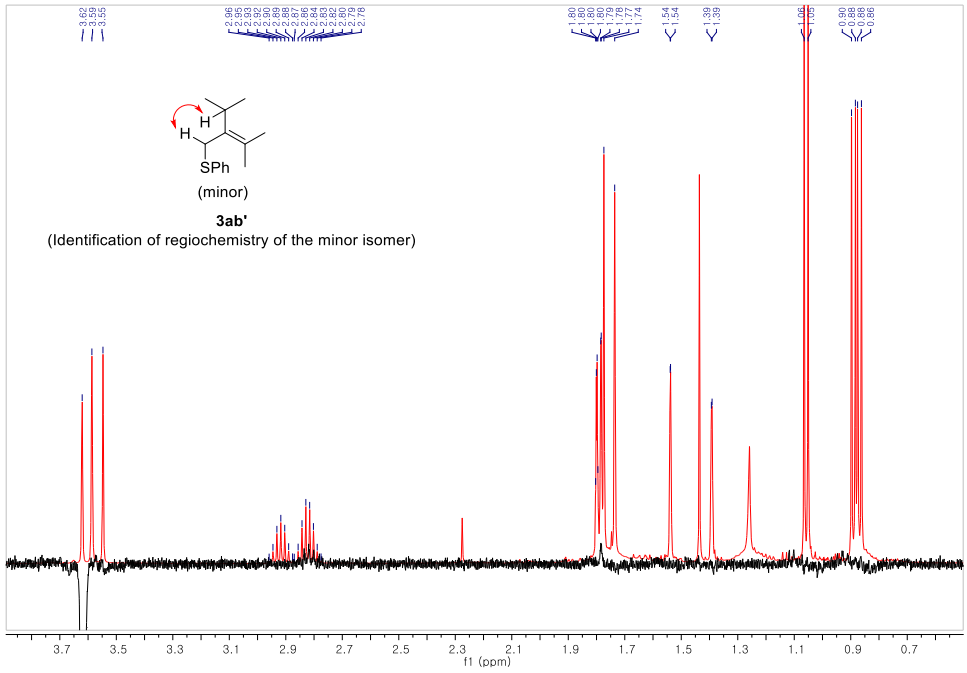
H
H
SPh
(minor)
3ab'
(Identification of regiochemistry of the minor isomer)
f1 (ppm)

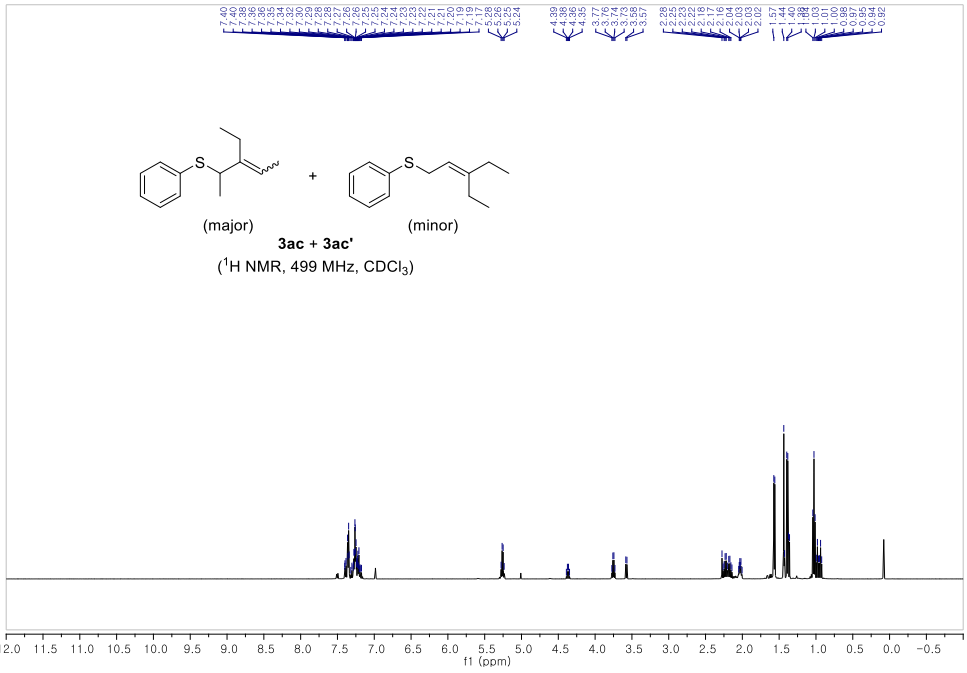
S
+
S
(major)
(minor)
3ac + 3ac'
(1H NMR, 499 MHz, CDCl3)
f1 (ppm)

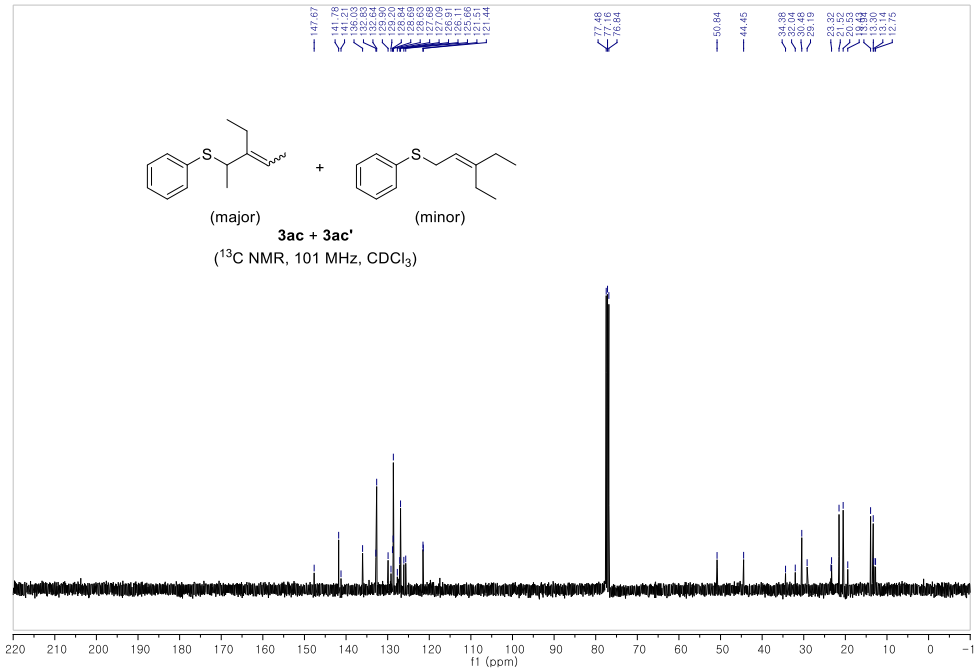
147.67
141.78
141.21
136.03
132.83
132.64
129.90
129.20
128.84
128.69
126.63
126.09
127.09
126.91
126.11
125.66
121.51
121.44
77.48
77.16
76.84
50.84
44.45
34.98
32.04
30.48
29.19
23.32
21.52
20.53
19.63
19.44
13.30
13.14
12.15
S
S
+
(major)
(minor)
3ac + 3ac'
(13C NMR, 101 MHz, CDCl3)
f1 (ppm)

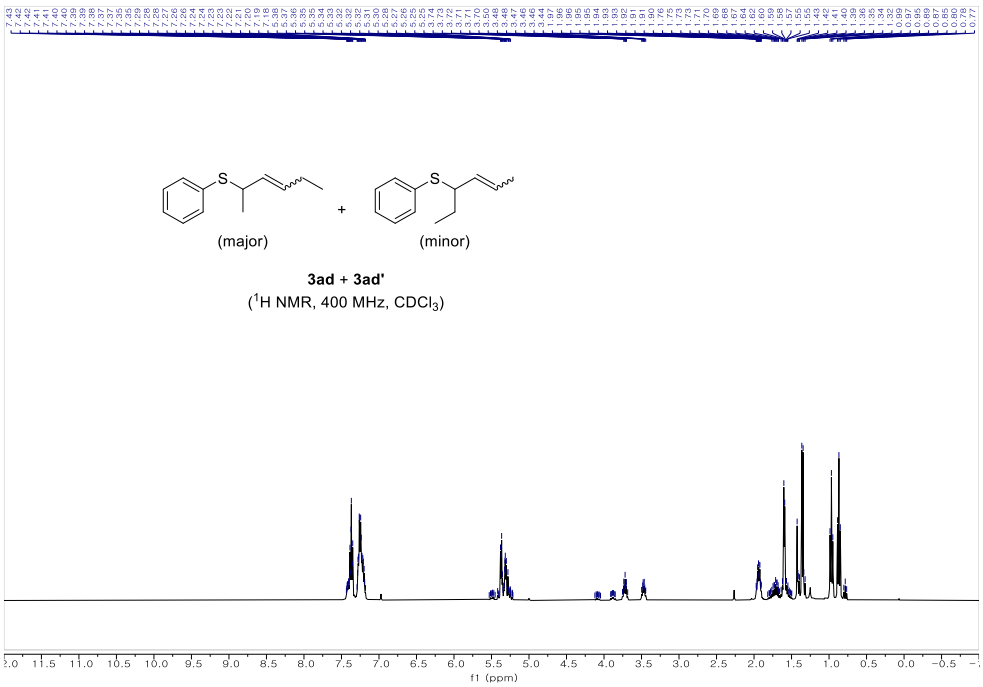
S
S
+
(major)
(minor)
3ad + 3ad'
(1H NMR, 400 MHz, CDCl3)
f1 (ppm)

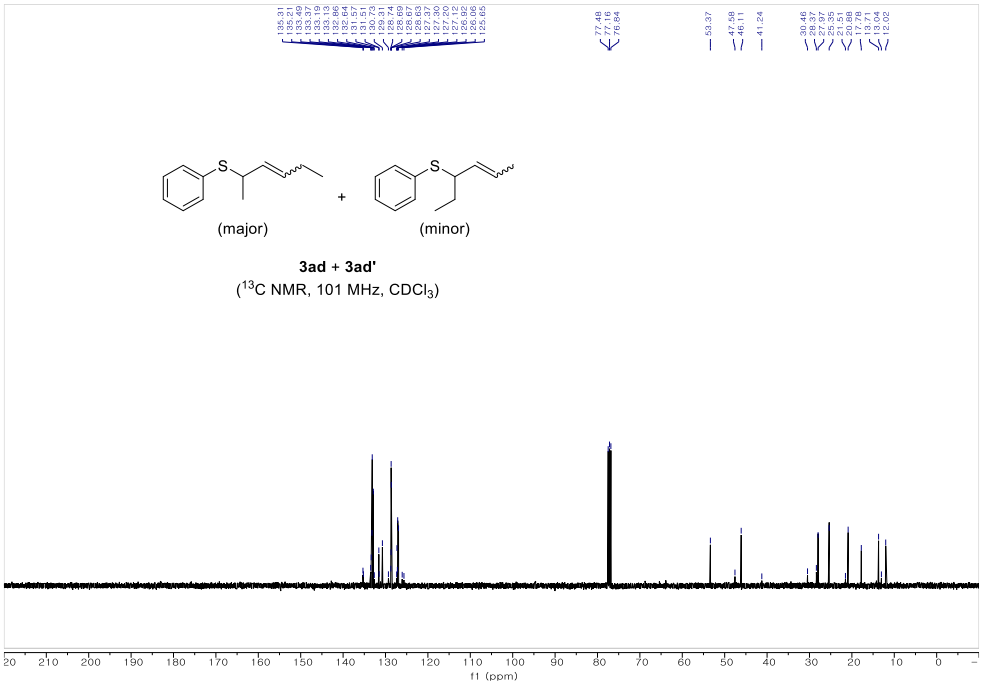
(major)
(minor)
3ad + 3ad'
(13C NMR, 101 MHz, CDCl3)
f1 (ppm)

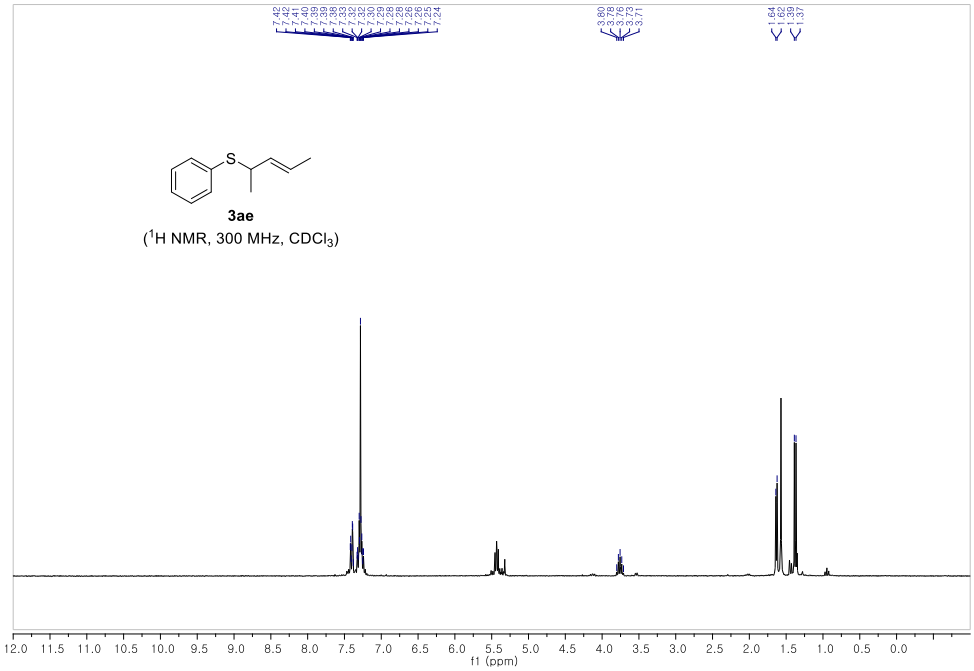
3ae
(1H NMR, 300 MHz, CDCl3)
f1 (ppm)

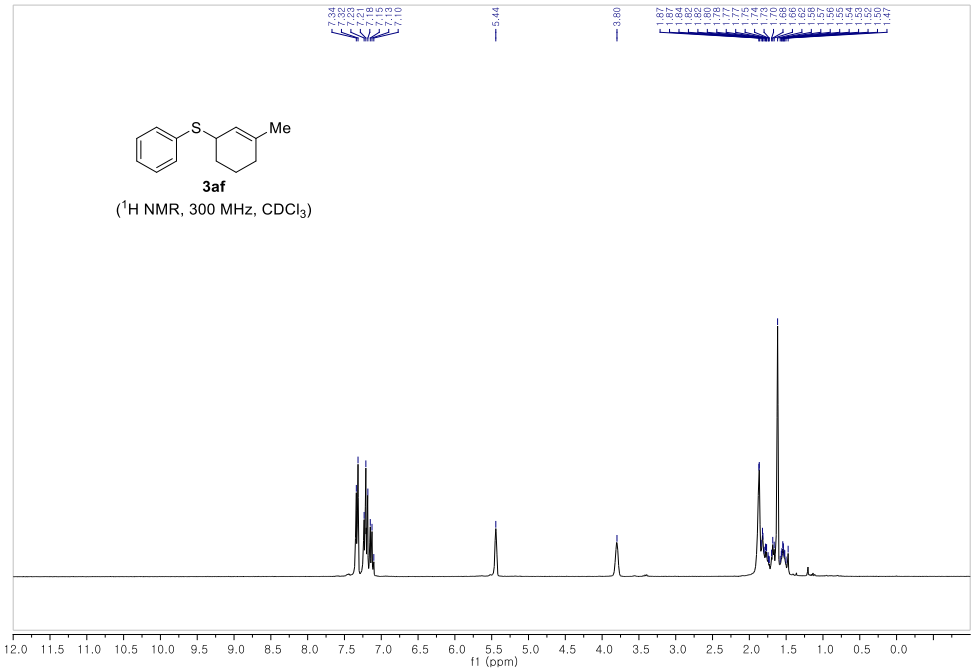
7.34
7.32
7.23
7.21
7.18
7.15
7.13
7.10
5.44
3.80
1.87
1.84
1.82
1.80
1.78
1.77
1.75
1.74
1.70
1.68
1.66
1.62
1.56
1.57
1.56
1.55
1.54
1.53
1.52
1.50
1.47
S
Me
3af
(1H NMR, 300 MHz, CDCl3)
12.0 11.5 11.0 10.5 10.0 9.5 9.0 8.5 8.0 7.5 7.0 6.5 6.0 5.5 5.0 4.5 4.0 3.5 3.0 2.5 2.0 1.5 1.0 0.5 0.0
f1 (ppm)

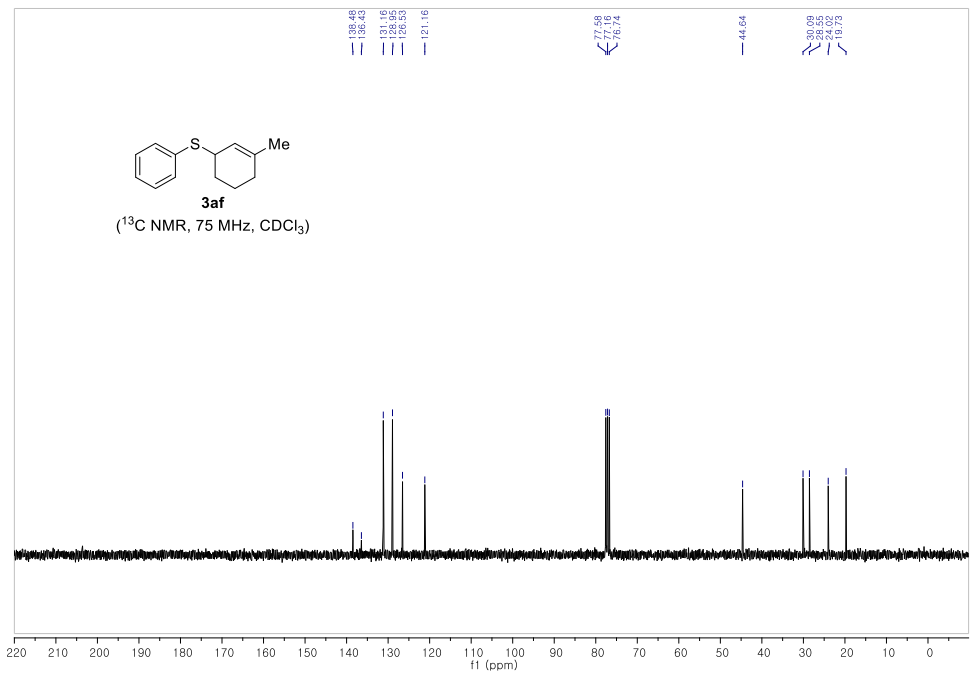
138.48
136.43
131.16
128.65
126.53
121.16
77.58
77.16
76.74
44.64
30.09
28.55
24.02
19.73
S
Me
3af
(13C NMR, 75 MHz, CDCl3)
220 210 200 190 180 170 160 150 140 130 120 110 100 90 80 70 60 50 40 30 20 10 0
f1 (ppm)

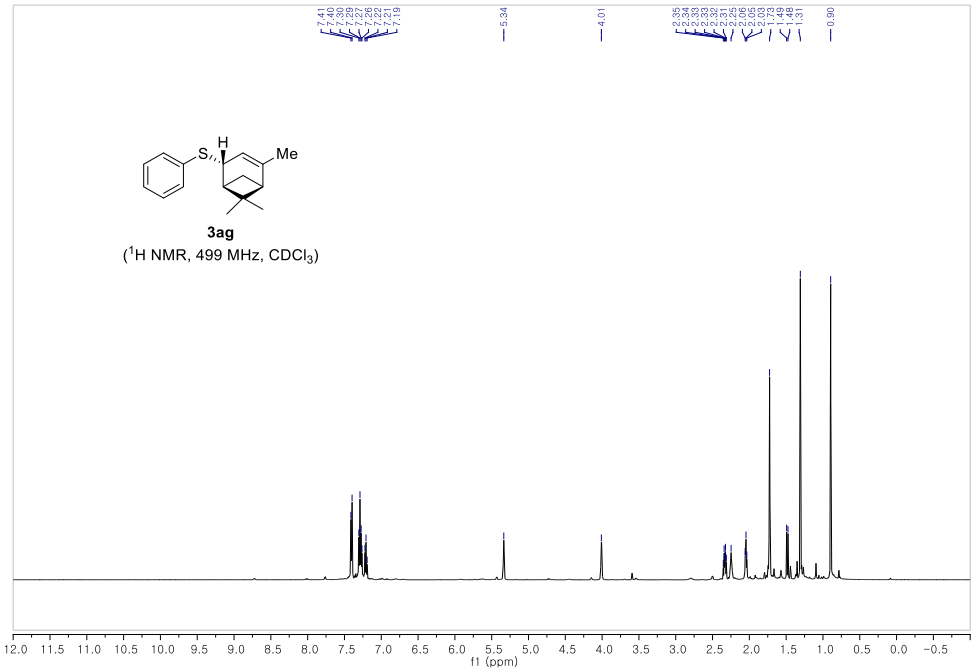
7.41
7.40
7.30
7.29
7.27
7.26
7.22
7.21
7.19
5.34
4.01
2.35
2.34
2.33
2.33
2.32
2.31
2.25
2.06
2.05
2.03
1.73
1.48
1.31
0.90
H
S
Me
3ag
(1H NMR, 499 MHz, CDCl3)
f1 (ppm)

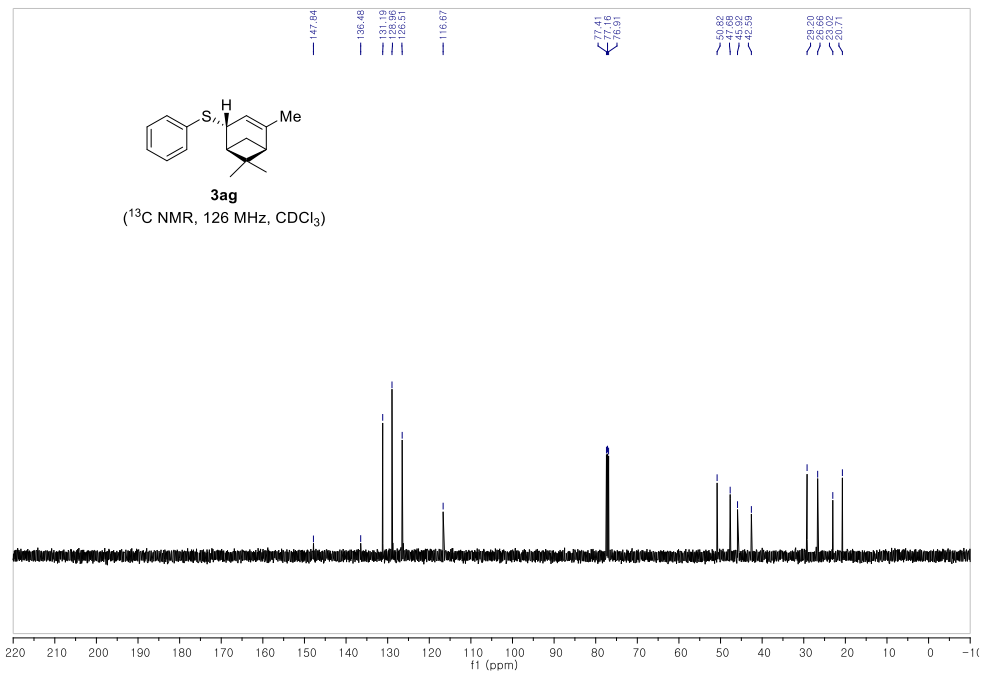
147.84
136.48
131.19
128.86
126.51
116.67
77.41
77.16
76.91
50.82
47.68
45.60
42.59
29.20
28.66
23.02
20.71
H
S
Me
3ag
(13C NMR, 126 MHz, CDCl3)
f1 (ppm)

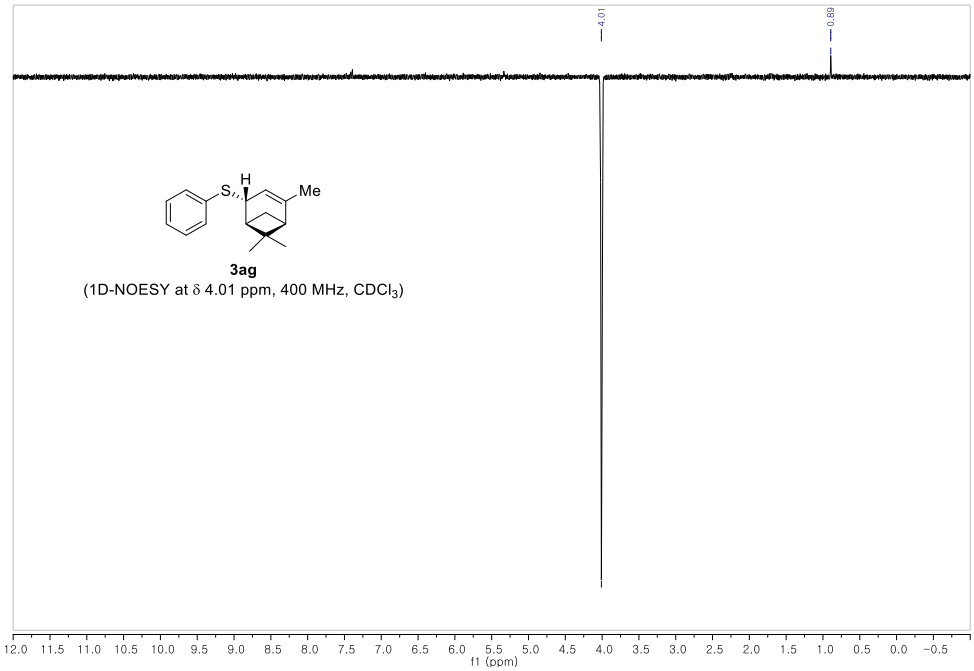

3ag

(1D-NOESY at δ 4.01 ppm, 400 MHz, $CDCl_3$)

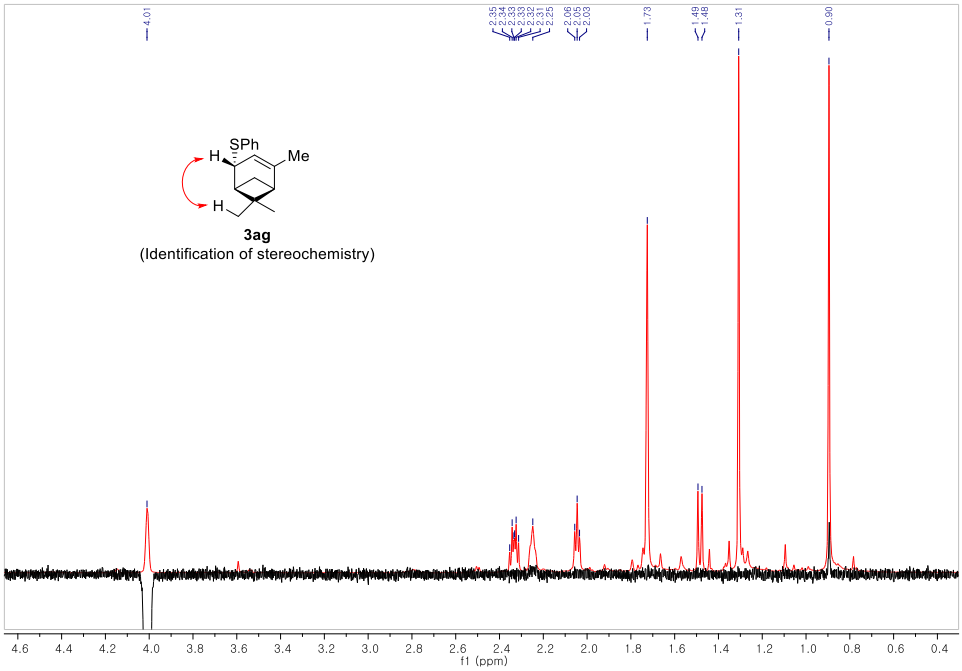

3ag

(Identification of stereochemistry)

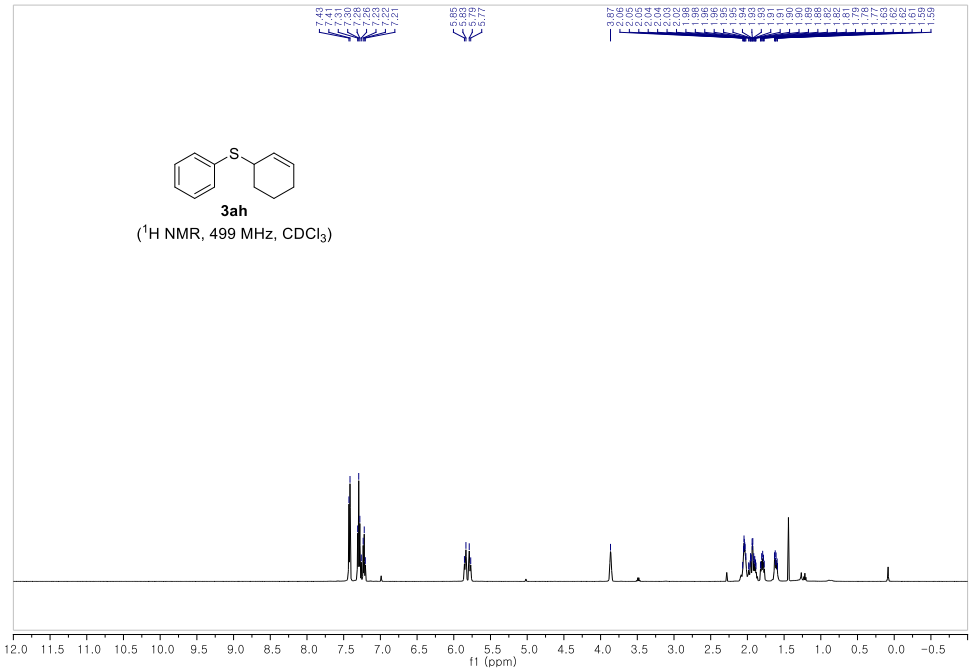

3ah

(^{1}H NMR, 499 MHz, $CDCl_3$)

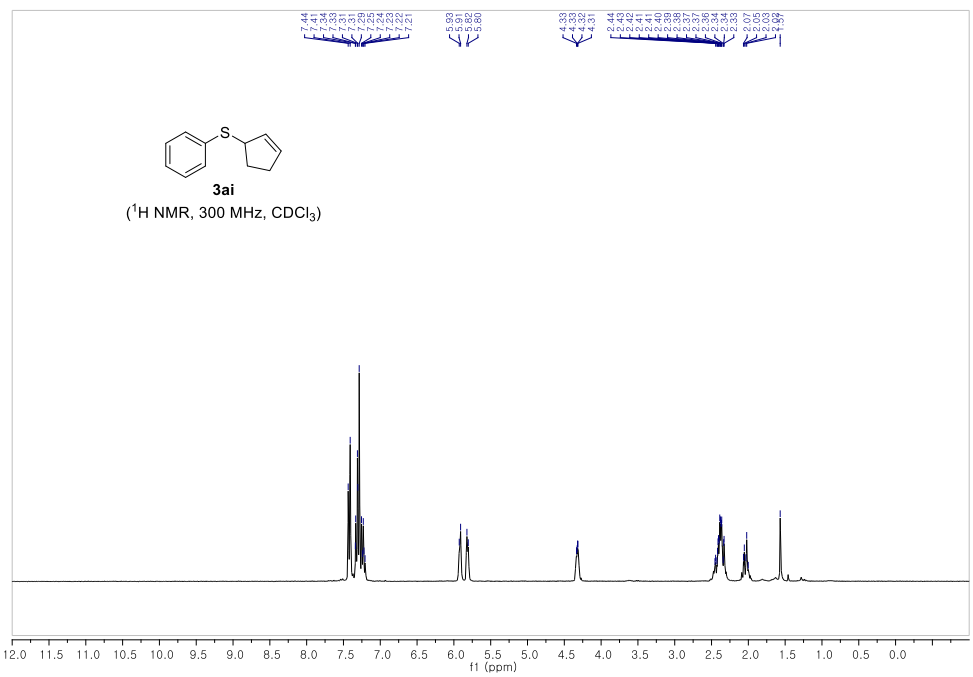

3ai

(^{1}H NMR, 300 MHz, $CDCl_3$)

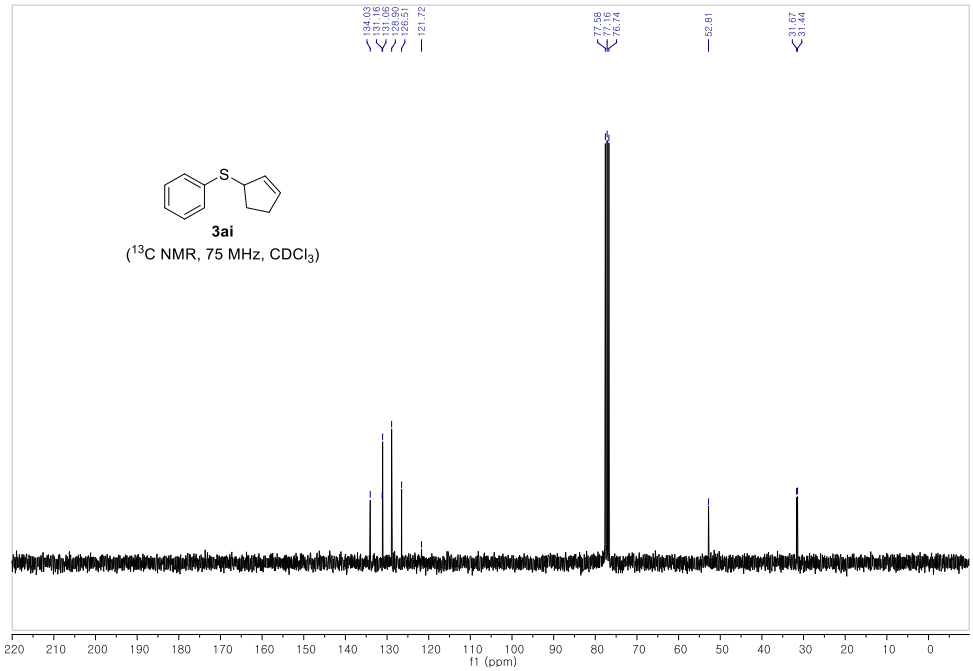
134.03
131.16
131.06
128.90
126.51
121.72
77.58
77.16
76.74
52.81
31.67
31.44
S
3ai
(13C NMR, 75 MHz, CDCl3)
f1 (ppm)

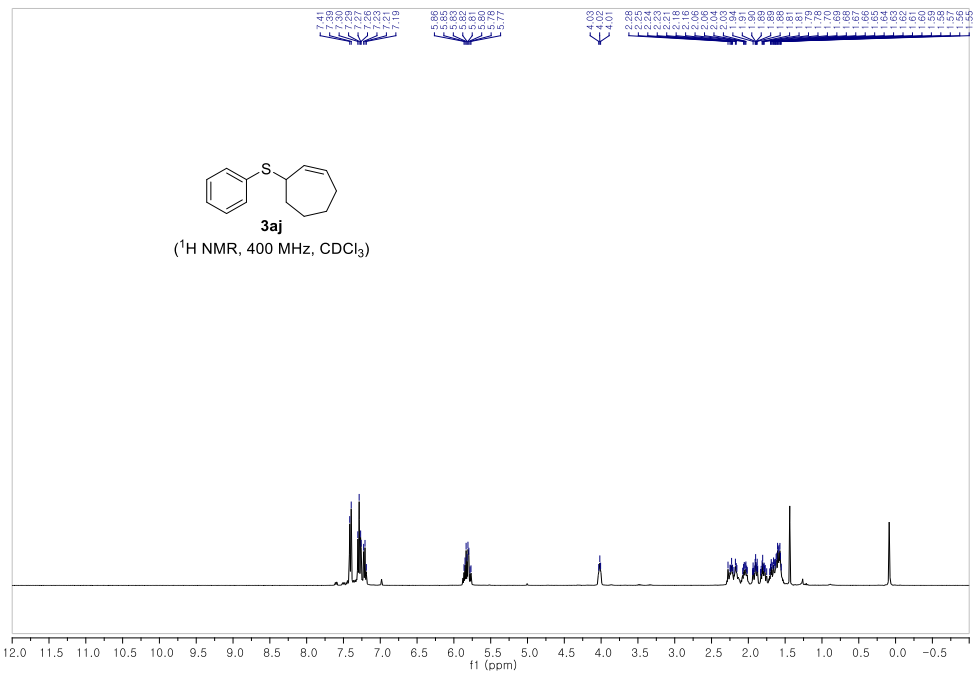
S
3aj
(1H NMR, 400 MHz, CDCl3)
f1 (ppm)

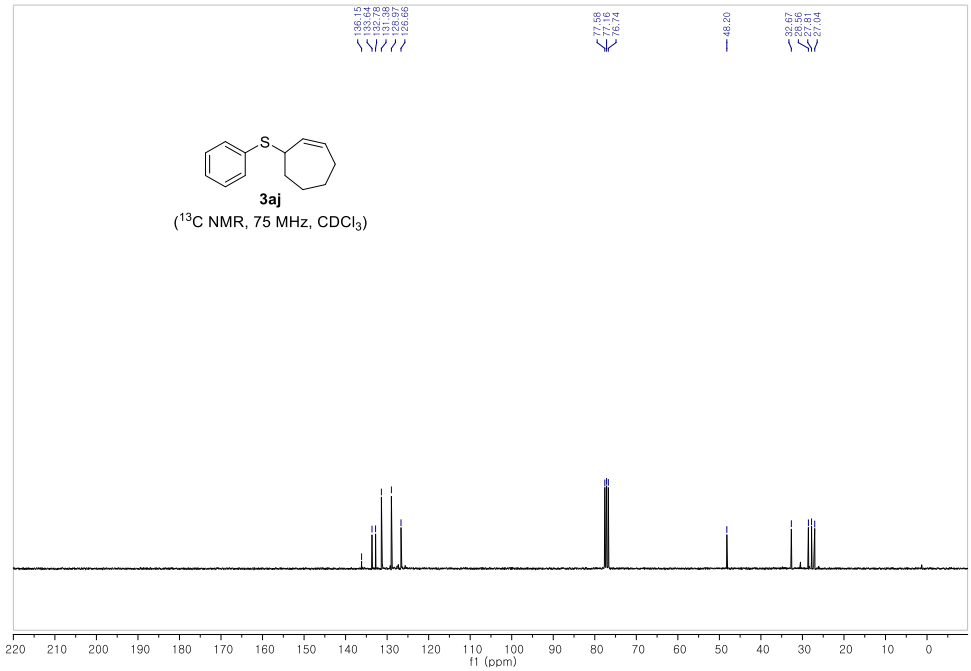
136.15
133.64
132.78
131.48
128.97
126.66
77.58
77.16
76.74
48.20
32.67
28.56
27.81
27.04
S
3aj
(13C NMR, 75 MHz, CDCl3)
220 210 200 190 180 170 160 150 140 130 120 110 100 90 80 70 60 50 40 30 20 10 0
f1 (ppm)

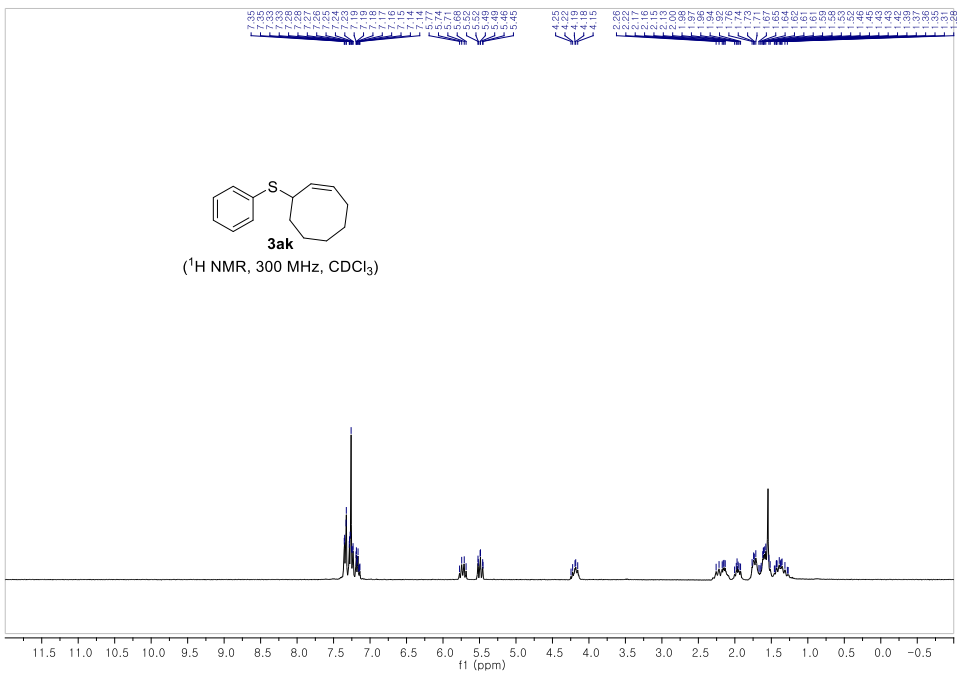
7.35
7.33
7.30
7.28
7.27
7.26
7.25
7.24
7.23
7.19
7.18
7.17
7.16
7.15
7.14
5.77
5.74
5.71
5.68
5.52
5.49
5.46
5.45
4.25
4.22
4.19
4.18
4.15
2.28
2.17
2.16
2.15
2.13
2.00
1.99
1.97
1.96
1.94
1.92
1.76
1.74
1.73
1.71
1.70
1.65
1.64
1.62
1.61
1.60
1.59
1.58
1.53
1.52
1.46
1.45
1.44
1.43
1.42
1.39
1.37
1.36
1.33
1.31
1.29
S
3ak
(1H NMR, 300 MHz, CDCl3)
11.5 11.0 10.5 10.0 9.5 9.0 8.5 8.0 7.5 7.0 6.5 6.0 5.5 5.0 4.5 4.0 3.5 3.0 2.5 2.0 1.5 1.0 0.5 0.0 -0.5
f1 (ppm)

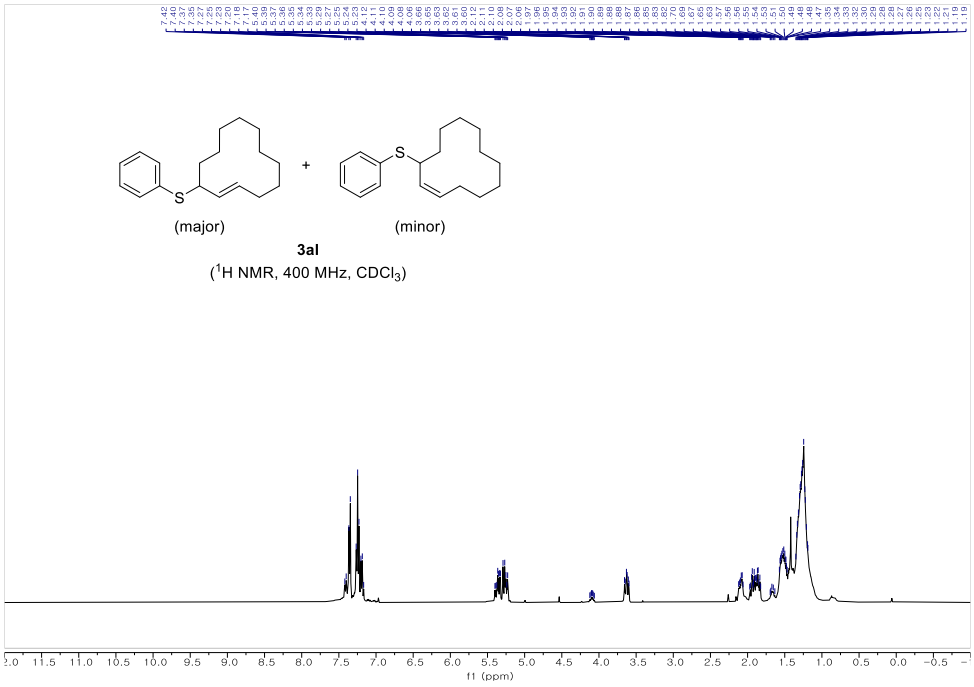
(major)
(minor)
3al
(^{1}H NMR, 400 MHz, $CDCl_3$)
f1 (ppm)

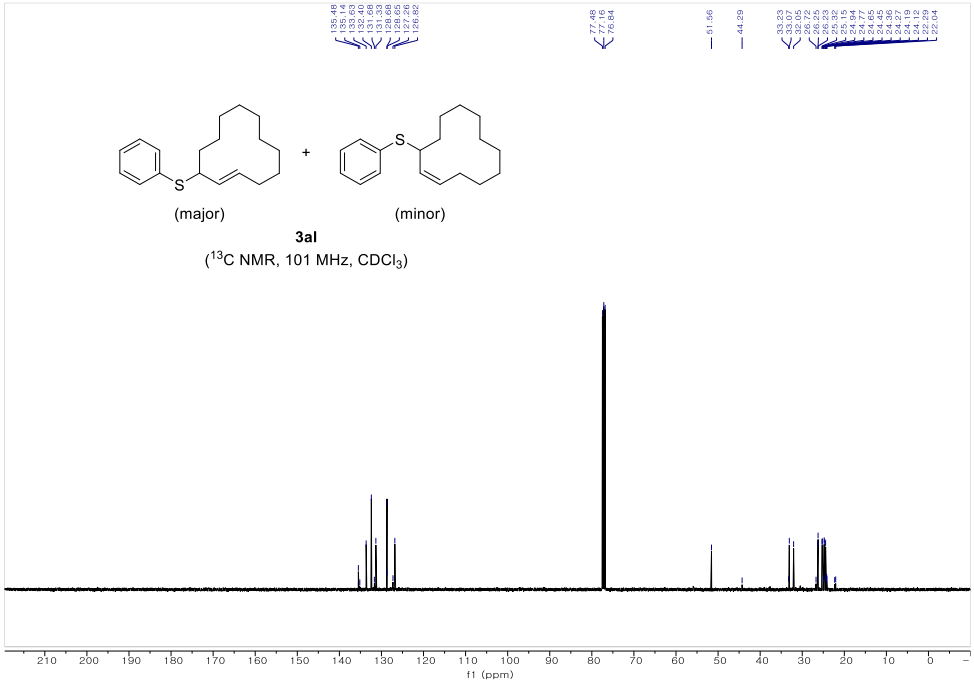
(major)
(minor)
3al
(^{13}C NMR, 101 MHz, $CDCl_3$)
f1 (ppm)

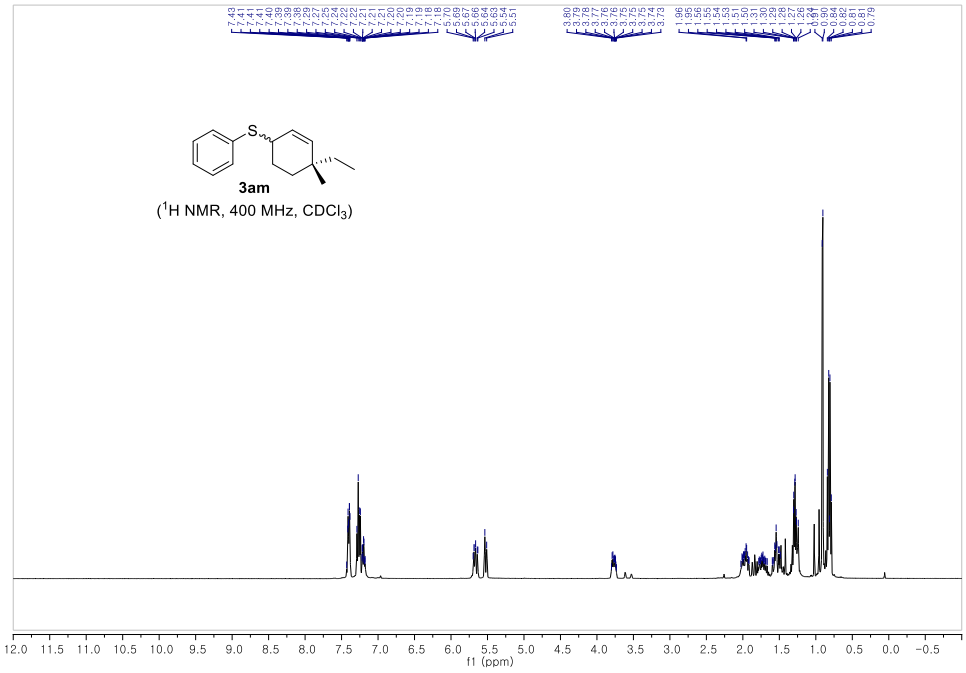
3am
(1H NMR, 400 MHz, CDCl3)
f1 (ppm)

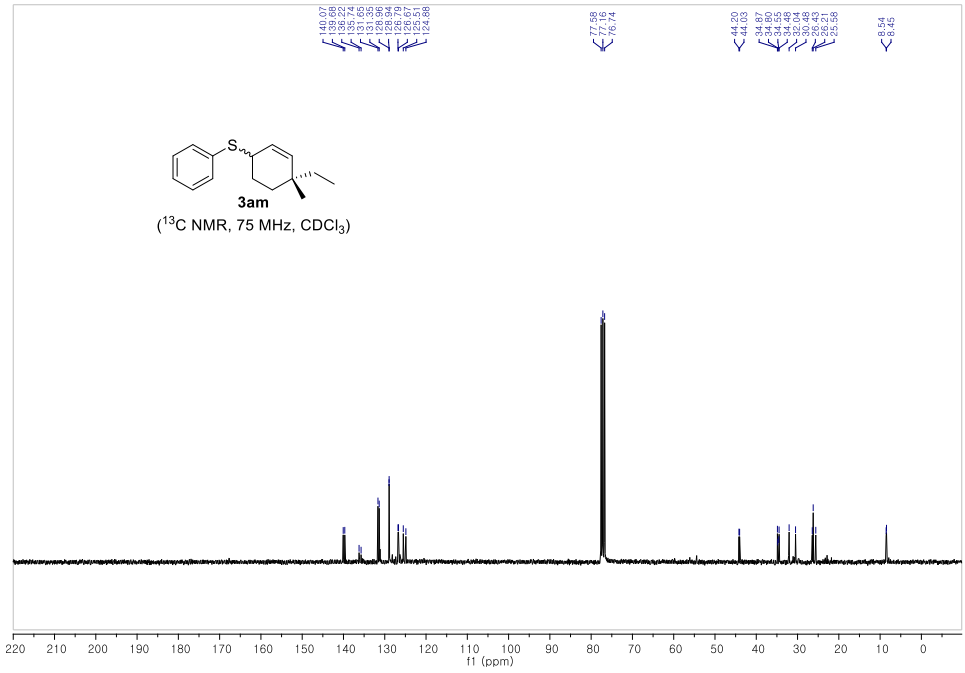
3am
(13C NMR, 75 MHz, CDCl3)
f1 (ppm)

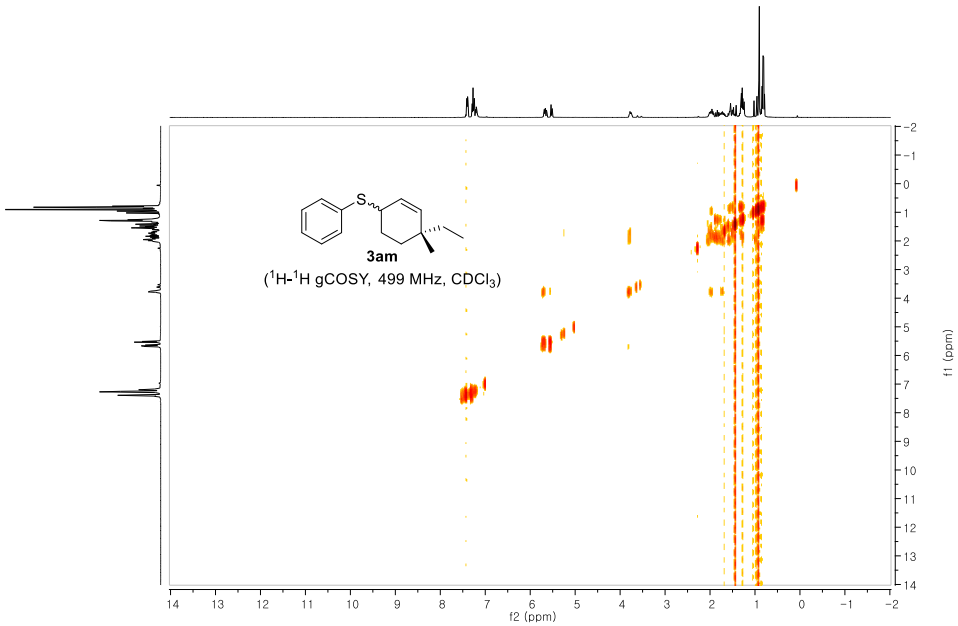
3am
(^{1}H-^{1}H gCOSY, 499 MHz, $CDCl_3$)
f2 (ppm)
f1 (ppm)

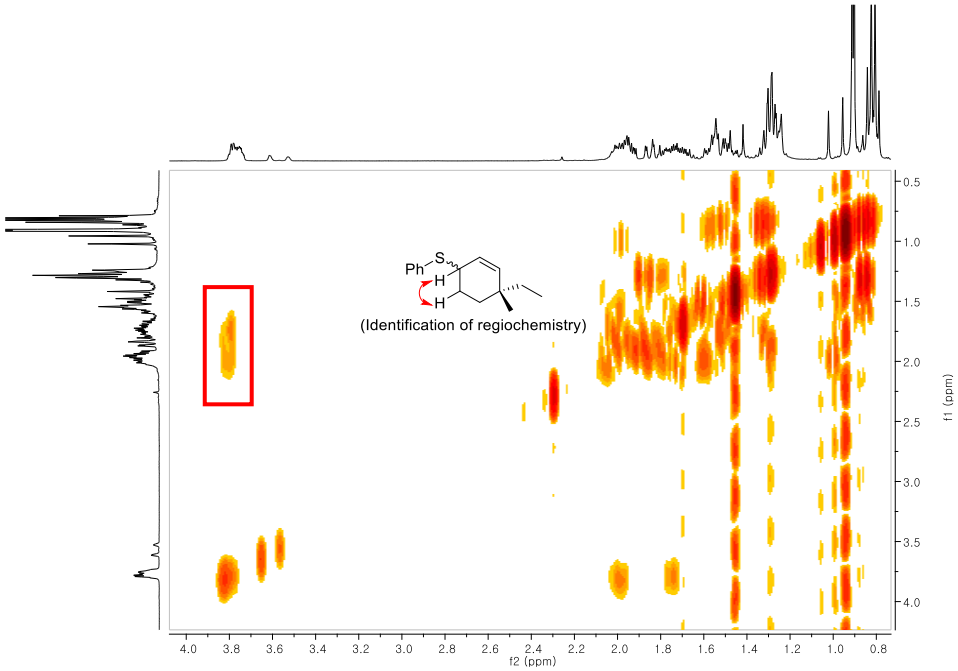
Ph
H
H
(Identification of regiochemistry)
f2 (ppm)
f1 (ppm)

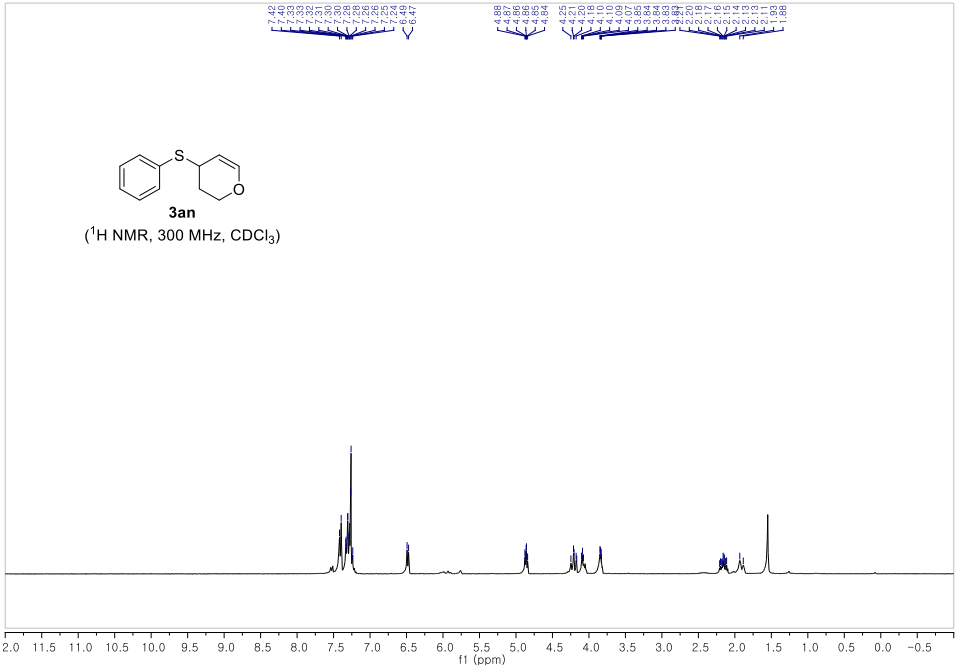
7.42
7.40
7.33
7.32
7.31
7.30
7.28
7.26
7.25
7.24
6.49
6.47
4.88
4.87
4.86
4.85
4.84
4.25
4.21
4.20
4.18
4.10
4.09
4.07
3.85
3.84
3.84
3.83
2.20
2.19
2.17
2.16
2.15
2.14
2.13
2.13
2.11
1.88
S
O
3an
(1H NMR, 300 MHz, CDCl3)
12.0 11.5 11.0 10.5 10.0 9.5 9.0 8.5 8.0 7.5 7.0 6.5 6.0 5.5 5.0 4.5 4.0 3.5 3.0 2.5 2.0 1.5 1.0 0.5 0.0 -0.5
f1 (ppm)

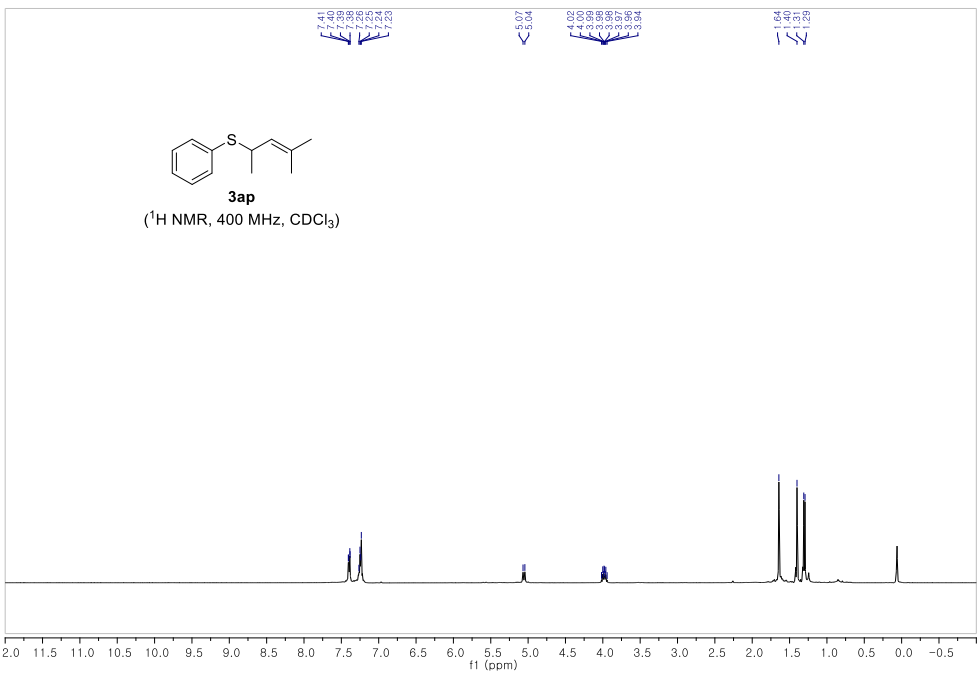
7.41
7.40
7.39
7.38
7.26
7.25
7.24
7.23
5.07
5.04
4.02
4.00
3.99
3.98
3.98
3.97
3.96
3.94
1.64
1.40
1.31
1.29
S
3ap
(1H NMR, 400 MHz, CDCl3)
12.0 11.5 11.0 10.5 10.0 9.5 9.0 8.5 8.0 7.5 7.0 6.5 6.0 5.5 5.0 4.5 4.0 3.5 3.0 2.5 2.0 1.5 1.0 0.5 0.0 -0.5
f1 (ppm)

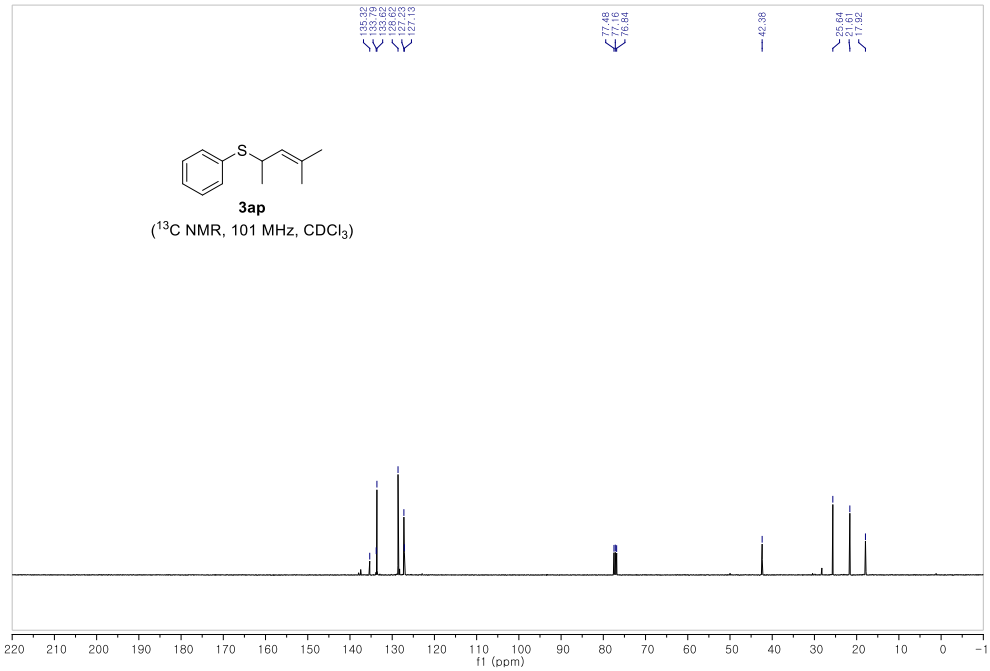

3ap

(^{13}C NMR, 101 MHz, $CDCl_3$)

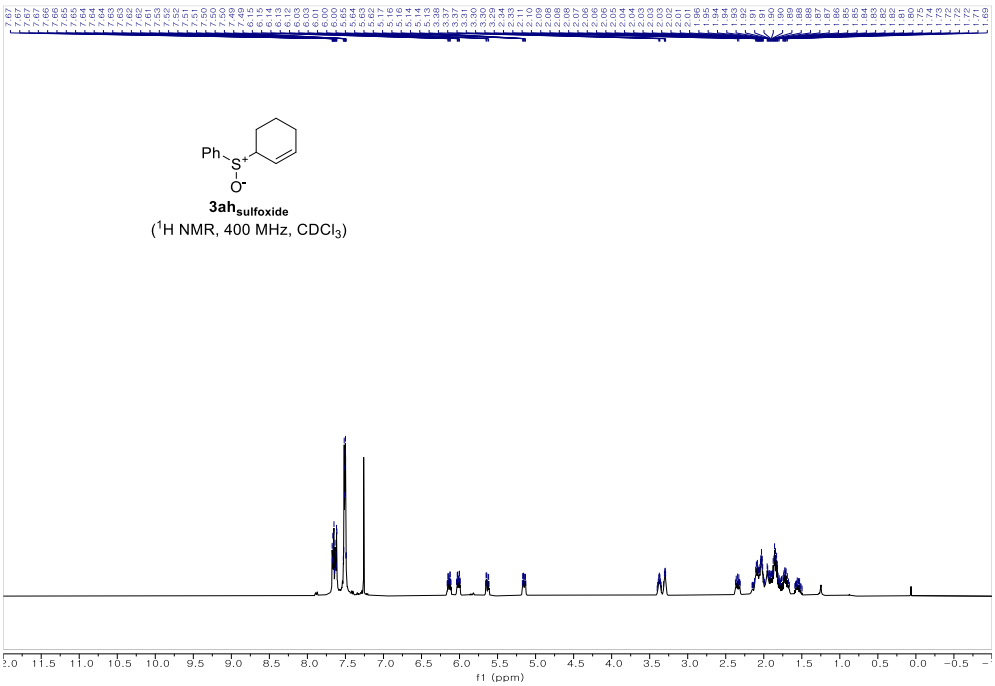

3ah$_{sulfoxide}$

(^{1}H NMR, 400 MHz, $CDCl_3$)

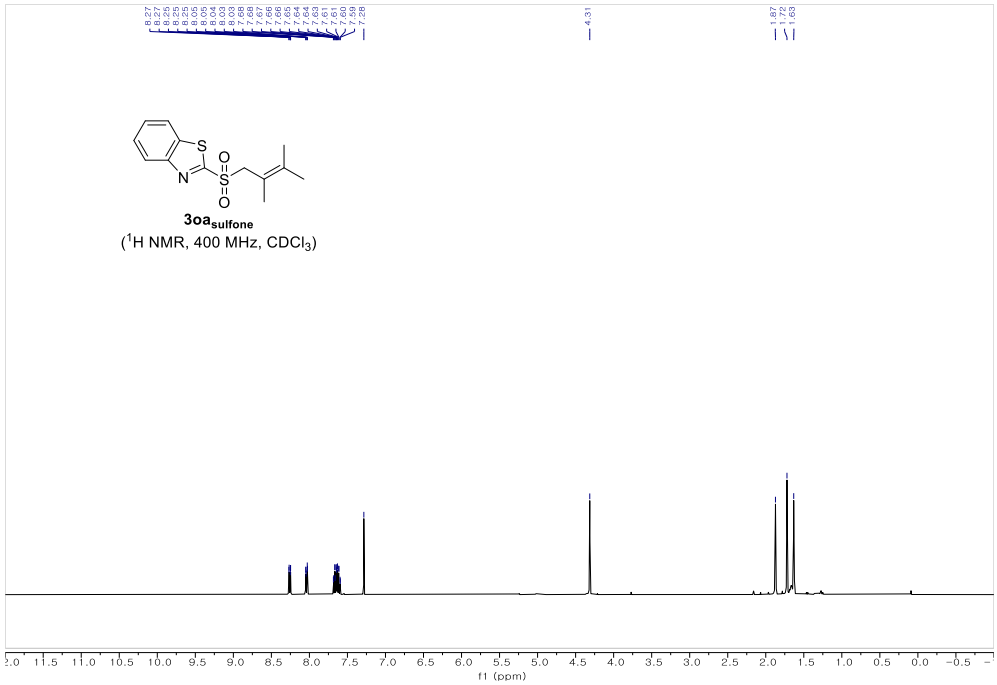

3oa$_{sulfone}$
(^{1}H NMR, 400 MHz, $CDCl_3$)

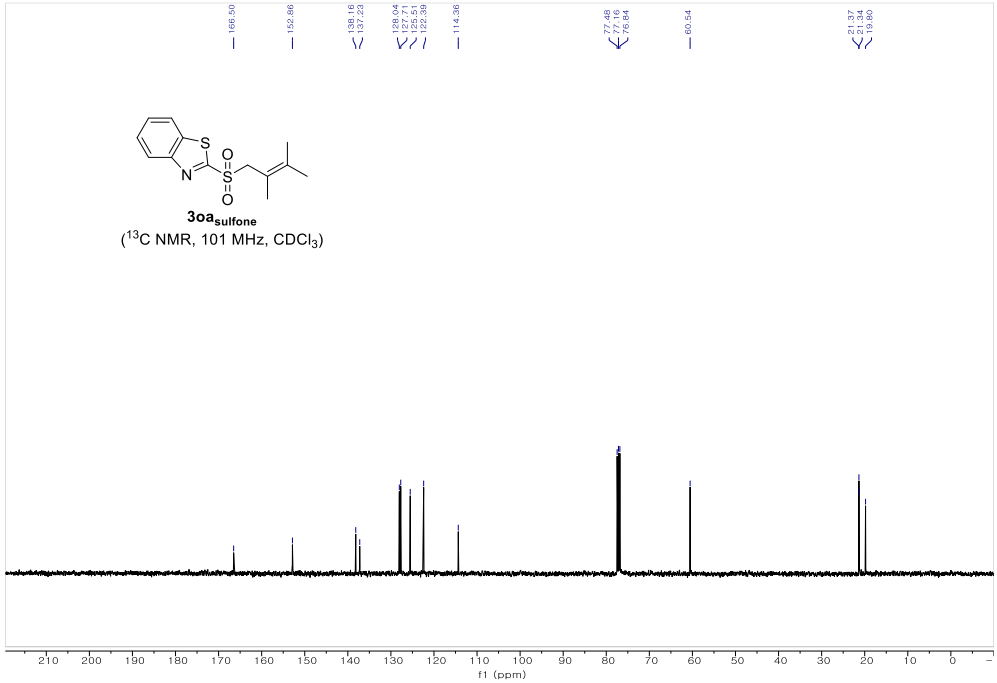

3oa$_{sulfone}$
(^{13}C NMR, 101 MHz, $CDCl_3$)

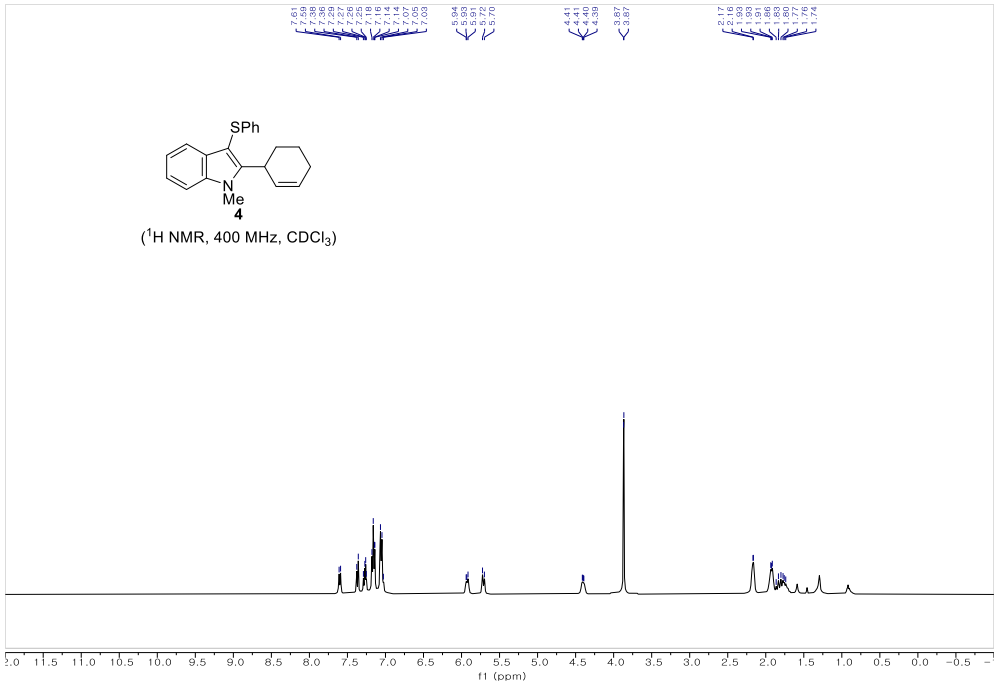

(^{1}H NMR, 400 MHz, $CDCl_3$)

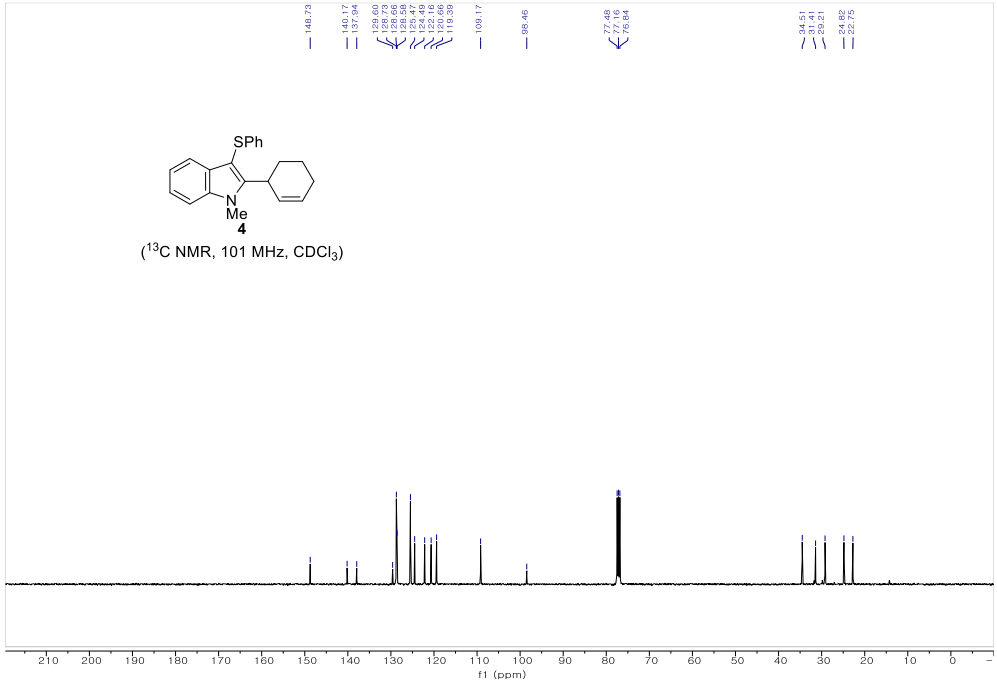

(^{13}C NMR, 101 MHz, $CDCl_3$)

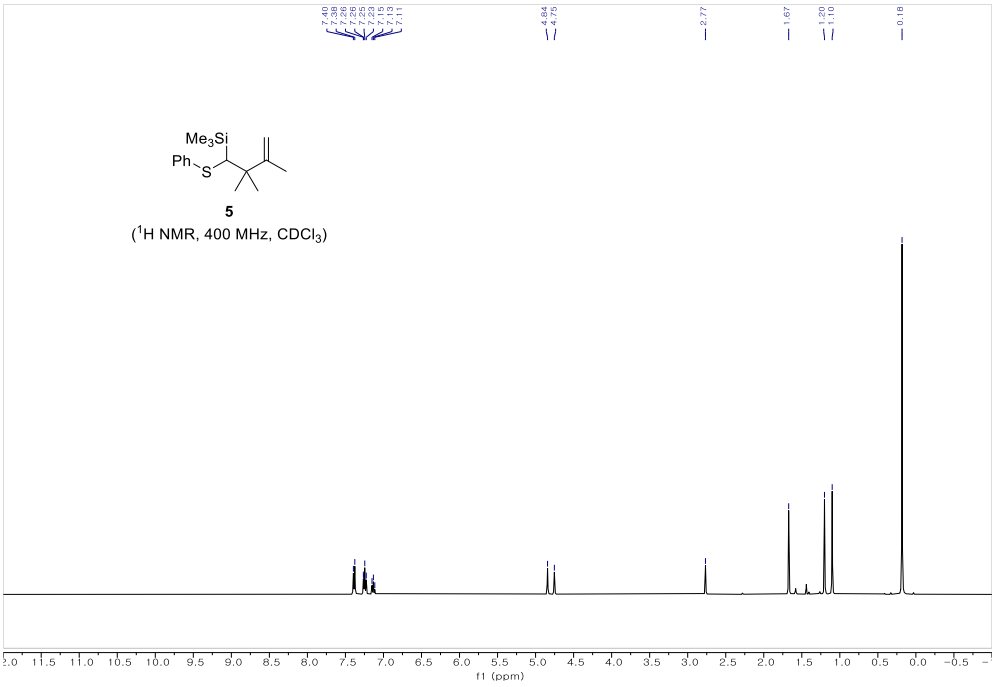

5

(^{1}H NMR, 400 MHz, $CDCl_3$)

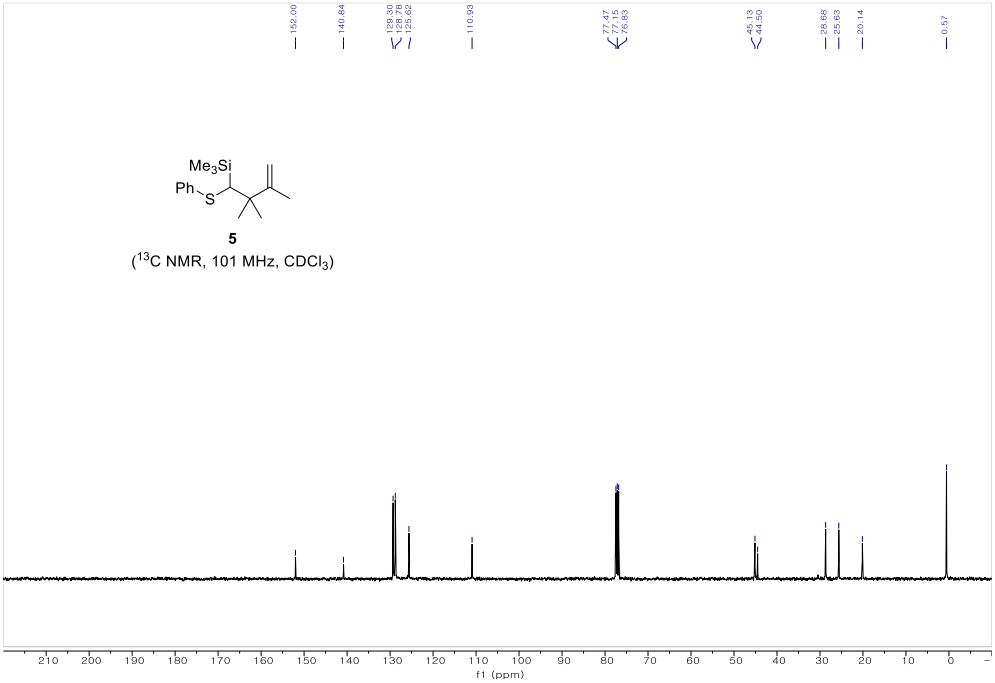

5

(^{13}C NMR, 101 MHz, $CDCl_3$)

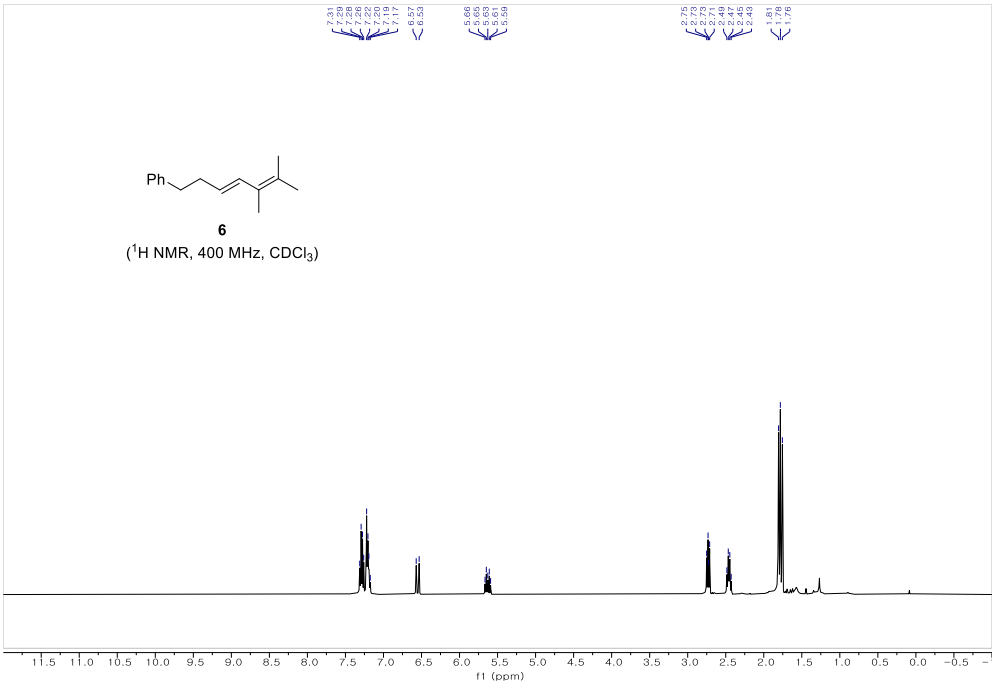

6

(^{1}H NMR, 400 MHz, $CDCl_3$)

Appendix – Cartesian Coordinates for DFT Calculation

Chapter 5

PhSH	C	0.196015	-1.210805	-0.000002
	C	1.590976	-1.207708	-0.000004
	C	2.297806	-0.005023	-0.000002
	C	1.595588	1.201429	-0.000003
	C	0.201953	1.209433	0.000004
	C	-0.506521	0.000404	0.000000
	H	-0.340536	-2.155158	-0.000012
	H	2.124161	-2.154084	0.000008
	H	3.383273	-0.007497	0.000003
	H	2.133243	2.145168	-0.000013
	H	-0.335167	2.153444	0.000020
	S	-2.293873	0.083520	-0.000002
	H	-2.517918	-1.244565	0.000015
PhS-	C	-0.164682	1.200768	-0.000001
	C	-1.557116	1.199982	-0.000001
	C	-2.279368	0.000395	0.000000
	C	-1.557368	-1.199891	0.000001
	C	-0.165436	-1.201173	0.000001
	C	0.598449	-0.000119	0.000000
	H	0.376671	2.143541	-0.000002
	H	-2.090395	2.151381	-0.000003
	H	-3.367357	0.000377	-0.000001
	H	-2.091443	-2.150831	0.000002
	H	0.376425	-2.143692	0.000002
	S	2.346826	-0.000034	0.000000
PhS·	C	-0.149684	1.219689	-0.000001
	C	-1.537703	1.215256	-0.000001
	C	-2.235646	0.000503	0.000000
	C	-1.538387	-1.214848	0.000001
	C	-0.150618	-1.220256	0.000001
	C	0.577665	-0.000436	0.000001
	H	0.403802	2.152639	-0.000003
	H	-2.083342	2.154044	-0.000002
	H	-3.321679	0.000850	0.000000
	H	-2.084717	-2.153247	0.000001
	H	0.402666	-2.153328	0.000002
	S	2.305594	-0.000026	0.000000
PhSSPh	C	2.645615	-1.877357	-0.712303
	C	1.713249	-0.875131	-0.984549
	C	1.855366	0.389689	-0.398193
	C	2.934913	0.644905	0.458605
	C	3.859530	-0.362133	0.730793
	C	3.716646	-1.622867	0.145659
	H	2.533989	-2.856053	-1.169800
	H	0.877658	-1.064623	-1.650150
	H	3.042287	1.628002	0.905228
	H	4.694911	-0.161802	1.395304
	H	4.441213	-2.403976	0.356501
	S	0.687881	1.692221	-0.805274
	S	-0.687867	1.692210	0.805300
	C	-1.855362	0.389695	0.398195
	C	-2.934867	0.644909	-0.458656
	C	-1.713295	-0.875112	0.984591
	C	-3.859493	-0.362117	-0.730856
	H	-3.042204	1.627997	-0.905309

	C	-2.645673	-1.877326	0.712335
	H	-0.877734	-1.064604	1.650229
	C	-3.716661	-1.622837	-0.145679
	H	-4.694842	-0.161787	-1.395408
	H	-2.534086	-2.856012	1.169865
	H	-4.441236	-2.403937	-0.356531
Ir(III)*	Ir	0.706696	-0.606817	0.135908
	C	-0.441857	-0.723836	-1.527762
	C	-1.844505	-0.656408	-1.586540
	C	0.246576	-0.914650	-2.759292
	C	-2.532218	-0.774128	-2.794389
	H	-2.409401	-0.492373	-0.676537
	C	-0.456212	-1.030696	-3.971752
	C	-1.840940	-0.962657	-3.996875
	H	0.074970	-1.173032	-4.907795
	C	1.711875	-0.975408	-2.696803
	C	2.568896	-1.113842	-3.801448
	C	3.944062	-1.145318	-3.615622
	H	2.154750	-1.189655	-4.799332
	C	3.568484	-0.898713	-1.269151
	C	4.462431	-1.034777	-2.322683
	H	4.606904	-1.250151	-4.469248
	H	3.912220	-0.803850	-0.244836
	H	5.529719	-1.049213	-2.132513
	N	2.237197	-0.876634	-1.444789
	C	-0.790164	-0.492253	1.425136
	C	-1.388594	0.662260	1.956504
	C	-1.305688	-1.817390	1.876068
	C	-2.441483	0.597245	2.864731
	H	-1.031000	1.634411	1.640238
	C	-2.400356	-1.846907	2.801336
	C	-2.942515	-0.683696	3.276165
	H	-2.812330	-2.795002	3.130591
	H	-3.774516	-0.721116	3.973448
	C	-0.668821	-2.965961	1.369759
	C	-1.004356	-4.322545	1.679746
	C	-0.328281	-5.363254	1.096870
	H	-1.805328	-4.519427	2.383486
	C	1.018687	-3.752150	-0.097481
	C	0.715280	-5.082050	0.170641
	H	-0.588473	-6.390030	1.334224
	H	1.806645	-3.493816	-0.799154
	H	1.265548	-5.873653	-0.324245
	N	0.388672	-2.719105	0.472824
	C	1.070238	1.396490	0.061532
	C	1.997660	1.892086	1.022723
	C	0.528608	2.330941	-0.835767
	C	2.342339	3.254762	1.066377
	C	0.880425	3.681253	-0.790354
	H	-0.192694	2.004512	-1.576434
	C	1.789771	4.151884	0.163772
	H	3.042622	3.627891	1.807604
	H	2.049046	5.203772	0.199287
	C	2.570247	0.912096	1.956766
	C	3.473641	1.203897	2.992628
	C	3.944541	0.187214	3.812537
	H	3.797106	2.224771	3.154969
	C	2.620962	-1.357976	2.559894
	C	3.513348	-1.124967	3.597512
	H	4.639096	0.414435	4.615783
	H	2.240506	-2.350381	2.342400
	H	3.851933	-1.945930	4.219439
	N	2.166774	-0.375304	1.764655
	C	0.326163	4.628533	-1.820294
	C	-3.052300	1.820958	3.456857
	F	-0.925028	4.294390	-2.200879
	F	0.286487	5.903461	-1.369582
	F	1.087195	4.636748	-2.943491
	F	-2.614742	2.957687	2.875090

	F	-2.785430	1.930776	4.789046
	F	-4.407982	1.809581	3.357707
	C	-4.037624	-0.763800	-2.798504
	F	-4.536300	-0.298876	-3.967589
	F	-4.541146	-2.011084	-2.630038
	F	-4.546211	0.000274	-1.809161
	H	-2.382918	-1.043996	-4.932085
Ir(II)	Ir	-0.962573	-0.000769	-0.001418
	C	0.084511	-0.594768	-1.631783
	C	1.221583	0.011612	-2.190359
	C	-0.408111	-1.769041	-2.290679
	C	1.858402	-0.504801	-3.325966
	H	1.629984	0.900272	-1.722374
	C	0.249321	-2.289087	-3.427950
	C	1.371997	-1.666320	-3.946430
	H	-0.112749	-3.195004	-3.907208
	C	-1.602054	-2.379239	-1.728131
	C	-2.274307	-3.508262	-2.243143
	C	-3.403142	-4.004474	-1.616189
	H	-1.897268	-3.988149	-3.139619
	C	-3.188587	-2.253472	0.005723
	C	-3.876793	-3.367583	-0.451559
	H	-3.914079	-4.875468	-2.017767
	H	-3.507562	-1.719206	0.895304
	H	-4.747672	-3.728389	0.084906
	N	-2.097932	-1.757866	-0.602109
	C	0.079797	1.710757	0.300812
	C	1.215835	1.893927	1.106105
	C	-0.415540	2.867606	-0.386268
	C	1.849151	3.137261	1.227944
	H	1.626209	1.045102	1.641445
	C	0.238352	4.114288	-0.266688
	C	1.360104	4.254490	0.532738
	H	-0.125709	4.981635	-0.811332
	H	1.863692	5.211965	0.616299
	C	-1.608275	2.682730	-1.197126
	C	-2.282837	3.691943	-1.917075
	C	-3.410015	3.394448	-2.661735
	H	-1.908878	4.709348	-1.883022
	C	-3.189272	1.114253	-1.958406
	C	-3.879567	2.065985	-2.694382
	H	-3.922731	4.176729	-3.215007
	H	-3.505147	0.075743	-1.942031
	H	-4.748944	1.779735	-3.276321
	N	-2.100291	1.395408	-1.223753
	C	0.081076	-1.115593	1.331072
	C	-0.415727	-1.099828	2.675965
	C	1.219119	-1.902071	1.088422
	C	0.238861	-1.824864	3.696699
	C	1.853159	-2.627444	2.105135
	H	1.630547	-1.940770	0.086051
	C	1.362716	-2.584709	3.419770
	H	-0.126329	-1.787492	4.719785
	H	1.866810	-3.134361	4.207872
	C	-1.610671	-0.308058	2.919824
	C	-2.286784	-0.190519	4.153090
	C	-3.416067	0.600303	4.266437
	H	-1.912319	-0.727489	5.017704
	C	-3.194328	1.131192	1.940130
	C	-3.886210	1.291324	3.131609
	H	-3.929970	0.687269	5.220005
	H	-3.510578	1.635290	1.032154
	H	-4.757244	1.936259	3.173631
	N	-2.103316	0.357021	1.817552
	C	3.014395	-3.512741	1.783599
	C	3.008071	3.301654	2.158275
	F	3.749194	-3.063099	0.740639
	F	3.866595	-3.653079	2.836020
	F	2.628561	-4.779667	1.454234

	F	3.741847	2.173332	2.293403
	F	2.619160	3.651447	3.418771
	F	3.861909	4.282348	1.754822
	C	3.018397	0.219170	-3.930877
	F	3.874998	-0.620452	-4.574916
	F	2.631319	1.134403	-4.866288
	F	3.748769	0.902177	-3.019907
	H	1.878285	-2.072910	-4.815742
2h	C	0.698390	-1.192370	-0.318162
	C	1.498329	0.047962	0.110584
	C	0.665914	1.305825	0.057057
	C	-0.665911	1.305827	-0.057058
	C	-1.498329	0.047966	-0.110581
	C	-0.698392	-1.192370	0.318160
	H	1.198254	2.254188	0.112672
	H	1.888580	-0.088670	1.131142
	H	2.385243	0.164368	-0.526290
	H	0.593871	-1.193252	-1.411364
	H	1.244359	-2.105160	-0.053572
	H	-1.198249	2.254190	-0.112679
	H	-2.385239	0.164373	0.526298
	H	-1.888587	-0.088665	-1.131137
	H	-0.593873	-1.193257	1.411361
	H	-1.244363	-2.105157	0.053566
TS-A	C	3.427770	-0.356934	-0.673901
	C	3.565700	1.163754	-0.493071
	C	2.393390	1.759217	0.237699
	C	1.543972	1.010822	0.996320
	C	1.690863	-0.412405	1.142757
	C	2.967893	-1.041200	0.622903
	H	2.250522	2.835926	0.178739
	H	4.487433	1.398655	0.064204
	H	3.685859	1.652870	-1.468204
	H	2.685182	-0.556679	-1.455468
	H	4.375670	-0.785361	-1.016328
	H	0.714457	1.496218	1.504709
	H	1.258563	-0.855868	2.040258
	H	3.748640	-0.948295	1.394418
	H	2.826397	-2.116150	0.460670
	H	0.691395	-0.992775	0.236785
	S	-0.342608	-1.718902	-0.641518
	C	-1.681619	-0.585191	-0.318927
	C	-1.650722	0.729448	-0.813734
	C	-2.798187	-1.009365	0.419632
	C	-2.708888	1.602030	-0.560821
	H	-0.796522	1.057081	-1.397013
	C	-3.861993	-0.138496	0.652874
	H	-2.822512	-2.023276	0.805683
	C	-3.818753	1.170699	0.168916
	H	-2.671655	2.617623	-0.945076
	H	-4.722589	-0.481170	1.220505
	H	-4.645658	1.849372	0.356520
2h-rad	C	-0.000815	-1.359834	-0.329946
	C	1.273520	-0.675110	0.195883
	C	1.218410	0.815349	0.003203
	C	0.000888	1.478032	-0.092050
	C	-1.217428	0.816809	0.003209
	C	-1.274333	-0.673586	0.195875
	H	2.148564	1.375202	-0.037200
	H	1.400341	-0.905766	1.267470
	H	2.159076	-1.093016	-0.299451
	H	-0.000779	-1.304878	-1.425496
	H	-0.001451	-2.422244	-0.062283
	H	0.001534	2.557485	-0.230898
	H	-2.146908	1.377781	-0.037173
	H	-1.401438	-0.904101	1.267458
	H	-2.160386	-1.090426	-0.299470
2h-cat	C	1.394023	0.000099	-0.291131
	C	0.663238	1.268842	0.168266

	C	-0.801619	1.193178	0.010723
	C	-1.497816	-0.000105	-0.137637
	C	-0.801452	-1.193289	0.010743
	C	0.663420	-1.268752	0.168256
	H	-1.370409	2.120795	0.076338
	H	0.828029	1.483358	1.243982
	H	1.038107	2.171077	-0.332029
	H	1.443865	0.000107	-1.385192
	H	2.422639	0.000171	0.074157
	H	-2.577551	-0.000181	-0.240809
	H	-1.370110	-2.120989	0.076322
	H	0.828254	-1.483259	1.243967
	H	1.038409	-2.170927	-0.332055
TS-C	C	-2.538270	-0.323227	-1.028926
	C	-2.660742	-1.704862	-1.423388
	C	-3.619322	-2.519841	-0.918622
	C	-4.628860	-2.064201	0.099400
	C	-4.195331	-0.771334	0.808944
	C	-3.649433	0.257805	-0.189835
	H	-3.690886	-3.544514	-1.277091
	H	-1.952065	-2.092010	-2.151002
	H	-5.598264	-1.917157	-0.404587
	H	-4.802863	-2.861726	0.832901
	H	-5.033749	-0.348173	1.372211
	H	-3.405067	-1.004857	1.531102
	H	-3.313469	1.165650	0.320681
	H	-4.454948	0.572739	-0.875078
	C	0.186779	4.203685	-0.401802
	C	-0.473458	3.788195	0.756788
	C	-0.714361	2.432585	0.979143
	C	-0.291027	1.477293	0.042839
	C	0.379215	1.899421	-1.115237
	C	0.611873	3.257672	-1.336294
	H	0.371597	5.260030	-0.573688
	H	-0.801379	4.520513	1.488982
	H	-1.217580	2.103936	1.882628
	H	0.719836	1.159099	-1.831956
	H	1.130626	3.575707	-2.236193
	H	-2.071024	0.346891	-1.746271
	S	-0.612871	-0.265889	0.310279
	S	1.229691	-0.779516	1.798236
	C	2.595476	-1.014527	0.697618
	C	3.367515	0.082663	0.269945
	C	2.946927	-2.305727	0.260968
	C	4.463033	-0.111086	-0.569053
	H	3.100325	1.078667	0.606581
	C	4.044326	-2.493240	-0.576000
	H	2.351564	-3.151717	0.588443
	C	4.804843	-1.397586	-0.993985
	H	5.054108	0.742332	-0.889509
	H	4.308106	-3.494932	-0.903560
	H	5.660928	-1.546124	-1.645846
3ah-rad	C	1.162953	-0.565394	-0.652589
	C	1.316694	0.869678	-0.933415
	C	2.391029	1.672211	-0.267135
	C	3.716174	0.896034	-0.141845
	C	3.483579	-0.510178	0.427159
	C	2.498058	-1.300769	-0.445789
	H	2.544610	2.616321	-0.803441
	H	0.490465	1.391612	-1.408596
	H	4.179254	0.810463	-1.134084
	H	4.418045	1.454826	0.487697
	H	4.432352	-1.055251	0.494067
	H	3.093342	-0.433449	1.450401
	H	2.315071	-2.296557	-0.028760
	H	2.056257	1.956665	0.747140
	H	2.943094	-1.448832	-1.439350
	S	0.119188	-0.829693	0.969799
	C	-4.057909	0.508662	-0.402001

	C	-3.584096	-0.761231	-0.738573
	C	-2.314523	-1.166978	-0.327836
	C	-1.499640	-0.300054	0.415992
	C	-1.981908	0.972897	0.751678
	C	-3.256243	1.372391	0.345851
	H	-5.049016	0.821281	-0.717517
	H	-4.206767	-1.440282	-1.314099
	H	-1.950454	-2.159962	-0.572957
	H	-1.355149	1.640970	1.333227
	H	-3.621440	2.359961	0.613072
	H	0.558314	-1.066283	-1.412550
TS-B	C	1.260443	-0.445481	-0.778115
	C	1.424767	0.946925	-0.846615
	C	2.588903	1.654461	-0.219594
	C	3.847520	0.772904	-0.135660
	C	3.509407	-0.631831	0.382023
	C	2.480346	-1.317879	-0.527248
	H	2.800060	2.581146	-0.768015
	H	0.600037	1.549444	-1.219369
	H	4.296446	0.689193	-1.134442
	H	4.595517	1.251383	0.506227
	H	4.415719	-1.244788	0.443878
	H	3.105878	-0.561072	1.400234
	H	2.174666	-2.284610	-0.116952
	H	2.298849	1.974316	0.795693
	H	2.940573	-1.523978	-1.505460
	S	0.023962	-0.746161	1.087492
	C	-4.105608	0.462523	-0.500577
	C	-3.597838	-0.811731	-0.765684
	C	-2.341537	-1.180001	-0.287584
	C	-1.568694	-0.275739	0.464524
	C	-2.090838	1.004017	0.725894
	C	-3.349205	1.367215	0.247808
	H	-5.085680	0.747046	-0.872120
	H	-4.183891	-1.521785	-1.342486
	H	-1.950256	-2.173673	-0.482692
	H	-1.502314	1.703196	1.311041
	H	-3.740173	2.358446	0.459878
	H	0.505172	-0.877980	-1.430319
3ah	C	1.179823	-0.575586	0.448894
	C	2.443722	-1.329426	0.141690
	C	3.639462	-0.739343	0.029279
	C	3.862408	0.743903	0.173701
	C	2.547300	1.535077	0.117286
	C	1.459444	0.848428	0.950449
	H	4.515944	-1.355353	-0.165298
	H	2.350657	-2.404239	0.005245
	H	4.382755	0.935507	1.125287
	H	4.550386	1.090236	-0.608394
	H	2.705676	2.561306	0.466231
	H	2.205797	1.599372	-0.922612
	H	0.534392	1.433528	0.952911
	H	1.790709	0.774939	1.996430
	S	0.124459	-0.614511	-1.106924
	C	-4.062042	0.370509	0.525230
	C	-3.361910	1.312181	-0.229308
	C	-2.082942	1.018728	-0.706828
	C	-1.498528	-0.227166	-0.441910
	C	-2.213507	-1.175258	0.304676
	C	-3.483951	-0.872626	0.793280
	H	-5.055162	0.601028	0.899447
	H	-3.807198	2.279542	-0.443496
	H	-1.532833	1.750577	-1.289598
	H	-1.774378	-2.150686	0.491025
	H	-4.028525	-1.612786	1.372639
	H	0.594757	-1.127327	1.192333
TS-D	C	0.523140	0.977073	0.121994
	C	-0.535188	1.721371	0.868503
	C	-0.417320	3.214649	1.009646

	C	0.041760	3.900060	-0.289865
	C	1.272514	3.202197	-0.885719
	C	0.999002	1.713724	-1.138399
	H	-1.366435	3.635729	1.361992
	H	-0.997924	1.184516	1.696702
	H	-0.778667	3.875395	-1.019361
	H	0.254973	4.956847	-0.094215
	H	1.564226	3.687727	-1.823909
	H	2.122143	3.304371	-0.198675
	H	1.883559	1.214461	-1.546657
	H	0.317951	3.428085	1.806498
	H	0.204422	1.613275	-1.891142
	S	1.943933	0.657599	1.355141
	H	0.171889	-0.028603	-0.128027
	H	-1.866337	1.538539	-0.117148
	S	-3.043883	1.257861	-0.913013
	C	2.815507	-0.674679	0.527444
	C	4.036824	-0.419830	-0.111738
	C	2.306228	-1.981552	0.543873
	C	4.737655	-1.459055	-0.726581
	H	4.432934	0.590465	-0.119188
	C	3.002835	-3.013307	-0.084212
	H	1.370228	-2.184437	1.055085
	C	4.220416	-2.754886	-0.718311
	H	5.685245	-1.253204	-1.215972
	H	2.599999	-4.021914	-0.068847
	H	4.764702	-3.561556	-1.200450
	C	-3.244185	-0.441915	-0.375775
	C	-3.006702	-1.490522	-1.275809
	C	-3.670507	-0.739422	0.927400
	C	-3.192278	-2.814983	-0.876865
	H	-2.677772	-1.260722	-2.284039
	C	-3.837172	-2.065359	1.326307
	H	-3.878138	0.070862	1.619037
	C	-3.601706	-3.106124	0.425250
	H	-3.009698	-3.619434	-1.583653
	H	-4.162339	-2.284934	2.339276
	H	-3.740703	-4.137477	0.735787
3ah'	C	-3.454990	-0.474792	-0.501656
	C	-2.496362	-1.332767	0.339808
	C	-1.135438	-0.655119	0.580502
	C	-1.311790	0.768694	1.133792
	C	-2.273439	1.624167	0.296265
	C	-3.628501	0.926568	0.103269
	H	-2.949188	-1.506744	1.326394
	H	-2.351217	-2.317296	-0.117815
	H	-3.067998	-0.385178	-1.524910
	H	-4.424934	-0.980030	-0.579482
	H	-1.710196	0.673474	2.155306
	H	-0.336647	1.258573	1.226188
	H	-2.411786	2.599430	0.777767
	H	-1.822383	1.817413	-0.684784
	H	-4.134010	0.839362	1.076203
	H	-4.281744	1.535548	-0.532826
	C	-0.156001	-0.704075	-1.013203
	H	-0.556563	-1.254411	1.290175
	C	1.482020	-0.259040	-0.428138
	C	2.033195	0.982485	-0.771794
	C	2.244342	-1.162390	0.326997
	C	3.326116	1.316211	-0.363275
	H	1.445723	1.680135	-1.359857
	C	3.529342	-0.819330	0.746092
	H	1.830910	-2.135396	0.574446
	C	4.074199	0.419352	0.399750
	H	3.744788	2.280248	-0.637631
	H	4.110705	-1.525259	1.332385
	H	5.078387	0.681101	0.719997

Acknowledgement (감사의 글)

6년에 걸친 학위과정을 무사히 마치고 학위 논문을 마무리 지을 수 있게 되었습니다. 한참 부족한 저였지만, 많은 분들의 도움과 관심이 있었기에 이 영광스러운 순간이 다가왔다고 생각합니다. 이 지면을 통해 감사의 인사를 드리고자 합니다.

제일 먼저, 대학원 진학이라는 선택에 무한한 지지와 지원을 아끼지 않아 주신 가족들에게 감사함을 전합니다. 긴 시간 동안 학업을 이어 나갈 수 있었던 가장 큰 원동력은 가족들의 응원이었습니다. 항상 저를 가장 아껴 주시며, 그 어떠한 결정도 믿어 주셨던 부모님께 진심으로 감사드리며, 사랑합니다. 동생 다영이에게는, 집 밖에서 지낸 시간이 길어 오빠 노릇을 제대로 못해서 미안한 마음이 큽니다. 그럼에도 착실하게 지내는 동생에게 고맙고 항상 응원한다는 말을 전하고 싶습니다.

2013년 학부 연구생 시절부터 지금까지 끊임없는 가르침과 조언을 주신 홍순혁 교수님께 무한한 감사의 말씀 올립니다. 연구 과정에서 여러 실수와 실패를 거듭 하는 와중에도 격려와 지지를 보내 주셨고, 새로운 아이디어와 실험들을 제안할 수 있는 환경을 만들어 주셨습니다. 교수님의 관심과 지도가 없었다면 학위 과정을 무사히 마칠 수 없었을 것입니다. 그동안 주신 은혜에 보답하는 마음으로 성장 해 나가겠습니다.

I would like to express my greatest appreciation to Professor David Yu-Kai Chen for his sincere guidance and advice to the so-called novice undergraduate researcher in 2012. His teaching and

training had let me know the beauty of organic chemistry and finally decide to be involved in this research field. Also, he was always willing to participate in my Ph.D. candidate proposal presentation and the Ph.D. thesis presentation as a co-advisor. I really thank him for his careful evaluations and advice throughout the Ph.D. course.

데이비드 첸 교수님과 함께 박사과정생 연구제안 발표와 박사학위 논문 발표에 심사위원으로 기꺼이 참석해 주신 정영근 교수님, 최태림 교수님, 그리고 이홍근 교수님께 감사의 말씀 올립니다. 제 연구 과제와 학위 논문에 관심을 가지고 많은 가르침들과 조언을 주셨습니다. 끊임없는 배움의 자세와 열정적인 연구 자세를 솔선수범하여 보여주신 교수님들의 모습을 본받고 명심하겠습니다.

한편으로는 단조롭고 고된 대학원 생활을 이어 나갈 수 있었던 것은 같은 연구실에서 동고동락했던 연구실 선후배님들이 있었기에 가능했습니다. 한창 모르는 것이 많던 신입생 시절에 했던 그 어떤 질문들도 친절하게 알려주셨던 선배님들이 계셨기에 실험실에 잘 적응할 수 있었습니다. 홍종태 박사님, 건중이형, 호성이형, 정빈누나, 승효형, 병준이형, 한수형, 상승이형, Benjamin Pooi, 기철이형, 재운이형, 그리고 민하누나 모두에게 진심 어린 감사의 말씀 전합니다. 2014년도에 대학원 생활을 같이 시작한 석순이와 상민이형으로부터 정말 많은 것들을 배웠습니다. 특히, 연구실 옆 자리였던 상민이형과 많은 이야기와 디스커션을 하면서 연구에 대한 애정과 즐거움을 배우고

느낄 수 있었습니다. 서울대에서 뿐만 아니라 카이스트에서도 같이 생활하고 있는 건순이, 다은이, 기택이형, 근호, 근석이에게는 특별한 애틋함이 있습니다. 실험실에 있었던 많은 대소사들을 경험하고 공유하며 생긴 유대감은 평생 갈 것입니다. 항상 연구에 열정적이며 기대 이상의 일들을 해 내는 동료들에게 많이 배울 수 있었고, 정말 고마웠습니다. 석사로 졸업하여 먼저 사회에 진출한 다본누나와 홍다은에게도 앞날의 발전을 기원합니다. 서울대에 남아있는 연구실 후배님들 (장우, 원정이, 수용이, 사벽이형, 호경이) 과 카이스트에서 만난 후배님들 (범순이, 세혜, 경민이, 선우) 과 함께 연구실 생활을 할 수 있어서 즐거웠습니다. 앞으로의 대학원 생활을 잘 해내며 각자의 위치에서 나날이 성장할 것으로 믿어 의심치 않습니다.

각자의 연구실에서 열심히 생활하며 서로를 응원 해 왔던 대학원 학우 분들에게도 감사의 말씀 전합니다. 항상 스스럼없이 먼저 다가와 때로는 시시콜콜한 이야기를, 때로는 한없이 진지한 이야기를 털어 놓던 상희에게 고마운 마음이 큽니다. 본인의 연구에 몰두하며 훌륭한 성과를 이루는 모습을 가까운 곳에서 지켜보며 많이 느끼며 배울 수 있었습니다. 같은 유기화학 분야의 선배로서 여러 가지 조언과 격려를 아끼지 않으셨던 김태훈 박사님께도 감사드립니다. 무엇보다도 경태, 도담이, 그리고 석희에게 특별한 감사의 마음을 전합니다. 평소에는 대학원 생활에 치이며 정신없이 지내도, 시간이 맞으면 모여서 마음 속 이야기들을 맥주 안주 삼아 회포를 풀던 그 때가 정말 행복했습니다. 본받고 싶은 점들이 많은 참으로 매력 넘치는 이 친구들과 함께 한

시간들이 있었기에 대학원 생활이 조금 더 윤택할 수 있었습니다. 비록 먼 거리에 있어 자주 만나지는 못하지만, 학부 시절부터 서로를 응원하며 같이 꿈을 키워 나갔던 은재에게도 진심으로 고마움을 전하고 싶습니다.

대전 카이스트로 자리를 옮기게 되었을 때 많은 도움을 주었던 분들에게 감사의 말씀을 드립니다. 특히, 실험실 셋업 과정에서 생겼던 여러 가지 문제들의 해결 등 여러 방면으로 도움을 주었던 박윤수 박사에게 많은 고마움을 느낍니다. 또한 서울에서 지내던 시절에도 대전을 방문할 때마다 반갑게 반겨주던 동형이, 영범이, 그리고 종호에게도 고맙다는 말을 전하고 싶습니다.

이제 학생이라는 신분에서 벗어나 또 다른 삶의 영역으로 들어가게 되었습니다. 항상 겸손하며 배움에 끊임이 없는 삶을 지향하겠습니다. 많은 분들에게 받은 과분한 관심과 도움 잊지 않고 보답 해 나아가겠습니다.

2020년 7월

학위 논문을 마무리하며

김 정 원

국문초록

아이소사이아나이드와 알릴 화합물의 촉매적 변환 개발

유기 화합물의 촉매적 변환은 가치가 높은 구조를 합성할 수 있는 유용한 전략이다. 기질의 화학적 특성과 이전에 구축되어 온 전략들을 기반으로 촉매 조건을 구성하여, 새롭고 독창적인 유기 변환들을 개발할 수 있다. 본 논문에서는 아이소사이아나이드와 알릴 화합물의 새로운 촉매적 변환의 개발을 통해 합성적으로 유용한 화학 구조를 얻기 위한 과정에 대해 논의한다.

논문의 첫 부분에서는 아이소사이아나이드의 화학적 특성과 촉매적 활용에 대해 논의한다. 친핵체와 친전자체 양쪽의 성질을 모두 가지는 아이소사이아나이드의 말단 탄소는 촉매적 변환에서 다양한 방식으로 활성화될 수 있다. 제1장에서는 아이소사이아나이드의 말단 탄소의 활성화를 유도하는 자세한 기작들을 대표적인 예시 반응들과 함께 소개한다. 제2장과 제3장에서는 아이소사이아나이드의 촉매적 친핵체 활성화를 위한 새로운 접근법을 소개한다. 특히, 질소고리화카벤(NHC)을 유기촉매로 활용하여 아이소사이아나이드의 새로운 변환

방식들을 제시한다. 케톤과의 반응을 통해 다양한 종류의 엔아민온을 높은 수율로 합성할 수 있으며 (2장), 인돌과 아이소사이나이드 사이의 반응을 통해 독특한 구조의 폼아미딘을 합성할 수 있었다 (3장).

논문의 두 번째 부분에서는 가시광 광산화환원 촉매 체계에서 sp^3 혼성 탄소-수소 결합의 작용기화를 논한다. 가시광선을 에너지원으로 도전적인 탄소-수소 결합을 활성화하는 전략은 유기 합성에서 널리 연구되고 있다. 제4장 에서는 sp^3 혼성 탄소-수소 결합 작용기화 반응을 위해 현재까지 개발된 가시광 광산화환원 촉매 체계를 전략별로 구분하여 대표적인 예시들과 함께 소개한다. 제5장 에서는 가시광 광산화환원 촉매 체계를 활용하여 간단한 알릴 화합물과 다이설파이드로부터 알릴 티오에터를 합성하는 새로운 방법론을 제시한다. 예상되는 부반응 (하이드로티올레이션)을 억제하는 촉매 순환을 구성하여 알릴 자리 탄소-수소 티오화 반응을 선택적으로 진행하였고, 깊이 있는 반응 기작 연구로부터 제시된 비대칭형 다이설파이드를 도입하여 반응 기질의 폭을 넓힐 수 있었다.

주요어 : 아이소사이아나이드, 친핵성 활성화, 유기촉매, 질소고리화카벤, 알릴 화합물, 가시광선, 광산화환원 촉매반응, 알릴 티오에터
학 번 : 2014-21250